Durham E-Theses

X-ray structural studies of lanthanide macrocycles and biological molecules

Moloney, Janet M.

How to cite:

Moloney, Janet M. (1999) *X-ray structural studies of lanthanide macrocycles and biological molecules*, Durham theses, Durham University. Available at Durham E-Theses Online: http://etheses.dur.ac.uk/4599/

Use policy

The full-text may be used and/or reproduced, and given to third parties in any format or medium, without prior permission or charge, for personal research or study, educational, or not-for-profit purposes provided that:

- a full bibliographic reference is made to the original source
- a link is made to the metadata record in Durham E-Theses
- the full-text is not changed in any way

The full-text must not be sold in any format or medium without the formal permission of the copyright holders.

Please consult the full Durham E-Theses policy for further details.

Academic Support Office, Durham University, University Office, Old Elvet, Durham DH1 3HP
e-mail: e-theses.admin@dur.ac.uk Tel: +44 0191 334 6107
http://etheses.dur.ac.uk

X-ray Structural Studies of Lanthanide Macrocycles and Biological Molecules

by Janet M. Moloney, B.Sc.

Thesis submitted in part fulfillment of the requirements for the degree of

Doctor of Philosophy

at the

University of Durham

Department of Chemistry

September 1999

The copyright of this thesis rests with the author. No quotation from it should be published without the written consent of the author and information derived from it should be acknowledged.

12 APR 2000

X-ray Structural Studies of Lanthanide Macrocycles and Biological Molecules

Submitted for the degree of Doctor of Philosophy, September 1999, by Janet M. Moloney, University of Durham.

ABSTRACT

The work described in this thesis is broadly divided into two sections. The structural study on the lanthanide macrocyclic complexes was afforded by means of X-ray crystallography. In this chapter, the molecules dota, the cationic enantiopure tetraamide europium and dysprosium complexes, the sodium complexes of the tetranaphthylamide and quinoyl derivative, the enantiopure gadolinium and europium complexes of the tetraamide series with esteratic sidechains, the lanathanum and ytterbium complexes of the dota derivative with benzyl phosphinate sidechains, and the tetracarboxyethyl series both as three uncomplexed stereoisomer and complexes of the *RRRR* stereoisomer with europium, gadolinium and terbium. These complexes exhibit quite a lot of structural diversity.

Chapter five deals with experiments carried out at ultra low temperatures. A phase transition that the molecule benzil undergoes is investigated on the *Fddd* diffractometer, a study of the interesting 1,12-dicarbonyl borane was undertaken to obtain precise values for the carbonyl bond lengths and the unprecedented structure of its hydrate was revealed to be a carbene diol and not the expected carboxylic acid complex. The standard for macromolecular tests for diffraction, chicken egg white lysozyme, was crystallised and used to optimise conditions for low-temperature data acquisition from macromolecular samples.

J. M. Moloney, 1999.

The work described in this Thesis was carried out in the Department of Chemistry, Durham University from October 1995 to January 1999, under the supervision of Professor J.A.K. Howard. All of the work is my own, unless stated to the contrary, and it has not been submitted previously for a degree at this or any other university.

J.M. Moloney, 1999

The copyright of this Thesis rests with the author. No quotation from it should be published without her prior written consent and information derived from it should be acknowledged.

Acknowledgements

I am eternally grateful and privileged to have had as a mentor Professor Judith Howard over the course of my Ph.D. Her dedication to science, to members of the group and hard-working attitude have been inspirational. Thank you also for your kindness to me, and constant words of encouragement during the writing of this thesis.

I am extremely grateful to Dr. Andrés Goeta for all the help he has given me over the past almost four years. I would like to thank Dr. Slimane Dahaoui, in particular, for being a brilliant teacher and for useful discussions and encouragement.

It has been a pleasure to have collaborated with many chemists in this department, in particular the group of Professor David Parker in the field of lanthanide complexation chemistry. I am especially grateful to Dr. Gareth Williams for his help and ideas on the investigations of lanthanide complex binding to DNA. Thank you to Dr. Rachel Dickins, Dr. Morag Easson, Dr. Clive Foster, Dr. Linda Govenlock, Dr. Alvaro de Sousa and Dr. Mark Woods.

I am very grateful to the chemist Dr. Mark Fox, whom I have enjoyed collaborating with on the boron cage project. Thank you to Dr. Simon Teat for much help and working long hours during visits to station 9.8 at Daresbury. Thank you to Dr. Harry Powell for advice on oligonucleotide crystallography.

I am very indebted to many members of the crystallography group, past and present, for what they have taught me. I would like to sincerely thank Dr. Andrei Batsanov, Dr. Roy Copley, Dr. Phillippe Guinneou, Dr. Mike Leech, Dr. Christian Lehmann, Dr. Claire Wilson, and Dr. Dmitrii Yufit. Thank you also for your friendship and good humour to many crystallographers and visitors to the group over the three-and-a-half years: Charlie Broder, Dr. Brian Bridgewater, John Cowan, Dr. Jacqui Cole, Dr. Pete Ford, Richard Hampshire, Andrew Hamilton, Dr. Mark Roden and Dr. Jing-Wen Yao, Professor Lyudmila Kuz'mina, Professor Sasha Bagatur'yants. Elena Alekseveya, , Dr. Andrei Churakov, Dr. Olga Gladkikh and Dr. Dmitrii Naumov. It has been a pleasure to know you all.

I must give a special mention to Andrew Johnson for genuine belief in me, extreme tolerance(!) and lots of good times inside and out of work, and to Jan Kelly for her friendship, support and for dragging me out of the lab.

Outside of work, I would like to mention for making my time in Durham a happy one. Adrian O' Halloran, Kim McGarry, Julian Cherryman, Caroline Williamson, Marcela Goeta, Jane Vear, Faye Buxton, Linda Gibbons. To friends from Cork – Sarah Keating, Sinead Jacob, Darren McAdam-O' Connell and Entesar Al-Balushi thank you very much.

Thank you to Dr. Yvonne Jones for understanding during the past few months, while I have finished writing. Thank you very much to Dr. Wai-Ching Hon for words of encouragement and ginseng tea, which kept me going. And last but not least, thank you to Dr. Lesley Greene for good times in Oxford and especially for keeping me on a writing timetable – you're a good kid!

To my parents,

Thomas and Mary Moloney.

Table of Contents

Chapter 1: Introduction 1

Chapter 2 Theory and Practice of Crystal Growth 4
2.1 Historical Background 5
2.2 Stages in Crystal Growth 6
2.2.1 Nucleation 6
2.2.2 Growth 10
2.2.2.1 Factors Affecting Growth 11
2.2.3 Cessation of Growth 13
2.3 Crystallisation Conditions 14
2.4 Precipitants 16
2.4.1 Salts 16
2.4.2 Volatile and involatile organic solvents 18
2.4.3 Polyethylene Glycols 18
2.5 Crystal Growth Set-up and Experimental Conditions 19
2.5.1 Liquid Diffusion 19
2.5.2 Vapour Diffusion 19
2.6 Industrial Methods 20
2.7 References 22

Chapter 3 The X-ray Diffraction Experiment 23
3.1 Introduction 24
3.2 Background 24
3.3 Generation of X-radiation 26
3.4 Monochromation and Absorption 28
3.4.1 The analytical absorption correction 30
3.4.2 The semi-empirical absorption correction 31
3.4.3 The empirical absorption correction 31
3.5 Instrumentation 33
3.5.1 The four-circle goniostat 33
3.5.2 The single crystal Rigaku AFC6S four-circle diffractometer 36

3.5.3 The *Fddd* four-circle diffractometer 39
3.5.4 The single crystal SMART three-circle diffractometer 43
3.5.4.1 The charge-coupled device area detector 49
3.6 Crystal Evaluation and Mounting 52
3.7 Unit Cell Determination 54
3.8 Data Collection 57
3.9 Data Reduction 57
3.10 Structure Solution and Refinement 58
3.10.1 Space group assignment 59
3.10.2 Patterson methods 60
3.10.3 Direct methods 61
3.10.4 Refinement of the trial structure 63
3.11 Low temperature attachments 64
3.11.1 The N_2 open flow cryostat 65
3.11.2 The closed cycle refrigerator 66
3.11.3 The open flow helium cryostat (Helix) 69
3.12 Synchrotron radiation at the Daresbury SRS 70
3.12.1 Background to synchrotron radiation crystallography 70
3.12.2 The Daresbury SRS 75
3.12.3 Station 9.8 75
3.13 Bibliography 79
3.14 References 80

Chapter 4 Structural Studies of Lanthanide Macrocylic Complexes 83
4.1 Introduction 84
4.2 Applications of lanthanide macrocyclic complexes 87
4.2.1 Luminescence 87
4.2.2. Spectroscopic applications 91
4.2.3 Tumour Imaging using Positron Imaging Tomography 94
4.3 Perspective 96
4.4 'DOTA' – The archetypal chelate 99
4.5 Characterisation of enantiopure lanthanide tetraamide compounds 110
4.5.1 Stereoisomers of lanthanide complexes of dota derivatives 110

4.5.2 Structural investigations of enantiopure lanthanide complexes incorporating phenyl chromophores 112
4.5.3 Structural investigations of enantiopure lanthanide complexes incorporating naphthyl and quinoline chromophores 119
4.5.4 Enantiopure complexes of tetraamide dota bearing esteratic groups 125
4.5.5 The macrocycle DTMA in its free and complexed forms 130
4.6 Lanthanide complexes with benzylphosphinate pendant groups 137
4.7 Lanthanide complexes with carboxyethyl pendant groups 142
4.7.1 Structures of the all the isomers of the free ligand. 156
4.8 Conclusions and the Future 161
4.9 References 169

Chapter 5 Low-temperature Studies on small and macromolecules 175
5.1 Introduction 176
5.2 Phase transition in benzil 180
5.3 The structures of 1,12-$B_{12}H_{10}(CO)_2$ and its tetrahydrate 183
5.3.1 The crystal structure of 1,12-$B_{12}H_{10}(CO)_2$ 183
5.3.2 The crystal structure of the tetrahydrate $C_2H_{14}B_{12}O_4 \cdot 4H_2O$ 188
5.4 Lysozyme 192
5.5 References 206

Appendix A Atomic Coordinates, Equivalent and Anisotropic Displacement Parameters for all Reported Structures A-1

Appendix B Conferences, Courses, Seminars attended and other periods spent working away from host institution and list of pulications arising from this thesis B-1

Tables Presented in this Thesis

Table 4.4.1 – Crystal data and refinement details for DOTA dichloride pentahydrate 104
Table 4.4.2 – Selected bond lengths [Å] for DOTA. 105
Table 4.4.3 – Selected bond angles [°] for DOTA. 106
Table 4.4.4 - Selected torsion angles [°] for DOTA 107

Table 4.5.2.1 – Selected crystal data for Eu·(SSSS)-L^2, Dy·(SSSS)-L^2, Eu·(RRRR)-L^2. 114

Table 4.5.2.2 – Selected bond lengths (Å) for Eu·(SSSS)-L^2, Dy·(SSSS)-L^2, Eu·(RRRR)-L^2 115

Table 4.5.3.1 - Selected torsion angles (°) for sodium complexes of L^3 and L^4. 121

Table 4.5.3.2 - Selected crystal data for $C_{64}H_{76}ClN_{14}NaO_5$ and $C_{68}H_{75}F_3N_9NaO_6$ 122

Table 4.5.3.3 – Selected bond lengths (Å) for $C_{68}H_{75}F_3N_9NaO_6$ and $C_{64}H_{76}ClN_{14}NaO_5$ the enantiopure S complexes of L^3 and L^4 respectively. 123

Table 4.5.4.1 - Selected torsion angles (°) for europium and gadolinium complexes of L^5. 125

Table 4.5.4.2 – Selected crystal for $C_{36}H_{69}EuF_{18}N_8O_{14.5}P_3$ and $C_{36}H_{68}F_{18}GdN_8O_{14}P_3$. 128

Table 4.5.4.3 – Selected bond lengths (Å) for $C_{36}H_{69}EuF_{18}N_8O_{14.5}P_3$ and $C_{36}H_{68}F_{18}GdN_8O_{14}P_3$ for the enantiopure complex of L^5. 129

Table 4.5.5.1 - Selected crystal data for DTMA and its dysprosium complex. 135

Table 4.5.4.2 – Selected bond lengths (Å) for $C_{20}H_{47}DyF_{18}N_8O_{7.50}P_3$ and $C_{20}H_{43}N_8O_{5.50}$. 136

Table 4.6.1 – Selected interatomic distances (Å) for the La and Yb complexes of L^7. (* denotes that there are two symmetrically independent molecules.) 138

Table 4.6.2 – The bite angles (°) for the La and Yb complexes of L^7. 139

Table 4.6.3 – Selected crystal data and structure refinement details for the ytterbium and lanthanum complexes of L^7. 141

Table 4.7.1 - Selected torsion angles (°) for europium, terbium and gadolinium complexes of L^8. 146

Table 4.7.2 – Intermolecular close contacts for the Gd-L^8 complex. 148

Table 4.7.3 - Selected torsion angles (°) for europium, terbium and gadolinium complexes of L^8 to illustrate their conformational preferences. 148

Table 4.7.4 - Selected crystal data for the europium, gadolinium and terbium complexes of 1,4,7,10-tetrakis(carboxyethyl)-1,4,7,10-tetraazacyclododecane. 149

Table 4.7.5 – Selected bond lengths (Å) for C28 H49 Eu N4 O20.25, C28 H49 Gd N4 O20 and C28 H49 N4 O20 Tb, the lanthanide complexes of L^8. 153

Table 4.7.1.1 – Selected crystal data and structure refinement details for the three diastereomers of L^8. 159

Table 4.7.1.2 – Selected bond lengths for three of the isomers of L^8. 160

Table 4.8.1 – Crystallisation conditions for the Eu RRR complex of N-methylated phenanthradine with $(CG)_6$ at pH 7.0 buffered with sodium cacodylate. 165

Table 4.8.2 – Crystallisation conditions for the Eu RRR complex of N-methylated phenanthradine with $(CG)_6$ at pH 6.4 buffered with sodium cacodylate. 165

Table 4.8.3 – Crystallisation conditions for the Eu RRR complex of N-methylated phenanthradine with $(AT)_6$ at pH 6.4 buffered with sodium cacodylate. 166

Table 4.8.4 – Crystallisation conditions for the Eu RRR complex of N-methylated phenanthradine with $(AT)_6$ at pH 7.0 buffered with sodium cacodylate. 166

Table 4.8.5 – Crystallisation conditions for the Eu SSS complex of N-methylated phenanthradine with $(CG)_6$ at pH 7.0 buffered with sodium cacodylate. 166

Table 4.8.6 – Binding characteristics for chiral europium complexes with $(CG)_6$ and $(AT)_6$ (0.1 M Hepes, 293 K, 10 mM NaCl) as performed by J.A.G. Williams. 167

Table 5.3.1 - Bond lengths [Å] for the independent part of C2 H10 B12 O2. 185

Table 5.3.2 - Data for the refinements of C2 H10 B12 O2 at 150 K and 100 K. 187

Table 5.3.3 - Bond lengths [Å] for C2 H22 B12 O8. 189

Table 5.3.4 - Crystal data and structure refinement for C2 H22 B12 O8. 191

Table 5.4.1 - Preliminary Results from the SMART 193

Figures Presented in this Thesis

Figure 2.2.1 - Regions of Saturation, Note that whilst [Protein] is denoted, this graph holds true for any sample. Reprinted from T. Arakawa and S.N. Timasheff, (1985), Methods in Enzymology, Vol. 114, 49-127. 7

Figure 2.4.1 - Kinetics and crystal quality as a function of salt and protein concentrations. 17

Figure 3.2.1 - Schematic representation of the Ewald (reflection) sphere. 25

Figure 3.3.1 – A schematic representation along the longitudinal axes of (a) a sealed tube and (b) a rotating anode X-ray sources (reprinted from Giacovazzo, 1992).27

Figure 3.3.2 – X-ray spectra of the output from a copper source (reprinted from Fundamentals of Crystallography by Giacovazzo, 1992). 27

Figure 3.4.1 – The indexed faces of $C_{14}H_{40}Br_{0.8}Cl_{1.2}N_8P_4S_4Cu_2$, measured on the SMART viewed perpendicular to the mounted axis. 30

Figure 3.5.1.1 - Schematic representation of a four-circle diffractometer, reprinted from J.P. Glusker and K.N. Trueblood (1985), Crystal Structure Analysis – A Primer, 2nd edition. Oxford University Press. 33

Figure 3.5.1.2 – Diagram of the normal - beam geometry of data collection. 34

Figure 3.5.1.3 – An illustration of how rotations through χ and ϕ bring a reflection in to the equatorial plane (reprinted from G.H. Stout and L.H. Jensen, 1968). 35

Figure 3.5.1.4 – Schematic representations of the (a) ω scanning mode and (b) ω-2θ scanning mode (reprinted from G.H. Stout and L.H. Jensen, 1968). 35

Figure 3.5.2 – The Rigaku AFC6S diffractometer with Oxford Cryosystems Cryostream. 36

Figure 3.5.3 – The Fddd four-circle diffractometer with closed cycle refrigerator. 41

Figure 3.5.4 – The SMART-CCD three-circle diffractometer with Oxford Cryosystems Cryostream. 43

Figure 3.5.4.1 - Schematic diagram of a water-cooled CCD detector design (reprinted from Westbrook and Naday, 1997). 50

Figure 3.7.1 – A 320° ϕ oscillation Polaroid photograph taking on the Rigaku AFC6S, used to index a crystal of $B_{12}H_{10}O_2$ at 150 K. 55

Figure 3.11.1 – A diagram of the Oxford Cryosystems Cryostream flow scheme (reprinted from the operating manual for the cryostream cooler, October 1992, Version 3.1). 66

Figure 3.11.2.1 – Schematic representation of the set-up of the compressor module of a close cycle refrigerator (reprinted from the APD Compressor Module Manual, 1986). 67

Figure 3.11.2.2 – A schematic diagram of the goniometer head construction. The key is: A: collet B: copper body C: spring D: ¼ in UNF E: spring tension adjust F: release button. The figure has been reprinted from reference 8 68

Figure 3.11.3 – The open flow helium gas cooler (Helix). 69

Figure 3.12.1.1 – Schematic representation of the construction of an electron storage ring [from J.R. Helliwell]. 72

Figure 3.12.1.2 – A schematic representation of the path an electron beam and radiation emitted from a dipole magnet and passing through a wiggler [from Catlow and Greaves]. 74

Figure 3.12.1.3 – Schematic representation of the layout of a generic insertion device [from J.R. Helliwell]. 74

Figure 3.12.1.4 – Operation of three types of insertion device: (a) wavelength shifter, (b) multipole wiggler, (c) undulator [from J.R. Helliwell]. 75

Figure 3.12.3.1 – A schematic representation of the layout of Station 9.8, Daresbury (reprinted from Station 9.8 World Wide Web homepage). 76

Figure 3.12.3.2 – The SMART diffractometer in place on its side at Station 9.8, Daresbury. 77

Figure 4.2.1.1 - Schematic diagram of electronic transitions for europium and terbium, depicting the strongly observed bands in the visible region (reprinted from R.S. Dickins (1997) Ph.D. Thesis, University of Durham.) 88

Figure 4.2.1.2 – Schematic representation of the principle of circular dichroism (CD) whereby the direction of propagation of plane polarised light is altered. 89

Figure 4.2.1.3 – Pictorial description of the two changes to the electric vector traversing a solution containing an excess of left-handed enantiomer, along the direction of propagation of plane-polarised light. 1→2: the resultant electric vector is tilted and (3→4) r and l will trace out an ellipse. 90

Figure 4.2.3 – (a) Schematic diagram illustrating the principle of PET. (b) Schematic diagram illustrating how a 3D image is built up, thus locating tumour position(s), by the simultaneous detection of pairs of photons by a set of cameras (reprinted from C.E. Foster (1996) Ph.D. Thesis, University of Durham.) 95

Figure 4.3.1 – Schematic representation of (a) 1,4,7,-triazacyclononane-N,N',N''-triacetic acid and (b) 1,4,7,-triazacyclononane-N,N',N''-tris (phenylphosphonic acid). 97

Figure 4.4.1 – Schematic representation of the macrocyclic ligand 'DOTA', or L^1.99

Figure 4.4.2 – The operations performed on a cube to become a square antiprism or a dodecahedron. 101

Figure 4.4.3 – The tetra-N 1,4,7,10-tetrakis(2-carbomoylethyl) derivative of cyclen.102

Figure 4.4.4 – The structure of 'DOTA' determined from the 150(2) K X-ray experiment projected on to the plane of the four nitrogen atoms. The anisotropic displacement parameters are drawn at 50% probability level. The broken lines indicate reasonably close intramolecular contacts to hydrogen (see **Table 4.4.2**).105

Figure 4.4.5 – The torsion angles [°] around the cyclen ring in the crystal structure of DOTA (g = gauche, a = anti). 108

Figure 4.5.1 – The chiral tetraamide ligands and their achiral analogue L^5. Lanthanide complexes of the chiral series have been enantiopure for employment as probes in circular dichroism and circular polarised luminescence spectroscopy. 110

Figure 4.5.1.1 - Stereoisomers of DOTA complex derivatives and their interconversions. The case of the stereocentre α to the ring nitrogen is depicted.111

Figure 4.5.2.1 - The monocapped square antiprismatic geometry in the structure of Eu·(S)-L^2. 113

Figure 4.5.2.2 –Thermal ellipsoid plot (50%) of L^3 complexes, above: Eu·(S), below: Eu·(R). 116

Figure 4.5.2.3 – A view of the Dy·(S)-L^2 complex, rotated by 90° from the orientation on the previous figure which is along the Ln-OH_2 bond. The chirality at the remote amide stereocentre dictates the helicity or handedness of the phenyl groups. Hydrogen atoms have been omitted for clarity. 117

Figure 4.5.2.4 – Three illustrations of the interactions / close contacts between the lanthanide ion bound water molecule and the counter ions or solvent molecules. In all cases, the macrocyclic 'shrubbery' has been removed for clarity. Top left: Eu·(S), top right: Dy·(S), bottom: Eu·(R). Note the similarity in the arrangement of the distinctly different anions about the water in the Eu·(R)-L^2 to the former two complexes. 118

Figure 4.5.3.1 – A view of the eight co-ordinate sodium tetraamide complex with naphthyl substituents. The co-ordination geometry about the metal is twisted square antiprismatic. The naphthyl groups, which engage in excimer coupling, are drawn with darker bonds. 120

Figure 4.5.3.2 – A view of the eight co-ordinate sodium tetraamide complex with quinoline functional groups. The structure is basket-shaped with the metal encapsulated in the centre. As is the case of the naphthyl complex analogue, the acetonitrile is inserted into the groove defined by the rings. 121

Figure 4.5.3.3 – A superimposition of sodium tetraamide complexes with naphthyl (in purple) and quinoline (colourless with red and blue heteroatoms) pendant arms reveals them to be isostructural, that main differences are observed in the orientations of the pendant arms which are relatively less rigid (Note. The co-ordinates of the tetranaphthylamide complex were first inverted). These differences cannot be attributed to a crystal packing effect. The sodium metal and heteroatoms on the cyclen alone are labelled for clarity. 124

Figure 4.5.4.1 – Two views of the isostructural europium (top) and gadolinium (bottom) complexes of L^5, (the bound water molecule is obscured in the gadolinium complex). 127

Figure 4.5.5.1 – A thermal ellipsoid plot of the DTMA ligand at 150(2) K with the anisotropic displacement parameters drawn at 50% probability level. 130

Figure 4.5.5.2 –The packing diagram for DTMA viewed along the [001] direction. 131

Figure 4.5.5.3 – A thermal ellipsoid plot of the monocapped square antiprismatic dysprosium complex of DTMA at 150(2) K with the anisotropic displacement parameters drawn at 50% probability level 133

Figure 4.5.5.4 – A view of the dysprosium complex of DTMA showing the bound water molecule above the O4 plane. 134

Figure 4.6.1 – Schematic diagram of the ligand L^7: 1,4,7,10-tetraazacyclododecane-1,4,7,10-tetrakismethylenebenzylphosphonic acid. 137

Figure 4.6.2 – Schematic diagram of definition of the N-Ln-O bite angle. 138

Figure 4.6.3 – A view of the ytterbium complex of L^7, which emphasises the eight co-ordinate geometry about the metal. 140

Figure 4.6.4 – A view of the lanthanum complex of L^7, emphasising the nine co-ordinate geometry about the metal, as a result of face-capping by a water molecule (O5). 140

Figure 4.7.1 – Schematic representation of L^8, the 1,4,7,10-tetrakis(carboxyethyl)-1,4,7,10-tetraazacyclododecane ligand that has been complexed with gadolinium, europium, terbium and ytterbium. 143

Figure 4.7.2 – A thermal ellipsoid plot drawn at 50% probability level of the structure of europium 1,4,7,10-tetrakis(carboxyethyl)-1,4,7,10-tetraazacyclododecane in the N4 plane projected along the Eu-OH_2 bond. The R isomer of this racemic crystal is depicted and the solvent water molecules have been excluded from the figure for clarity. 144

Figure 4.7.3 – A connectivity plot of the structure in the crystal of terbium 1,4,7,10-tetrakis(carboxyethyl)-1,4,7,10-tetraazacyclododecane 144

Figure 4.7.4 – A thermal ellipsoid plot drawn at 50% probability level of the structure of gadolinium 1,4,7,10-tetrakis(carboxyethyl)-1,4,7,10-tetraazacyclododecane in the N4 plane projected along the H_2O-Gd bond. The R isomer of this racemic crystal is depicted and the solvent water molecules have been excluded from the figure for clarity. 145

Figure 4.7.6 – A photograph of the crystal used for data collection of the terbium complex of L^8 displaying the morphology that typifies this series. 146

Figure 4.7.7 – A difference electron density (Fo-Fc) contouring plot of the final model in the refinement of terbium 1,4,7,10-tetrakis(carboxyethyl)-1,4,7,10-tetraazacyclododecane in the plane of the four nitrogen atoms. A new contour is drawn every 0.1 e/Å^3 Positive residuals are drawn with unbroken lines and negative residuals with broken lines. The colour code in e/Å^3 is: -0.8 green, -0.7 red, -0.6 blue, -0.5 yellow, -0.4 pink, -0.3 white, -0.2 grey, -0.1 blue, 0.1 green, 0.2 purple, 0.3 mustard, 0.4 bright blue, 0.5 brown, 0.6 dark grey, 0.7 red, 0.8 green, 0.9 red, 1.0 blue, 1.1 yellow, 1.2 pink. 150

Figure 4.7.8 - Selected bond lengths for europium, terbium and gadolinium complexes of L^8, where 1 = Eu, 2 = Gd and 3 = Tb. 152

Figure 4.7.9 – A photograph of the mounted crystal of Yb-L^8 that was measured on Station 9.8, Daresbury SRS. The extremely thin fibre is glue to the stouter fibre to facilitate crystal mounted and to reduce the amount of amorphous glass scatter from the intense source. 154

Figure 4.7.10 – Samples that were screened by Philip Pattison on the Swiss-Norwegian beamline (BM1B) at the ESRF. (a) The sample of Yb-L^8 crystals. (b) The mounted plate-like crystal on the fibre end. 154

Figure 4.7.1.1 – Diagrams of the crystal structures of RSRS (top) and RRRS (bottom) isomers of 1,4,7,10-tetrakis(carboxyethyl)-1,4,7,10-tetraazacyclododecane. 157

Figure 4.7.1.2 – Diagram of the RRSS isomer of 1,4,7,10-tetrakis(carboxyethyl)-1,4,7,10-tetraazacyclododecane (dashed lines indicate close contacts to hydrogen and atoms are symmetry related about an inversion centre to their equivalent atoms with a letter suffix). 158

Figure 4.8.1 - Schematic representation of the putative complex that would bind to an oligonucleotide, where Ln = Eu^{3+} or Tb^{3+}. 163

Figure 4.8.2 - Diagram of the molecular packing viewed along the b axis. Antiparallel chains are formed mediated by strong OH..O interactions of 1.43(4) Å along [001]. 164

Figure 5.2.1 – Schematic representation of 1,2 di-phenyl ethanedione or 'benzil'. 180

Figure 5.2.2 – Phase transition in benzil, tracked by monitoring the β angle in the monoclinic cell setting. 182

Figure 5.3.1 - Crystal structure of $C_2H_{10}B_{12}O_2$ (50% ellipsoids) at 100(2) K. Dashed atoms represent those that are generated by a symmetry element. 184

Figure 5.3.2 – Reaction scheme for the hydration of para di-carbonyl borane by six molecules of water to give the bis-carbene species. 188

Figure 5.3.3. - Crystal structure of $B_{12}H_{22}C_2O_6$ (50% ellipsoids) at 90(2) K. Important interatomic distances (Å) are: O(1)-H(10)..O(2S) 1.73(2), O(2)-H(20)..O(1S) 1.80(2). Angles (°): O(1)-H(10)-O(2S) 159(2), O(2)-H(20)-O(1S) 173(2). 190

Figure 5.3.4 - Packing diagram of the extended crystal structure of $B_{12}H_{22}C_2O_6$ viewed along the [010] direction. The supramolecular structure consists of sheets of cages mediated by water molecules, on the (101) plane. Hydrogen bond distances (O..H, Å) are 1.92(2) and 1.97(2) between the water molecules. There is a weak B..H interaction between B(5) and one of the water protons of 2.62(2) Å. 190

Figure 5.4.1 – Cartoon representation depicting the secondary structure (the coils are α helices and the flat arrows are β sheets) in the 1.9 Å resolution crystal structure of the tetragonal form of CEW lysozyme at 100 K. There are three disulphide bridges. The solvent water molecules are not shown in this figure. 192

Figure 5.4.2 - Methodology of preparing a sample mount for macromolecular or air-sensitive crystals on the Fddd diffractometer. 195

Figure 5.4.3 – The physical set-up for taking Polaroid photographs on the Fddd diffractometer. The sample is mounted inside the beryllium cans. The beam stop,

which casts a shadow on the photograph, is visible here. The camera is clamped to the 2θ arm. 196

Figure 5.4.4 – (a) 1.0 x 0.8 x 0.4 mm crystal mounted on graphite with 24-hour glue, left to harden measured at room temperature with $\phi = 0 - 5°$ in 0.05° steps at a rate of two seconds per step and (b) Using the new sample mount scanned over the same range as the last photograph. 197

Figure 5.4.5 – Labelled from the top left. (a) The first photograph of the crystal at room temperature with out the cans at $\chi = 0°$. (b) The cans are added. (c) The Displex is switched on 296 K and $\chi = 267°$. 198

Figure 5.4.6 – (a) → (f) are labelled from the top left. (a) The first photograph of the 0.7 x 0.4 x 0.4 mm crystal at room temperature. (b) A 1° oscillation photograph with the cans and pumping apparatus in position. (c) The Displex was switched on and the reading was 10^{-2} mbar. (d) After 20 minutes at 3 x 10^{-3} mbar. (e) After 45 minutes at 4 x 10^{-4} mbar. (f) After 95 minutes at 1.4 x 10^{-5} mbar. 199

Figure 5.4.7 – (a) → (f) are labelled from the top left. (a) The first photograph was the crystal at room temperature. (b) A 1° oscillation photograph with the cans and pumping apparatus in position, the Displex had been switch on for 5 minutes. (c) The Displex had been on for 35 minutes, the vacuum reading was 5.2 x 10^{-6} mbar. (d) A photograph after the pump had been removed. (e) The image at 12 K before the crystal was recentred in the beam using the intensities. (f) The diffraction from the crystal at 12 K, the graphite lines have returned. Note the camera was clamped further back on the 2θ arm in this case. 201

Figure 5.4.8 – (a) The crystal at room temperature before the Displex was switched on. The diffraction remained unchanged until 250 K in (b) where ice diffraction is visible and more intense than the reflections from lysozyme and the protein intensities are markedly broader in full width at half maximum. This is after height and lateral recentring. 202

Figure 5.4.9 – (a) The measurement of the temperature inside a system sealed in this manner (b). The sample is surrounded by transparent cannister whilst nitrogen gas cools it. The thermocouple reading at the crystal position is 263.1 K here. 204

Figure 5.4.10 – A frame of CEW-lysozyme data from the SMART at 60 K. The outer rings on the frame have arisen from the beryllium nozzle on the Helix. 205

List of Abbreviations *

Å	Angstrom, 10^{-10} m
CCD	charge coupled device
CCR	closed cycle refrigerator
CFOM	combined figure of merit
cyclen	1,4,7,10-tetraazacyclododecane
DNA	deoxyribonucleic acid
DOTA	1,4,7,10-tetraazacyclododecane-1,4,7,10-tetraacetic acid
DTMA	Dota tetrakis(methylamide)
EM	electromagnetic
esd	estimated standard deviation, esds given for refined parameters are from the least-squares refinements, esds for average values are variances of the mean
FSD	fast scintillation detector
FT	Fourier transform
fwhm	full width at half maximum
L	shorthand for a ligand
Ln	generic term for an element of the lanthanide series
MRI	magnetic resonance imaging
MPD	2-methyl-2,4-pentanediol
NMR	nuclear magnetic resonance
PEG	polyethylene glycol
ppm	parts per million
SR	synchrotron radiation
SRS	synchrotron radiation source
VT	variable temperature

* Note that all the standard symbols herein follow the IUPAC convention

Chapter 1

Introduction

Crystals are the foundation upon which this work is built. A theoretical overview of crystal growth is presented, outlining the three stages of this process: nucleation, growth and cessation of growth. The key factors that may be explored to improve crystal quality are discussed.

The experimental procedures underlying this body of work are presented in detail. Most importantly are the following geometries and key features: the SMART-CCD, Rigaku AFC6S and *Fddd* diffractometers, crystal screening and unit cell determination, data reduction including absorption corrections, crystal structure solution, low temperature attachments and how they work and the production and nature of synchrotron radiation.

The lanthanide complexation investigation sheds light on its structure and from there, attempts to explain some of the solution-state behaviour of these important *in vivo* probes. The framework upon which all of these macrocyclic compounds are based namely dota, or 1,4,7,10-tetraazacyclodocane-1,4,7,10-tetraacetate, is studied from the point of view of its uncomplexed conformation and how this changes on ligating an element of the lanthanide series or in some cases a smaller sodium ion. The dota derivatives presented have been each in turn rationally designed and synthesised by David Parker and coworkers. The crystallographic structures presented herein give insights into the nature and chemistry of these molecules and in some instances verified their architecture in a way that no other structural probe has achieved previously. For example the unambiguous determination of the absolute configuration for the europium and dysprosium complexes of the enantiopure tetraamide series.

The *Fddd* diffractometer is a unique design by Judith Howard and coworkers. This has the ability of cooling the crystal to temperatures as low as 9 K. For the precise measurements that are routinely made on this instrument, it is very important to calibrate the temperature. Studies were conducted to verify the temperature at the crystal by using benzil, a molecule known to undergo a transition from a hexagonal to a monoclinic setting in the region of 83 K. The effect of d-block elements and the

icosahedral B_{12} cage on the carbonyl group was investigated. In order to obtain very precise values for the bond lengths, which correlate with the bond energies, low-temperature data were collected. This revealed some interesting results on the structures of these borane cages and how changing the substituent can change the geometry of the cluster. A standard crystal was employed to test the suitability of measuring biological molecules on this instrument. Chicken egg white lysozyme was crystallised and several methods to cool them were employed and yielded varying results.

Chapter 2

Theory And Practice Of Crystal Growth

2.1 Historical Background

The endeavour to transform liquid and gaseous substance in to the solid, pure state, thereby immobilising them, has permeated the whole of chemistry from the days of the early alchemists.[1] The word crystal is derived from the Greek word "krustallos" meaning "clear ice". The word "crystal" implies a clear, unblemished substance and the process of crystallisation has been called "*...one of the most perfect of purification operations...*" Crystallisation was used before the advancement of X-ray structural analysis, to resolve enantiomers by the crystallisation of the enantiomers as salts.

The first reported crystallisation of protein crystals was over a hundred years ago by Funke *et al.*[2] This was before the concept of using X-rays as a tool to determine molecular structure in the solid state had even been put forward. They crystallised haemoglobin from the blood of various vertebrates and invertebrates. Northrop crystallised pepsin and a series of other proteolytic enzymes in 1926 and drew the conclusion that enzymes are proteins. Influenced by this, Stanley crystallised Tobacco Mosaic Virus (TMV) in 1935 and showed that it retained its infectivity after several recrystallisations, thus developing the theory that biological molecules retain their activity in the solid state, for which he was awarded the Nobel Prize for Chemistry in 1946. The first diffraction of pattern of a biological molecule was produced by J.D. Bernal and D. Crowfoot in 1934, that being pepsin. With the advent of protein crystallography, a lot of effort was put into the crystallisation of various heavy-atom isomorphous derivatives of proteins.

The need for a reliable method for the production of high quality, suitably sized crystals remained. A major breakthrough occurred in the 1960's with the development of micromethods (e.g. vapour diffusion) which were suited to crystallisation where only limited amount of sample is available. It became apparent that certain additives were good precipitants, and that under the correct conditions (i.e. concentration, pH, and temperature) would yield monocrystals of the substance. Despite this advance, the total number of variables were so large and combinatorial that a complete exhaustive screen of crystallisation conditions were rendered too time consuming and wasteful of the substance. An incomplete factorial method was proposed in 1979 by Carter and Carter[3] in which a coarse matrix of crystallisation

conditions was initially screened and this was refined depending on the success of the individual trials. This method has been used with great success and in 1991, Jancarik and Kim[4] proposed an empirically derived set of fifty crystallisation conditions based on published results. Proteins that failed to crystallise under any of these conditions were later proven non-homogenous by techniques such as gel-electrophoresis and isoelectric focussing. With the development of the macromolecular crystallisation database, it is sometimes feasible to predict *a priori* the conditions to crystallise a given molecule using the conditions used in the crystallisation of related substances.

2.2 Stages in Crystal Growth

The stages of crystal growth can be divided into the following categories:

2.2.1 Nucleation

Nucleation is the formation of a 'seed nucleus' from which, by a process of molecular aggregation, a crystal of the material will form. The ideal nucleus, or start point, for monocrystal formation is a seed of the same material. The material, typically in solution, must become supersaturated before it spontaneously forms nucleation sites for crystal growth. Saturation is reached when the solvent contains a certain amount of solute such that on any further addition of crystals there will be neither growth nor dissolution. Here, the liquid and solid phases are said to be in dynamic equilibrium, i.e. their chemical potentials are equal.

$$\mu_{ic} = \mu_{is} = \mu_{i0} + RT \ln\gamma c_i \qquad (2.1)$$

where μ_{ic} and μ_{is} are the potentials of the crystal and the solution respectively, μ_{i0} is the standard potential of species i, R is the gas constant, γ is the activity coefficient and c_i = concentration of species i. Supersaturation is reached when the chemical potential of the solute in solution is greater than that of the crystal. Supersaturation can be divided into two regions. The metastable region is where nucleation is not spontaneous but crystals can grow, and the labile is where nuclei can form and grow. These are shown in ***Figure 2.2.1***.

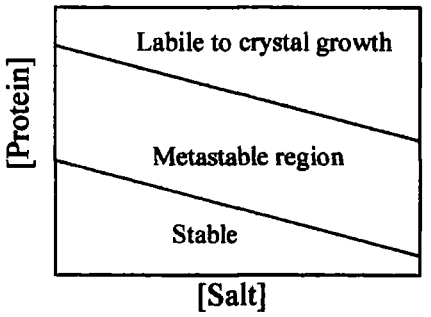

***Figure 2.2.1** - Regions of Saturation, Note that whilst [Protein] is denoted, this graph holds true for any sample.*

The stable region is undersaturated and no nucleation will occur. The dotted line represents the supersolubility curve and the continuous line represents the solubility curve. Nucleation of a new phase originates from energy fluctuations about the mean value of the free energy induced by supersaturation. Nucleation is said to be homogeneous when it occurs in the bulk of the solution and heterogeneous when it occurs on solid particles (e.g. dust, glass etc.) Furthermore, it is called primary in all cases when it occurs where there is no crystalline matter and secondary when it grows out of a parent crystal (e.g. branching). There is an interesting analogy between the concepts of molecular synthesis and controlled crystallisation. The production of a single point nucleus from which a crystal may grow is compared to the starting point of a radical chain reaction. Once a critical nucleus has been reached, continuing accretion of molecules to the macroscopic crystal becomes the growth phase.

For nucleation to occur from a supersaturated solution, the free energy of germination, ΔG_g, must be overcome i.e. supersaturation must be great enough to overcome this energy barrier. Crystallisation is a non-equilibrium process of a heterogeneous system whereby $\Delta G_g(N \rightarrow C) = G_C - G_N < 0$ (C = crystal, N = nutrient phase). The final condition for the growth of a macroscopic crystal results from a local deviation from equilibrium, ΔG, the removal of the heat of crystallisation, the inflow of lattice components and the outflow of dispersive and other components which are not taken up in the lattice. If nucleation and subsequent volume growth take place at high/low temperatures (pressures), attention must be given to the defect equilibria on returning to normal conditions. (Schottky defects). Crystals may grow by a process of homogeneous or heterogeneous nucleation. Starting from the statistically disordered nutrient phase N ($T > T_{equilibrium}$), where T is the temperature

and $T_{equilibrium}$ is the temperature when the solid and liquid are at the same potential, the mechanism of homogeneous nucleation involves the structure forming self organisation of 'components' (i.e. atoms or molecules). This process can take place under conditions of supercooling or supersaturation, the process that occurs involves elementary steps when infinitely repeated lead to a "macromolecular" crystal. The four stages of nucleation are shown starting from initial nucleation to the formation of the first unit cell. Here, the NaCl structure is calculated from Quantum Mechanics of clusters. The four stages are: a) formation of small first-order aggregates, b) cluster formation, c) transition to NaCl lattice structure, d) first unit cell.

An equilibrium exists between the two phases where, liquid $\leftrightarrow$ solid. For a heterogeneous, multiphase system the Clausius-Clapeyron equation states that:

$$(\delta p/\delta T)_{coex} = \Delta H/T\Delta V \qquad (2.2)$$

allows for the coexistence of two phases for specific p, V and T only, where p is the pressure, T is the temperature, H is the enthalpy of the system, and V is the volume. They may coexist in any ratio. The Gibbs equation (2.3), is composed of two terms.

$$\Delta G = \Delta H - T\Delta S \qquad (2.3)$$

where ΔS = the entropy change, ΔH is the sum of the enthalpies of desolvation, that is the removal of molecules from the solvent sphere and their addition to the growing crystal(s). The $T\Delta S$ term will be negative because crystallisation is an anti-entropic ordering process. If crystal growth is to occur the ΔH_{desolv} must be more negative than $T\Delta S$. For a nucleus to form and grow it must overcome the cluster radius critical size, r^*. Crystal aggregates with a radius less than this will tend to redissolve being unstable from a thermodynamic point of view. The cluster formation energy, ΔG_c, must be overcome to form a nucleus of critical radius. For a nucleus, assumed spherical in solution, the 'Classical Capillary Approximation' is used to describe the nucleation process. The first transition that of small molecular agglomerates to clusters (c) leads to the formation of a phase boundary surface. ΔG_c, is described in equation 2.4 which is composed of volume and surface area terms. This is the energy required to form a crystal of volume and surface area described by the first and second terms of the equation respectively.

$$\Delta G_c = \Delta G_c(r) = -\frac{4}{3}\pi r^3[k_B T \ln(\sigma+1)]/v + 4\pi r^2\gamma \qquad (2.4)$$

where σ is the relative supersaturation given by $[(X-X_0)/X_0]$, X_0 is the equilibrium concentration, X is the concentration, v is the molar volume of the cluster, γ represents the interface surface energy per unit area and k_B is the Boltzmann constant. ΔG_c decreases with supersaturation and increases with interfacial/solution free energy. The presence of foreign particles reduces the interfacial free energy and increases the nucleation rate. Alternatively, this can be written as:

$$\Delta G_c = \Delta G_c(r) = -\frac{4}{3}\pi r^3[k_B T \ln(\beta)]/v + 4\pi r^2\gamma \qquad (2.5)$$

where β, the supersaturation, $= (\sigma+1)$. This is a special case of (4). The critical radius and the critical radius energy of formation are given by (2.6) and (2.7) respectively. For transition from nucleation to the growth of macroscopic crystals the two terms, r^*, and ΔG_c^* must be overcome.

$$r^* = 2v\gamma/[k_B T \ln(\sigma+1)] \qquad (2.6)$$

$$\Delta G_c^* = 16\pi v^2\gamma^3/[3k_B^2T^2 \ln^2(\sigma+1)] \qquad (2.7)$$

Secondary nucleation, that is, surface curvature anisotropy, (e.g. the attachment of a cluster to a macroscopic surface such as a larger nucleus) leads to the thermodynamic stabilisation of small clusters with $r < r^*$. In real systems in the supersaturated state there exists metastable and stable, but subcritical, nuclei of varying size r. Since r depends on the relative supersaturation, the construction of the first cell does not always lead to a critical nucleus. The number of clusters that exist with ΔG_c^* is proportional to $\exp(\Delta G_c^*/k_B T)$. The nucleation rate, J, in $cm^{-3}s^{-1}$, is given by the Arrhenius law.

$$J = \exp(-\Delta G_D^*/k_B T)\exp(-\Delta G_C^*/k_B T)\, k_B T/h v_L \qquad (2.8)$$

where ΔG_D is the contribution made by diffusion, v_L is the molar volume of the solvent, h is Planck's constant. J can show a sharp maximum where the optimum temperatures for maximum nucleation and maximum growth do not overlap. These then have to be optimised separately.

A clean surface will reduce the number of nucleation sites. Aqueous solutions tend to adhere to a glass surface and this can promote nucleation on the side of the vessel. This can be prevented by silanising the test tubes or cover slips to be used. A 5% v/v solution of dimethyl-dichlorosilane is made up in toluene. The glassware is treated with a bath of this solution for 10 minutes, then washed with a soapy solution, rinsed with water and then ethanol. This leaves the glass surface chemically clean. The water drops are not attracted to the glass surface thus drops of water behave like a beads of mercury while flowing along the surface.

2.2.2 Growth

Once the critical nucleus has been reached, continued accretion becomes the growth stage. Growth proceeds by a mechanism of stepped growth or by means of a screw dislocation. In the nucleation and growth stages, the surface smoothness is an important factor in determining this. Growth by means of a screw dislocation is much more favourable than by direct accretion onto a two-dimensional sheer surface because in the former mechanism there are more contact points between the molecule and the surface of the crystal. The nuclei adsorb onto surfaces so that the least number of faces as possible can be exposed. The substance in position 3 is the most stable of the all. The crystallite in position 1 stands a greater chance of disconnecting again or being lost due to collisions. The surface free energy is increased much more by a nucleus bonding to a sheer surface (i.e. with five faces exposed) than if it attached to a ledge. This serves as an explanation as to why crystal growth by a mechanism of screw dislocation is a more favourable mechanism. A defect occurring in the lattice provides a 'haven' for this particular defect occurring. If the lattice is sheared along an axis, the cut produced, called the axis of screw dislocation, will result in a ledge forming about which growth will occur. The morphology of the crystal will appear spiralled or stepped as incoming nuclei have ramped around the axis. The growth rate onto natural faces is slower than for growth onto crystal faces of high index. The faster growth rate can lead to the incorporation of errors or defects into the growing lattice.

The step velocity, υ, and the surface growth velocity, R, are functions of the supersaturation. In the case of growth driven by adsorption onto a growth surface and growth by means of a screw dislocation, the growth rate, R, is given by (2.9)

$$R = k_2 \sigma^2 \tanh(\sigma^{-1} \frac{k_1}{k_2}) \quad (2.9)$$

where k_1 and k_2 are kinetic temperature-dependent constants. For small values of σ, a parabolic rate relationship would be expected and for larger values, it is linear. Above σ^1 (critical supersaturation) the growth, R, increases considerably. This shows the importance of prior purification of the solute and solvent and the use of vessels, which have chemically clean surfaces. Some impurities are present down to a ppm level which is why sometimes under conditions of supercooling and supersaturation (large ΔT, σ) no growth can be observed. Most problems are associated not with growth though but with nucleation, which can proceed at too fast a rate at high supersaturation, resulting in volume growth from most nuclei and none attaining the desired size. It is often useful to produce the seeds in separate vessels and to add the seed(s) to the supersaturated solution. The presence of foreign materials can reduce the growth rate even when they are not incorporated onto the growing surface. When $k_0 < 1$ (Nernst distribution coefficient, $\frac{X_C}{X_N}$) the foreign material including dispersive components becomes concentrated in the vicinity of the growing surface, this leads to a reduction in the liquid temperature and reduces the growth rate. When the temperature is held constant there is a reduction in the supercooling and supersaturation (ΔT, σ) and the growth rate decreases (9). The general rule that crystal growth should take place slowly is confirmed in that too rapid a growth rate would lead to macroscopic inclusion of nutrient phase in the cluster.

2.2.2.1 Factors Affecting Growth

If the major stabilising factors are maintained the chances of obtaining X-ray quality crystals from post-critical nuclei are maximised. These main factors are summarised below. The factors, which affect small molecule crystallisation, are then listed followed by the additional factors for the special case of macromolecular crystallisation. A discussion of the different types of precipitants and their individual uses is at the end of this section.

The factors that influence the stability of macromolecular crystals include:

1. Purity: The processes of purification and crystallisation are often mutually beneficial. Crystallisation of molecules can be used as a tool for purification and *vice versa*. Because biological molecules are often extracted from complex mixtures, purification is an important consideration. Incorporation of impurities into the lattice can result in crystals which do not attain minimum size (0.2 mm at least for the dimension of a face) or polycrystalline precipitation. A typical cubic crystal of 1 mm^3 contains 10^{20} molecules so impurities at the ppm level are important. The two most common methods of purification prior to crystallisation are centrifugation and isoelectric focussing. Crystallography grade purity of proteins refers not only to the absence of contaminants but to the quaternary structure remaining intact, i.e. it has to be conformationally pure. In general, this factor adversely affects crystal growth more so than does unrelated molecules. A distinction must be made between purity and homogeneity, which refers to the absolute identity of all macromolecules in the sample.

2. Supersaturation: Molecules must be brought to a thermodynamically unstable state of supersaturation to induce crystallisation. The most frequent method of reaching this, used by macromolecular crystallographers, is salting out using e.g. ammonium sulphate.

3. Packing: Intermolecular interactions between proteins are important in determining packing and morphology. The forces stabilising macromolecules in a crystal are weak compared to small molecule interactions but despite their individual weaknesses are collectively strong. These are: Salt bridges - Amino acids exist in their zwitterionic form at certain pH's and salt bridges can form between charged residues e.g. CO_2^- and NH_3^+. Dipole-dipole interactions - These includes two different types of interaction, that is, H-bonding which can be to the solvent water molecules or intra or intermolecular (e.g. C=O..H-N). and van der Waals, non bonded interactions are also important. Non-covalent bonds: This is the major force in small molecules and is important in macromolecules. An example of this is the stacking of base pairs in DNA.

4. It is worth mentioning the effect that H-bond competitors have. Molecules having hydrogen bonding potential (formamide, urea, guanidinium salts) compete at high concentration ($\geq$ 4 M) with hydrogen bonds to water and also

the intramolecular hydrogen bonds. In the latter case these competitors could be acting as denaturants but conversely they may stabilise hydrophobic interactions.

5. Temperature: The higher the temperature, the more disorder the incoming molecules will have.

6. pH: This is one of the most important factors affecting the growth of macromolecules. pH changes (that is altering the proton and hydroxyl concentrations) of the solute and solvent are minor changes compared to the protonation and deprotonation of titratable groups along the protein backbone. Proteins are not stable over large pH ranges. If one wants to change the pH of a protein during a crystallisation trial this incurs a change of buffer which means that two variables have been changed so valid comparisons cannot be made. pH changes can lead to crystals forming with different space groups which was seen in the case of HEW lysozyme.

7. Salts: Salts may interact with the macromolecule in a number of different ways:

8. They are responsible for the ionic strength and affect macromolecular electrostatic interactions by charge shielding. They reduce the repulsions between polyelectrolytes of the same net charge.

9. They interact directly with the macromolecule by monopole-monopole interactions e.g. anions with lysine or arginine sidechains.

10. Salts are involved in monopole-dipole interactions with dipolar groups (e.g. peptide bonds, carboxyl group.) These interactions lead to partial denaturation.

11. There are also non-polar interactions between the hydrophobic part of the salts (e.g. carboxylates) and the solvent exposed hydrophobic residue of the protein. These are stabilising interactions and aid in solubilising solvent-exposed hydrophobic residues. Here, the salt acts as an ionic detergent.

2.2.3 Cessation of Growth

Not much is known about this process. It is generally accepted that the accumulation of impurities about the growing surface, or the poisoning of the crystal surface, is one of the major factors contributing to the growth stage ending. The faster the rate that crystals grow, the larger the number and the smaller their terminal size. This affect is particularly pronounced when the solution is agitated.

2.3 Crystallisation conditions

The factors, which affect crystallisation, are:

1. Relative solubility of the material in the solvent.
2. Solvent combinations.
3. Volatility of the solvents.
4. Concentration of the molecule in the drop.
5. Purity of the solvent.
6. Purity of the molecule.
7. Temperature.
8. Concentration of the precipitant.
9. Pressure.
10. Volume of the crystallisation sample.
11. Seeding.
12. Amorphous precipitate.

Additionally, the factors, which particularly influence macromolecular crystallisation include:

1. Preparation and storage of macromolecules: Storage buffers whose pK is only weakly affected by temperature must be chosen so that samples stored at -20°C and assayed at room temperature are not subjected to important pH variations. Ionic strength should be controlled since macromolecules may require a minimal salt concentration to stay soluble. Denaturation of proteins during storage can be prevented by avoiding denaturing treatments (e.g. extremes of temperature, pH, organic solvents and or reducing agents.) Proteins should not be stored as dilute solutions because they may adsorb to the vessel wall. Glycerol at high concentrations (e.g. 50-60% v/v) is a stabilising agent for the storage of proteins. It has the advantage in that it is liquid at -20°C thus the risk of denaturation due to ice formation is eliminated and its high viscosity reduces diffusion by two orders of magnitude. Storage as a suspension in ammonium sulfate is also sometimes recommended. Ligands and cocrystallisation agents (e.g.

cyclosporin A) can also increase protein stability and lengthen the lifetime while in storage.

2. Substrates, coenzymes, ligands and metal ions.
3. Level of reducing agent or oxidant.
4. Proteolysis and fragmentation.
5. Age of the macromolecule.
6. Degree of denaturation.
7. Vibration and sound.
8. Buffers.
9. Organism, or species, from which the macromolecule was extracted.

2.4 Precipitants

The three types of precipitants used are outlined in the following sections.

2.4.1 Salts

These are very frequently used in the crystallisation of macromolecules. The most widely used and successful of all precipitants is ammonium sulfate. Other salts used are sodium chloride, lithium sulfate, sodium formate, sodium citrate, magnesium formate, sodium potassium formate, ammonium phosphate, magnesium sulfate and imidazole. The nature of these salts was ranked by Hofmeister,[5] in 1888, (lyotropic series) depending on their ability to precipitate HEW proteins. More recently it has been shown that these ions act as reinforcants or denaturants of the native biological macromolecular conformation. Here, the ions are ranked in order of decreasing ability to reinforce the native conformation.

- cations: $Li^+ > Na^+ > K^+ > NH_4^+ > Mg^{2+}$
- anions: $SO_4^{2-} > PO_4^{3-} > CH_3CO_2^- >$ citrate^{3-} > tartrate^{2-} > bicarbonate$^-$ > chromate^{2-} > Cl^- > nitrate$^-$ >> chlorate$^-$ > SCN^-

Sulfate ions are called lyotropic (stabilising the native form) whereas ClO_3^- and SCN^- are chaotropic agents, which have a disruptive effect on water structure and promote denaturation at high concentrations.

The change of protein solubility, when increasing salt concentrations has been studied in terms of salting-in and salting-out.

Salting-in: Proteins are highly complex polyelectrolytes carrying both positive and negative charges. At low salt concentrations (< 0.5 M) the protein is surrounded by an ionic atmosphere described by the Debye-Hückel theory. Here, there are non-specific electrostatic interactions between the charged protein and the ionic species of the salt. The ionic strength, I, of an electrolyte solution increases due to these interactions.

$$I = \tfrac{1}{2}\Sigma\, m_i.Z_i^2 \qquad (2.10)$$

where m = the molality of species i and z = the number of charges. The effect the ionic strength has is described in the Debye-Hückel limiting law (2).

$$\log_{10} \gamma \pm = -A |z^+.z^-| \sqrt{I} \qquad (2.11)$$

where $\gamma \pm$ is the mean ionic activity coefficient, A is -0.509 at 298 K. As the activity coefficient decreases due to the ionic strength, the solubility, s, increases to keep the solubility product, k_{sp} constant (2.12). Hence, salting-in is an electrostatic effect.

$$k_{sp} = s^2\gamma^2 \qquad (2.12)$$

Salting-out occurs at high salt concentrations whereby the protein solubility is known to decrease. The protein at high ionic strengths behaves as a neutral dipole. Protein solubility decreases at high salt concentrations according to the Cohn-Green empirical linear equation.

$$\log S = \beta - K_S\, m, \text{ or } \log S = \beta - K_S'\, I \qquad (2.13)$$

where β and K_S are empirical constants, K_S being the salting-out constant. As the ionic strength increases so does the solubility decrease. ***Figure 2.4.1*** illustrates the variation of protein concentration with salt concentration. This is a schematic map of the crystallisation kinetics as a function of both concentrations.

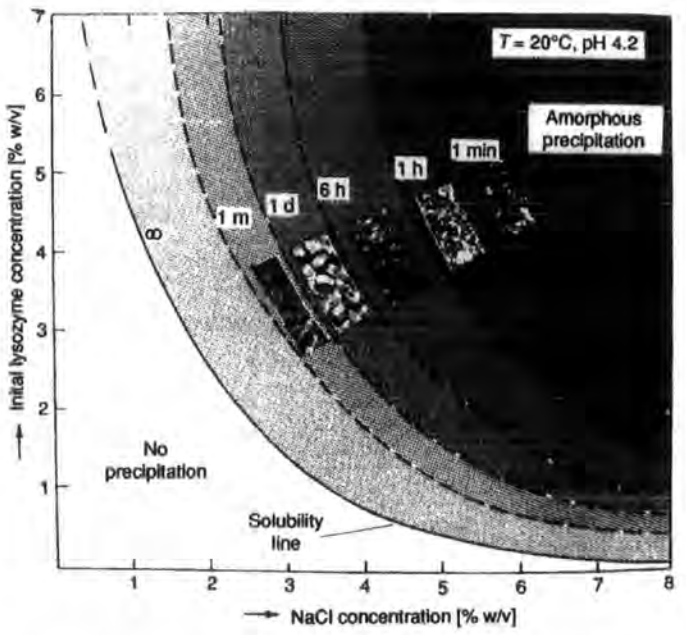

Figure 2.4.1 *- Kinetics and crystal quality as a function of salt and protein concentrations. Reprinted from T. Arakawa and S.N. Timasheff, (1985), Methods in Enzymology, Vol. 114, 49-127.*

2.4.2 Volatile and involatile organic solvents

These are volatile solvents (isopropanol, ethanol and t-butanol) and involatile (2-methyl-2,4-pentanediol (MPD), ethylene gylcol, glycerol, dioxane and 1,6 hexanediol.) These are more suited to use with small or intermediate length molecules. These molecules reduce the dielectric constant, D, of the medium, below.

$$A \propto 1/(DT)^{\frac{3}{2}} \qquad (2.14)$$

where A is a constant in the Debye-Hückel limiting law and T is the temperature. They bind water molecules and to some extent prevent decreases the capacity of the system to solvate the macromolecule fully.

2.4.3 Polyethylene glycols

This polymer is commonly called PEG but is more accurately described as $(\text{ethylene glycol})_n$ where n takes values between 1000 and 20000. The range from 4000 to 8000 is most prevalently used. As the concentration of PEG increases it perturbs the natural structure of the water and replaces it with a more complex structure having both water and itself as structural elements. The mechanism by which PEG induces crystallisation is not fully understood. PEG has a volume exclusion property, which means that it restructures the solvent, and causes the macromolecule to be excluded and phase separation is promoted. It shares some characteristics with salts in that it competes for water and dehydrates the protein and additionally, acts in a similar manner to organic solvents, which modify the dielectric properties of the medium. PEG provides a low electron dense medium and is most effective at low ionic strength. Its dehydrating property is important since this means low background noise in the difference density map and thus for protein structures easier solution, as they are more readily interpreted. The latter is important because this facilitates the formation of isomorphous heavy-atom derivatives and ligand binding for cocrystallisation because metal ions and ligands can interact with the protein without being perturbed by charged ions. Proteins grown from PEG tend not to be disturbed from their native conformation. An advantage of PEG is that most proteins crystallise in a narrow range of PEG concentration; this being from about 4-18%. If one is within 3% of the optimal PEG concentration for crystallisation, some success can usually be achieved. Thus an initial crude grid can be set up varying PEG concentration and from there, the conditions specialised. The

time for growth to occur with PEG is usually shorter than for salts but longer than for volatile organic solvents (e.g. ethanol.) Since PEG is involatile with a boiling point ~120°C it is suited to hanging drop techniques where a drop (2-10 µl) is suspended over a reservoir. PEGs are suited to low ionic strength systems and work well over the whole pH and temperature range.

2.5 Crystal Growth Set-up and Experimental Conditions

The techniques employed during this project for the growth of organic and oligopeptide crystals have been liquid-liquid diffusion and vapour diffusion.

2.5.1 Liquid diffusion

This works on the principle that a substance slowly diffuses from one solvent it is soluble in to another in which it is not[6]. Solubility tests are carried out on the molecule in question. It is dissolved in a suitable solvent and a second solvent is chosen in which it is insoluble. This is the precipitant. The denser liquid is added to the test-tube (typically 20 cm x 1 cm) first and the second dropped on at a rate of approximately. 1 drop per 5 sec so that a visible interface forms. An advisable starting volume ratio of solvent to precipitant is 1:3 and from here this can be varied. The test-tube is sealed and left in an upright position and checked at regular intervals.

2.5.2 Vapour diffusion

This is a more specialised technique and ideally suited to the crystallisation of larger molecules where the sample is in short supply. A 24-well Linbro plate (used also for the growth of biological cultures) is used. Three variations can be carried out, depending on the amount of sample available and the volatility of the solvent used.

1. Sitting drop diffusion: Sitting drop plates are equipped with a well in the reservoir which can hold up to 35 µl of sample.
2. Micro-bridge drop vapour diffusions are an adaptation of vapour diffusions. Here, a microbridge is added to the reservoir. It can hold up to 20 µl of sample.

An advantage of this setup is that the microbridge can be removed from the reservoir for the inspection of the sample.

3. Hanging-drop vapour diffusion is ideal when the material is in very short supply (i.e. < 4 mg). A drop containing the molecule in solution, buffer and an equal volume of precipitant is syringed onto a silanised coverslip. All deliveries of this nature in the experiments in this thesis were carried out using an Eppendorf micropipette, which can deliver accurately volumes of 2-20 µl. The reservoir solution is added to the well and this is commonly 1 ml of precipitant. Hence, the ratio of precipitant concentration between the drop and the reservoir is 1:2. Vacuum grease is applied in a thin layer to the rim of the well and the coverslip is inverted and depressed gently to form an airtight seal. All vapour diffusions described here were carried out in an air-conditioned room, held at 12 °C. Trays could be transferred to room temperature or a ~4° C refrigerator, if necessary. Water from the drop, being less volatile than the precipitant, diffuses to the region of lower water concentration (i.e. the reservoir) and the precipitant concentration in the drop increases, slowly solubilising the macromolecule. If the precipitant is more volatile than water, it will still tend not to diffuse as it forms a charged species with the macromolecule.

2.6 Industrial Methods

In this section, a few other methods of crystal growth will be reviewed briefly. The almost universally used, method is that of Czochralski. Here, the crystal is grown from the melt. The principle is that of controlled freezing under as near to thermal equilibrium conditions as can be achieved. The freezing is started at the solid-liquid interface and moved through the molten mass. There is a 25% increase in volume in the case of silicon, and this allows for the expansion by not using a crucible. Again, this is carried out in an atmosphere of pure argon. A small seed crystal is mounted with the desired growth plane parallel to the melt surface. This is dipped in the liquid and the temperature dropped until the silicon starts to crystallise on it. Pulling then starts as the crystal is withdrawn and more material freezes on it. Crystallisation is the basis of the production of silicon for the microchip. Silicon dioxide is reduced in a furnace to produce silicon at 98% purity. The purity requirements are less than one impurity in 10^9. The most successful method of

purification and crystallisation is zone refining. This relies on the fact that the solubility of the impurities is much greater when the material is liquid than when it is solid. To prevent oxidation of the material the process is carried out in an inert atmosphere of argon. To improve uniformity the silicon rod is rotated by two rotating chucks at the top and bottom, whilst the molten zone is traversed up through it.

2.7 References

[1] J. Hulliger, *Angew. Chem. Int. Ed. Engl.* **1994**, 33, 143 - 162.

[2] A. Ducruix and R. Giegé (1992). Editors *Crystallization of Nucleic Acids and Proteins, - A Practical Approach*, IRL press at Oxford University Press, pp. 219.

[3] C. Carter JR. and C.W. Carter (1979). *J. Biol. Chem.* **254**, 12219 - 12223.

[4] J. Jancarik and S.-H. Kim (1991). *J. Appl. Cryst,* **24**, 409 - 411.

[5] F. Hofmeister (1888) *Arch. Exp. Pathologie und Pharmakologie* (Leipzig), **24**, 247.

[6] P.G. Jones (1981) *Chem. Br.*, **17**, pp. 222 - 225.

Chapter 3

The X-ray Diffraction Experiment

3.1 Introduction

The phenomenon of single-crystal X-ray diffraction is a constructive and destructive interference process. A distinctive property of the crystalline state, is the regular repetition in three-dimensional space of an atom, molecule, or group of molecules. The unit cell is the repeat unit of the lattice. The size and shape of the unit cell can be described by three vectors a, b and c and their interaxial angles α, β and γ with one corner taken as the origin. Miller indices (h, k, l) are a means of referring unambiguously to sets of planes running through the crystal and to the faces of the crystal where the planes terminate. These indices are defined as the reciprocals of the fractional intercepts, which the planes make with the crystallographic axes. X-rays are scattered predominantly by the electron density, which can be viewed as constructing these imaginary sets of planes. Each diffracted intensity or 'reflection' is thus denoted with its particular (h, k, l) value.

X- radiation is the atomic probe of choice because it has a similar wavelength to interatomic distances. The aim of an X-ray crystallographic experiment is to measure accurately and precisely a unique set of integrated intensities, which have been scattered by the electron density, using an automated diffractometer.

The diffractometers used for these purposes were the single-crystal Siemens SMART, Rigaku AFC6S and *Fddd* diffractometers at Durham and station 9.8 at the Daresbury SRS. Details of the experimental set up and procedure, employed for the X-ray and synchrotron experiments investigated in this thesis, will be briefly described in this chapter, and further information is available in general texts (see bibliography).

3.2 Background

The first X-ray photograph was taken in 1912, and was based on an idea of Max von Laue, using a stationary copper sulfate crystal. This experiment involved the use of continuous, or white, radiation and proved the theory that crystals diffracted X-rays. The Braggs viewed this phenomenon as the reflecting planes, corresponding to the *hkl*

reflections, being fixed in direction. They used monochromatic radiation, which resulted in discrete diffracted intensities and from this derived Braggs' relationship,

$$n\lambda = 2\, d_{hkl} \sin\theta_{hkl} \qquad (3.1)$$

where n can be any integer but in practice is always set to 1, λ is the wavelength used, d_{hkl} is the interplanar spacing, and θ is the 'Bragg angle' between the incident beam and the set of planes in the diffracting position. This relationship is most clearly illustrated by P.P. Ewald's sphere, which is a reciprocal lattice interpretation of the process of diffraction, depicted in ***Figure 3.2.1***.

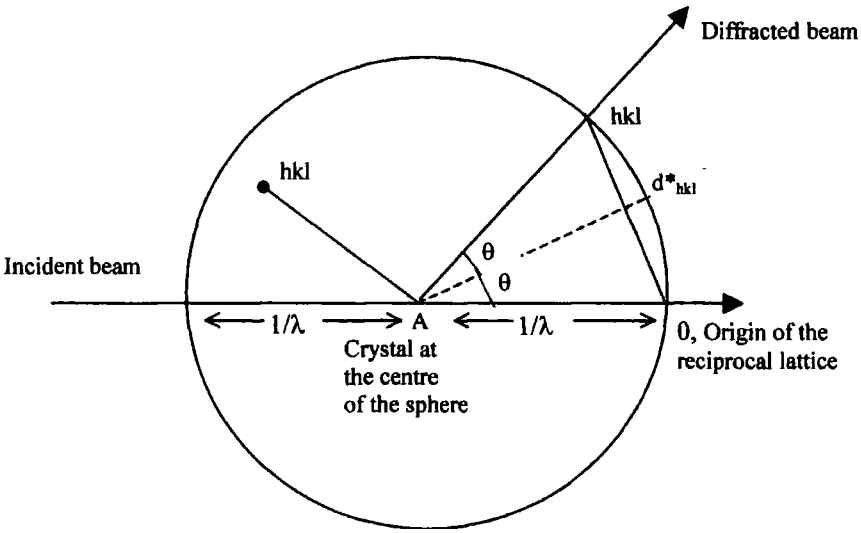

Figure 3.2.1 *- Schematic representation of the Ewald (reflection) sphere.*

From the diagram, it can be seen that $\sin\theta = (d^*/2).\lambda$. This is rearranged to give Bragg's law. The diffracted intensities allow the calculation of the electron density distribution at any point in the unit cell:

$$\rho_{xyz} = \frac{1}{V}\sum_{hkl}(F_{hkl})\exp[-2\pi i\,(hx + ky + lz)] \qquad (3.2)$$

where ρ is the electron density at any point x, y, z, V is the unit cell volume ($Å^3$) and F_{hkl} is the calculated structure factor. The relationship exists whereby the measured intensity is the square of the structure factor amplitude, $I_{hkl} = |F_{hkl}|^2$, thus the magnitude of the structure factors amplitudes can be obtained directly but not their phases. The

structure factor has two components and is expressed in terms of its amplitude and phase angle, (ϕ).

$$F_{hkl} = |F_{hkl}| \exp[(i\phi_{hkl})] \tag{3.3}$$

The structure factor is calculated from:

$$F_{hkl} = \sum_{n=1}^{n=N} f_n \exp[2\pi i(hx_n+ky_n+lz_n)] \tag{3.4}$$

where f_n is the scattering factor for the n^{th} atom. This is a function of atomic number and for X-rays there is an exponential decrease in scattering with increasing $(\sin\theta)/\lambda$. The process of crystal structure solution and refinement (described in section 3.10) is an iterative one and involves the location of a partial structure or just a heavy atom position. If this initial start-point is sufficiently correct, the calculated phases are hence largely correct, enabling the remainder of the structure to be found and refined.

3.3 Generation of X-radiation

The X-ray region of the electromagnetic spectrum lies between ultraviolet and gamma radiation in the 0.1-100 Å range. X-rays are produced by decelerating rapidly moving electrons onto a rectangular metal target whose K_α line is at a practical wavelength for an X-ray diffraction experiment to be performed and converting approximately 1% of them into quanta of energy. Within the sealed tube, electrons are accelerated by an electric field and directed towards a water-cooled metal anodic target. A continuum of X-radiation is emitted. A high vacuum is necessary because gas molecules reduce the efficiency of the generator due to collisions with the electrons and generated X-rays. The typical continuous power output from a laboratory based sealed tube is 2 – 3 kW, determined from the product of the voltage (kV) and current (mA) settings. Obviously, a more intense source, to illuminate the sample, will be obtained by increasing these settings. A practical limit is reached whereby the anode will not be cooled sufficiently and this is overcome by an alternative source design.

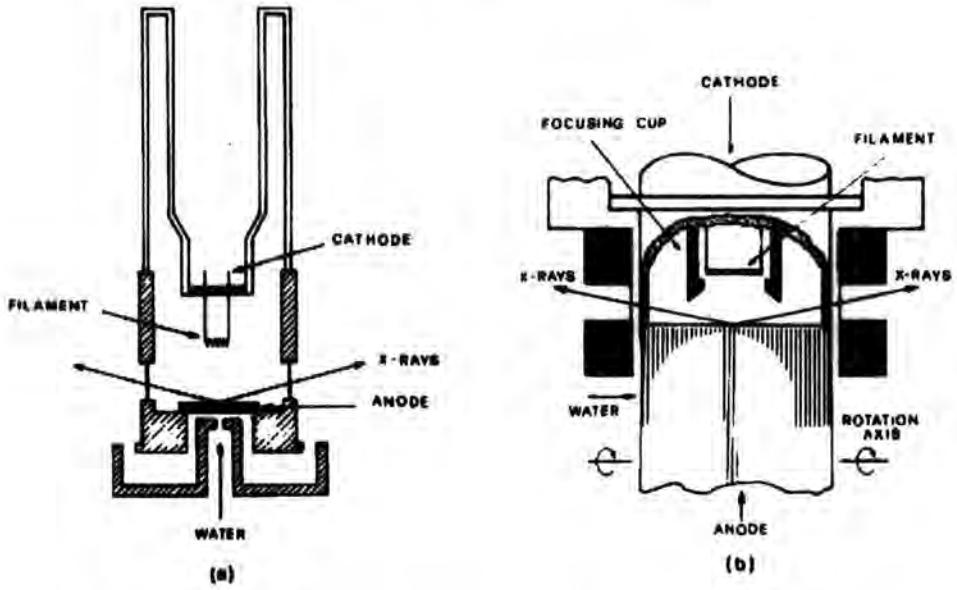

***Figure 3.3.1** – A schematic representation along the longitudinal axes of (a) a sealed tube and (b) a rotating anode X-ray sources (reprinted from Fundamentals of Crystallography by Giacovazzo, 1992).*

The most intense laboratory based X-ray source is the rotating anode generator. Here a new target is constantly presented to the electrons since the anode is constantly rotated. In both designs, the beam leaves the generator via beryllium windows. The output from a rotating anode is usually 18 kW. A cross-section of the construction of an X-ray tube and rotating anode is drawn in ***Figure 3.3.1***. As the accelerating voltage increases to 50 kV, the peak intensity shifts to shorter wavelength. Within this distribution, X-ray spectra show characteristic lines whose positions (i.e. wavelength) are target metal dependent. ***Figure 3.3.2*** shows the lines observed for Cu radiation. In practice, the wavelength produced by metal target sealed tubes used in laboratory X-ray source range from the harder, more penetrating, X-rays from a silver tube (Ag $K\bar{\alpha}$ = 0.5608) to the longer wavelength chromium radiation (Cr $K\bar{\alpha}$ = 2.2909). At energies ca. 10 k eV electrons are knocked out of the *K* shells and replaced by higher energy *L* (to give K_α radiation) or *M* electrons (to give K_β radiation). These lines are both close doublets since the transitions can occur from two possible electronic configurations. These are only distinguishable in high angle data, and in practice, a weighted average of the two is used ($K\bar{\alpha}$).

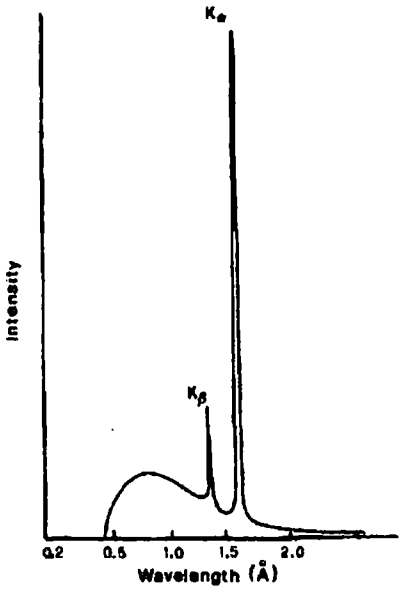

***Figure 3.3.2** – X-ray spectra of the output from a copper source (reprinted from Fundamentals of Crystallography by Giacovazzo, 1992).*

3.4 Monochromation and absorption

Monochromation is the removal of the weaker K_β lines using either selective filters or a monochromator crystal. The incident beam cross-section is then determined by the size of collimator used. A flat single-crystal of pyrolytic graphite is employed to monochromate the beam on both the SMART and Rigaku instruments. The (*0002*) reflection for this crystal is strongly allowed and the crystal is orientated with the X-ray beam incident on the {0002} surface. This crystal has approximately 50% reflectivity and is mosaic enough to diffract a divergent primary beam. Here, K_β radiation is removed and there is almost no white radiation background. The take-off angle allows the diffracted beam to pass into the collimator, which is an aperture that controls its size and divergence. The SMART and Rigaku are fitted with 0.8 mm and 1.0 mm collimators respectively as standard. In circumstances where only a much smaller crystal is available, a 0.5 mm or 0.2 mm collimator can be attached to the SMART to improve the signal to background ratio. Generally, the maximum sample size should not exceed 60% of the beam cross-section. The absorption of X-rays is crystal thickness, element type and density and wavelength dependent, and follows a Beer-Lambert type equation:

$$\frac{I}{I_0} = \exp(-\mu\tau) \tag{3.5}$$

and

$$\mu_m = kZ^3\lambda^3 \tag{3.6}$$

where I is the transmitted intensity, I_0 is the incident intensity, μ is the linear absorption coefficient (mm^{-1}), τ (mm) is the path length travelled by the diffracted beam through the crystal, k is a constant and Z is the atomic number of the element. Since the value of μ depends on the density of the material it is tabulated as μ_m, where $\mu_m = \mu/\rho$, in the *International Tables for X-ray Crystallography, Vol. III.* While shorter wavelengths reduce the absorption effects, they also reduce the diffracted intensity, which is proportional to λ^3. Thus, it is important to select an approximately equi-dimensional crystal (which comes close to the spherical ideal) to avoid a large variation in the transmitted intensity and the wavelength of choice for heavier scatterers is usually imposed as molybdenum. However, there are often substantial absorption errors in a data set due to the use of a plate or needle-like crystal or the presence of heavy atoms. A rule - of - thumb as to whether or not it is necessary to apply a correction can be determined from the value of μ for heavy scatterers. A molecule with a value less than 10 mm^{-1} suffers from negligible absorption, a value of $10 \leq \mu \leq 20$ indicates that it is not necessary to apply a correction and a value greater than 20 mm^{-1} means that substantial absorption errors exist and a correction should be applied. If a correction is not applied, a biased result will be obtained from the crystal structure refinement. This is often most obvious from the shape of the anisotropic displacement parameter (U_{ij}) values and distortions in molecular geometry. An absorption correction is applied by calculating the integral:

$$A = \frac{1}{V}\int \exp(-\mu\tau)dv \tag{3.7}$$

This may be done in several ways: analytically by describing the crystal faces, experimentally by measuring the variation in transmission to apply relative transmission factors or empirically by the comparison of symmetrically equivalent reflection. Three

possible types of correction exist and the choice often depends on the instrument upon which the data were collected.

3.4.1 The analytical absorption correction

This type of correction involves the measurement of the real crystal faces and from this, the calculation of the path length travelled by the X-ray beam through the crystal. Hitherto, the application of this correction was only possible by using an optical goniometer. The *Siemens* SMART diffractometer has an inbuilt microscope, which allows the indexing of the faces and the measurement of their distance from the centre of mass of the crystal. It is only advisable to carry out this measurement on crystals that have some well defined natural faces and which are mounted using glue or a very *thin* film of oil. This analytical correction is applied to the integrated intensities with knowledge of the incident and diffracted beam positions. This correction only corrects the data above a user-defined (I/σI) for absorption depending on the atomic types, crystal size and shape and wavelength. It does not take into account diffuse scattering from the crystal mount. ***Figure 3.4.1*** shows a view of a crystal of a copper complex whose faces have been described in terms of its Miller indices (*hkl*).

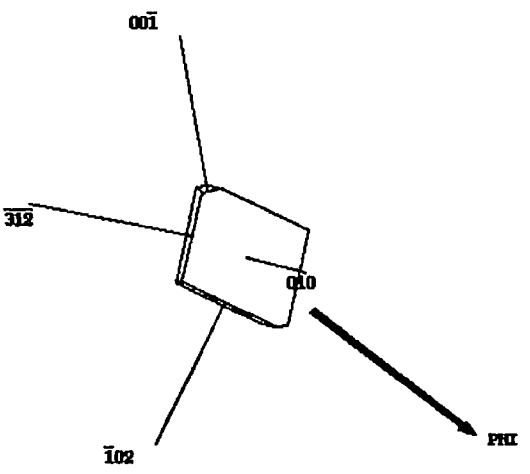

Figure 3.4.1 *– The indexed faces of* $C_{14}H_{40}Br_{0.8}Cl_{1.2}N_8P_4S_4Cu_2$*, measured on the SMART viewed perpendicular to the mounted axis.*

3.4.2 The semi-empirical absorption correction

The ψ (or azimuthal) scan correction is an experimental absorption correction carried out after data collection, that involves the rotation of the crystal about its ψ - axis on a four-circle diffractometer.[1] This axis is defined as $\chi = 90°$. Here a reflection is maintained in the diffracting position by presenting one face to the incident beam. The crystal is rotated about the ψ-axis thus varying the path length to yield a transmission profile that can be fitted to the raw intensities. The relative transmission factors for all data are calculated from:

$$T = \frac{I(\phi)}{I_{max}(\phi)} \qquad (3.8)$$

In practice, only values of $80° \leq \chi \leq 100°$ are useable for this purpose. No Rigaku measured crystal described in this thesis displayed markedly large absorption, hence this correction was not applied.

3.4.3 The empirical absorption correction

An empirical absorption correction does not require the measurement of any data after data collection. It involves taking the raw intensities after data reduction and applying a correction. The two empirical absorption corrections used in this thesis were the ψ-scan correction in XPREP[2] and the CCD correction Sadabs.[3] The ψ-scan routine reads the integrated peak intensities and, from the direction cosines of the incident and diffracted beams, calculates the mean path length (τ) through the crystal for every reflection as in (3.7). The transmission factor for every reflection is calculated and thus the intensities are adjusted.

The other program of this type used in this thesis is the relatively recent program 'Sadabs'. This program was written exclusively for Siemens SMART data. This is a multi-purpose program with the aim of correcting charge-coupled device (CCD) area detector data for the numerous systematic problems that effect them and which have been demonstrated to have a negative effect on the quality of both standard crystal

structure analyses and very accurate electron density studies. There are two components to this correction:-

1) The incident beam correction – This employs a 7-point Savitsky-Golay filter to smooth individual scale factors for each frame. The correction covers

- Crystal decay throughout the experiment, or time-dependent decay.
- Incident beam absorption – scattering from the crystal mount. One of the advantages of using a CCD detector is that it gives a direct impression of the effect of the crystal mount. Attenuation of the primary beam is at its greatest when the glass fibre passes under the collimator. In the ω-scan mode, this is unavoidable in the 250-290° range. Sadabs is the only program to account for this. Naturally, ϕ-scan data can also be corrected which removes this altogether and this is becoming an increasingly popular data collection mode.
- Reduction in the intensity of the incident beam – This is applicable when the data have been collected at a synchrotron central facility. In this case, there is an exponential decay in intensity. It is possible to scale the intensities using SADABS. All the data sets collected using synchrotron radiation during this thesis were scaled using Sadabs.
- A correction is also made for batches of data that have been collected at different generator settings in this program.

2) The diffracted beam correction – The absorption correction component employed is the methods of spherical harmonics.[4] This is an alternative method to performing an azimuthal scan that models an empirical transmission surface by a procedure of restrained full-matrix least squares. True absorption by the crystal components and anisotropy in the intensity of the equivalent reflections due to the crystal morphology can only be accurately estimated if there is a high redundancy in the data. In theory, it is best to aim to have at least four times redundancy in the data. If it *is* to be applied in triclinic cases, it is imperative that a full sphere of data is available. In some cases where the absorption is negligible, it is often advisable not to apply this particular absorption

correction component. The two pieces of information that are required by Sadabs are the Laue group and a value for μ*d (where d is the smallest crystal thickness). This value has a very substantial effect on the anisotropy of the atomic displacement parameters in the refinement and thus, if atoms do go non-positive definite, it may be necessary to increase this value.

To conclude, it can be seen that Sadabs aims to correct for far more than attenuation of the beam by the crystal. The maximum and minimum transmission factors given by the program are therefore not true transmission factors and should not be treated as such. It is important to bear these pitfalls in mind when using the program.

3.5 Instrumentation

3.5.1 The four-circle goniostat

This is so called because it contains four arcs designed to adjust the orientation of the crystal to bring the required set of *hkl* planes into the diffracting position. ***Figure 3.5.1.1*** shows a schematic representation of the design of a four-circle diffractometer with full χ circle.

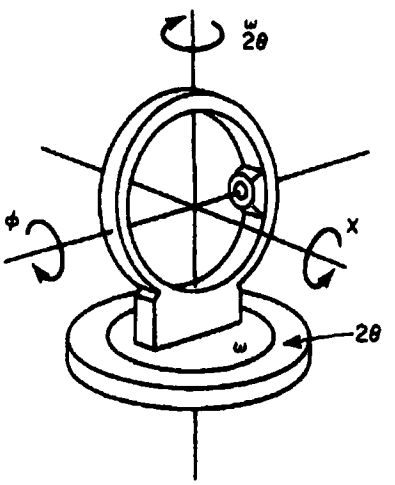

Figure 3.5.1.1 *- Schematic representation of a four-circle diffractometer, reprinted from J.P. Glusker and K.N. Trueblood (1985), Crystal Structure Analysis – A Primer, 2nd edition. Oxford University Press.*

The four circles are 2θ, ω, χ and φ. A standard arcless head was used for all the Rigaku and SMART experiments since no axial alignment of the crystal is required. The

head is attached directly to the ϕ circle. A four-circle diffractometer has four independently driven shafts. Most four-circle diffractometers operate with equatorial geometry meaning that the detector can only rotate in one plane, thus the reflecting must be brought into the diffracting position in that plane to be measured. The crystal orienter contains the ϕ and χ circles. The base circles, ω and 2θ, are mounted on a common axis with the χ circle mounted on ω and the detector on 2θ. When $\chi = 0$, the ϕ axis coincides with ω. Two equatorial geometries are used for data collection on the Rigaku and *Fddd* diffractometers. The normal beam mode of data collection is whereby a reflection is measured by oscillating the crystal through the diffracting position with both the incident and diffracted beams normal to the oscillation axis or χ circle. The diffraction vector is defined parallel to the plane of the χ circle. An illustration of this geometry is provided in ***Figure 3.5.1.2***.

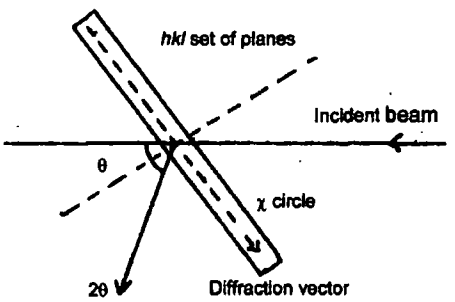

Figure 3.5.1.2 *– Diagram of the normal - beam geometry of data collection.*

However, it can be seen that as the data collection proceeds to measure higher angle reflections the χ circle obstructs the diffracted beam. This is overcome by then switching to an alternative setting of the circles whereby $\omega = \theta$. This is known as the bisecting geometry. The movements of ω and 2θ are correlated here. This case arises routinely on the Rigaku since it employs Cu K_α radiation. Due to the longer wavelength, reflections are more spatially resolved (equation 3.1) and thus data collection extends to higher 2θ angles. The *Fddd* operates with Mo K_α radiation but data are collected in this mode for part of the collection too due to the necessity of using well-formed crystals that diffract to high-angle for charge density data collection. A combination of rotations of ω, χ and ϕ are required to bring a reciprocal lattice point into the equatorial plane.

The function of χ and ϕ in bringing a reciprocal lattice point into the equatorial plane can be seen in ***Figure 3.5.1.3***.

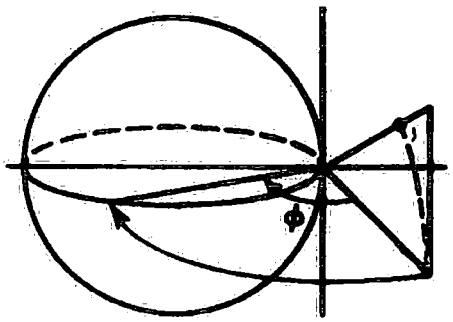

Figure 3.5.1.3 *– An illustration of how rotations through χ and ϕ bring a reflection in to the equatorial plane (reprinted from G.H. Stout and L.H. Jensen, 1968).*

The intensity measurements can then be acquired by a number of different scanning methods. The ω scan is useful for reducing the overlap between neighbouring reflections, which can be a problem due to the presence of either at least one long unit cell axis or a large degree of mosaicity. Scan modes other than this one are often precluded when using Mo K_α for these reasons. The ω-2θ involves movement of both ω and 2θ. This collection mode scans diagonally through a reflection and is advised for accurate measurements when the unit cell is determined reliably. Since more than one Ewald sphere is present, the dangers of overlap are high and it is not suited to situations with high background or diffuse scattering. ***Figure 3.5.1.4*** shows both these scanning modes.

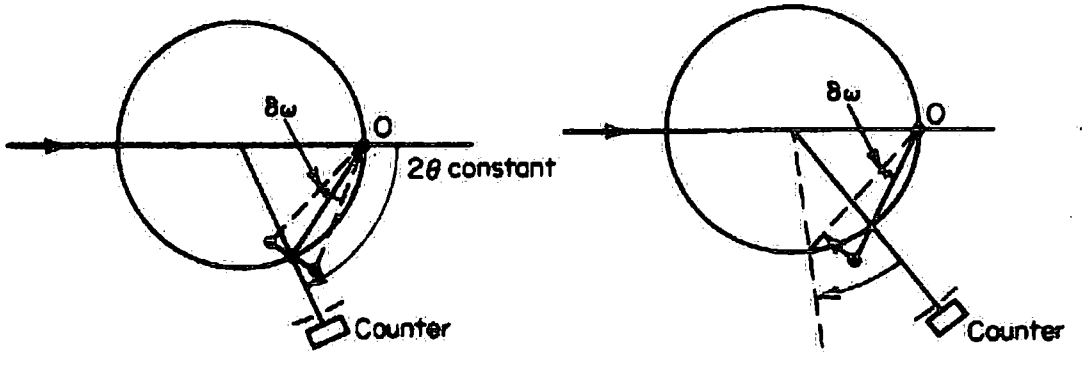

(a) *(b)*

Figure 3.5.1.4 *– Schematic representations of the (a) ω scanning mode and (b) ω-2θ scanning mode (reprinted from G.H. Stout and L.H. Jensen, 1968).*

3.5.2 The single-crystal Rigaku AFC6S four-circle diffractometer

The Rigaku AFC6S diffractometer (***Figure 3.5.2***) is a four-circle diffractometer equipped with a copper K_α source. This diffractometer is suited to the measurement of organic crystals or any weakly diffracting materials. It is necessary to use this instrument when the absolute configuration is required, due to the enhanced intensity of the copper source. It is not the ideal instrument for the measurement of metal containing compounds or any very strong scatterers due to the anisotropy of the absorption effect with Cu K_α radiation, or for fluorescent materials.

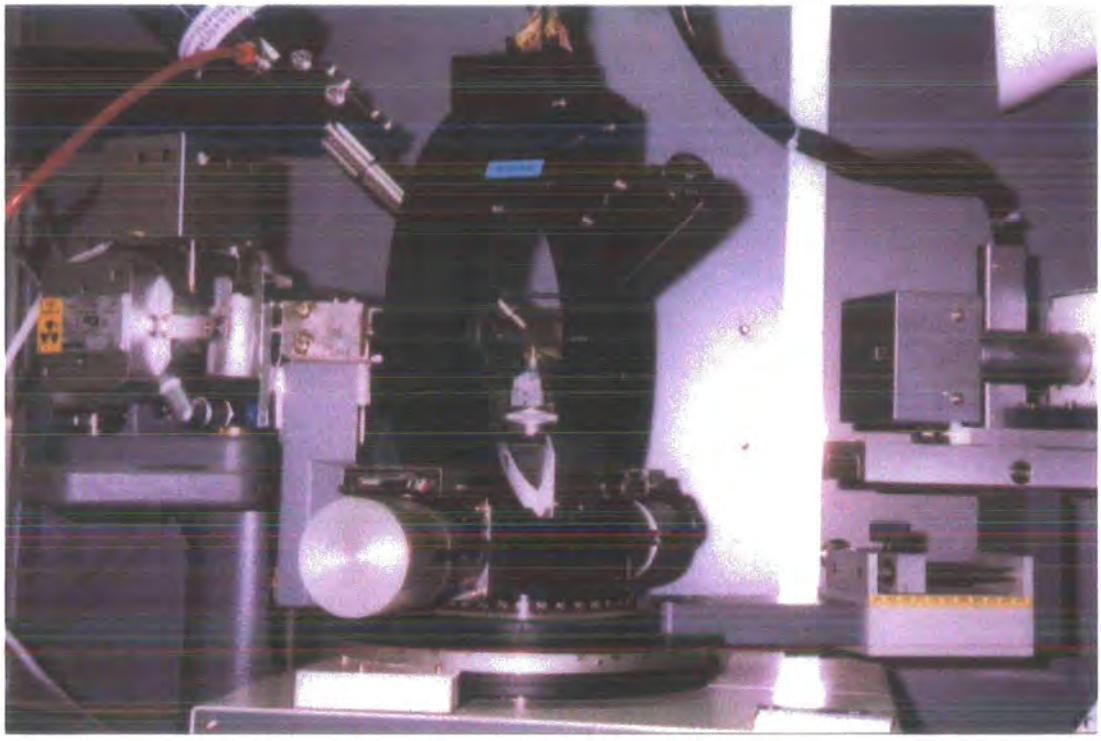

***Figure 3.5.2** – The Rigaku AFC6S diffractometer with Oxford Cryosystems Cryostream.*

As with all modern diffractometers it is computer – controlled, and writes the data to a local PC. The MSC created instrument specific software is the 'MSC/AFC Diffraction Control Software'[5] is used for all diffractometer operations.

The X-rays are incident on the {0002} surface of a graphite monochromator crystal. A 1 mm collimator aperture determines the beam diameter. Whilst this has a disadvantageous effect on the signal to noise ratio, it is necessary due to the greater loss of X-rays from a softer Cu source as a consequence of air absorption. This sealed tube

operates normally with generator settings of 45 kV and 40 mA. A perspex-glass panelled interlock system is present to prevent user intervention while the shutter is open and a lead curtain is attached to the right hand wall of the enclosure opposite the direct beam. A scintillation counter point detector is used. It operates on the principle of an X-ray photon hitting a thallium doped sodium iodide crystal, where its energy is converted to visible light. The light photons are picked up by a photomultiplier tube, the signal is amplified and a corresponding voltage results as output. An energy discriminator is used to differentiate between X-ray reflections arising from λ and harmonics of λ. The limitation on this set-up is the maximum time delay between X-rays hitting the detector necessary to separate the pulses. The dynamic range of a type is usually 50000 counts per second meaning that above this value the detector becomes saturated. The readout time refers to the response time of the photomultiplier and the speed of the subsequent electronics.

The diffractometer is fitted with an Oxford Cryosystems Cryostream[6] which is positioned diagonally above the sample, are data collections are normally carried out at 150(2) K. This has a temperature range of 90 – 373 K in practice. A crystal is 'centred' on a diffractometer of this type by a series of fine x, y and z translations of the goniometer head in order to position the sample at the centre of the four circles. When centred, the crystal should not precess when ϕ, χ or ω are moved. The central positions is estimated visually using a microscope with graduated x and y axes (1 division = 0.025 mm) and then the translational degrees of freedom in all directions are locked. A blind zigzag search of reciprocal space is commonly used to locate 20 – 50 reflections to calculate an initial unit cell. The search limits that are set up for this are $20 \leq 2\theta \leq 55$, $-20 \leq \chi \leq 80$, $-20 \leq \phi \leq 110$. For a reasonably well diffracting crystal, 20 reflections should be located within two hours. These are searched for without the presence of horizontal or vertical slits which are often placed before the detector to reduce the area upon which the photons are incident and therefore to increase the signal to background ratio. This maximises the chances of locating a reflection. Alternatively, a Polaroid photograph can be taken (***Figure 3.7.1***). This is a good method of saving time in the

early stages of an experiment since it gives irrefutable evidence of crystal quality and information on the positions of the reflections. This is usually an oscillation over 320° in ϕ with 3-8 exposures depending on how strongly diffracting the crystal might be. A good quality crystal exhibits intense diffraction spots past the resolution of the Polaroid which should not show smearing or lines, indicative of disorder or an incommensurate structure. By measuring the positions of the reflections on the photograph and entering their x and y co-ordinates the angular positions are calculated and these serve as start points for a search. From here the unit cell is determined and once it is verified that this is sufficiently precise and reasonable for the size of molecule under investigation, a Laue symmetry check is performed by measuring equivalent reflections in the expected Laue group (e.g. 2/m). This information is required prior to data collection for all four-circle diffractometers because each reflections must be consecutively acquired and to be economical with time on routine data collections the unique data for a particular crystal may only be measured (e.g. it is only necessary to collect a quadrant of a sphere $0 \rightarrow h$, $0 \rightarrow k$, $-l \rightarrow l$ for the point group 2/m). It is should be noted that in order to determine the absolute configuration of a molecule it is advisable to measure Friedel equivalents. If there is any doubt about the symmetry of a crystal, a data collection for a centrosymmetric triclinic crystal system, that is a hemisphere, should be recorded if not a full sphere. In the case of higher symmetries, this will have a beneficial effect on the data precision and hence the reliability of the results since the merging statistics will be improved. Higher angle reflections ($40 \geq 2\theta \geq 60°$) are then measured since the relative error in their measurement decreases as θ tends to higher angle which are refined to give a more accurate unit cell. Prior to data collection, standard reflections (typically 3 - 8) are selected to monitor the crystal throughout the collection, which can take up to one week depending on the scan speed. These are usually selected by taking one with a large h index, one with a large k index and one with a large l index. A high χ value reflection is chosen to follow the crystal centring. These are usually set to be measured every 100 – 150 reflections. Depending on the peak intensity and width, the slits may be used. These are available in sizes of 1.0 and 1.3 cm and reduce the detector area on which an

X-ray can be recorded in the vertical and horizontal directions. In all cases except where there is a problem with peak broadness, the 1.3 cm slits give a substantial improvement in integrated intensity and full scale deflection whereas the 1.0 cm slits often truncate the peaks. It has been observed for the Rigaku determined structures in this thesis that for ω scans it is beneficial to use the vertical 1.3 cm slits. These reduce the possibility of neighbouring reflections overlapping and improve the signal to background ratio. For data beyond 120° in 2θ it helps to add the horizontal 1.3 cm slits to bring the weakly observed intensities above a fluctuating background. The data collection scan width, Δω, is determined from

$$\Delta\omega = A + B \tan\theta \qquad (3.9)$$

where A is the largest peak width found and B tanθ is a term that compensates for peak broadening as a function of θ. Once these parameters have been determined, data collection can be commenced. It must be borne in mind that the accuracy of the measurement is proportional to the square root of the measuring time thus as on all instruments it is important not to use exposure times that are adequate for the particular crystal and realistic for the required accuracy of the final results.

Data are reduced from the Rigaku using the TEXSAN package.[7] Here the integrated intensities are converted to structure factors by performing Lorentz and polarisation corrections (Lp) and if necessary for absorption.

3.5.3 The *Fddd* four-circle cryo-diffractometer

The *Fddd* four-circle diffractometer[8] (shown in ***Figure 3.5.3***) has been developed specifically to perform accurate low temperature measurements in the 9 – 300 K ranges. This enables it to follow low temperature phase transitions, to attain much more high-angle data for charge-density studies, and the ultra low temperatures reduce thermal vibration, which allows the analysis of anisotropic displacement parameters. It has an identical geometry to the aforementioned Rigaku AFC6S instrument and operates using the data collection modes previously cited. Due to the

requirements of supporting the bulky and heavy Displex cooling device on the χ circle, the position of the circles with $\chi = 180°$ is conventionally renamed the zero positions. The implication that this has is that what would be a left – handed geometry on a conventional four-circle geometry is obtained. For indexing reflections, the transformation $x \rightarrow -y$ and $y \rightarrow -x$ is applied to the orientation matrix and a corresponding transformation is applied to the direction cosines in order to apply an absorption correction.

The complete instrument is an in-house design. X-rays are produced by a Siemens Molybdenum-target belt driven rotating anode generator. This offers a beam of greatly enhanced intensity in comparison to a standard laboratory sealed tube. It was previously fitted with a 0.1 x 1.0 mm filament and operated with generator settings of 52 kV and 76 mA. This gave an approximately 4 kW output. After this work, this was replaced and it now employs a 0.3 x 3.0 mm filament with generator settings of 40 kV and 160 – 180 mA, giving a power output of 7.2 kW. The incident beam is monochromated using a Huber '151' graphite monochromator operating in parallel mode. Due to its size, the instrument is enclosed in a room by an interlocking system of patio doors. Cooling is attained by an 'Air Products and Chemicals' (APD) '202' two stage closed cycle Displex He cryogenic refrigerator[9] (CCR).

The diffractometer is a 300 kg Huber four-circle goniometer that was connected to the χ-circle via high-pressure rotary joints, now replaced by lightweight nylon coils. Precise movement of the diffractometer for beam alignment is facilitated by means of support from three compressed air pads on a polished surface. A fast readout is insured by using a 'Siemens Fast Scintillation Detector' (FSD) fitted with a 3 mm entrance aperture, which is capable of recording 4×10^6 counts per second. In the experiments described in this thesis, the crystal-detector distance is 35 cm (it has a range of 35-70 cm). The crystal is mounted on a sharpened graphite pencil lead usingthe commercially available methyl acrylate '24 hour' glue, which has been proven to be stable and thermally conducting down to 4 K. It is thermally coupled to the second stage of the Displex.

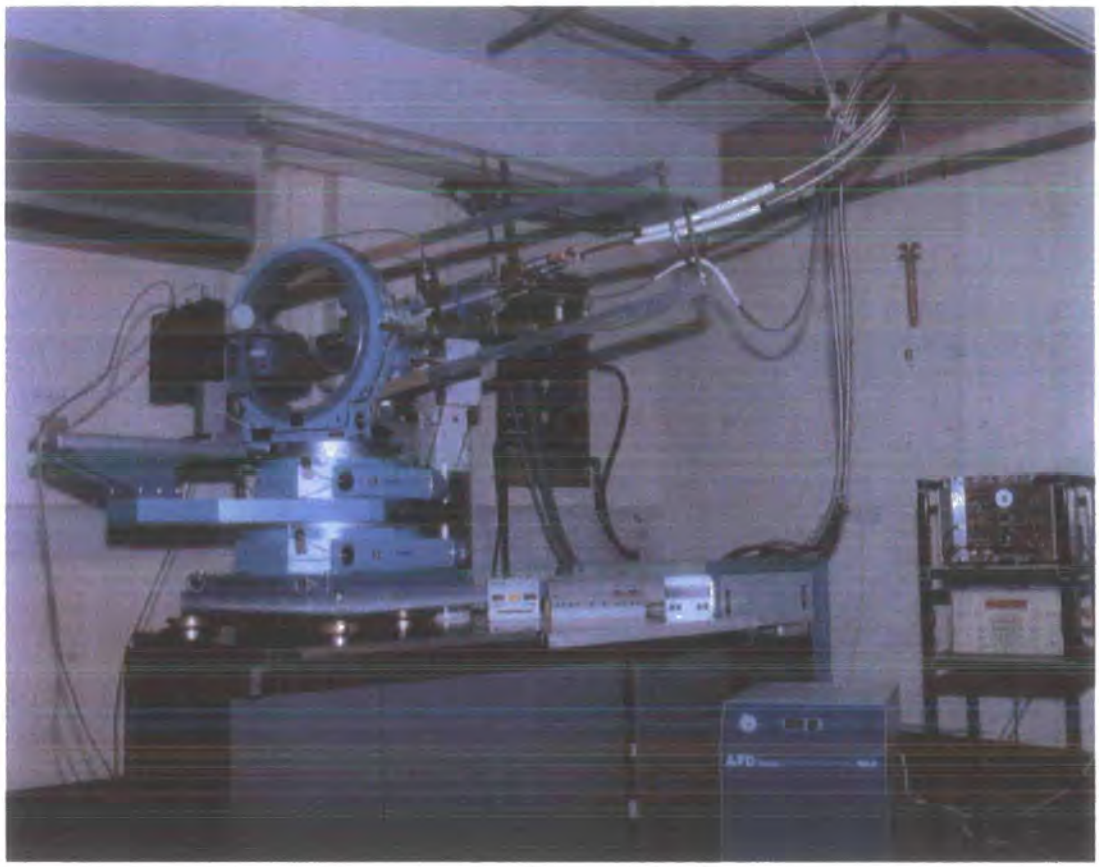

***Figure 3.5.3** – The Fddd four-circle diffractometer with closed cycle refrigerator.*

Crystals are mounted, as standard, in glue. It is crucial that good thermal contact is maintained between the cryostat and the graphite. An efficient heat transfer from the 2nd stage of the Displex to the crystal is attained by using a copper goniometer head. The graphite is attached to this by a spring-mounted mechanism. The process of mounting crystals on this instrument and cooling to cryogenic temperature does not allow 'flash - cooling'. This is because the crystal must first be mounted and optically centred, two concentric cylindrical beryllium shrouds (with diameters of 6.5 and 5.0 cm) attached and the interior evacuated for thermal insulation. Cooling then begins at a maximum rate of ca. 3.2° min^{-1} which clearly renders fast cooling impossible.

The procedure for cooling crystals on the *Fddd* is to screw the goniometer head onto the second stage of the Displex at room temperature. An oscillation or rotation photograph is often taken first as a means of preliminary crystal screening and as on the Rigaku AFC6S as a means of finding the positions of reflections for unit cell determination. For macromolecular compounds, a rotation over a large portion of

reciprocal space would contain too much information; thus, an oscillation over 5° in ϕ in 0.02° steps with an exposure time of 2 seconds is deemed more appropriate. The *(0002)* graphite lines are quite visible on Polaroid photographs at 12.1° in 2θ and their intensities serve as a diagnostic crystal height marker when centring the crystal using X-rays. The beryllium shrouds are added and the pump switched on, which achieves a vacuum of 10^{-2} mbar. The Displex is switched on and cooling begins. Without any contra-heating, 9 K is attained within several hours. When the Leybold 'Turbovac 361' turbomolecular pump (TMP) is switched on, vacuums of the order of 10^{-5} mbar are maintained. The connection with the pump is closed and the vacuum is maintained within the Displex and the goniometer head due to cryosorption. The principle of the operation of Displexes is discussed further in section 3.11.2. The crystal quality can be monitored during cooling by taking successive Polaroid photographs as the crystal passes through the water/ice freezing point since it is not visible to the experimentalist as this stage.

The instrument was controlled and data collected remotely using a DEC Alpha 200 workstation operating VMS 5.1 and CAMAC electronics. All data are written locally to the VAX. The software that controls the movement of the circles data collection is the 'Multi-detector Acquisition of Data'[10] (MAD) program.

3.5.4 The single-crystal SMART three-circle diffractometer

The Bruker (née Siemens) SMART diffractometer[11], shown in ***Figure 3.5.4*** is a three – circle diffractometer that operates with a Mo K_α sealed tube X-ray source. It has an area detector, which is a 512 x 512 pixel (1K) charge - coupled device (CCD). This allows the acquisition of a large amount of data in a relatively short period. A larger 2K CCD detector is also available, which collects higher resolution data and is suitable for measuring data from macromolecular crystals where copper radiation is invariably employed, since there is increased spatial resolution of the diffraction spots.

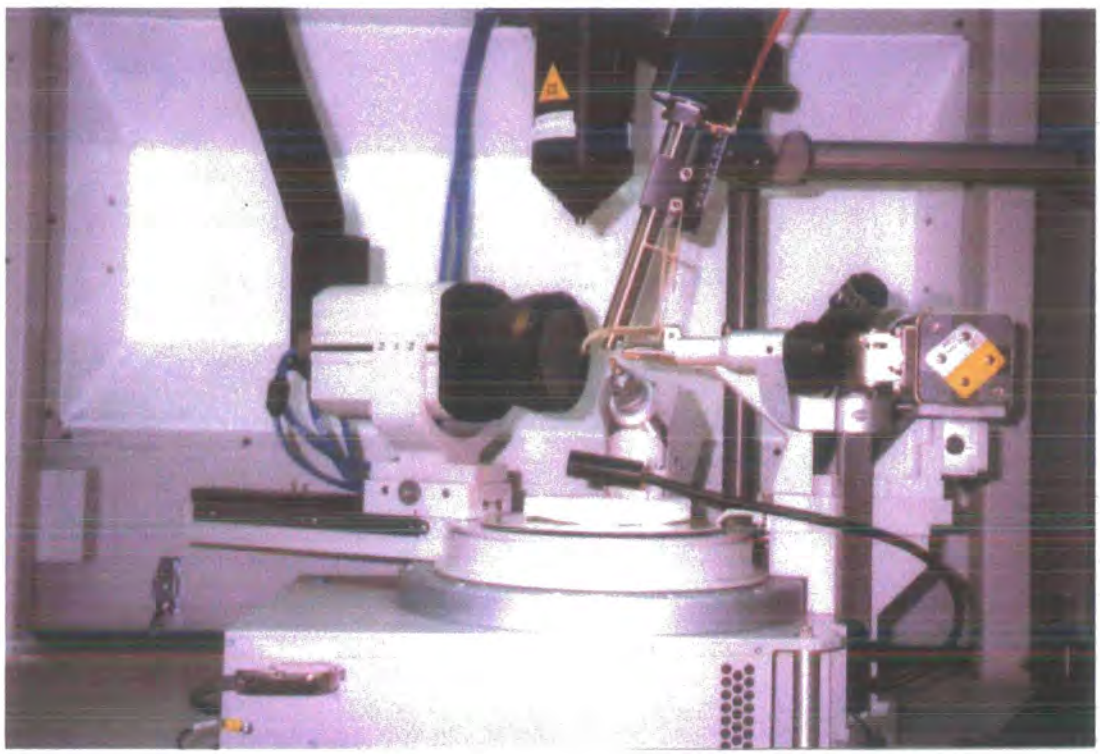

Figure 3.5.4 *– The SMART-CCD three-circle diffractometer with Oxford Cryosystems Cryostream.*

A molybdenum source often precludes the study of compounds with exclusively light atoms or small crystals. However, due to the opportunity of collecting data using longer exposure times it is possible to overcome this factor. The majority of the crystal structure determinations reported in this thesis were from data measured using the SMART instrument, therefore it is worth discussing here the data collection and processing procedures as well the unique design features of this diffractometer.

The main advantage of the SMART system is that many data covering large portions of reciprocal space can be recorded simultaneously with the advent of this position - sensitive detector. Because of using this detector instead of a scintillation counter as in a four-circle diffractometer, the number of rotational axes can be reduced. Due to the size of the detector, the function of the χ circle becomes redundant to a certain resolution. The χ arc is fixed at 54.71°. Data are measured with a stationary detector at -29° in 2θ, as default. This detector position means that some Friedel equivalents at low angle are measured. The crystal is rotated through ϕ or more usually ω to collect a unique set of data. An Oxford Cryosystems Cryostream[6] is positioned diagonally above the crystal to provide cooling to 150 K as in the case of the Rigaku AFC6S. The beam is monochromated using the {0002} surface of a graphite monochromator. Beam alignment is achieved by fine movements to the monochromator position using the larger 0.8 mm collimator. A fluorescent cover is placed over the collimator tip, which enables the beam position to be located by the presence of green emission lines. For reasons of safety and to prevent detector saturation and melting, low generator settings of 40 kV and 5 mA are used and the x and y positions of the primary beam are input into the software. For all alignment or diffractometer stability tests the standard 'ylid' crystal, 2-Dimethylsulfuranylidene-indan-1,3-dione,[12] is used whose previously determined unit cell dimensions indicates the accuracy of the instrument alignment.

The SMART has generator settings of 50 kV and 40 mA in normal operation. A perspex glass panelled interlock system prevents user intervention while the shutter is open as in the previously cited instruments. The evaluation of crystal quality and diffracting strength is quickly determined in this case. An electronic rotation, or oscillation, photograph taken for exposure time of 60 seconds over 360° in ϕ is informative since an indication of mosaicity from the appearance of the reflections and the resolution that the data set might extend to is obtained. Although, determining the unit cell is not a prerequisite to data collection, an initial search of reciprocal space for reflections to calculate the unit cell is always carried out. Three batches of 15 – 30

frames are usually collected. The first batch is at $\omega = 2\theta = -29°$ and $\phi = 0°$. The second batch involves the rotation of ϕ through 90° which means that two volumes of reciprocal space are scanned that are mutually orthogonal. The third batch of data is collected at $\omega = 2\theta = 29°$ to obtain Friedel equivalents. If the crystal is of reasonable quality, the correct unit cell will be obtained at this stage. Data collection can then be commenced. The two parameters that must first be decided upon are the exposure time and the scan width. This refers to the angular rotation or increment by which the scan axis is moved. A scan width of 0.3° for ω scans is the optimal value for most situations. This is sometimes varied to between 0.2 and 0.4° depending on the peak width. To calculate the positions of the peaks accurately it is best to have 5 – 6 data points, which describe their profiles. This should be borne in mind when deciding on the scan width while taking into account peak broadening at high angle and the fact that reflections close to the rotation axis on the SMART appear broader. An exposure time of 20 seconds is usually used on the SMART. In practice, this is varied between 10 – 40 seconds. If a crystal is very strongly diffracting and saturates the detector, a frame will be retaken at 8 x speed. This may only be the case for a few strong reflections, however if this is a frequent occurrence in the early stage of data collection, the collection should be restarted with a slower speed. Due to the readout time efficiency, a standard data collection over a hemisphere with the additional collection of Friedel equivalents takes 8 hours using 10 second exposures and 12 hours using 20 second exposures. As with all diffractometers, a data collection strategy must be set up prior to collection. The suggested SMART hemisphere and quadrant of a sphere offer sensible strategies for the collection of data covering that portion of reciprocal space. At a crystal – detector distance of 4.5 cm, a resolution of 0.77 Å is attained in the corners of the square detector and 0.87 Å along the edge. The default hemisphere gives this coverage or completeness to 2θ and there is some redundancy in the measurement to improve the merging statistics. It is rare to measure less than a hemisphere of data on the SMART. For data collections that require more data, it is possible to determine a good strategy using the program ASTRO.[13] This can work out detector positions where very high

angle data is required that give some overlap. This interactive program updates the coverage and redundancy values as the proposed data collection set-up is changed. It is advisable here as on all the other instruments to check the circles for any positional errors prior to commencing a data collection by driving 2θ, ω and ϕ to the zero positions. Since reflections are not collected individually as in a four-circle diffractometer, standard reflections are not measured in the same way. However, the first ca. 50 frames are usually recollected afterwards which serves as an indication of the extent of any crystal decay, movement, or any axial misalignment that might have happened during the course of the experiment.

There is a '$\lambda/2$' problem inherent in area detector data since this offers no means of energy discrimination. When the primary beam leaves the monochromator crystal, it is well known that there are harmonics present. For copper radiation these are present up to $\lambda/6$ and for molybdenum they are not appreciably intense beyond $\lambda/2$. These harmonics are therefore incident on the crystal. Following Bragg's law any reflection *2h, 2k, 2l* arising from λ will contribute to the intensity of a reflection *h, k, l* arising from $\lambda/2$. When these $\lambda/2$ contaminant reflections are strong and not removed, it is possible that they will result in systematic absences being apparently observed leading to an incorrect space group assignment and a doubling of one or all unit cell axes.[14] This problem can be removed by either the reduction in the accelerating voltage or the use of another type of monochromator. The threshold voltage can be calculated below which half-integral intensities are not observed

$$\lambda_{min} = hc/eV = 12398(1/V) \qquad (3.10)$$

where h is Planck's constant, c is the speed of light, e is the charge on the electron and V is the accelerating potential in volts. For Mo K_α, $\lambda/2 = 0.3554$ Å. The accelerating voltage for this is 34.9 kV. However operating a sealed tube at these reduced voltages would result in an unacceptable loss of intensity:

$$I(K_\alpha) = k(V - V_0)^{1.63} \qquad (3.11)$$

where k is a constant, V is the accelerating potential and V_0 is the minimum voltage required for K_α generation. From this, there is a 68% loss in intensity of the primary beam when operating at 34.9 kV. It is possible to use alternative monochromators such as silicon or germanium. In these cases, the F_{222} is very weak therefore the contribution to the *(111)* intensity is very small resulting in virtually $\lambda/2$ free radiation. However, for routine data collections using the SMART-CCD device it has been found that the $\lambda/2$ problem has a negligible effect.

Data reduction from the SMART involves the integration of all the frames using the program SAINT[15] to yield a set of integrated Lp corrected intensities. This is a Fortran program developed for the reduction of single-crystal diffraction data from a series of adjacent rotation frames recorded with a fixed wavelength by an area detector.[16] Before the frames are integrated, it is imperative that the accuracy of the unit cell is optimised. The orientation matrix dictates the calculated positions of the reflections and the SAINT program reads the two-dimensional frames and does a 'box' integration for the volume where they should be. The 'start' unit cell for integration is calculated using up to a maximum of 512 reflections thus the unit cell from the initial pre-data collection search is improved by successive least squares refinements. The extra reflections are located by manually 'thresholding' frames from well separated areas of reciprocal space and adding intensities above a specified $I/\sigma(I)$ threshold into the 'reflection array'. During the course of these refinements, the agreements of the *h, k* and *l* indices are observed in conjunction with the estimated standard deviations in the unit cell parameters. The unit cell is often transformed to a higher symmetry setting or a centred cell may be located (C, F or I) using the 'Bravais' option, due to the addition of extra reflections. If relatively high angle reflections are observed ($2\theta \geq 30°$ Mo K_α), these should be used for the unit cell refinement since they yield more accurate values.

The user must specify a few parameters before integration begins: (i) The approximate beam divergence and mosaic spread. The profiles of many reflections are measured using the SMART software to get an overall impression of the broadness of the reflections for inputting into SAINT. They are firstly measured in terms of their

width in the x and y directions (i.e. in the plane of the frame). A value for their spread in z must be estimated; this represents the peak width or crystalline mosaicity as the crystal is turned through ω, i.e. perpendicular to the other two directions and is referred to as the full-width-at-half-maximum (FWHM). A well-formed periodic crystal that is not perturbed by any disorder, or imperfections, will have an average z value of 0.5-0.8°. The user specified box size remains constant during the course of integration. It is possible to refine this as the integration proceeds, whereby an updated value is used for each batch of data. This is not recommended in most cases as it can lead to non-sensible box sizes because of a poorly determined orientation matrix or another problem with the data set. (ii) The second parameter that must be specified is the name of the spatial calibration frame used to calculate positional corrections of detector images. (iii) The constant part of the filenames of input and output files. (iv) The wavelength, direction and polarization of the direct beam. (v) The unit cell dimensions.

There are two stages in the integration process. In the first stage, reflection profiles are learnt as a function of detector position and spindle angle within the data collection range. The first 25 frames are used to locate strong diffraction spots and to estimate the background. In this learning phase the profiles of the strong reflections are normalised and added to the nearest reference profile boxes. The contributions are weighted according to their distance from the box and each grid point within the box is classified as signal if it is above 2% of the peak maximum. Thus the importance of a good starting orientation matrix can be seen and also how adept SAINT is at located weak reflections hardly above background.

In the second stage, intensities are estimated for each peak using the nearest reflection profile. In general, the correlation coefficients are higher for the stronger reflections, which have been more reliably determined.

As the integration proceeds, a few figures of merit are monitored which are indicative of the suitability of the user-defined parameters and the quality of the data set. The 'correlation coefficient' values for each frame are a fractional measure of how close the peak position is to its expected position and should ideally be close to 1. In

practice values greater than 0.5 indicate that the integration is satisfactory. A box of 9 x 9 x 9 grid points is used to show how the initial reflections fit the box. There are nine such boxes and the step sizes between grid points and between the boxes are derived from the approximate values of the beam divergence and crystal mosaicity. This profile should be inspected and, if necessary, changed. The root-mean-square values in x, y, and z should be less than 0.4 approximately. If these are large, the unit cell may not be very accurate or wrong.

The integrated intensities, produced by SAINT, are directly related to the square of the structure factor amplitudes. Before these can be used for structure solution, several geometrical factors must be corrected. These corrections, once applied give a data set of relative intensities. These are the generic Lorentz and polarization corrections (Lp), an absorption correction (T), and the scaling of one or more data sets, if necessary, resulting from either crystal decay or data acquired from different crystals of the same compound. These corrections take the same form for all single-crystal X-ray diffractometers thus will be discussed in more detail in section 3.9.

3.5.4.1 The charge-coupled device area detector

Nowadays, virtually all macromolecular data are recorded on some kind of area detector and this trend is also revolutionising small-molecule crystallography. This recent development is different from the conventional photon counting devices (i.e. scintillation counters and multiwire proportional gas chambers). The data collection speed for scintillation counters is not limited by count rate limits but by their need to examine each data point sequentially. Multiwire detectors examine many Bragg reflections simultaneously and therefore result in a markedly accelerated data collection. All counting detectors have what is called a 'dead time' which means that the electronic processes involved in discriminating each incoming X-ray photon require a finite time. Dead times of 2-5 μsec are achieved by diffractometers in service today permitting reasonably efficient and accurate operation of multiwire detectors up to count rates of

10^{-6} sec^{-1}. Beyond these count rates the efficiency drops. However, for CCD detectors the counting efficiency increases with increasing count/sec.[17]

CCD detectors are integrating detectors. These have no upper rate limits and measure the total energy during an exposure. Individual pixels become saturated when the signal exceeds their storage capacity. The heating caused by the strong diffracted beam is dissipated by heating neighbouring pixels. The factors to be considered when choosing a detector are expense, spatial resolution, efficiency and dynamic range. The other type of integrating detector, film, is inexpensive and offers good spatial resolution (2-5 μm). However, the dynamic range is poor, and film development is slow and thus film is not used for quantitative data collections today. The dynamic range of a detector refers to its ability to measure both strong and weak reflections simultaneously. The CCD is the only area detector to offer a good dynamic range. ***Figure 3.5.4.1*** shows a schematic diagram of a typical CCD detector design.

The CCD design is based on direct contact between the CCD and the fibre-optic taper. Although the signal levels in this type of detector are low, CCDs have such low noise levels and exhibit such electronic perfection that the signal from each incident X-ray photon equals exceeds the total noise of the detector.

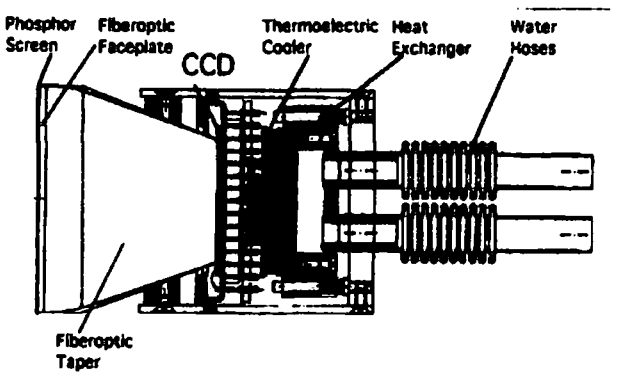

Figure 3.5.4.1 *- Schematic diagram of a water-cooled CCD detector design (reprinted from Westbrook and Naday, 1997[17]).*

The X-rays pass through the beryllium window that protects the phosphor surface and is X-ray transparent. The X-ray sensitive phosphor surface converts X-rays into visible light photons. If the X-rays struck the CCD directly, it would suffer from

radiation damage and signal saturation. The generated visible light photons are then passed through visible light fibre-optic tapers to process the signal. The CCD is placed tightly against the end of the taper to maintain a good focus.

Fibre-optic tapers induce a slight image distortion, and this is corrected for by a factory performed spatial calibration correction. Due to the construction of the CCD camera, some distortions occur between the position of an X-ray beam hitting the beryllium front window and the position of the corresponding visible light photon being stored in a pixel well on the CCD-chip. These non-linear distortions originate mainly from the glass taper connecting the X-ray phosphor and the CCD chip. In order to correct these distortions an algorithm is used to map each pixel on the detector with a position on the beryllium window. This map is established by using the brass 'fiducial' plate, which consists of a regular pattern of drilled holes. A distorted image is recorded on the detector and an algorithm is used which will alter the image until the same regular pattern as the brass plate is observed. The regular diffraction image from a crystal is taken and this correction is applied resulting in an image of the undistorted diffraction pattern. This correction in practice is never changed. If data are to be measured with a significantly different detector distance, a new correction may then be carried out and applied.

A random error associated with CCDs is natural background radiation such as cosmic rays, producing spurious signals called 'zingers'. This problem is more or less eliminated by collecting every frame twice, meaning that, every frame is collected in two half exposures which are summed together. The CCD is coupled to the taper by means of experimental grease on the SMART instrument, which is periodically replaced to ensure good contact.

The formation of an image by a CCD has two stages: (i) charge generation and accumulation, and (ii) charge transfer and detection.

(i) Charge generation and accumulation: The light captured in a CCD generates electron-hole pairs. An incident visible light photon (energies between 1.1 and 5

eV) excites a valence electron into the conduction band, forming a free electron in silicon.

(ii) Charge transfer and detection: When a frame has been taken the X-ray shutter is closed and each pixel is read out one at a time. The charge is passed along a 16-bit analog-to-digital converter on the SMART instrument.

The SMART CCD[18] is cooled to a temperature of -50° C in normal operation and this temperature is displayed by a LCD. Even with no light coming into the CCD chip, the pixels slowly accumulate electrons with time. A dark time, or current, is a frame taken for the same time as the exposure with the X-ray shutter closed. This is used as a correction for every data collection frame.

3.6 Crystal evaluation and mounting

The most informative method of deciding on crystal suitability is usually to visually inspect the crystals. The ideal crystal for an X-ray diffraction experiment has well-formed sheer faces and sharp edges. A crystal should be of one uniform colour or be completely colourless. Surface staining may indicate that it is not chemically homogenous or may be reacting with moisture in the atmosphere. The crystal should be examined under a polarising microscope for any cracks. Since crystals act as diffraction gratings for visible light, a crystal can extinguish and let light pass through as it is rotated about plane polarised light. This optical property of crystalline materials is known as 'birefringence'. A single crystal will be illuminated and disappear uniformly and sharply as it is rotated. If this does not happen, it is probable that the crystal has a twinning component, and it should be disregarded. This is not a completely failsafe method of detecting twinning however as cubic crystals, hexagonal crystal when viewed along the c direction and deeply coloured crystals do not exhibit any birefringence.

When cleaving a large crystal, an effort should be made to cut along the natural faces of the crystal. This makes it possible to index the faces of the crystal and reduces stress within the crystal, which could cause cracking on cooling.

Crystals are usually mounted on a glass fibre, which should be as thin as possible to reduce background scatter while remaining strong enough to support the crystal's weight and not to shake in the gas stream of an open flow N_2 cryostat. The choice of the means of attaching the crystal to the fibre is usually dictated by the stability of the crystal and the required temperature of the measurement. The method of choice has previously been to attach the crystal using a small covering of glue on the end of the glass fibre. The use of epoxy-resin glue means that the crystal is fixed rigidly in 4-5 minutes. However, if the crystal is air-sensitive this offers no means of protection from moisture in the atmosphere. There are many previously described methods of handling crystals that are air or moisture-sensitive. They can be mounted in a glove box under a positive flow of nitrogen. The more usual route to mounting air-sensitive crystals that have come from a synthetic chemistry laboratory is to attach a Schlenk tube directly to a vacuum line with a nitrogen flow. This allows the atmosphere within the container to be purged with nitrogen gas. Most gaseous nitrogen contains a small percentage of oxygen gas, thus all of these procedures should be carried out as rapidly as possible. Historically, crystals that exhibited sensitivity were mounted in thin-walled Lindemann capillaries. This method, although reasonably effective, does result in a considerable and unavoidable glass scatter. The use of inert oils to protect macromolecular crystals has been pioneered by Håkon Hope.[19] Here, the oil used was Paratone-N (Exxon) mixed with 25-50% mineral oil to yield a suitable viscosity which offers a unique means of protecting crystals by the method of 'flash-cooling'. Nowadays, the oil of choice is per-fluoropolyether (MW 2700, purchased from Riedel-de Haën or Fluorochem). It exhibits a marked increase in viscosity below 230 K. These oils operate on the principle that a crystal is covered in a very thin oil film and is attached to the fibre by capillary action. The crystal, mounted to the goniometer head, is then placed on the diffractometer in a N_2 gas stream, which cools it to below 200° C in 1-2 sec. Per-fluoropolyether vitrifies at approximately 200° C, forming a solid glassy matrix. The advantage that this method offers is that the crystal is protected at room temperature while being handled and the oil has some cryoprotective properties, which will be discussed further in more detail in chapter 7. When the covering of oil is kept to

a minimum, its contribution to the background scatter, which can be significant, is very much reduced. However, the method does not allow data to be measured at room temperature because the oil is liquid. The crystal can be removed easily after the experiment and if it does not suffer unduly from X-radiation induced decay, it can be preserved for another measurement under the protection of oil. It should be borne in mind that once covered in oil, the crystals are invariably unsuitable for other solid or solution-state measurements due to this surface 'contamination'. The current belief is that crystals benefit from being additionally handled and mounted at cryogenic temperatures, following examples by Kottke and Stalke.[20]

3.7 Unit cell determination

The reciprocal lattice is a convenient means of performing calculations of diffraction geometry. Each reciprocal lattice point or node represents the position of a Bragg reflection. The reciprocal cell parameters are used in diffractometer control in setting the circles to measure the intensity of a reflection *(h, k, l)* because they are directly related to these Miller indices. The distance of a reciprocal lattice point from the origin is the length of the vector:

$$1/d_{hkl} = (\mathbf{ha^*} + \mathbf{kb^*} + \mathbf{lc^*}) \qquad (3.12)$$

The direct lattice is the lattice of the crystal structure. A unit cell will normally contain an integer number of unique atoms, ions or molecules within its volume. One necessary task in four-circle diffractometry is to obtain the unit cell and orientation matrix of the single crystal under investigation. Although, as previously stated, this is not a prerequisite to data collection using an area detector system, it is strongly advised. ***Figure 3.7.1*** shows a 320° oscillation Polaroid photograph taking on the Rigaku AFC6S. Since this covers a large portion of reciprocal space, the reflections that are located from it are used to calculate the unit cell.

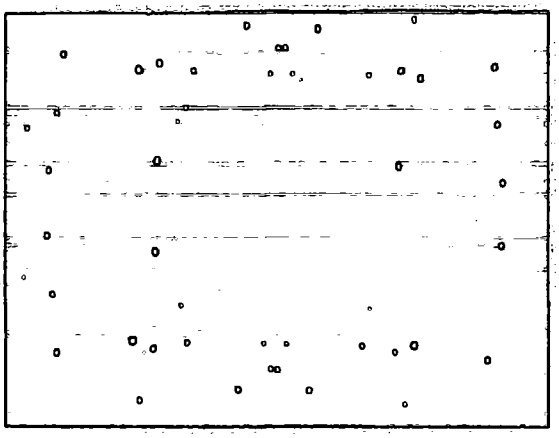

***Figure 3.7.1** – A 320° ϕ oscillation Polaroid photograph taking on the Rigaku AFC6S, used to index a crystal of $B_{12}H_{10}O_2$ at 150 K.*

There are two sets of axes important in diffractometry. Firstly, the crystal-fixed reciprocal axes a*, b* and c*. As mentioned before, the co-ordinates of this axial system are the Miller indices *hkl* and these are denoted by **h**. The second set of axes are orthogonal and fixed to the crystal mounting. The z axis is coincident with ϕ and x and y are defined arbitrarily to complete a right handed-set. This set is denoted as **x**. The relationship between the two sets of axes is given by:

$$\mathbf{x} = \mathbf{A}\mathbf{h} \tag{3.13}$$

The orientation matrix is **A**. Thus, once **A** is known, the correct diffractometer angle can be calculated for any reflection, *(h, k, l)*:

$$\mathbf{h} = \mathbf{A}^{-1}\mathbf{x} \tag{3.14}$$

The orientation matrix, **A**, is a 3 x 3 matrix and its components are the reciprocal cell axes along each of the three orthogonal axes.

$$\mathbf{A} = \begin{pmatrix} a_x^* & b_x^* & c_x^* \\ a_y^* & b_y^* & c_y^* \\ a_z^* & b_z^* & c_z^* \end{pmatrix} \tag{3.15}$$

The six cell parameters can be extracted from this. Obtaining an orientation matrix and unit cell means that a set unindexed reflections found in a search of reciprocal space are assigned *(h, k, l)* indices.

There are two methods for unit cell and orientation matrix determination. One operates in real space and the other in reciprocal space. Both methods aim to determine the simplest matrix and cell, which assign indices to all reflections. A search for reflections covering a subset of reciprocal space is carried out with the crystal mounted in a random orientation.

The reciprocal space method[21] operates on the principle that the observed vectors, **x**, must correspond to reciprocal lattice points. The vectors, $x_i \pm x_j$, are all added to the list of vectors from the initial search. From this new list, the three shortest non-coplanar vectors are selected as the reciprocal cell axes. The nine xyz coordinates are the nine elements of **A**. The indices of every reflection of the diffraction pattern can then be generated. These indices should be at least within 5% of integer values prior to unit cell refinement. If they are simple fractions (i.e. ½ or ¼) one or more cell axes may simply be too short. If there is no obvious means of obtaining integer values for all reflections, it is very probably that the crystal is twinned. The unit cell obtained from this procedure is primitive and may have to be transformed to the conventional cell that represents the metric symmetry of the lattice. The transformation may involve conversion to a centred lattice or a cell that represents a higher symmetry setting. The assignment of a unit cell usually involves the choice of the smallest possible unit cell with angles close to 90°, known as a Delauney reduction.

The real-space method[22,23] (also known as 'auto-indexing') is used to index reflections from the SMART diffractometer. There is also a useful alternative description.[24] This method involves the selection of three non-coplanar vectors and arbitrarily assigning them vectors 100, 010 and 001 to generate an orientation matrix. Although, this cell a′, b′, c′, is not correct it must be a subcell of the real lattice are also vectors in the lattice described by the subcell. This method generates real space vectors:

$$t = ua + vb + wc \qquad (3.16)$$

where u, v and w are all integer values. These vectors are found up to a maximum specified length. Each one is then tested to ascertain whether it is a real lattice vector, for which t.x must be an integer. The correct cell can then be chosen by hand or

automatically by the particular program, which tends to be reliable, if perhaps 'black-box', for a well-formed strongly diffracting crystal.

A development of this method, which is complementary to the use of area detectors, is the use of 'difference vectors' instead of the reciprocal lattice vectors, **x**. From a list of **x** vectors, all difference vectors, $x_i - x_j$, are generated. This is effective where many reflections have been collected, as is the case with area detectors, since some differences will result more than once. Such vectors are averaged, thus improving their accuracy. Like any other method, there are pitfalls associated with this. Firstly if only a small, or biased, subset has been measured, an incorrect cell may result. This can be caused by all reflections having an even *h*, *k* or *l* index or in the case where heavy atoms are in special positions as in the case of pseudosymmetric structures. This method frequently fails in the case where there are spurious reflections from a twinning component. This enhanced real space method is incorporated in the SMART software[22,23]. As default in the program the cell is automatically reduced by specifying a range that the unit cell angles must fall within. The 'Bravais' option is then used, if necessary, to transform to the lattice based on the metric symmetry. The real space indexing method is also employed by the Rigaku AFC6S software. The *Fddd* diffractometer now employs the Siemens $P2_1$ suite of programs for autoindexing only.

3.8 Data collection

This procedure has been outlined for all the instruments individually.

3.9 Data reduction

Relative structure factor amplitudes, which were corrected for polarization, Lorentz and absorption errors, were obtained from the raw intensities using the SAINT software[15] for SMART data, the TEXSAN suite for Rigaku AFC6S data[7] and DREAM for F*ddd* collected data.

$$I_H = k\, I_o\, LPTE\, |F_H|^2 \qquad (3.17)$$

where I_H is the integrated intensity, L is the Lorentz factor, P is the polarization factor, T is the transmission and E is the extinction coefficient.

Extinction can take one of two forms. Primary extinction refers to the decrease in diffracted intensity due to multiple reflections arising from individual blocks within the crystal. Secondary extinction takes account of the fact that lattice planes near the crystal surface will reflect a certain amount of primary beam. Thus, the centre of the crystal receives less intensity.

Crystallography involves measuring the diffracted intensities as they cross the Ewald sphere. Due to the nature of the methods used to record these intensities, nodes, they are not all in the diffracting position for the same amount of time. This is the Lorentz factor and in its simplest form, it is:

$$L = (\sin 2\theta)^{-1} \tag{3.18}$$

The polarization factor corrects for the polarization of the beam by the crystal monochromator. This factor is equal to

$$P = \tfrac{1}{2}(1+\cos^2 2\theta) \tag{3.19}$$

The other corrections that can be applied at the data reduction stage are absorption corrections, which have been described in section 3.4, and scaling of subsets of data from more than one crystal.

3.10 Structure solution and refinement

Following data reduction and the correction of the structure factor amplitudes for geometrical factors, a set of relative structure factor amplitudes are obtained. As can be seen from equation 3.2 and 3.3, the structure factors are used to calculate the electron density distribution within the unit cell, via a Fourier transform. Because the measured intensity is related to the square of the structure factor, the phases can not be measured directly. There are two methods to overcome the 'phase problem' in chemical crystallography and the method of structure solution employed is largely dependent on

the molecule under investigation. The option to perform either of these structure solutions is contained within the program, SHELXS-86.[25]

3.10.1 Space group assignment

Following data reduction, the intensity relationships of reflections are examined in order to determine the actual symmetry of the crystal. Here, one of the 230 space groups is assigned whose symmetry elements describe the three-dimensional arrangement of independent atoms within the crystal. Firstly, it is necessary to examine for general systematic absences in all the data, which indicate lattice centring (i.e. the presence of an extra lattice point in the centre of a face or the cell). The possible lattice types are P, C (alternatively A or B), F, I, or R. The diffraction symmetry is then grouped by the corresponding crystal system, i.e. triclinic, monoclinic, orthorhombic, tetragonal, trigonal, hexagonal and cubic. It can be useful to bear in mind the external crystal morphology here if a crystal with natural faces was used, e.g. the characteristic 'coffin' shape of crystals with tetragonal symmetry. The assignment of a space group involves the search for special systematic absences in lines or planes of data. These absences indicate translational symmetry elements, i.e. screw axes and glide planes. If these translational symmetry elements are not found the corresponding point group symmetry elements are assigned, i.e. rotation and/or inversion axes. The presence or absence of inversion centres can be more difficult to recognise. This indicates a centrosymmetric space group. Other factors such as physical properties and type of molecule are a useful indication. Crystals with a large secondary harmonic generation (SHG) output crystallise in noncentrosymmetric space groups and biological molecules crystallise in chiral space groups only. The presence of an inversion centre is often most clearly indicated by statistics. This test involves converting the intensity data (F_{hkl}) to normalised structure factors (E_{hkl}). This is calculated from $E^2(hkl) = F^2(hkl)/\langle F^2 \rangle$. The mean value of $E^2(hkl)$ should be 1 for all ranges of $\sin\theta$. In practice, the values for centric and acentric crystal structures vary significantly. This test is based on the fact that where an inversion centre is present, the relationship between atoms in pairs gives

rise to more strong and weak intensities than the comparatively featureless diffraction pattern for noncentrosymmetric structures. The $|E^2-1|$ values are diagnostic, tending to 0.74 for noncentrosymmetric structures and 0.97 for centrosymmetric structures. Whilst this test is a useful indicator, it is important to bear in mind that the values can vary significantly from the expected ones, especially if heavy atoms are present.

It is important that the correct space group selection is made prior to the attempted structure solution, as this dictates the relationship between the atoms in the unit cell. An incorrect choice will lead to the wrong calculation of the interatomic vectors in Patterson methods and direct methods, which relies on the atomic distribution being correct, is very unlikely to be successful. If the space group choice proves difficult, it is often useful to try to solve the structure in a lower symmetry setting and examine the relationship between molecules at a later stage.

3.10.2 Patterson methods

Although direct methods are the means used most often in chemical crystallography for structure solution nowadays, Patterson methods[26] work especially well in the case of mononuclear organometallic complexes where the relative molecular weights of the constituent atoms are disparate. One of the original structures to be solved by this method was nickel sulfate heptahydrate,[27] and for a detailed account of the development of this method in the solution of heavy atom derivatives of cholesterol and penicillan.[28] Here the phase problem is simply ignored by using the square of the structure factor amplitudes. This is a Fourier summation over all data, which gives the vector density at any point in Patterson space, u, v, w. The height, P_{uvw}, of the peak is proportional to the product of the atomic numbers of atoms. From the Patterson synthesis, the heavy atom position is obtained. Since its electron density represents a large proportion of the independent structure, the structure factor phases obtained will be largely correct.

$$P_{uvw} = \frac{1}{V}\sum_{hkl}(F_{hkl})^2 \exp[-2\pi i(hu + kv + lw)] \qquad (3.20)$$

where V is the volume of the unit cell ($Å^3$), F_{hkl} is the structure factor amplitude and $i = \sqrt{-1}$. The Patterson vector map has a peak for every pair of atoms in the unit cell or in other words, n^2 peaks for n atoms. This results in the largest peak being on the origin, which serves to scale the map, since each peak is related to its inversion equivalent through the origin. All Patterson maps are thus centrosymmetric. The height of the remainder of the atoms is proportional to the product of the atomic numbers of the atoms giving rise to them. The list of Patterson vectors are also useful to identify the point group symmetry elements present, and to verify the space group assignment since all screw axes and glide planes reduce to rotation axes and mirror planes respectively. The other main application of Pattersons is in 'Patterson search' methods where a fragment or an arrangement of atoms with a well known geometry is known to be part of the molecule. Here a rotation and translation search is performed for this fragment.

3.10.3 Direct methods

Direct Methods[29,30,31,32] is used to solve structures of small organic molecules and macromolecules. It is a statistical method relying on the fact that the amplitudes of the structure factors contain information on their phases, which are determined *directly* from the measured X-ray intensities.[33] Fortunately, the amplitude and phase of a structure factor are related quantities. If the phases are known, the magnitudes can be calculated and *vice versa*. There are several features of the electron density, which can be expressed as constraints on the function ρ_{xyz}. These constraints are all included in the previously mentioned SHELXS-86[25] package. Some of the constraints rely on the structure being chemically sensible i.e. all atoms are treated as discrete using normalised structure factors and the electron density must be positive or zero everywhere, and $\int\rho^3(x)dV$ must equal a maximum which leads to the tangent formula that has formed the basis of direct methods to the present day. Closely related to the tangent formula is Sayre's equation. This applies the constraint of all atoms being equal. After the constraints have been applied, the next stages of structure determination are as follows: the phase relationship is set up – proper assignment of space group symmetry to phase

relationships leads to more accurate phases. Reflections are then selected for phase determination by eliminating some reflections whose phases have been poorly determined. The phases that are assigned are random values. These are unlikely to be correct or in any way representative of their true values obtained after phase refinement. The procedure of assigning phases is carried out normally between 60 and 200 times. As this proceeds there are some figures of merit that are used to identify the best solution. The combined figure of merit (CFOM) should be close to zero but in practice values < 0.2 often mean that the correct phases have been calculated. The are two extra quick tests on the quality of the phases: Rα is based on the agreement between triplets and takes strong reflections only into account should ideally be small. NQUAL is based on negative quartets are should be –1 in ideal cases. All reflections into account here and if the data are weak, this term becomes less reliable.

If direct methods does not yield a solution in a centrosymmetric space group, it is often useful to lower the symmetry to a non-centrosymmetric space group because the phases in the former are constrained to be 0 or 180 whereas they can takes any value in between in the non-centrosymmetric case. It is more important to use the correct molecular formula in direct methods since normalised structure factors are used as opposed to the square of the structure factor as in Patterson methods. Direct methods normally yield the positions for the majority of the non-hydrogen atoms in a small molecule structure. The remainder is located by a series of Fourier syntheses are least squares refinements performed simultaneously.

In the case of isomorphous structures, it is possible to use the calculated phases from a previously solved structure and the measured structure factor amplitudes for the system under investigation. Following a series of least squares refinements, where the data are first scaled, the electron density is obtained. This method of 'molecular replacement' arises in the case of 'isomorphous' macromolecules where most of the structure is chemically and conformationally identical, variable temperature studies and in the case of ligands derivatised from different metals.

3.10.4 Refinement of the trial structure

The trial solution obtained is next refined, to determine the complete structure of the molecule. This is done by Fourier, least squares or conjugate gradients methods and all of these options are incorporated within the SHELXL-93[34] program. The refinement of small molecule crystal structures is accomplished, in the most part, by the method of full-matrix least-squares.[35,36] For the majority of structures, this is a relatively straightforward iterative process that involves the location of all the atoms in the initial stages by calculated a series of difference Fourier syntheses. The practice of structure refinement against F^2 is now widely used.

The minimisation function in least-square refinement is $\sum w(Yo-Yc)^2$ where Y = |F| or F^2. The correct weighting of reflections is important in a successful refinement. The weighting should be $w=\frac{1}{\sigma^2}(Fo^2)$ where the variance on F^2 is derived from counting statistics. However, the variance changes with resolution and it is standard practise for X-ray data to discard unit weights in favour of a weighting scheme that does not treat all reflections equally once all of the atoms have been located. The *R*-indices are monitored throughout the refinement to indicate that the structure is progressing toward convergence. The conventional free *R* index is calculated from

$$R=\frac{\sum||Fo|-k|Fc||}{\sum|Fo|} \tag{3.21}$$

However, the more significant index is *wR* or *wR2,* depending on whether the refinement is based on F or F^2.

$$wR2=\left[\frac{\sum w(Fo^2-Fc^2)^2}{\sum w(Fo^2)^2}\right]^{\frac{1}{2}} \tag{3.22}$$

The goodness-of-fit (S) value is defined as

$$S=\left[\frac{\sum w\left(Fo^2-Fc^2\right)^2}{(N-P)}\right]^{\frac{1}{2}} \tag{3.23}$$

This is correlated with the weighting scheme and its value is one when the correct weights are used. These figures of merit give an indication of the validity of the refinement, but it is important to check for likely sources of error. The anisotropic displacement parameters are a sensitive means of checking for the correctness of structures. Lists of 'bad' reflections should be checked if the space group assignment is in doubt. It is also important not to over-parameterise the model where there is not sufficient data to justify this.

3.11 Low temperature attachments

The benefits of collecting data at low temperatures are manifold. There is a reduction in dynamic disorder. It is possible to acquire higher angle data. Low angle scattering is predominantly derived from the valence electron density whereas the higher order reflections, in general above 1.5 Å, are due to the core electrons. The structure factor equation (3.4), is expanded to incorporate the Debye-Waller factor, T_n, which takes thermal smearing into account.

$$F_{hkl} = \sum_{n=1}^{n=N}\sum_{n=1}^{n=N} f_n T_n \exp[2\pi i(hx_n + ky_n + lz_n)] \qquad (3.22)$$

$$\text{where} \quad T_n = \exp(-8\pi^2 < u_{T,j}^2 > \sin^2\theta/\lambda^2) \qquad (3.23)$$

Thus, lowering the temperature reduces the effect of the Debye-Waller factor on a structure factor and makes it possible to distinguish between core and valence electrons. It has also been shown that there is a reduction in X-ray radiation damage at low temperatures.[37,38,39] In no area has this been more beneficial than in macromolecular crystallography. The advent of low temperature devices means that it is now possible to measure entire data sets from viruses or proteins with a very high (i.e. > 70%) water content whereas without this facility it would not be feasible. Three cryostats have been employed for sample cooling in the course of this work and the principles of their operation and their advantages are now outlined briefly.

3.11.1 The N_2 open flow cryostat

As mentioned previously, the Oxford Cryosystems Cryostream[6] is a liquid nitrogen open flow cryostat and is fitted to both the Rigaku and SMART diffractometers. The principle of the cryostream operation is as follows. Unpressurised liquid nitrogen (LN_2) is pumped from the metal liquid Dewar (V) through a vacuum-insulated supply line (L). The liquid flows past the evaporator coil (E), which converts most of the liquid into a vapour. The vapour flows along one path of the heat exchanger (HX) to the diaphragm pump (P) at 10 K below room temperature and back to the heat exchanger to be re-cooled. The flow rate is pre-set by a needle valve (NV). The gas passes through a heating coil (H) and a thermosensor (T) and emerges from the delivery nozzle to cool the sample. The heater regulates the temperature of the emerging gas. The cryostream can reliably maintain temperatures from 90 to 373 K within a margin of error of ± 0.2 K. The crystal should typically be less than 10 mm from the nozzle. The flow rate has been designed to produce a laminar flow for a few millimetres from the nozzle tip. Beyond this, there will be turbulence in the stream, causing icing on the crystal. To overcome this there is a laminar flow of dry air around the nitrogen stream to the crystal. One of the advantages of this method of cooling is that the Dewar can be refilled with liquid nitrogen without any interruption to the experiment. To operate at more reduced temperatures ($T < 90$ K) the amount of heating from the evaporator can be reduced manually. This should only be carried out when the cryostream has been in operation for a few hours at a temperature of less that 100 K. ***Figure 3.11.1*** is a schematic representation of the flow scheme in this apparatus.

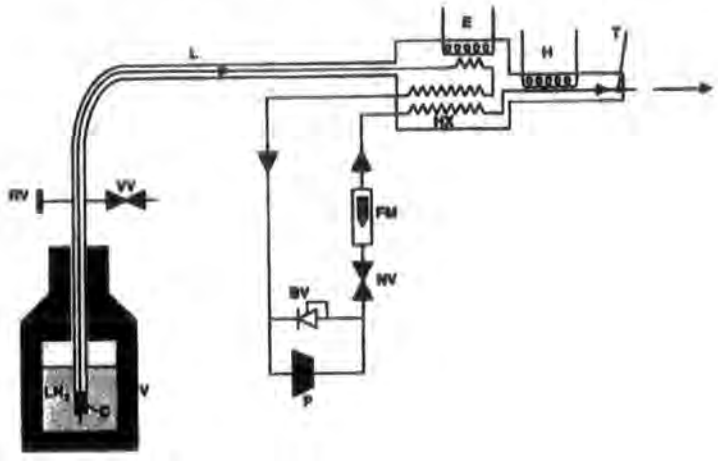

***Figure 3.11.1** – A diagram of the Oxford Cryosystems Cryostream flow scheme (reprinted from the operating manual for the cryostream cooler, October 1992, Version 3.1).*

3.11.2 The closed cycle refrigerator

The limitation of an open flow N_2 cryostat is that the base temperature is above the liquefaction temperature of N_2 (77 K at atmospheric pressure). One means of overcoming this limitation and attaining ultra low temperatures and is to use helium as the cryogen. One of the most stable cryostats is one that utilises helium, as the cryogen is the closed cycle refrigerator. This means of cooling is performed by means of thermal conductivity through the goniometer head to the crystal. This is accomplished by means of an 'Air Products and Chemicals' (APD) '202' two-stage closed cycle Displex cryogenic refrigerator. As the name suggests, the system is completely shielded from the outer atmosphere. One of the advantages of this design condition is the absence of any icing on the crystal or mount surface. The helium is constantly recycled during operation. These cryostats are not very widely used being more technically complex than cryostreams. Single stage CCRs have been used on neutron diffractometers[40]. However, the *Fddd* is equipped with a two-stage system, which is coupled to the χ circle.[9] The refrigerator is comprised of two basic modules, which are connected by nylon coils.

The compressor module supplies refrigerant (He_g) to the expander. It is comprised of a surge bottle, compressor, oil separator and adsorber components. The reservoir of helium gas enters the system as can be seen from ***Figure 3.11.2.1***. The

surge bottle dampens gas pulses prior to entering the compressor where it is injected with oil, cleaned and compressed. The compressor is surrounded by heat exchanger coils that cool the helium, compressor and oil.

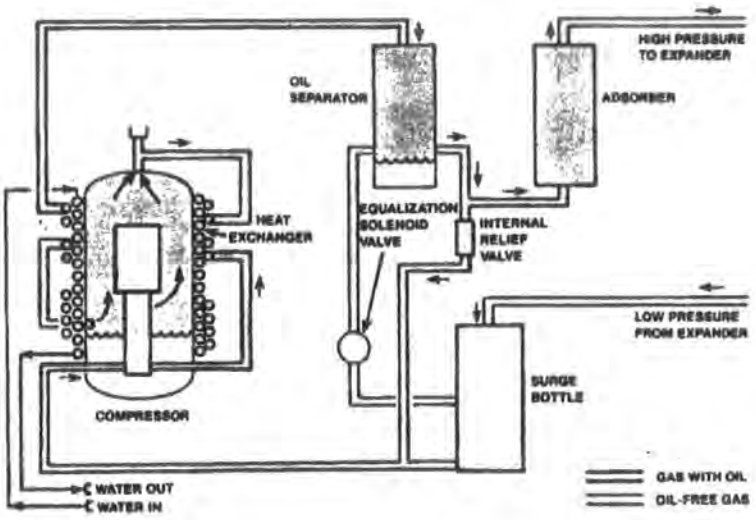

Figure 3.11.2.1 *– Schematic representation of the set-up of the compressor module of a close cycle refrigerator (reprinted from the APD Compressor Module Manual, 1986).*

The expander module or Displex is the refrigerator and consists of two stages. The first stage, the warmer of the two stages, operates in the 50-75 K range and in the cryostat and is used to cool the outer cryopanel onto which water vapour will freeze out. The vapour pressures of neon, hydrogen and helium are too high at temperatures greater than 20 K to be condensed onto a bare surface. For this reason, activated charcoal is used to adsorb these gases due to its large surface to volume ratio. The second stage reaches 10-20 K. This is used to cool the inner cryopanels. Any gases not yet frozen onto a panel lastly will be adsorbed, in a process known as cryosorption. The temperature at the crystal is controlled by a heater, which counteracts the cooling from the second stage of the Displex. This always reaches 10 K. The Displex works on the principle of Joule-Thomson expansion cooling. The compressed gas is cooled as it enters the Displex since if a gas expands on passing through a throttle without doing any work on its surroundings it generally exhibits a lowering of its temperature. The cooling is attributed to overcoming the intermolecular attractions. Thus by using a standard rotary pump and attaining a reasonable vacuum of the order of 10^{-2} Pa cooling occurs. An enhanced vacuum in the Displex is additionally maintained at $3x10^{-5}$ Pa by the

turbomolecular pump. The work done by one mole of gas after expansion is $\Delta P.\Delta V$. Since this is an adiabatic system:

$$-\Delta E = \Delta P.\Delta V \text{ and } \Delta H = E_1+w_1 = E_2+w_2. \qquad (3.24)$$

The Joule-Thomson coefficient $(\delta T/\delta p)_H$ is the quantity observed[41]. This is zero for an ideal gases and non-zero for a real gas resulting in a reduction in temperature. The decrease in temperature in an adiabatic expansion is greater the larger the difference between the initial and final pressures. Two concentric beryllium shrouds are used for thermal insulation, which are effectively X-ray-transparent.

Efficient cooling relies on good conductivity. A copper goniometer head is used, which is thermally coupled to the 2nd stage of the Displex, and the crystal mounted in low temperature glue which remains thermally conducting at temperatures down to 4 K. This is illustrated in ***Figure 3.11.2.2***, which has been reproduced from (8).

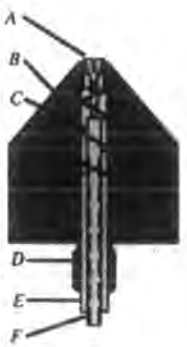

Figure 3.11.2.2 *– A schematic diagram of the goniometer head construction. The key is: A: collet B: copper body C: spring D: ¼ in UNF E: spring tension adjust F: release button. The figure has been reprinted from reference 8.*

3.11.3 The open flow helium cryostat (Helix)

The Oxford Helix, produced by Oxford Cryosystems, is an open flow helium gas cooler. It is supplied with bottled helium gas, which last for durations of 15 hours and are periodically replaced as the experiment progresses. It consists of a compressor and cold-head containing a Displex. The compressor delivers helium gas to the Displex, which reaches a temperature of 10 K. A turbomolecular vacuum pump evacuates the Displex and thus the helium gas passing through the cryostat is cooled and this gas stream cools the crystal. A heater heats the gas stream to the required temperature. A thermocouple close to the nozzle measures the temperature at the crystal. The device has a base temperature in the 28-33 K range and above this has a temperature stability of ±0.3 K. This cryostat has been used in this thesis to follow phase transitions that occur below the temperature of boiling nitrogen. The main advantage apart from the availability of these reduced temperatures is the opportunity to 'flash-cool' the crystal.

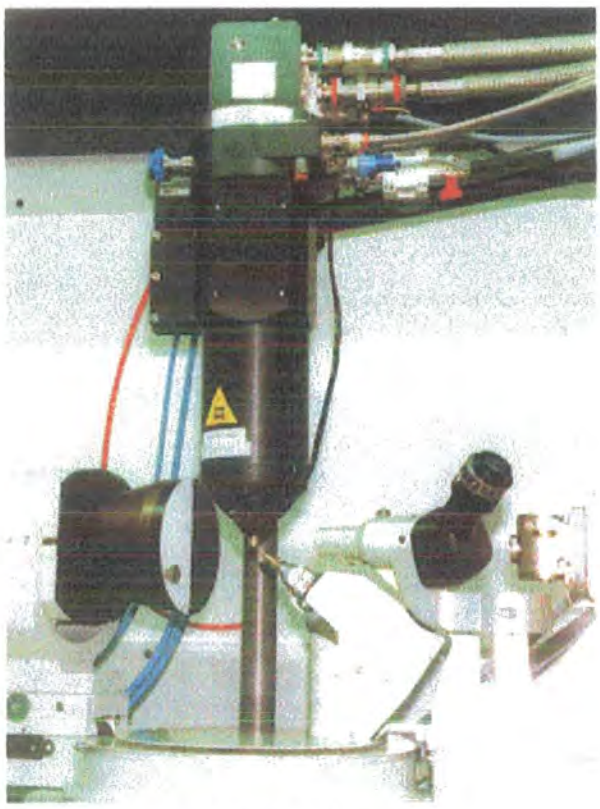

***Figure 3.11.3** – The open flow helium gas cooler (Helix).*

3.12 Synchrotron radiation at the Daresbury SRS

3.12.1 Background to SR crystallography

The past twenty years has seen the scope of X-ray crystallography transformed by the coming online of intense tuneable and collimated X-ray beams to allow rapid structure determinations as well as the acquisition of higher resolution data. This has also allowed the determination of the structure of viruses containing up to a million atoms.

The advantages of synchrotron radiation are:

- The X-rays are more intense.
- There is enhanced flux, brightness and brilliance in comparison to a laboratory source.
- It is much more collimated, resulting in improved sharpness of the reflections.
- It offers a choice from a continuum of wavelengths. The experimental technique that has benefited most from this opportunity is Multiwavelength Anomalous Dispersion (MAD). This is a method of phasing reliant on making a series of measurements close to the absorption edge of a designated atomic type in the structure. The useful wavelength range for experiments of this kind can be considered to be in the window from ~0.3 to ~3.0 Å.[42]
- It is the ideal means of collecting data from crystals containing a small number of unit cells. Protein crystals as small as 20 μm^3 have been measured and successful structure determinations performed on small molecular crystals whose dimensions do not exceed 10 μm^3. The average intensity is estimated from $\langle F_{hkl} \rangle^2 . \frac{Vsample}{Vcell^2}$ (where $\langle F_{hkl} \rangle^2 = \sum f^2$ ignoring the effect of atomic displacement), which demonstrates the effect of unit cell volume.[43]

- There is reduced radiation damage. This is particularly relevant to the time dependent component of the radiation damage effect. This is the process whereby incident photons cause radiolysis of water molecules of crystallisation. Gradually, the radicals diffuse through the crystal causing it to shatter. Since data collection times are reduced, this effect is minimised.
- Absorption errors can be reduced.
- There is no α_1/α_2 splitting which is present in radiation from a sealed tube.

Synchrotron radiation is a completely different means of producing X-radiation. Here electrons or positrons are accelerated in discrete bunches in a closed orbit. In the more common case where electrons are used, a linear accelerator injects an electron beam into the storage ring at precise time intervals so that discrete bunches are circulated. An extremely high vacuum is required to prevent the particles being lost through collisions with atoms in the ring. They are 'steered' in a closed trajectory by a set of magnetic fields perpendicular to the plane of the orbit called a 'lattice' and are accelerated to near the speed of light by a radio frequency electric field. As the electrons or positrons are experiencing centripetal acceleration, (i.e. towards the centre of the orbit) they radiate light. As they approach the speed of light, the emission of this light becomes highly compressed in the forward direction. The radiation produced varies from infrared to the hard X-ray region of the EM spectrum. The highly collimated beam is emitted tangential to the orbit. ***Figure 3.12.1.1*** gives a schematic representation of the construction of an electron storage ring.

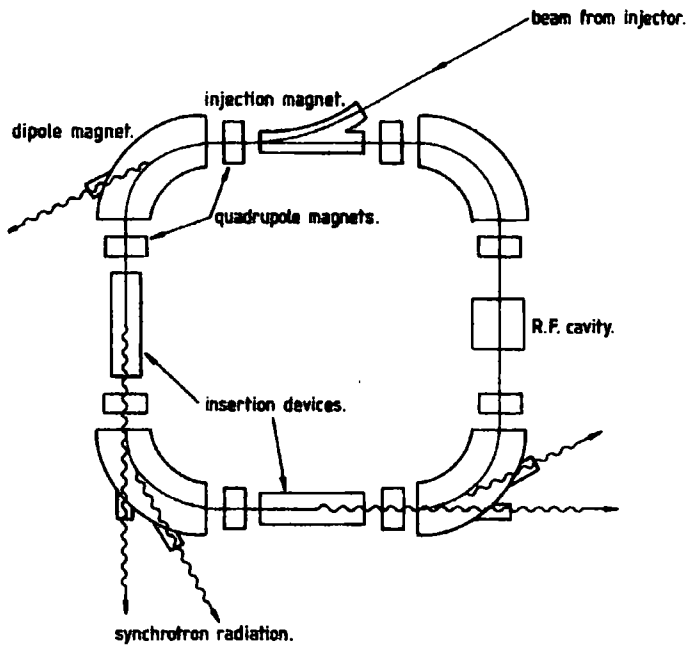

***Figure 3.12.1.1** – Schematic representation of the construction of an electron storage ring [from J.R. Helliwell[44]].*

The power emitted by a charged particle per unit time following a circular orbit is given by:

$$P = \frac{2e^2cE^4}{3R^2(m_0c^2)^4} = \frac{2e^2c\gamma^4}{3R^2} \qquad (3.25)$$

where P = energy emitted per unit time; c = speed of light; m_0= mass at rest; R = bending radius of the orbit; γ = ratio of total energy to rest energy and is inversely proportional to the angular deflection, δ. It is worth explaining the terminology that apply to all X-ray sources, but particularly define the unique characteristics of synchrotron radiation:

The spectral flux, N, is the number of photons emitted per unit time interval into a relative bandwidth $\Delta\lambda / \lambda$ into an angle element $d\theta$ in the plane of the electron orbit and integrated in the vertical plane. It can be shown that the flux of the radiation normalised to the ring current generated by the bending magnets.

$$N(h\upsilon) = 1.256 \times 10^7 \gamma G_1(y) \text{ photons } s^{-1}(0.1\% \delta\lambda/\lambda)^{-1} \qquad (3.26)$$

where the factor $G_1(y)$ is a energy dependent function

$$y = h\upsilon/E_c \qquad (3.27)$$

The critical energy, E_c, is associated with the magnetic field, and this, together with its related function λ_c are parameters that define characteristics of synchrotron sources.

The intensity defines the flux per unit area of the wave front some distance from the source. If there is a high flux spread over a large area of the beam incident on the crystal the sample will only intercept a small portion of the crystal.

The brightness is the number of photons per second per $mrad^2$ per 0.1% of the relative bandwidth ($\Delta\lambda / \lambda$).

The brilliance is the number of photons per second per $mrad^2$ per mm^2 per 0.1% of the relative bandwidth ($\Delta\lambda / \lambda$), that is, the brightness per unit area. Where a high flux brought to a small focus is required, a beam with a small divergence angle and a small source size is used to ensure a large brilliance. The advance in the available brilliance in sources worldwide is best emphasised by example: In the 1960', the most brilliant sources were rotating anode generators, which gave an output of 10^7 photons s^{-1} (0.1% $\delta\lambda/\lambda$) (mm mrad)$^{-2}$. By 1975 the Stanford SRL was online delivering 10^{12} photons s^{-1} (0.1% $\delta\lambda/\lambda$) (mm mrad)$^{-2}$. In 1985, 6 GeV sources with undulator being developed which produced beams with a brilliance of 10^{19} photons s^{-1} (0.1% $\delta\lambda/\lambda$) (mm mrad)$^{-2}$.

'Third-generation' insertion devices have revolutionised SR crystallography. These are found on the straight section of the storage ring; and are magnetic structures, which enhance certain characteristics of the SR. Their capabilities are to:

- Extend the spectral range to a shorter λ.
- Increase the available intensity.
- Provide an intense quasi-monochromatic beam.
- Provide a different polarisation.

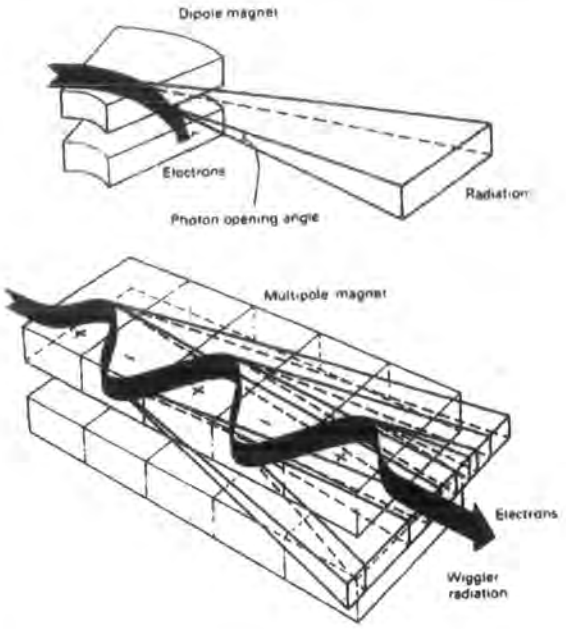

***Figure 3.12.1.2** – A schematic representation of the path an electron beam and radiation emitted from a dipole magnet and passing through a wiggler [from Catlow and Greaves[45]].*

Figure 3.12.1.2 shows the effect an insertion device has on an electron beam. The simplest insertion device is a 3-pole wiggler, which acts as a wavelength shifter. A multipole wiggler or an undulator (***Figure 3.12.1.3***) will increase the light magnification. As the beam changes direction or accelerates, this is accompanied by a change in energy and thus wavelength.

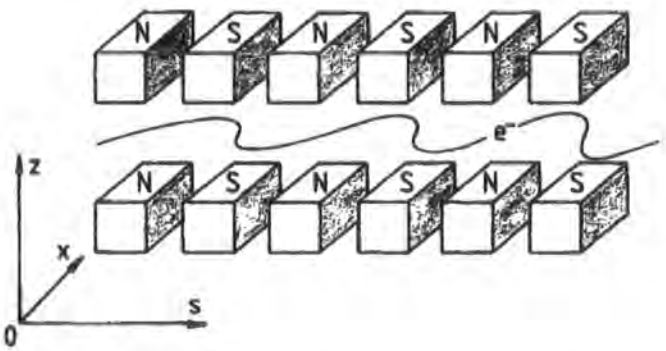

***Figure 3.12.1.3** – Schematic representation of the layout of a generic insertion device [from J.R. Helliwell[46]].*

The classification of an insertion device as a wiggler or undulator depends on the interference effects. The interference effects for a wiggler are smoothed out. An undulator has large interference effects

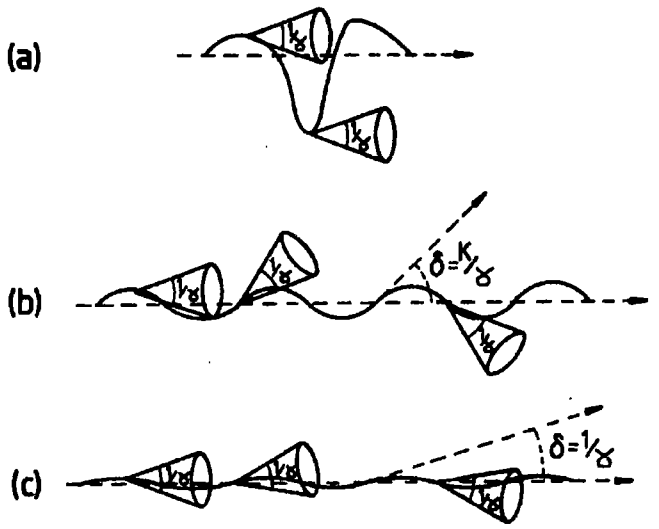

Figure 3.12.1.4 *– Operation of three types of insertion device: (a) wavelength shifter, (b) multipole wiggler, (c) undulator [from J.R. Helliwell[47]].*

3.12.2 The Daresbury SRS

In the 1970's, SR became popular as a means of determining protein structure. The SRS at Daresbury, opened in the 1960's, was the first purpose built storage ring in the world. The advent of third generation insertion devices revolutionised the experimental capabilities of the facility. The beam is steered by 16 dipole magnets, which constrain it to a roughly circular path of 96 m. Two superconducting wiggler magnets produce a more intense output of 2 GeV and critical energy 13.3 keV. The energy of the storage ring is approximately 598 MeV and with a current setting of 200 mA, this results in a beam lifetime of 25 hours. The beam is 'refilled' daily.

3.12.3 Station 9.8

The gap left in the area of chemistry and materials science was addressed by the construction of a dedicated chemical crystallography facility, station 9.8. The applications and opportunities of this instrument are obvious and vast. Minerals and zeolites often form extremely small yet single crystals. The improvement in the measured intensity is also evident in the case of weak scatterers. The highly collimated and tuneable X-ray wavelength means that electron density studies are not only feasible

but in theory preferential using data acquired on a SR source. The station construction is illustrated in ***Figure 3.12.3.1.***

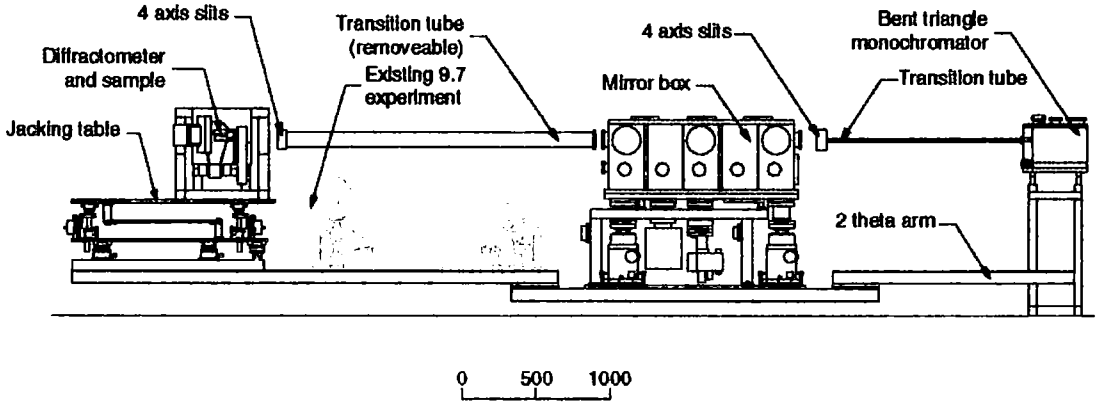

Figure 3.12.3.1 *– A schematic representation of the layout of Station 9.8, Daresbury (reprinted from Station 9.8 World Wide Web homepage[46]).*

The beam on this line is provided by a 5 Tesla superconducting wiggler magnet. The station is, in fact, comprised of two facilities: 9.7 is a multiwavelength station and used for Laue or energy-dispersive work[47] and heavy-atom containing clusters have been solved using the Laue method since the early 1990's.[48] It operates while in multibunch mode. Single-crystal measurements are performed on station 9.8 when the storage ring produces SR in single bunch mode. Two available diffractometers may be coupled to the beam line. The Enraf-Nonius CAD-4 is a four-circle diffractometer with a point detector. It has been adopted for high pressure measurements entailing the use of a diamond anvil cell since the intense diamond reflections would damage severely the SMART-CCD. It is also used to monitor phase transitions whereby individual reflections may be followed[49,50] and high temperature measurements up to 1000 K. The SMART diffractometer is the more widely used instrument due its wide ranging advantages, predominantly the improved speed of data collection. The arrangement of this diffractometer on the station is depicted in ***Figure 3.12.3.2.***

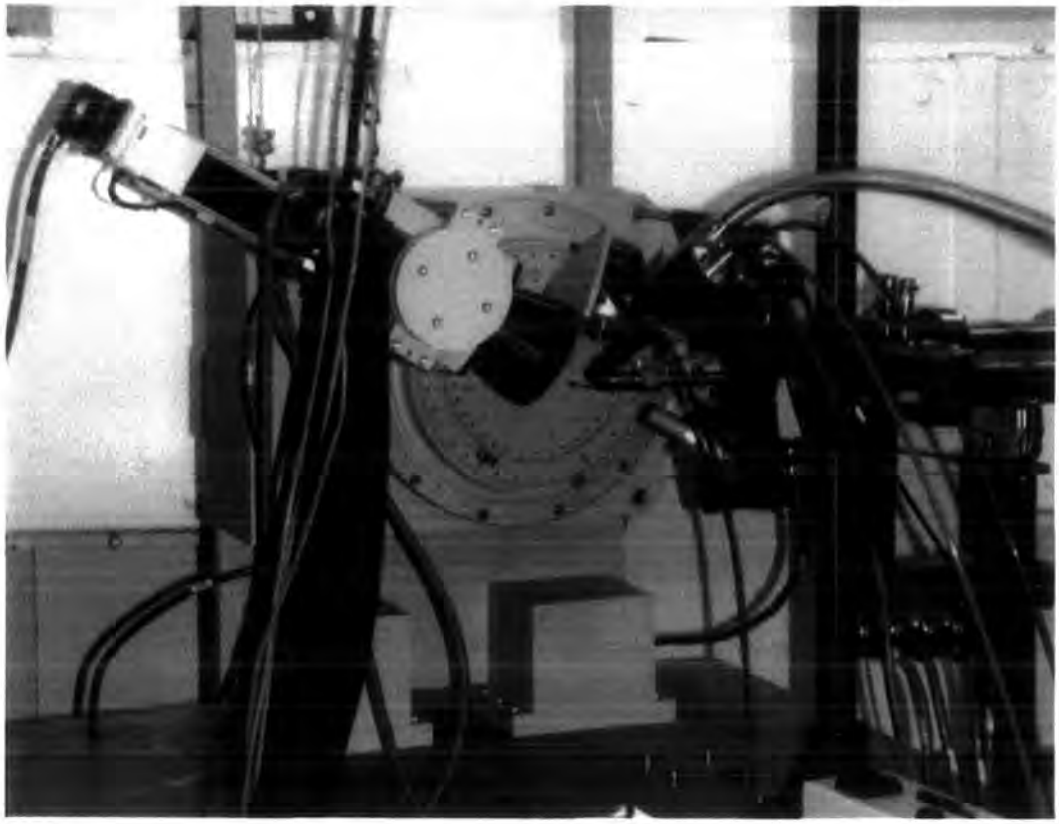

***Figure 3.12.3.2** – The SMART diffractometer in place on its side at Station 9.8, Daresbury.*

The incident beam can be attenuated either by a set of source slits 5.2 m from the tangent point or by a set of pre-monochromatic slits at 10.3 m. The first optical device is the monochromator crystal which provides focus in the vertical plane or brings the divergent beam to a line focus. There is a choice of two available monochromators, which provides wavelengths in the 0.3-1.5 Å range. The {111} surface of a triangular bent silicon crystal is used to provide in the upper wavelength range up to 1.5 Å. The asymmetric cut in the crystal of 1° allows compression of the beam. Higher energies are delivered by the {220} surface of the second monochromator. These are both cooled using a Ga/In/Sn coolant. Just over 50% of the crystal is in contact with the coolant and the heat extracted by the eutectic mixture is dissipated in the water-cooled copper block. A turbomolecular pump vacuum of 10^{-7} torr is maintained in the vessel. The full experimental assembly swings out to scan the wavelength range, referred to as 2θ arm rotation. The well known unit cell dimensions of a ruby crystal is used as a standard to obtain a wavelength calibration. Beam realignment is necessary after this procedure.

Focusing in the vertical plane is provided by a cylindrically bent zerodur mirror with a 300 μm thick palladium coating. This focuses the beam and removes harmonics. A possibly strong λ/3 contamination is removed by the correct positioning of this mirror.

There are two motors on the SMART, which allow movement in the vertical and lateral directions for beam alignment. The crystal to detector distance is also easily adjustable due to the attachment of a motor on the detector shaft. The radiation emitted by an individual electron is 100% polarised in the plane of the electron orbit. The total polarisation for the full beam is reduced by the beam size and its oscillations. Since radiation is horizontally polarised a vertical plane of diffraction is desirable and so for a conventional serial diffractometer, the 2θ and ω axes are oriented horizontally rather than vertically as in the usual arrangement. This arrangement is also used for the SMART. Counter weights attached to the 2θ axis are used to balance the weight of the detector.

3.13 Bibliography

1. C. Giacovazzo, H.L. Monaco, D. Viterbo, F. Scordari, G. Gilli, G. Zanotti, and M. Catti (1992). *Fundamentals of Crystallography*, edited by C. Giacovazzo. IUCr Texts on Crystallography, OUP.
2. G.H. Stout and L.H. Jensen (1968). *X-ray Structure Determination – A Practical Guide*, The Macmillan Company.
3. U.W. Arndt and B.T.M. Willis (1966). *Single Crystal Diffractometry*. Cambridge University Press.
4. M.M. Woolfson (1997). *An Introduction to X-ray Crystallography*, 2nd edition. Cambridge University Press.
5. C.W. Bunn (1961). *Chemical Crystallography – An Introduction to Optical and X-ray Methods*, Oxford University Press.
6. *International Tables for X-ray Crystallography, Vol. III Physical and Chemical Tables*, edited by Kathleen Lonsdale, 2nd edition reprinted (1985). Kluwer Academic Publishers Group.
7. J.P. Glusker and K.N. Trueblood (1985). *Crystal Structure Analysis – A Primer*, 2nd edition. Oxford University Press.

3.14 References

[1] A.C.T. North, D.C. Phillips and F.S. Matthews (1968). *Acta Crystallogr.*, **A24**, 351 – 359.

[2] G.M. Sheldrick (1985). XPREP – Data preparation and reciprocal space exploration, Version 5.04/VMS, Siemens Analytical X-ray Instruments Inc., Madison, Wisconsin, U.S.A.

[3] G.M. Sheldrick (1996). Sadabs – Program for the refinement of area detector data. University of Göttingen, Germany. To be published.

[4] R.H. Blessing (1995). *Acta. Crystallogr.*, **A51**, 33 – 38.

[5] Molecular Structure Corporation (1991). *MSC/AFC Diffractometer Control* Software. MSC. 3200 Research Forest Drive, The Woodlands, TX77381, U.S.A.

[6] J. Cosier and A. M. Glazer (1986). *J. Appl. Cryst.*, **19**, 105 – 107.

[7] Molecular Structure Corporation (1989). TEXSAN. Version 5.0, TEXRAY Structure Analysis Package. MSC, 3200 Research Drive, The Woodlands, TX77381, U.S.A.

[8] R.C.B. Copley, A.E. Goeta, C.W. Lehmann, J.C. Cole, D.S. Yufit, J.A.K. Howard, and J.M. Archer (1997). *J. Appl. Cryst.*, **30**, 413 – 417.

[9] J.M. Archer and M.S. Lehmann (1986). *J. Appl. Cryst.*, **19**, 456 – 458.

[10] J.R. Allibon (1996). *MAD Diffractometer Control Software – AlphaVMS Version.* Institut Laue-Langevin (DPT/SCI), Grenoble, France.

[11] Siemens Analytical X-ray Instruments (1995). SMART. Version 4.050. Siemens Analytical X-ray Instruments Inc., Madison, Wisconsin, U.S.A.

[12] M. Webster (1998). *J. Appl. Cryst.*, **31**, 510 – 514.

[13] Siemens Analytical X-ray Instruments (1995). ASTRO. Version 4.050. Siemens Analytical X-ray Instruments Inc., Madison, Wisconsin, U.S.A.

[14] K. Kirschbaum, A. Martin and A.A. Pinkerton (1997). *J. Appl. Cryst.*, **30**, 514 – 516.

[15] Siemens Analytical X-ray Instruments (1995). SAINT. Version 4.050. Siemens Analytical X-ray Instruments Inc., Madison, Wisconsin, U.S.A.

[16] W. Kabsch (1988). *J. Appl. Cryst.*, **21**, 916 – 924.

[17] E.M. Westbrook and I. Naday (1997). *Charge-coupled device-based area detectors* in *Methods in Enzymology*, Volume 276, Part 2.

[18] Siemens SMART Software References Manual (1994). Siemens Industrial Business Unit, Madison, Wisconsin, U.S.A.

[19] H. Hope (1988). *Acta Cryst.* **B44**, 22 – 26.

[20] T. Kottke and D. S. Stalke (1993). *J. Appl. Cryst.*, **26**, 615 – 619.

[21] J. Hornstra and H. Vossers (1974). *Philips Tech. Rundschau*, **33**, 65 – 78.

[22] R.A. Sparks (1976). *Crystallographic Computing Techniques*. ed. F.R. Ahmed, Munksgard, Copenhagen, pp. 452 – 467.

[23] R.A. Sparks (1982). *Computational Crystallography*, ed. D. Sayre, Clarendon Press, Oxford, pp. 1 – 18.

[24] W. Clegg (1984). *J. Appl. Cryst.*, **17**, 334 – 336.

[25] G. M. Sheldrick (1990). *Acta. Cryst.* **A46**, 467-473.

[26] A.L. Patterson (1944). *Phys. Rev.*, **65**, 195.

[27] C.A. Beevers and C.M. Schwartz (1935). *Z. Krist.*, **91**, 157 – 169.

[28] J.P. Glusker, B.K. Patterson and M. Rossi (1987). An offprint from *Patterson and Pattersons – Fifty Years of the Patterson Function.*, pp 167 – 192, IUCr, OUP.

[29] D. Harker and J.S. Kasper (1947). *J. Chem. Phys.*, **15**, 882.

[30] D. Harker and J.S. Kasper (1948). *Acta Crystallogr.*, **1**, 70 – 75.

[31] J. Karle and J.S. Kasper (1950). *Acta Crystallogr.*, **3**, 181 – 187.

[32] D. Sayre (1952). *Acta Crystallogr.*, **5**, 60 – 65.

[33] P. Main (1997). Notes from *The 6th BCA Intensive Teaching School in X-ray Structure Analysis*.

[34] G. M. Sheldrick (1993). SHELXL-93. Program for the Refinement of Crystal Structures. University of Göttingen, Germany.

[35] D. Watkin (1994). *Acta Cryst.*, **A50**, 411 – 437.

[36] M.A. Leech (1991). B.A. (Hons.) Part II Thesis, University of Oxford.

[37] E.F. Garman and T.R. Schneider (1997). *J. Appl. Cryst.*, **30**, 211 – 237.

[38] E.F. Garman. From: *Methods in Molecular Biology*, Volume 56: *Crystallographic Methods and Protocols*. Edited by: C. Jones, B. Molloy, and M. Sanderson. Humana Press Inc., Totowa, NJ.

[39] A. Gonzalez and C. Nave (1994). *Acta Cryst.*, **D50**, 874 – 877.

[40] J.R. Allibon, A. Filhol, M.S. Lehmann, S.A.Mason and P. Simms (1981). *J. Appl. Cryst.*, **14**, 326 – 328.

[41] R. Rudman (1976). *Low-Temperature X-ray Diffraction – Apparatus and Techniques*, Plenum Press.

[42] W.A. Hendrickson (1991). *Science*, **261**, 51 – 58.

[43] M.M. Harding (1995). *Acta Cryst.* **B51**, 432 – 446.

[44] J.R. Helliwell (1992). *Macromolecular Crystallography with Synchrotron Radiation*, Cambridge University Press.

[45] C.R.A. Catlow and G.N. Greaves (1990). Editors. *Applications of Synchrotron Radiation*. Glasgow and London: Blackie.

[46] http://www.dl.ac.uk/SRS/XRD/9.8.dir/

[47] S.M. Clark, R.J. Cernik and P. Pattison (1989). *Rev. Sci. Instrum.* **60**, 2376 – 2379.

[48] M.M. Harding (1990). *Chem. Br.*, **26**, 10, 956-958.

[49] R.J. Cernik, W. Clegg, C.R.A. Catlow, G. Busnell-Wye, J.V. Flaherty, G.N. Greaves, I. Burrows, D.J. Taylor, S.J. Teat and M. Hamichi (1997). *J. Synchrotron Rad.*, **4**, 279 – 286.

[50] D.R. Allan (1998). *Personal Communication*, Department of Physics and Astronomy, The University of Edinburgh, U.K.

Chapter 4

Structural Studies of Lanthanide Macrocyclic Complexes

4.1 Introduction

In 1971, it was said of the chemistry of the lanthanide ions that:

"...Lanthanum has only one important oxidation state in aqueous solution, the +3 state. With few exceptions, this tells the whole boring story about the other 14 Lanthanides..."[1](!)

While this viewpoint may seem shortsighted, it was in fact indicative of the state of advancement of lanthanide chemistry and its applications at the time. Indeed there are several properties that hold true for the entire lanthanide series notably the stability and predominance of the tripositive lanthanide ion species.

There is certainly a striking structure/property correlation within the lanthanide series in terms of their physical and chemical properties in both elemental and complexed form. The lanthanide series refers to the fourteen elements with occupied f orbitals and the rare earth label refers to these fourteen in addition to lanthanum, yttrium and scandium. The presence of these elements was confirmed in the mid eighteenth century. The first rare earth element to be isolated was yttrium by J. Gadolin in 1794. For the next century, there were many claims of new rare earth elements. The confusion can be attributed to the fact that these occur together as mixtures. Due to their similar properties, they are difficult to separate; e.g., monazite is a mixture of primarily lanthanum, cerium and neodymium phosphates. They also have negligible differences in solubility due to ionic size effects. The phenomenon known as the 'lanthanide contraction' refers to the fact that the ionic radius steadily decreases across the series. This is because of the poor nuclear shielding provided by the electrons in the 4f shell.[2,3] The effective ionic radii for eight co-ordinate La^{+3} and Lu^{+3} are 1.216 Å and 0.977 Å respectively.[4]

Prior to the advent of X-ray spectroscopy, their presence and place in the periodic table could not be proved conclusively. In 1913, W. Moseley showed that there were fourteen elements between lanthanum and hafnium by their characteristic X-ray patterns. Many of the lanthanide elements' properties arise from having occupied f orbitals, accommodating up to fourteen electrons. They do not extend far from the

nucleus and thus unlike the transition metal 5d lobes, their interactions with ligands are largely ionic and thus lacking structural implications. The lanthanide ions are hard and polarising, and thus bind more strongly to hard bases like oxygen and nitrogen rather than sulfur. Unlike the d-block elements, the lanthanides display very little tendency towards variable valence with the aforementioned 3+ oxidation state dominating in complexes. The chemistry of the lanthanide ions is principally that of Ln^{3+} because of the considerable energy stabilisation in forming this oxidation state. In terms of ionisation potential it is much more energetically favourable to remove the 5d and 6s electrons from the neutral lanthanide elements, resulting Ln^{3+} with the remaining 4f electrons virtually incapable of modification by chemical means. Their electronic configuration in complexed form is thus $[Xe]4f^n$. The enthalpy of atomisation shows an inverse trend to the ionisation energies whereby it becomes progressively more difficult to oxidise the elements with ΔH_{atm} for $Ln^{3+} > Ln^{2+} > Ln^{+}$. The energies of hydration across the series for Ln^{3+} show a smooth trend with a more favourable ΔH_{hyd} (Ln^{3+}) as the ionic radius decreases. Generally, the overriding energy correlation is with the ionisation potential for the removal of three electrons.

The Ln^{3+} ions do not emit brightly in the visible region of the electromagnetic spectrum, as is the case with the transition metals. Most of the ions are colourless. Some complexes of europium and terbium are pale pink and those of dysprosium are yellow arising from Laporte forbidden f → f transitions. However, all the lanthanide complexes studied during the course of this work were without doubt colourless.

In reality, elements of the rare earth series have relatively high natural abundances. Lanthanum, cerium and neodymium are incidentally more common than lead in the earth's crust. The majority of the rare earth metals occur as oxides. The mineral bastnasite, which is found in the Sierra Nevadas, is composed of mostly lanthanum and cerium fluorocarbonate supplying most of the world's demand. One of the methods of separation of these metals gives information on the ligand binding trends across the series. The 'Ion Exchange Displacement Column' method whereby a chelating ligand like ethylenediaminetetraacetic acid (EDTA) displays stronger binding

capacity with increasing atomic number and decreasing atomic size across the series. Consequently, this determines the elution times of the ions.

The complexation chemistry of the lanthanide series has undergone a recent resurgence of interest, largely due to the opportunities of performing new diagnostic and imaging studies *in vivo* and *in vitro*. The reasons for designing new lanthanide ion complexes are manifold and research is now focussing on the development of specially tailored complexes as probes in the following techniques:

1. Europium, praseodymium and ytterbium complexes are used as shift reagents in NMR spectroscopy.
2. Paramagnetic gadolinium complexes are used as contrast agents in Magnetic Resonance Imaging (MRI).
3. Luminescence research has shifted from the development of solid-state phosphors (e.g. TV screens) and lasers (yttrium aluminium garnet, YAG) to the use of solution-state luminescent probes exemplified by the development of time-resolved luminescent assays.

The aim of this chapter is to provide a fresh insight, into the behavioural properties of the candidate probes under investigation in the aforementioned techniques, using X-ray crystallography. To this end, first the background to lanthanide complexation chemistry and their recent applications will be reviewed generally. The results of the crystallographic experiments will be presented and the structural insights gathered will be discussed. Finally, some avenues of further research will be suggested in terms of other recent developments in using lanthanide complexes *in vivo*.

4.2 Applications of lanthanide macrocyclic complexes

The conventional uses of lanthanide metals are widely known. Mischmetall ($LnCl_3$ / NaCl) is used to improve the strength of pipes. When alloyed with 30% iron, it becomes pyrophoric and is used in lighter flints. However their applications, when complexed with specially tailored ligands, have attracted much attention over the past ten years...

4.2.1 Luminescence

Luminescence is the generic term for the emissive process whereby when electrons having absorbed energy to be promoted to excited electronic states, revert to their ground states. The loss in energy in reverting to their ground states can take one of two de-excitation pathways. If a pathway is between states of the same spin, fluorescence occurs and if it is between states of opposing spin, phosphorescence occurs. These are non-radiative pathways and radiative luminescence occurs if it can compete with them. Luminescent labels are becoming more prevalent for use in *in vitro* diagnostics.[5] A plethora of molecules ranging from naturally-occurring proteins as enzyme labels (e.g. horseradish peroxidase in immunoassay) to conjugated heterocycles for fluorescence studies and main group complexes, such as [*tris*-(bipy) ruthenium]$^{2+}$ in electrochemiluminescence have been used. Interest has focussed on the lanthanides as luminescent labels because they are prone to luminesce strongly because of the large band gaps present between the ground and excited states of the elements in the series. Here the radiative pathways are to the lower lying f orbitals, shielded behind the p orbitals, and are in the UV-visible region of the electromagnetic spectrum. The main attraction of these complexes is the sensitivity of fluorescence immunoassays. Research has recently focussed on complexes of trivalent europium and terbium that have relatively large energy gaps and emit relatively strongly in the visible region, which is illustrated in ***figure 4.2.1.1*** for europium and terbium. The unique fluorescent properties of these ions include having long lifetimes (microsecond to millisecond range as

opposed to the microsecond to nanosecond range for the biological background). They have sharp emission lines imparting the complexes with high sensitivity.

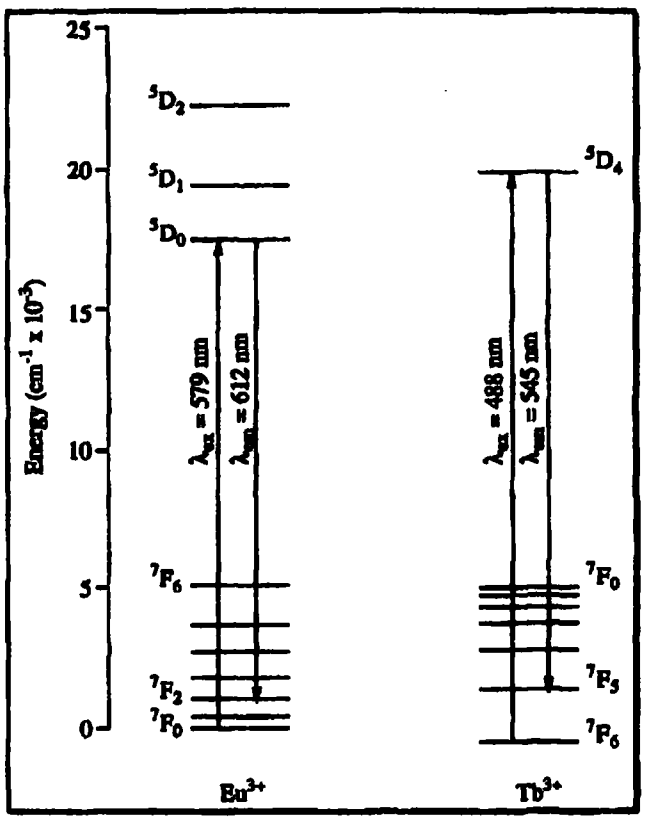

Figure 4.2.1.1 *- Schematic diagram of electronic transitions for europium and terbium, depicting the strongly observed bands in the visible region (reprinted from R.S. Dickins (1997) Ph.D. Thesis, University of Durham.)*

Luminescence studies have been used to investigate the *inter*molecular interactions of the complexes with other chiral molecules and circularly polarised luminescence experiments have been used to probe the chiral environment about the metal ion. Most lanthanides do absorb visible or ultra-violet light but the electronic transitions within a $4f^n$ configuration are Laporte forbidden causing low molar absorptivities and weak luminescence.

For Eu^{3+} the relative intensities of the $^5D_0 \rightarrow {}^7F_1$ and $^7F_2$ emissions are sensitive to the ligand environment. The $^5D_0 \rightarrow {}^7F_1$ transition is magnetic dipole in character; the transition is sensitive to the symmetry of the complex, two bands being observed if a C_3 or C_4 axis is present. The $^5D_0 \rightarrow {}^7F_2$ (and $^7F_4$) transitions are electric dipole in character and their transition probabilities are sensitive to the ligand environment. $^5D_0 \rightarrow {}^7F_2$ is

absent if europium lies on an inversion centre. The number, energy spacing and relative intensities of these components can provide detailed information about the symmetry and structural nature of the Eu^{3+} co-ordination site.

Circular dichroism (CD) is a powerful structural probe, which is widely in use to investigate the secondary structure of polypeptides/proteins in the far UV (180-260 nm) region. Like proteins, small chiral molecules can be studies using CD in the same wavelength range. The spectra of resolved enantiomeric pairs are equal and opposite in intensity to each other. CD refers to the phenomenon whereby the plane of polarisation of plane polarised light is rotated on passing through a solution containing one or an excess of one of two enantiomers. The resultant of plane polarised light is comprised of right and left-circularly polarised components (***Figure 4.2.1.2***).

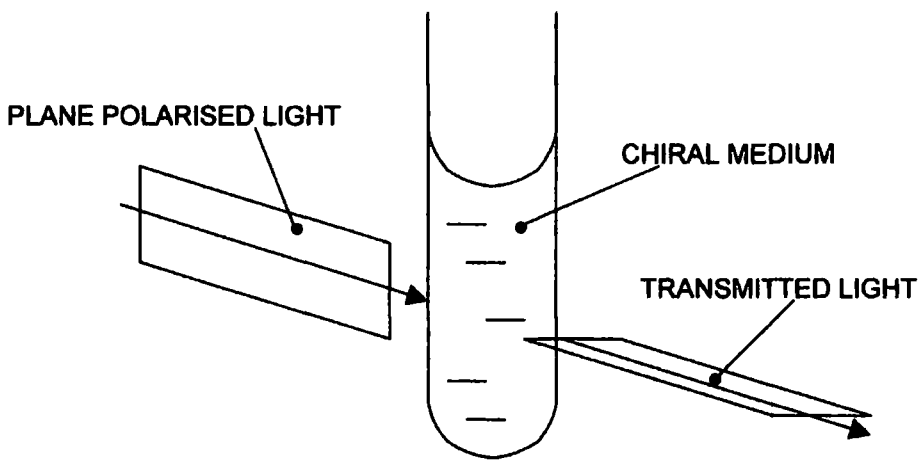

Figure 4.2.1.2 *– Schematic representation of the principle of circular dichroism (CD) whereby the direction of propagation of plane polarised light is altered.*

These are oscillating in-phase sine waves yet one rotates the plane of polarised light in a clockwise manner and the other in an anticlockwise manner. The physical interaction of a given circularly polarised component with a given enantiomer will be different. The important differences are in the refractive indices, n_l and n_r, leading to a change in the measured resultant defined by the tilt angle α, and the molar absorbances ε_l and ε_r which gives rise to the resultant $\varepsilon_l - \varepsilon_r$ tracing an elliptical rather than circular path.[3,6] See ***Figure 4.2.1.3*** for a schematic representation of this process.

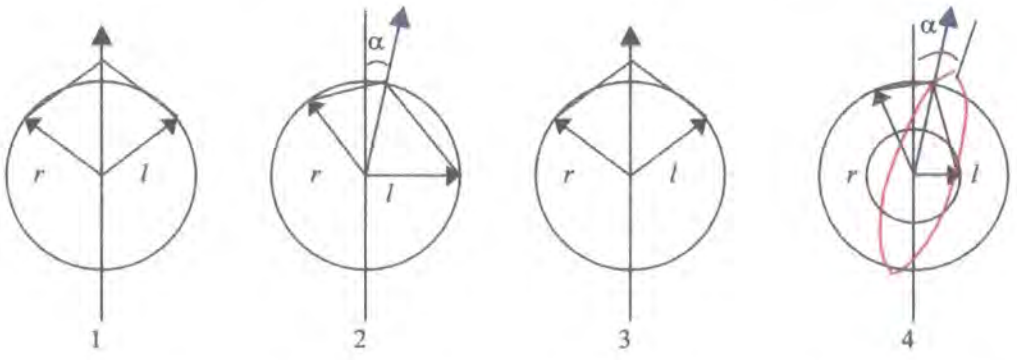

Figure 4.2.1.3 *– Pictorial description of the two changes to the electric vector traversing a solution containing an excess of left-handed enantiomer, along the direction of propagation of plane-polarised light. 1→2: the resultant electric vector is tilted and (3→4) r and l will trace out an ellipse.*

The other technique used to study chiral metal complexes is Circularly Polarised Luminescence (CPL) which is the emission analogue of circular dichroism. Chiral luminescent molecules have the ability to display CPL. It is spontaneous emission of right and left-circularly polarised light by chiral luminescent systems and the technique measures the difference in intensity between left and right circularly polarised light in the emission spectrum instead of the difference in absorption between two circular polarisations. Again, this method can only be applied to optically active or chiral molecules. Even though transition metal complexes with overall chirality (e.g. *tris* chromium and ruthenium complexes of bidentate ligands such as 1,10-phenanthroline, bipyridine, and ethylenediamine) are at first glance good candidates for this application, they must be disregarded due to the fact that they do not emit strongly unless at reduced temperatures in glassy media.[7] This focussed attention on complexes of tripositve europium, dysprosium and terbium as replacements for Fe^{2+} and Ca^{2+}. As can be seen from ***Figure 4.2.1.1***, the transitions for Eu^{3+} and Tb^{3+} are $^5D_0 \rightarrow {}^7F_2$ and $^5D_4 \rightarrow {}^7F_5$ respectively. Incidentally, europium also emits with less intensity for the $^5D_0 \rightarrow {}^7F_1$ transition at 594 nm. For Tb^{3+}, the transition at 545 nm displays an intense CPL structured band. A pioneering study in 1976,[8] saw that terbium displayed CPL in over one quarter of the test cases when added to over 30 proteins. The ion was excited by aromatic residues at 280 nm and structural insights on the intermolecular interactions were gained from these measurements. When comparing CPL spectra the most striking

feature is the degree of structure in contrast to the analogous total luminescence profile. The CPL spectra are slightly changed in the case of different proteins and importantly the traces of the enantiomers are mirror images of one another.[9]

4.2.2 Spectroscopic applications

The NMR spectra of paramagnetic lanthanide ions differ from diamagnetic ions in that the spatial resolution of the peaks is vastly expanded due to the large magnetic moment of the unpaired electrons. This renders lanthanide ion complexes very useful as NMR shift reagents, because of the paramagnetism of the ions. This effects the resonances of organic molecules that are co-ordinated to the metal in that they are spread in the ^{1}H NMR spectrum.

The ability of paramagnetic complexes to catalyse nuclear relaxation is termed relaxivity and this property of altering the proton relaxation rates has earned lanthanide complexes the title 'contrast agents'. When a paramagnetic ion such as Ln^{3+} interacts with an NMR active nucleus (e.g. ^{1}H, ^{13}C) the interaction between the unpaired electrons on both atoms results in broadening, enhanced relaxation of the nucleus and sometimes shifting of the resonances. The large magnetic moment of the tripositive lanthanide ions results in an expanded range of the chemical shift, δ, and ^{1}H shifts of 200 ppm or more.[10] Signal broadening in the NMR is a disadvantage, which can result in the loss of fine detail in the multiplet region. This effect is most pronounced for the dysprosium and terbium ions. Attention has focussed on the Gd^{3+} ion in recent years because of its large magnetic moment (7/2) and its long electron spin relaxation time ($10^{-9.5}$ s) which has a noticeable effect on the ^{1}H nuclear spin relaxation time.[11] This is one of the most powerful proton relaxation agents, increasing the speed of ^{1}H relaxation by a factor of 10^{6}. The observed longitudinal relaxation of proton nuclei because of interaction with a paramagnetic ion is described by the theory of Soloman, Bloembergen and Morgan[12,13,14,15] (equation 4.1),

$$R_i^{obs} = R_{ip}^{is} + R_{ip}^{os} + R_{ip}^{0} \qquad (4.1)$$

where R_1^{obs} is the overall observed relaxivity, R_{lp}^{is} and R_{lp}^{os} are inner sphere and outer sphere contributions respectively, and R_{lp}^{0} is the water proton relaxation rate in the absence of a paramagnetic ion. There are two mechanisms by which the lanthanide contrast agents alters the ^1H relaxation rates, i.e., the inner sphere and outer sphere. The inner sphere contribution is described in equation 4.2

$$R_{lp}^{is} = \frac{Cq}{55.6} \frac{1}{T_{1M} + \tau_M} \qquad (4.2)$$

where C is the molar concentration of the paramagnetic ions, q is the number of co-ordinated water molecules and τ_M is the mean co-ordinated lifetime. The T_{1M} term is the longitudinal proton relaxation time and is inversely proportional to the sixth power to the metal-bound water distance. The inner sphere contribution originates from the dipolar interaction between the paramagnetic metal ion and the bound water proton nuclei. As can be seen from equation 4.2, the number of bound water molecules, q, has a direct effect on R_{lp}^{is}. The time for chemical exchange or the mean residence lifetime is the means of transferring the relaxation effect to the bulk solvent. The outer sphere mechanism is the only means of transferring the relaxivity effect to the bulk in the absence of a bound water molecule and takes place via diffusion of proximal solvent water to allow electron-nuclear magnetic dipole coupling. The relaxivities of the nuclei are highly sensitive to the structural, dynamic and electronic aspects of the complex. Thus, the measurement of relaxivities can give vital information on these features. Recently it has been shown,[16] that when a Gd^{3+} chelate is interacting with a slowly tumbling substrate like a protein, the optimal value of τ_M, the mean co-ordinated lifetime, is a few tenths of a nanosecond to maximise the relaxivity. The nuclear magnetic relaxation dispersion (NMRD) technique is used to determine which paramagnetic metal complexes are good relaxation agents and to what extent. Contrast agents that have been previously investigated were the complexes of lanthanide ions with BzDOTP or 1,4,7,10-tetraazacyclododecanetetrakis(benzylmethylenephosphinic acid) have been investigated. The structures have been elucidated using X-ray

crystallography[16] and will be discussed further in light of the related structures done in this thesis in the experimental section.

Magnetic Resonance Imaging (MRI) is a diagnostic technique relying on the detection of spatially localised NMR signals. The body is composed of about 60% water hence the ^1H is an abundant resonance for which to scan. The signal intensity is dependent mainly on the proton relaxation times (T_1 and T_2), as in equation 4.3.

$$\text{Signal intensity} = [H_2O]\, H_v\, (\exp\{-T_E/T_2\})\, (1-\exp\{-T_R/T_1\}) \qquad (4.3)$$

where H_v = motion factor, T_E = echo delay time, T_R = pulse repetition time, T_1 = longitudinal relaxation time, T_2 = transverse relaxation time.

Although the tripositive gadolinium ion does not have NMR shift properties, it is a very powerful contrast agent in MRI. The resolution of the information obtained from NMR images of biological tissues can be enhanced by the use of a Gd^{3+} complex, which decreases the ^1H relaxation. Since the free ion is toxic, with an LD_{50} of 0.1 mm/kg, a kinetically stable, water-soluble complex of low toxicity is desirable for *in vivo* administration. These NMR contrast agents are more versatile than isotope imaging agents and have low toxicity.

The tetraazacyclododecane complexes of lanthanide ions are all kinetically stable with respect to the dissociation of the metal, undergo rapid excretion after administration, are water-soluble and can accumulate in specific target tissues and exhibit high relaxivity.

The NMR shift ability of lanthanide ions fluctuates throughout the series because of the distribution of the unpaired f electrons affecting their capability to shift resonances. Gd^{3+} has seven unpaired electrons, which are isotropically or evenly distributed into the available orbitals so $\delta p = 0$, and hence it does not shift resonances of bound atoms. In n-hexanol, europium and promethium shift the resonances to higher and lower frequencies respectively. The criteria for an effective NMR shift reagent are a high magnetic moment (e.g. Dy^{3+}, Tb^{3+} and Tm^{3+}) and a high overall negative charge (i.e. the lanthanide complex should ideally be appended with negatively charged

functionalities such as carboxylic, phosphonic). To date, dysprosium complexes have been the more suitable shift reagents[15]. In recent years, chiral NMR shift reagents have been used, including chiral molecules where the stereogenic centre(s) are defined by phosphorus atoms.[16] The use of chiral molecules results in interactions that are more specific and the obvious application of this is the use of chiral lanthanide complexes as a means of interrogating macromolecular structure. The first chiral lanthanide complexes to be used in the analysis of chiral molecules such as sulfoxides and diastereotopic methyl groups were europium and praseodymium complexes of camphor derivatives.[17]

4.2.3 Tumour imaging using Positron Emission Tomography

Lanthanide complexes have been synthesised and utilised successfully in the clinical application positron emission tomography (PET) imaging. This imaging technique is gaining popularity as a non-invasive alternative to X-rays for the detection of tumours. The method harnesses the fact that the radionuclide ^{134}La is a suitable nucleus for PET imaging. Its half-life ($t_{1/2}$) of 6.7 minutes is short enough for repeated imaging and long enough to be incorporated into complexes and administered *in vivo*. The complexes have low toxicity, are stable to acid and cation mediated dissociation and are water stable.

In PET, a positron (anti-electron) emitted during the decay process of ^{134}La collides with an electron and in the subsequent annihilation reaction two collinear γ-rays are produced travelling at 180° with respect to each other. These are both detected simultaneously by external cameras, thus defining a line passing through the location of the complex. ***Figure 4.2.3*** overleaf is a pictorial description of this process.

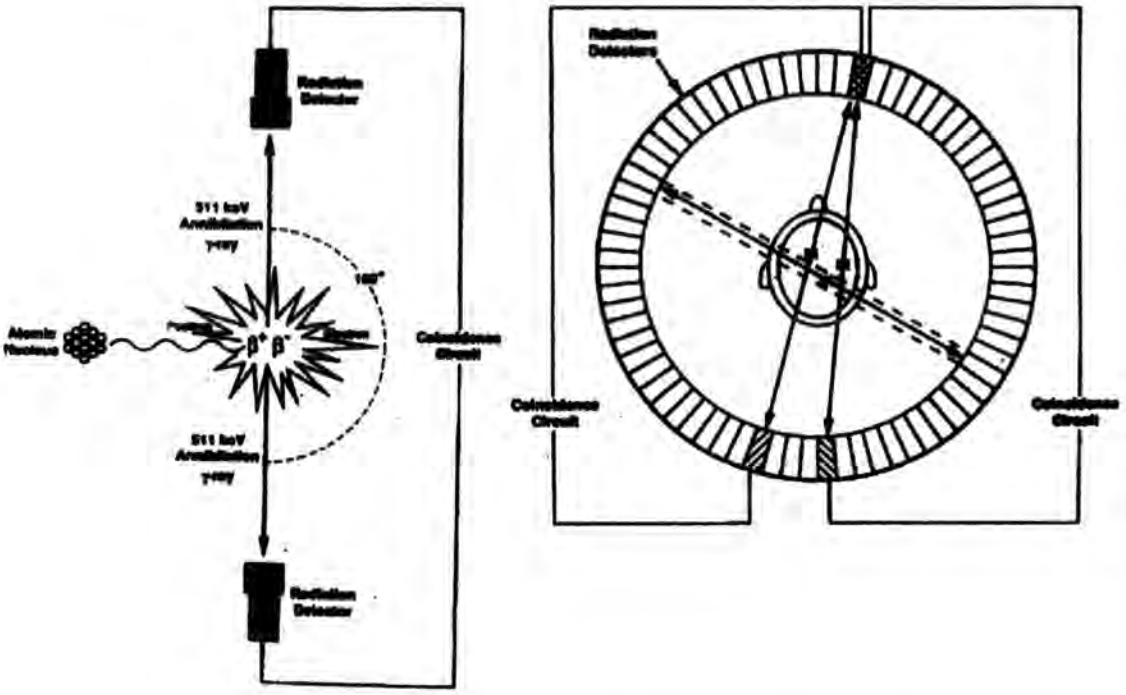

(a) *(b)*

***Figure 4.2.3** – (a) Schematic diagram illustrating the principle of PET. (b) Schematic diagram illustrating how a 3D image is built up, thus locating tumour position(s), by the simultaneous detection of pairs of photons by a set of cameras (reprinted from C.E. Foster (1996) Ph.D. Thesis, University of Durham.)*

A set of such lines allows a 3 D picture to be built up describing the position of the complex with a resolution of approximately 3 mm allowing a diagnosis of which organ is affected to be made. If a series of these events can be detected and the intersections calculated, a distribution of the radioisotope in the body can be built up. Non-metallic radionuclides have played a vital role in the development of PET as an imaging technique. Such nuclei (e.g. ^{15}O, ^{13}N, ^{11}C) have very short half-lives which necessitate the use of an expensive on-site cyclotron. An alternative option to this is to use generator-produced nuclides, which have short lived daughter isotopes of longer-lived parent isotopes. A candidate nuclide is ^{134}La because of the aforementioned reasons.

4.3 Perspective

The late 1980's witnessed an explosive revival in the chemistry of the lanthanide elements when their potential as diagnostic tools was realised. This resulted in renewed interest in their complexation chemistry.

In the rational design of lanthanide ion complexes for *in vivo* applications, their toxicity, behaviour and interactions with biological molecules must be considered. The complexation chemistry of lanthanide tetraaza compounds was triggered by the requirement to devise complexes of the β-emitting isotope ^{90}Y that were stable with respect to dissociation *in vivo*. Yttrium-90 is a therapeutic radioisotope that has sufficient energy (2.25 MeV, ca. 3.6 x 10^{-13} J) to cause cell death following double-stranded DNA cleavage. Effective radiotherapy results in targeting the cytotoxic isotope selectively to the tumour cell provided it has not been prematurely released by the targeting vector. The requirements of the designated ligand for lanthanide complexation were rapid binding of ^{90}Y in aqueous solution (^{90}Y, t½ = 16 h) to form a cation or acid-mediated decomplexation resistant compound, rapid excretion after administration and good water solubility. In no environment was this more crucial than *in vivo,* due to the high toxicity of the unbound metals. The kinetic pathway for metal ion dissociation is cation or acid mediated, thus it was decided to focus on the design and synthesis of neutral or anionic complexes.

The mode of interaction of these complexes with biological molecules such as proteins, DNA and RNA depends largely on their charge and chirality. The overall charge on a compound dictates its relative tissue distribution. The chirality of these complexes is similarly of the utmost importance, since biological processes are achieved by means of precise molecular recognition between chiral molecules. These interactions can be followed by measuring the metal-based luminescence.

It is known that many stable unidentate lanthanide ion complexes with eight and nine co-ordination number exist. To take full advantage of this in the design of stable macrocyclic complexes, a suitable ligand could organise its donor atoms at the vertices

of one of the common geometries. Not withstanding this, many of these ligands are very flexible, as can be seen from the copper and nickel complexes of TETA where two perchlorate molecules positions themselves above and below the square planar N4 donor set to form octahedral complexes.[18]

In the chromium complex of the tris-carbamoylethyl derivative of NOTA, the mean Cr-N distance is 2.042(4) Å and the mean Cr-O distance is 1.955(4) Å. When one of the carbamoyl oxygen atoms is replaced by a deprotonated amide nitrogen, the distance from chromium to this nitrogen atom is 1.963(4) Å.[19]

The smaller triazacyclononane ring, when tris-*N* substituted with carboxamide groups readily forms C_3 symmetric mononuclear complexes with V^{3+} (pentagonal bipyramid), V^0, Cr^{3+}, These complexes display oxophilicity but also in the case of Cr^{3+} binding of an amide N when deprotanated. When the ligand is methylated at the amide nitrogen, the N_3O_3 donor set is reformed. Octahedral complexes of divalent Cu, Ni, Co, Zn and trivalent Fe, Co, Ga and In are formed with the triazacyclononane based fragment when it is tris-N substituted with methylene phosphinate groups. Like the carboxamide series, the complexed triazacyclononane is the same 'triangular' framework. The N-M-O 'bite' angle is sensitive to the functionality at the ring nitrogen and expands when derivatised with the bulkier phosphinate groups as can be seen for the analogous Cu^{2+}, Ni^{2+}, Fe^{2+} and Gd^{3+} complexes of the triaza heterocycles depicted in ***Figure 4.3.1***.

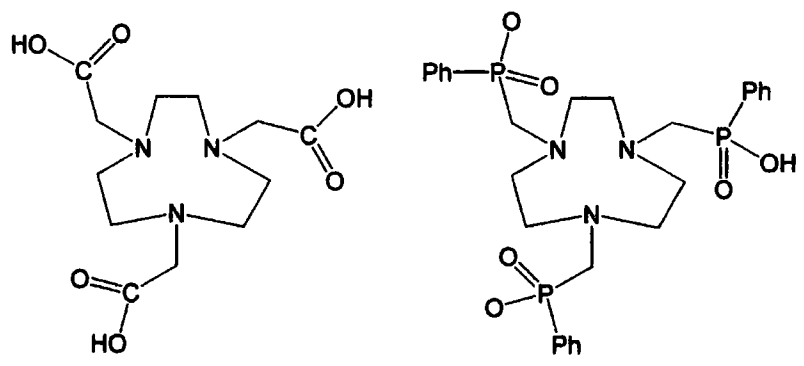

(a) *(b)*

Figure 4.3.1 *– Schematic representation of (a) 1,4,7,-triazacyclononane-N,N',N''-triacetic acid and (b) 1,4,7,-triazacyclononane-N,N',N''-tris (phenylphosphonic acid).*

The cyclen (1,4,7,10-tetrazacyclododecane) ligand when tetra-*N* substituted with suitable donor groups forms chelates for complexation to the lanthanide ions which invariably form high co-ordination number mononuclear complexes. When tetra-*N* substituted with acetate groups, the ligand DOTA is formed. This molecule has a high affinity for most metals, notably binding Ca^{2+} with a binding constant of $10^{17.2}$. It is known that lanthanide ions complex ligands in a similar manner to calcium, for example europium can exchange for calcium in proteins, rendering the free ion toxic to the body.

Chiral molecules of europium, terbium and dysprosium, which luminesce strongly were synthesised and their crystal structures obtained to verify that one enantiomer was present which contributed solely to this signal. The choice of which 'pendant arms' to attach to the ring nitrogen atoms was governed by two considerations. An electron donating functionality would act as a strong chromophore and increase the intensity of the metal-based luminesce making it more discernible in biological media. Secondly, the long-term aim is the reaction of these lanthanide probes with biological molecules and so the choice of functional group to form a covalent linkage to should be a relevant one. The amide group, present in every protein residue, fitted both these criteria satisfactorily.

The design of ligands with nitrogen and oxygen donor atoms yields readily formed complexes of not only lanthanides but also transition metal ions. The macrocycle DOTA was used in the course of this work for lanthanide ion complexation when derivatised with functional groups that alter the lipophilicity, charge or impart inherent chirality on the molecule. They also form kinetically stable complexes for *in vivo* administration. The fine-tuning of the complex as a probe for a given application is also possible. This may take the form of ensuring that a mono-hydrated complex forms which facilitates the transfer of the relaxivity effect to the bulk solvent in MRI. The structural investigations by means of X-ray crystallography are therefore of the extremely useful in both structural characterisation and in the analysis of the molecules' properties.

4.4 'DOTA' - The archetypal chelate

The ligand 'DOTA' or 1,4,7,10-tetrazacyclododecanetetraacetate (***Figure 4.4.1***) is the ideal macrocycle for co-ordinating virtually all metals, possessing a mixture of both hard and soft donor atoms and a rigid framework that creates an encapsulating co-ordination sphere defined by its octadenticity. It forms one of the most stable complexes known to date with calcium over a large pH range. Its synthesis was reported in 1990 by Cox *et al.*[20] Surprisingly the crystal structure had not been reported in the literature and thus the X-ray structure determination was undertaken to ascertain whether this tetraaza ligand predisposed towards metal binding. The molecule was synthesised and crystallised by Mark Woods from the chemistry department at the University of Durham. The molecule is based on the '[12]ane N_4' heterocyclic ring cyclen and it, like phthalocyanine or tetrathiocyclotetradecane, is a tetradentate macrocycle. The cyclen ring when tetra-*N* appended with acetate side chains forms DOTA. The commonly observed 'flattening' of the N-C-C-O 5-ring in the presence of large metal ions renders the complex nine co-ordinate as a result of the binding of a water molecule.

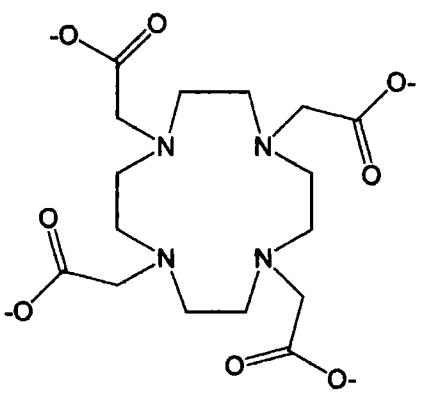

***Figure 4.4.1** – Schematic representation of the macrocyclic ligand 'DOTA', or* L^1.

Interest in the co-ordination behaviour of this ligand was fuelled predominantly by the search for kinetically and thermodynamically stable complexes in MRI. The rate of complexes formation is thus of considerable importance and this, for macrocycles, is additionally regulated cavity size, steric factors, conformation, preorganisation and, if necessary, reorganisation. The complexation chemistry thus far reported of this ligand is

substantial. The close relatives of DOTA, the siderophores, are naturally occurring chelators produced by micro-organisms, which use them as iron transport agents. The complexation chemistry of the siderophore analogue TETMAHA or 1,4,8,11-tetraazacyclotetradecane-N,N',N''-tris(N-methylacetohydroxamic acid) emphasises the variable co-ordination geometry possible in these systems, it binds divalent iron, aluminium and copper in an octahedral manner.[21] Kinetics studies found a high correlation between rate of formation and pH for Gd^{3+} complexes of DO3A[22] and DOTA[23] with complex formation rates increasing at high pH. Gd^{3+}·DOTA is now routinely used as a contrast agent in MRI.[23] It was proposed that the binding mechanism progressed via an intermediate whereby the metal bound the oxygen donors in the O4 plane, which is free to expand, and from there moved into the centre of the macrocycle. This would allow for reorganisation of the cyclen ring. The synthesis and crystal structures of trivalent iron and gadolinium complexes of DO3A and the trivalent iron, yttrium, gadolinium and europium complexes of DOTA have been reported.[24,25] This study revealed the effect of metal on co-ordination geometry. The geometries of Fe·DO3A and Fe·DOTA were face-capped trigonal prisms. In the Fe·DOTA compound, one of the carboxylate arms does not co-ordinate to the central metal, the unco-ordinated carboxylate is turned away from the metal and accepts two hydrogen bonds from the water of crystallisation. The Gd^{3+} complexes of DO3A and DOTA are nine co-ordinate. The DO3A ligand itself is heptadentate with the eight and ninth co-ordination sites filled by a single carbonate ion. Not surprisingly, the Y^{3+}, Eu^{3+} and Gd^{3+} complexes of DOTA are all crystallographically isostructural. These C_4 symmetric ligands bind the lanthanide ion and are capped above the O4 plane by a water molecule.

The co-ordination geometry adopted by complexes of octadentate DOTA is usually one of two types. For co-ordination number eight, there are three idealised structures: the cube (square prismatic geometry) O_h, the square antiprism (D_{4d}), and the dodecahedron (D_{2d}). The latter two are attained by simple distortions of the cube, see ***Figure 4.4.2***). The square antiprism is achieved by a simple rotation of the top face of a cube with respect to the 'stationary' bottom square face. A rotation of 45° gives an idealised square antiprism. A dodecahedron is formed by the folding back of two

opposite faces from the opposite diagonal in each case. The cuboid structure occurs rarely, notably in the case of continuous solids e.g. CsCl. The other two geometries are more common, offering the additional advantage of reduced ligand-ligand repulsions.

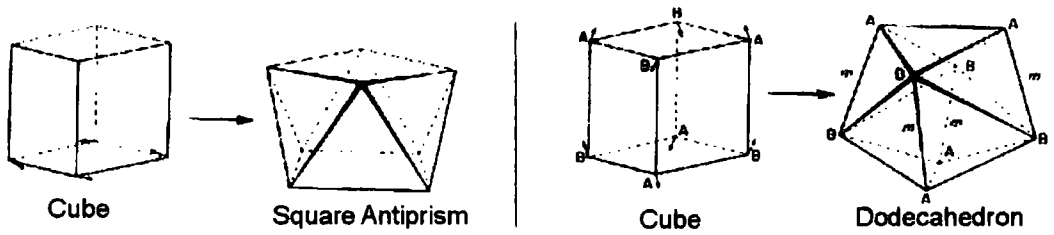

***Figure 4.4.2** – The operations performed on a cube to become a square antiprism or a dodecahedron, figure reprinted from reference 3.*

The dodecahedron and the other geometry the bicapped trigonal antiprism are suitable geometries for bidentate chelates, in particular, with small 'bite' angles (e.g. nitrate or carboxylate) which happen to fit reasonably well to the dimensions of the smaller faces present. The dodecahedron has also been observed for homoleptic Ln^{3+} complexes with ligands incorporating virtually no steric bulk, for example $Yb(MeCN)_9$.[26] Two geometries predominate for nine co-ordinate complexes, the trigonal tricapped prism and the square antiprism with one ligand capping a rectangular face. The trigonal tricapped prism is quite common for mononuclear unidentate complexes as in the case of the eight co-ordinate dodecahedra, it is prevalent for Ln^{3+} complexes with 'small' ligands such as $Pr(MeCN)_9$.[26] The square antiprism has eight triangular and three rectangular faces. It is the common co-ordination geometry for Ln complexes of DOTA and its derivatives. For nine co-ordinate Ln^{3+}·DOTA complexes, the capping of one rectangular face is commonly observed. The complexes of DOTA with gadolinium, yttrium,[24] and europium[27] are nine co-ordinate with square antiprismatic geometry. Lanthanum forms an interesting square antiprismatic complex with the related ligand 1,4,7,10-tetrakis(2-carbomoylethyl)-1,4,7,10-tetraazacyclododecane[28] (see ***Figure 4.4.3***). It is eight co-ordinate due to the flexibility of the now extended amide pendant arms to completely encapsulate the metal. This is reflected in the large 'bite' angle (N_x-Ln-O_x) averaging at 71.8°. It is a distorted square antiprism with a 'twist' angle of 26.5° from cuboid structure. The 'twist' angle is

defined as the angle between two planes, one containing the two nitrogen atoms on opposite sides of the ring and the metal, and the other plane containing the two oxygen atoms on the same pendant arms as the two previously defined nitrogen atoms and the metal. As will be described later, there is an alternative way of calculating the twist angle that only holds true where the ring nitrogen is connected to the oxygen atom via two (carbon) atoms.

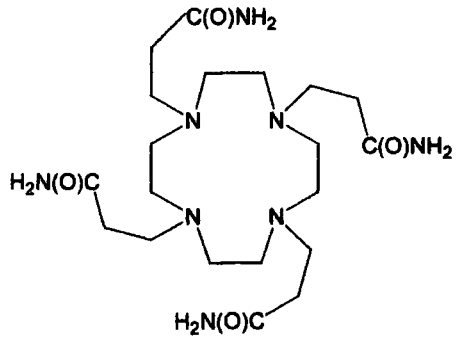

***Figure 4.4.3** – The tetra-N 1,4,7,10-tetrakis(2-carbomoylethyl) derivative of cyclen.*

The hardness of the lanthanide ions is emphasised by the mean Ln-O and Ln-N averaging at 2.42(3) and 2.72(1) Å respectively. No unusual bond lengths were reported in this considerably strain-free complex where the metal moves significantly toward the O4 plane. In the crystal structure of the europium complex with THP[29] (1,4,7,10-tetrakis(2-hydroxypropyl)-1,4,7,10-tetraazacyclododecane) in which the four acetate groups on DOTA were replaced by hydroxypropyl groups to form an overall tricationic complex, there are two molecules contained in the asymmetric unit based on square antiprismatic geometry. One is square antiprismatic and the other is twisted square antiprismatic (see ***Figure 4.5.1***) and each has a capping water molecule above the O4 face. In aqueous solution, lanthanide complexes of DOTA exist as a mixture of two stereoisomers. Incidentally, a parallel ^{1}H and ^{13}C NMR study of Ln^{3+}·DOTA complexes in solution indicated the presence of a major and a minor isomer.[30] The bond lengths and angles were identical in both isomers in the NMR solution. The most significant disparity was the difference in N-C-C-O (where the oxygen is the one turned toward the metal) which was 8.9° for the major (square antiprism) and –28.3° for the minor (twisted square antiprism) isomer. [Note. Estimated standard deviations are not obtainable from

NMR]. Later studies found the relative concentrations of twisted square antiprism or the Δ(δδδδ) isomer (see ***Figure 4.5.1***) decreases with decreasing ionic radius. For Eu·DOTA a 1:4 mixture was observed. The fastest process for the interconversion to the major isomer, seen in the crystal structure, was via rotation of the four acetate groups.[31] It has also been reported that the free energy of conversion of the minor isomer to the major was higher than for the reverse process.[32] Hence, it was very interesting to investigate the subtleties of the DOTA structure by solving the crystal structure. As mentioned previously, the structures of DOTA complexes have been cited in the literature and in addition to the abovementioned complexes, these include the main group copper,[33,34] zinc[35] and nickel[34] complexes. The structures of a considerable number of related free ligands have also been reported, which include the tetraethoxycarbonylmethyl derivative of diazonicyclododecane.[36]

The data collection and structural refinement details for this structure are presented in ***Table 4.4.1***. Data were collected from a large sample on the Rigaku AFC6S 4-circle diffractometer to avail of the increased intensity of its copper source for this putative exclusively light atom structure. However, the molecule crystallised as the dihydrochloride salt with a solvent channel containing approximately five disordered water molecules of crystallisation. The presence of disordered heavy atom scatterers impeded the refinement. In retrospect, it would have been more beneficial to collect the data using molybdenum radiation. ψ-scans were not performed following data collection and thus the data from this reasonably strongly absorbing (μ = 2.852 mm^{-1}) crystal has unfortunately not been absorption corrected. The hydrogen atoms were placed in supposed positions and were not included in the structure factor calculation on the water molecules. Nevertheless, the experiment has yielded interesting information on the structure of this free ligand. This molecule is C_4 symmetric, and this point group symmetry is maintained upon complexation to form eight co-ordinate compounds, although this four-fold symmetry is invariably not crystallographic.

***Table 4.4.1** – Crystal data and refinement details for DOTA dichloride pentahydrate*

COMPOUND	$[C_{16}H_{29}Cl_2N_4O_8].(4.H_2O).(H_3O)^+$
Formula weight	567.42
Temperature	150(2) K
Wavelength	1.54178 Å
Crystal system	Monoclinic
Space group	$P2_1/n$
Unit cell dimensions	a = 11.018(2) Å $\alpha = 90°$
	b = 20.019(4) Å $\beta = 91.30(3)°$
	c = 11.822(2) Å $\gamma = 90°$
Volume	2606.9(9) $Å^3$
Z	4
Density (calculated)	1.446 g/cm^3
Absorption coefficient	2.852 mm^{-1}
F(000)	1208
Crystal size	0.750 x 0.675 x 0.375 mm^3
Theta range for data collection	4.34 to 74.98°.
Index ranges	0<=h<=13, 0<=k<=24, -14<=l<=14
Reflections collected	5021
Independent reflections	4801 [R(int) = 0.0355]
Absorption correction	Not applied
Refinement method	Full-matrix least-squares on F^2
Data / restraints / parameters	4801 / 0 / 316
Goodness-of-fit on F^2	1.090
Final R indices [I>2sigma(I)]	R1 = 0.0815, wR2 = 0.2293
R indices (all data)	R1 = 0.0888, wR2 = 0.2501
Largest diff. peak and hole	0.846 and -0.981 $e.Å^{-3}$

A selection of bond lengths and angles are presented in ***Tables 4.4.2-4.4.3*** and the full list of atomic co-ordinates, bond lengths and angles and anisotropic displacement parameters are in ***Appendix A.4.1***. The molecule crystallises as a mixture of stereoisomers in the centrosymmetric space group $P2_1/n$. Although the dimensions along the a and c axes are similar, no transformation to a tetragonal setting was found. Interestingly, this family of ligands and their complexes do not crystallise in tetragonal space groups. This is reminiscent of the structure of 1,4,7,10-tetraethyl-1,4,7,10-tetraazacyclododecane[37] where a pseudo-tetragonal structure was found in the enantiomorphous space group $P4_12_12$. This structure turned out to be an average structure of two independent molecules and the true space group was $P2_12_12_1$.

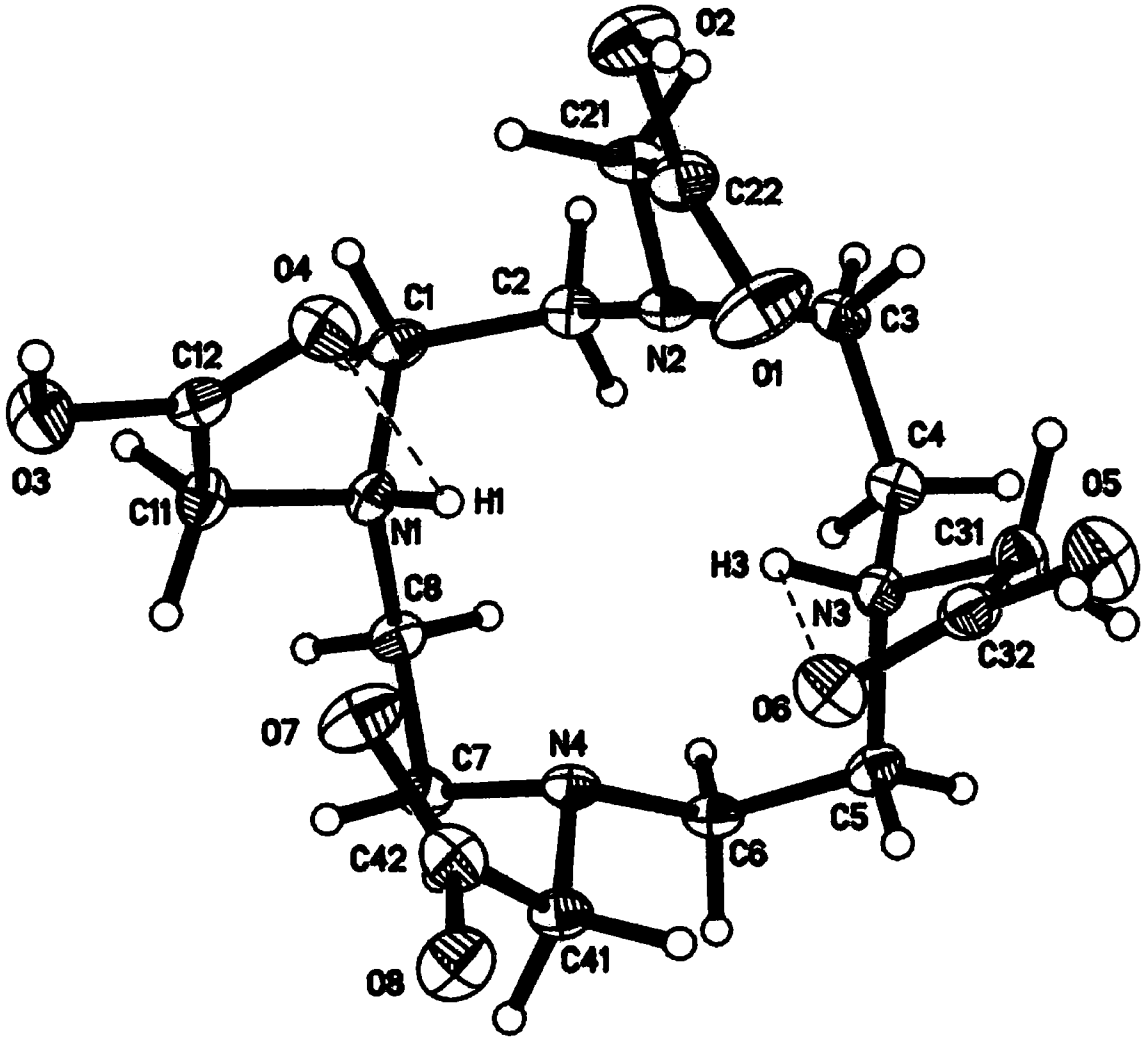

Figure 4.4.4 *– The structure of 'DOTA' determined from the 150(2) K X-ray experiment projected on to the plane of the four nitrogen atoms. The anisotropic displacement parameters are drawn at 50% probability level. The broken lines indicate reasonably close intramolecular contacts to hydrogen (see* ***Table 4.4.2****).*

Table 4.4.2 *– Selected bond lengths [Å] for DOTA.*

BOND LENGTH	Å	N(1)-C(1)	1.510(4)	C(3)-C(4)	1.515(4)
O(1) - C(22)	1.208(5)	N(2)-C(21)	1.463(4)	C(5)-C(6)	1.528(5)
O(2) - C(22)	1.325(4)	N(2)-C(2)	1.475(5)	C(7)-C(8)	1.523(4)
O(3) - C(12)	1.320(4)	N(2)-C(3)	1.476(4)	C(11)-C(12)	1.519(5)
O(4) - C(12)	1.202(4)	N(3)-C(4)	1.502(4)	C(21)-C(22)	1.499(5)
O(5) - C(32)	1.312(4)	N(3)-C(31)	1.493(4)	C(31)-C(32)	1.516(5)
O(6) - C(32)	1.202(4)	N(3)-C(5)	1.503(4)	C(41)-C(42)	1.491(5)
O(7) - C(42)	1.261(5)	N(4)-C(6)	1.468(4)	NH..O CONTACT	Å
O(8) - C(42)	1.284(4)	N(4)-C(7)	1.469(4)	N1-H1..O4	2.3526
N(1) - C(11)	1.492(4)	N(4)-C(41)	1.471(4)	N3-H3..O6	2.4512
N(1)-C(8)	1.502(4)	C(1)-C(2)	1.524(5)		

***Table 4.4.3** – Selected bond angles [°] for DOTA.*

C(11)-N(1)-C(8)	111.9(3)	N(1)-C(1)-C(2)	111.9(3)	N(2)-C(21)-C(22)	111.2(3)
C(11)-N(1)-C(1)	110.5(2)	N(2)-C(2)-C(1)	111.3(3)	O(1)-C(22)-O(2)	122.7(4)
C(8)-N(1)-C(1)	111.7(3)	N(2)-C(3)-C(4)	111.6(3)	O(1)-C(22)-C(21)	125.0(3)
C(21)-N(2)-C(2)	111.7(3)	N(3)-C(4)-C(3)	111.3(3)	O(2)-C(22)-C(21)	112.3(3)
C(21)-N(2)-C(3)	109.9(3)	N(3)-C(5)-C(6)	112.4(3)	N(3)-C(31)-C(32)	111.0(3)
C(2)-N(2)-C(3)	110.9(3)	N(4)-C(6)-C(5)	111.6(3)	O(6)-C(32)-O(5)	126.6(4)
C(31)-N(3)-C(4)	111.3(2)	N(4)-C(7)-C(8)	111.9(3)	O(6)-C(32)-C(31)	123.7(3)
C(31)-N(3)-C(5)	110.1(2)	N(1)-C(8)-C(7)	111.5(3)	O(5)-C(32)-C(31)	109.7(3)
C(4)-N(3)-C(5)	111.6(3)	N(1)-C(11)-C(12)	110.0(3)	N(4)-C(41)-C(42)	113.7(3)
C(6)-N(4)-C(7)	110.4(3)	O(4)-C(12)-O(3)	126.1(3)	O(7)-C(42)-O(8)	123.0(4)
C(6)-N(4)-C(41)	110.6(2)	O(4)-C(12)-C(11)	123.2(3)	O(7)-C(42)-C(41)	120.8(3)
C(7)-N(4)-C(41)	110.0(3)	O(3)-C(12)-C(11)	110.6(3)	O(8)-C(42)-C(41)	116.3(3)

The point group symmetries of the related NOTA (1,4,7-triazacyclononane) complexes have been reported as maintained on complexation. For example, the nickel complex of NOTA crystallises in the trigonal space group, *R*3c,[38] and the cobalt, nickel, copper and zinc complexes of tris(phenylphosphonic acid) crystallise in $P\bar{3}$[39] where one third of these molecule are independent. In the case of DOTA, one must ascribe the loss of four-fold symmetry to the presence of counter ions and water of crystallisation, as was seen for the tris(amide) derivatives of NOTA.[19]

A 1 mm collimator was used and although the crystal was within the specifications that would be acceptable, had it been cleaved the anisotropic absorption profile could have been improved. The structure was solved using direct methods. One fifth of the scattering density (hydrogen atoms excluded) is contained in the solvent channel with is the chloride counter ions and water molecules, all of which are disordered. This has certainly contributed to the larger than normal residual electron density peaks. The macrocycle is an overall cation (***figure 4.4.2***) due to the protonation of N1 and N3 on the ring. These hydrogen atoms form weak hydrogen bonds with the carbonyl group of their respective *N*-substituted acetic acid. This is reflected in the lengthening of the bond lengths from these nitrogen atoms to their neighbouring carbon atoms by 0.02 Å on average. Three of the carbonyl groups are protonated whilst the group at C42 is an anion and not involved in hydrogen bonding. As can be seen from ***Figure 4.5.1***, DOTA, its derivatives and in complexed form can be described as square

antiprism or twisted square antiprisms. As a rough visual estimation, a conformation can be described as a square antiprism when the (oxygen) atom donors pass over a central ring carbon atom when viewed on projection on the N4 plane. A twisted square antiprismatic conformation is assigned when the oxygen atom passes over a carbon atom at a corner. A more quantitative description can be applied using the rule that when the torsion angles of the N-C-C-N and the N-C-C-O entities are of the same parity the twisted square antiprism isomer is formed and when they are of the opposite parity the square antiprism is formed. Whilst DOTA looks very like a twisted square antiprism, these particular dihedral angles are of the same parity (***Table 4.4.4***), and it is thus a square antiprism by definition. However, it is only just so and may be regarded as an intermediate state between the two structures. This result is further substantiated by previously reported structures of DOTA and its derivatives where both conformations have been seen adopted. It is certainly more preorganised towards octadentate metal complexation than some related macrocycles.

Table 4.4.4 *- Selected torsion angles [°] for DOTA.*

N-C-C-O angle (°)		N-C-C-N angle (°)	
4.21(0.45)	N1-C11-C12-O4	-53.62(0.37)	N1-C1-C2-N2
6.47(0.53)	N2-C21-C22-O1	-59.77(0.36)	N2-C3-C4-N3
7.38(0.47)	N3-C31-C32-O6	-57.11(0.36)	N3-C5-C6-N4
10.73(0.47)	N4-C41-C42-O7	-60.37(0.37)	N4-C7-C8-N1

The tetracyanoethylated derivatives of cyclam[40] (1,4,7,10-tetraazacyclotetradecane) in both neutral and diprotonated states are also stabilised by intramolecular hydrogen bonding but two pendant arms on opposite sides of the ring are extended away from the cycle.[41] The deciding factor for this may be the minimisation of steric hindrance between four pendant arms, which are at least 1.5 Å longer than in the case of DOTA. This also holds true for the tetra-2-carboxyethyl derivatives of cyclam where every other pendant arm is extended outwards.[42] The structure of BzDOTP[16] is actually completely preorganised for octadentate binding in a twisted square antiprismatic conformation. However, there is a large variation in the values of the N-C-P-O torsion angles, as much as 59.8° between the largest and the smallest. The

intramolecular hydrogen bonds in DOTA may be structure determining. A molecular modelling study using the molecular electrostatic potential performed on DOTA[43] resulted in a structure with all the four acetate groups extended outwards from the ring. The crystal structure of DOTA does not reveal any significant intermolecular contacts with a solvent channel in between layers of ligands. The structure appears to be quite flexible and an inspection of the bond lengths and angles (***tables 4.4.2 and 4.4.3***) reveals no strained or surprising dimensions. Despite not being in the complexed form, the geometry of the eight potential donor atoms two rather regular square bases. The angles of intercept between the lines joining N2 to N4 and N3 to N1, and O1 to O7 and O4 to O6 are effectively 90° in both cases. The maximum deviation out of the N4 plane is 0.002 Å and 0.04 Å for the O4 plane. The distance of the N4 plane from the O4 plane is 2.50 Å and they can be referred to as coplanar with an angle of 0.7° between them. The pore or cavity size is estimated to be 4.33 Å in diameter from the average of the four distances not at corners between opposite atoms around the ring. The implication this has for complexation is that cyclen could not accommodate a lanthanide ion in its centre, the smallest lanthanide ion covalent radius is 1.117 Å for lutetium^{3+}, and it therefore must be displaced out of it.

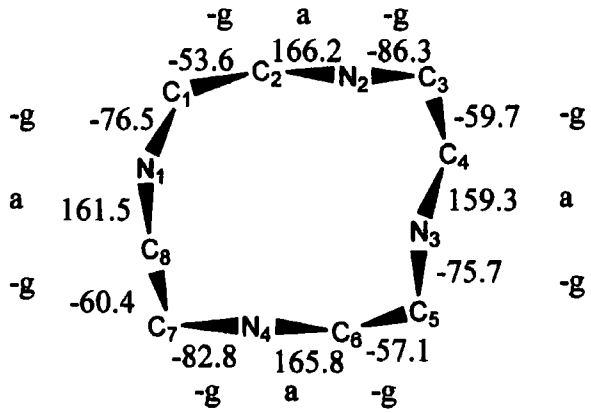

Figure 4.4.5 *– The torsion angles [°] around the cyclen ring in the crystal structure of DOTA (g = gauche, a = anti).*

The conformation of this ring is most effectively interpreted in terms of its torsion angles (***Figure 4.4.3***) and an unmistakable pattern is revealed on examining these angles. The experiment confirmed that the cyclen ring adopts the energetically favoured quadrangular conformation introduced by Johannes Dale in his seminal review

of the conformation of free and complexes oligoethers, which used results from X-ray crystallography and ^{13}C NMR.[44] This described the preference of acyclic and heterocyclic 1,4 dioxa groupings to forming rings and fragments with 'genuine corners'. It was observed that the crown ethers were not perfect circular macrocycles and indeed this was first established firmly by the proclamation that the X-ray structure of 1,4,7,10,13,16-hexaoctacyclooctadecane or 18-crown-6[45] as a rectangle. Following this, the structures of 2,3,11,12-tetraphenyl-[18]crown-6 compounds, showed a distinct tendency for large ring systems to 'fill their own cavity'.[46] The cyclen ring in DOTA can be classified as having the [3333] conformation where each digit refers to the *number of bonds between bends*. The structure of the cyclam ring in TETA[47] (1,4,7,10-tetraazacyclotetradecane) has the [3434] conformation. The tetraaza ring has $(-g\ a\ -g)_4$ conformation. Note that its mirror image is present in equal amount, generated by the inversion centre, having the $(g\ a\ g)_4$ conformation. Upon complexation with lanthanide ions forming the compounds that will be described in this chapter this conformation undergoes only negligible changes. The tetraoxa analogue (12-crown-4) also has the [3333] conformation and is stabilised by two intramolecular CH..O contacts but changes from $[(-g\ a\ -g)_2(g\ a\ g)_2]$ to $(g\ a\ g)_4$ on binding a sodium ion. In this respect, the tetraaza ring resembles more the cyclododecane hydrocarbon in conformation than the tetraether. Molecular orbital *ab initio* calculations performed on tetraaza cyclic amines[48] revealed the minimum energy conformations adopted by these molecules at different protonation states. These do not differ significantly from the crystallographically observed conformational preferences and for the neutral tetraaza ring the N-C-C-N torsion angles were (-62.2, -56.9, -62.2, -56.9), which correlate well with the results in ***table 4.4.4***. The study also showed that conformation and the position of the heteroatoms were very sensitive to the protonation state. These finding was corroborated by the results of an X-ray study of TETP for the tetraprotonated, pentaprotonated and octaprotonated forms where the ring nitrogens 'moved' from the straight sections to the corners in the octaprotonated form.[42]

4.5 Characterisation of enantiopure lanthanide tetraamide complexes

Chiral complexes of these ions were investigated by circularly polarised luminescence and circular dichroism in a parallel study of the X-ray determined structures of chiral tetraamides. These chiroptical methods are a means of studying chiral complexes. When DOTA is unsubstituted, it exists as a pair of enantiomers. When it becomes derivatised, at the carbon α to the ring nitrogen (as in ***Figure 4.5.1.1***) or further along the pendant arm, it exists as a mixture of diastereomers.

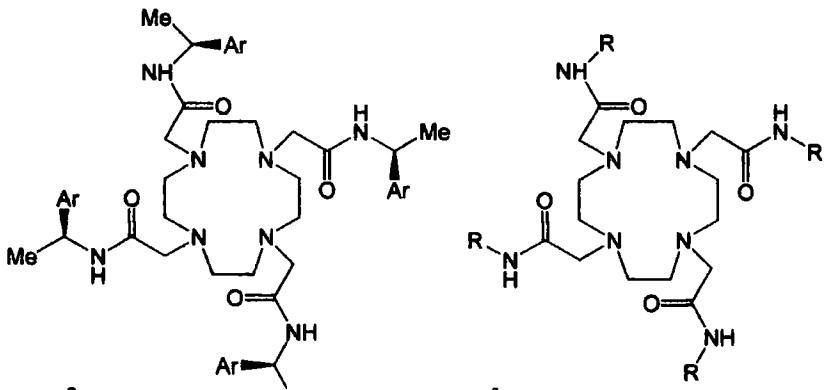

Figure 4.5.1 *– The chiral tetraamide ligands and their achiral analogue L^5. Lanthanide complexes of the chiral series have been enantiopure for employment as probes in circular dichroism and circular polarised luminescence spectroscopy.*

4.5.1 Stereoisomers of lanthanide complexes of DOTA derivatives

It is worth briefly reviewing the rules that apply when specifying the configuration at a stereocentre. A molecule and its non-identical mirror image are a pair of enantiomers. One will rotate the plane of polarised light to the right (clockwise); and it is dextrorotatory, defined as (+). The second will rotate the plane of polarised light to the left (counterclockwise); it is levorotatory, defined as (-). The R, S convention specifies unambiguously the absolute configuration of the four groups attached to a stereocentre. A racemic compound has equimolar quantities of the two enantiomers in the crystal. When more than one stereocentre is present, the molecule has 2^n

stereoisomers for n stereocenters. Compounds that are stereoisomers of one another, but are not enantiomers, are called diastereomers.

In the case of the tetraazacyclododecane derivatives, there is potential for 16 diastereomers. However, the inclusion of a remote stereocentre δ to the ring nitrogen incorporating bulky aryl groups effectively reduces the number of stereoisomers to a pair of enantiomers.

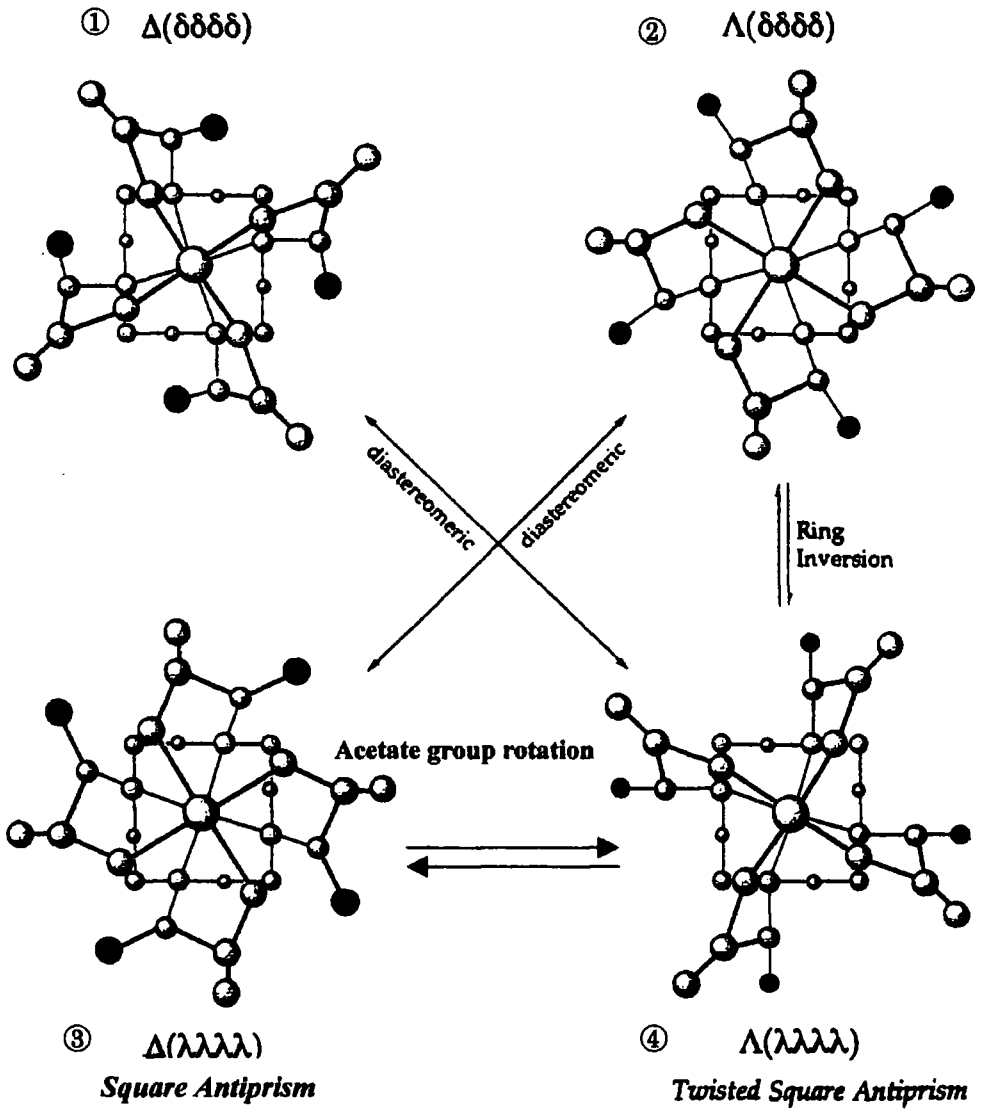

Figure 4.5.1.1 *- Stereoisomers of DOTA complex derivatives and their interconversions. The case of the stereocentre α to the ring nitrogen is depicted. Taken from reference 49.*

The chirality of the stereocentre, even in the case of the remote amide stereocentre of this series determines the conformation of the twelve membered tetraaza macrocycle. The second element of chirality is the conformation of the '[12]ane N_4'

cyclen ring. Ring inversion yields an alternate co-ordination polyhedron, the twisted square antiprism. The ring conformation is denoted δ or λ where δ is defines a positive N-C-C-N torsion angle and λ is defines a negative N-C-C-N torsion angle. The terms Δ/Λ refer to the handedness or helicity of the pendant arms. The opposite sign in the stereocentre on the pendant arms to the cyclen ring defines a square antiprism. The stereoisomers are summarised in ***Figure 4.5.1.1***.

4.5.2 Structural investigations of enantiopure lanthanide complexes incorporating phenyl chromophores

The study of the enantiopure series of complexes where the aryl group is a substituent on a remote stereocentre δ to the ring nitrogen yielded many structural insights. The tricationic complexes studied were the Eu·(*RRRR*)-L^2, Eu·(*SSSS*)-L^2 and Dy·(*SSSS*)-L^2.* These complexes were synthesised and crystallised by Rachel Dickins from the chemistry department at the University of Durham. Their structures adopt a square antiprismatic geometry whereby the tetraaza group and the four carboxy groups bind co-operatively to form this polyhedron. In the complexes of europium and dysprosium, this is monocapped by the binding of one water molecule above the plane of the four donor oxygen atoms.[9,10,50] ***Figure 4.5.2.1*** of Eu·(*S*) typifies the monocapped square antiprismatic co-ordination geometry Both the Eu·(*S*) and the Dy·(*S*) complexes of L^2 crystallise as trifluoromethanesulfonate salts with two additional acetonitrile and one water molecule in the asymmetric unit. The Eu·(*R*) complex of L^2 crystallises as the trifluoroacetate salt with four trifluoroacetate molecules and one hydroxyl anion per independent lanthanide complex. There is a consistent trend in all the complexes described herein whereby they do not crystallise in tetragonal crystal systems that contain the molecular four-fold symmetry elements. This is due in part to the effect of the other molecules that co-crystallise and break this symmetry.

*In this section, the notation will be abbreviated to Eu(*R*)-L^2 etc. since all the compounds are enantiopure.

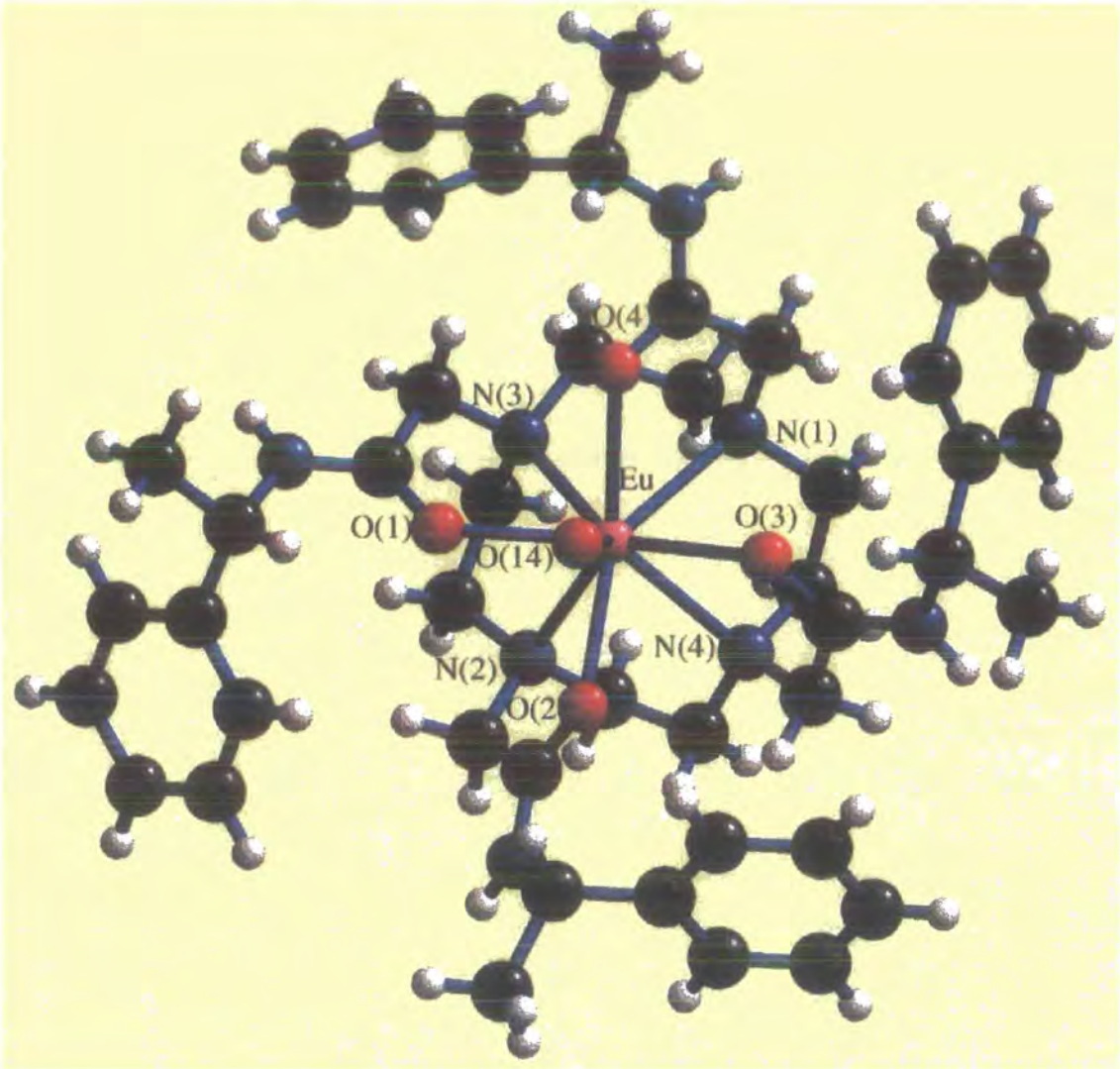

Figure 4.5.2.1 *- The monocapped square antiprismatic geometry in the structure of Eu·(S)-L*^{2}.

Details of the data collection and structural refinement of these three complexes are summarised in ***Table 4.5.2.1***. The data collections were carried out on the Siemens SMART-CCD device at 150(2) K according to the procedures set out in section 5.4 of chapter 3. All the crystals had well-defined sheer faces and were stable to atmospheric exposure. Fortunately, they formed reasonably equidimensional crystals that did not require potentially damaging cleavage. Thus, the anisotropy of the absorption effect was minimised. As can be seen from ***Figure 4.5.2.2***, the Dy·(*S*) and Eu·(*S*) complexes are crystallographically isostructural. The small differences in the unit cell dimensions can be attributed to the decrease in ionic radius from europium to dysprosium. All three molecules crystallise in the non centrosymmetric space group $P2_12_12_1$. The Eu·(*R*) complex is a mirror image of its Eu·(*S*) enantiomer and adopts an identical packing

motif. The overall loss of crystallographic isostructure is due to the incorporation of the reasonably bulky trifluoroacetate anions in the lattice.

***Table 4.5.2.1** – Selected crystal data for Eu·(SSSS)-L^2, Dy·(SSSS)-L^2, Eu·(RRRR)-L^2.*

Empirical formula	$C_{57}H_{75}EuF_9N_{11}O_{14}S_3$	$C_{57}H_{75}DyF_9N_{11}O_{14}S_3$	$C_{60}H_{73}EuF_{12}N_{10}O_{13}$
Formula weight	1557.42	1567.96	1522.24
Temperature	150(2) K	150 (2) K	150(2) K
Wavelength	0.71073 Å	0.71073 Å	0.71073 Å
Crystal system	Orthorhombic	Orthorhombic	Orthorhombic
Space group	$P2_12_12_1$	$P2_12_12_1$	$P2_12_12_1$
Unit cell dimensions	a = 15.7764(2) Å α= 90°. b = 20.4123(2) Å β= 90°. c = 21.7840(2) Å γ = 90°.	a = 15.7679(4) Å α= 90°. b = 20.3133(4) Å β= 90°. c = 21.7304(4) Å γ = 90°.	a = 14.9659(1) α= 90°. b = 18.4204(1) β= 90°. c = 24.9210(3) Å γ = 90°.
Volume	7015.2(1) $Å^3$	6960.2(3) $Å^3$	6870.2(1) $Å^3$
Z	4	4	4
Density (calculated)	1.475 g/cm^3	1.496 g/cm^3	1.472 g/cm^3
Absorption coefficient	1.074 mm^{-1}	1.255 mm^{-1}	1.011 mm^{-1}
Absorption correction	Empirical ψ-scans	Empirical ψ-scans	Empirical ψ-scans
Max. & min. transm.	0.70 and 0.61	0.60 and 0.75	0.28 and 0.23
F(000)	3192	3204	3112
Crystal size	0.4 x 0.3 x 0.2 mm^3	0.3 x 0.3 x 0.2 mm^3	0.4 x 0.3 x 0.3 mm^3
Theta range	1.37 to 28.16°.	1.37 to 25.79°	1.37 to 25.72°
Index ranges	-19<=h<=18, -24<=k<=26, -28<=l<=26	-18<=h<=11, -24<=k<=23, -26<=l<=26	-17<=h<=16, -22<=k<=21, -29<=l<=26
Reflections collected	55315	31346	36069
Independent reflects.	14735 [R(int) = 0.0709]	12047 [R(int) = 0.0590]	11766 [R(int) = 0.0303]
Refinement method	Full-matrix least-squares, F^2	Full-matrix least-squares, F^2	Full-matrix least-squares, F^2
Data/restrs./parameters	14735 / 0 / 860	12047 / 0 / 857	11766 / 2 / 839
Goodness-of-fit on F^2	1.045	1.129	1.030
R indices [I>2σ(I)]	R1 = 0.0491, wR2 = 0.1009	R1 = 0.0419, wR2 = 0.0989	R1 = 0.0298, wR2 = 0.0843
R indices (all data)	R1 = 0.0735, wR2 = 0.1145	R1 = 0.0495, wR2 = 0.1058	R1 = 0.0310, wR2 = 0.0859
Abs. structure parameter	-0.020(10)	-0.022(9)	-0.010(8)
Extinction coefficient	not refined	not refined	not refined
Largest peak and hole	0.909 and -1.599 $e.Å^{-3}$	0.976 and -1.064 $e.Å^{-3}$	0.912 and –0.604 $e.Å^{-3}$

The full list of atomic co-ordinates, bond lengths and angles and anisotropic displacement parameters can be found in the Appendices (***A.4.2-A.4.4***).

***Table 4.5.2.2** – Selected bond lengths (Å) for Eu·(SSSS)-L², Dy·(SSSS)-L², Eu·(RRRR)-L²*

Eu·(SSSS)-L²		Dy·(SSSS)-L²		Eu·(RRRR)-L²	
Eu(1)-O(4)	2.349(4)	Dy(1)-O(3)	2.308(4)	Eu(1)-O(2)	2.352(2)
Eu(1)-O(3)	2.365(4)	Dy(1)-O(2)	2.325(4)	Eu(1)-O(4)	2.356(2)
Eu(1)-O(2)	2.384(4)	Dy(1)-O(1)	2.342(4)	Eu(1)-O(1)	2.374(3)
Eu(1)-O(1)	2.427(4)	Dy(1)-O(4)	2.382(4)	Eu(1)-O(3)	2.384(3)
Eu(1)-O(5)	2.442(4)	Dy(1)-O(5)	2.422(3)	Eu(1)-O(5)	2.426(2)
Eu(1)-N(1)	2.641(4)	Dy(1)-N(4)	2.609(4)	Eu(1)-N(3)	2.688(3)
Eu(1)-N(4)	2.677(5)	Dy(1)-N(3)	2.647(5)	Eu(1)-N(1)	2.693(3)
Eu(1)-N(2)	2.685(4)	Dy(1)-N(1)	2.656(5)	Eu(1)-N(4)	2.694(3)
Eu(1)-N(3)	2.710(5)	Dy(1)-N(2)	2.676(4)	Eu(1)-N(2)	2.716(3)
O(1)-C(12)	1.231(7)	O(1)-C(12)	1.251(7)	O(1)-C(12)	1.246(5)
O(2)-C(22)	1.275(7)	O(2)-C(22)	1.260(7)	O(2)-C(22)	1.262(4)
O(3)-C(32)	1.253(7)	O(3)-C(32)	1.249(7)	O(3)-C(32)	1.244(5)
O(4)-C(42)	1.260(6)	O(4)-C(42)	1.234(7)	O(4)-C(42)	1.256(4)
N(1)-C(8)	1.493(7)	N(1)-C(11)	1.475(7)	N(1)-C(11)	1.484(5)
N(1)-C(1)	1.499(7)	N(1)-C(1)	1.480(8)	N(1)-C(1)	1.485(5)
N(1)-C(11)	1.502(8)	N(1)-C(8)	1.496(7)	N(1)-C(8)	1.499(5)
N(2)-C(21)	1.472(7)	N(2)-C(21)	1.458(7)	N(2)-C(3)	1.491(5)
N(2)-C(3)	1.477(8)	N(2)-C(3)	1.479(7)	N(2)-C(21)	1.484(5)
N(2)-C(2)	1.502(7)	N(2)-C(2)	1.499(7)	N(2)-C(2)	1.494(5)
N(3)-C(31)	1.462(7)	N(3)-C(31)	1.486(7)	N(3)-C(31)	1.481(5)
N(3)-C(5)	1.491(6)	N(3)-C(5)	1.489(7)	N(3)-C(4)	1.490(5)
N(3)-C(4)	1.503(7)	N(3)-C(4)	1.495(8)	N(3)-C(5)	1.482(5)
N(4)-C(6)	1.477(8)	N(4)-C(7)	1.481(7)	N(4)-C(7)	1.484(5)
N(4)-C(7)	1.485(7)	N(4)-C(6)	1.490(7)	N(4)-C(41)	1.487(5)
N(4)-C(41)	1.496(7)	N(4)-C(41)	1.512(7)	N(4)-C(6)	1.491(5)
N(5)-C(12)	1.332(7)	N(5)-C(12)	1.314(8)	N(5)-C(12)	1.323(5)
N(5)-C(13)	1.477(7)	N(5)-C(13)	1.489(8)	N(5)-C(13)	1.467(5)
N(6)-C(22)	1.302(8)	N(6)-C(22)	1.307(8)	N(6)-C(22)	1.309(5)
N(6)-C(23)	1.468(8)	N(6)-C(23)	1.491(8)	N(6)-C(23)	1.485(5)
N(7)-C(32)	1.334(7)	N(7)-C(32)	1.316(7)	N(7)-C(32)	1.320(5)
N(7)-C(33)	1.498(8)	N(7)-C(33)	1.476(7)	N(7)-C(33)	1.469(6)
N(8)-C(42)	1.320(7)	N(8)-C(42)	1.343(8)	N(8)-C(42)	1.320(5)
N(8)-C(43)	1.476(7)	N(8)-C(43)	1.467(8)	N(8)-C(43)	1.475(6)
C(1)-C(2)	1.515(8)	C(7)-C(8)	1.509(8)	C(1)-C(2)	1.518(6)
C(3)-C(4)	1.521(8)	C(1)-C(2)	1.519(9)	C(3)-C(4)	1.525(5)
C(5)-C(6)	1.518(8)	C(3)-C(4)	1.514(8)	C(5)-C(6)	1.528(6)
C(7)-C(8)	1.533(7)	C(5)-C(6)	1.529(8)	C(7)-C(8)	1.532(6)
C(11)-C(12)	1.530(8)	C(11)-C(12)	1.509(8)	C(11)-C(12)	1.523(5)
C(21)-C(22)	1.511(9)	C(21)-C(22)	1.528(8)	C(21)-C(22)	1.516(5)
C(31)-C(32)	1.528(8)	C(31)-C(32)	1.516(8)	C(31)-C(32)	1.522(5)
C(41)-C(42)	1.519(8)	C(41)-C(42)	1.514(8)	C(41)-C(42)	1.518(6)

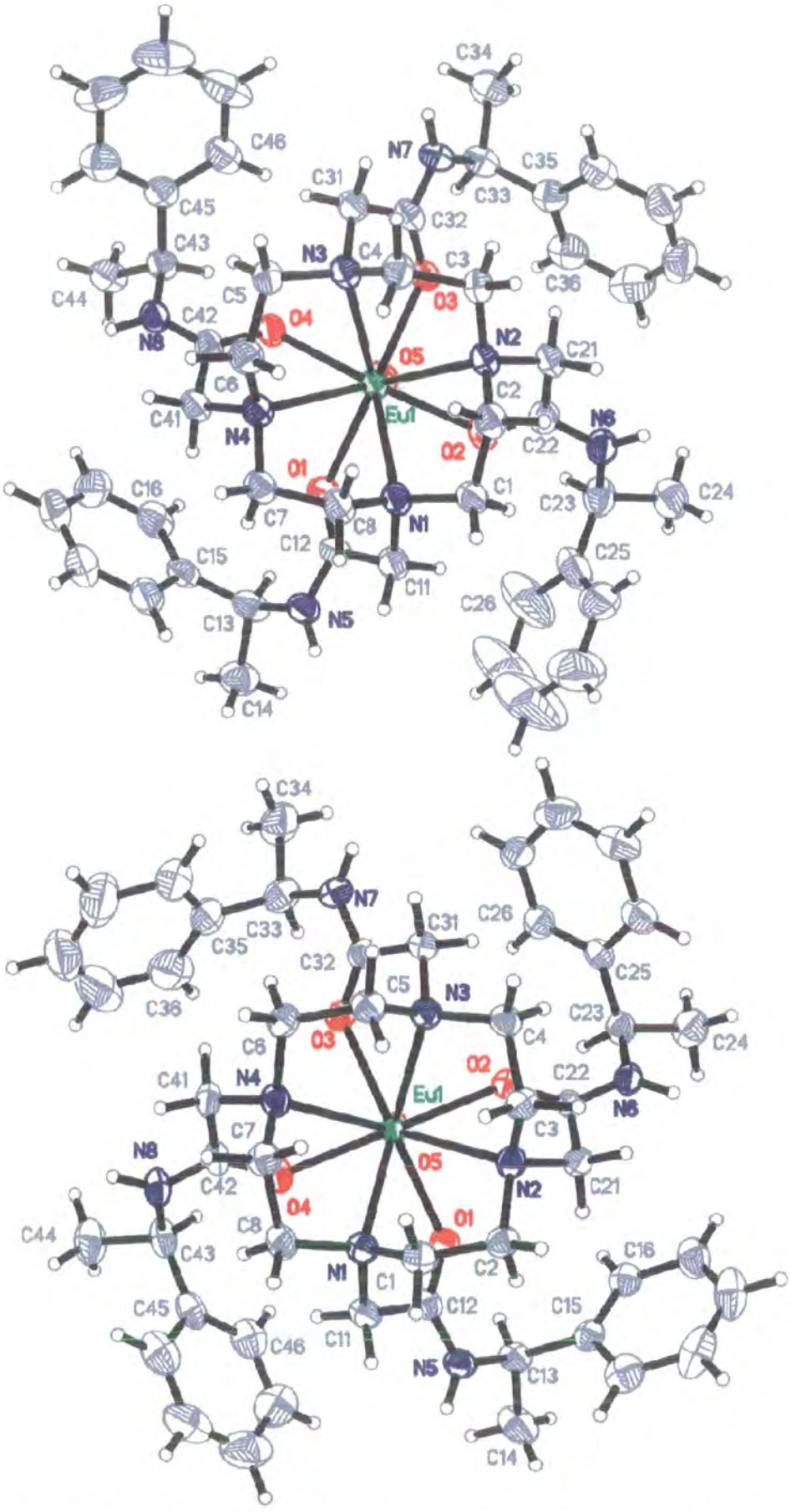

***Figure 4.5.2.2** –Thermal ellipsoid plot (50%) of* L^3 *complexes, above: Eu·(S), below: Eu·(R).*

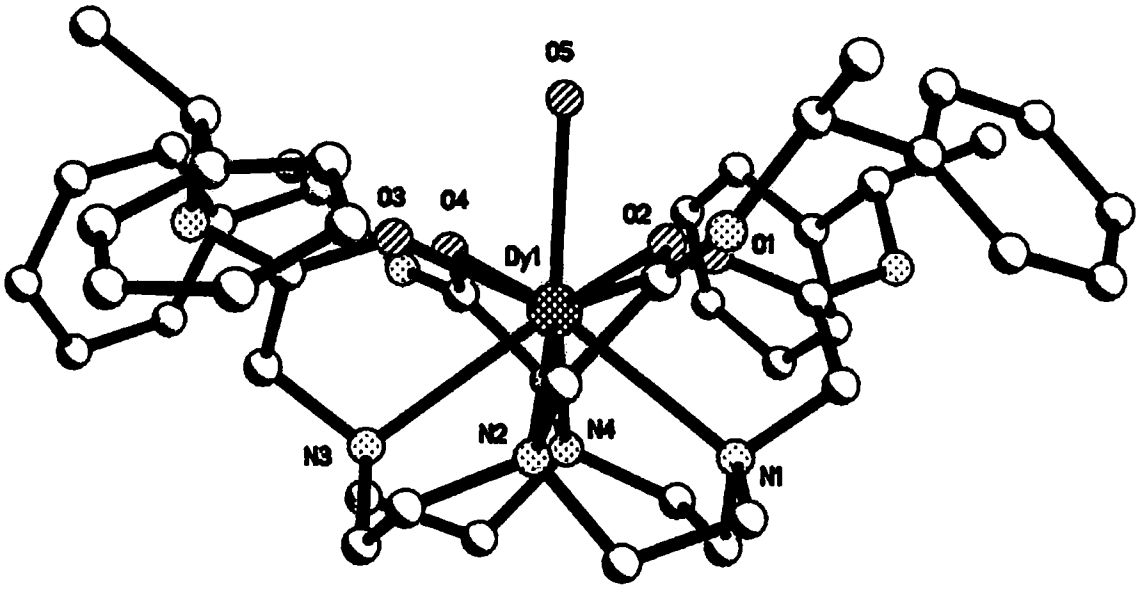

***Figure 4.5.2.3** – A view of the Dy·(S)-L² complex, rotated by 90° from the orientation on the previous figure which is along the Ln-OH₂ bond. The chirality at the remote amide stereocentre dictates the helicity or handedness of the phenyl groups. Hydrogen atoms have been omitted for clarity.*

The values for the absolute structure (Flack) parameter in ***Table 4.5.2.1*** confirm that all the refinements were carried out with the correct polarity and that the data were also of good enough quality to determine these values to a high precision. The N-C-C-N and N-C-C-O torsion angles averaged at -59.5 and 31.9° for Eu·(*SSSS*)-L^2, -58.5 and 29.7° for Dy·(*SSSS*)-L^2 and 58.7 and –30.2° for Eu·(*RRRR*)-L^2 consistent with a square antiprismatic geometry. The twist angle of the N4/O4 planes with respect to each other were 38.3° for Eu·(*SSSS*)-L^2, 39.0° for Dy·(*SSSS*)-L^2 and 38.5° for Eu·(*RRRR*)-L^2

On viewing the complexes' bond lengths in ***Table 4.5.2.2***, it is clear that in all cases the lanthanide ion is not equidistant from both the N4 and O4 planes. There is a range of 0.08(4) Å between the closest and the furthest oxygen atoms from the metal in Eu·(*SSSS*)-L^2. There is a contraction of 0.02 Å of the ligand donor atoms toward the metal in the Dy·(*SSSS*)-L^2 complex because of the lanthanide contraction. The mean Ln-N bond lengths decrease from 2.68 to 2.65 Å from Eu·(*SSSS*)-L^2 to Dy·(*SSSS*)-L^2 and the mean Ln-O bond length (excluding the bound water molecule) decreases from 2.38 to 2.34 Å for the same two molecules. The Yb·(*RRRR*)-L^2 complex recently appeared in the literature[51] has mean Yb-N and Yb-O bond lengths of 2.62 and 2.28 Å respectively.

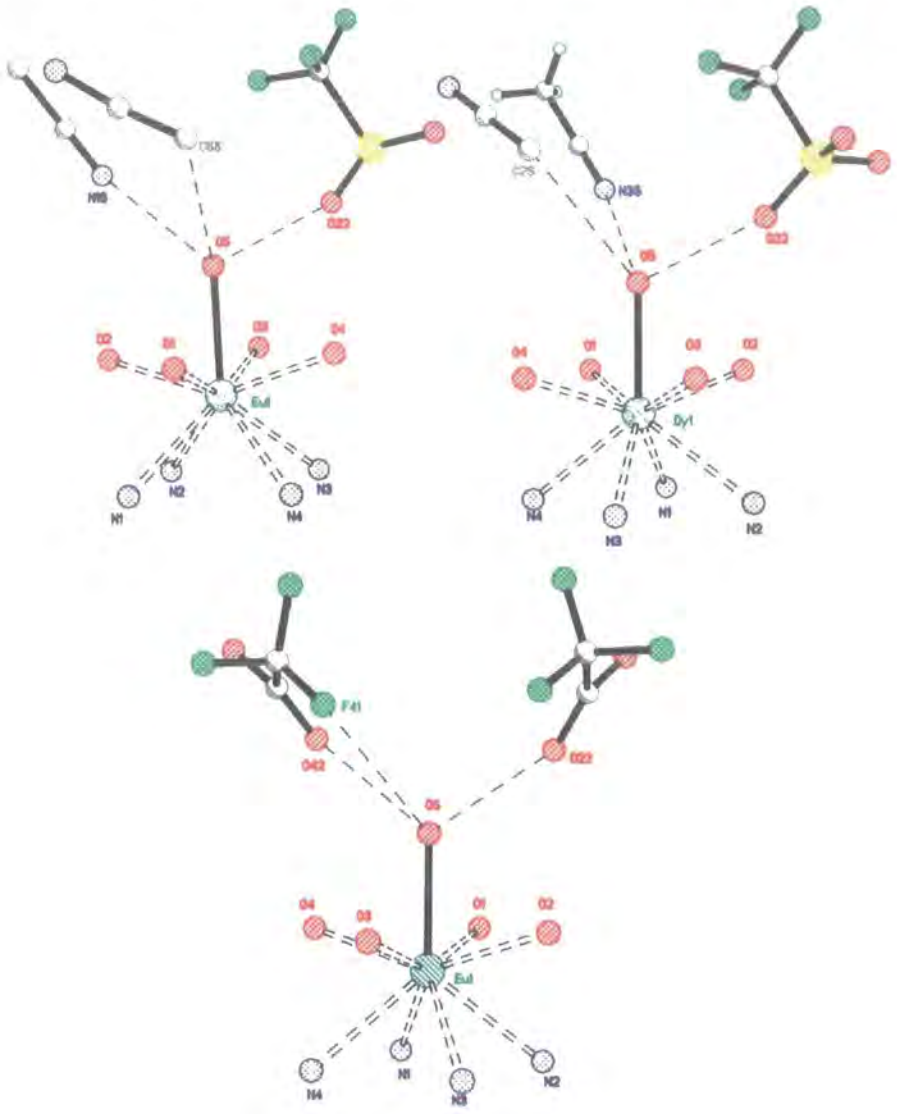

Figure 4.5.2.4 *– Three illustrations of the interactions / close contacts between the lanthanide ion bound water molecule and the counter ions or solvent molecules. In all cases, the macrocyclic 'shrubbery' has been removed for clarity. Top left: Eu·(S), top right: Dy·(S), bottom: Eu·(R). Note the similarity in the arrangement of the distinctly different anions about the water in the Eu·(R)-L² to the former two complexes.*

These do not appear to be very strained complexes and chemically equivalent bond lengths around the cyclen ring are equal within experimental precision. Despite the presence of a very different counter ion in the Eu·(*RRRR*)-L^2 complex, the molecular packing remains unchanged and it also crystallises in $P2_12_12_1$. The reason for this is revealed in looking at the close contacts between the bound water molecule and the counter ions and solvent molecules in ***Figure 4.5.2.4.*** When the Eu·(*RRRR*)-L^2 complex is juxtaposed along side the Eu·(*SSSS*)-L^2 and Dy·(*SSSS*)-L^2 complexes, it is

clear that the trifluroacetates bind in the same manner and occupy an approximately equal volume.

4.5.3 Structural investigations of enantiopure tetraamide ligands incorporating naphthyl and quinoline chromophores

The investigations of the structures of enantiopure lanthanide complexes derived from DOTA next focussed on the naphthyl and quinoline analogues of the tetraamide series. The naphthyl complex was synthesised and crystallised by Rachel Dickins and the quinoline derivative by Linda Govenlock from the chemistry department at the University of Durham. Again the placement of a stereogenic centre δ to the ring nitrogen imparts conformational rigidity and leads to the formation of an enantiopure complex that as before crystallises in the chiral space group $P2_12_12_1$. Both the naphthyl and quinoline analogues are eight co-ordinate, which can be attributed to the decrease in ionic radius for sodium and the increased bulk of this ligand. From ***figures 4.5.3.1*** and ***4.5.3.2*** showing both complexes, it can be seen that the sodium ion is encapsulated completely by its co-ordination sphere and then the naphthyl and quinoline groups fold in on it. Lanthanide complexes bearing naphthyl and quinoline aromatic groups are known to luminesce strongly.[52,53,54] The remote naphthyl group has been shown to act as an antenna for energy transfer to the europium ion.[55,56] The strong metal binding capability of these macrocycles is exemplified by the fact that what should have been the structures of free ligands here has turned out to be complexes since they ligated sodium ions in solution. Data for the naphthyl complex was collected on a laboratory source SMART instrument using Mo Kα radiation,[57,58] whereas the quinoline complex was collected at Daresbury station 9.8.[59] The data collection details on station 9.8 and structure solution using Professor George Sheldrick's program HALF BAKED are presented elsewhere.[59] Selected data collection and structure refinement details are presented in ***Table 4.5.3.1***. It is interesting to note that virtually the same amount of data could be acquired from the quinoline crystal at the synchrotron source although the crystal of naphthyl analogue has a volume four times its size.

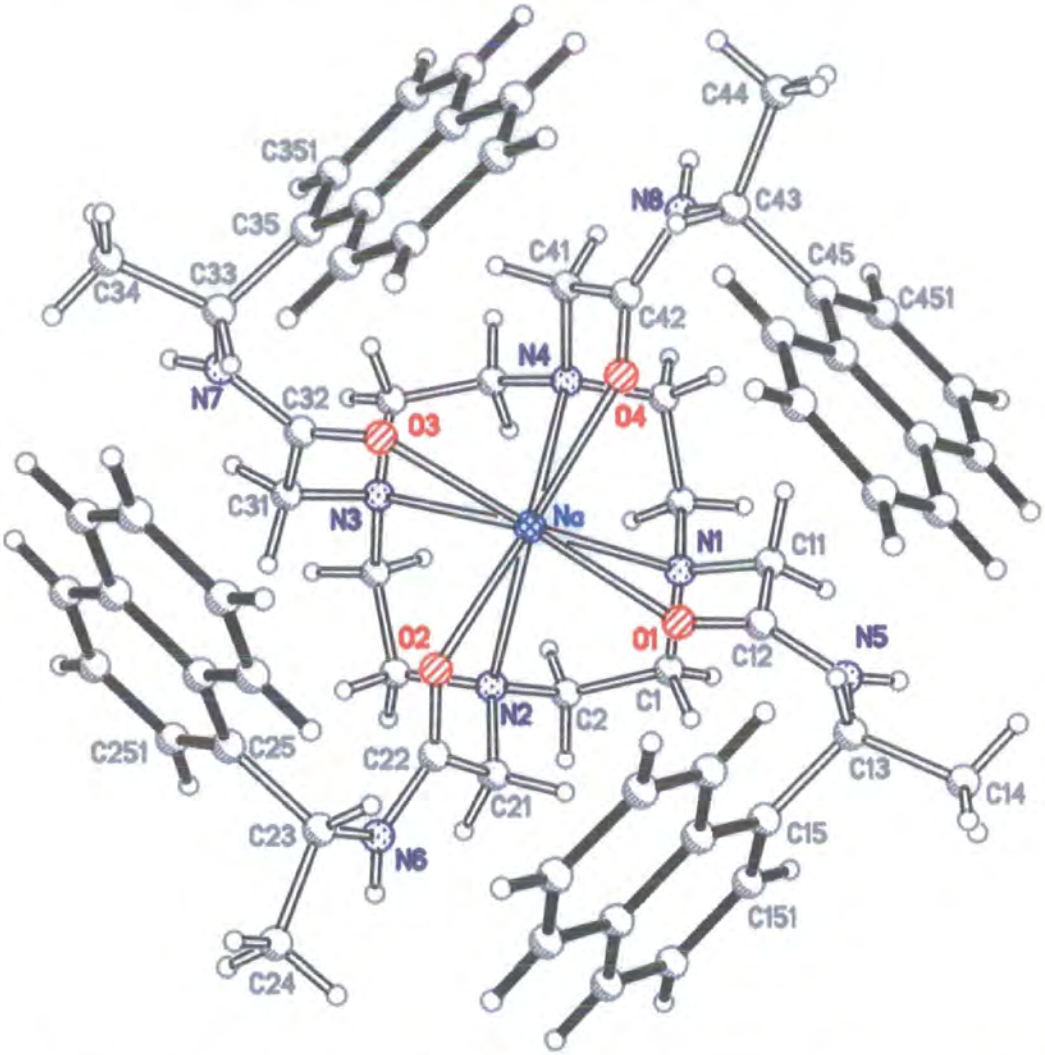

Figure 4.5.3.1 *– A view of the eight co-ordinate sodium tetraamide complex with naphthyl substituents. The co-ordination geometry about the metal is twisted square antiprismatic. The naphthyl groups, which engage in excimer coupling, are drawn with darker bonds.*

The absolute configuration of the naphthyl complex could not be determined reliably from the X-ray data. It was known to be the (*RRRR*)- isomer from the synthetic route and it is therefore refined with this polarity. The absolute structure of the quinoline analogue was determined from the crystallographic experiment (see the Flack parameter in ***Table 4.5.3.2***) to be the (*SSSS*)-isomer and thus the mirror image of the naphthyl derivative.

Both complexes crystallise as twisted square antiprisms, which are not at all uncommon for eight coordinate complexes of DOTA-like ligands. The torsion angles, defining the absolute configuration of the cyclen ring and the four pendant arms, are shown in ***Table 4.5.3.1***.

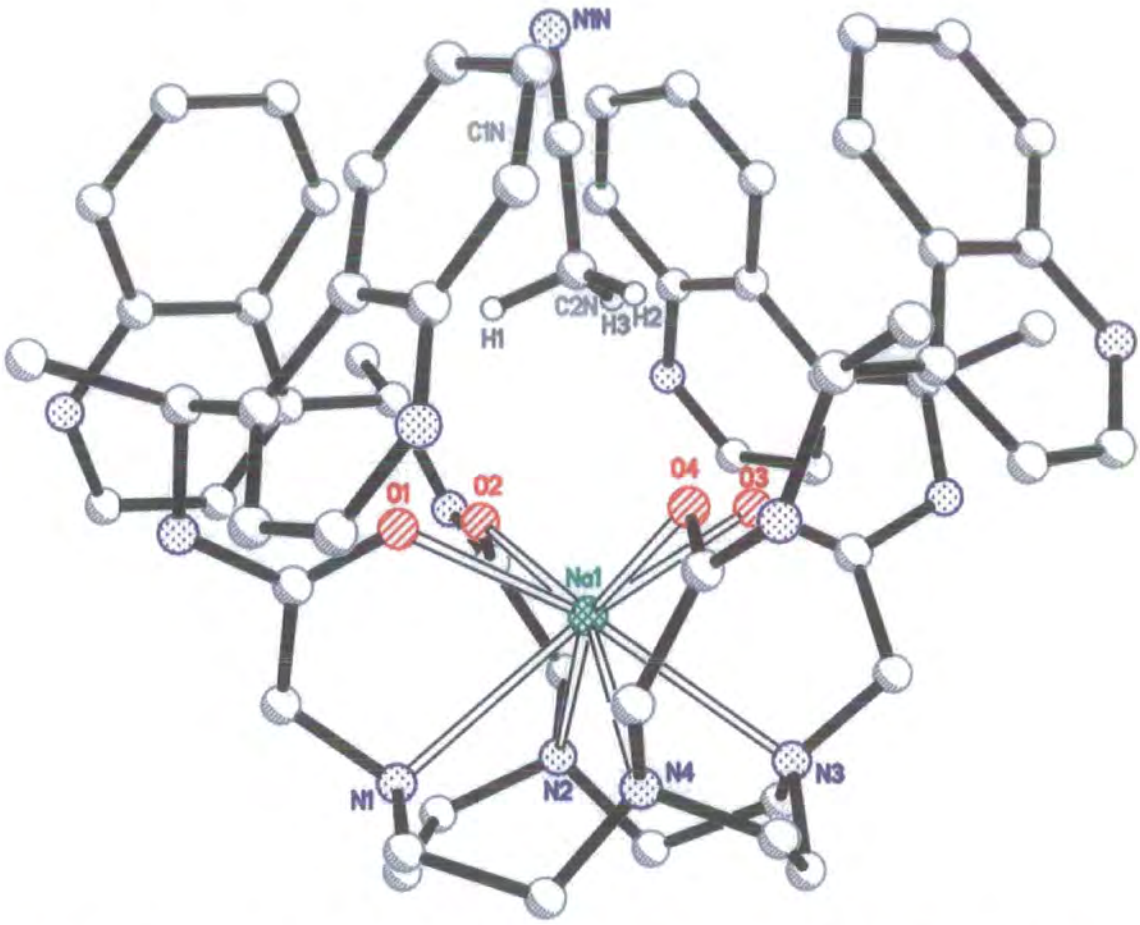

Figure 4.5.3.2 *– A view of the eight co-ordinate sodium tetraamide complex with quinoline functional groups. The structure is basket-shaped with the metal encapsulated in the centre. As is the case of the naphthyl complex analogue, the acetonitrile is inserted into the groove defined by the rings.*

The sign on both sets of angles for each complex are the same defining them as twisted square antiprisms.

Table 4.5.3.1 *- Selected torsion angles (°) for sodium complexes of L^3 and L^4.*

	Na·*(RRRR)*-L^3	Na·*(SSSS)*-L^4
N(1)-C(1)-C(2)-N(2)	-58.5 (6)	60.0 (1.0)
N(2)-C(3)-C(4)-N(3)	-61.1 (7)	59.1 (9)
N(3)-C(5)-C(6)-N(4)	-59.0 (7)	60.7 (1.0)
N(4)-C(7)-C(8)-N(1)	-61.7 (6)	62.6 (1.0)
N(1)-C(11)-C(12)-O(1)	-40.0 (8)	32.3 (1.2)
N(2)-C(21)-C(22)-O(2)	-37.1 (8)	32.7 (1.1)
N(3)-C(31)-C(32)-O(3)	-42.0 (8)	38.5 (1.1)
N(4)-C(41)-C(42)-O(4)	-37.4 (8)	42.5 (1.1)

The bond lengths to the atoms of the co-ordination sphere are in ***Table 4.5.3.2***. This shows the oxophilicity of the metal, qualifying it as a hard acid and hence it is displaced toward the O4 plane. The distances are very similar to those in lanthanide complexes.

***Table 4.5.3.2** - Selected crystal data for $C_{64}H_{76}ClN_{14}NaO_5$ and $C_{68}H_{75}F_3N_9NaO_6$*

Empirical formula	$C_{64}H_{76}ClN_{14}NaO_5$	$C_{68}H_{75}F_3N_9NaO_6$
Formula weight	1179.83	1194.36
Temperature	150(2) K	150(2) K
Wavelength	0.6875 Å	0.71073 Å
Crystal system	Orthorhombic	Orthorhombic
Space group	$P2_12_12_1$	$P2_12_12_1$
Unit cell dimensions	a = 12.0573(14) Å α= 90°. b = 14.6746(17) Å β= 90°. c = 34.231(4) Å γ = 90°.	a = 15.0215(12) Å α= 90°. b = 17.1363(14) Å β= 90°. c = 23.8997(14) Å γ = 90°.
Volume	6056.7(12) $Å^3$	6152.1(8) $Å^3$
Z	4	4
Density (calculated)	1.294 g/cm^3	1.290 g/cm^3
Absorption coefficient	0.133 mm^{-1}	0.096 mm^{-1}
F(000)	2504	2528
Crystal size	0.25 x 0.15 x 0.10 mm^3	0.30 x 0.25 x 0.20 mm^3
θ range for data collection	1.15 to 22.52°.	1.46 to 22.50°.
Index ranges	-13<=h<=13, -16<=k<=13, -18<=l<=37	-18<=h<=18, -20<=k<=19, -27<=l<=28
Reflections collected	31543	26944
Independent reflections	8734 [R(int) = 0.0738]	8046 [R(int) = 0.0748]
Absorption correction	Multiscan – Sadabs	Empirical
Max. and min. transmission	0.99 and 0.97	0.78 and 0.71
Refinement method	Full-matrix least-squares on F^2	Full-matrix least-squares on F^2
Data / restraints / parameters	8734 / 4 / 757	7364 / 0 / 745
Goodness-of-fit on F^2	1.092	1.037
Final R indices [I>2sigma(I)]	R1 = 0.1044, wR2 = 0.2813	R1 = 0.0705, wR2 = 0.1713
R indices (all data)	R1 = 0.1243, wR2 = 0.2916	R1 = 0.1149, wR2 = 0.2096
Absolute structure parameter	-0.1(2)	-0.5(9)
Extinction coefficient	0.0048(9)	None
Largest diff. peak and hole	0.537 and –0.519 $e.Å^{-3}$	0.654 and -0.526 $e.Å^{-3}$

The full list of atomic co-ordinates, bond lengths and angles and anisotropic displacement parameters can be found in the Appendices (***A.4.5-A.4.6***).

Table 4.5.3.3 *– Selected bond lengths (Å) for $C_{68}H_{75}F_3N_9NaO_6$ and $C_{64}H_{76}ClN_{14}NaO_5$ the enantiopure S complexes of L^3 and L^4 respectively.*

The sodium complex with naphthyl sidechains				*The sodium complex with quinoyl sidechains*			
Na-O(4)	2.443(5)	C(5)-C(6)	1.510(8)	Na(1)-O(3)	2.404(6)	C(5)-C(6)	1.531(12)
Na-O(3)	2.453(4)	C(7)-C(8)	1.522(8)	Na(1)-O(2)	2.411(6)	C(7)-C(8)	1.512(13)
Na-O(2)	2.454(5)	C(11)-C(12)	1.528(8)	Na(1)-O(4)	2.433(6)	C(11)-C(12)	1.481(12)
Na-O(1)	2.493(4)	C(13)-C(14)	1.527(8)	Na(1)-O(1)	2.459(6)	C(13)-C(15)	1.502(13)
Na-N(1)	2.700(5)	C(13)-C(15)	1.527(9)	Na(1)-N(4)	2.649(7)	C(13)-C(14)	1.589(13)
Na-N(3)	2.712(5)	C(15)-C(151)	1.365(8)	Na(1)-N(1)	2.671(7)	C(15)-C(151)	1.363(13)
Na-N(4)	2.728(5)	C(15)-C(159)	1.443(8)	Na(1)-N(2)	2.693(7)	C(15)-C(159)	1.457(14)
Na-N(2)	2.733(5)	C(21)-C(22)	1.536(8)	Na(1)-N(3)	2.715(7)	C(21)-C(22)	1.545(12)
O(1)-C(12)	1.227(7)	C(23)-C(24)	1.524(9)	O(1)-C(12)	1.231(10)	C(23)-C(25)	1.482(12)
O(2)-C(22)	1.228(7)	C(23)-C(25)	1.536(9)	O(2)-C(22)	1.203(10)	C(23)-C(24)	1.529(13)
O(3)-C(32)	1.233(7)	C(25)-C(251)	1.380(9)	O(3)-C(32)	1.212(10)	C(25)-C(251)	1.346(14)
O(4)-C(42)	1.239(7)	C(25)-C(259)	1.425(9)	O(4)-C(42)	1.211(10)	C(25)-C(259)	1.406(13)
N(1)-C(11)	1.441(7)	C(31)-C(32)	1.507(8)	N(1)-C(1)	1.458(11)	C(31)-C(32)	1.519(11)
N(1)-C(1)	1.465(7)	C(33)-C(35)	1.501(8)	N(1)-C(11)	1.461(11)	C(33)-C(34)	1.518(14)
N(1)-C(8)	1.470(7)	C(33)-C(34)	1.525(8)	N(1)-C(8)	1.491(11)	C(33)-C(35)	1.516(14)
N(2)-C(21)	1.458(7)	C(35)-C(351)	1.388(8)	N(2)-C(21)	1.458(11)	C(35)-C(351)	1.395(13)
N(2)-C(3)	1.463(7)	C(35)-C(359)	1.456(9)	N(2)-C(3)	1.460(11)	C(35)-C(359)	1.416(14)
N(2)-C(2)	1.473(7)	C(41)-C(42)	1.519(8)	N(2)-C(2)	1.478(11)	C(41)-C(42)	1.482(13)
N(3)-C(4)	1.461(7)	C(43)-C(45)	1.538(9)	N(3)-C(31)	1.434(11)	C(43)-C(45)	1.475(13)
N(3)-C(31)	1.467(7)	C(43)-C(44)	1.544(9)	N(3)-C(5)	1.442(10)	C(43)-C(44)	1.537(13)
N(3)-C(5)	1.469(7)	C(45)-C(451)	1.384(8)	N(3)-C(4)	1.464(11)	C(45)-C(451)	1.372(14)
N(4)-C(6)	1.459(7)	C(45)-C(459)	1.427(9)	N(4)-C(7)	1.448(10)	C(45)-C(459)	1.432(13)
N(4)-C(41)	1.475(7)	C(151)-C(152)	1.418(9)	N(4)-C(6)	1.464(11)	C(151)-C(152)	1.416(15)
N(4)-C(7)	1.476(7)	C(152)-C(153)	1.370(9)	N(4)-C(41)	1.479(11)	N(153)-C(152)	1.291(15)
N(5)-C(12)	1.344(7)	C(153)-C(154)	1.418(9)	N(5)-C(12)	1.354(11)	N(153)-C(154)	1.358(14)
N(5)-C(13)	1.468(7)	C(251)-C(252)	1.383(9)	N(5)-C(13)	1.453(12)	C(251)-C(252)	1.459(16)
N(6)-C(22)	1.342(7)	C(252)-C(253)	1.365(10)	N(6)-C(22)	1.373(11)	N(253)-C(252)	1.327(17)
N(6)-C(23)	1.469(8)	C(253)-C(254)	1.402(10)	N(6)-C(23)	1.449(12)	N(253)-C(254)	1.366(16)
N(7)-C(32)	1.356(7)	C(351)-C(352)	1.427(9)	N(7)-C(32)	1.393(12)	C(351)-C(352)	1.419(15)
N(7)-C(33)	1.472(7)	C(352)-C(353)	1.359(9)	N(7)-C(33)	1.439(12)	N(353)-C(352)	1.273(14)
N(8)-C(42)	1.342(8)	C(353)-C(354)	1.400(9)	N(8)-C(42)	1.341(11)	N(353)-C(354)	1.409(13)
N(8)-C(43)	1.489(7)	C(451)-C(452)	1.409(9)	N(8)-C(43)	1.497(12)	C(451)-C(452)	1.346(15)
C(1)-C(2)	1.520(8)	C(452)-C(453)	1.362(9)	C(1)-C(2)	1.488(13)	N(453)-C(454)	1.324(13)
C(3)-C(4)	1.510(8)	C(453)-C(454)	1.418(9)	C(3)-C(4)	1.565(12)	N(453)-C(452)	1.338(14)

The eight co-ordinate complexes have twisted square anti-prismatic geometry, where the mean N-Na-O twist angle is 36°. These complexes are isostructural, which is best shown by superimposing the two complexes, in ***Figure 4.5.3.3***.

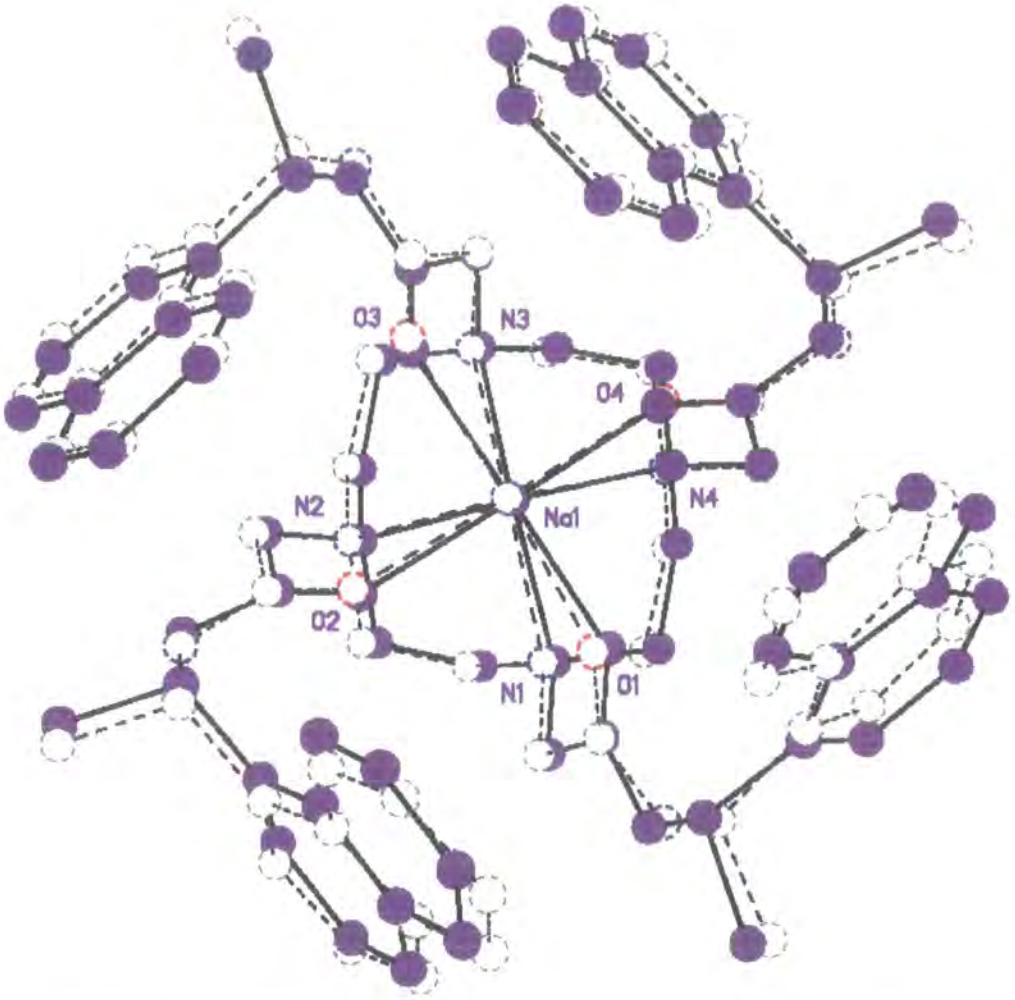

Figure 4.5.3.3 *– A superimposition of sodium tetraamide complexes with naphthyl (in purple) and quinoline (colourless with red and blue heteroatoms) pendant arms reveals the sodium complexes themselves to be isostructural, that main differences are observed in the orientations of the pendant arms which are relatively less rigid (Note. The co-ordinates of the tetranaphthylamide complex were first inverted). These differences cannot be attributed to a crystal packing effect. The sodium metal and heteroatoms on the cyclen alone are labelled for clarity.*

A chloride counter ion, one well-ordered water molecule and two molecules of acetonitrile are also present in the asymmetric unit of the quinoline structure, whereas the naphthyl structure crystallises with one trifluoroacetate and one acetonitrile per independent molecule. As can be seen from ***Figure 4.5.3.2***, one of the acetonitrile molecules is inserted into the groove defined by the quinoline groups, the nearest solvent hydrogen being 3.38(1) Å from the metal atom. This provides a stabilising effect and the lower thermal motion in these particular solvent molecule atoms is reflected in the reduced values of their thermal parameters. The fact that this overall

structure is not crystallographically isostructural with its tetranaphthylamide analogue cannot be ascribed to any structure determining intermolecular interactions or conformational changes between the two complexes. One must assume that this is because of the presence of a relatively bulky trifluoroacetate counter ion in the lattice of the quinoline crystal structure.

4.5.4 Enantiopure complexes of tetraamide DOTA bearing ester groups

The europium and gadolinium complexes of L^5 are isostructural[60] and crystallise in the chiral space group $P2_12_12_1$. These complexes were synthesised and crystallised by Alvaro de Sousa from the chemistry department at the University of Durham. They are enantiopure complexes with the remote stereocentre δ to the ring nitrogen and the (*SSSS*)- isomers are reported here. The overall structure of the central part of the co-ordination complexes agree well with the other tetraamide derivatives that have been studied here and as can be seen from ***Table 4.5.4.1*** the torsion angles are equal to those reported for the tetraamide complexes bearing phenyl, naphthyl and quinoline chromophores. The absolute configuration can therefore be designated as Δ(λλλλ) here. The Flack parameter of -0.03(1) for Eu·*(SSSS)*-L^5 and -0.03(1) for Gd·*(SSSS)*-L^5 shown that the refinements have been carried out with the correct polarity and that the level of precision is satisfactory here.

Table 4.5.4.1 *- Selected torsion angles (°) for europium and gadolinium complexes of L^5.*

	Eu·*(SSSS)*-L^5	Gd·*(SSSS)*-L^5
N(1)-C(1)-C(2)-N(2)	-57.7(8)	-56.4(13)
N(2)-C(3)-C(4)-N(3)	-58.4(9)	-56.2(16)
N(3)-C(5)-C(6)-N(4)	-60.1(8)	-58.5(13)
N(4)-C(7)-C(8)-N(1)	-59.3(1)	-60.6(14)
N(1)-C(11)-C(12)-O(1)	32.8(8)	32.2(12)
N(2)-C(21)-C(22)-O(2)	22.5(9)	23.8(14)
N(3)-C(31)-C(32)-O(3)	30.3(9)	28.2(14)
N(4)-C(41)-C(42)-O(4)	28.7(9)	29.1(14)

The complexes are monocapped square antiprisms and the twist angle of the O4 plane with respect to the N4 plane is 39.6° for both the complexes and the 'bite' angle (N-Ln-O) is 66.29° for the europium complex and 66.13° for the gadolinium complex, effectively the same within experimental error.

These are tricationic complexes and co-crystallise with three well-ordered hexafluorophosphate anions in the asymmetric unit and a water molecule. The refinement of the both models were carried out with all of the lanthanide complex and the three hexafluorophosphates, excluding the water with anisotropic displacement parameters. The hydrogen atoms were placed in calculated positions (riding model). It was also possible to locate the water protons from these difference Fourier syntheses.

The bond lengths for both complexes are in ***Table 4.5.4.3***. The europium complex binds the water molecule more tightly with the interatomic distance to O5 shorter by 0.02 Å. The mean lanthanide distance to the N4 and O4 donor sets decreases by 0.01 Å on going from europium to gadolinium. This is a consequence of the larger ionic size and larger bite angle in the europium complex. Interestingly, there is a distortion in the mono-capped square antiprismatic geometry. The europium and gadolinium distances to the O(1) are longer by 0.04 Å. This is not unusual for these complexes and has been observed for all the tetraamide derivatives including the eight co-ordinate sodium derivatives. For these two complexes however the distances to the 'distorted' oxygen are longer than the distances to the bound water molecule. Larger fluctuation is generally observed with the O4 plane than the N4 plane. There is also a trend of the longest distance to oxygen, being on the carboxyl group appended to the ring nitrogen atom that has the shortest distance to the metal, and *vice versa*. Thus, the square antiprism is not a distorted polyhedron but the lanthanide ion has some flexibility to move within it.

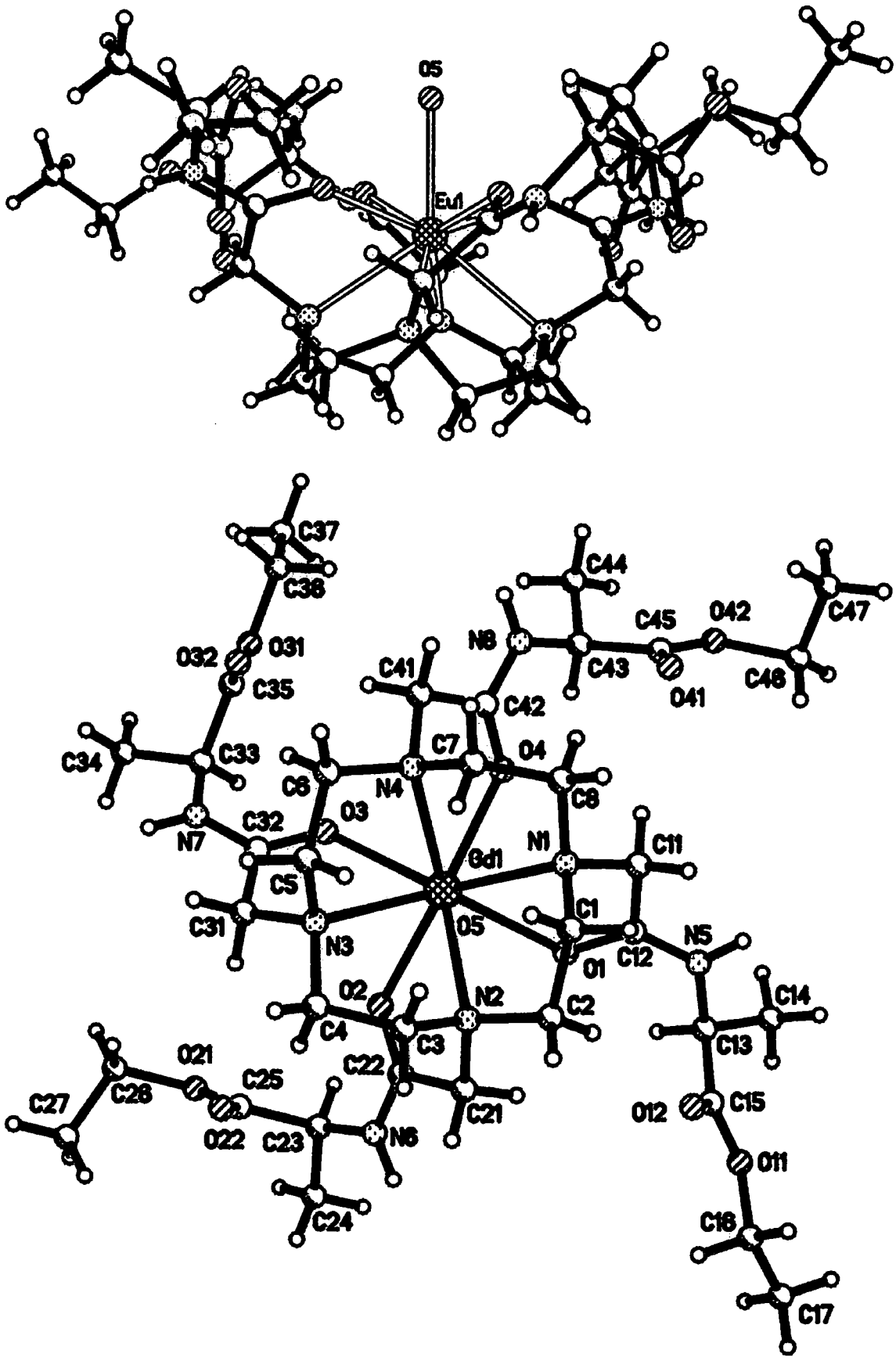

Figure 4.5.4.1 *– Two views of the isostructural europium (top) and gadolinium (bottom) complexes of L^5, (the bound water molecule is obscured in the gadolinium complex).*

***Table 4.5.4.2** – Selected crystal for $C_{36}H_{69}EuF_{18}N_8O_{14.5}P_3$ and $C_{36}H_{68}F_{18}GdN_8O_{14}P_3$.*

Empirical formula	$C_{36}H_{69}EuF_{18}N_8O_{14.5}P_3$	$C_{36}H_{68}F_{18}GdN_8O_{14}P_3$
Formula weight	1432.86	1429.14
Temperature	150(2) K	150(2) K
Wavelength	0.71073 Å	0.71073 Å
Crystal system	Orthorhombic	Orthorhombic
Space group	$P2_12_12_1$	$P2_12_12_1$
Unit cell dimensions	a = 12.5731(4) Å α= 90°.	a = 12.5908(2) Å α= 90°.
	b = 15.4085(5) Å β= 90°.	b = 15.3906(2) Å β= 90°.
	c = 29.7563(10) Å γ = 90°.	c = 29.8194(4) Å γ = 90°.
Volume	5764.8(3) $Å^3$	5778.4(1) $Å^3$
Z	4	4
Density (calculated)	1.651 g/cm^3	1.643 g/cm^3
Absorption coefficient	1.294 mm^{-1}	1.352 mm^{-1}
F(000)	2908	2892
Crystal size	0.36 x 0.24 x 0.07 mm^3	0.58 x 0.12 x 0.06 mm^3
Crystal colour	Colourless	Colourless
Experimental device	Siemens SMART-CCD	Siemens SMART-CCD
θ range for data collection	1.37 to 27.47°.	1.37 to 27.50°.
Index ranges	-15<=h<=16,	-16<=h<=16,
	-19<=k<=16,	-20<=k<=19,
	-38<=l<=38	-38<=l<=37
Reflections collected	47368	50047
Independent reflections	13218 [R(int) = 0.0727]	13273 [R(int) = 0.1420]
Absorption correction	Multiscan - Sadabs	Multiscan - Sadabs
Max. and min. transmission	0.915 and 0.653 (xstal size)	0.923 and 0.508 xstal size)
Refinement method	Full-matrix least-squares on F^2	Full-matrix least-squares on F^2
Data / restraints / parameters	13218 / 0 / 786	13273 / 0 / 722
Goodness-of-fit on F^2	1.071	1.063
Final R indices [I>2σ(I)]	R1 = 0.0491, wR2 = 0.0940	R1 = 0.0720, wR2 = 0.1337
R indices (all data)	R1 = 0.0840, wR2 = 0.1083	R1 = 0.1530, wR2 = 0.1656
Absolute structure parameter	-0.03(1)	-0.00(2)
Extinction coefficient	not refined	not refined
Largest diff. Peak and hole	0.919 and -0.775 $e.Å^{-3}$	0.976 and -1.492 $e.Å^{-3}$

The full list of atomic co-ordinates, bond lengths and angles and anisotropic displacement parameters can be found in the Appendices (***A.4.7 - A.4.8***).

***Table 4.5.4.3** – Selected bond lengths (Å) for $C_{36}H_{69}EuF_{18}N_8O_{14.5}P_3$ and $C_{36}H_{68}F_{18}GdN_8O_{14}P_3$ for the enantiopure complex of L^5.*

$C_{36}H_{69}EuF_{18}N_8O_{14}$				$C_{36}H_{68}F_{18}GdN_8O_{14}P_3$			
Eu(1)-O(2)	2.381(4)	N(3)-C(4)	1.497(11)	Gd(1)-O(2)	2.399(6)	N(3)-C(31)	1.517(11)
Eu(1)-O(3)	2.393(4)	N(4)-C(41)	1.490(10)	Gd(1)-O(4)	2.400(7)	N(4)-C(41)	1.464(15)
Eu(1)-O(4)	2.394(4)	N(4)-C(7)	1.507(9)	Gd(1)-O(3)	2.406(6)	N(4)-C(6)	1.489(13)
Eu(1)-O(5)	2.429(4)	N(4)-C(6)	1.507(9)	Gd(1)-O(5)	2.447(6)	N(4)-C(7)	1.507(13)
Eu(1)-O(1)	2.454(4)	N(5)-C(12)	1.332(8)	Gd(1)-O(1)	2.457(6)	N(5)-C(12)	1.312(11)
Eu(1)-N(1)	2.625(5)	N(5)-C(13)	1.469(8)	Gd(1)-N(1)	2.641(8)	N(5)-C(13)	1.449(13)
Eu(1)-N(2)	2.635(6)	N(6)-C(22)	1.324(8)	Gd(1)-N(2)	2.647(9)	N(6)-C(22)	1.303(13)
Eu(1)-N(4)	2.649(6)	N(6)-C(23)	1.457(9)	Gd(1)-N(4)	2.667(9)	N(6)-C(23)	1.452(13)
Eu(1)-N(3)	2.659(5)	N(7)-C(32)	1.345(8)	Gd(1)-N(3)	2.670(8)	N(7)-C(32)	1.331(12)
O(1)-C(12)	1.253(7)	N(7)-C(33)	1.452(8)	O(1)-C(12)	1.285(11)	N(7)-C(33)	1.440(13)
O(2)-C(22)	1.265(7)	N(8)-C(42)	1.330(9)	O(2)-C(22)	1.260(11)	N(8)-C(42)	1.317(13)
O(3)-C(32)	1.252(7)	N(8)-C(43)	1.461(9)	O(3)-C(32)	1.263(11)	N(8)-C(43)	1.466(14)
O(4)-C(42)	1.244(7)	C(1)-C(2)	1.524(12)	O(4)-C(42)	1.237(11)	C(1)-C(2)	1.539(16)
O(11)-C(15)	1.321(8)	C(3)-C(4)	1.518(10)	O(11)-C(15)	1.325(13)	C(3)-C(4)	1.537(16)
O(11)-C(16)	1.486(8)	C(5)-C(6)	1.523(12)	O(11)-C(16)	1.476(13)	C(5)-C(6)	1.510(18)
O(12)-C(15)	1.209(8)	C(7)-C(8)	1.523(10)	O(12)-C(15)	1.218(13)	C(7)-C(8)	1.521(14)
O(21)-C(25)	1.332(9)	C(11)-C(12)	1.505(9)	O(21)-C(25)	1.326(14)	C(11)-C(12)	1.512(13)
O(21)-C(26)	1.564(15)	C(13)-C(15)	1.523(10)	O(21)-C(26)	1.504(17)	C(13)-C(15)	1.532(15)
O(22)-C(25)	1.217(9)	C(13)-C(14)	1.542(9)	O(22)-C(25)	1.195(15)	C(13)-C(14)	1.533(15)
O(31)-C(35)	1.337(9)	C(16)-C(17)	1.488(11)	O(31)-C(35)	1.344(14)	C(16)-C(17)	1.456(17)
O(31)-C(36)	1.453(9)	C(21)-C(22)	1.520(10)	O(31)-C(36)	1.468(15)	C(21)-C(22)	1.535(15)
O(32)-C(35)	1.210(8)	C(23)-C(25)	1.522(11)	O(32)-C(35)	1.219(13)	C(23)-C(24)	1.507(17)
O(41)-C(45)	1.188(9)	C(23)-C(24)	1.530(11)	O(41)-C(45)	1.185(15)	C(23)-C(25)	1.553(18)
O(42)-C(45)	1.333(9)	C(26)-C(27)	1.423(19)	O(42)-C(45)	1.333(15)	C(26)-C(27)	1.48(2)
O(42)-C(46)	1.534(11)	C(31)-C(32)	1.513(9)	O(42)-C(46)	1.554(17)	C(31)-C(32)	1.483(14)
N(1)-C(11)	1.482(7)	C(33)-C(35)	1.533(9)	N(1)-C(1)	1.493(13)	C(33)-C(35)	1.533(15)
N(1)-C(1)	1.497(9)	C(33)-C(34)	1.537(9)	N(1)-C(11)	1.496(11)	C(33)-C(34)	1.544(13)
N(1)-C(8)	1.506(10)	C(36)-C(37)	1.505(13)	N(1)-C(8)	1.497(13)	C(36)-C(37)	1.52(2)
N(2)-C(21)	1.492(10)	C(41)-C(42)	1.507(9)	N(2)-C(3)	1.488(13)	C(41)-C(42)	1.529(15)
N(2)-C(2)	1.501(9)	C(43)-C(44)	1.522(10)	N(2)-C(21)	1.499(15)	C(43)-C(44)	1.491(16)
N(2)-C(3)	1.503(8)	C(43)-C(45)	1.528(11)	N(2)-C(2)	1.502(13)	C(43)-C(45)	1.563(16)
N(3)-C(5)	1.485(10)	C(46)-C(47)	1.448(14)	N(3)-C(4)	1.485(17)	C(46)-C(47)	1.41(2)
N(3)-C(31)	1.494(7)			N(3)-C(5)	1.485(16)		

4.5.5 The macrocycle DTMA in its free and complexed forms

Dota tetrakis(methylamide) or DTMA and its dysprosium complex were synthesised and crystallised by Alvaro de Sousa from the chemistry department at the University of Durham and were studied using X-ray crystallography, and revealing many interesting insights.[61] DTMA is the precursor compound and the optically inactive analogue of the chiral tetraamides ligands that have been described here. It acts as an octadentate ligand towards Ln^{3+} ions forming cationic complexes. The data were recorded on the Rigaku AFC6S four-circle diffractometer to take advantage of the increased intensity of the Cu Kα source for these small crystals with only light atom scatterrers present. The combination of this with cooling the crystal to 150(2) K allowed enough reflections to be obtained for a full anisotropic refinement of the non-hydrogen atoms including the two water molecules in the lattice (see ***Figure 4.5.5.1***).

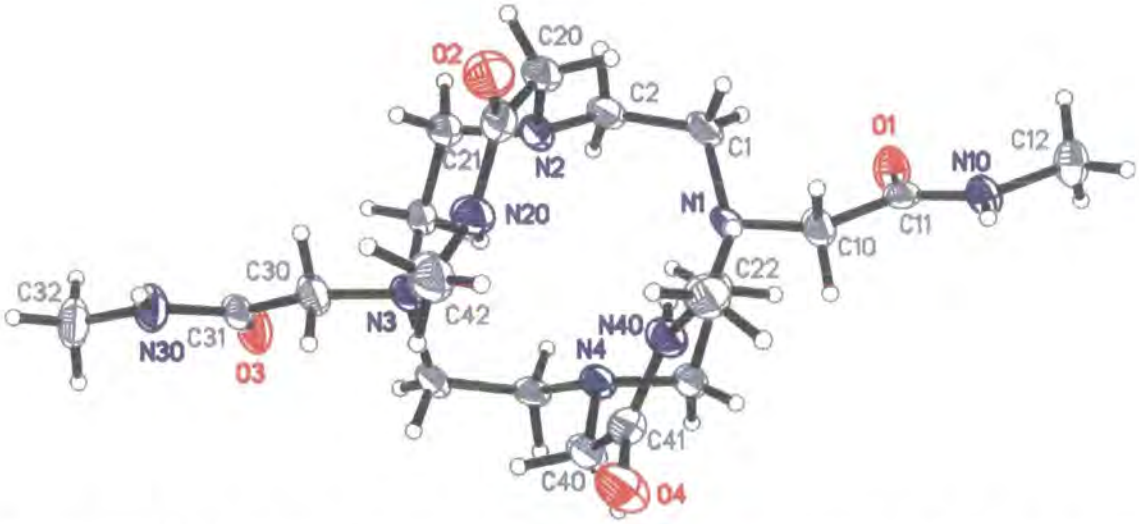

Figure 4.5.5.1 *– A thermal ellipsoid plot of the DTMA ligand at 150(2) K with the anisotropic displacement parameters drawn at 50% probability level.*

An interesting hydrogen-bonded packing motif is present here, which is a consequence of the protonation state of the ligand. Since this is a neutral ligand, and not an overall zwitterion like the stereoisomers of the ligand L^8 in section 4.7, there is not any interaction between the protonated aza groups and their respective appended carboxyl groups. The ligand DOTA also has two alternate intramolecular transannular hydrogen bonds. However, the remaining two carboxylate groups adopt a similar

conformation defining an overall preorganised twisted square antiprism. In the case of the DTMA molecule, in addition to the absence of any stabilising effect hydrogen-bonded contact involving the aza groups, the pendant arms are bulkier and longer by approximately 1.5 Å. The configuration at the carbon atom α to the ring nitrogen atom determines the layout of the pendant arms since the atoms after these on the chain do not have the option to sample other conformations due to the planar nature of the peptide bond. The hydrogen bond acceptor groups are the amide oxygen atoms and they adopt the position facing outward from the cyclen ring. The N-C-C-O torsion angles are informative. The N1-C10-C11-O1 and N3-C30-C31-O3 groups have values of -2.8(7) and 3.4(8)° respectively, since the pendant arms extend away from the ring. This departure from the conventional conformation is due to two strong intermolecular (N-H..O) interactions (N30-H30..O1 2.030 Å; N10-H10..O4 2.00 Å). The N2-C20-C21-O2 and N4-C40-C41-O4 groups have values of -173.8(5) and -179.0(5)° respectively. The latter two values shown are where the possible twisted square antiprismatic preorganisation is rejected to form hydrogen bonds with the water molecules that are reasonably short and structure defining.

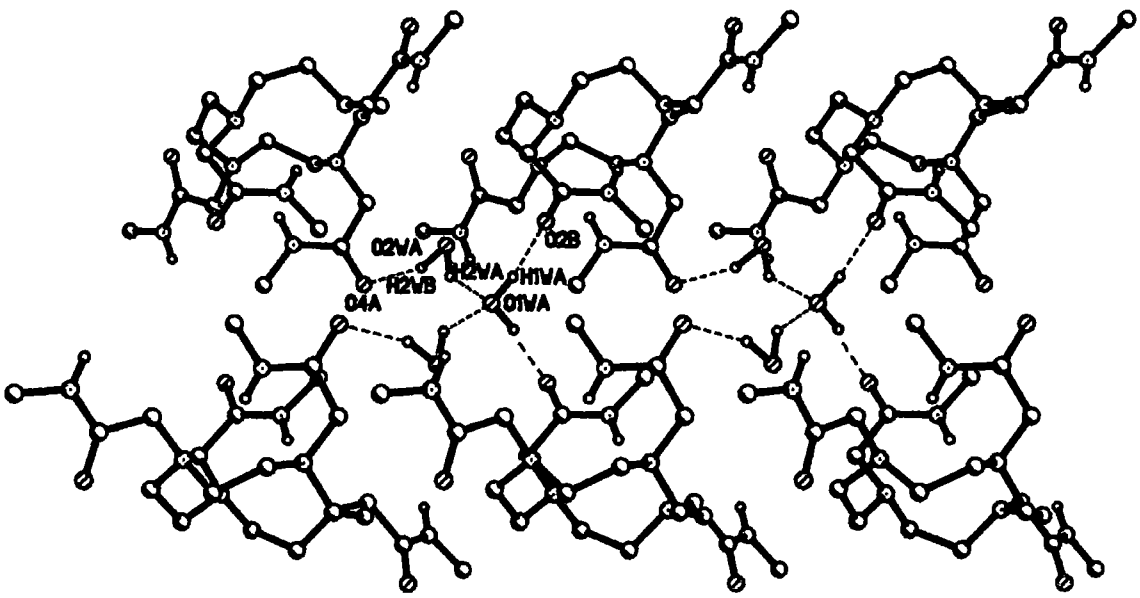

***Figure 4.5.5.2** –The packing diagram for DTMA viewed along the [001] direction*

Contacts between the layers are provided by the water molecules. The network that forms (in ***Figure 4.5.5.2***) involves the water molecule, O1w, being positioned on a two-fold axis of symmetry and hydrogen bonding directly to molecules in one layer

(O1w-H1wa..O2 1.84 Å) while it links via a contact of 2.04 Å to the second water molecule to the layer below (O2w-H2wb..O4a 1.94 Å). All the hydrogen atoms were placed in calculated position in the refinement of this structure and the distances to hydrogen presented here should therefore not be overinterpreted.

The cyclen ring in DTMA does not depart from the [3333] conformation although there is a slight variation. The torsion angles around the ring are 56.6(6), 67.5(6), 57.3(6), 65.4(6) Å for the four N-C-C-N groups.

The structure of the dysprosium complex of DTMA was then investigated. It is depicted in ***Figure 4.5.5.3***, showing it to be a monocapped square antiprism much like the dysprosium (*S*) complex of the tetraamide ligand, L^2. The distances to the nine donor atoms are equal within experimental precision to the distances to the nitrogen and oxygen atoms bind dysprosium in the complex of L^2.

Good quality colourless single crystals of dimensions 0.30 x 0.30 x 0.30 mm^3 were used to collect data on SMART diffractometer with Mo Kα. The data collection and structure refinement details for this complex and its ligand are shown in ***Table 4.5.5.1***. The asymmetric unit also contains three molecules of hexafluorophosphate and diffuse water molecules. One of the counter ions is statically disordered and it was thought that the symmetry might actually have been non centrosymmetric caused by the anions not being related via an inversion centre. A reciprocal space plot revealed a centric distribution of intensity at the k = 3 layer however and the structure was refined successfully in the centrosymmetric space group with the anion modelled with three statically disordered components.

The average twist angle of the N4/O4 planes is 38.7° and the average bite angle that the donor nitrogen and oxygen atoms subtend at the metal is 66.81°. The torsion angles around the cyclen ring are –58.6, -58.1, -59.9 and –58.1° for the four N-C-C-N groups thus the cyclen ring has a more rigid structure in the complexed form than as a free ligand. The N-C-C-O torsion angles show much more fluctuation with values of 33.5, 29.8, 24.5 and 34.6° for the four N-C-C-O arms.

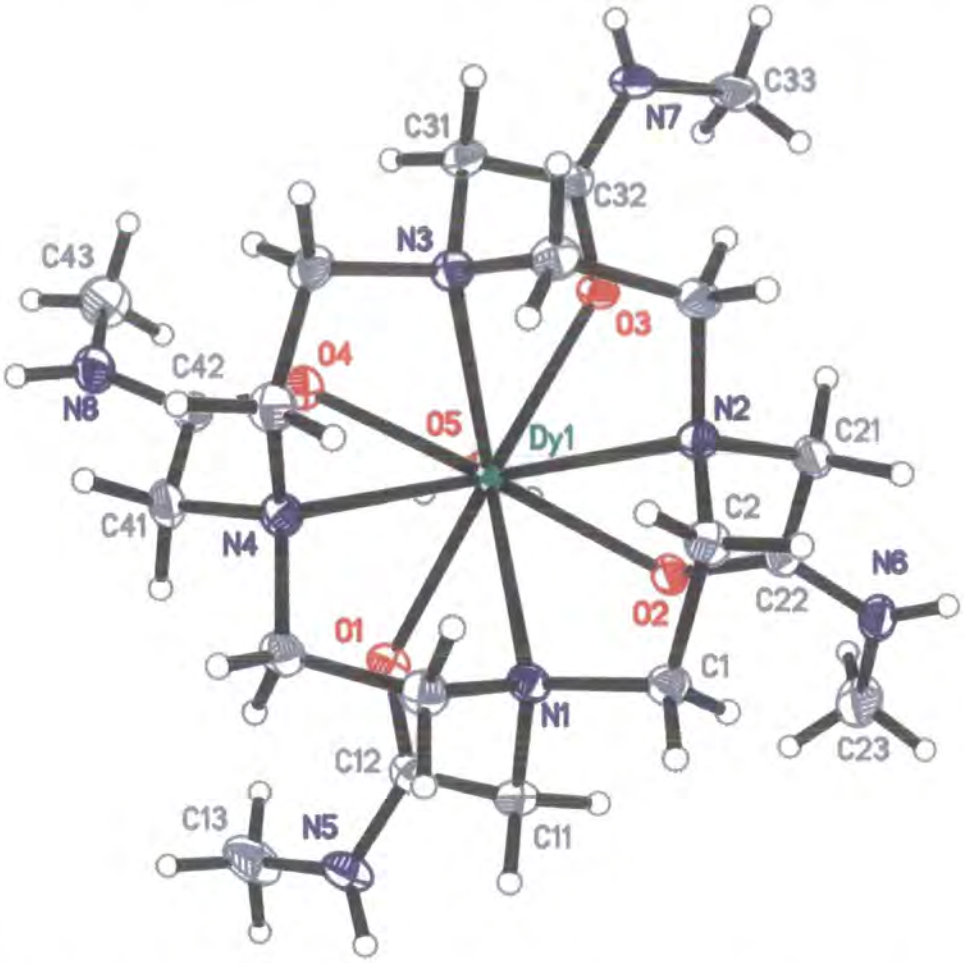

Figure 4.5.5.3 *– A thermal ellipsoid plot of the monocapped square antiprismatic dysprosium complex of DTMA at 150(2) K with the anisotropic displacement parameters drawn at 50% probability level*

The ability of Gd^{3+} complexes to enhance the nuclear relaxivity of solvent water protons can occur by an inner-sphere mechanism, an outer-sphere mechanism or via prototropic exchange. The cationic gadolinium complex of this ligand was chosen for NMR studies because it was shown that and the exchange lifetime, τ_M, increases with decreasing negative charge.[62] Thus, the exchange should proceed via an outer sphere route. The distance to the bound water molecule was of interest because of the contribution it could make to the exchange, and the dysprosium complex was obtained for X-ray analysis. The distance from the metal to the bound water protons is 2.82 and 2.87 Å, and the protons were refined without being placed in calculated positions (***Figure 4.5.5.4***).

It has been suggested that in this case, exchange could proceed faster by conversion in solution to the minor (10%) twisted square antiprismatic isomer.[9] From the structural data this seems unlikely as for a given lanthanide ion complex the isomeric form does not affect the bite angles or cause a significant trend in the distances to the donor set as was seen when twisted square antiprismatic and square antiprismatic isomers of the Eu·THP complex cocrystallised in the asymmetric unit.[29]

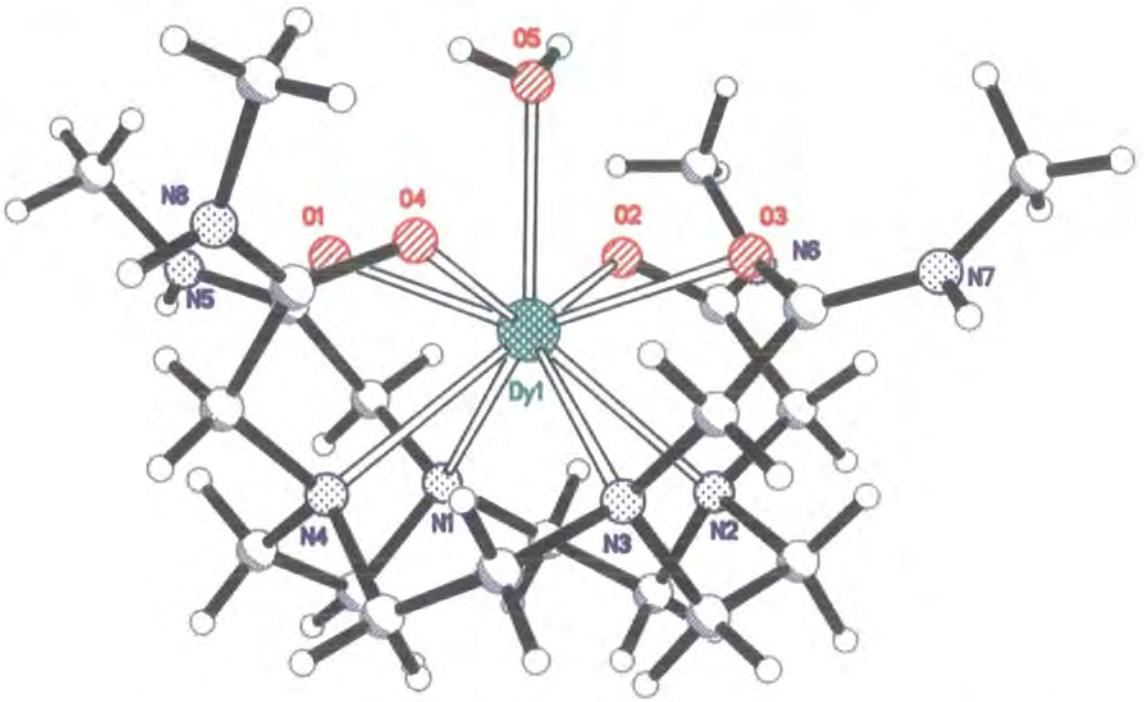

Figure 4.5.5.4 *– A view of the dysprosium complex of DTMA showing the bound water molecule above the O4 plane.*

***Table 4.5.5.1** - Selected crystal data for DTMA and its dysprosium complex.*

Empirical formula	$C_{20}H_{43}N_8O_{5.50}$	$C_{20}H_{47}DyF_{18}N_8O_{7.50}P_3$
Formula weight	483.62	1117.07
Temperature	150(2) K	150(2) K
Wavelength	1.54184 Å	0.71073 Å
Crystal system	Monoclinic	Triclinic
Space group	C2/c	P-1
Unit cell dimensions (Å/°)	a = 32.517(7) α= 90 b = 8.723(2) β= 106.13(3) c = 18.638(4) γ = 90	a = 12.7068(2) α= 70.130(1) b = 13.0137(2) β= 72.953(1) c = 14.3285(2) γ = 65.408(1)
Volume	5078.5(17) $Å^3$	1994.07(5) $Å^3$
Z	8	2
Density (calculated)	1.265 g/cm^3	1.860 g/cm^3
Crystal colour	Colourless	Colourless
Experimental device	Rigaku AFC6S	Siemens SMART-CCD
Absorption coefficient	0.769 mm^{-1}	2.128 mm^{-1}
Absorption correction	Not applied	Integration
Max. and min. transmission	–	0.632 and 0.443
F(000)	2104	1112
θ range for data collection	4.94 to 49.99°.	1.54 to 30.27°.
Index ranges	0<=h<=32, 0<=k<=8, -18<=l<=17	-17<=h<=17, -18<=k<=17, -19<=l<=20
Reflections collected	2676	28728
Independent reflections	2618 [R(int) = 0.0884]	10729 [R(int) = 0.0237]
Refinement method	Full-matrix least-squares on F^2	Full-matrix least-squares on F^2
Data / restraints / parameters	2618 / 0 / 331	10723 / 0 / 794
Goodness-of-fit on F^2	1.086	1.064
Final R indices [I>2σ(I)]	R1 = 0.0765, wR2 = 0.1956	R1 = 0.0234, wR2 = 0.0563
R indices (all data)	R1 = 0.0952, wR2 = 0.2179	R1 = 0.0271, wR2 = 0.0589
Extinction coefficient	not refined	not refined
Largest diff. Peak and hole	0.424 and -0.375 $e.Å^{-3}$	0.795 and -1.210 $e.Å^{-3}$

The full list of atomic co-ordinates, bond lengths and angles and anisotropic displacement parameters can be found in the Appendices (***A.4.9 - A.4.10***).

***Table 4.5.4.2** – Selected bond lengths (Å) for $C_{20}H_{47}DyF_{18}N_8O_{7.50}P_3$ and $C_{20}H_{43}N_8O_{5.50}$.*

$C_{20}H_{47}DyF_{18}N_8O_{7.50}P_3$		N(4)-C(6)	1.491(3)	N(2)-C(2)	1.462(7)
Dy(1)-O(2)	2.3096(15)	N(5)-C(13)	1.459(3)	N(2)-C(3)	1.477(7)
Dy(1)-O(4)	2.348(2)	N(6)-C(22)	1.307(3)	N(3)-C(30)	1.442(6)
Dy(1)-O(1)	2.3495(14)	N(6)-C(23)	1.457(3)	N(3)-C(5)	1.464(6)
Dy(1)-O(3)	2.4139(14)	N(7)-C(32)	1.309(3)	N(3)-C(4)	1.474(7)
Dy(1)-O(5)	2.427(2)	N(7)-C(33)	1.461(3)	N(4)-C(40)	1.454(7)
Dy(1)-N(3)	2.605(2)	N(8)-C(42)	1.315(3)	N(4)-C(6)	1.468(7)
Dy(1)-N(4)	2.640(2)	N(8)-C(43)	1.459(3)	N(4)-C(7)	1.473(6)
Dy(1)-N(1)	2.643(2)	C(1)-C(2)	1.514(3)	N(10)-C(11)	1.315(7)
Dy(1)-N(2)	2.654(2)	C(3)-C(4)	1.520(3)	N(10)-C(12)	1.473(7)
O(1)-C(12)	1.257(3)	C(5)-C(6)	1.512(3)	N(20)-C(21)	1.336(7)
O(2)-C(22)	1.263(2)	C(7)-C(8)	1.514(3)	N(20)-C(22)	1.449(7)
O(3)-C(32)	1.262(2)	C(11)-C(12)	1.510(3)	N(30)-C(31)	1.336(7)
O(4)-C(42)	1.254(3)	C(21)-C(22)	1.519(3)	N(30)-C(32)	1.460(7)
N(1)-C(11)	1.485(3)	C(31)-C(32)	1.510(3)	N(40)-C(41)	1.343(7)
N(1)-C(1)	1.490(3)	C(41)-C(42)	1.509(3)	N(40)-C(42)	1.448(7)
N(1)-C(8)	1.491(3)	$C_{20}H_{43}N_8O_{5.50}$		C(1)-C(2)	1.515(8)
N(2)-C(21)	1.482(3)	O(1)-C(11)	1.235(6)	C(3)-C(4)	1.513(7)
N(2)-C(3)	1.489(3)	O(2)-C(21)	1.235(6)	C(5)-C(6)	1.512(7)
N(2)-C(2)	1.490(3)	O(3)-C(31)	1.224(6)	C(7)-C(8)	1.510(7)
N(3)-C(31)	1.480(3)	O(4)-C(41)	1.255(6)	C(10)-C(11)	1.542(7)
N(3)-C(4)	1.491(3)	N(1)-C(10)	1.448(7)	C(20)-C(21)	1.518(8)
N(3)-C(5)	1.495(3)	N(1)-C(8)	1.465(7)	C(30)-C(31)	1.540(8)
N(4)-C(41)	1.479(3)	N(1)-C(1)	1.475(7)	C(40)-C(41)	1.488(8)
N(4)-C(7)	1.490(3)	N(2)-C(20)	1.453(7)		

4.6 Lanthanide complexes with benzylphosphinic acid pendant groups

The use of the imaging technique positron emission tomography (PET) has become widespread in the past decade in the study of brain function[63] and tumour imaging.[64,65] For reasons already stated the choice of radioisotope is important. The radioisotopes ^{111}In, ^{67}Ga and ^{64}Cu are suitable for PET imaging.[66] It is know that elements of the lanthanide series form kinetically stable complexes that allow repeated measurements in vivo before excretion (5-15 sec). It is of interest to target these PET imaging complexes to a designated organ and to this end, the hydrophobicity of the complex can be fine-tuned.[67] The need to design lipophilic complexes that cleared the body via the biliary route (from the liver to the gall bladder to the small intestine) for PET and MRI analyses focussed on anionic gadolinium complexes of L^7 (1,4,7,10-tetraazacyclododecane-1,4,7,10-tetrakismethylenebenzylphosphinic acid).[68,69]

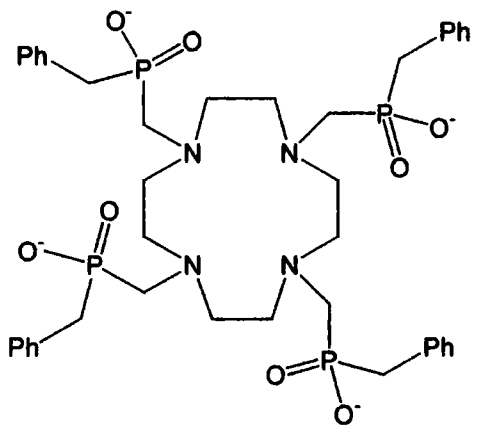

***Figure 4.6.1** – Schematic diagram of the ligand L^7: 1,4,7,10-tetraazacyclododecane-1,4,7,10-tetrakismethylenebenzylphosphinic acid.*

Experiments by David Parker *et al* with the gadolinium complex showed that it cleared tumour tissue slower than healthy tissue.[70,71] This led to an investigation of this ligand and its lanthanide complexes.[72] The lanthanum and ytterbium complexes of L^7 were synthesised and crystallised by Clive Foster from the chemistry department at the University of Durham. The use of phosphinate groups to bind to metals results in a larger 'bite' angle at the metal than with carboxylate groups, thus burying it and

forming a more stable complex. It has already been seen that the substitution of benzyl phosphinate for carboxylate in NOTA complexes, derivatised with copper, gallium, iron and indium resulted in the opening of the 'bite' angle by several degrees.[73,39] The lanthanum and ytterbium complexes of L^7 were investigated by X-ray crystallography. The isomer present was a twisted square antiprism in the case of both metals as was the case with the yttrium and europium complexes of L^7, which had already been shown.[16,71] The twist angle is 29.4° for the lanthanum complex and 30.5° for the ytterbium complex. The lanthanum complex is the only nine co-ordinate complex in this series, with the smaller ytterbium ion retaining an eight co-ordinate geometry. The distances of the two metals to the donor atoms are listed in ***Table 4.6.1***

***Table 4.6.1** – Selected interatomic distances (Å) for the La and Yb complexes of L^7. (* denotes that there are two symmetrically independent molecules.)*

	La – L^7	Yb1*-L^7	Yb2*-L^7
Ln-N1	2.84(3)	2.626(7)	2.668(7)
Ln-N2	2.69(3)	2.620(7)	2.715(8)
Ln-N3	2.83(3)	2.615(7)	2.590(6)
Ln-N4	2.84(3)	2.639(6)	2.550(7)
Ln-O11	2.41(2)	2.215(5)	2.270(5)
Ln-O21	2.42(2)	2.231(5)	2.227(5)
Ln-O31	2.47(2)	2.256(5)	2.256(5)
Ln-O41	2.50(2)	2.287(5)	2.241(5)
Ln-O5	2.66(2)	—	—

The 'bite' angles, defined as α in ***Figure 4.6.2,*** for both complexes are presented in ***Table 4.6.1***. A comparison with the bite angles for lanthanum and ytterbium carboxylate complex derivatives is not possible since the structures of these have not been reported in the literature (The Yb·DOTA structure from ^{1}H NMR and 2D EXSY spectroscopy has been reported but this data would not yield sufficient information to calculate those angles accurately.[30,32])

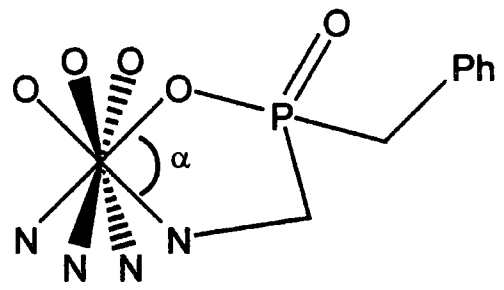

***Figure 4.6.2** – Schematic diagram of definition of the N-Ln-O bite angle.*

As an indication of the phosphinate's effect, the average bite angle for Eu·DOTA[27] is 72.3°, although this compound was a monocapped square antiprism and there was very large variation in the bite angles in this distorted complex Y·DOTA has a mean bite angle of 66.8° and Gd·DOTA has a mean bite angle of 66.1°.[24] These complexes, however, are again nine co-ordinate square antiprisms.

***Table 4.6.2** – The bite angles (°) for the La and Yb complexes of L^7.*

α	La – L^7	Yb1-L^7	Yb2-L^7
N1-Ln-O11	65.4(7)	72.2(2)	70.4(2)
N2-Ln-O21	64.6(8)	69.7(2)	71.2(2)
N3-Ln-O31	68.5(8)	69.9(2)	68.1(2)
N4-Ln-O41	66.6(7)	69.7(2)	72.3(2)

The variation in angles for both complexes here is much less than for the other cited square antiprismatic complexes. Clearly, the angles are significantly more acute for the lanthanum complex. This is because of the bound water molecule, which causes the N4 and O4 donor atoms to move toward one another. This structural change causes the phenyl groups of the ytterbium complex to extend outwards from the metal. The mean distance from La to a central point in the rings was 5.8 Å whereas for Yb it was 6.0 Å, averaged over two molecules. It must be stressed that these data sets had many inherent problems and the final structures reported have been determined with low precision. Both complexes, despite growing as what appeared as good quality crystals from a visual inspection under cross-polarised light, gave rise to very mosaic reflections in one direction. The high proportion of solvent water (nine water molecules per independent lanthanum complex and a potassium hexa-aquo species and fifteen water molecules per two independent ytterbium complexes) may have contributed to the increased mosaicity at low temperature although ice rings were not visible on any of the frames. These structures were refined isotropically with the exceptions of the metal atom and the phosphorus atoms for the ytterbium complex and the metal atom, the phosphorus atoms and the oxygen donor atoms for the lanthanum complex. The hydrogen atoms were placed in calculated positions and the phenyl rings were refined as rigid groups.

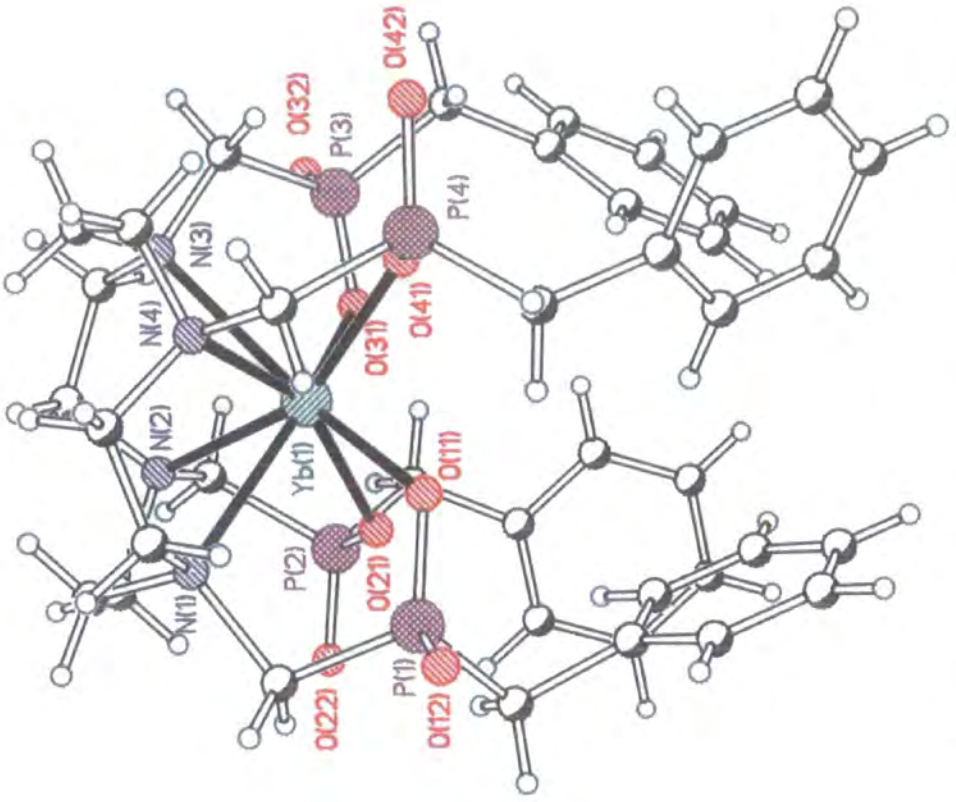

***Figure 4.6.3** – A view of the ytterbium complex of L^7, which emphasises the eight co-ordinate geometry about the metal.*

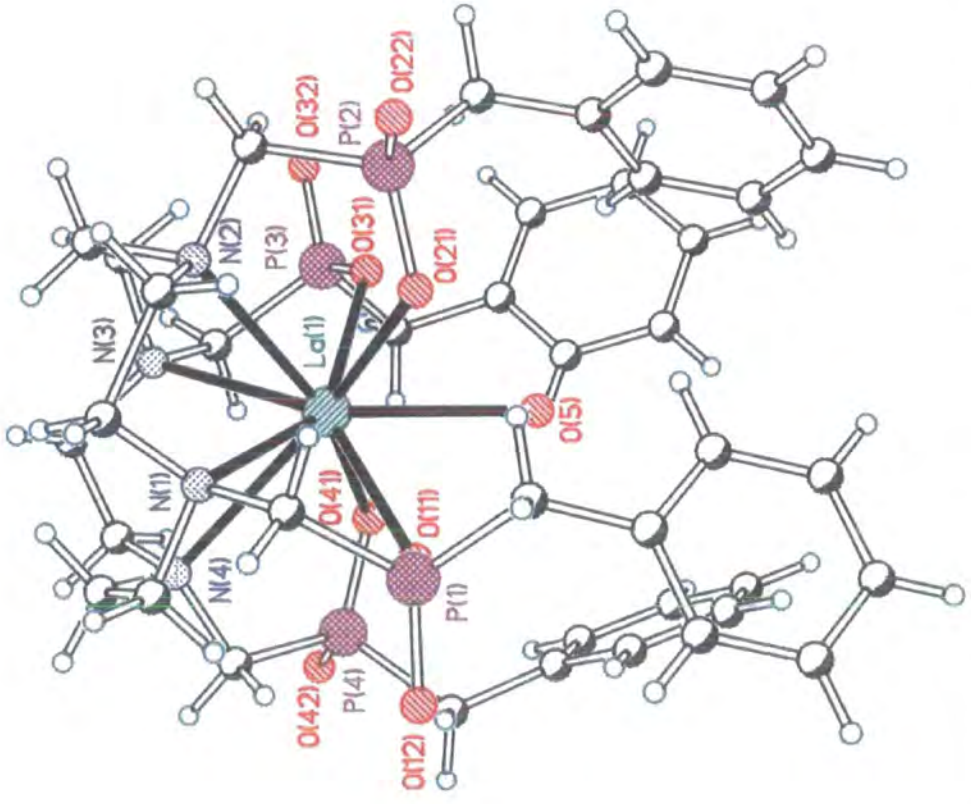

***Figure 4.6.4** – A view of the lanthanum complex of L^7, emphasising the nine co-ordinate geometry about the metal, as a result of face-capping by a water molecule (O5).*

***Table 4.6.3** – Selected crystal data and structure refinement details for the ytterbium and lanthanum complexes of L^7.*

Empirical formula	$C_{80}H_{148}K_1N_8O_{33}P_8Yb_2$	$C_{40}H_{66}LaN_4O_{17}P_4$
Formula weight	2383.00	1137.76
Temperature	150(2) K	150(2) K
Wavelength	0.71073 Å	0.71073 Å
Crystal system	Monoclinic	Orthorhombic
Space group	C2/c	Pbcn
Unit cell dimensions (Å/°)	a = 32.1349(1) α= 90 b = 31.4465(3) β= 93.984(1) c = 21.4508(2) γ = 90	a = 22.7440(4) α= 90 b = 23.1243(5) β= 90 c = 21.1979(4) γ = 90
Volume	21624.3(3) $Å^3$	11148.8(4) $Å^3$
Z	16	8
Density (calculated)	1.498 g/cm^3	1.356 g/cm^3
Absorption coefficient	1.957 mm^{-1}	0.945 mm^{-1}
F(000)	10040	4696
Crystal size	0.40 x 0.40 x 0.25 mm^3	0.25 x 0.25 x 0.25 mm^3
θ range for data collection	0.91 to 27.58°.	1.26 to 18.90°.
Index ranges	-41<=h<=41, -38<=k<=40, -27<=l<=27	-16<=h<=20, -21<=k<=20, -19<=l<=19
Reflections collected	87025	27104
Independent reflections	24920 [R(int) = 0.0822]	4432 [R(int) = 0.1044]
Refinement method	Full-matrix least-squares on F^2	Full-matrix least-squares on F^2
Data/restraints/ parameters	21467 / 0 / 497	4429 / 0 / 308
Goodness-of-fit on F^2	5.216	3.309
Final R indices [I>2σ(I)]	R1 = 0.2496, wR2 = 0.4653	R1 = 0.1992, wR2 = 0.4741
R indices (all data)	R1 = 0.2942, wR2 = 0.4832	R1 = 0.2171, wR2 = 0.4816
Largest diff. peak and hole	9.230 and -6.270 $e.Å^{-3}$	1.375 and -1.055 $e.Å^{-3}$

The full list of atomic co-ordinates, bond lengths and angles and anisotropic displacement parameters can be found in the Appendices (***A.4.11 - A.4.12***).

The final cycles of refinement for the ytterbium crystal structure were performed with damping and this resulted in an "artificially" precise structure, which should not be over-interpreted.

4.7 Lanthanide compounds with carboxyethyl pendant groups

There is a considerable interest in the structure and behaviour of gadolinium complexes in light of their potential use as ^1H relaxometric agents *in vivo*. Recent work has underlined the effect of exchange in the transfer of paramagnetism to the bulk solvent via an inner-sphere contribution, as in Soloman-Bloembergen-Morgan theory.[49,74] It has already been shown for the europium complex of L^4 that the rate of water exchange is heavily dependent on the isomer present in solution. The square antiprismatic isomer has a water exchange rate of 6×10^{-3} s^{-1} at 298 K which undergoes a fifty fold increase on conversion to the twisted square antiprismatic isomer. These two isomers are interconverted by means of either ring inversion [$\Lambda(\delta\delta\delta\delta) \rightarrow \Lambda(\lambda\lambda\lambda\lambda)$] or arm rotation [$\Lambda(\delta\delta\delta\delta) \rightarrow \Delta(\delta\delta\delta\delta)$]. The average twist angle is 40° for a regular square antiprism and 29° for a twisted square antiprism. Either process must happen in isolation for the other isomer to be reached and as previously explained the isomer in question is defined by the N-C-C-N and N-C-C-O torsion angles. A ^1H NMR spectrum is completely diagnostic of the isomeric composition where ring inversion is fast and precludes conversion via the slower arm rotation route. The conversion between a square antiprism and twisted square antiprism results in a change in proton environment from axial to equatorial when cyclen ring flip yields the other isomer. This has been shown for europium complexes of L^8. Rationalisation of why there is increased speed of interconversion via cyclen ring flip is difficult. Cyclen ring flip can only occur through an uncomplexed intermediate to avoid collision between the carbonyl group and the methylene bond. The change in geometry about the metal ion has implications in water bonding reflected in the Ln-water bond lengths and thus the rate of exchange. It was interesting to probe the structure of lanthanide complexes of the tetrakis(carboxyethyl) derivatives to ascertain which isomer was giving rise to the paramagnetism, how abundant the isomer was in solution and in the crystal structure, and the co-ordination number of its complexes across the series. The lanthanide complexes and the free ligands were synthesised and crystallised by Mark Woods from the University of Durham. Here the stereogenic centre is α to the ring nitrogen, as can be seen from

Figure 4.7.1. As has been demonstrated in previous sections, placement of a stereogenic centre β (as in the case of the tetraphosphenoxymethyl complexes, L^7) or δ (for the tetraamide ligands, L^2, L^3, L^4) imparts considerable rigidity to the complexes.

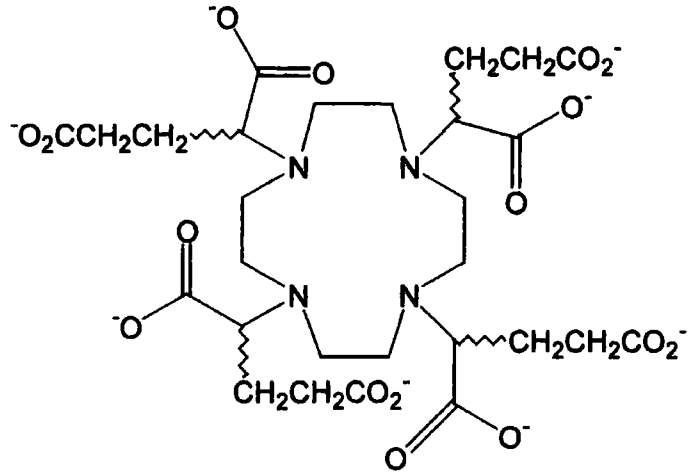

Figure 4.7.1 *– Schematic representation of L^8, the 1,4,7,10-tetrakis(carboxyethyl)-1,4,7,10-tetraazacyclododecane ligand that has been complexed with gadolinium, europium, terbium and ytterbium.*

There are six ligand stereoisomers of L^8: RRRR (SSSS), RSSS (SRRR), RSRS, RRSS. Each of these can exist as one of four possible isomers, obtained from either ring inversion or arm rotation, as in ***Figure 4.5.1.1.*** In the absence of any external influence on the ratio of stereoisomers present, the enantiomeric pairs RRRR (SSSS) and RSSS (SRRR) would be expected to be present in considerable excess to the achiral RSRS and RRSS stereoisomers. Additionally, a ^1H NMR spectrum revealed that for these particular two stereoisomers, the twisted square antiprism predominates in solution by factor of 4:1 for the RRRR enantiomer. The structural investigation of the europium, gadolinium, ytterbium and terbium complexes of L^8 was afforded by means of X-ray crystallography. The crystallisation forces in action proved to be the nemesis of a solid-state structure determination of the predominant isomer in solution. It was quite surprising to observe that the europium, gadolinium and terbium complexes for the *R*-enantiomer all crystallise as the minor isomer, i.e. the square antiprism. Moreover, the degree of isostructure exhibited was interesting. ***Figures 4.7.2-4*** show three perspectives related by 90° to give different views of these virtually identical compounds.

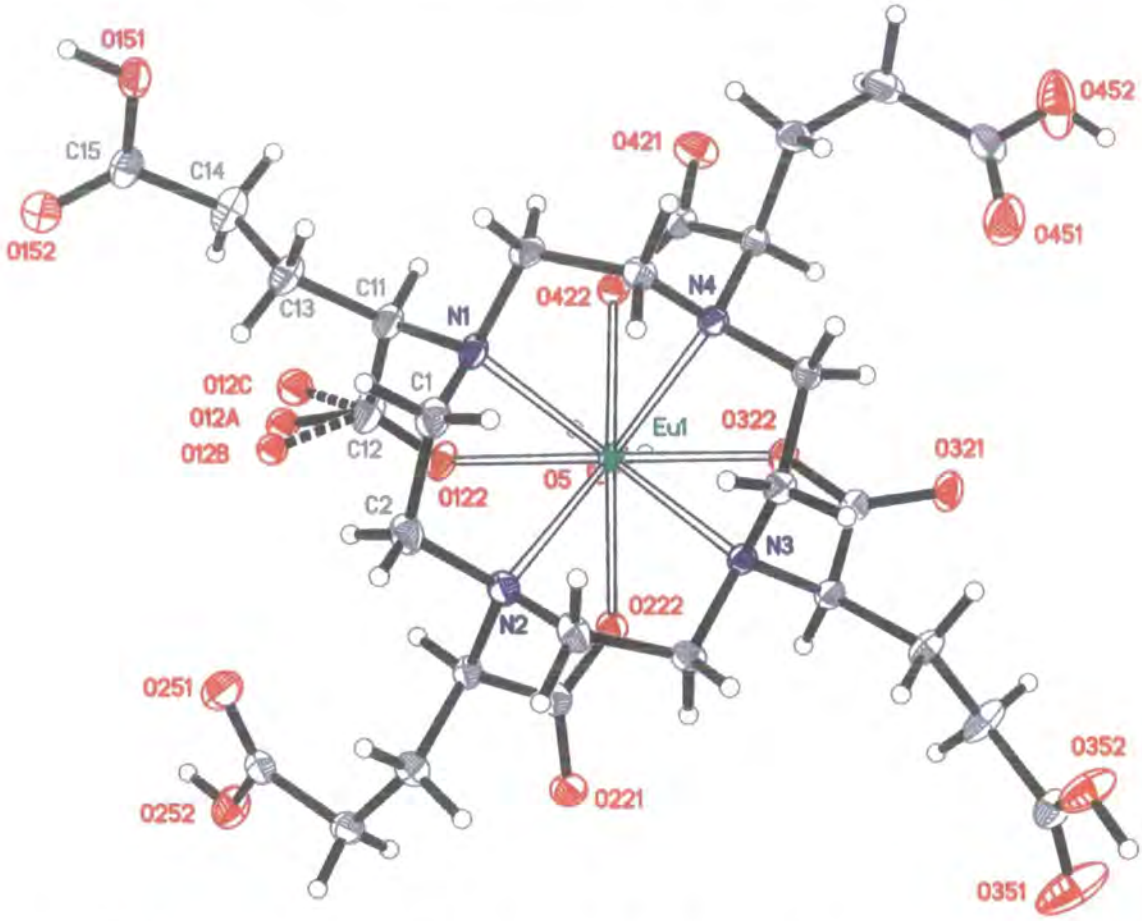

Figure 4.7.2 *– A thermal ellipsoid plot drawn at 50% probability level of the structure of europium 1,4,7,10-tetrakis(carboxyethyl)-1,4,7,10-tetraazacyclododecane in the N4 plane projected along the Eu-OH_2 bond. The R isomer of this racemic crystal is depicted and the solvent water molecules have been excluded from the figure for clarity.*

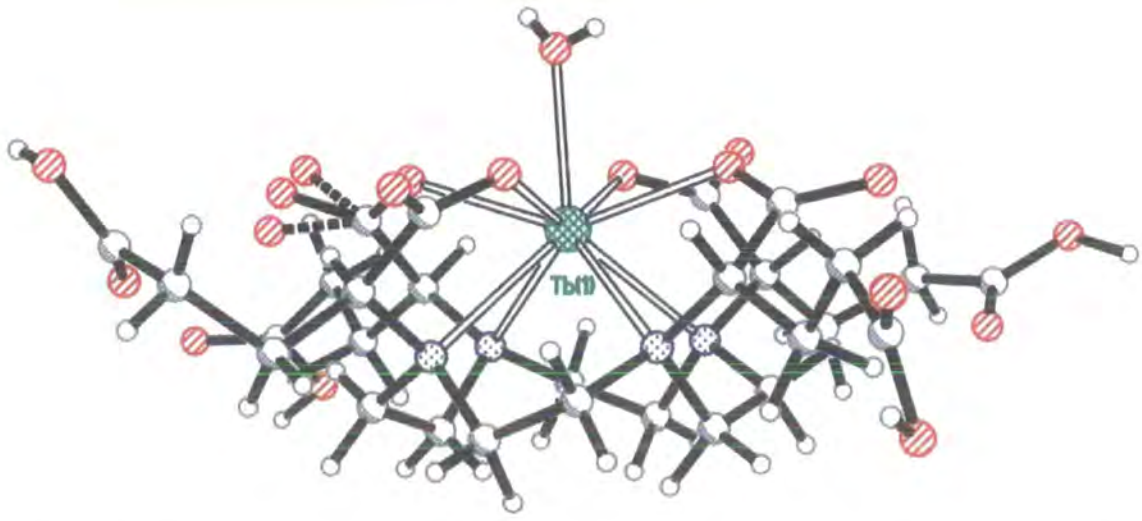

Figure 4.7.3 *– A connectivity plot of the structure in the crystal of terbium 1,4,7,10-tetrakis(carboxyethyl)-1,4,7,10-tetraazacyclododecane.*

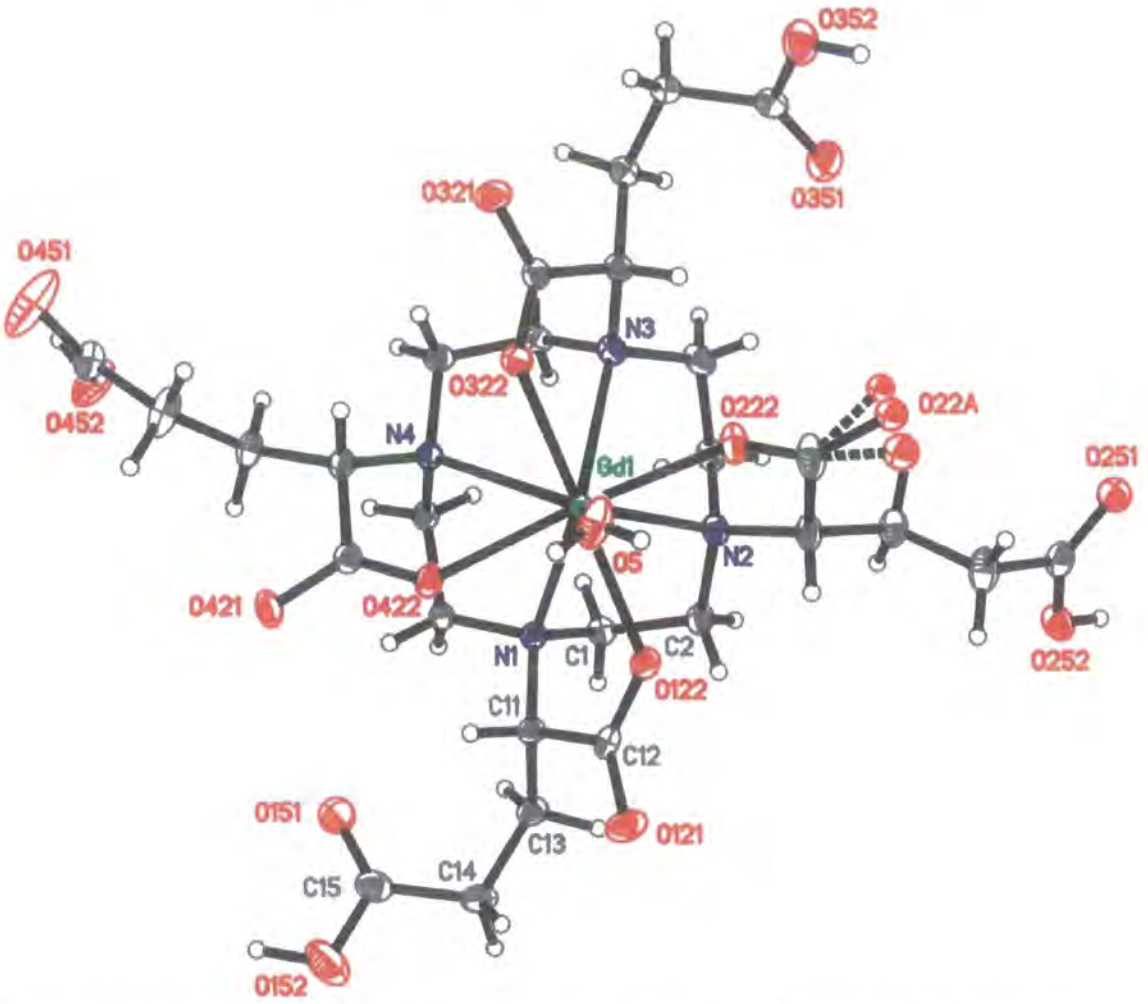

Figure 4.7.4 *– A thermal ellipsoid plot drawn at 50% probability level of the structure of gadolinium 1,4,7,10-tetrakis(carboxyethyl)-1,4,7,10-tetraazacyclododecane in the N4 plane projected along the H_2O-Gd bond. The R isomer of this racemic crystal is depicted and the solvent water molecules have been excluded from the figure for clarity.*

The three complexes are isostructural and crystallise as racemic RRRR/SSSS compounds in the centrosymmetric space group $P\bar{1}$. All three complexes crystallised as square antiprisms with the donor oxygen atoms over a carbon atom in the centre of the cyclen [3333] square. The twist angle is 38.4° for the europium complex, 38.6° for the gadolinium complex and 38.6° for the terbium complex, as an indication of the extent of isostructure and that these complexes are close to the ideal square antiprism twist angle of 40°. The torsion angles that define the independent elements of chirality are presented in ***Table 4.7.1***. Symmetry related atoms were inadvertently chosen for the europium enantiomer, but this does not effect the accuracy of the structural and a comparison of the torsion angles is achieved by negating the signs.

Table 4.7.1 *- Selected torsion angles (°) for europium, terbium and gadolinium complexes of* L^8.

	Eu·*(RRRR)*-L^8	Tb·*(RRRR)*-L^8	Gd·*(RRRR)*-L^8
N(1)-C(1)-C(2)-N(2)	59.5(4)	-61.1(6)	-61.5(2)
N(2)-C(3)-C(4)-N(3)	58.4(4)	-58.7(6)	-59.6(3)
N(3)-C(5)-C(6)-N(4)	58.7(4)	-59.0(6)	-58.1(2)
N(4)-C(7)-C(8)-N(1)	60.9(4)	-58.1(6)	-58.9(2)
N(1)-C(11)-C(12)-O(122)	-38.5(5)	18.2(6)	17.5(3)
N(2)-C(21)-C(22)-O(222)	-39.7(4)	38.1(8)	37.6(3)
N(3)-C(31)-C(32)-O(322)	-40.6(4)	39.2(6)	39.5(2)
N(4)-C(41)-C(42)-O(422)	-17.5(4)	40.6(6)	40.6(2)

The three complexes formed distinctive crystals (***Figure 4.7.6***) with sheer faces and an almost characteristic tetragonal, coffin-like morphology, but in this case, it can be viewed as a skewed coffin. Therefore, the inherent stability and persistence of the square antiprismatic structure for the *RRRR*-enantiomer is the driving force in crystallisation.

Figure 4.7.6 *– A photograph of the crystal used for data collection of the terbium complex of* L^8 *displaying the morphology that typifies this series.*

The data collected from these three complexes were intense and extended beyond 0.8 Å and this resulted in accurate structures. Absorption errors were corrected for by indexing the crystal faces for the europium complex and the program Sadabs was used for the gadolinium and terbium complexes. These refinements converged well and the positions and isotropic displacement parameters of all hydrogen atoms were determined in the gadolinium and terbium complexes whereas some hydrogen atoms were placed in calculated positions in the europium complex.

One curious feature seen in all these structures, is the static disorder in one of the proximate carbonyl oxygen atoms. There are three discrete sites with occupancies of

50%, 30% and 20%. These three partially occupied atoms were modelled with isotropic displacement parameters whereas the remainder of the non-hydrogen atoms on the macrocycle were given anisotropic motion. It is difficult to explain the reoccurrence of this disorder. It does not appear to have a dynamic component since the anisotropic displacement parameters of the carbon atom it is attached to are reasonably spherical. The nature of the disorder is that the two oxygen sites of lesser occupancy are situated at almost equal distances above and below the plane defined by the three atoms of the carboxy group. ***Table 4.7.3*** presents some bond lengths for the three complexes and this shows that in all cases the distances to the oxygen sites of lower occupancy are significantly longer, by approximately 0.06 Å. This is why one of the dihedral N-C-C-O angles presented in ***Table 4.7.1*** averages at 17.7° rather than the conventional value that is closer to 40°. A probable explanation behind the reoccurrence of these multiple occupancy oxygen atom sites can be proposed from studying the intermolecular contacts in the crystal. There are several potential hydrogen bond donors and acceptors in these molecules. The carboxy groups α to the ring nitrogen atoms are anionic and those at the extremities are protonated. In total the potential number of donors and acceptors in the eight carboxy groups are four hydrogen bond donors and twelve acceptor atoms. A frequently occurring interaction for such functional groups is packing via the classical carboxylic acid dimers where either one or both OH..O hydrogen bonds can form.[75] In this case, neither of these interactions occur and terminal carboxylic acid groups form close contacts with the non-protonated carboxy groups or water molecules in the asymmetric unit. The contacts are listed in ***Table 4.7.2***. All values here are for the gadolinium complex because this sample yielded the best data and the most successful refinement. It is fully representative of the situation for the other two structures. As can be seen these are short contacts. The interaction with the water molecule has been deemed to be a consequence of the other packing effects and not structure determining in itself. Surprisingly, the water molecule is disordered over two positions and not confined to a single site by the interaction with the carboxylic acid. There are three contacts between the carboxylic acids and the carboxy groups, one to the anionic oxygen atom (O352-H352..O122) and the other two to the carbonyl groups. The fifth

close contact in these molecules is between the disordered oxygen atom and the ordered oxygen atom on that same parent carbon atom. The distances are quite short. This contact must be a forced one, like that of H152 to the water molecule, which arises from the overall packing motif. The distance to the two sites of lesser occupancy is 0.2 Å longer, thus it is proposed that this disorder facilitates the crystallisation of a stable complex by minimising steric hindrance.

***Table 4.7.2** – Intermolecular close contacts for the Gd-L^8 complex.*

OH..O / O..O contact	Distance / Å	OH..O / O..O contact	Distance / Å
O352-H352..O122	1.88(5)	O452-H452..O121	1.69(5)
O252-H252..O321	1.70(4)	O222..O22A	2.83(1)
O152-H152..O1WA	1.55(7)	O222..O22B	2.60(1)
O152-H152..O1WB	1.65(7)	O222..O22C	2.78(1)

It is noticeable in all three complexes that the anisotropic displacement parameters on the two alternate pendant arms (for example the top and bottom fragments starting at N1 and N3 in ***Figure 4.7.4***) have smaller, more spherical anisotropic displacement parameters that the other two side arms. This is more than likely because of the effect of the intermolecular contacts. The side arms starting at N1 and N3 have three and two strong OH..O mediated contacts respectively whereas the other two side arms have only one such contact each. Additionally, the conformation of the two alternate side arms with reduced thermal motion is different. They diverge fully from the cyclen ring and when viewed in its N4 plane are practically at 180° with respect to one other whereas the other two atoms twist after the carbon atom γ to the ring nitrogen. The conformational preferences are most effectively described in terms of the torsion angle about the penultimate methylene group in ***Table 4.7.3***.

***Table 4.7.3** - Selected torsion angles (°) for europium, terbium and gadolinium complexes of L^8 to illustrate their conformational preferences.*

	Eu·(*RRRR*)-L^8	Tb·(*RRRR*)-L^8	Gd·(*RRRR*)-L^8
Cα-Cβ-Cγ-Cδ	178.2(3)	-178.9(5)	-178.5(5)
Cα-Cβ-Cγ-Cδ	-64.1(4)	63.8(6)	64.1(3)
Cα-Cβ-Cγ-Cδ	-156.8(3)	157.0(5)	156.8(2)
Cα-Cβ-Cγ-Cδ	-71.0(4)	71.5(6)	71.3(3)

These conformational effects are solid-state phenomena in order to facilitate the formation of close intermolecular contacts.

***Table 4.7.4** - Selected crystal data for the europium, gadolinium and terbium complexes of 1,4,7,10-tetrakis(carboxyethyl)-1,4,7,10-tetraazacyclododecane.*

Empirical formula	C28 H49 Eu N4 O20.25	C28 H49 Gd N4 O20	C28 H49 N4 O20 Tb
Formula weight	917.67	918.96	920.63
Temperature	150(2) K	150(2) K	150(2) K
Wavelength	0.71073 Å	0.71073 Å	0.71073 Å
Crystal system	Triclinic	Triclinic	Triclinic
Space group	$P\bar{1}$	$P\bar{1}$	$P\bar{1}$
Cell dimensions (Å/°)	a = 9.637(2) α = 102.47(2)	a =9.6460(5) α=102.652(4)	a =9.6289(1) α=102.7389(8)
	b = 12.690(4) β = 101.28(2)	b=12.6915(7) β=101.192(4)	b=12.6877(2) β=101.2348(9)
	c = 16.186(5) γ = 110.42(2)	c=16.2000(11) γ=110.446(3)	c=16.2170(2) γ=110.5812(4)
Volume	1729.84(3) $Å^3$	1731.9(2) $Å^3$	1726.76(4) $Å^3$
Z	2	2	2
Density (calculated)	1.762 g/cm^3	1.762 g/cm^3	1.771 g/cm^3
Absorption coefficient	1.906 mm^{-1}	2.007 mm^{-1}	2.141 mm^{-1}
Absorption correction	Integration	Empirical – Sadabs	Empirical – Sadabs
Max. & min. transmiss.	0.835 and 0.713	0.610 and 0.491	0.677 and 0.419
F(000)	940	938	940
Crystal size	0.16 x 0.16 x 0.10 mm^3	0.34 x 0.32 x 0.18 mm^3	0.10 x 0.20 x 0.25 mm^3
θ range for collection	1.35 to 27.45°.	1.35 to 27.50°.	1.35 to 27.53°.
Index ranges	-11<=h<=12,	-12<=h<=12,	-11<=h<=12,
	-15<=k<=16,	-16<=k<=16,	-16<=k<=16,
	-20<=l<=20	-13<=l<=21	-21<=l<=20
Reflections collected	13944	14872	13969
Independent reflects.	7826 [R(int) = 0.0310]	7843 [R(int) = 0.0251]	7856 [R(int) = 0.0381]
Refinement method	Full-matr least-squares on F^2	Full-matr least-squares on F^2	Full-matr least-squares on F^2
Data/restrs/parameters	7797 / 0 / 627	7843 / 0 / 651	7856 / 0 / 610
Goodness-of-fit on F^2	1.094	1.046	1.085
R indices [I>2σ(I)]	R1 = 0.0305, wR2 = 0.0670	R1 = 0.0211, wR2 = 0.0511	R1 = 0.0442, wR2 = 0.1057
R indices (all data)	R1 = 0.0364, wR2 = 0.0747	R1 = 0.0242, wR2 = 0.0523	R1 = 0.0601, wR2 = 0.1177
Extinction coefficient	Solvent water only	Solvent water only	Solvent water only
Largest residuals	0.979 and -0.950 $e.Å^{-3}$	0.656 and -0.714 $e.Å^{-3}$	2.683 and -2.362 $e.Å^{-3}$

The full list of atomic co-ordinates, bond lengths and angles and anisotropic displacement parameters can be found in the Appendices (***A.4.13** - **A.4.15***). The final cycles of least-squares of the terbium complex illuminated a problem with the model, as can be seen from ***Figure 4.7.7***. The maximum and minimum values of residual electron density were +2.683 and –2.362 $e/Å^3$ respectively, which is higher than what would be acceptable for an absorption corrected and otherwise error free structure.

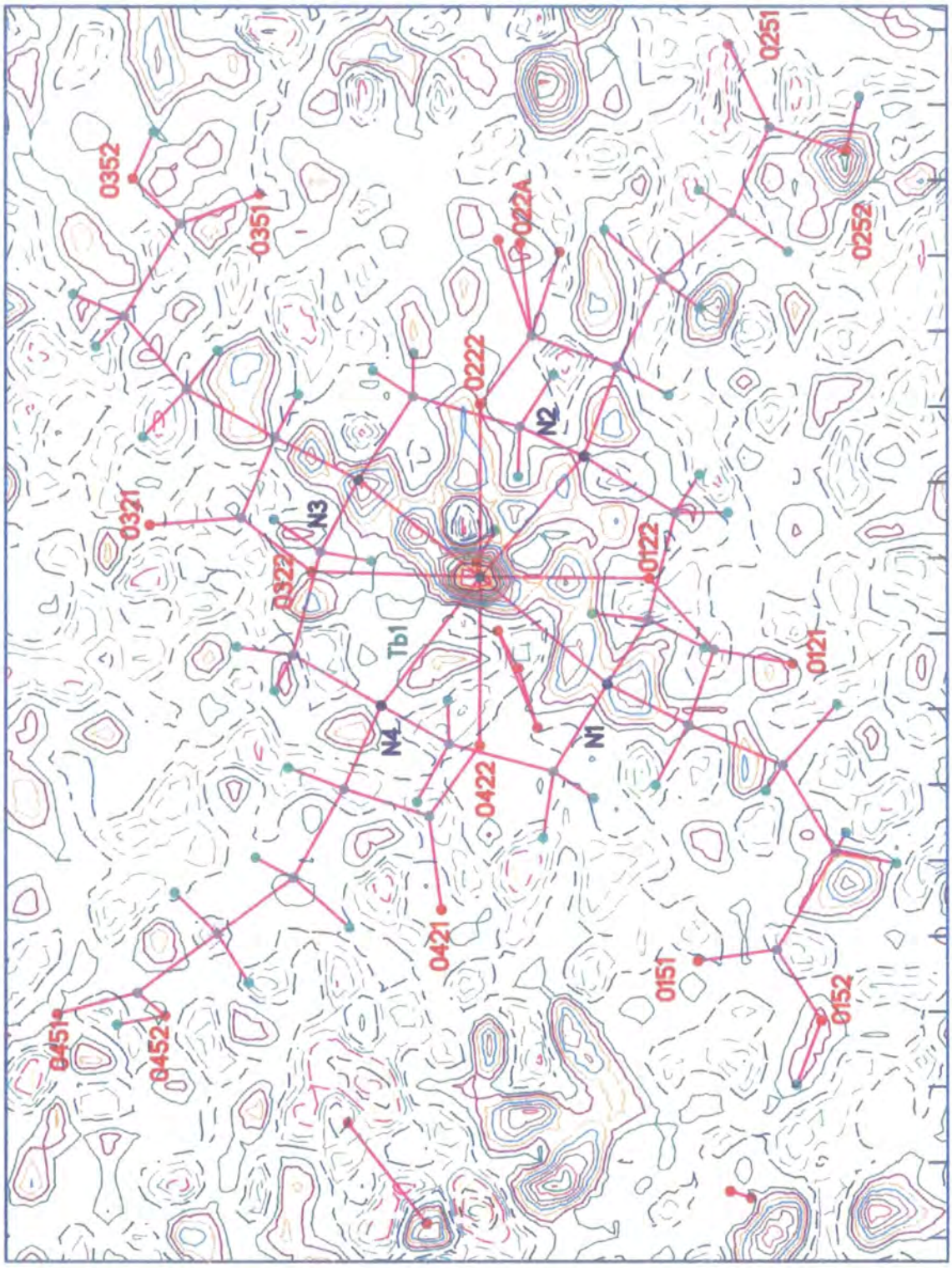

***Figure 4.7.7** – A difference electron density (Fo-Fc) contouring plot of the final model in the refinement of terbium 1,4,7,10-tetrakis(carboxyethyl)-1,4,7,10-tetraazacyclododecane in the plane of the four nitrogen atoms. A new contour is drawn every 0.1 e/Å^3 Positive residuals are drawn with unbroken lines and negative residuals with broken lines. The colour code in e/Å^3 is: -0.8 green, -0.7 red, -0.6 blue, -0.5 yellow, -0.4 pink, -0.3 white, -0.2 grey, -0.1 blue, 0.1 green, 0.2 purple, 0.3 mustard, 0.4 bright blue, 0.5 brown, 0.6 dark grey, 0.7 red, 0.8 green, 0.9 red, 1.0 blue, 1.1 yellow, 1.2 pink.*

This electron density takes the form of a ripple on the metal with the highest electron density peak 0.89 Å from the metal and the second highest peak 0.93 Å from the metal. The problem was not encountered for the gadolinium and europium complexes in this series, which have virtually the same absorption coefficient values. Similarly, the data for the gadolinium complex was absorption corrected using Sadabs. Such termination waves around heavy metal sites are common before the data are absorption corrected but in this case, the problem remained unchanged when no absorption correction was applied and also when an empirical ψ-scan correction was applied. On viewing the difference electron density (Fo-Fc) in the N4 plane in ***Figure 4.7.7***, it became clear that the largest peaks by far were located on the terbium metal position. After that the next highest peaks were in the lattice near solvent water and therefore very likely to have arisen from the disordered water molecules that could not be modelled very well. It was thought that the scattering factors for terbium might not be determined accurately, which would lead to unusually high residuals around the atomic position, but this was refuted on noting that the structure of terbium vanadate did not exhibit this problem.[76] The scattering factors for the tri-cationic terbium were also used, since neutral scattering factors are used as default in the SHELXL-93 refinement software,[77] but made no impression on the model.

The complexes were all monoanions with approximately three independent water molecules, one of which was a counter ion. There is a steady decline in bond length to the nine donor atoms from europium, through gadolinium to terbium. It is more sensitive to atom type, as can be seen in the case of the ring nitrogen atoms, in ***Figure 4.7.8***. This shows that with increasing atomic number across the lanthanide series, the metal moves towards the centre of the square antiprismatic core. The oxygen donors and bound water molecule 'follow it in' as the metal approaches the N4 plane. The changes in distances to water are of the same magnitude as to the other atom type even though it is arguably less constrained and thus freer to vary. Despite this tendency for the lanthanide ion to drop into the macrocyclic core with increasing atomic number,

there is no significant change in the overall shape of the complex and the water molecules remain also disordered in the lattice, indicating that these are not structural.

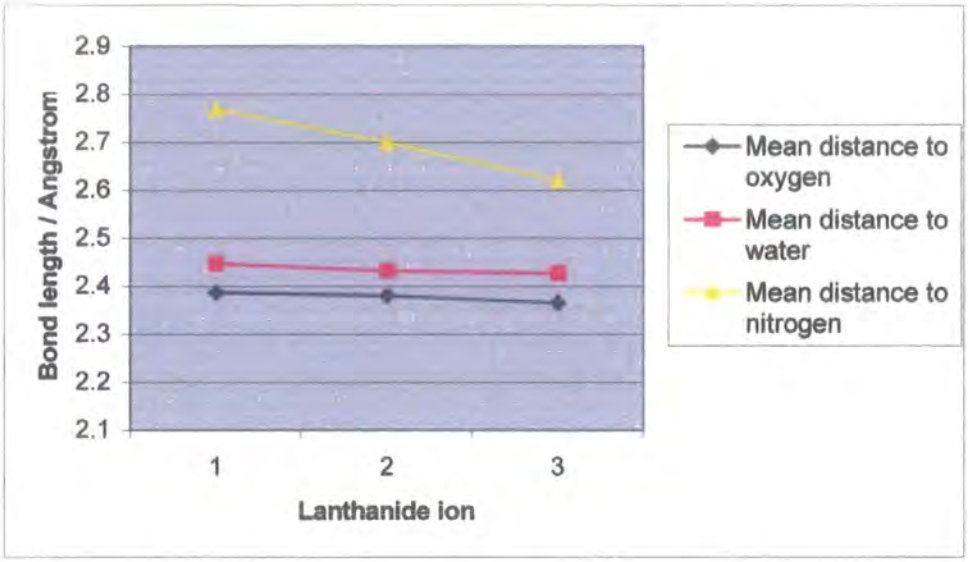

Figure 4.7.8 *- Selected bond lengths for europium, terbium and gadolinium complexes of L^8, where 1 = Eu, 2 = Gd and 3 = Tb.*

It was thought that the use of the ligand, L^8, with oxygen atom donors having formal negative charges would form stronger lanthanide ion complexes and that this would be reflected in the metal-donor atom bond lengths. This was not the case and a comparison of the distance to the nine donor atoms from europium in Eu·(*SSSS*)-L^2 with the Eu·(*RRRR*)-L^8 showed no significant difference in the bond lengths. Certainly, there is a lot of strain in the square antiprismatic geometries of these complexes, as can be seen from ***Table 4.7.5*** there is a significant variation in both the metal-N distances and the metal-O distances.

***Table 4.7.5** – Selected bond lengths (Å) for C28 H49 Eu N4 O20.25, C28 H49 Gd N4 O20 and C28 H49 N4 O20 Tb, the lanthanide complexes of L^8.*

C28 H49 Eu N4 O20.25		C28 H49 Gd N4 O20		C28 H49 N4 O20 Tb	
Eu(1)-O(222)	2.354(2)	Gd(1)-O(322)	2.3492(15)	Tb(1)-O(322)	2.335(3)
Eu(1)-O(422)	2.391(2)	Gd(1)-O(222)	2.383(2)	Tb(1)-O(122)	2.368(4)
Eu(1)-O(122)	2.393(2)	Gd(1)-O(122)	2.385(2)	Tb(1)-O(222)	2.371(3)
Eu(1)-O(322)	2.412(2)	Gd(1)-O(422)	2.4028(15)	Tb(1)-O(422)	2.386(3)
Eu(1)-O(5)	2.447(3)	Gd(1)-O(5)	2.432(2)	Tb(1)-O(5)	2.427(4)
Eu(1)-N(3)	2.664(3)	Gd(1)-N(4)	2.655(2)	Tb(1)-N(4)	2.644(4)
Eu(1)-N(4)	2.667(3)	Gd(1)-N(1)	2.662(2)	Tb(1)-N(1)	2.654(4)
Eu(1)-N(1)	2.681(3)	Gd(1)-N(2)	2.674(2)	Tb(1)-N(2)	2.665(4)
Eu(1)-N(2)	2.696(3)	Gd(1)-N(3)	2.689(2)	Tb(1)-N(3)	2.686(4)
O(12A)-C(12)	1.274(6)	O(121)-C(12)	1.235(3)	O(121)-C(12)	1.238(6)
O(12B)-C(12)	1.367(9)	O(122)-C(12)	1.282(3)	O(122)-C(12)	1.296(6)
O(12C)-C(12)	1.343(14)	O(151)-C(15)	1.213(3)	O(151)-C(15)	1.218(7)
O(122)-C(12)	1.249(4)	O(152)-C(15)	1.307(3)	O(152)-C(15)	1.298(7)
O(151)-C(15)	1.300(4)	O(22A)-C(22)	1.275(4)	O(22A)-C(22)	1.292(9)
O(152)-C(15)	1.227(4)	O(22B)-C(22)	1.363(6)	O(22B)-C(22)	1.353(14)
O(221)-C(22)	1.242(4)	O(22C)-C(22)	1.346(9)	O(22C)-C(22)	1.366(18)
O(222)-C(22)	1.277(4)	O(222)-C(22)	1.250(3)	O(222)-C(22)	1.249(7)
O(251)-C(25)	1.213(4)	O(251)-C(25)	1.225(3)	O(251)-C(25)	1.231(7)
O(252)-C(25)	1.331(4)	O(252)-C(25)	1.305(3)	O(252)-C(25)	1.289(7)
O(321)-C(32)	1.275(4)	O(321)-C(32)	1.244(3)	O(321)-C(32)	1.242(6)
O(322)-C(32)	1.248(4)	O(322)-C(32)	1.275(3)	O(322)-C(32)	1.276(6)
O(351)-C(35)	1.193(5)	O(352)-C(35)	1.330(3)	O(352)-C(35)	1.331(7)
O(352)-C(35)	1.319(4)	O(351)-C(35)	1.216(3)	O(351)-C(35)	1.207(7)
O(421)-C(42)	1.230(4)	O(421)-C(42)	1.280(3)	O(421)-C(42)	1.284(6)
O(422)-C(42)	1.287(4)	O(422)-C(42)	1.246(3)	O(422)-C(42)	1.247(6)
O(451)-C(45)	1.214(5)	O(452)-C(45)	1.313(3)	O(451)-C(45)	1.191(7)
O(452)-C(45)	1.304(5)	O(451)-C(45)	1.198(3)	O(452)-C(45)	1.312(7)
N(1)-C(1)	1.488(5)	N(1)-C(8)	1.495(3)	N(1)-C(1)	1.492(6)
N(1)-C(11)	1.494(4)	N(1)-C(1)	1.497(3)	N(1)-C(8)	1.505(6)
N(1)-C(8)	1.501(4)	N(1)-C(11)	1.501(3)	N(1)-C(11)	1.507(6)
N(2)-C(3)	1.489(4)	N(2)-C(3)	1.492(3)	N(2)-C(3)	1.487(7)
N(2)-C(2)	1.497(4)	N(2)-C(21)	1.498(3)	N(2)-C(21)	1.495(6)
N(2)-C(21)	1.507(4)	N(2)-C(2)	1.500(3)	N(2)-C(2)	1.508(6)
N(3)-C(5)	1.483(4)	N(3)-C(5)	1.496(3)	N(3)-C(5)	1.490(7)
N(3)-C(4)	1.501(4)	N(3)-C(4)	1.498(3)	N(3)-C(31)	1.496(6)
N(3)-C(31)	1.503(4)	N(3)-C(31)	1.500(3)	N(3)-C(4)	1.501(6)
N(4)-C(7)	1.496(4)	N(4)-C(7)	1.491(3)	N(4)-C(7)	1.483(6)
N(4)-C(41)	1.500(4)	N(4)-C(6)	1.497(3)	N(4)-C(6)	1.500(6)
N(4)-C(6)	1.501(4)	N(4)-C(41)	1.507(3)	N(4)-C(41)	1.507(6)

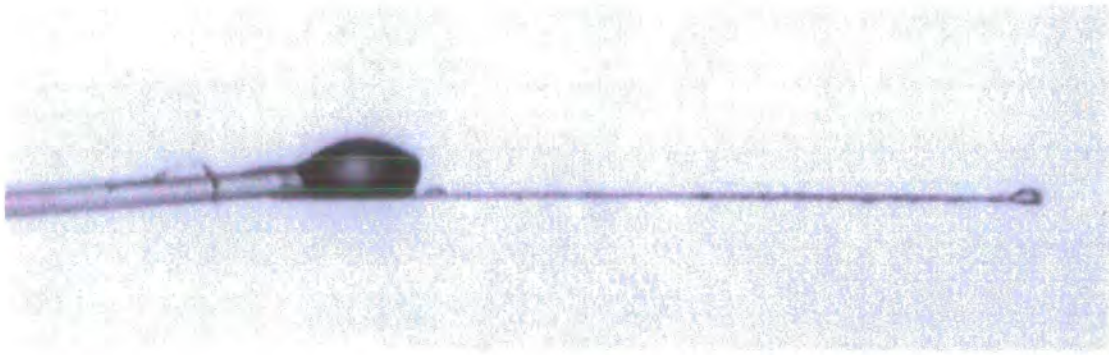

***Figure 4.7.9** – A photograph of the mounted crystal of Yb-L^8 that was measured on Station 9.8, Daresbury SRS. The extremely thin fibre is glue to the stouter fibre to facilitate crystal mounted and to reduce the amount of amorphous glass scatter from the intense source.*

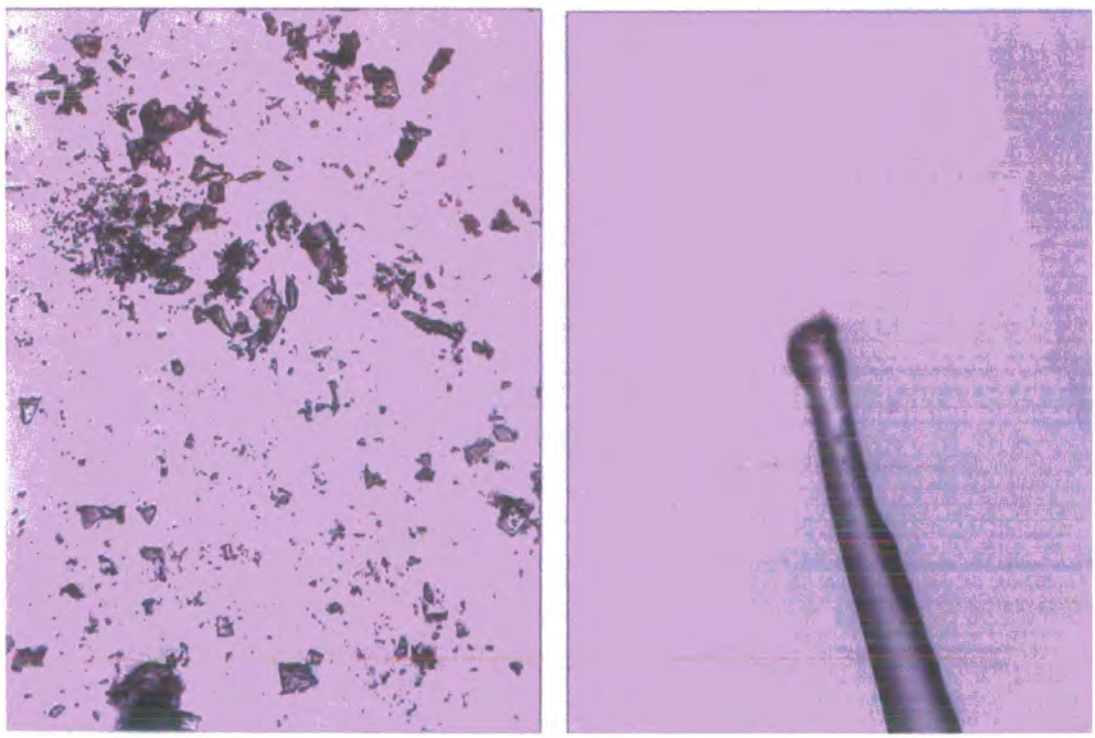

(a) *(b)*

***Figure 4.7.10** – Samples that were screened by Philip Pattison on the Swiss-Norwegian beamline (BM1B) at the ESRF. (a) The sample of Yb-L^8 crystals. (b) The mounted plate-like crystal on the fibre end.*

The solid-state structure of the ytterbium complex of L^8 was of considerable interest because results from a ^{1}H NMR experiment gave a ration of 1:15 for the mole ratio of square antiprism: twisted square antiprism for this complex.[78] This was the biggest swing in favour of the twisted square antiprismatic isomer. It was also suspected that the complex would not bind a water molecule as in the twisted square antiprismatic

ytterbium complex of L^7. The ytterbium complex structure remains unsolved but the strategies tried will be outlined here. The X-ray crystal structure of the ytterbium derivative of L^8 was attempted by collecting data on both a laboratory SMART source and a SMART-CCD installed on station 9.8 at Daresbury SRS. The crystals of this sample were all minute and plate like. Initial crystal screening on the laboratory source revealed no intensities above background level. The data were then collected at station 9.8 at a wavelength setting calibrated at 0.6878 Å in a beamtime allocation from 2/7/98 – 4/7/98. A photograph of the mounted crystal is shown in ***Figure 4.7.9***. Some tests were also performed at the European Synchrotron Radiation Facility (ESRF) by Philip Pattison but the reflections were too weak to obtain a data set. The crystals and the mount are shown in ***Figure 4.7.10***. The stout glass fibre also contributed to the amorphous scatter in this case.

A small (0.05 x 0.05 x 0.02 mm3) crystal was mounted on an extremely thin glass fibre (Figure 4.7.9) and flash cooled to 100 K The unit cell dimensions from an initial search of reciprocal space were a = 22.464(3), b = 22.476(2), c = 16.623(2) Å, α = 90.03(7), β = 89.99(8), γ = 90.06(10)°, V = 8392(1) $Å^3$. A hemisphere of data was collected with an ω scan width of 0.15° and a 2 sec exposure time. A Niggli reduced cell of a = 15.8472(1), b = 15.8519(1), c = 16.5913(1) Å, α = 90.0147(4), β = 90.0470(4), γ = 89.9858(6)° was obtained after processing the data. 28130 reflections were recorded in total. There was a rapid drop off in intensity with increasing $\sin\theta/\lambda$ and the data were weak with 21087 having $I/\sigma(I) \leq 2$. 11184 unique data were obtained when merged with the point group –4. The redundancy was satisfactory with 6479 unique data measured three or more times. The data flow protocol for the treatment of outliers and negative intensities developed for charge density analysis[79] was followed. SADABS[80] was used to correct for incident beam decay only. The program SORTAV[81,82] merges data whilst being a very effective means of identifying outliers and rejecting reflections. The program BAYES[83] was then used to treat negative intensities. The space group was unclear but fragments of the structure emerged by finding the ytterbium position by Patterson methods in $P\bar{4}$ and P4/nmm. In P-4, the

refinement looked most encouraging and two molecules were built through a series cycles of Fourier syntheses. For 11184 unique data, R_1 was 0.1476, wR_2 = 0.3683 and most of the core of the structure was found. However, the solution was wrong since the cyclen ring contained ten atoms in both molecules and the pendant arms collided into one another. In P4/nmm, two ytterbium atoms were located, one on a four fold with one quarter occupancy and one on a four fold inversion centre with a quarter occupancy. It was not possible to find anymore of the molecule. Solutions in these two space groups assume molecular and crystallographic four-fold symmetry. The symmetry was lowered to $P\bar{1}$ but this did not yield a solution. It is believed that this structure is twinned but it is highly likely to have crystallographic four-fold symmetry. It remains for new crystals to be grown.

4.7.1 Structures of the all the isomers of the free ligand.

The structures of *all* of the isomers of 1,4,7,10-tetrakis(carboxyethyl)-1,4,7,10-tetraazacyclododecane were determined by X-ray crystallography, as a means to understanding the conformational changes that occur upon metal-binding. There are four stereogenic centres α to the cyclen ring nitrogen atom, which leads to four isomers in solution, which can interconvert by ring inversion or pendant arm rotation. The structures of the RRRR isomeric complexes of europium, gadolinium and terbium show a monocapped square antiprismatic geometry with a characteristic pendant arm conformation. Crystals of the remaining RSRS, RRRS and RRSS isomers were obtained and measured on the Siemens SMART diffractometer at 150(2) K.

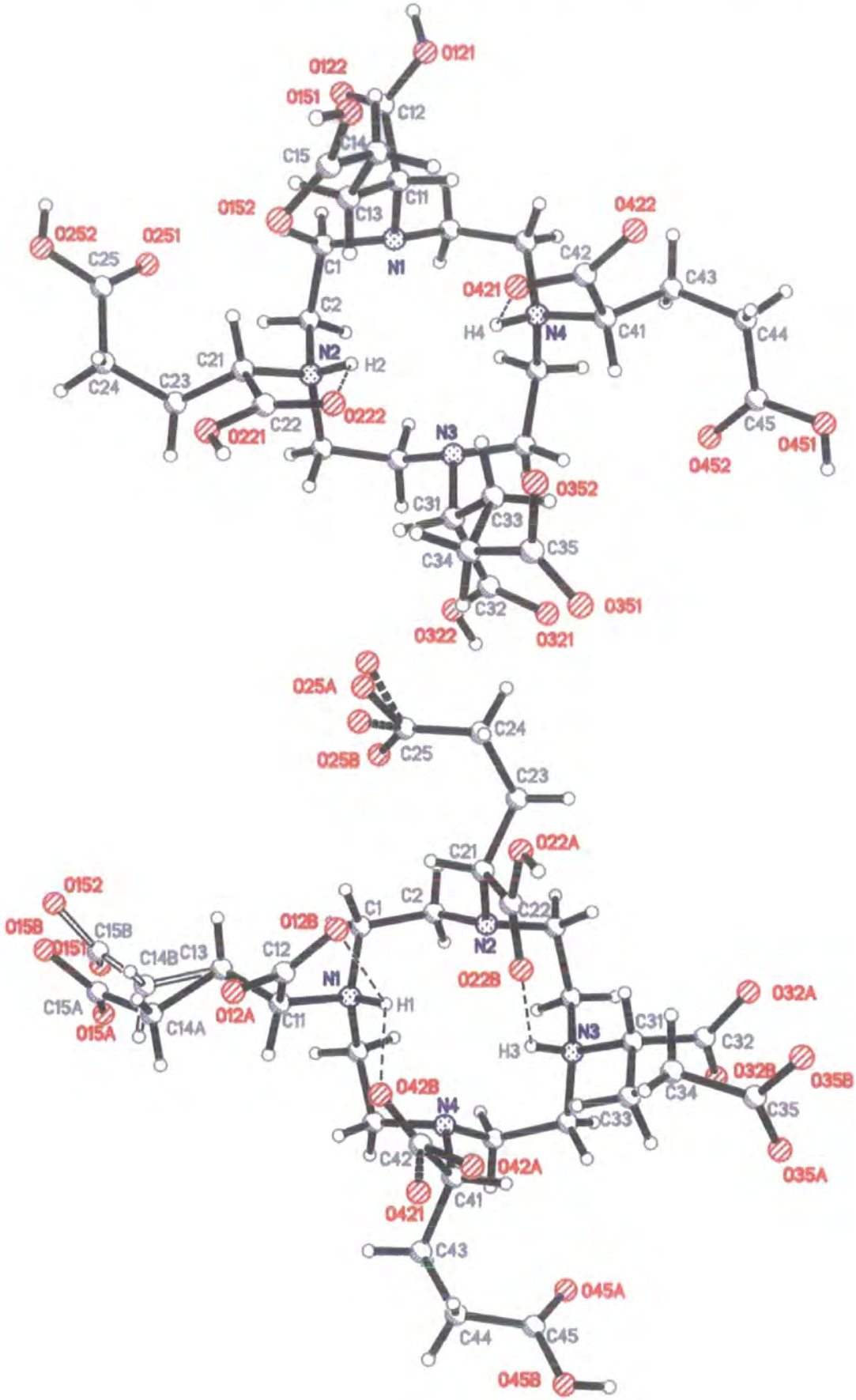

Figure 4.7.1.1 *– Diagrams of the crystal structures of RSRS (top) and RRRS (bottom) isomers of 1,4,7,10-tetrakis(carboxyethyl)-1,4,7,10-tetraazacyclododecane.*

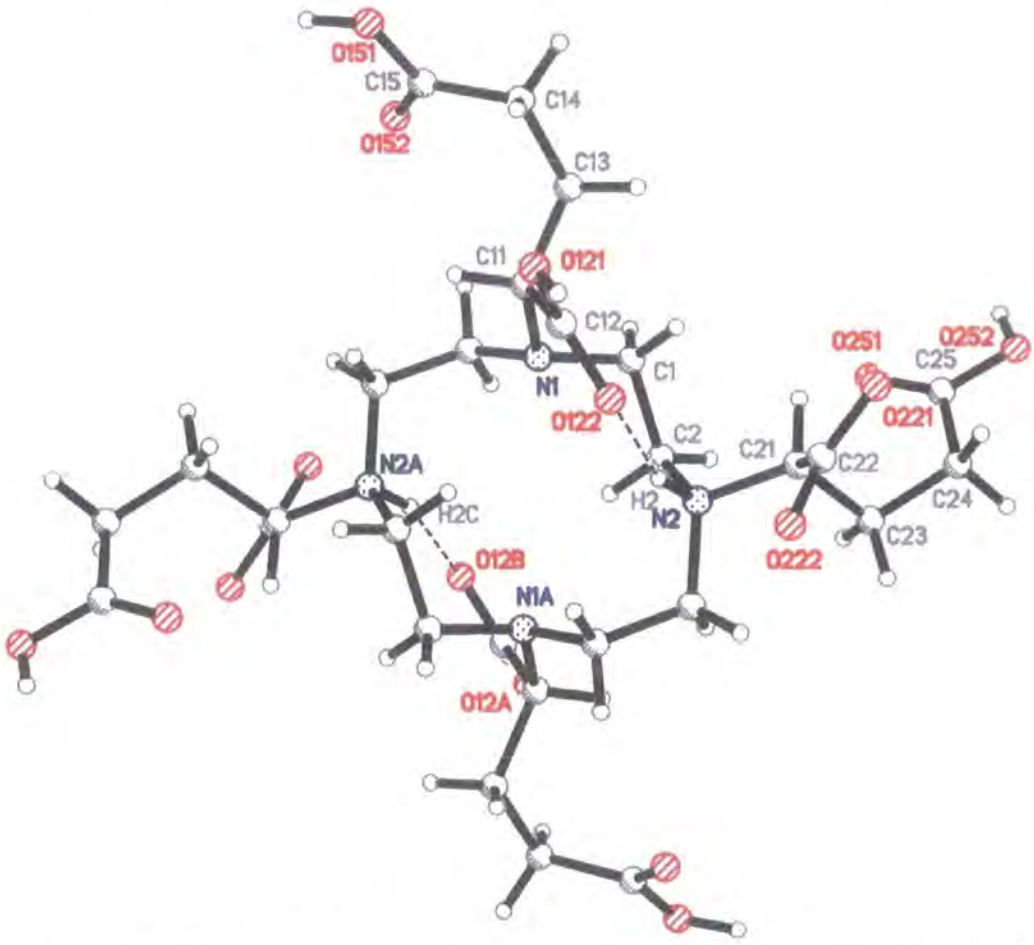

Figure 4.7.1.2 *– Diagram of the RRSS isomer of 1,4,7,10-tetrakis(carboxyethyl)-1,4,7,10-tetraazacyclododecane (dashed lines indicate close contacts to hydrogen and atoms are symmetry related about an inversion centre to their equivalent atoms with a letter suffix).*

They all diffracted weakly due to only light atom scatterrers being present and small crystal size. Additionally, the RRRS isomer has three parts of the molecule that are disordered. The ligands (***figures 4.7.1.1 - 4.7.1.2*** and ***tables 4.7.1.1-4.7.1.2***) all have some intramolecular transannular hydrogen bonded contact, which takes a different form in each structure since the carboxylic acid hydrogen bond acceptor position is dictated by the chirality at the stereogenic centre. The interactions in the RSRS isomer are reminiscent of those observed in DOTA whereby the contact is between an aza group and the carboxylic acid group that branches off it. In all three complexes, alternate ring nitrogen atoms were protonated. The RRSS isomer crystallised on an inversion centre. The structural implication that this has is that the classic [3333] conformation was lost and the ring distorted considerably.

Table 4.7.1.1 *– Selected crystal data and structure refinement details for the three diastereomers of* L^8.

ISOMER	*RSRS*	*RRRS*	*RRSS*
Empirical formula	C28 H67 N4 O23.5	C29 H54.5 N4 O20.25	C28 H60 N4 O22
Formula weight	835.86	783.27	804.80
Temperature	150(2) K	150(2) K	150(2) K
Wavelength	0.71073 Å	0.71073 Å	0.71073 Å
Crystal system	Monoclinic	Monoclinic	Triclinic
Space group	$P2_1/c$	$P2_1/c$	P-1
Cell dimensions (Å/°)	a = 21.4038(1) α = 90	a = 16.7042(1) α= 90	a = 9.2517(2) α = 97.19(2)
	b = 10.1930(1) β = 109.425(1)	b = 10.7222(1) β= 102.746(1)	b = 9.7886(3) β = 106.94(2)
	c = 18.5358(2) γ = 90	c = 21.1538(2) γ = 90	c = 12.2960(4) γ = 113.08(2)
Volume, Z	3813.74(6) $Å^3$, 4	3695.40(5) $Å^3$, 4	942.99(5) $Å^3$, 1
Density (calculated)	1.456 g/cm^3	1.408 g/cm^3	1.417 g/cm^3
Absorption coefficient	0.126 mm^{-1}	0.120 mm^{-1}	0.122 mm^{-1}
Absorption correction	Not applied	Sadabs, Sortav & Bayes	Multiscan (Sadabs)
F(000)	1804	1674	432
Crystal size	0.40 x 0.30 x 0.25 mm^3	0.20 x 0.20 x 0.20 mm^3	0.25 x 0.20 x 0.10 mm^3
θ range for data coll.	1.01 to 27.56°.	1.97 to 27.47°.	1.80 to 25.00 °
Index ranges	-27<=h<=27,	-21<=h<=21,	-9<=h<=11,
	-12<=k<=13,	0<=k<=13,	-12<=k<=9,
	-24<=l<=21	0<=l<=27	-15<=l<=15
Reflections collected	29672	25267	8066
Independent reflections	8759 [R(int) = 0.0722]	8402 [R(int) = 0.0772]	3321 [R(int) = 0.0943]
Max. & min. transm.	0.862 and 1.000		0.977 and 0.636
Refinement method	Full-matrix least-squares on F^2	Full-matrix least-squares on F^2	Full-matrix least-squares on F^2
Data / parameters	8759 / 519	8402 / 496	3321 / 267
Goodness-of-fit on F^2	1.169	0.954	1.052
R indices [I>2σ(I)]	R1 = 0.0887, wR2 = 0.2024	R1 = 0.0839, wR2 = 0.2150	R1 = 0.0795, wR2 = 0.1711
R indices (all data)	R1 = 0.1212, wR2 = 0.2200	R1 = 0.1593, wR2 = 0.2742	R1 = 0.1741, wR2 = 0.2310
Extinction coefficient	Not refined	Solvent water correction	Not refined
Largest residuals	0.900 and -0.647 $e.Å^{-3}$	0.960 and -0.599 $e.Å^{-3}$	0.555 and -0.406 $e.Å^{-3}$

The full list of atomic co-ordinates, bond lengths and angles and anisotropic displacement parameters can be found in the Appendices (***A.4.16 - A.4.18***).

***Table 4.7.1.2** – Selected bond lengths for three of the isomers of L^8.*

RSRS		*RRRS*		*RRSS*	
O(121)-C(12)	1.336(5)	O(12B)-C(12)	1.267(7)	O(121)-C(12)	1.321(6)
O(122)-C(12)	1.201(5)	O(12A)-C(12)	1.245(7)	O(121)-H(121)	0.84
O(151)-C(15)	1.327(5)	O(22B)-C(22)	1.218(5)	O(122)-C(12)	1.221(6)
O(152)-C(15)	1.221(5)	O(22A)-C(22)	1.327(5)	O(151)-C(15)	1.331(6)
O(221)-C(22)	1.266(5)	O(25A)-C(25)	1.355(9)	O(151)-H(151)	0.97(7)
O(222)-C(22)	1.241(5)	O(251)-O(252)	1.31(2)	O(152)-C(15)	1.214(6)
O(251)-C(25)	1.205(5)	O(251)-C(25)	1.409(13)	O(221)-C(22)	1.262(7)
O(252)-C(25)	1.337(5)	O(252)-C(25)	1.435(16)	O(222)-C(22)	1.251(7)
O(321)-C(32)	1.216(5)	O(25B)-C(25)	1.213(5)	O(251)-C(25)	1.211(7)
O(322)-C(32)	1.307(5)	O(32B)-C(32)	1.261(4)	O(252)-C(25)	1.306(7)
O(351)-C(35)	1.198(5)	O(32A)-C(32)	1.270(5)	O(252)-H(252)	0.72(8)
O(352)-C(35)	1.348(5)	O(35B)-C(35)	1.353(5)	N(1)-C(4)	1.465(7)
O(421)-C(42)	1.262(5)	O(35A)-C(35)	1.213(5)	N(1)-C(1)	1.474(7)
O(422)-C(42)	1.258(5)	O(42B)-C(42)	1.168(6)	N(1)-C(11)	1.486(6)
O(451)-C(45)	1.324(5)	O(42A)-O(421)	1.049(13)	N(2)-C(3)	1.511(6)
O(452)-C(45)	1.236(5)	O(42A)-C(42)	1.437(11)	N(2)-C(2)	1.512(6)
N(1)-C(8)	1.479(4)	O(421)-C(42)	1.326(10)	N(2)-C(21)	1.529(7)
N(1)-C(11)	1.480(5)	O(45B)-C(45)	1.338(5)	C(1)-C(2)	1.528(7)
N(1)-C(1)	1.486(5)	O(45A)-C(45)	1.224(5)	C(3)-C(4)#1	1.511(8)
N(2)-C(2)	1.511(5)	N(1)-C(1)	1.510(5)	C(4)-C(3)#1	1.511(8)
N(2)-C(3)	1.514(5)	N(1)-C(8)	1.522(5)	C(11)-C(12)	1.523(7)
N(2)-C(21)	1.521(5)	N(1)-C(11)	1.525(5)	C(11)-C(13)	1.555(8)
N(3)-C(4)	1.476(5)	N(2)-C(2)	1.467(5)	C(13)-C(14)	1.535(7)
N(3)-C(5)	1.478(5)	N(2)-C(3)	1.475(5)	C(14)-C(15)	1.494(8)
N(3)-C(31)	1.492(5)	N(2)-C(21)	1.479(5)	C(21)-C(22)	1.529(7)
N(4)-C(7)	1.508(5)	N(3)-C(4)	1.507(5)	C(21)-C(23)	1.538(7)
N(4)-C(6)	1.520(5)	N(3)-C(5)	1.519(4)	C(23)-C(24)	1.521(8)
N(4)-C(41)	1.531(5)	N(3)-C(31)	1.524(5)	C(24)-C(25)	1.520(8)
		N(4)-C(7)	1.477(5)		
		N(4)-C(6)	1.482(5)		
		N(4)-C(41)	1.483(5)		
		C(15A)-O(15A)	1.273(15)		
		C(15A)-O(15B)	1.307(16)		
		C(15B)-O(151)	1.251(9)		
		C(15B)-O(152)	1.302(9)		

4.8 Conclusions and The Future

"Nothing holds up the progress of science so much as the right idea at the wrong time." – *Vincent de Vigneaud, 1901 – 1978.*

This chapter has shown the rich diversity in structures adopted by lanthanide macrocyclic complexes within an eight or nine co-ordination sphere. It also has shown how making small changes to lanthanide complexes built on the DOTA framework can render complexes that are optimised for use as *in vivo* probes in MRI, PET imaging or luminescence experiments.

The interactions between the chiral molecules of the tetraamide series are highly specific. Molecular recognition in biological systems is also achieved through specific interactions between chiral molecules. All of the common amino acids are chiral molecules and the oligonucleotides that form the DNA helix form either a right-handed (B-DNA) or left-handed (A-DNA or Z-DNA) turn.

There has been much speculation about the form of the interactions between small molecules and DNA. Recent experiments have begun to shed light on this. The organometallic chelate Ru^{2+}tris(phenanthroline) is a chiral molecule, i.e. the bidentate ligands can arrange themselves in a Δ or Λ manner about the metal. One of the phenanthroline ligands intercalates between the base pairs in DNA and it has been shown that the interaction is enantioselective with the Δ isomer intercalating between the nitrogenous bases in the similarly right-handed B-DNA.[84] The potential use for chiral lanthanide luminescent complexes in nucleic acid chemistry is obviously enormous. They are employed as luminescent markers, The chemical properties of successful luminescent markers[85] are (i) a photochemically and kinetically stable compound (ii) a long wavelength of excitation (> 350 nm) (iii) high absorptivity at the wavelength of excitation (iv) efficient energy transfer from the ligand to the central ion (v) long luminescence lifetime (vi) good water solubility (vii) do not influence the structure and binding behavior of the nucleic acid. The europium and terbium complexes of the tetraamide series are good candidates and fit these criteria well.

It has been shown by Jacqueline Barton that chiral rhodium and ruthenium chelates bind selectively to DNA, intercalating the flat hydrocarbon rings on the pendant arms between the DNA base pairs. When irradiated with ultra-violet light, the complex is reduced, removing electrons from neighbouring nucleotides. Certain DNA sequences are more susceptible to oxidation and it has been shown that G sites are more easily oxidised in addition to GG and GGG.[86] Inserting extra bases into one of the strands of the double helix thus creating a bend can protect these. The distance dependence of photoinduced electron transfer along the DNA helix has been investigated. It has shown to fall off linearly with distance in acridine-DNA conjugates.[87] The implications of this are vast considering that mutations caused by ultra-violet radiation alter the reading frame and can lead to skin cancers. One such mutation is the formation of thymine dimers. The metallointercalator $Rh(phi)_2DMB^{3+}$ (phi = 9,10-phenanthrenequinone diimine; DMB = 4,4'-dimethyl-2,2'-bipyridine) has been shown to repair the thymine dimer by oxidising it.[88,89] Complexes involving osmium and ruthenium have also been investigated here.

There has been an explosion in the structural investigations of DNA and RNA structure since the landmark paper of James Watson and Francis Crick in 1953, which revealed that the coiled helical chains consisted of phosphodiester groups lined to β-D-deoxyribofuranose residues with 3',5' linkages. The purine and pyrimidine bases pairs stack in the centre of the helix forming 'the rungs of the ladder' and associated by means of specific hydrogen bonds. Because of size constraints, cytosine pairs with guanine and adenine pairs with thymine. Work has also been done on the sequence specific design of intercalators.[90,91] The modes of binding of these complexes to DNA is not fully understood. ^1H NMR has been used to demonstrate that the octahedral complex Δ-$[Ru(phen)_2dppz]^{2+}$ binds in the major groove of B-DNA.[92]

It had been proposed that the octahedral Λ isomer of Ru^{2+}(4,7-diphenylphenanthroline)$_3$ bound Z-DNA enantioselectively[93] but this was later refuted by absorption spectra which showed equal binding by both isomers.[94]

It would therefore be of interest to obtain the crystal structure of a DNA molecule with a chiral molecule that would have the potential to intercalate or to bind to the minor or major grooves of the sequence. The chiral lanthanide complexes have this potential and are useful *in vivo* probes as has already been discussed. It was decided to begin investigation on DNA binding with the enantiopure tetraamide complexes, as is shown in ***Figure 4.8.1***. Both the *S*- and the *R*- isomers of this complex were used.

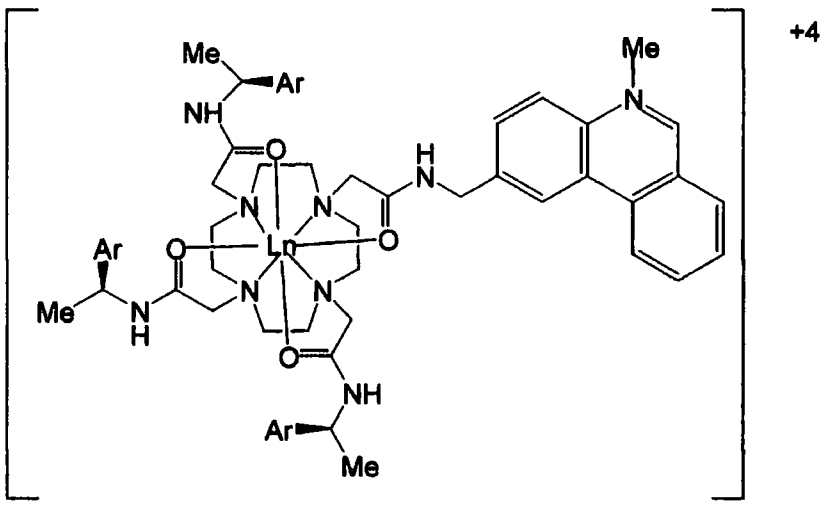

Figure 4.8.1 *- Schematic representation of the putative complex that would bind to an oligonucleotide, where Ln = Eu^{3+} or Tb^{3+}.*

It was thought that the helicity of the three pendant arms with stereogenic centres would be sufficient to force the fourth arm with the methylated phenanthridinium group to adopt the same conformation. The molecule is an overall cation and it was thought that it would therefore interact more strongly with the polyanionic DNA. The europium complex of the related phosphinate ligand with one phenanthroline pendant arm shows strong luminescence.[95]

It is known that phenanthroline group itself is very prone to pack via π-stacking interactions. This was seen when the structure of the compound 1,10-bis(phenylphosphinic acid)-2,9-bis(phenanthroline) was solved. A packing view along [010] is depicted in ***Figure 4.8.2***, showing the strong interactions between the planar aromatic phenanthroline groups and the OH..O hydrogen bonded contacts.

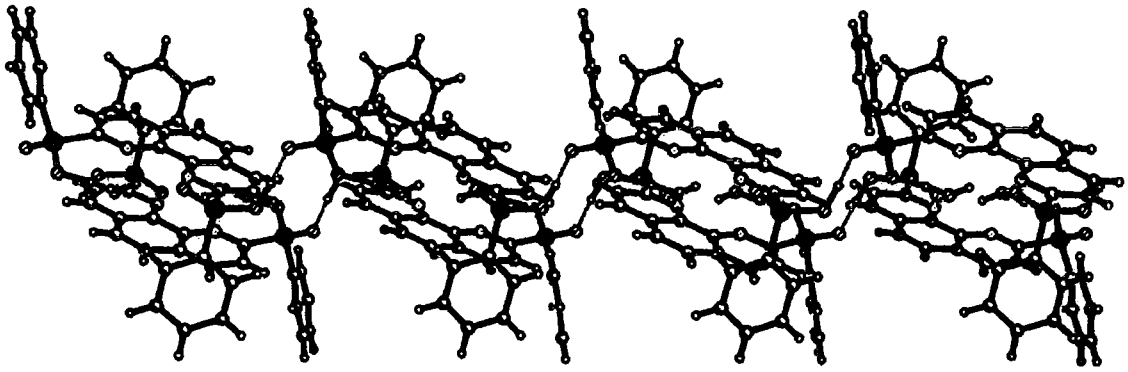

***Figure 4.8.2** - Diagram of the molecular packing viewed along the b axis. Antiparallel chains are formed mediated by strong OH..O interactions of 1.43(4) Å along [001].*

When viewed along the c axis the nitrogen containing six-membered rings completely obscure one another, being related by an inversion centre. The distance between the planes was 3.70(4) Å.

The acquisition of X-ray data that extends to atomic resolution for oligonucleotides up to dodecamer length is now feasible and there is a wealth of structures now available in the Nucleic Acid Database[96] which have many DNA drug complexes with the organic molecules bound in the groove,[97,98] such as the recent NMR determined structure of the 1:1 nogalamycin:d(ATGCAT)$_2$ structure.[99] The structure of the B-DNA dodecamer, CGCGAATTCGCG,[100,101] reported in 1981 by Richard Dickerson was followed by many structures of the structures of B-DNA oligonucleotides.[102] There are also many Z-DNA structures since the first oligonucleotide comprised of the complementary sequence $(CG)_3$ was published[103,104,105] and A-DNA.[106] This was followed by the discovery that additives of such as $[Co(NH_3)_6]^{3+}$ and $[Mg(H_2O)_6]^{2+}$ stabilised the Z-DNA structure, thus aiding in the crystallisation and they are now routinely used in the crystallisation of such sequences.[107]

In order to address the question as to whether the chiral europium tetraamide complex with the phenanthradinium group was an intercalator, major groove binder, minor groove binder or associated in a non-specific manner with DNA oligonucleotides of the sequence $(AT)_6$ and $(CG)_6$ were purchased from a commercial company with a view to co-crystallising with the europium complex.

The crystallisation experiments were carried out at 285 K and later at 277 K. For all crystallisation trials, micro-bridges were used in 6 x 4 well Linbro plates with the cover slips sealed with silicon grease. The drop volume was 3 μL. Crystallisations were performed in the absence of polyamines such as the commonly employed spermine, which is known to bind in the DNA groove. Stocks of DNA solution at 0.5 mM and the Eu *RRR* complex of N-methylated phenanthradine at 3.2 mM were used and dilutions made from there. The precipitant used was 2-methyl-2,4-pentanediol (MPD). The strategy was to add the DNA to a buffered Ln complex and then to add the preconcentrated magnesium dichloride. The Eu *RRR* complex of N-methylated phenanthradine was first screened with $(CG)_6$ and $(AT)_6$.

Table 4.8.1 *– Crystallisation conditions for the Eu RRR complex of N-methylated phenanthradine with $(CG)_6$ at pH 7.0 buffered with sodium cacodylate.*

	[DNA]/mM	[Ln]/mM	[Ln]:[DNA]	$[Mg^{2+}]$/mM
1	0.27	0.27	1:1	0
2	0.27	0.27	1:1	2.43 (0.75 per PO_4^{3-})
3	0.26	0.51	2:1	0
4	0.26	0.51	2:1	2.33 (0.75 per PO_4^{3-})
5	0.15	0.15	1:1	2.35 (1.30 per PO_4^{3-})
6	0.15	0.15	1:1	0

The conditions were also carried out at pH 6.4 (see ***Table 4.8.2***), buffered with sodium cacodylate. In both cases they were each set with MPD precipitant concentrations of 35%, 40%, 45%, 50% and 55%. The source of Mg^{2+} was $MgCl_2$. It was observed that larger crystals grew in the presence of magnesium ions so the mole fraction of magnesium chloride was increased for the pH 6.4 trials.

Table 4.8.2 *– Crystallisation conditions for the Eu RRR complex of N-methylated phenanthradine with $(CG)_6$ at pH 6.4 buffered with sodium cacodylate.*

	[DNA]/mM	[Ln]/mM	[Ln]:[DNA]	$[Mg^{2+}]$/mM
7	0.25	0.49	2:1	3.77 (1.26 per PO_4^{3-})
8	0.27	0.53	2:1	0
9	0.27	0.27	1:1	4.08 (1.26 per PO_4^{3-})
10	0.29	0.29	1:1	0
11	0.14	0.14	1:1	2.77 (1.53 per PO_4^{3-})
12	0.16	0.16	1:1	0

After four days, in both cases, the micro crystals were stopped growing. The best crystals were colourless and 'surf-board' like with tapered ends. They formed very thin plates with the longest dimension 0.2 mm.

Table 4.8.3 *– Crystallisation conditions for the Eu RRR complex of N-methylated phenanthradine with $(AT)_6$ at pH 6.4 buffered with sodium cacodylate.*

	[DNA]/mM	[Ln]/mM	[Ln]:[DNA]	$[Mg^{2+}]$/mM
13	0.30	0.34	1:1	0
14	0.27	0.30	1:1	3.23 (0.5 per PO_4^{3-})
15	0.27	0.30	1:1	6.26 (1.0 per PO_4^{3-})
16	0.27	0.30	1:1	9.68 (1.5 per PO_4^{3-})

The conditions in ***Table 4.8.3*** were incubated at 287 K overnight and then transferred to 277 K. They were screened with MPD precipitant concentrations of 35%, 40%, 45%, 50% and 55%. This was also repeated at pH 7.0 with MPD precipitant concentrations of 40%, 45%, 50% and 55%, summarised in ***Table 4.8.4***.

Table 4.8.4 *– Crystallisation conditions for the Eu RRR complex of N-methylated phenanthradine with $(AT)_6$ at pH 7.0 buffered with sodium cacodylate.*

	[DNA]/mM	[Ln]/mM	[Ln]:[DNA]	$[Mg^{2+}]$/mM
17	0.26	0.37	1.39:1	6.27 (1.0 per PO_4^{3-})
18	0.26	0.37	1.39:1	9.41 (1.5 per PO_4^{3-})
19	0.26	0.37	1.39:1	12.87 (2.0 per PO_4^{3-})

The Eu *SSS* complex of N-methylated phenanthradine was then screened with $(CG)_6$ in ***Table 4.8.5***. It was screened with MPD precipitant in the 40 – 55% range. As before the tray was placed at 287 K for 16 h and then stored in the fridge at 277 K.

Table 4.8.5 *– Crystallisation conditions for the Eu SSS complex of N-methylated phenanthradine with $(CG)_6$ at pH 7.0 buffered with sodium cacodylate.*

	[DNA]/mM	[Ln]/mM	[Ln]:[DNA]	$[Mg^{2+}]$/mM
20	0.25	0.32	1:1.30	6.27 (1.0 per PO_4^{3-})
21	0.25	0.32	1:1.30	9.41 (1.5 per PO_4^{3-})
22	0.25	0.32	1:1.30	12.87 (2.0 per PO_4^{3-})

Small crystals grew under all conditions except in the final tray, which was the Eu SSS complex of N-methylated phenanthradine with (CG)6 at pH 7.0 co-crystallisation. It was hoped that a magnesium complex was not crystallising and the fact that no crystals grew in the final experiment when there was the same concentration of magnesium was encouraging. The set-up in ***Table 4.8.4*** yielded plate like crystals at

all precipitant concentrations. One of these was screened on the SMART diffractometer and the unit cell obtained, whilst being found in a search of the CSD, appears to be a small molecule salt with a volume of 480.3(4) $Å^3$. Crystals were also screened that had been grown at all conditions at station 9.8 at the Daresbury SRS. The intensity was not enough to index the reflections.

Intrinsic binding constants were measured by Dr. J.A. Gareth Williams from the chemistry department, University of Durham and revealed an interesting trend as can be seen from ***Table 4.8.6***.

Table 4.8.6 *– Binding characteristics for chiral europium complexes with $(CG)_6$ and $(AT)_6$ (0.1 M Hepes, 293 K, 10 mM NaCl) as performed by J.A.G. Williams.*[108]

Complex	Oligonucleotide	*n'*	10^{-5} K / $dm^3mol^{-1}duplex^{-1}$
[*R*-Eu-phen]	$(CG)_6$	3.98	87
[*S*-Eu-phen]	$(CG)_6$	3.96	36
[*R*-Eu-phen]	$(AT)_6$	1.52	1.6
[*S*-Eu-phen]	$(AT)_6$	1.82	8.0
N-ethylphenanthridinium iodide	$(AT)_6$	~	<0.3
N-ethylphenanthridinium iodide	$(CG)_6$	3.88	6.8
Ethidium bromide	$(CG)_6$	2.26	31

The term, *n'*, is the site size or number of moles of complex per mole of duplex. The $(CG)_6$ sequence binds almost enantioselectively to the *R* isomer of the complex. The next avenue should be optimising the crystallisation conditions with this isomer and $(CG)_6$. Values were obtained here for comparison for the model DNA intercalators *N*-ethylphenanthridinium iodide and ethidium bromide.

It is believed that the ytterbium complex of 1,4,7,10-tetrakis(carboxyethyl)-1,4,7,10-tetraazacyclododecane is an eight co-ordinate twisted square antiprism from solution-state measurements and preliminary X-ray data, and it remains for a sample displaying enhanced crystallinity to be obtained to answer this question through a crystallographic experiment. The results from Daresbury station 9.8 have been limited but encouraging and now that this station has been commissioned, opportunity should be made of this resource to study small crystals. Lanthanide macrocyclic complexes are ideal for this station.

This project has been a collaborative study involving a parallel approach to investigating the structures of the complexes. Spectroscopic techniques have not only given information on the isomer present in solution, but also on the ratio of isomers. It has been proven here repeatedly in the case of the tetracarboxyethyl derivative complexes that it cannot be assumed that the major isomer will crystallise. These complexes epimerise in the solution prior to crystallisation to reduce steric hindrance in the solid-state or to take advantage of stabilising non-bonded contacts. Crystallographic studies in conjunction with molecular mechanics calculations is advised as a means of doing conformational analyses. These calculations are economical on computer time and memory. It would be interesting to apply this approach to the chiral tetraphenyl amide (L^2) lanthanide complexes. In this enantiopure series only one stereoisomer formed (i.e. $\Delta(\lambda\lambda\lambda\lambda)$ or $\Lambda(\delta\delta\delta\delta)$). The co-ordinates for one of the chiral Eu^{3+} complexes could be used and the conformation of the ring changed, then the conformation of the arms changed. Here conformational space is searched without changing the connectivities and relative energies for each structure generated. An analysis of these structures should reveal the reason why one stereoisomer is favoured.

The carboxyethyl series of complexes all formed square antiprismatic complexes with the twisted square antiprism epimerising in solution. It is proposed that the twisted square antiprism gives rise to enhanced relaxivity due to the decreased lifetime of the bound water molecule. This should be manifested by a lengthened distance from the metal to the bound water molecule compared to the distance in the square antiprismatic isomer. It would be useful to test this idea by obtaining two relative energy profiles for each isomer as the bound water is moved alone the Ln-O (water) vector. It is also thought that recrystallising the europium, gadolinium and terbium complexes of the tetracarboxyethyl series in the presence of alternate counter ions could yield the major isomer.

4.9 References

[1] G.C. Pimentel and R.D. Sprately (1971). *Understanding Chemistry*, Holden-Day, p.862.

[2] N.N. Greenwood and A. Earnshaw (1994). *Chemistry of the Elements*, Pergamon Press.

[3] F. Albert Cotton and Geoffrey Wilkinson (1988). *Advanced Inorganic Chemistry*. Fifth Edition, Wiley Interscience.

[4] R.D. Shannon (1976). *Acta Cryst.*, **A32**, 751.

[5] A. Mayer and S. Neuenhofer (1994), *Angew. Chem. Int. Ed. Engl.*, **33**, 1044-1072.

[6] Molecular Optical Activity and the Chiral Discrimination. (1982), S.F. Mason, Cambridge University Press.

[7] J.P. Riehl and F.S. Richardson, (1993), *Methods in Enzymology*, **226**, 539-553.

[8] H.G. Brittain, F.S. Richardson and R.B. Martin, (1976), *J. Am. Chem. Soc.*, *98*, 8255.

[9] R.S. Dickins, J.A.K. Howard, C.W. Lehmann, J. Moloney, D. Parker and R.D. Peacock, (1997), *Angew. Chem. Int. Ed. Engl.*, **36**, No. 5, 521-523.

[10] R.S. Dickins (1997) Ph.D Thesis, University of Durham.

[11] S. Aime, M. Botta, G. Ermondi, F. Fedeli and F. Uggeri, (1992), *Inorg. Chem.*, **31**, 1100-1103.

[12] I. Soloman, (1955), *Phys. Rev.*, **99**, 559.

[13] N. Bloembergen and L.O. Morgan (1961), *J. Chem. Phys.*, **34**, 842.

[14] D. Parker and J.A.G. Williams (1996), *J. Chem. Soc., Dalton Trans.*, 3613-3628.

[15] S. Aime, M. Botta, M. Fasano and E. Terreno, (1998), *Chem. Soc. Rev.*, **27**, 19-29.

[16] S. Aime, A.S. Batsanov, M. Botta, J.A.K. Howard, D. Parker, K. Senanayake and J.A.G. Williams (1994). *Inorg. Chem.*, **33**, 4696 – 4706.

[17] D. Parker (1991). *Chem. Rev.*, **91**, 1441 – 1457. And references therein.

[18] J. Chapman, G. Ferguson, J.F. Gallagher, M.C. Jennings and D. Parker (1992) *J. Chem. Soc., Dalton Trans.*, 345-353.

[19] T. Weyhermüller, K. Weighardt and P. Chaudhuri, (1998), *J. Chem. Soc., Dalton Trans.*, 3805-3813.

[20] J.P.L. Cox, A.S. Craig, I.M. Helps, K.J. Janskowski, D. Parker, M.A.W. Eaton, A.T. Millican, K. Millar, N.R.A. Beeley and B.A. Boyce (1990). *J. Chem. Soc. Perkin Trans.*, 1, 2567 – 2576.

[21] M. Gaspar, R. Grazina, A. Bodor, E. Farkas and M.A. Santos, (1999), *J. Chem. Soc., Dalton Trans.*, 799-806.

[22] K. Kumar and M.F. Tweedle, (1993), *Inorg. Chem.*, **32**, 4193-4199.

[23] X. Wang, T. Jin, V. Comblin, A. Lopez-Mut, E. Merciny and J.F. Desreux, (1992), *Inorg. Chem.*, **31**, 1095-1099.

[24] C.A. Chang, L.C. Francesconi, M.F. Malley, K. Kumar, J.Z. Gougoutas and M.F. Tweedle, (1993), *Inorg. Chem.*, **32**, 3501-3508.

[25] D. Parker, K. Pulukkody, F.C. Smith, A. Batsanov and J.A.K. Howard, (1994), *J. Chem. Soc., Dalton Trans.*, 689-693.

[26] G.B. Deacon, B. Görtler, P.C. Junk, E. Lork, R. Mews, J. Peterson and B. Zemva, (1998), *J. Chem. Soc., Dalton Trans.*, 3887-3891.

[27] M.-R. Spirlet, J. Rebizant, J.F. Desreux and M.-F. Loncin, (1984), *Inorg. Chem.*, **23**, 359-363.

[28] J.R. Morrow, S. Amin, C.H. Lake and M.R. Churchill, (1993), *Inorg. Chem.*, **32**, 4566-4572.

[29] K.A.O. Chin, J.R. Morrow, C.H. Lake and M.R. Churchill, (1994), *Inorg. Chem.*, **33**, 656-664.

[30] S. Aime, M. Botta and G. Ermondi, (1992), *Inorg. Chem.*, **31**, 4291-4299.

[31] S. Hoeft and K. Roth, (1993), *Chem. Ber.*, **126**, 869-873.

[32] V. Jacques and J.F. Desreux, (1994), *Inorg. Chem.*, **33**, 4048-4053.

[33] A. Riesen, M. Zehnder and T.A. Kaden (1986) *Helv. Chim. Acta.*, **69**, 2074.

[34] A. Riesen, M. Zehnder and T.A. Kaden (1986) *Helv. Chim. Acta.*, **69**, 2067.

[35] A. Riesen, M. Zehnder and T.A. Kaden (1991) *Acta.* Cryst., **C47**, 531.

[36] K. Kobayashi, S. Tsuboyama, K. Tsuboyama, T. Sakurai (1994) *Acta.* Cryst., **C50**, 306.

[37] T. Sakurai, K. Kobayashi, K. Tsuboyama and S. Tsuboyama, (1978), *Acta.* Cryst., **B34**, 1144-1148.

[38] M.J. van der Merwe, J.C.A. Boeyens and R.D. Hancock, (1983), *Inorg. Chem.*, **22**, 3490-3492.

[39] E. Cole, R.C.B. Copley, J.A.K. Howard, D. Parker, G. Ferguson, J.F. Gallagher, B. Kaitner, A. Harrison and L. Royle, (1994), *J. Chem. Soc., Dalton Trans.*, 1619-1629.

[40] M. Meyer, V. Dahaoui-Gindrey, C. Lecomte and L. Guilard, (1998), *Coord. Chem. Rev.*, **180**, No. Pt2, 1313 – 1405.

[41] V. Dahaoui-Gindrey, C. Lecomte, C. Gros, A.K. Mishra, and R. Guilard (1995) *New. J. Chem,* **19**, 831-838.

[42] V. Dahaoui-Gindrey, C. Lecomte, H. Chollet, A.K. Mishra, C. Mehadji and R. Guilard (1995) *New. J. Chem,* **19**, 839-850.

[43] C. Lecomte, V. Dahaoui-Gindrey, H. Chollet, C. Gros, A.K. Mishra, F. Barbette, P. Pullumbi and R. Guilard (1997) *Inorg. Chem.*, **36**, 3827-3838.

[44] J. Dale (1980), *Isr. J. Chem.*, **20**, 3-11.

[45] J.D. Dunitz and P.Seiler, (1974), *Acta.* Cryst., **B30**, 2739-2741.

[46] G. Weber, G.M. Sheldrick, Th. Burgemeister, F. Dietl, A. Mannschreck and A. Merz, (1984), *Tetrahedron*, **40**, 855-863.

[47] V. Dahaoui-Gindrey, S. Dahaoui, C. Lecomte, F. Barbette and R. Guilard (1997) *Acta.* Cryst., **C53**, 1797-1799.

[48] P.J.A. Ribeiro-Claro, A.M. Amado, M.P.M. Marques and J.J.C. Teixeira-Dias (1996). *J. Chem. Soc., Perkin Trans. 2*, 1161 – 1167.

[49] J.A.K. Howard, A.M. Kenwright, J.M. Moloney, D. Parker, M. Port, M. Navet, O. Rousseau and M. Woods, (1998), *J. Chem. Soc. Chem. Commun.*, 1381.

[50] R.S. Dickins, J.A.K. Howard, C.L. Maupin, J.M. Moloney, D. Parker, J.P. Riehl, G. Siligardi, and J.A.G. Williams, (1999), *Chem. Eur. J.*, **5**, No. 3, 1095 – 1105.

[51] A.S. Batsanov, A. Beeby, J.L.Bruce, J.A.K. Howard, A.M. Kenwright and D. Parker, (1999), *J. Chem. Soc. Chem. Commun.*, 1011.

[52] A. Beeby, D. Parker and J.A.G. Williams, (1996), *J. Chem. Soc., Perkin Trans. 2*, 1565 – 1579.

[53] T. Gunnlaugsson and D. Parker, (1998), *J. Chem. Soc., Chem. Commun.*, 511.

[54] C. Piguet, A.F. Williams, G. Bernardinelli and J.-C.G. Bünzli, (1993), *Inorg. Chem.*, **32**, 4139 – 4149.

[55] D. Parker and J.A.G. Williams, (1995), *J. Chem. Soc., Perkin Trans. 2*, 1305 – 1314.

[56] D. Parker and J.A.G. Williams, (1996), *J. Chem. Soc., Perkin Trans. 2*, 1581 – 1586.

[57] R.S. Dickins, J.A.K. Howard, J.M. Moloney, D. Parker, R.D. Peacock and G. Siligardi, (1997) *J. Chem. Soc., Chem. Commun.*, 1747.

[58] R.S. Dickins, J.A.K. Howard, C.L. Maupin, J.M. Moloney, D. Parker, R.D. Peacock, J.P. Riehl and G. Siligardi, (1998), *New J. Chem.*, 891 – 899.

[59] L.J. Govenlock, J.A.K. Howard, J.M. Moloney, D. Parker, R.D. Peacock and G. Siligardi, (1999), *J. Chem. Soc., Perkin Trans. 2,* 2415-2418.

[60] S. Aime, A. Barge, M. Botta, J.A.K. Howard, R. Kataky, M.P. Lowe, J.M. Moloney, D. Parker and A.S. de Sousa, (1999), *J. Chem. Soc., Chem. Commun.*, 1047.

[61] M. Woods, S. Aime, A. Barge, M. Botta, J.A.K. Howard, J.M. Moloney, D. Parker and A.S. de Sousa, (1999), *J. Am. Chem. Soc.*, **121**, 5762-5772.

[62] S. Aime, A. Barge, M. Botta, D. Parker and A.S. de Sousa, (1997), *J. Am. Chem. Soc.*, **119**, 4767 – 4768.

[63] S. Greenfield, *The Independent*, 11 June 1999.

[64] D. Parker, (1990), *Chem. Br.*, **26**, No. 10, 942 – 945.

[65] D. Parker, (1994), *Chem. Br.*, 818 – 822.

[66] D. Parker, (1990), *Chem. Soc. Rev.*, **19**, 271 – 291.

[67] K.P. Pulukkody, T.J. Norman, D. Parker, L. Royle and C.J. Broan, (1993), *J. Chem. Soc., Perkin Trans. 2.*, 605 - 620.

[68] C.J. Broan, K.J. Jankowski, R. Kataky, D. Parker, A.M. Randall and A. Harrison, (1990), *J. Chem. Soc., Chem. Commun.*, 1739.

[69] D. Parker, K. Pulukkody, T.J. Norman, A. Harrison, L. Royle and C. Walker, (1992), *J. Chem. Soc., Chem. Commun.*, 1441.

[70] C.E. Foster (1996) Ph.D. Thesis, University of Durham, U.K.

[71] S. Aime, A.S. Batsanov, M. Botta, R.S. Dickins, S. Faulkner, C.E. Foster, A. Harrison, J.A.K. Howard, J.M. Moloney, T.J. Norman, D. Parker, L. Royle and J.A.G. Williams, (1997), *J. Chem. Soc., Dalton Trans.*, 3623 – 3636.

[72] G.B. Bates, E. Cole, D. Parker and R. Kataky, (1996), *J. Chem. Soc., Dalton Trans.*, 2693 – 2698.

[73] E. Cole, D. Parker, G. Ferguson, J.F. Gallagher and B. Kaitner, (1991), *J. Chem. Soc., Chem. Commun.*, 1473.

[74] M. Woods, S. Aime, M. Botta, J.A.K. Howard, J.M. Moloney, M. Navet, D. Parker, M. Port, O. Rousseau, (2000), *J. Am. Chem. Soc.*, 121, Submitted.

[75] Z. Berkovich, (1982), *J. Am. Chem. Soc.*, **104**, 4052.

[76] A.E. Goeta, (1998), *Personal Communication*. University of Durham, U.K.

[77] G. M. Sheldrick (1993). SHELXL-93. Program for the Refinement of Crystal Structures. University of Göttingen, Germany.

[78] M. Woods, (1998), Ph. D. Thesis, University of Durham.

[79] S. Dahaoui, (1998), *Personal Communication*, University of Durham. U.K.

[80] G.M. Sheldrick (1996). SADABS – Program for the refinement of area detector data. University of Göttingen, Germany. Unpublished.

[81] R.H. Blessing and C. Lecomte, (1991), from *The Application of Charge Density Research to Chemistry and Drug Design*, NATO ASI Series, Series B, Vol. **250**, Edited by G.A. Jeffrey and J.F. Piniella, Plenum Press, New York, 155.

[82] R.H. Blessing, (1987), *Cryst. Rev.*, **1**, 3-58.

[83] S. French and K. Wilson, (1978), *Acta Cryst.*, A**34**, 517 – 525.

[84] J.K. Barton, (1986), *Science*, **233**, 727.

[85] V.-M. Mukkala, H. Takalo, P. Liitti, J. Kankare, S. Kuusela and H. Lönnberg, (1994), *Lanthanide Chelates as a Tool in Nucleic Acid Chemistry* from *Metal-Based Drugs*, **1**, Nos. 2 – 3, 201 – 211.

[86] J. Thomas, (1998), *New Scientist*, 37 - 39.

[87] K. Fukui and K. Tanaka, (1998), *Angew. Chem. Int. Ed. Engl.*, **37**, No.1/2, 158 – 161.

[88] P.J. Dandliker, R.E. Holmlin and J.K. Barton, (1997), *Science*, **275**, 1465 – 1468.

[89] R.E. Holmlin, P.J. Dandliker, and J.K. Barton, (1997), *Angew. Chem. Int. Ed. Engl.*, **36**, 2714 - 2730.

[90] B.P. Hudson, .M. Dupureur and J.K. Barton, (1995), *J. Am. Chem. Soc.*, **117**, 9379 – 9380.

[91] T.W. Johann and J.K. Barton, (1996), *Phil. Trans. R. Soc. Lond. A,*. **354**, 299 – 324.

[92] C.M. Dupureur and J.K. Barton, (1994), *J. Am. Chem. Soc.*, **116**, 10286 – 10287.

[93] J.K. Barton, (1986), *Science*, **233**, 727 – 734.

[94] H.-K. Kim, P. Lincoln, B. Nordén and E. Tuite, (1997), *J. Chem. Soc., Chem. Commun.*, 2375.

[95] D. Parker, K. Senanyake and J.A.G. Williams, (1997), *J. Chem. Soc., Chem. Commun.*, 1777.

[96] ©1995,1996. The Nucleic Acid Database Project Rutgers, The State University of New Jersey. http://www.ebi.ac.uk/NDB/

[97] S. Neidle and C.M. Nunn, (1998), *Natural Products Reports*, 1-15.

[98] M.C. Wahl and M. Sundaralingam, (1995), *Curr. Opin. Struc. Biol.*, **5**, 282 – 295.

[99] H.E.L. Williams and M.S. Searle, (1999), *J. Mol. Biol.*, **290**, 699 – 716.

[100] H.R. Drew, R.M. Wing, T. Takano, C. Broka, S. Tanaka, K. Itakura and R.E. Dickerson, (1981), *Proc. Natl. Acad. Sci. USA*, **78**, No. 4, 2179 – 2183.

[101] S.R. Holbrook, R.E. Dickerson and S.-H. Kim, (1985), *Acta Cryst.*, **B41**, 255 – 262.

[102] D. Vlileghe, J.P. Turkenbourg and L. van Meervelt, (1999), *Acta Cryst.*, **D55**, 1495 – 1502.

[103] A. H.-J. Wang, G.J. Quigley, F.J. Kolpak, J.L. Crawford, J.H. van Boom, G. van der Marel and A. Rich, (1979), *Nature*, **282**, 680 – 686.

[104] S. Fujii, A. H.-J. Wang, G. van der Marel, J.H. van Boom and A. Rich, (1982), *Nucleic Acids Research*, **10**, No. 23, 7879 – 7892.

[105] A. H.-J. Wang, T. Hakoshima, G. van der Marel, J.H. van Boom and A. Rich, (1984), *Cell*, **37**, 321 – 331.

[106] D.J. Wilcock, A. Adams, C.J. Cardin and L.P.G. Wakelin, (1996), *Acta Cryst.*, **D52**, 481 – 485.

[107] R.V. Gessner, G.J. Quigley, A. H.-J. Wang, G. van der Marel, J.H. van Boom and A. Rich, (1985), *Biochemistry*, **24**, No.2, 237 – 240.

[108] L.J. Govenlock, C.E. Mathieu, C.L. Maupin, D. Parker, J.P. Riehl, G. Siligardi and J.A.G. Williams, (1999), *J. Chem. Soc., Chem. Commun.*, 1699 – 1700.

Chapter 5

Ultra-Low Temperature Crystallographic Studies on the *Fddd* Diffractometer

5.1 Introduction

The proportion of X-ray diffraction data being measured from small-moiety and macromolecular crystals at low temperatures (200>T>100 K) and at temperatures below that of boiling N_2 (77 K) has shown an exponential increase in recent years. Research has focussed on developing reliable and facile techniques for the acquisition of high quality data in both the small-molecule and macromolecular crystallographic fields.[1,2]

The benefits in crystallography of cryogenic data collection are:

1. Data sets at extended resolutions are obtained, due to the reduction in atomic motion.[3] As has been mentioned in chapter three, data acquisition at low temperatures has a beneficial effect on the quality of the data. High order reflections can be measured that would not be detectable above background noise due to thermal smearing at room temperature. The decrease in intensity with increasing ($\sin\theta/\lambda$) can be directly attributed to the parameter B, where $B = 8\pi^2u^2$. It has been shown on numerous occasions that measuring data at cryogenic temperatures allows loosely bound parts of a protein molecule to be identified, e.g. the structure of crambin measured at 130 K allowed the location of a hydrogen-bonded array of water molecules, all in close contact.[4,5] Although crystals of this protein diffract strongly at all temperatures, solvent water molecules can not be located at room temperature.

2. A substantial reduction in radiation decay process can be achieved by collecting at cryogenic temperatures.[6] In macromolecular X-ray crystallography, the effects of reducing the temperature are even more beneficial as the *time-dependent* component of the radiation decay process is reduced to an almost negligible quantity.[7] Radiation damage can be divided into a dose-dependent and a time dependent component. The former component can be defined as the number of chemical reactions per incident X-ray photon. These events occur at the crystal surface and their number depends on the beam intensity. The process of radiation

damage is the production of free radicals within the crystal by the X-ray beam. Macromolecular crystals are particularly susceptible to a deleterious effect as a result of radiation damage due to being comprised of 30-75% solvent water molecules which serve to transport the generated oxygen, hydroxyl or hydroperoxyl radicals in a 'domino' effect which shatters the crystal. The temperature of the data collection does not affect the dose-dependent component but the time-dependent component of the decay is minimised effectively since the transfer of free-radicals is decelerated at cryogenic temperatures and the enhanced intensity allows reduced X-ray exposure times.

3. One position of a disordered site may be frozen out at low-temperatures; e.g., the phosphate backbones of oligonucleotides are prone to flip between two positions.
4. The structures of reaction intermediates have been determined by isolating them at low-temperatures and crystallising them *in situ*. The gives a new chemical insight to the reaction mechanism and allow further reactions to be designed. The structures of organometallic reaction intermediates and metastable compounds such as butyllithium and lithium silylcuprates have been reported by Dietmar Stalke.[8] In the macromolecular field, this philosophy extends to the study of enzyme–substrate complexes.[9,10]

The aforementioned benefits prompted advances in the available technologies and experimental techniques to ensure successful cryogenic experiments were accomplished:

1. Open-flow nitrogen cryostats, which can collect data in the 90-373 K range[11] and closed-cycle helium refrigerators with a temperature range of 9-300 K[12,13] are now available and widely used.
2. The surfaces of the proteins can be cross-linked with glutaraldehyde, which 'buttresses' the crystal and keep it intact during cooling.
3. The problem that accompanies the nucleation and growth of hexagonal ice crystals is the 9% increase in specific volume, which disrupts the crystal lattice.

Formation of the high-pressure modification of ice at ~250 MPa which has a specific volume more similar to water prior to cooling has been reported by Thomanek *et al.*[14] This approach has now, however, gained popularity. At atmospheric pressure, nucleation of ice crystals occurs at 233 K for pure water (homogenous nucleation) and this temperature is elevated when heterogeneities are present. Supercooling water results in its vitrification and the glass transition for pure water is 136 K.[15]

4. It is now almost universally acknowledged that rapid or 'flash-cooling' is the best method of cooling crystals using an open-flow nitrogen cryostat, which causes the solvent of crystallisation to vitrify. In macromolecular samples, slow cooling causes ice crystallites to grow which manifests itself as an increase in mosaicity[16] and ice scatter at low angle prior to the disintegration of the crystal. Crystals can also be plunged into liquid propane that causes almost instantaneous crystal freezing and prevents ice formation. The method of cooling, which has gained almost universal approval in small molecule and also in protein crystallography, is the cooling of the crystalline sample in a gaseous N_2 stream in a drop of inert oil such as per-fluoropolyether (MW 2700, purchased from Riedel-de Haën or Fluorochem), which solidifies, acting as an adhesive.[4,17] The advantages this offers are that delicate crystal can be mounted on glass fibres by first placing them in a drop of oil, avoiding mechanical stresses. In addition, air-sensitive samples are hermetically sealed from the atmosphere. When the sample is mounted on the diffractometer, the gaseous stream should first be deflected with a piece of sturdy card and the card then swiftly removed when the sample has been attached to allow cooling as rapidly as possible.[18] The method has now dispensed with the requirement to mount air-sensitive crystals in Lindemann capillaries. It has been shown to work very well for the relatively dry (30% solvent water) protein crystal crambin[4], bovine pancreatic trypsin inhibitor, form II[4] and chicken egg white lysozyme as will be reported in this chapter. In a few cases in the literature, it has been reported that 'flash-cooling' was not necessary or damaging to protein crystals. The structure of the B-DNA dodecamer[19] was

solved and refined successfully following extremely slow cooling to 16 K. In the case of bovine heart cytochrome C oxidase, slow cooling was better for the crystals since on cooling the b axis shrank rapidly and when flash frozen this effect was faster near the surface and cracks formed there due to the stresses on the crystal and continued in to the centre of the crystal, causing it to shatter.[20]

5. Cryoprotection, as first described by Petsko[21,22] involves the replacement of the mother liquor by organic solvents which vitrify at low temperature. The most commonly used cryoprotectants are glycerol, 2-methyl-2,4-pentanediol, ethylene glycol, PEG 400, xylitol, (2R,3R)-(-)-butane 2,3-diol, erythritol and glucose.[23] The cryoprotectant acts to slow ice nucleation inside the crystal so that the aqueous solution can be transformed in to a glass before ice crystals form.

This chapter focuses on three disparate themes, which are nonetheless linked to the development of methods to study molecules by low-temperature X-ray crystallography and the study of their thermal motion at low temperature. The temperature calibration of the *Fddd* diffractometer is performed by taking crystals of molecules that are known to undergo phase transitions and following that transition. 1,2 di-phenyl ethanedione or benzil was used as it undergoes a transition from a hexagonal to a monoclinic cell setting in the region of 83 K. The structure of the icosahedral borane cluster 1,12-$B_{12}H_{12}(CO)_2$ was investigated at low-temperature to determined an accurate value for the carbonyl bond length, and to study the effects of low-temperature on it thermal motion. The development of protocols to study air-sensitive, macromolecular or delicate molecules using a closed-cycle helium refrigerator was required and to this end the *de facto* standard for crystallisation and data collection trials, chicken egg white (CEW) lysozyme, was employed.

5.2 Phase transition in benzil

Crystal cooling on the *Fddd* diffractometer is achieved in a closed-cycle helium cryogenic refrigerator as has been mentioned previously. The crystal is not directly exposed to the flow of gaseous coolant in this apparatus as in open-flow cryostats. Accurate cooling of the sample to the temperature that is designated on the readout is reliant on exceptionally good conduction to the crystal. The goniometer head is made from copper, and crystals are mounted on sharpened graphite pencil leads – both of these materials are good conductors. However, the question of what the temperature was at the crystal remained. The logical strategy was to take a series of crystals that were known to undergo solid-solid phase transitions at precise temperatures and to monitor the temperature at which these occurred. This could easily be accomplished by following the appearance or disappearance of a reflection (such that would accompany the doubling or tripling of cell axes). Ideally, a phase transition for such a study would be reversible, would occur within a fraction of a degree, the change would be very significant and thus it would not be difficult to quantify where it commenced, and the crystals would not be delicate or air-sensitive.

Benzil was proposed as a model crystal that underwent a phase transition and for this reason could be used as a temperature calibrant. The initial structural investigations on benzil were reported in *Nature* in 1939.[24,25] It was studied at the time because of its characteristic of being a 'skew' molecule, that is, the angle of rotation was about the central ethylene bond was determined the overall twist of the molecule and its macroscopic structure.

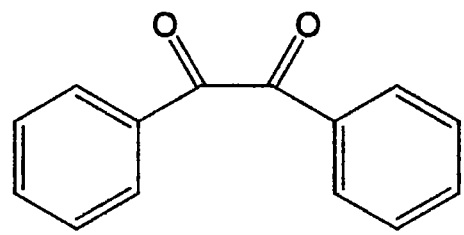

***Figure 5.2.1** – Schematic representation of 1,2 di-phenyl ethanedione or 'benzil'.*

The unit cell and space group were first reported by Becker and Rose in 1923,[26] who obtained a = 8.15 and c = 13.46 Å in the trigonal enantiomorphous space groups $P3_121$ and $P3_221$. The crystal structure was finally solved in 1965 to reveal three molecules in the unit cell each on a dyad.[27] The phenomena of benzil crystals giving rise to diffuse scattering in the form of streaks along layer lines, which was much reduced at low temperatures, was investigated in 1973[28] using optical methods to reveal a phase transition at 84.0(5) K. The first crystallographic study of this transition was carried out by Odou *et al*[29] to show that the transition involved a change from a hexagonal to a monoclinic setting.

Crystals were grown using the liquid-liquid diffusion technique. Water was deemed a good co-solvent so solvents that are miscibilities with water were tested, namely ethanol, tetrahydrofuran, methanol, acetonitrile and acetone. Water is denser so this formed the bottom layer in the tube. Crystals were obtained from the ethanol, methanol and acetone combinations with water within six days. A yellow crystal suitable for X-ray diffraction was obtained from the methanol/water combination.

At 100 K a hexagonal cell of 8.360(3), 8.363(3), 13.383(4) Å, 90.01(2), 89.99(1), 119.98(1)° was obtained from indexing eighteen reflections The cell was transformed to the monoclinic setting using the matrix $a_m = a_h - b_h$, $b_m = a_h + b_h$, $c_m = c_h$, where h is hexagonal and m is monoclinic.

A unit cell of 14.4794(4), 8.363(2), 13.371(4) Å, 89.99(2), 89.99(1), 90.02(1)° was obtained and the emergence of the monoclinic angle tracked by remeasuring these reflections every degree. As can be seen from ***Figure 5.2.2*** this is a gradual phase transition and its commencement has been defined as when the angle starts to deviate from 90°. The phase transition temperature was defined as having happened at 83.0 (1.4) K.

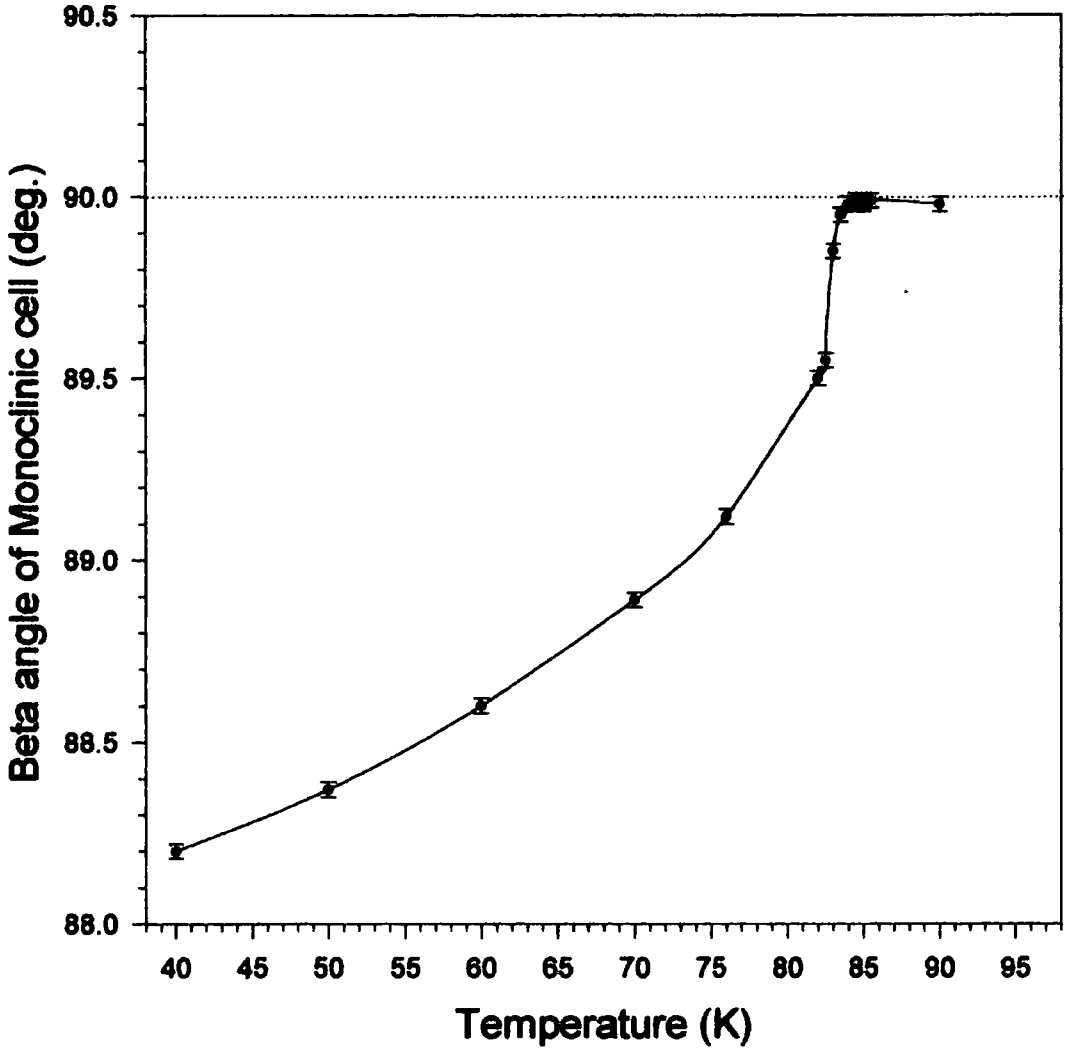

***Figure 5.2.2** – Phase transition in benzil, tracked by monitoring the β angle in the monoclinic cell setting.*

From the temperature of this phase transition and that of terbium vanadate[30] at 33 K, the temperature error on the *Fddd* diffractometer was determined as 1.4 K.

5.3 The structures of 1,12-$B_{12}H_{10}(CO)_2$ and its tetrahydrate

This study stemmed from the interest in the proposed inverse correlation between bond strength and bond length in metal clusters. Catherine Housecroft *et al* refuted assumptions that metal-metal energies in high-nuclearity clusters were independent of nuclearity and bond length.[31] They suggested that there was a straightforward relationship between metal-metal distances and their energies, as in covalent two-electron two-centre bonds. One of the most common ligands for transition metal clusters is the carbonyl group, e.g. $M_3(CO)_9$ where, for example, M is iron, ruthenium or osmium. Thus, the determination of M-C and C≡O bond lengths in metal clusters gives useful information on the metal-metal bond strengths.

The carbonyl ligand, however, is capable of accepting an appreciable amount π^* electron density from the metal resulting in a lengthening in the C≡O bond. This is a synergic effect whereby in the first place σ electron density is donated from the carbonyl ligand to the metal resulting in an electropositive carbon centre. This electron density is dispersed by back-bonding from the $d\pi$ metal orbitals to the $p\pi$ carbon orbitals, resulting in an almost electroneutral M-C bond. Calculations of the metal-metal bond energies in metal-carbonyl systems involve making assumptions due to the back-bonding effect, hence a replacement group for the metal or metal cluster would eliminate this uncertainty. In this instance, the icosahedral B_{12} cage was used. The most reliable method of estimating the metal-metal energies is from the accurate measurement of the bond lengths by X-ray crystallography.

5.3.1 The crystal structure of 1,12-$B_{12}H_{10}(CO)_2$

As part of this ongoing project, the structure of the icosahedral B_{12} complex with two carbonyl groups para substituted on the cage were investigated. The B-C and C≡O distances were of interest in comparison with the analogous dimensions in d-block transition metal cluster carbonyl complexes. Low temperature X-ray

diffraction data were collected and some preliminary data at liquid helium temperatures are reported.

It is known that the B_{12} moiety has icosahedral symmetry. The substitution of two carbonyl groups at the 1- and 12- positions on the cage reduces the symmetry. There are two valid space group options for this well-ordered 1,12-dicarbonyl borane complex in the 100 to 150 K range, where the crystals have been investigated.[32] Data collection and structure refinement details were presented in ***Table 5.3.2***. The monoclinic setting in the space group $P2_1/n$ involved the placement of the cage on an inversion centre. The structure refined to convergence in this setting. The other option was a higher symmetry setting and for this reason, it was chosen. The structure was solved in the orthorhombic space group Cmca with nine unique atoms. The molecule has 2/m site symmetry. Equivalent atoms within this molecule were generated by means of an inversion centre, a mirror plane of symmetry and two-fold axis of symmetry. The structure of molecule is depicted in ***Figure 5.3.1***.

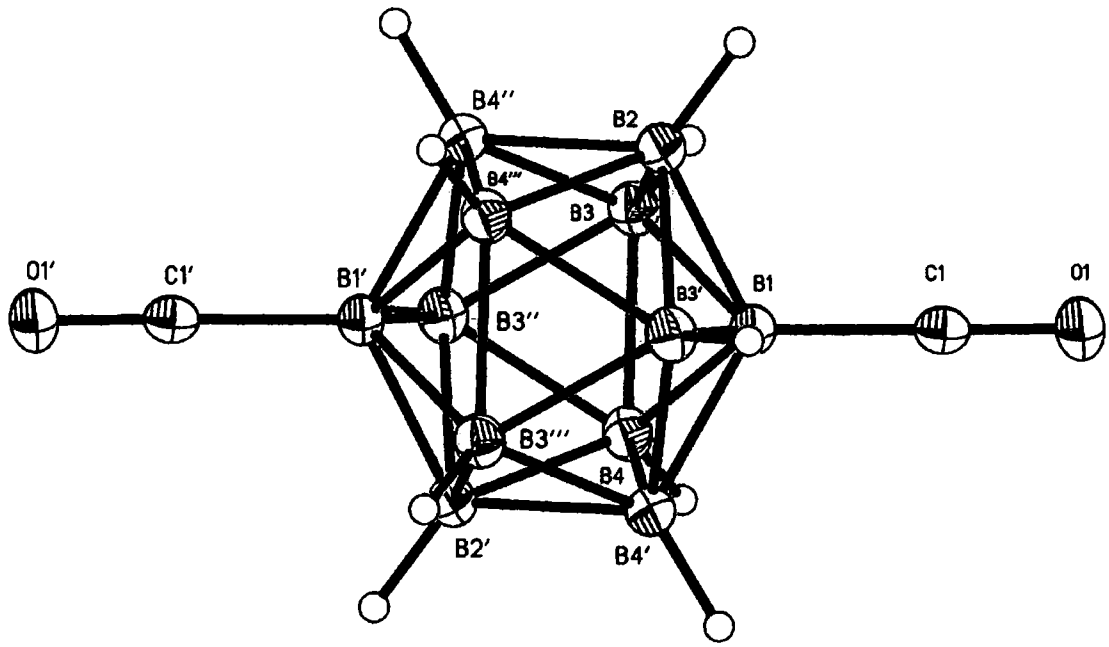

Figure 5.3.1 *- Crystal structure of $C_2H_{10}B_{12}O_2$ (50% ellipsoids) at 100(2) K. Dashed atoms represent those that are generated by a symmetry element.*

It is interesting that the structure departs from ideal icosahedral structure. If the twelve-membered cage is viewed as a globe, with the substituted groups the north and south poles, and the remainder of the boron atoms occupying tropical sites, it can

be seen that there is significant lengthening within the tropics, by approximately 0.05 Å. Thus, the molecule exhibits a flattened structure. The B-C≡O bond angle in this dicarbonyl complex, at 179.4(2)°, is effectively linear.

***Table 5.3.1** - Bond lengths [Å] for the independent part of C2 H10 B12 O2.*

O(1)-C(1)	1.119(2)	B(2)-B(3)	1.8214(12)
C(1)-B(1)	1.543(2)	B(2)-H(2)	1.09(2)
B(1)-B(2)	1.764(2)	B(3)-B(4'')	1.7782(14)
B(1)-B(3')	1.7681(12)	B(3)-B(3'')	1.779(2)
B(1)-B(3)	1.7681(12)	B(3)-B(4)	1.8269(13)
B(1)-B(4)	1.7695(14)	B(3)-H(3)	1.060(14)
B(1)-B(4')	1.7695(14)	B(4)-B(3'')	1.7782(14)
B(2)-B(4'')	1.782(2)	B(4)-B(2''')	1.782(2)
B(2)-B(4''')	1.782(2)	B(4)-B(4')	1.824(2)
B(2)-B(3')	1.8214(12)	B(4)-H(4)	1.105(12)

There have been very few boron cages with an exo-carbonyl bond reported in the literature to date. A search of the Cambridge Structural Database (October 1997 release)[33] for all B-C≡O contacts, not specifying the boron atom as part of a cage yielded 30 hits. The mean *d*(B-C) distance was 1.627(1) Å and the mean *d*(C≡O) distance was 1.402(8) Å, however the distribution for both these distances showed double maxima. The structures which contained boron cages were clustered in the upper end of these distributions, giving an average *d*(B-C) of 1.703(5) Å and a *d*(C≡O) of 1.436(2) Å. As can be seen from ***Table 5.3.1***, the experimentally determined values for these two bond lengths are significantly shorter than this. However, they do agree well with the gas – phase *ab – initio* Hartree Fock calculation that was carried out using the 6-31G force field.

Theoretical data corroborated the experimental findings. Dr. Mark Fox using the program MOPAC[34] that uses the AM1 force-field calculated the bond lengths and orders. The bond order for O1≡C1 was 1.328 and 1.274 for O2≡C1. The carbonyl group of the 1, 12-$B_{12}H_{10}(CO)_2$ complex exhibited the most π bond order at 1.464 whereas the values for the ene-diol were tetrahydrate 0.407 and 0.369.

Attempts were made to collect data for 1, 12-$B_{12}H_{10}(CO)_2$ at temperatures below that of boiling nitrogen. In both cases, the experiment was hampered by poor crystal quality and it remains for the molecule to be recrystallised for the recollection of ultra-low temperature data, which will lead to more accurate and reliable structural details. The structure was solved at 40 K using data collected on the *Fddd* diffractometer. Here there were one and a half molecules in the asymmetric unit, with one sitting on an inversion centre.

The structure was also solved at 40 K from data collected on the SMART diffractometer, equipped with the Helix open-flow cryostat. The crystal was an irregular plate of dimensions 0.1 x 0.1 x 0.05 mm. A unit cell of a = 9.1931(6), b = 10.6348(8), c = 10.9578(7) Å was obtained and the structure was solved in the space group Cmca and refined to give a R_1 value of 0.0735 for 473 reflections and wR_2 of 0.2431 for all data. Surprisingly, given the dataset's limitations in comparison to the 100 K data the anisotropic thermal displacement parameters are only slightly larger in magnitude than from the 100 K data set and they are all essentially spherical.

***Table 5.3.2** - Data for the refinements of C2 H10 B12 O2 at 150 K and 100 K.*

Compound	C2 H10 B12 O2	C2 H10 B12 O2	C2 H10 B12 O2
Formula weight	195.82	195.82	195.82
Temperature	150(2) K	100(2) K	100(2) K
Wavelength	1.54178 Å	0.71073 Å	0.71073 Å
Crystal system	Monoclinic*	Monoclinic	Orthorhombic
Space group	$P2_1/n$	$P2_1/n$	Cmca
Unit cell dimensions (Å/°)	a = 7.0608(14) α= 90	a = 7.0538(2) α= 90	a = 9.2538(3) α= 90
	b = 10.904(2) β= 97.83(3)	b = 10.9415(2) β= 98.01	b = 10.6482(3) β= 90
	c = 7.0677(14) γ = 90	c = 7.0535(2) γ = 90	c = 10.9415(2) γ = 90
Volume	539.1(2) $Å^3$	539.07(2) $Å^3$	1078.14(5) $Å^3$
Z	2	2	4
Density (calculated)	1.206 g/cm^3	1.206 g/cm^3	1.206 g/cm^3
Absorption coefficient	0.479 mm^{-1}	0.064 mm^{-1}	0.064 mm^{-1}
F(000)	196	196	392
Crystal size	0.20 x 0.40 x 0.70 mm^3	0.35 x 0.20 x 0.20 mm^3	0.35 x 0.20 x 0.20 mm^3
θ range for data collection	7.52 to 49.84°.	3.46 to 27.46°.	3.46 to 27.46°.
Index ranges	0<=h<=7	-9<=h<=8,	-12<=h<=11
	0<=k<=12	-14<=k<=14,	-10<=k<=13
	-7<=l<=7	-7<=l<=9	-14<=l<=14
Reflections collected	600	4049	3942
Independent reflections	548 [R(int) = 0.0312]	1224 [R(int) = 0.0411]	654 [R(int) = 0.0428]
Absorption correction	Not applied	Not applied	Not applied
Refinement method	Full-matrix L-S on F^2	Full-matrix L-S on F^2	Full-matrix L-S on F^2
Data / restraints / parameters	548 / 0 / 64	1222 / 0 / 93	653 / 0 / 54
Goodness-of-fit on F^2	1.045	1.073	1.101
Final R indices [I>2σ(I)]	R1 = 0.0416, wR2 = 0.1132	R1 = 0.0347, wR2 = 0.0931	R1 = 0.0323, wR2 = 0.0899
R indices (all data)	R1 = 0.0432, wR2 = 0.1154	R1 = 0.0399, wR2 = 0.1038	R1 = 0.0354, wR2 = 0.0951
Extinction coefficient	0.0123(32)	Not refined	Not refined
Largest diff. Peak and hole	0.204 and –0.135 $e.Å^{-3}$	0.188 and -0.250 $e.Å^{-3}$	0.178 and -0.219 $e.Å^{-3}$

The full list of atomic co-ordinates, anisotropic and isotropic displacement parameters are presented in ***Appendices A.5.1 and A.5.2*** for this structure at 150 and 100 K. * Note: There is also an alternative orthorhombic cell setting for the structure at 150 K.

5.3.2 The crystal structure of the tetrahydrate $C_2H_{14}B_{12}O_4 \cdot 4H_2O$

A crystal of the hydrate of 1,12-dicarbonyl carborane, $C_2H_{14}B_{12}O_4 \cdot 4H_2O$, was obtained in a recrystallisation from water. The reaction scheme for its formation is shown in ***Figure 5.3.2***.

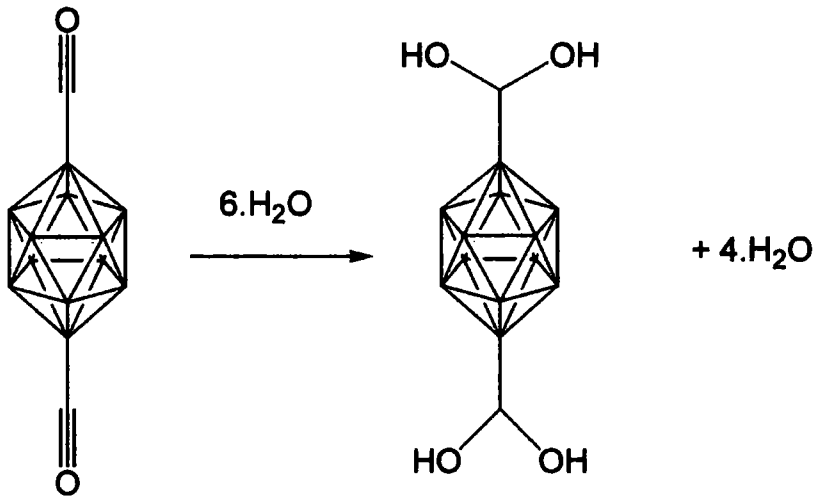

Figure 5.3.2 *– Reaction scheme for the hydration of para di-carbonyl borane by six molecules of water to give the bis-carbene species.*

The crystal structure of this compound disproved what had been generally accepted as being the outcome of the reaction between 1, 12-$B_{12}H_{10}(CO)_2$ and water since Knoth *et al* reported in 1967 that the carboxylic acid had been formed.[35] Given that the molecule had four water molecules per one boron cage, if the aforementioned proposed structure was taken as fact, two water molecules must be protonated with a -4 charge on the cage and each carboxylic acid having a positive charge. It has been decided that this is not the situation. Surprisingly, two ene-diols formed as opposed to carboxylic acid dimers, which would interact with hydroxyl groups in the lattice. The structure of the hydrate is shown in ***Figure 5.3.3***. The packing diagram explains the disposition of the water molecules, which are there to mediate strong hydrogen bond contacts. This is shown in ***Figure 5.3.4*** where there are three important intermolecular interactions, the OH..O mediated diol to water molecule contact, the water to water contact and the water molecule to boron cage contact. The data collection and structure refinement details are in ***Table 5.3.4*** and

the tables of bond lengths are in ***Table 5.3.3***. The range of interatomic distances exhibited within the dicarbonyl cluster are not in evidence in this structure with the largest although again the largest bond lengths are within the tropics of the cage.

***Table 5.3.3** - Bond lengths [Å] for C2 H22 B12 O8.*

O(1)-C(1)	1.2885(12)	B(3)-B(4)	1.808(2)
O(1)-H(10)	0.86(2)	B(3)-H(3)	1.092(14)
O(2)-C(1)	1.2868(12)	B(4)-B(2')	1.785(2)
O(2)-H(20)	0.84(2)	B(4)-B(6')	1.787(2)
C(1)-B(1)	1.5887(14)	B(4)-B(5)	1.799(2)
B(1)-B(6)	1.774(2)	B(4)-H(4)	1.077(14)
B(1)-B(3)	1.776(2)	B(5)-B(3')	1.779(2)
B(1)-B(4)	1.779(2)	B(5)-B(2')	1.781(2)
B(1)-B(5)	1.781(2)	B(5)-B(6)	1.795(2)
B(1)-B(2)	1.784(2)	B(5)-H(5)	1.103(13)
B(2)-B(5')	1.781(2)	B(6)-B(3')	1.785(2)
B(2)-B(4')	1.785(2)	B(6)-B(4')	1.787(2)
B(2)-B(3)	1.794(2)	B(6)-H(6)	1.096(14)
B(2)-B(6)	1.809(2)	O(1S)-H(1SB)	0.83(2)
B(2)-H(2)	1.091(14)	O(1S)-H(1SA)	0.86(2)
B(3)-B(5')	1.779(2)	O(2S)-H(2SB)	0.84(2)
B(3)-B(6')	1.785(2)	O(2S)-H(2SA)	0.82(2)

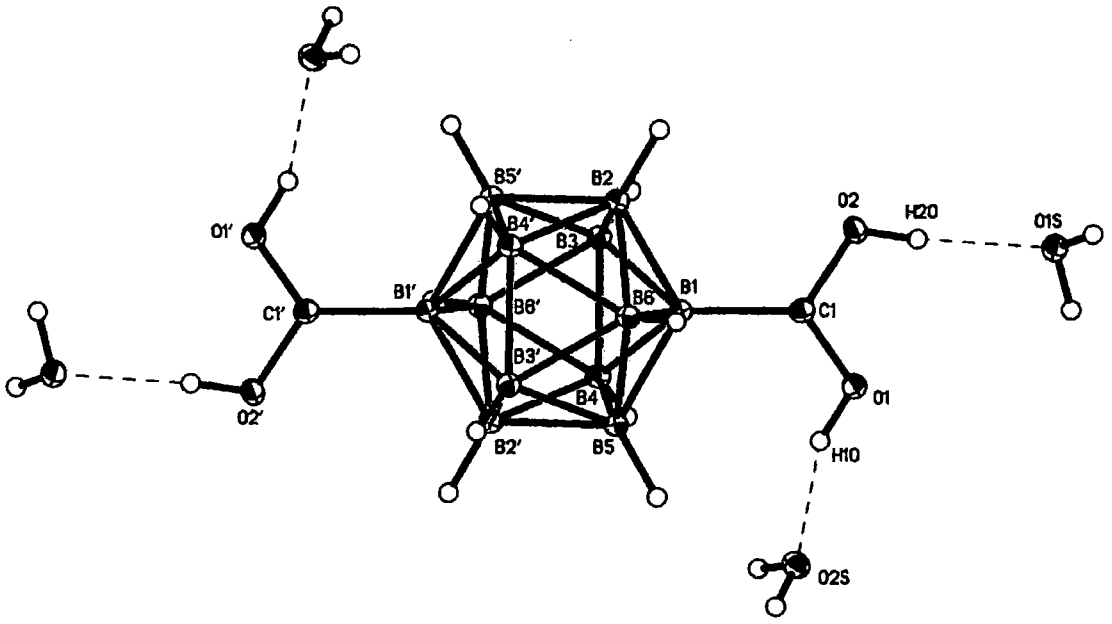

Figure 5.3.3. *- Crystal structure of $B_{12}H_{22}C_2O_6$ (50% ellipsoids) at 90(2) K. Important interatomic distances (Å) are: O(1)-H(10)..O(2S) 1.73(2), O(2)-H(20)..O(1S) 1.80(2). Angles (°): O(1)-H(10)-O(2S) 159(2), O(2)-H(20)-O(1S) 173(2).*

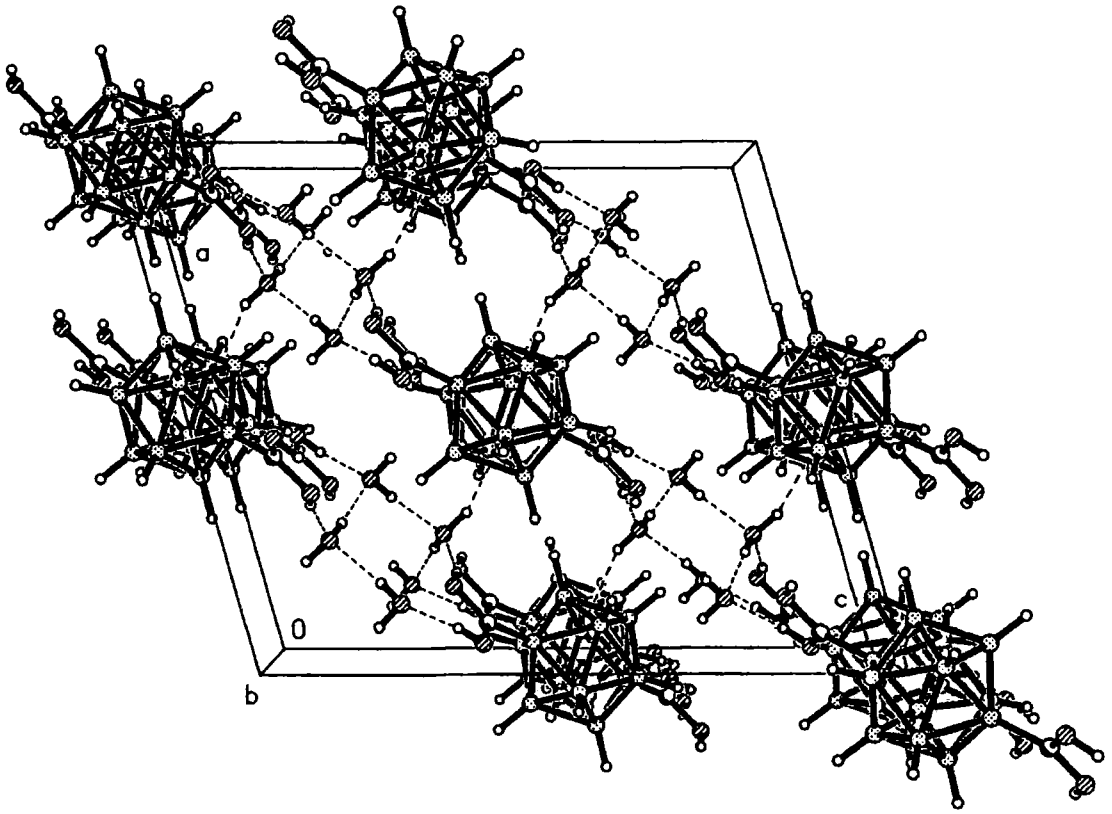

Figure 5.3.4 *- Packing diagram of the extended crystal structure of $B_{12}H_{22}C_2O_6$ viewed along the [010] direction. The supramolecular structure consists of sheets of cages mediated by water molecules, on the (101) plane. Hydrogen bond distances (O..H, Å) are 1.92(2) and 1.97(2) between the water molecules. There is a weak B..H interaction between B(5) and one of the water protons of 2.62(2) Å.*

***Table 5.3.4** - Crystal data and structure refinement for C2 H22 B12 O8.*

Compound	C2 H22 B12 O8
Formula weight	303.92
Temperature	90(2) K
Wavelength	0.71073 Å
Crystal system	Monoclinic
Space group	C2/c
Unit cell dimensions	a = 13.6298(2) Å α= 90°. b = 7.30180(10) Å β= 105.720(1)° c = 15.92440(10) Å γ = 90°.
Volume	1525.55(3) $Å^3$
Z	4
Density (calculated)	1.323 g/cm^3
Absorption coefficient	0.099 mm^{-1}
F(000)	632
Crystal size	0.35 x 0.20 x 0.20 mm^3
Theta range for data collection	2.66 to 27.49°.
Index ranges	-17<=h<=17, -8<=k<=9, -20<=l<=20
Reflections collected	5412
Independent reflections	1749 [R(int) = 0.0290]
Absorption correction	Not applied
Refinement method	Full-matrix least-squares on F^2
Data / restraints / parameters	1746 / 0 / 144
Goodness-of-fit on F^2	1.132
Final R indices [I>2sigma(I)]	R1 = 0.0286, wR2 = 0.0747
R indices (all data)	R1 = 0.0335, wR2 = 0.0814
Extinction coefficient	Not refined
Largest diff. peak and hole	0.357 and -0.192 $e.Å^{-3}$

The full list of atomic co-ordinates, anisotropic and isotropic displacement parameters are presented in ***Appendix A.5.3***.

5.4 Lysozyme

Lysozyme is the *de facto* standard for all trials of this nature. It is used for both theoretical studies on the mechanism of crystallisation of globular proteins[36] and optimising methods of crystallisation of other proteins.[37] Its function is to break down cell walls by hydrolysing glycosidic bonds. The structure was solved by David Phillips in 1965.[38,39] Single crystals grow rapidly that have well-defined morphologies. The morphology will depend on the polymorph, which is largely controlled by the crystallisation conditions and can crystallise in either a tetragonal, orthorhombic, monoclinic or triclinic space group. These polymorphs do not interconvert in a temperature-dependent manner, although all but the triclinic form do show reversible phase transitions in controlled relative humidity conditions.[40] These are manifested as fluctuations in unit cell volume, by as much as 50% in the monoclinic case.[41] They each have also a characteristic and significantly different percentage of solvent water in the lattice.

***Figure 5.4.1** – Cartoon representation depicting the secondary structure (the coils are α helices and the flat arrows are β sheets) in the 1.9 Å resolution crystal structure of the tetragonal form of CEW lysozyme at 100 K.[42] There are three disulphide bridges. The solvent water molecules are not shown in this figure.*

The test crystals in this study were the tetragonal modification having 41% solvent content in the asymmetric unit, which is the most for any of the four polymorphs.

Crystallisation of CEW lysozyme is known to occur at temperatures up to 333 K. The crystallisation of this protein was carried out at 298 K as follows. 100 mg of protein were dissolved in 1.25 cm^3 of sodium acetate buffer at pH 4.7. The mixture was stirred gently and 1.25 cm^3 of 10% (w/v) sodium chloride added slowly with continuous stirring. The solution was filtered using a 2 μm Amicon and covered with parafilm. Crystals of the tetragonal habit grew to an average dimension of 0.4 mm within 16 hours and larger if left for longer. They proved to be stable when removed from the mother liquor and placed in per-fluoropolyether oil overnight. The same crystallisation was carried out 285 K and the crystals that grew were plates originating from one nucleation point.

The crystal mount was first investigated. Crystals that are sensitive to exposure to the atmosphere or solvent loss had not previously been studied on the *Fddd* diffractometer.

A large crystal of dimensions 0.8 x 0.5 x 0.5 mm^3 was first flash-cooled to 150(2) K on a Siemens SMART-CCD. It was mounted on a glass fibre in perfluoro polyether oil and cooled using an Oxford Cryosystems open-flow N_2 cryostat. The crystal was indexed successfully (see ***Table 5.4.1***). Clearly, it was not surprising that this test yielded a positive result since the crystal was instantaneously cooled.

Table 5.4.1 *- Preliminary Results from the SMART*

Compound	CEW-lysozyme
Temperature / K	150(2)
Wavelength / Å	0.71073
Unit cell dimensions	a = 77.163(44) Å α = 90.02(4) °
	b = 77.266(20) Å β = 90.14(5) °
	c = 37.286(14) Å γ = 90.70(4) °
Collimator / mm	0.8
Crystal – detector / cm	12.00
Number of Reflections	77
Scan Width / °ω	-0.03
Exposure time / seconds	20.0(1)

The sample's mosaicity was then tested on the SMART using various cooling rates. Here, the crystal was again mounted on a fibre in oil. It was ramped at 30K/hr through the freezing point, which is a normal cooling rate for the *Fddd*. Frames were collected at an ω scan width of –0.03° and an exposure time of 10 seconds to follow the progress of the cooling. At 270(2) K the reflections had an average ω half width of 0.3°. At 253(2) K this had not changed. At 250(2) K, there started a gradual increase in the ω half width. The reflections were double their previous width at this stage. At 247(2) K there was a dramatic increase in mosaicity with the reflections having an average half width of 1.8° in ω and the frames of data contained rings which had not been there previously. This was accompanied by the appearance of some intense spots, resulting from ice formation.

A mount was developed (*see* ***Figure 5.4.2***) for macromolecular and air-sensitive crystals on the *Fddd*. It aims to protect the crystals from exposure to air and the drop of mother liquor adjacent to the crystal in the Lindemann capillary keeps the internal atmosphere hydrated, thus preventing the crystal from dehydrating. The Lindemann capillary used was either 0.5 mm or 0.8 mm in diameter depending on the crystal size. The crystal is protected from the low-pressure inside the beryllium cans and good contact with the graphite is still maintained to ensure cooling by conduction. It is crucial that good thermal contact is maintained between the cryostat and the graphite, and the graphite and the crystal. It was observed that good contact between the graphite and the crystal was invariably obtained using this mount since the crystal had several sheer faces and it adhered to the fibre by means of capillary action alone. Screening on the SMART showed that a crystal survived overnight in this mount. The conventional method of mounting crystals on this instrument and cooling to cryogenic temperature does not allow for rapid cooling. This is because the crystal must first be mounted and centred optically, two concentric cylindrical beryllium shrouds (with diameters of 6.5 and 5.0 cm) attached and the interior evacuated. Cooling then begins at a maximum rate of ca. 3.2° min^{-1} which clearly renders fast cooling impossible.

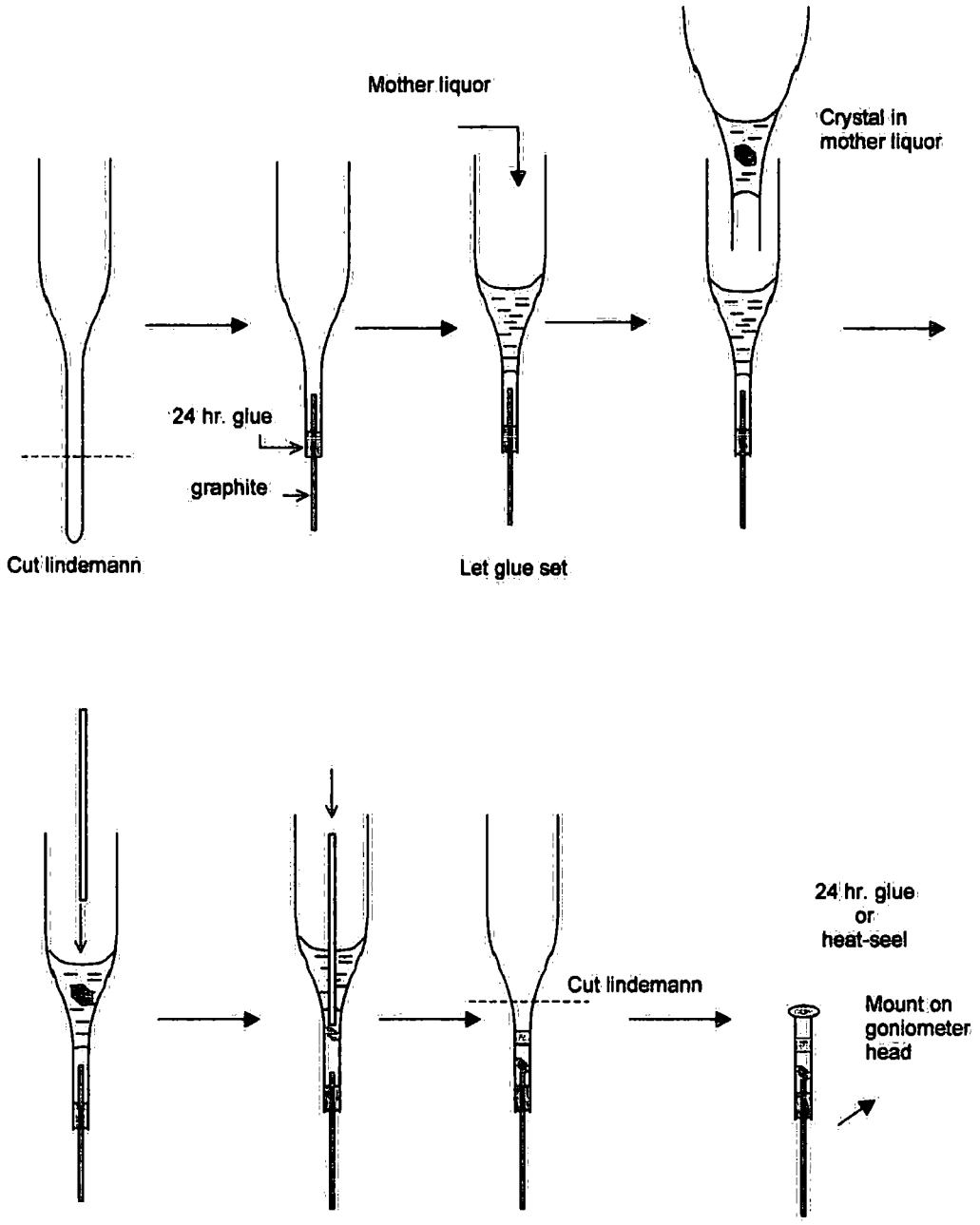

***Figure 5.4.2** - Methodology of preparing a sample mount for macromolecular or air-sensitive crystals on the Fddd diffractometer.*

SMART tests also showed that crystals that had been flash-cooled could not be re-measured once brought to room temperature, although the crystals appear undamaged from visual inspection. This problem can be attributed to radiation damage, which has a much more deleterious effect at room temperature when the free-radicals propagate faster through the crystal.

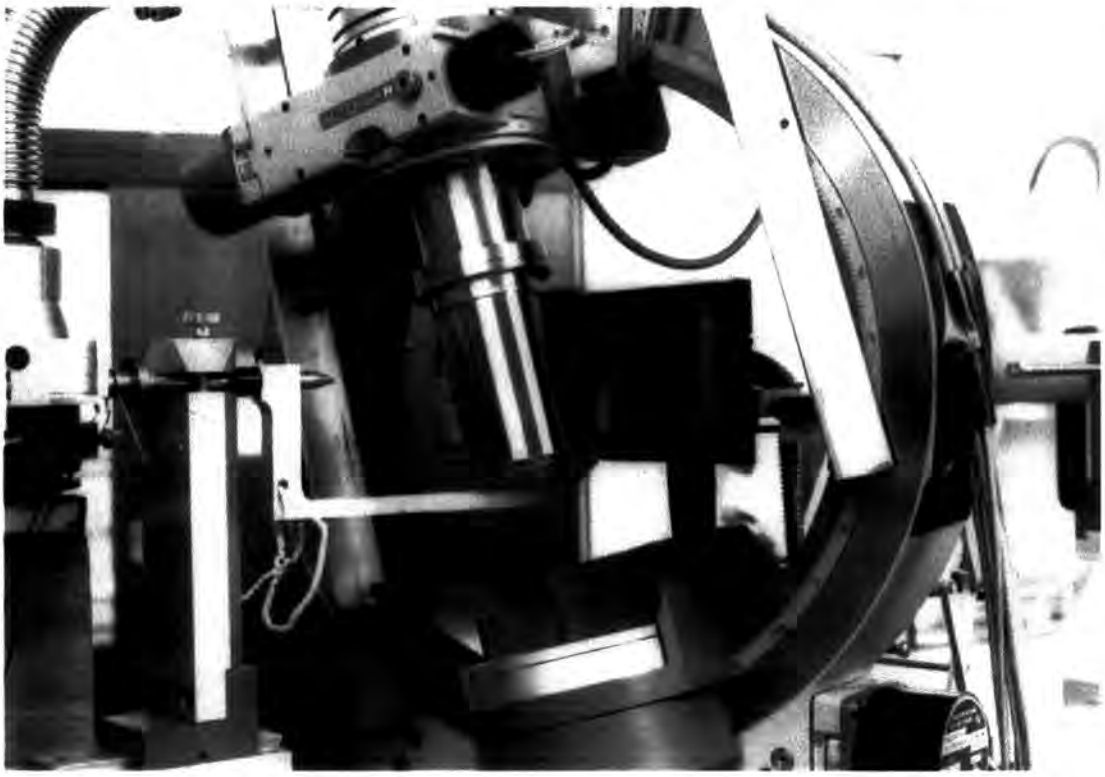

***Figure 5.4.3** – The physical set-up for taking Polaroid photographs on the Fddd diffractometer. The sample is mounted inside the beryllium cans. The beam stop, which casts a shadow on the photograph, is visible here. The camera is clamped to the 2θ arm.*

The rotating anode on the *Fddd* diffractometer operated at generator settings of 52 kV and 76 mA during the course of this work. The first test on the *Fddd* involved taking a large (1.0 x 0.8 x 0.4 mm) crystal mounted on sharpened graphite with 24-hour glue and leaving to harden. A room temperature rotation photograph showed no protein diffraction but numerous peaks due to the formation of sodium chloride and ice crystals ***Figure 5.4.4(a)***. The checks for diffraction described here were all done by collecting an oscillation photograph using a Polaroid camera by rotating through $\phi = 0 - 5°$ in 0.05° steps at a rate of two seconds per step repeated five times (see ***Figure 5.4.3***). The first crystal to be screened on the *Fddd* using the new sample mount described was a small crystal and the results shown in ***Figure 5.4.4(b)*** were somewhat some encouraging.

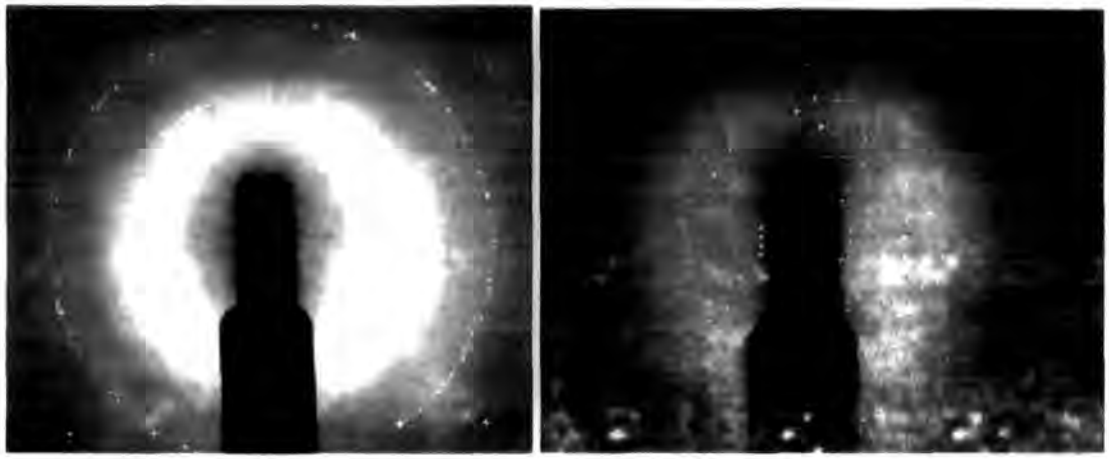

(a) *(b)*

Figure 5.4.4 *– (a) 1.0 x 0.8 x 0.4 mm crystal mounted on graphite with 24-hour glue, left to harden measured at room temperature with ϕ = 0 - 5° in 0.05° steps at a rate of two seconds per step and (b) Using the new sample mount scanned over the same range as the last photograph.*

The conventional χ = 180° position in a conventional four-circle diffractometer is 0° on this instrument due to the physical restrictions the cumbersome Displex imposes. These tests were carried out at χ = 180°. A new crystal was mounted in a Lindemann capillary and showed good diffraction from a Polaroid photograph, the graphite lines from the mount are clearly visible at 12.1° in 2θ, which is a resolution of 3.37 Å. The maximum resolution of these Polaroid photographs at this crystal-detector distance is 1.83 Å. The beryllium cans were added and there were at least 12 lines that appeared on the photograph, the protein diffraction remained unaltered. The χ circle was manually moved to a position above the horizontal plane, at approximately χ = 267° to allow the attachment of the pump. The Displex was switched on at 296 K and the photograph that was taken from a 5° oscillation as before showed complete loss of crystalline diffraction. These three photographs are depicted in ***Figure 5.4.5 a, b and c***. When the cans were removed, it could be seen that the crystal was no longer attached to the fibre. It was in a few pieces and in the drop. It must be concluded that either the movement of the χ circle or the vibrations due to the pump caused it to dissociate from the mount.

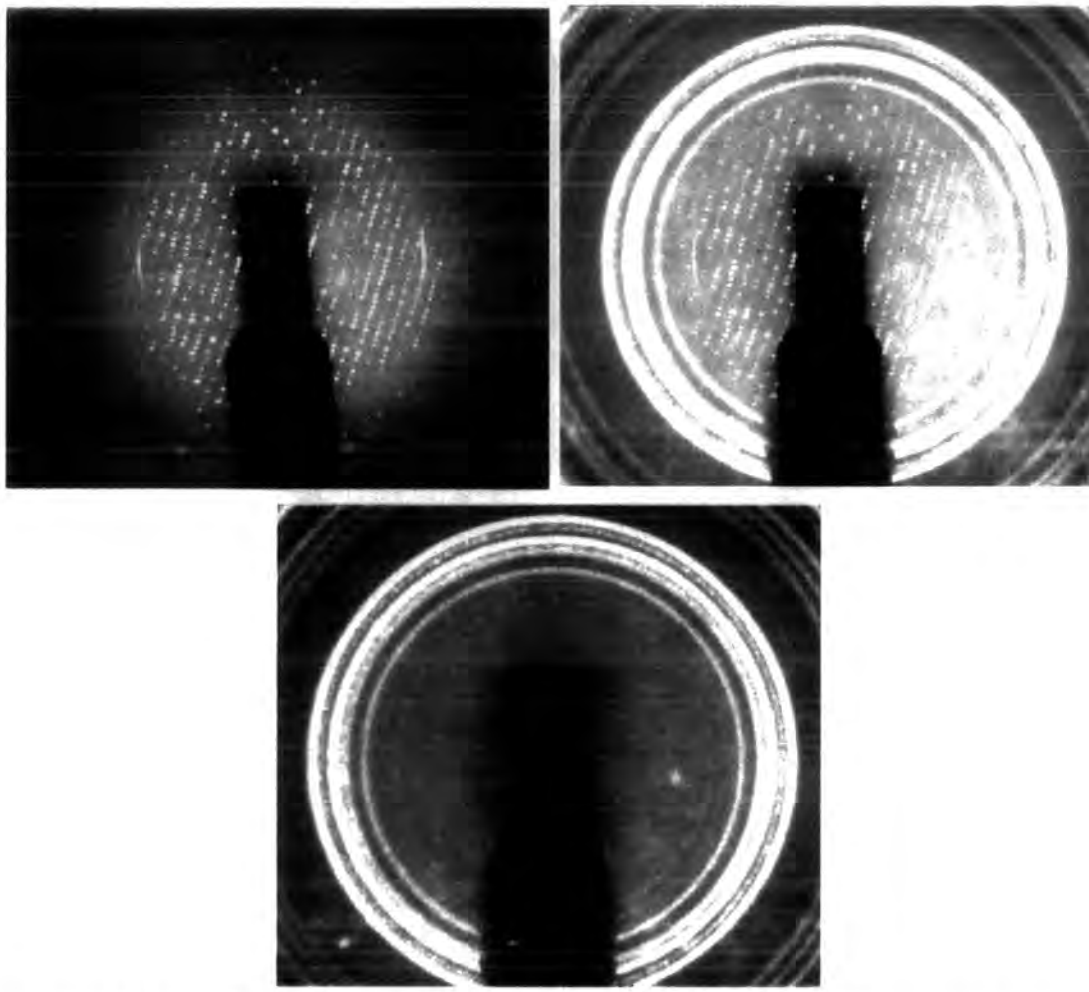

Figure 5.4.5 *– Labelled from the top left. (a) The first photograph of the crystal at room temperature with out the cans at* $\chi = 0°$*. (b) The cans are added. (c) The Displex is switched on 296 K and* $\chi = 267°$*.*

The results of the next attempted are tracked over six Polaroid photographs in ***Figure 5.4.6***. A large (0.7 x 0.4 x 0.4 mm) crystal was next used and this showed intense diffraction. The oscillation was of the same type as before taken over the range of ϕ = -90 to -85° in 0.05° steps at a rate of two seconds per step repeated five times. This time the χ circle was moved to a position 15° off the vertical to minimise the chances of crystal loss and the cans were attached. Oscillation photographs over 1° in ϕ in 0.01° steps and two second exposures were then taken owing to restrictions placed on its movement. A photograph was then taken using the thinner slice oscillation with the cans and pumping apparatus in place. The third photograph was taken when the pump was switch on. It is obvious form this that the crystal could withstand any vibrations with the χ circle in this position.

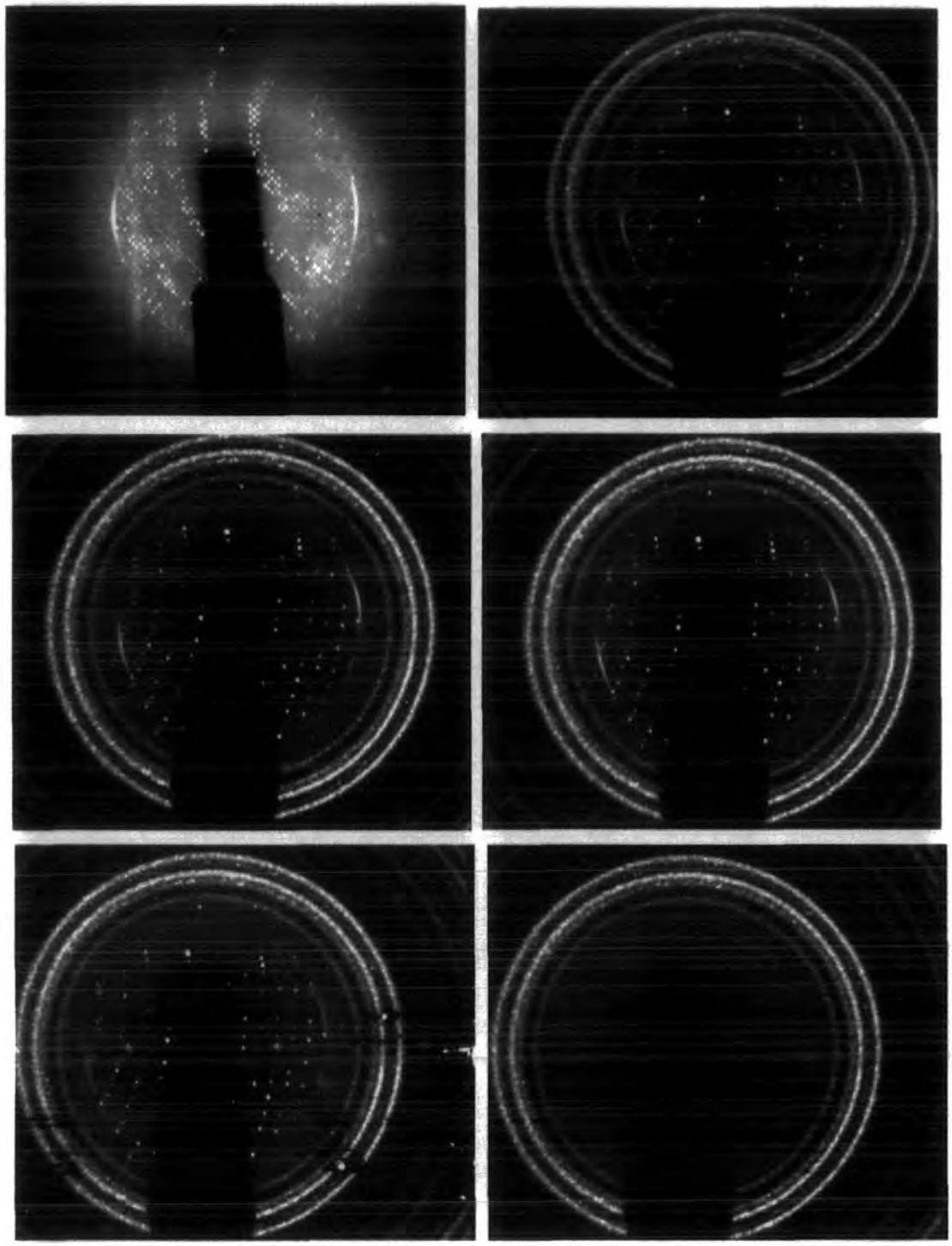

Figure 5.4.6 *– (a) → (f) are labelled from the top left. (a) The first photograph of the 0.7 x 0.4 x 0.4 mm crystal at room temperature. (b) A 1° oscillation photograph with the cans and pumping apparatus in position. (c) The Displex was switched on and the reading was 10^{-2} mbar. (d) After 20 minutes at 3 x 10^{-3} mbar. (e) After 45 minutes at 4 x 10^{-4} mbar. (f) After 95 minutes at 1.4 x 10^{-5} mbar.*

Crystals mounted in the upright position remained intact at room temperature with the Displex switched on. The heater temperature was set to and remained at 296

K for all of these tests. After 20 minutes, as the inner chamber was evacuated another Polaroid photograph was taken, which showed that the crystal appeared to be intact still. After 45 minutes, a further Polaroid of a 1° in ϕ oscillation showed diffraction as before. After 95 minutes, the chamber was evacuated enough to maintain cryogenic temperatures below 30 K. The Polaroid taken then showed complete loss of the crystalline diffraction and characteristic powder lines arising from the graphite fibre. The vacuum reading was 1.4×10^{-5} mbar. Again, the crystal fell off the mount and moved 2 mm down the capillary but this time it remained intact. It was decided to repeat this procedure but with cooling as an attempt to secure the crystal in place.

The χ circle was moved to a position 1° above the horizontal plane. In these trials, the inner beryllium can was not used and this was found to be beneficial because vacuums that could achieve cryopumping capability were obtained and also the background caused by the multiple powder lines were removed. Only one relatively faint line remained. The same procedure as before was followed and when the vacuum gauge read 5.2×10^{-6} mbar the heater was switched off to allow for maximum rate of cooling. Polaroid photographs were taken to track the crystal quality during cooling. The graphite lines and diffraction intensity steadily disappeared during the cooling process due to the temperature-induced contraction of the graphite fibre. Here 12 K was achieved in 70 minutes. When the temperature at the crystal was 12 K, some low angle intensities and their Friedel pairs with 2θ values less than 5° were located in order to recentre the crystal at 12 K. Some very weak diffraction reappeared and there was an absence of powder lines or diffraction of the type that ice crystallites would generate. These stages are shown in the photographs in ***Figure 5.4.7***.

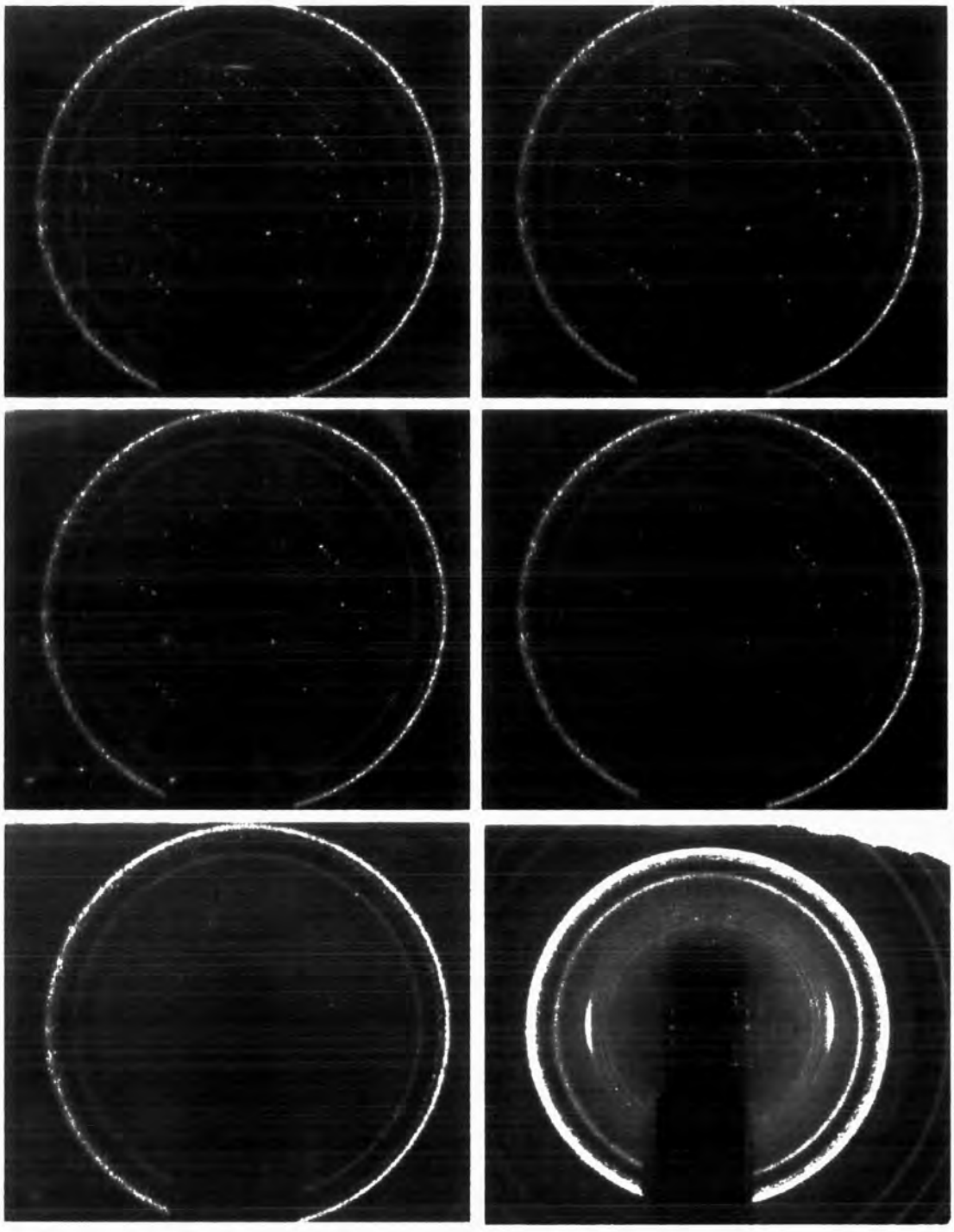

Figure 5.4.7 *– (a) → (f) are labelled from the top left. (a) The first photograph was the crystal at room temperature. (b) A 1 ° oscillation photograph with the cans and pumping apparatus in position, the Displex had been switch on for 5 minutes. (c) The Displex had been on for 35 minutes, the vacuum reading was 5.2 x 10^{-6} mbar. (d) A photograph after the pump had been removed. (e) The image at 12 K before the crystal was recentred in the beam using the intensities. (f) The diffraction from the crystal at 12 K, the graphite lines have returned. Note the camera was clamped further back on the 2θ arm in this case.*

This crystal had been reasonably small. It was thought that since the thermal gradient across the crystal would be less, therefore the crystal would be under less stress and not as likely to shatter. Although, the crystal was still diffracting, there has been a decrease in intensity and a loss of the higher order intensities. The centring of two of the eight reflections that were located at 12 K did not converge fully due to their broadness.

A large crystal of dimensions 0.7 x 0.5 x 0.4 mm was cooled slowly at 0.5 K/min in the next case to reduce the thermal gradient across the crystal. Again 1° oscillations in ϕ in 0.01° steps and two second exposures were taken. Reflections were centred during the cooling process between 293 K and 265 K. The average value of full width at half peak maximum during the ω scan, which is a very diagnostic measure of the crystalline mosaicity, was 0.11°. At 250 K, it suddenly became difficult to centre reflections and their full width at half peak maximum increased to an average value of 2.85°.

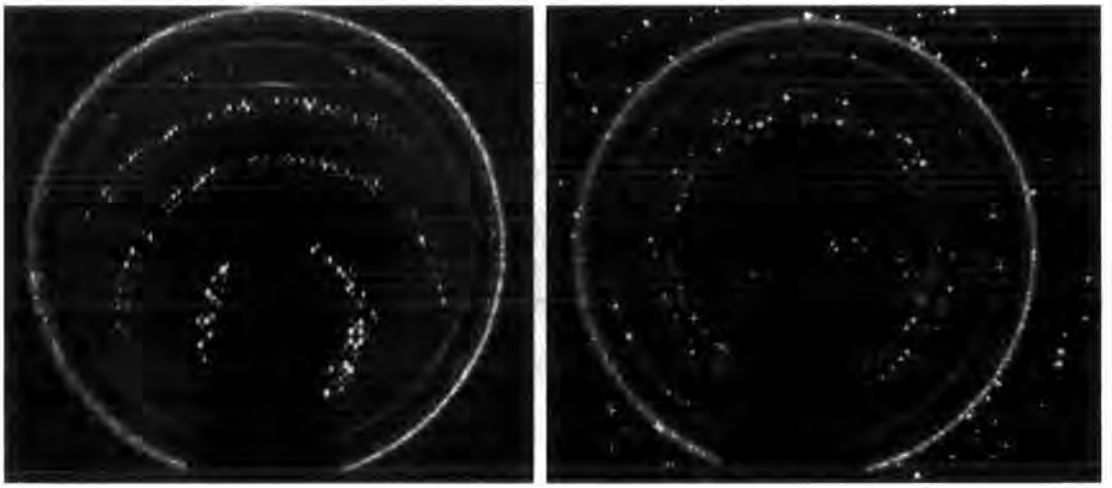

(a) *(b)*

***Figure 5.4.8** – (a) The crystal at room temperature before the Displex was switched on. The diffraction remained unchanged until 250 K in (b) where ice diffraction is visible and more intense than the reflections from lysozyme and the protein intensities are markedly broader in full width at half maximum. This is after height and lateral recentring.*

Twelve reflections were located and centred but they failed to index to yield the correct unit cell. A test was carried out on the SMART diffractometer. A crystal

(soaked in 25% MPD) was cooled at a rate of 6K/hour. The crystal cracked and much ice formed. It had been hoped that using this cryoprotectant would allow for slow cooling on the *Fddd* diffractometer.

It appeared that slow cooling would not work and that the cooling protocol on the *Fddd* diffractometer would have to be modified to allow for flash-cooling. The maximum cooling rate was approximately 3.2° min^{-1}, which clearly rendered flash-cooling impossible.

A crystal on a graphite fibre in a Lindemann capillary as in ***Figure 5.4.2*** was flash-cooled on the SMART to 150(2) K. It was not possible to measure data above background and ice crystals had grown. This was because the glass had slowly cooling and insulating the crystal. Therefore this sample mount could not be used for any modified cooling method involving partial cooling using a gaseous stream on the *Fddd*. Lysozyme crystals after this point were mounted on a graphite fibre using per-fluoropolyether oil.

This procedure effectively aimed at flash–cooling using a Displex. A nitrogen gas flow was attached to the upper stage of the Displex and passing it down inside the upper can. A transparent cannister was added in place of the outer beryllium can, leaving a 2 cm gap as an exit point for the nitrogen gas. A thermocouple used to measure the temperature near where the crystal would be was attached. The goniometer head with the crystal mounted in oil was attached loosely such that the copper section would become cold but the heat transfer would not extend to the crystal. Once the temperature had reached 138 K, the goniometer head was quickly screwed tightly with the crystal in oil and the beryllium can sealed. Cooling by means of the Displex then took over and the nitrogen supply was removed. The rotary pump was switched on and the temperature held at 177 K. The crystal did not show any diffraction above background.

(a) *(b)*

Figure 5.4.9 *– (a) The measurement of the temperature inside a system sealed in this manner (b). The sample is surrounded by transparent cannister whilst nitrogen gas cools it. The thermocouple reading at the crystal position is 263.1 K here.*

CEW-Lysozyme was later successfully indexed on the SMART instrument at 60(2) K using the Helix, helium open-flow cryostat. A loop was made from a strand of hair and superglued to a stout glass fibre. The crystal was pipetted from the mother liquor into oil and scooped into the loop. It was flash-cooled to 60(2) K and optically centred. The crystal to detector distance employed was 16 cm and frames of data were collected at a scan width of 0.3° in ω and an exposure time of 40 seconds (see ***Figure 5.4.10*** for an example of one such frame of data). The unit cell obtained from sixty centred reflections was 76.30(6), 76.56(7), 32.22(4) Å, 90.31(4), 85.66(5), 89.89(3)°, 205,718(544) $Å^3$. There is a significant decrease in the unit cell volume and one of the angles has deviated from 90° suggesting a monoclinic setting. However, this needs further investigation to confirm the existence of a temperature-dependent phase transition.

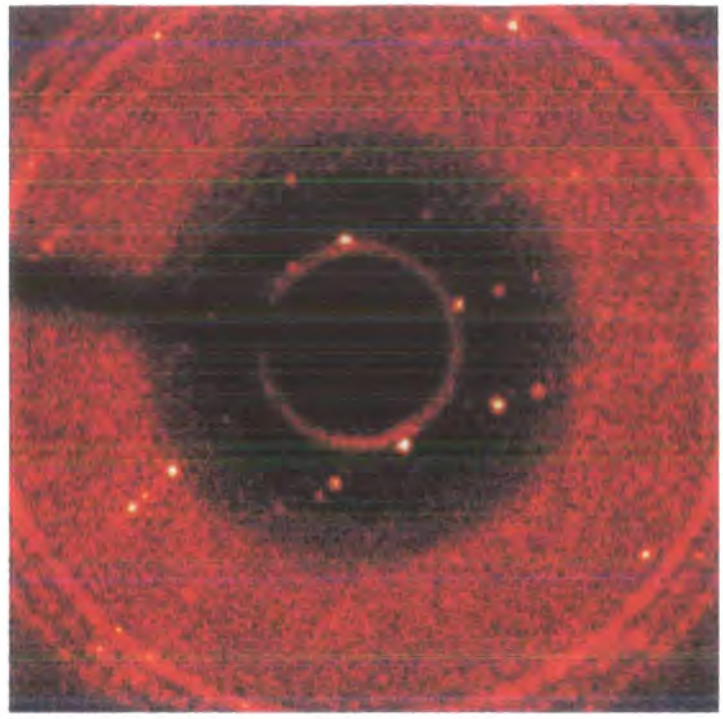

***Figure 5.4.10** – A frame of CEW-lysozyme data from the SMART at 60 K. The outer rings on the frame have arisen from the beryllium nozzle on the Helix.*

The conclusions that can be made at this stage are that the estimated ten minutes it takes between attaching the head and turning on the pump is too long a period of time to allow the crystal to be exposed to X-rays. It is very likely that redoing this using a crystal that has been modified with cryoprotectant will work, since the organic compounds that replace surface moisture and diffuse partially into the lattice does not crystallise on experiencing temperatures below 250 K. Crystals soaked in 20% 2,5-methyl pentane diol and 15% glycerol for a few seconds were also successfully indexed at 291 K.

It has been shown that larger protein crystals are more problematic than small ones at cooling. This is because of the larger thermal gradient across the sample.

This method for rapid cooling on the *Fddd* diffractometer works well for air-sensitive crystals, as has been shown by some recent work at Durham, but is not as yet suitable for proteins.

5.5 References

[1] D.W. Rodgers, (1994), *Structure*, **2**, 1135 – 1139.

[2] K.D. Watenpaugh, (1991), *Curr. Opin. Struct. Biol.*, **1**, 1012 – 1015.

[3] R. Rudman, (1976), *Low-temperature X-ray diffraction*, Plenum Press, New York.

[4] H. Hope, (1988), *Acta Crystallogr.*, **B44**, 22-26.

[5] M.M. Teeter and H. Hope, (1986), *Ann. N.Y. Acad. Sci.*, **482**, 163-165.

[6] K. Moffat and R. Henderson, (1995), *Current Opinion in Structural Biology*, **5**, 656-663.

[7] E.F. Garman and T.R. Schneider, (1997), *J. Appl. Cryst.*, **30**, 211-237.

[8] D. Stalke, (1998), *Chem. Soc. Rev.*, **27**, 171-178.

[9] A. Gonzalez and C. Nave, (1994), *Acta Crystallogr.* **D50**, 874 – 877.

[10] A.L. Fink and A.I. Ahmed, (1976), *Nature*, **263**, 294 – 300.

[11] J. Cosier and A. M. Glazer, (1986). *J. Appl. Cryst.*, **19**, 105 – 107.

[12] J.R. Allibon, A. Filhol, M.S. Lehmann, S.A. Mason and P. Simms (1981). *J. Appl. Crystallogr.*, **14**, 326 – 328.

[13] R.C.B. Copley, A.E. Goeta, C.W. Lehmann, J.C. Cole, D.S. Yufit, J.A.K. Howard, and J.M. Archer (1997). *J. Appl. Cryst.*, **30**, 413 – 417.

[14] U.F. Thomanek, F. Parak, R.L. Mössbauer, H. Formanek, P. Schwager and W. Hoppe, (1973), *Acta Crystallogr.*, **A29**, 263 – 265.

[15] S. Sastry (1999), *Nature*, **398**, 467-470.

[16] E.P. Mitchell and E.F. Garman, (1994), *J. Appl. Cryst.*, **27**, 1070-1074.

[17] T. Kottke and D. Stalke, (1993), *J. Appl. Cryst.*, **26**, 615-619.

[18] E.F. Garman from *Methods in Molecular Biology*, **Vol. 56**: *Crystallogrpahic Methods and Protocols*, 87-126. Edited by C. Jones, B. Molloy and M. Sanderson, Humana Press Inc., Totowa, N.J.

[19] H.R. Drew, S. Samson and R.E. Dickerson, (1982), *Proc. Natl. Acad. USA*, **79**, 4040-4044.

[20] T. Tsukihara, R. Nakashima, E. Yamashita, M. Yao, T. Mizushima, M. Odoko, K. Shinzawa-Itoh and S. Yoshikawa, (1999), Abstract **M05.OB.004**, IUCR Congress, Glasgow.

[21] P. Douzou, G. Hui Bon Hoa and G.A. Petsko (1974), *J. Mol. Biol.*, **96**, 367-380.

[22] G.A. Petsko (1974), *J. Mol. Biol.*, **96**, 381-392.

[23] D.W. Rodgers (1996), *Synchrotron Radiation News*, **9**, 6, 3-11.

[24] C.C. Caldwell and R.J.W. Le Févre, (1939), *Nature*, **143**, 803.

[25] I.E. Knaggs and K. Lonsdale, (1939), *Nature*, **143**, 1023-1024.

[26] K. Becker and H. Rose, (1923), *Z. Phys.*, **14**, 369.

[27] C.J. Brown and R. Sadanaga, (1965), *Acta Cryst.*, **18**, 158.

[28] P. Esherick and B.E. Kohler, (1973), *J. Chem. Phys.*, **59**, 12, 6681 – 6682.

[29] G. Odou, M. More and V. Warin, (1978), *Acta Cryst.*, A**34**, 459 – 462.

[30] G. Will, H. Göbel, C.F. Sampson and J.B. Forsyth, (1972), *Phys. Lett.*, **38**A, 207–208.

[31] C.E. Housecroft, K. Wade and B.C. Smith, (1978), *J. Chem. Soc., Chem. Commun.*, 765 – 766.

[32] M.A. Fox, J.A.K. Howard, J.M. Moloney and K. Wade, (1998), *J. Chem. Soc., Chem. Commun.*, 2487 – 2488.

[33] F.H. Allen & O. Kennard, *Chemical Design Automation News* (1993), 8(1) 1-37.

[34] J.J.P. Stewart, MOPAC 6.0, Frank Seiler Research Lab., USAF Academy, Colarado 1992; and M.J.S. Dewar, E.G.Zoebisch, E.F. Healy, J.J.P. Stewart, *J. Am. Chem. Soc.*, **1985**, *107*, 3902. M.J.S. Dewar & E.G.Zoebisch, *Theochem*, **1988**, *180*, 1.

[35] W.H. Knoth, J.C. Sauer, J.H. Balthis, H.C. Miller and E.L. Muetterties, (1967), *J. Amer. Chem. Soc.*, **89:19**, 4842 – 4850.

[36] F. Rosenberger, P.G. Vekilov, M. Muschol and B.R. Thomas, (1996) *J. Cryst. Growth*, **168**, 1 – 27.

[37] E.H. Snell, T.J. Boggon, J.R. Helliwell, M.E. Moskowitz and A. Nadarajah, (1997), *Acta Cryst.*, D**53**, 747 – 755.

[38] CC. Blake, D.F. Koenig, G.A. Mair, A.C.T North, D.C. Phillips and V.R. Sarma, (1965), *Nature* (London), **206**, 757 – 763.

[39] D.C Phillips, (1966), *Sci. Amer.*, **215**, No. 5, 78 – 90.

[40] D.M. Salunke, B. Veerapandian, R. Kodandapani and M. Vijayin, (1985), *Acta Cryst.*, B**41**, 431 – 436.

[41] Madhusudan, R. Kodandapani and M. Vijayin, (1993), *Acta Cryst.*, D**49**, 234 – 245.

[42] J.C. Dewan, A.C.M. Young and R.F. Tilton, (1993), *J. Appl. Cryst.*, **26**, 309.

Appendix A

Atomic Coordinates, Equivalent And Anisotropic Displacement Parameters For All Reported Structural Determinations.

***Table 4.1.2** - Atomic coordinates (x 10^4) and equivalent isotropic displacement parameters ($Å^2$x 10^3) for DOTA. U(eq) is defined as one third of the trace of the orthogonalized U^{ij} tensor.*

	x	y	z	U(eq)
O(1)	4799(3)	2588(2)	11061(3)	39(1)
O(2)	3499(3)	3013(1)	9787(2)	31(1)
O(3)	415(2)	2841(1)	13147(2)	27(1)
O(4)	1957(2)	2576(1)	12016(2)	25(1)
O(5)	7566(2)	2964(1)	12026(2)	28(1)
O(6)	6132(2)	2667(1)	13250(2)	26(1)
O(7)	3152(3)	2580(1)	14325(2)	29(1)
O(8)	4489(2)	3013(1)	15572(2)	26(1)
N(1)	2109(2)	1303(2)	12804(2)	18(1)
N(2)	3763(3)	1340(2)	10923(2)	17(1)
N(3)	5975(2)	1398(2)	12369(2)	17(1)
N(4)	4311(2)	1364(2)	14289(2)	17(1)
C(1)	1765(3)	1012(2)	11663(3)	21(1)
C(2)	2875(3)	793(2)	11011(3)	21(1)
C(3)	4945(3)	1086(2)	10547(3)	19(1)
C(4)	5727(3)	845(2)	11536(3)	18(1)
C(5)	6338(3)	1130(2)	13515(3)	19(1)
C(6)	5258(3)	856(2)	14157(3)	18(1)
C(7)	3174(3)	1052(2)	14644(3)	20(1)
C(8)	2449(3)	768(2)	13644(3)	19(1)
C(11)	1118(3)	1740(2)	13221(3)	21(1)
C(12)	1219(3)	2432(2)	12708(3)	20(1)
C(21)	3329(3)	1865(2)	10155(3)	21(1)
C(22)	3961(3)	2515(2)	10395(3)	23(1)
C(31)	6927(3)	1863(2)	11955(3)	21(1)
C(32)	6815(3)	2545(2)	12499(3)	21(1)
C(41)	4702(3)	1872(2)	15119(3)	19(1)
C(42)	4066(3)	2525(2)	14979(3)	23(1)
Cl(1A)	4294(3)	-701(1)	12616(2)	21(1)
Cl(1B)	4539(2)	-711(1)	12573(2)	19(1)
Cl(2A)	4143(3)	4817(2)	7951(4)	23(1)
Cl(2B)	4083(3)	4947(2)	8328(3)	34(1)
Cl(2C)	4011(3)	4694(2)	7598(3)	26(1)
O(1SA)	2232(4)	5856(2)	7098(4)	29(1)
O(1SB)	1953(16)	5864(9)	7225(14)	24(4)
O(2SA)	9946(6)	1032(4)	-1506(6)	47(2)
O(2SB)	8420(11)	1134(6)	-2420(9)	37(3)
0(2SC)	8815(18)	1299(10)	-2434(14)	39(4)
O(3SA)	7551(5)	1156(3)	-826(5)	33(1)
O(3SB)	8428(5)	871(3)	-89(5)	37(1)
O(4SA)	10000	0	0	63(3)
O(4SB)	9557(16)	15(9)	219(14)	82(4)
O(5SA)	4745(6)	4096(4)	10290(5)	52(2)
O(5SB)	4042(10)	4254(5)	10178(9)	58(2)

***Table 4.1.3** - Bond lengths [Å] and angles [°] for DOTA.*

O(1)-C(22)	1.208(5)	O(6)-C(32)	1.202(4)	N(2)-C(2)	1.475(5)
O(2)-C(22)	1.325(4)	O(7)-C(42)	1.261(5)	N(2)-C(3)	1.476(4)
O(2)-H(2)	0.8400	O(8)-C(42)	1.284(4)	N(3)-C(31)	1.493(4)
O(3)-C(12)	1.320(4)	N(1)-C(11)	1.492(4)	N(3)-C(4)	1.502(4)
O(3)-H(3C)	0.8400	N(1)-C(8)	1.502(4)	N(3)-C(5)	1.503(4)
O(4)-C(12)	1.202(4)	N(1)-C(1)	1.510(4)	N(3)-H(3)	0.9300
O(5)-C(32)	1.312(4)	N(1)-H(1)	0.9300	N(4)-C(6)	1.468(4)
O(5)-H(5)	0.8400	N(2)-C(21)	1.463(4)	N(4)-C(7)	1.469(4)

N(4)-C(41)	1.471(4)	C(1)-N(1)-H(1)	107.5	N(4)-C(7)-H(7B)	109.2
C(1)-C(2)	1.524(5)	C(21)-N(2)-C(2)	111.7(3)	C(8)-C(7)-H(7B)	109.2
C(1)-H(1A)	0.9900	C(21)-N(2)-C(3)	109.9(3)	H(7A)-C(7)-H(7B)	107.9
C(1)-H(1B)	0.9900	C(2)-N(2)-C(3)	110.9(3)	N(1)-C(8)-C(7)	111.5(3)
C(2)-H(2A)	0.9900	C(31)-N(3)-C(4)	111.3(2)	N(1)-C(8)-H(8A)	109.3
C(2)-H(2B)	0.9900	C(31)-N(3)-C(5)	110.1(2)	C(7)-C(8)-H(8A)	109.3
C(3)-C(4)	1.515(4)	C(4)-N(3)-C(5)	111.6(3)	N(1)-C(8)-H(8B)	109.3
C(3)-H(3A)	0.9900	C(31)-N(3)-H(3)	107.9	C(7)-C(8)-H(8B)	109.3
C(3)-H(3B)	0.9900	C(4)-N(3)-H(3)	107.9	H(8A)-C(8)-H(8B)	108.0
C(4)-H(4A)	0.9900	C(5)-N(3)-H(3)	107.9	N(1)-C(11)-C(12)	110.0(3)
C(4)-H(4B)	0.9900	C(6)-N(4)-C(7)	110.4(3)	N(1)-C(11)-H(11A)	109.7
C(5)-C(6)	1.528(5)	C(6)-N(4)-C(41)	110.6(2)	C(12)-C(11)-H(11A)	109.7
C(5)-H(5A)	0.9900	C(7)-N(4)-C(41)	110.0(3)	N(1)-C(11)-H(11B)	109.7
C(5)-H(5B)	0.9900	N(1)-C(1)-C(2)	111.9(3)	C(12)-C(11)-H(11B)	109.7
C(6)-H(6A)	0.9900	N(1)-C(1)-H(1A)	109.2	H(11A)-C(11)-H(11B)	108.2
C(6)-H(6B)	0.9900	C(2)-C(1)-H(1A)	109.2	O(4)-C(12)-O(3)	126.1(3)
C(7)-C(8)	1.523(4)	N(1)-C(1)-H(1B)	109.2	O(4)-C(12)-C(11)	123.2(3)
C(7)-H(7A)	0.9900	C(2)-C(1)-H(1B)	109.2	O(3)-C(12)-C(11)	110.6(3)
C(7)-H(7B)	0.9900	H(1A)-C(1)-H(1B)	107.9	N(2)-C(21)-C(22)	111.2(3)
C(8)-H(8A)	0.9900	N(2)-C(2)-C(1)	111.3(3)	N(2)-C(21)-H(21A)	109.4
C(8)-H(8B)	0.9900	N(2)-C(2)-H(2A)	109.4	C(22)-C(21)-H(21A)	109.4
C(11)-C(12)	1.519(5)	C(1)-C(2)-H(2A)	109.4	N(2)-C(21)-H(21B)	109.4
C(11)-H(11A)	0.9900	N(2)-C(2)-H(2B)	109.4	C(22)-C(21)-H(21B)	109.4
C(11)-H(11B)	0.9900	C(1)-C(2)-H(2B)	109.4	H(21A)-C(21)-H(21B)	108.0
C(21)-C(22)	1.499(5)	H(2A)-C(2)-H(2B)	108.0	O(1)-C(22)-O(2)	122.7(4)
C(21)-H(21A)	0.9900	N(2)-C(3)-C(4)	111.6(3)	O(1)-C(22)-C(21)	125.0(3)
C(21)-H(21B)	0.9900	N(2)-C(3)-H(3A)	109.3	O(2)-C(22)-C(21)	112.3(3)
C(31)-C(32)	1.516(5)	C(4)-C(3)-H(3A)	109.3	N(3)-C(31)-C(32)	111.0(3)
C(31)-H(31A)	0.9900	N(2)-C(3)-H(3B)	109.3	N(3)-C(31)-H(31A)	109.4
C(31)-H(31B)	0.9900	C(4)-C(3)-H(3B)	109.3	C(32)-C(31)-H(31A)	109.4
C(41)-C(42)	1.491(5)	H(3A)-C(3)-H(3B)	108.0	N(3)-C(31)-H(31B)	109.4
C(41)-H(41A)	0.9900	N(3)-C(4)-C(3)	111.3(3)	C(32)-C(31)-H(31B)	109.4
C(41)-H(41B)	0.9900	N(3)-C(4)-H(4A)	109.4	H(31A)-C(31)-H(31B)	108.0
Cl(2A)-Cl(2C)	0.503(4)	C(3)-C(4)-H(4A)	109.4	O(6)-C(32)-O(5)	126.6(4)
Cl(2A)-Cl(2B)	0.522(4)	N(3)-C(4)-H(4B)	109.4	O(6)-C(32)-C(31)	123.7(3)
Cl(2B)-Cl(2C)	1.002(5)	C(3)-C(4)-H(4B)	109.4	O(5)-C(32)-C(31)	109.7(3)
O(2SA)-0(2SC)	1.726(19)	H(4A)-C(4)-H(4B)	108.0	N(4)-C(41)-C(42)	113.7(3)
O(2SB)-0(2SC)	0.546(19)	N(3)-C(5)-C(6)	112.4(3)	N(4)-C(41)-H(41A)	108.8
O(3SA)-O(3SB)	1.406(8)	N(3)-C(5)-H(5A)	109.1	C(42)-C(41)-H(41A)	108.8
O(4SA)-O(4SB)#1	0.559(18)	C(6)-C(5)-H(5A)	109.1	N(4)-C(41)-H(41B)	108.8
O(4SA)-O(4SB)	0.559(18)	N(3)-C(5)-H(5B)	109.1	C(42)-C(41)-H(41B)	108.8
O(4SB)-O(4SB)#1	1.12(4)	C(6)-C(5)-H(5B)	109.1	H(41A)-C(41)-H(41B)	107.7
O(5SA)-O(5SB)	0.845(11)	H(5A)-C(5)-H(5B)	107.9	O(7)-C(42)-O(8)	123.0(4)
		N(4)-C(6)-C(5)	111.6(3)	O(7)-C(42)-C(41)	120.8(3)
C(22)-O(2)-H(2)	109.5	N(4)-C(6)-H(6A)	109.3	O(8)-C(42)-C(41)	116.3(3)
C(12)-O(3)-H(3C)	109.5	C(5)-C(6)-H(6A)	109.3	Cl(2C)-Cl(2A)-Cl(2B)	155.9(10)
C(32)-O(5)-H(5)	109.5	N(4)-C(6)-H(6B)	109.3	Cl(2A)-Cl(2B)-Cl(2C)	11.8(5)
C(11)-N(1)-C(8)	111.9(3)	C(5)-C(6)-H(6B)	109.3	Cl(2A)-Cl(2C)-Cl(2B)	12.3(5)
C(11)-N(1)-C(1)	110.5(2)	H(6A)-C(6)-H(6B)	108.0	O(2SB)-0(2SC)-O(2SA)	111(3)
C(8)-N(1)-C(1)	111.7(3)	N(4)-C(7)-C(8)	111.9(3)	O(4SB)-O(4SA)-O(4SB)	180(5)
C(11)-N(1)-H(1)	107.5	N(4)-C(7)-H(7A)	109.2	O(4SA)-O(4SB)-O(4SB)	0(3)
C(8)-N(1)-H(1)	107.5	C(8)-C(7)-H(7A)	109.2		

***Table 4.1.4** - Anisotropic displacement parameters ($Å^2 x\ 10^3$) for DOTA. The anisotropic displacement factor exponent takes the form: $-2\pi^2[h^2 a^{*2} U^{11} + ... + 2 h k a^* b^* U^{12}]$*

	U^{11}	U^{22}	U^{33}	U^{23}	U^{13}	U^{12}
O(1)	41(2)	26(2)	49(2)	-2(1)	-24(1)	-1(1)
O(2)	36(1)	18(1)	37(2)	9(1)	-10(1)	-3(1)
O(3)	34(1)	17(1)	31(1)	4(1)	7(1)	7(1)
O(4)	30(1)	21(1)	24(1)	1(1)	2(1)	0(1)
O(5)	33(1)	20(2)	33(1)	-2(1)	7(1)	-8(1)
O(6)	31(1)	20(1)	25(1)	-2(1)	3(1)	-2(1)
O(7)	34(1)	17(1)	35(1)	0(1)	-14(1)	2(1)
O(8)	28(1)	17(1)	32(1)	-8(1)	-5(1)	-2(1)
N(1)	15(1)	18(2)	22(1)	-1(1)	-2(1)	0(1)
N(2)	23(1)	15(2)	14(1)	1(1)	-2(1)	1(1)
N(3)	16(1)	16(2)	19(1)	3(1)	0(1)	-1(1)
N(4)	22(1)	15(2)	13(1)	-1(1)	-3(1)	-1(1)
C(1)	22(2)	19(2)	21(2)	-2(1)	-7(1)	-2(1)
C(2)	26(2)	15(2)	20(2)	-1(1)	-1(1)	-1(1)
C(3)	26(2)	14(2)	17(2)	1(1)	1(1)	2(1)
C(4)	24(2)	10(2)	20(2)	-1(1)	1(1)	0(1)
C(5)	20(2)	15(2)	21(2)	-1(1)	-4(1)	3(1)
C(6)	25(2)	15(2)	15(1)	0(1)	-3(1)	1(1)
C(7)	23(2)	19(2)	18(2)	2(1)	0(1)	-1(1)
C(8)	22(2)	13(2)	21(2)	3(1)	-2(1)	-1(1)
C(11)	18(2)	18(2)	26(2)	2(1)	1(1)	2(1)
C(12)	21(2)	20(2)	19(2)	2(1)	-4(1)	2(1)
C(21)	26(2)	22(2)	16(1)	3(1)	-5(1)	0(1)
C(22)	27(2)	18(2)	23(2)	2(1)	-2(1)	2(1)
C(31)	19(2)	21(2)	23(2)	-3(1)	3(1)	-4(1)
C(32)	20(2)	24(2)	19(2)	2(1)	-3(1)	-3(1)
C(41)	23(2)	17(2)	17(1)	-4(1)	-4(1)	-3(1)
C(42)	28(2)	17(2)	23(2)	3(1)	4(1)	-1(1)

***Table 4.1.5** - Hydrogen coordinates ($x\ 10^4$) and isotropic displacement parameters ($Å^2 x\ 10^3$) for DOTA.*

	x	y	z	U(eq)
H(2)	3876	3367	9945	46
H(3C)	483	3221	12854	41
H(5)	7502	3342	12329	42
H(1)	2790	1570	12709	22
H(3)	5262	1640	12445	20
H(1A)	1309	1351	11214	25
H(1B)	1224	623	11769	25
H(2A)	3262	408	11402	25
H(2B)	2617	646	10243	25
H(3A)	5377	1445	10145	23
H(3B)	4808	712	10010	23
H(4A)	5311	473	11920	22
H(4B)	6506	673	11252	22
H(5A)	6727	1491	13966	22
H(5B)	6943	770	13424	22
H(6A)	4912	468	13742	22
H(6B)	5538	700	14913	22
H(7A)	2676	1389	15035	24
H(7B)	3364	689	15188	24
H(8A)	2937	422	13266	22
H(8B)	1702	553	13920	22
H(11A)	1175	1771	14056	25

H(11B)	320	1543	13011	25
H(21A)	2444	1924	10240	25
H(21B)	3474	1730	9364	25
H(31A)	6844	1908	11123	25
H(31B)	7740	1676	12134	25
H(41A)	5587	1945	15051	23
H(41B)	4559	1700	15889	23

***Table A.4.2.2** - Atomic coordinates (x 10^4) and equivalent isotropic displacement parameters ($Å^2$x 10^3) for C57H75EuF9N11O14S3. U(eq) is defined as one third of the trace of the orthogonalized U^{ij} tensor.*

	x	y	z	U(eq)
Eu(1)	1181(1)	88(1)	866(1)	30(1)
O(1)	210(3)	-832(2)	804(2)	37(1)
O(2)	-24(3)	758(2)	661(2)	40(1)
O(3)	1643(3)	982(2)	1470(2)	34(1)
O(4)	1885(3)	-526(2)	1622(2)	34(1)
O(5)	319(2)	142(2)	1796(2)	39(1)
O(13)	177(5)	2130(4)	-1125(3)	121(3)
O(12)	-691(4)	2897(3)	-1705(2)	97(2)
O(11)	-857(4)	2811(2)	-605(2)	66(2)
O(23)	3850(4)	-3279(3)	997(2)	82(2)
O(22)	4086(4)	-2107(2)	946(3)	77(2)
O(21)	3507(3)	-2616(2)	1881(2)	53(1)
O(33)	1718(6)	1019(3)	3647(3)	116(3)
O(32)	1249(5)	268(4)	2853(2)	126(3)
O(31)	1789(3)	-131(3)	3815(2)	69(1)
N(1)	716(3)	-207(2)	-266(2)	33(1)
N(2)	1488(3)	1077(2)	84(2)	32(1)
N(3)	2855(3)	364(2)	759(2)	33(1)
N(4)	2085(3)	-913(2)	415(2)	33(1)
N(5)	-635(3)	-1520(2)	264(2)	38(1)
N(6)	-660(3)	1650(2)	264(2)	41(1)
N(7)	2627(3)	1619(2)	1941(2)	39(1)
N(8)	2547(3)	-1422(2)	1988(2)	35(1)
C(1)	623(4)	395(3)	-654(3)	37(1)
C(2)	1361(4)	860(3)	-568(2)	37(1)
C(3)	2361(4)	1331(3)	150(3)	35(1)
C(4)	3014(4)	786(3)	206(3)	37(1)
C(5)	3360(4)	-249(2)	693(2)	35(1)
C(6)	2961(4)	-730(3)	246(3)	39(1)
C(7)	1669(4)	-1195(3)	-137(2)	36(1)
C(8)	1341(4)	-654(2)	-564(2)	38(2)
C(11)	-138(4)	-531(3)	-231(3)	41(1)
C(12)	-162(4)	-984(3)	328(3)	34(1)
C(13)	-757(4)	-1999(3)	765(3)	44(2)
C(14)	-1494(5)	-2456(3)	599(3)	56(2)
C(15)	57(4)	-2373(2)	892(3)	42(1)
C(16)	371(5)	-2416(3)	1493(3)	52(2)
C(17)	1115(6)	-2759(3)	1618(3)	66(2)
C(18)	1550(5)	-3077(3)	1140(4)	64(2)
C(19)	1220(6)	-3038(3)	553(3)	60(2)
C(20)	490(5)	-2693(3)	431(3)	49(2)
C(21)	876(4)	1596(3)	238(3)	36(1)
C(22)	17(4)	1312(3)	390(3)	38(1)
C(23)	-1513(4)	1423(3)	429(3)	52(2)
C(24)	-2109(5)	2020(3)	438(4)	60(2)
C(25)	-1822(5)	884(3)	-6(5)	69(2)
C(26)	-2229(7)	348(5)	251(7)	117(4)
C(27)	-2540(10)	-144(8)	-174(10)	168(8)
C(28)	-2412(8)	-68(8)	-774(10)	163(8)
C(29)	-2015(6)	448(5)	-1014(6)	112(4)
C(30)	-1709(5)	935(4)	-635(5)	74(3)
C(31)	3120(4)	706(3)	1317(3)	36(1)
C(32)	2401(4)	1126(3)	1574(3)	35(2)
C(33)	1965(4)	1993(3)	2289(3)	43(2)
C(34)	2440(5)	2411(3)	2762(3)	55(2)

C(35)	1418(4)	2392(3)	1858(3)	43(2)
C(36)	538(4)	2312(4)	1882(3)	54(2)
C(37)	14(5)	2691(4)	1492(4)	70(2)
C(38)	376(6)	3144(4)	1095(4)	69(2)
C(39)	1243(6)	3221(3)	1082(3)	61(2)
C(40)	1762(5)	2857(3)	1453(3)	52(2)
C(41)	2096(4)	-1415(2)	915(3)	37(1)
C(42)	2195(4)	-1088(3)	1537(3)	33(1)
C(43)	2622(4)	-1168(3)	2620(2)	37(1)
C(44)	2491(5)	-1721(3)	3073(3)	49(2)
C(45)	3470(4)	-815(3)	2683(3)	41(2)
C(46)	3489(5)	-129(3)	2703(3)	54(2)
C(47)	4256(6)	202(4)	2712(3)	74(3)
C(48)	5018(6)	-151(5)	2711(3)	81(3)
C(49)	5002(5)	-822(5)	2710(4)	70(2)
C(50)	4229(5)	-1156(4)	2690(3)	57(2)
C(100)	486(6)	3370(7)	-1003(5)	111(4)
C(200)	5074(6)	-2775(5)	1604(4)	78(3)
C(300)	312(7)	378(5)	3825(5)	91(3)
S(1)	-313(2)	2725(1)	-1132(1)	74(1)
S(2)	4017(1)	-2707(1)	1339(1)	60(1)
S(3)	1374(2)	370(1)	3491(1)	69(1)
F(13)	1090(4)	3342(6)	-1409(4)	195(4)
F(12)	132(4)	3966(3)	-1054(5)	160(4)
F(11)	826(4)	3321(4)	-447(3)	123(2)
F(23)	5137(5)	-3308(3)	1994(3)	132(3)
F(22)	5631(3)	-2861(3)	1141(2)	96(2)
F(21)	5339(3)	-2294(3)	1949(2)	86(2)
F(33)	-169(5)	809(5)	3545(3)	175(4)
F(32)	-48(5)	-190(4)	3747(5)	175(4)
F(31)	318(4)	539(4)	4408(2)	114(2)
N(1S)	-1223(7)	953(4)	2058(4)	103(3)
N(2S)	-2880(17)	-1314(13)	1049(12)	362(19)
N(3S)	-2571(14)	-605(10)	2375(14)	253(12)
C(1S)	-1912(7)	984(5)	2243(4)	77(3)
C(2S)	-2772(6)	1018(6)	2481(5)	98(3)
C(3S)	-3539(15)	-1053(9)	1073(7)	171(8)
C(4S)	-4432(10)	-808(9)	1044(9)	173(7)
C(5S)	-1790(20)	-737(7)	2373(9)	188(13)
C(6S)	-1015(9)	-914(6)	2424(7)	107(4)

***Table A.4.2.3** - Bond lengths [Å] and angles [°] for C57 H75 Eu F9 N11 O14 S3.*

Eu(1)-O(4)	2.349(4)	O(13)-S(1)	1.439(6)	N(3)-C(5)	1.491(6)
Eu(1)-O(3)	2.365(4)	O(12)-S(1)	1.428(5)	N(3)-C(4)	1.503(7)
Eu(1)-O(2)	2.384(4)	O(11)-S(1)	1.446(5)	N(4)-C(6)	1.477(8)
Eu(1)-O(1)	2.427(4)	O(23)-S(2)	1.411(5)	N(4)-C(7)	1.485(7)
Eu(1)-O(5)	2.442(4)	O(22)-S(2)	1.499(5)	N(4)-C(41)	1.496(7)
Eu(1)-N(1)	2.641(4)	O(21)-S(2)	1.439(4)	N(5)-C(12)	1.332(7)
Eu(1)-N(4)	2.677(5)	O(33)-S(3)	1.471(7)	N(5)-C(13)	1.477(7)
Eu(1)-N(2)	2.685(4)	O(32)-S(3)	1.417(5)	N(6)-C(22)	1.302(8)
Eu(1)-N(3)	2.710(5)	O(31)-S(3)	1.405(5)	N(6)-C(23)	1.468(8)
Eu(1)-C(42)	3.234(6)	N(1)-C(8)	1.493(7)	N(7)-C(32)	1.334(7)
Eu(1)-C(32)	3.252(6)	N(1)-C(1)	1.499(7)	N(7)-C(33)	1.498(8)
Eu(1)-C(12)	3.263(6)	N(1)-C(11)	1.502(8)	N(8)-C(42)	1.320(7)
O(1)-C(12)	1.231(7)	N(2)-C(21)	1.472(7)	N(8)-C(43)	1.476(7)
O(2)-C(22)	1.275(7)	N(2)-C(3)	1.477(8)	C(1)-C(2)	1.515(8)
O(3)-C(32)	1.253(7)	N(2)-C(2)	1.502(7)	C(3)-C(4)	1.521(8)
O(4)-C(42)	1.260(6)	N(3)-C(31)	1.462(7)	C(5)-C(6)	1.518(8)

C(7)-C(8)	1.533(7)	O(4)-Eu(1)-O(5)	72.88(13)	C(32)-O(3)-Eu(1)	125.2(4)
C(11)-C(12)	1.530(8)	O(3)-Eu(1)-O(5)	70.99(13)	C(42)-O(4)-Eu(1)	124.4(3)
C(13)-C(15)	1.518(9)	O(2)-Eu(1)-O(5)	71.68(13)	C(8)-N(1)-C(1)	108.7(4)
C(13)-C(14)	1.534(8)	O(1)-Eu(1)-O(5)	74.33(13)	C(8)-N(1)-C(11)	110.2(4)
C(15)-C(20)	1.379(9)	O(4)-Eu(1)-N(1)	131.63(12)	C(1)-N(1)-C(11)	107.5(4)
C(15)-C(16)	1.402(9)	O(3)-Eu(1)-N(1)	141.36(13)	C(8)-N(1)-Eu(1)	111.2(3)
C(16)-C(17)	1.395(11)	O(2)-Eu(1)-N(1)	74.62(14)	C(1)-N(1)-Eu(1)	111.6(3)
C(17)-C(18)	1.406(11)	O(1)-Eu(1)-N(1)	66.20(13)	C(11)-N(1)-Eu(1)	107.6(3)
C(18)-C(19)	1.385(10)	O(5)-Eu(1)-N(1)	129.05(13)	C(21)-N(2)-C(3)	109.7(4)
C(19)-C(20)	1.377(10)	O(4)-Eu(1)-N(4)	66.33(13)	C(21)-N(2)-C(2)	109.8(4)
C(21)-C(22)	1.511(9)	O(3)-Eu(1)-N(4)	128.93(14)	C(3)-N(2)-C(2)	108.6(4)
C(23)-C(25)	1.533(11)	O(2)-Eu(1)-N(4)	142.55(14)	C(21)-N(2)-Eu(1)	106.2(3)
C(23)-C(24)	1.538(9)	O(1)-Eu(1)-N(4)	74.10(14)	C(3)-N(2)-Eu(1)	111.8(3)
C(25)-C(30)	1.384(12)	O(5)-Eu(1)-N(4)	129.45(13)	C(2)-N(2)-Eu(1)	110.7(3)
C(25)-C(26)	1.387(12)	N(1)-Eu(1)-N(4)	68.40(14)	C(31)-N(3)-C(5)	109.2(4)
C(26)-C(27)	1.451(19)	O(4)-Eu(1)-N(2)	139.49(14)	C(31)-N(3)-C(4)	110.2(4)
C(27)-C(28)	1.33(2)	O(3)-Eu(1)-N(2)	73.57(13)	C(5)-N(3)-C(4)	108.3(4)
C(28)-C(29)	1.332(18)	O(2)-Eu(1)-N(2)	66.00(14)	C(31)-N(3)-Eu(1)	107.9(3)
C(29)-C(30)	1.380(12)	O(1)-Eu(1)-N(2)	131.35(14)	C(5)-N(3)-Eu(1)	110.7(3)
C(31)-C(32)	1.528(8)	O(5)-Eu(1)-N(2)	126.30(13)	C(4)-N(3)-Eu(1)	110.5(3)
C(33)-C(35)	1.513(9)	N(1)-Eu(1)-N(2)	68.30(13)	C(6)-N(4)-C(7)	108.1(4)
C(33)-C(34)	1.535(8)	N(4)-Eu(1)-N(2)	104.18(13)	C(6)-N(4)-C(41)	110.0(5)
C(35)-C(36)	1.400(9)	O(4)-Eu(1)-N(3)	73.15(14)	C(7)-N(4)-C(41)	109.1(4)
C(35)-C(40)	1.405(9)	O(3)-Eu(1)-N(3)	65.61(13)	C(6)-N(4)-Eu(1)	113.4(3)
C(36)-C(37)	1.416(11)	O(2)-Eu(1)-N(3)	129.88(13)	C(7)-N(4)-Eu(1)	110.9(3)
C(37)-C(38)	1.388(12)	O(1)-Eu(1)-N(3)	140.47(13)	C(41)-N(4)-Eu(1)	105.2(3)
C(38)-C(39)	1.376(12)	O(5)-Eu(1)-N(3)	127.14(13)	C(12)-N(5)-C(13)	122.6(5)
C(39)-C(40)	1.368(10)	N(1)-Eu(1)-N(3)	103.79(13)	C(12)-N(5)-H(5)	118.7
C(41)-C(42)	1.519(8)	N(4)-Eu(1)-N(3)	66.93(14)	C(13)-N(5)-H(5)	118.7
C(43)-C(44)	1.513(8)	N(2)-Eu(1)-N(3)	67.26(14)	C(22)-N(6)-C(23)	122.2(5)
C(43)-C(45)	1.525(9)	O(4)-Eu(1)-C(42)	18.75(13)	C(22)-N(6)-H(6)	118.9
C(45)-C(50)	1.384(9)	O(3)-Eu(1)-C(42)	99.69(15)	C(23)-N(6)-H(6)	118.9
C(45)-C(46)	1.401(9)	O(2)-Eu(1)-C(42)	154.84(15)	C(32)-N(7)-C(33)	120.1(5)
C(46)-C(47)	1.387(10)	O(1)-Eu(1)-C(42)	76.30(14)	C(32)-N(7)-H(7)	120.0
C(47)-C(48)	1.402(12)	O(5)-Eu(1)-C(42)	86.21(14)	C(33)-N(7)-H(7)	120.0
C(48)-C(49)	1.369(13)	N(1)-Eu(1)-C(42)	112.97(14)	C(42)-N(8)-C(43)	123.1(5)
C(49)-C(50)	1.399(10)	N(4)-Eu(1)-C(42)	48.41(14)	C(42)-N(8)-H(8)	118.4
C(100)-F(13)	1.303(11)	N(2)-Eu(1)-C(42)	139.07(15)	C(43)-N(8)-H(8)	118.4
C(100)-F(11)	1.328(12)	N(3)-Eu(1)-C(42)	73.20(14)	N(1)-C(1)-C(2)	111.6(4)
C(100)-F(12)	1.343(13)	O(4)-Eu(1)-C(32)	74.64(14)	N(1)-C(1)-H(1A)	109.3
C(100)-S(1)	1.843(13)	O(3)-Eu(1)-C(32)	18.35(14)	C(2)-C(1)-H(1A)	109.3
C(200)-F(21)	1.305(9)	O(2)-Eu(1)-C(32)	100.74(15)	N(1)-C(1)-H(1B)	109.3
C(200)-F(22)	1.349(10)	O(1)-Eu(1)-C(32)	154.70(14)	C(2)-C(1)-H(1B)	109.3
C(200)-F(23)	1.383(11)	O(5)-Eu(1)-C(32)	84.62(14)	H(1A)-C(1)-H(1B)	108.0
C(200)-S(2)	1.772(9)	N(1)-Eu(1)-C(32)	139.08(13)	N(2)-C(2)-C(1)	113.9(5)
C(300)-F(32)	1.302(12)	N(4)-Eu(1)-C(32)	110.83(16)	N(2)-C(2)-H(2A)	108.8
C(300)-F(31)	1.312(11)	N(2)-Eu(1)-C(32)	72.75(14)	C(1)-C(2)-H(2A)	108.8
C(300)-F(33)	1.312(11)	N(3)-Eu(1)-C(32)	47.80(14)	N(2)-C(2)-H(2B)	108.8
C(300)-S(3)	1.826(12)	C(42)-Eu(1)-C(32)	88.65(14)	C(1)-C(2)-H(2B)	108.8
N(1S)-C(1S)	1.161(13)	O(4)-Eu(1)-C(12)	101.61(14)	H(2A)-C(2)-H(2B)	107.7
N(2S)-C(3S)	1.17(2)	O(3)-Eu(1)-C(12)	156.51(14)	N(2)-C(3)-C(4)	112.5(5)
N(3S)-C(5S)	1.26(3)	O(2)-Eu(1)-C(12)	78.48(15)	N(2)-C(3)-H(3A)	109.1
C(1S)-C(2S)	1.455(14)	O(1)-Eu(1)-C(12)	18.48(14)	C(4)-C(3)-H(3A)	109.1
C(3S)-C(4S)	1.50(2)	O(5)-Eu(1)-C(12)	88.11(14)	N(2)-C(3)-H(3B)	109.1
C(5S)-C(6S)	1.28(3)	N(1)-Eu(1)-C(12)	48.06(14)	C(4)-C(3)-H(3B)	109.1
		N(4)-Eu(1)-C(12)	72.72(15)	H(3A)-C(3)-H(3B)	107.8
O(4)-Eu(1)-O(3)	82.83(14)	N(2)-Eu(1)-C(12)	113.20(14)	N(3)-C(4)-C(3)	111.7(5)
O(4)-Eu(1)-O(2)	144.54(13)	N(3)-Eu(1)-C(12)	137.85(14)	N(3)-C(4)-H(4A)	109.3
O(3)-Eu(1)-O(2)	84.66(14)	C(42)-Eu(1)-C(12)	89.20(15)	C(3)-C(4)-H(4A)	109.3
O(4)-Eu(1)-O(1)	85.69(13)	C(32)-Eu(1)-C(12)	172.54(14)	N(3)-C(4)-H(4B)	109.3
O(3)-Eu(1)-O(1)	145.29(14)	C(12)-O(1)-Eu(1)	122.8(4)	C(3)-C(4)-H(4B)	109.3
O(2)-Eu(1)-O(1)	86.03(14)	C(22)-O(2)-Eu(1)	123.7(4)	H(4A)-C(4)-H(4B)	107.9

N(3)-C(5)-C(6)	112.6(5)	C(18)-C(19)-H(19)	119.3	C(35)-C(33)-H(33)	108.7
N(3)-C(5)-H(5A)	109.1	C(19)-C(20)-C(15)	121.2(6)	C(34)-C(33)-H(33)	108.7
C(6)-C(5)-H(5A)	109.1	C(19)-C(20)-H(20)	119.4	C(33)-C(34)-H(34A)	109.5
N(3)-C(5)-H(5B)	109.1	C(15)-C(20)-H(20)	119.4	C(33)-C(34)-H(34B)	109.5
C(6)-C(5)-H(5B)	109.1	N(2)-C(21)-C(22)	111.2(4)	H(34A)-C(34)-H(34B)	109.5
H(5A)-C(5)-H(5B)	107.8	N(2)-C(21)-H(21A)	109.4	C(33)-C(34)-H(34C)	109.5
N(4)-C(6)-C(5)	113.1(5)	C(22)-C(21)-H(21A)	109.4	H(34A)-C(34)-H(34C)	109.5
N(4)-C(6)-H(6A)	109.0	N(2)-C(21)-H(21B)	109.4	H(34B)-C(34)-H(34C)	109.5
C(5)-C(6)-H(6A)	109.0	C(22)-C(21)-H(21B)	109.4	C(36)-C(35)-C(40)	119.0(7)
N(4)-C(6)-H(6B)	109.0	H(21A)-C(21)-H(21B)	108.0	C(36)-C(35)-C(33)	118.6(6)
C(5)-C(6)-H(6B)	109.0	O(2)-C(22)-N(6)	121.7(6)	C(40)-C(35)-C(33)	122.3(6)
H(6A)-C(6)-H(6B)	107.8	O(2)-C(22)-C(21)	119.1(6)	C(35)-C(36)-C(37)	119.5(7)
N(4)-C(7)-C(8)	111.2(4)	N(6)-C(22)-C(21)	119.1(5)	C(35)-C(36)-H(36)	120.2
N(4)-C(7)-H(7A)	109.4	O(2)-C(22)-Eu(1)	37.4(3)	C(37)-C(36)-H(36)	120.2
C(8)-C(7)-H(7A)	109.4	N(6)-C(22)-Eu(1)	159.0(4)	C(38)-C(37)-C(36)	119.9(8)
N(4)-C(7)-H(7B)	109.4	C(21)-C(22)-Eu(1)	81.9(3)	C(38)-C(37)-H(37)	120.1
C(8)-C(7)-H(7B)	109.4	N(6)-C(23)-C(25)	111.5(6)	C(36)-C(37)-H(37)	120.1
H(7A)-C(7)-H(7B)	108.0	N(6)-C(23)-C(24)	108.3(5)	C(39)-C(38)-C(37)	119.8(8)
N(1)-C(8)-C(7)	113.5(4)	C(25)-C(23)-C(24)	112.5(6)	C(39)-C(38)-H(38)	120.1
N(1)-C(8)-H(8A)	108.9	N(6)-C(23)-H(23)	108.2	C(37)-C(38)-H(38)	120.1
C(7)-C(8)-H(8A)	108.9	C(25)-C(23)-H(23)	108.2	C(40)-C(39)-C(38)	121.4(7)
N(1)-C(8)-H(8B)	108.9	C(24)-C(23)-H(23)	108.2	C(40)-C(39)-H(39)	119.3
C(7)-C(8)-H(8B)	108.9	C(23)-C(24)-H(24A)	109.5	C(38)-C(39)-H(39)	119.3
H(8A)-C(8)-H(8B)	107.7	C(23)-C(24)-H(24B)	109.5	C(39)-C(40)-C(35)	120.4(7)
N(1)-C(11)-C(12)	109.1(5)	H(24A)-C(24)-H(24B)	109.5	C(39)-C(40)-H(40)	119.8
N(1)-C(11)-H(11A)	109.9	C(23)-C(24)-H(24C)	109.5	C(35)-C(40)-H(40)	119.8
C(12)-C(11)-H(11A)	109.9	H(24A)-C(24)-H(24C)	109.5	N(4)-C(41)-C(42)	110.5(4)
N(1)-C(11)-H(11B)	109.9	H(24B)-C(24)-H(24C)	109.5	N(4)-C(41)-H(41A)	109.6
C(12)-C(11)-H(11B)	109.9	C(30)-C(25)-C(26)	121.2(9)	C(42)-C(41)-H(41A)	109.6
H(11A)-C(11)-H(11B)	108.3	C(30)-C(25)-C(23)	121.1(7)	N(4)-C(41)-H(41B)	109.6
O(1)-C(12)-N(5)	124.1(5)	C(26)-C(25)-C(23)	117.6(10)	C(42)-C(41)-H(41B)	109.6
O(1)-C(12)-C(11)	120.5(5)	C(25)-C(26)-C(27)	116.4(13)	H(41A)-C(41)-H(41B)	108.1
N(5)-C(12)-C(11)	115.3(5)	C(25)-C(26)-H(26)	121.8	O(4)-C(42)-N(8)	121.6(5)
O(1)-C(12)-Eu(1)	38.7(3)	C(27)-C(26)-H(26)	121.8	O(4)-C(42)-C(41)	119.4(5)
N(5)-C(12)-Eu(1)	162.2(4)	C(28)-C(27)-C(26)	119.6(14)	N(8)-C(42)-C(41)	118.8(5)
C(11)-C(12)-Eu(1)	82.2(3)	C(28)-C(27)-H(27)	120.2	O(4)-C(42)-Eu(1)	36.8(3)
N(5)-C(13)-C(15)	110.9(5)	C(26)-C(27)-H(27)	120.2	N(8)-C(42)-Eu(1)	158.3(4)
N(5)-C(13)-C(14)	109.0(5)	C(27)-C(28)-C(29)	123.3(16)	C(41)-C(42)-Eu(1)	82.6(3)
C(15)-C(13)-C(14)	112.2(5)	C(27)-C(28)-H(28)	118.3	N(8)-C(43)-C(44)	109.5(5)
N(5)-C(13)-H(13)	108.2	C(29)-C(28)-H(28)	118.4	N(8)-C(43)-C(45)	108.6(5)
C(15)-C(13)-H(13)	108.2	C(28)-C(29)-C(30)	119.9(15)	C(44)-C(43)-C(45)	114.4(5)
C(14)-C(13)-H(13)	108.2	C(28)-C(29)-H(29)	120.0	N(8)-C(43)-H(43)	108.0
C(13)-C(14)-H(14A)	109.5	C(30)-C(29)-H(29)	120.0	C(44)-C(43)-H(43)	108.0
C(13)-C(14)-H(14B)	109.5	C(29)-C(30)-C(25)	119.5(10)	C(45)-C(43)-H(43)	108.0
H(14A)-C(14)-H(14B)	109.5	C(29)-C(30)-H(30)	120.2	C(43)-C(44)-H(44A)	109.5
C(13)-C(14)-H(14C)	109.5	C(25)-C(30)-H(30)	120.2	C(43)-C(44)-H(44B)	109.5
H(14A)-C(14)-H(14C)	109.5	N(3)-C(31)-C(32)	111.1(5)	H(44A)-C(44)-H(44B)	109.5
H(14B)-C(14)-H(14C)	109.5	N(3)-C(31)-H(31A)	109.4	C(43)-C(44)-H(44C)	109.5
C(20)-C(15)-C(16)	118.4(6)	C(32)-C(31)-H(31A)	109.4	H(44A)-C(44)-H(44C)	109.5
C(20)-C(15)-C(13)	121.6(6)	N(3)-C(31)-H(31B)	109.4	H(44B)-C(44)-H(44C)	109.5
C(16)-C(15)-C(13)	120.0(6)	C(32)-C(31)-H(31B)	109.4	C(50)-C(45)-C(46)	118.9(6)
C(17)-C(16)-C(15)	120.8(7)	H(31A)-C(31)-H(31B)	108.0	C(50)-C(45)-C(43)	121.5(5)
C(17)-C(16)-H(16)	119.6	O(3)-C(32)-N(7)	122.7(6)	C(46)-C(45)-C(43)	119.5(6)
C(15)-C(16)-H(16)	119.6	O(3)-C(32)-C(31)	120.7(5)	C(47)-C(46)-C(45)	120.5(7)
C(16)-C(17)-C(18)	119.8(7)	N(7)-C(32)-C(31)	116.4(6)	C(47)-C(46)-H(46)	119.8
C(16)-C(17)-H(17)	120.1	O(3)-C(32)-Eu(1)	36.5(3)	C(45)-C(46)-H(46)	119.8
C(18)-C(17)-H(17)	120.1	N(7)-C(32)-Eu(1)	159.1(5)	C(46)-C(47)-C(48)	119.8(7)
C(19)-C(18)-C(17)	118.4(7)	C(31)-C(32)-Eu(1)	84.3(3)	C(46)-C(47)-H(47)	120.1
C(19)-C(18)-H(18)	120.8	N(7)-C(33)-C(35)	111.0(5)	C(48)-C(47)-H(47)	120.1
C(17)-C(18)-H(18)	120.8	N(7)-C(33)-C(34)	106.4(5)	C(49)-C(48)-C(47)	120.0(8)
C(20)-C(19)-C(18)	121.5(7)	C(35)-C(33)-C(34)	113.2(5)	C(49)-C(48)-H(48)	120.0
C(20)-C(19)-H(19)	119.3	N(7)-C(33)-H(33)	108.7	C(47)-C(48)-H(48)	120.0

C(48)-C(49)-C(50)	120.2(8)	F(21)-C(200)-S(2)	115.5(6)	O(23)-S(2)-O(21)	115.9(3)
C(48)-C(49)-H(49)	119.9	F(22)-C(200)-S(2)	112.3(6)	O(23)-S(2)-O(22)	112.8(3)
C(50)-C(49)-H(49)	119.9	F(23)-C(200)-S(2)	109.2(7)	O(21)-S(2)-O(22)	113.8(3)
C(45)-C(50)-C(49)	120.7(7)	F(32)-C(300)-F(31)	110.6(12)	O(23)-S(2)-C(200)	106.4(4)
C(45)-C(50)-H(50)	119.7	F(32)-C(300)-F(33)	106.6(10)	O(21)-S(2)-C(200)	105.6(4)
C(49)-C(50)-H(50)	119.7	F(31)-C(300)-F(33)	106.5(8)	O(22)-S(2)-C(200)	100.4(4)
F(13)-C(100)-F(11)	108.7(9)	F(32)-C(300)-S(3)	109.9(8)	O(31)-S(3)-O(32)	116.7(4)
F(13)-C(100)-F(12)	106.7(9)	F(31)-C(300)-S(3)	112.4(8)	O(31)-S(3)-O(33)	111.5(4)
F(11)-C(100)-F(12)	108.1(12)	F(33)-C(300)-S(3)	110.6(9)	O(32)-S(3)-O(33)	114.2(5)
F(13)-C(100)-S(1)	111.4(11)	O(12)-S(1)-O(13)	116.2(4)	O(31)-S(3)-C(300)	103.5(4)
F(11)-C(100)-S(1)	111.2(7)	O(12)-S(1)-O(11)	114.6(3)	O(32)-S(3)-C(300)	105.3(5)
F(12)-C(100)-S(1)	110.5(7)	O(13)-S(1)-O(11)	114.4(4)	O(33)-S(3)-C(300)	103.9(5)
F(21)-C(200)-F(22)	108.6(8)	O(12)-S(1)-C(100)	104.1(5)	N(1S)-C(1S)-C(2S)	179.2(13)
F(21)-C(200)-F(23)	102.4(7)	O(13)-S(1)-C(100)	103.6(5)	N(2S)-C(3S)-C(4S)	171(3)
F(22)-C(200)-F(23)	108.1(7)	O(11)-S(1)-C(100)	101.4(4)	N(3S)-C(5S)-C(6S)	173(3)

***Table A.4.2.4** - Anisotropic displacement parameters ($Å^2 x\ 10^3$) for C57H75EuF9N11O14S3. The anisotropic displacement factor exponent takes the form: $-2\pi^2[h^2 a^{*2} U^{11} + ... + 2 h k a^* b^* U^{12}]$*

	U^{11}	U^{22}	U^{33}	U^{23}	U^{13}	U^{12}
Eu(1)	37(1)	25(1)	28(1)	0(1)	1(1)	-1(1)
O(1)	43(2)	33(2)	34(2)	-1(2)	-3(2)	-5(2)
O(2)	48(3)	32(2)	38(2)	5(2)	3(2)	1(2)
O(3)	37(3)	30(2)	36(2)	-8(2)	2(2)	-2(2)
O(4)	45(3)	27(2)	30(2)	0(2)	-5(2)	4(2)
O(5)	44(2)	37(2)	36(2)	2(2)	5(2)	-9(2)
O(13)	166(7)	136(6)	62(3)	-7(4)	-13(4)	120(6)
O(12)	92(5)	145(6)	53(3)	28(4)	4(3)	70(4)
O(11)	86(4)	50(3)	62(3)	7(2)	25(3)	13(3)
O(23)	78(4)	85(3)	84(4)	-35(3)	18(3)	-3(3)
O(22)	91(4)	68(3)	71(4)	26(3)	5(3)	12(3)
O(21)	72(3)	42(2)	44(2)	-5(2)	12(2)	14(2)
O(33)	177(8)	54(4)	115(5)	-8(4)	26(5)	-9(4)
O(32)	160(6)	176(7)	42(3)	-39(3)	-38(4)	103(6)
O(31)	77(3)	77(4)	54(3)	4(3)	-17(2)	28(3)
N(1)	41(3)	25(2)	33(2)	3(2)	0(2)	-1(2)
N(2)	38(3)	23(2)	35(2)	0(2)	2(2)	0(2)
N(3)	39(3)	27(2)	33(3)	1(2)	1(2)	0(2)
N(4)	43(3)	28(2)	27(2)	1(2)	-1(2)	-1(2)
N(5)	49(4)	32(3)	34(3)	1(2)	-5(2)	-8(2)
N(6)	36(3)	36(3)	50(3)	6(2)	0(2)	4(2)
N(7)	41(3)	36(3)	39(3)	-8(2)	-3(2)	-8(2)
N(8)	43(3)	28(2)	33(3)	-3(2)	-2(2)	4(2)
C(1)	47(4)	30(3)	34(3)	-3(2)	-4(2)	-2(3)
C(2)	49(4)	33(3)	28(3)	4(2)	2(3)	1(3)
C(3)	39(4)	29(3)	36(3)	5(2)	0(3)	2(3)
C(4)	35(4)	36(3)	40(3)	5(2)	4(3)	-1(3)
C(5)	36(3)	31(3)	38(3)	1(2)	3(2)	2(2)
C(6)	42(4)	37(3)	37(3)	1(2)	2(3)	-1(3)
C(7)	48(4)	30(3)	31(3)	-3(2)	0(3)	1(3)
C(8)	54(5)	29(3)	31(3)	0(2)	-2(3)	0(3)
C(11)	50(4)	33(3)	39(3)	1(2)	-2(3)	1(3)
C(12)	38(4)	31(3)	34(3)	-5(2)	1(3)	-5(3)
C(13)	65(4)	37(3)	31(3)	3(2)	0(3)	-17(3)
C(14)	59(5)	53(4)	56(4)	5(3)	-3(3)	-17(3)
C(15)	60(4)	29(3)	38(3)	2(3)	-6(3)	-12(2)
C(16)	75(5)	39(3)	43(4)	10(3)	0(3)	-11(3)

C(17)	80(6)	52(4)	66(5)	26(3)	-26(5)	-11(5)
C(18)	69(6)	33(3)	89(6)	9(3)	-10(5)	0(3)
C(19)	74(5)	40(3)	67(4)	-1(3)	3(4)	8(4)
C(20)	64(5)	36(3)	47(4)	0(3)	-3(3)	2(3)
C(21)	43(4)	26(3)	41(3)	3(2)	1(2)	-1(2)
C(22)	43(4)	36(3)	35(3)	4(3)	-1(3)	2(3)
C(23)	41(4)	47(4)	67(4)	13(3)	6(3)	4(3)
C(24)	43(4)	51(4)	88(6)	1(4)	6(4)	9(3)
C(25)	46(5)	34(4)	127(8)	-4(4)	4(5)	3(3)
C(26)	90(8)	62(6)	200(13)	-18(7)	41(8)	-26(5)
C(27)	112(11)	78(8)	310(20)	-41(13)	73(14)	-55(8)
C(28)	80(8)	109(10)	300(20)	-61(17)	31(13)	-53(8)
C(29)	70(7)	105(8)	161(12)	-48(8)	-31(7)	5(6)
C(30)	51(5)	64(5)	107(7)	-16(5)	-24(5)	9(4)
C(31)	39(4)	32(3)	37(3)	-1(2)	-1(3)	-2(3)
C(32)	48(4)	25(3)	31(3)	0(2)	4(3)	-4(3)
C(33)	48(4)	40(3)	41(3)	-7(3)	3(3)	-8(3)
C(34)	68(5)	53(4)	45(4)	-19(3)	-1(3)	0(4)
C(35)	45(4)	43(3)	40(3)	-10(3)	5(3)	2(3)
C(36)	48(4)	56(4)	59(4)	-20(3)	10(3)	2(3)
C(37)	50(5)	79(6)	80(6)	-32(5)	1(4)	13(4)
C(38)	84(7)	57(5)	67(5)	-6(4)	-13(4)	24(4)
C(39)	74(6)	45(3)	66(4)	-3(3)	0(4)	4(4)
C(40)	61(5)	44(4)	52(4)	-4(3)	0(3)	-10(3)
C(41)	54(4)	26(2)	29(3)	-1(2)	-4(3)	-1(2)
C(42)	42(4)	29(3)	29(3)	4(2)	2(3)	1(3)
C(43)	47(4)	36(3)	28(3)	-5(2)	-2(3)	-1(3)
C(44)	68(5)	48(4)	32(3)	4(3)	-5(3)	-11(3)
C(45)	51(4)	44(3)	30(3)	-2(3)	-4(3)	-2(3)
C(46)	84(5)	40(3)	38(3)	5(3)	-13(3)	-9(4)
C(47)	124(8)	58(5)	42(4)	8(3)	-18(4)	-43(5)
C(48)	78(6)	110(8)	54(4)	5(5)	-1(4)	-48(6)
C(49)	40(5)	101(7)	68(5)	-22(5)	-1(4)	-7(5)
C(50)	56(5)	61(4)	53(4)	-18(3)	7(3)	0(4)
C(100)	60(6)	168(11)	106(9)	77(8)	24(6)	34(7)
C(200)	84(7)	83(6)	68(5)	-26(5)	-5(5)	28(5)
C(300)	78(7)	79(6)	116(9)	-18(6)	-18(6)	27(6)
S(1)	84(2)	89(2)	49(1)	17(1)	10(1)	53(1)
S(2)	66(1)	68(1)	47(1)	-11(1)	8(1)	9(1)
S(3)	105(2)	66(1)	35(1)	-6(1)	-7(1)	35(1)
F(13)	67(4)	368(13)	151(6)	130(7)	31(5)	33(6)
F(12)	64(4)	123(5)	291(11)	104(6)	-41(5)	-28(4)
F(11)	70(4)	174(6)	124(5)	37(5)	-8(3)	18(4)
F(23)	195(7)	82(4)	118(5)	6(3)	-45(5)	65(4)
F(22)	66(3)	131(5)	92(4)	-42(3)	3(3)	32(3)
F(21)	81(3)	94(4)	82(3)	-33(3)	-20(3)	19(3)
F(33)	171(7)	242(9)	112(5)	-45(5)	-45(5)	155(7)
F(32)	117(6)	131(6)	277(11)	-52(7)	-17(6)	-41(5)
F(31)	84(4)	201(7)	58(3)	-22(4)	8(3)	24(4)
N(1S)	95(7)	120(7)	94(6)	-7(5)	7(6)	9(7)
N(2S)	390(30)	390(30)	310(30)	0(20)	-20(20)	290(30)
N(3S)	240(20)	145(15)	380(30)	-3(16)	-30(20)	-30(15)
C(1S)	96(8)	83(6)	53(5)	-22(4)	6(5)	0(6)
C(2S)	71(7)	125(9)	98(7)	-19(6)	-1(6)	23(6)
C(3S)	260(30)	143(13)	110(11)	8(9)	-17(13)	52(15)
C(4S)	124(12)	186(15)	207(18)	36(13)	46(12)	69(11)
C(5S)	360(40)	63(9)	143(14)	9(9)	-80(20)	-47(17)
C(6S)	120(11)	84(8)	119(10)	38(7)	13(8)	-22(7)

***Table A.4.2.5** - Hydrogen coordinates (x 10^4) and isotropic displacement parameters ($Å^2$x 10^3) for C57 H75 Eu F9 N11 O14 S3.*

	x	y	z	U(eq)
H(5)	-885	-1592	-90	46
H(6)	-605	2027	72	49
H(7)	3165	1725	1980	46
H(8)	2748	-1815	1909	42
H(1A)	89	621	-545	44
H(1B)	587	265	-1091	44
H(2A)	1885	643	-713	44
H(2B)	1268	1252	-827	44
H(3A)	2391	1613	519	42
H(3B)	2499	1605	-212	42
H(4A)	2996	511	-168	44
H(4B)	3587	981	236	44
H(5A)	3415	-461	1099	42
H(5B)	3936	-137	548	42
H(6A)	2958	-533	-169	46
H(6B)	3313	-1131	230	46
H(7A)	1190	-1476	-7	44
H(7B)	2080	-1472	-361	44
H(8A)	1829	-392	-711	45
H(8B)	1073	-860	-927	45
H(11A)	-242	-787	-610	49
H(11B)	-587	-194	-196	49
H(13)	-914	-1753	1146	53
H(14A)	-2025	-2207	599	84
H(14B)	-1529	-2810	902	84
H(14C)	-1398	-2642	190	84
H(16)	74	-2208	1818	63
H(17)	1328	-2779	2026	79
H(18)	2058	-3313	1219	76
H(19)	1504	-3255	226	73
H(20)	281	-2674	22	58
H(21A)	821	1899	-114	44
H(21B)	1089	1849	594	44
H(23)	-1489	1238	853	62
H(24A)	-1890	2347	727	91
H(24B)	-2676	1881	567	91
H(24C)	-2139	2211	26	91
H(26)	-2301	306	682	141
H(27)	-2834	-518	-24	201
H(28)	-2613	-398	-1044	196
H(29)	-1943	481	-1446	134
H(30)	-1422	1302	-804	89
H(31A)	3614	988	1223	43
H(31B)	3297	381	1629	43
H(33)	1595	1674	2512	52
H(34A)	2030	2639	3024	83
H(34B)	2794	2733	2549	83
H(34C)	2799	2128	3016	83
H(36)	293	2005	2158	65
H(37)	-583	2636	1501	84
H(38)	27	3400	832	83
H(39)	1486	3533	811	73
H(40)	2358	2919	1435	63
H(41A)	2572	-1723	847	44
H(41B)	1562	-1669	906	44
H(43)	2160	-839	2685	45
H(44A)	2451	-1542	3489	74

H(44B)	2971	-2025	3050	74
H(44C)	1966	-1954	2973	74
H(46)	2973	110	2710	65
H(47)	4265	667	2720	89
H(48)	5545	74	2710	97
H(49)	5519	-1061	2723	84
H(50)	4224	-1621	2681	68

***Table A.4.3.2** - Atomic coordinates (x 10^4) and equivalent isotropic displacement parameters ($Å^2$x 10^3)for C57 H75 Dy F9 N11 O14 S3. U(eq) is defined as one third of the trace of the orthogonalized U^{ij} tensor.*

	x	y	z	U(eq)
Dy(1)	6201(1)	5088(1)	10835(1)	27(1)
O(1)	5001(3)	5735(2)	10640(2)	34(1)
O(2)	6623(3)	5975(2)	11438(2)	34(1)
O(3)	6891(3)	4490(2)	11587(2)	31(1)
O(4)	5257(2)	4174(2)	10782(2)	34(1)
O(5)	5339(2)	5123(2)	11757(2)	35(1)
N(1)	6498(3)	6084(2)	10074(2)	29(1)
N(2)	7853(3)	5371(2)	10741(2)	31(1)
N(3)	7098(3)	4093(2)	10394(2)	29(1)
N(4)	5742(3)	4805(2)	9713(2)	31(1)
N(5)	4342(3)	6632(3)	10269(3)	41(1)
N(6)	7585(3)	6611(3)	11934(2)	38(1)
N(7)	7544(3)	3594(2)	11967(2)	33(1)
N(8)	4382(3)	3485(3)	10258(2)	37(1)
C(7)	5642(4)	5404(3)	9330(3)	34(1)
C(8)	6377(4)	5869(3)	9421(3)	35(1)
C(1)	7364(4)	6355(3)	10144(3)	33(1)
C(2)	8012(4)	5804(3)	10195(3)	34(1)
C(3)	8370(4)	4766(3)	10680(3)	34(1)
C(4)	7984(4)	4285(3)	10227(3)	34(1)
C(5)	6683(4)	3811(3)	9838(3)	33(1)
C(6)	6358(4)	4353(3)	9410(2)	35(1)
C(11)	5873(4)	6596(3)	10232(3)	34(1)
C(12)	5029(4)	6288(3)	10388(3)	32(1)
C(13)	3489(4)	6376(4)	10438(4)	51(2)
C(14)	2890(4)	6972(4)	10467(4)	61(2)
C(15)	3193(5)	5847(4)	10000(5)	68(3)
C(16)	2785(8)	5309(5)	10238(7)	115(4)
C(17)	2471(11)	4830(10)	9806(11)	182(10)
C(18)	2605(9)	4896(9)	9213(12)	177(9)
C(19)	2998(7)	5422(6)	8979(7)	114(5)
C(20)	3291(5)	5910(5)	9373(5)	74(3)
C(21)	8099(4)	5716(3)	11302(3)	33(1)
C(22)	7376(4)	6131(3)	11564(3)	30(1)
C(23)	6925(4)	6988(3)	12276(3)	42(2)
C(24)	7373(5)	7396(4)	12760(3)	53(2)
C(25)	6388(4)	7400(3)	11840(3)	41(2)
C(26)	5508(4)	7324(4)	11861(4)	52(2)
C(27)	5006(5)	7718(5)	11467(4)	69(2)
C(28)	5375(6)	8167(4)	11073(4)	66(2)
C(29)	6245(6)	8237(4)	11065(3)	58(2)
C(30)	6740(5)	7851(4)	11442(3)	51(2)
C(31)	7117(4)	3592(3)	10893(3)	31(1)
C(32)	7188(4)	3925(3)	11515(3)	31(1)
C(33)	7610(4)	3856(3)	12598(2)	34(1)
C(34)	7473(5)	3297(4)	13053(3)	46(2)
C(35)	8464(4)	4215(3)	12667(3)	38(1)
C(36)	9214(4)	3867(4)	12677(3)	52(2)
C(37)	9995(5)	4195(5)	12703(4)	68(3)
C(38)	9997(6)	4873(6)	12702(3)	75(3)
C(39)	9259(6)	5226(4)	12704(3)	61(2)
C(40)	8476(5)	4885(4)	12694(3)	51(2)
C(41)	4886(4)	4472(3)	9752(3)	37(1)
C(42)	4863(4)	4027(3)	10311(3)	30(1)
C(43)	4273(4)	3011(3)	10761(3)	40(1)
C(44)	3541(5)	2553(4)	10598(3)	55(2)
C(45)	5080(4)	2637(3)	10887(3)	42(1)

C(46)	5511(5)	2308(4)	10425(3)	50(2)
C(47)	6262(5)	1970(3)	10554(4)	56(2)
C(48)	6565(5)	1927(4)	11141(4)	60(2)
C(49)	6143(6)	2253(4)	11622(4)	60(2)
C(50)	5401(5)	2599(4)	11491(3)	50(2)
C(100)	439(6)	6697(7)	11036(5)	108(5)
C(200)	4699(6)	10396(5)	11195(5)	75(3)
C(300)	5085(6)	2766(5)	8377(4)	80(3)
S(1)	-377(1)	7324(1)	11139(1)	68(1)
S(2)	3639(2)	10368(1)	11525(1)	63(1)
S(3)	4024(1)	2700(1)	8659(1)	58(1)
F(11)	1043(4)	6749(6)	11460(4)	190(5)
F(12)	123(4)	6092(4)	11092(5)	152(4)
F(13)	808(4)	6742(4)	10485(3)	120(2)
F(21)	5084(4)	9840(5)	11278(5)	164(4)
F(22)	5174(5)	10832(5)	11480(3)	149(4)
F(23)	4698(4)	10546(4)	10613(3)	107(2)
F(31)	5123(5)	3297(3)	7991(3)	132(3)
F(32)	5640(3)	2858(3)	8838(3)	92(2)
F(33)	5348(3)	2277(3)	8048(2)	83(2)
O(11)	91(5)	7935(4)	11133(3)	100(3)
O(12)	-769(4)	7151(4)	11707(3)	92(2)
O(13)	-891(4)	7216(3)	10603(2)	62(1)
O(21)	3274(5)	11011(3)	11365(3)	95(2)
O(22)	3768(5)	10266(4)	12163(2)	108(3)
O(23)	3238(3)	9848(3)	11201(2)	64(1)
O(31)	4105(4)	2099(3)	9056(3)	71(2)
O(32)	3510(3)	2604(2)	8120(2)	53(1)
O(33)	3862(4)	3274(3)	9005(3)	82(2)
N(1S)	2343(11)	4416(10)	12357(13)	252(12)
N(2S)	7110(20)	1365(16)	8963(13)	400(20)
N(3S)	3812(6)	5941(4)	12046(4)	91(2)
C(1S)	3078(14)	4296(7)	12378(7)	128(6)
C(2S)	3950(8)	4109(5)	12415(6)	93(3)
C(3S)	6495(19)	1068(10)	8936(8)	184(9)
C(4S)	5595(10)	789(10)	8949(8)	161(7)
C(5S)	3141(7)	5992(5)	12228(4)	73(3)
C(6S)	2278(7)	6051(6)	12458(5)	101(4)

Table A.4.3.3 - Bond lengths [Å] and angles [°] for C57 H75 Dy F9 N11 O14 S3.

Dy(1)-O(3)	2.308(4)	N(3)-C(31)	1.486(7)	C(13)-C(15)	1.509(12)
Dy(1)-O(2)	2.325(4)	N(3)-C(5)	1.489(7)	C(13)-C(14)	1.536(10)
Dy(1)-O(1)	2.342(4)	N(3)-C(4)	1.495(8)	C(15)-C(16)	1.371(13)
Dy(1)-O(4)	2.382(4)	N(4)-C(7)	1.481(7)	C(15)-C(20)	1.378(13)
Dy(1)-O(5)	2.422(3)	N(4)-C(6)	1.490(7)	C(16)-C(17)	1.44(2)
Dy(1)-N(4)	2.609(4)	N(4)-C(41)	1.512(7)	C(17)-C(18)	1.31(3)
Dy(1)-N(3)	2.647(5)	N(5)-C(12)	1.314(8)	C(18)-C(19)	1.34(2)
Dy(1)-N(1)	2.656(5)	N(5)-C(13)	1.489(8)	C(19)-C(20)	1.389(14)
Dy(1)-N(2)	2.676(4)	N(6)-C(22)	1.307(8)	C(21)-C(22)	1.528(8)
O(1)-C(12)	1.251(7)	N(6)-C(23)	1.491(8)	C(23)-C(24)	1.514(9)
O(2)-C(22)	1.260(7)	N(7)-C(32)	1.316(7)	C(23)-C(25)	1.521(9)
O(3)-C(32)	1.249(7)	N(7)-C(33)	1.476(7)	C(25)-C(30)	1.376(10)
O(4)-C(42)	1.234(7)	N(8)-C(42)	1.343(8)	C(25)-C(26)	1.397(9)
N(1)-C(11)	1.475(7)	N(8)-C(43)	1.467(8)	C(26)-C(27)	1.416(11)
N(1)-C(1)	1.480(8)	C(7)-C(8)	1.509(8)	C(27)-C(28)	1.378(12)
N(1)-C(8)	1.496(7)	C(1)-C(2)	1.519(9)	C(28)-C(29)	1.380(12)
N(2)-C(21)	1.458(7)	C(3)-C(4)	1.514(8)	C(29)-C(30)	1.377(10)
N(2)-C(3)	1.479(7)	C(5)-C(6)	1.529(8)	C(31)-C(32)	1.516(8)
N(2)-C(2)	1.499(7)	C(11)-C(12)	1.509(8)	C(33)-C(34)	1.521(9)

C(33)-C(35)	1.539(9)	O(4)-Dy(1)-N(3)	73.82(14)	C(8)-C(7)-H(7B)	109.4
C(35)-C(40)	1.362(10)	O(5)-Dy(1)-N(3)	128.49(14)	H(7A)-C(7)-H(7B)	108.0
C(35)-C(36)	1.377(9)	N(4)-Dy(1)-N(3)	68.99(15)	N(1)-C(8)-C(7)	113.9(5)
C(36)-C(37)	1.402(11)	O(3)-Dy(1)-N(1)	139.36(14)	N(1)-C(8)-H(8A)	108.8
C(37)-C(38)	1.378(14)	O(2)-Dy(1)-N(1)	73.18(14)	C(7)-C(8)-H(8A)	108.8
C(38)-C(39)	1.367(13)	O(1)-Dy(1)-N(1)	66.55(14)	N(1)-C(8)-H(8B)	108.8
C(39)-C(40)	1.415(10)	O(4)-Dy(1)-N(1)	132.35(14)	C(7)-C(8)-H(8B)	108.8
C(41)-C(42)	1.514(8)	O(5)-Dy(1)-N(1)	126.31(14)	H(8A)-C(8)-H(8B)	107.7
C(43)-C(45)	1.507(9)	N(4)-Dy(1)-N(1)	68.51(14)	N(1)-C(1)-C(2)	110.8(5)
C(43)-C(44)	1.525(9)	N(3)-Dy(1)-N(1)	105.15(14)	N(1)-C(1)-H(1A)	109.5
C(45)-C(46)	1.384(10)	O(3)-Dy(1)-N(2)	73.02(14)	C(2)-C(1)-H(1A)	109.5
C(45)-C(50)	1.408(9)	O(2)-Dy(1)-N(2)	66.33(14)	N(1)-C(1)-H(1B)	109.5
C(46)-C(47)	1.398(11)	O(1)-Dy(1)-N(2)	130.70(15)	C(2)-C(1)-H(1B)	109.5
C(47)-C(48)	1.364(11)	O(4)-Dy(1)-N(2)	140.51(14)	H(1A)-C(1)-H(1B)	108.1
C(48)-C(49)	1.405(12)	O(5)-Dy(1)-N(2)	127.14(13)	N(2)-C(2)-C(1)	112.2(5)
C(49)-C(50)	1.394(11)	N(4)-Dy(1)-N(2)	104.22(14)	N(2)-C(2)-H(2A)	109.2
C(100)-F(11)	1.329(12)	N(3)-Dy(1)-N(2)	67.38(14)	C(1)-C(2)-H(2A)	109.2
C(100)-F(12)	1.330(13)	N(1)-Dy(1)-N(2)	67.48(14)	N(2)-C(2)-H(2B)	109.2
C(100)-F(13)	1.334(13)	C(12)-O(1)-Dy(1)	123.7(4)	C(1)-C(2)-H(2B)	109.2
C(100)-S(1)	1.824(14)	C(22)-O(2)-Dy(1)	125.9(4)	H(2A)-C(2)-H(2B)	107.9
C(200)-F(21)	1.293(12)	C(32)-O(3)-Dy(1)	124.9(4)	N(2)-C(3)-C(4)	112.0(5)
C(200)-F(23)	1.302(10)	C(42)-O(4)-Dy(1)	122.9(4)	N(2)-C(3)-H(3A)	109.2
C(200)-F(22)	1.315(11)	C(11)-N(1)-C(1)	109.3(5)	C(4)-C(3)-H(3A)	109.2
C(200)-S(2)	1.819(10)	C(11)-N(1)-C(8)	110.0(4)	N(2)-C(3)-H(3B)	109.2
C(300)-F(33)	1.291(10)	C(1)-N(1)-C(8)	108.9(4)	C(4)-C(3)-H(3B)	109.2
C(300)-F(32)	1.343(10)	C(11)-N(1)-Dy(1)	105.9(3)	H(3A)-C(3)-H(3B)	107.9
C(300)-F(31)	1.367(12)	C(1)-N(1)-Dy(1)	112.4(3)	N(3)-C(4)-C(3)	112.7(5)
C(300)-S(3)	1.787(10)	C(8)-N(1)-Dy(1)	110.3(3)	N(3)-C(4)-H(4A)	109.1
S(1)-O(12)	1.424(6)	C(21)-N(2)-C(3)	109.2(4)	C(3)-C(4)-H(4A)	109.1
S(1)-O(13)	1.437(5)	C(21)-N(2)-C(2)	109.6(4)	N(3)-C(4)-H(4B)	109.1
S(1)-O(11)	1.443(6)	C(3)-N(2)-C(2)	108.9(4)	C(3)-C(4)-H(4B)	109.1
S(2)-O(22)	1.417(5)	C(21)-N(2)-Dy(1)	107.3(3)	H(4A)-C(4)-H(4B)	107.8
S(2)-O(23)	1.419(5)	C(3)-N(2)-Dy(1)	111.4(3)	N(3)-C(5)-C(6)	111.3(5)
S(2)-O(21)	1.468(7)	C(2)-N(2)-Dy(1)	110.4(3)	N(3)-C(5)-H(5A)	109.4
S(3)-O(33)	1.412(6)	C(31)-N(3)-C(5)	109.7(4)	C(6)-C(5)-H(5A)	109.4
S(3)-O(32)	1.437(5)	C(31)-N(3)-C(4)	109.7(4)	N(3)-C(5)-H(5B)	109.4
S(3)-O(31)	1.501(6)	C(5)-N(3)-C(4)	108.3(5)	C(6)-C(5)-H(5B)	109.4
N(1S)-C(1S)	1.19(2)	C(31)-N(3)-Dy(1)	105.6(3)	H(5A)-C(5)-H(5B)	108.0
N(2S)-C(3S)	1.14(3)	C(5)-N(3)-Dy(1)	110.7(3)	N(4)-C(6)-C(5)	113.2(4)
N(3S)-C(5S)	1.135(13)	C(4)-N(3)-Dy(1)	112.8(3)	N(4)-C(6)-H(6A)	108.9
C(1S)-C(2S)	1.43(2)	C(7)-N(4)-C(6)	109.1(4)	C(5)-C(6)-H(6A)	108.9
C(3S)-C(4S)	1.53(3)	C(7)-N(4)-C(41)	107.7(4)	N(4)-C(6)-H(6B)	108.9
C(5S)-C(6S)	1.454(14)	C(6)-N(4)-C(41)	109.3(5)	C(5)-C(6)-H(6B)	108.9
		C(7)-N(4)-Dy(1)	112.0(3)	H(6A)-C(6)-H(6B)	107.7
O(3)-Dy(1)-O(2)	82.79(15)	C(6)-N(4)-Dy(1)	111.5(3)	N(1)-C(11)-C(12)	110.4(5)
O(3)-Dy(1)-O(1)	143.56(14)	C(41)-N(4)-Dy(1)	107.0(3)	N(1)-C(11)-H(11A)	109.6
O(2)-Dy(1)-O(1)	84.15(15)	C(12)-N(5)-C(13)	120.7(5)	C(12)-C(11)-H(11A)	109.6
O(3)-Dy(1)-O(4)	85.32(14)	C(12)-N(5)-H(5)	119.6	N(1)-C(11)-H(11B)	109.6
O(2)-Dy(1)-O(4)	144.08(14)	C(13)-N(5)-H(5)	119.6	C(12)-C(11)-H(11B)	109.6
O(1)-Dy(1)-O(4)	85.65(15)	C(22)-N(6)-C(23)	120.9(5)	H(11A)-C(11)-H(11B)	108.1
O(3)-Dy(1)-O(5)	72.26(13)	C(22)-N(6)-H(6)	119.5	O(1)-C(12)-N(5)	122.3(6)
O(2)-Dy(1)-O(5)	70.83(14)	C(23)-N(6)-H(6)	119.5	O(1)-C(12)-C(11)	120.1(5)
O(1)-Dy(1)-O(5)	71.33(13)	C(32)-N(7)-C(33)	122.7(5)	N(5)-C(12)-C(11)	117.5(5)
O(4)-Dy(1)-O(5)	73.28(14)	C(32)-N(7)-H(7)	118.7	N(5)-C(13)-C(15)	111.8(6)
O(3)-Dy(1)-N(4)	132.57(14)	C(33)-N(7)-H(7)	118.7	N(5)-C(13)-C(14)	106.9(6)
O(2)-Dy(1)-N(4)	140.99(14)	C(42)-N(8)-C(43)	122.7(5)	C(15)-C(13)-C(14)	113.4(6)
O(1)-Dy(1)-N(4)	74.34(15)	C(42)-N(8)-H(8)	118.7	N(5)-C(13)-H(13)	108.2
O(4)-Dy(1)-N(4)	67.04(14)	C(43)-N(8)-H(8)	118.7	C(15)-C(13)-H(13)	108.2
O(5)-Dy(1)-N(4)	128.62(13)	N(4)-C(7)-C(8)	111.0(4)	C(14)-C(13)-H(13)	108.2
O(3)-Dy(1)-N(3)	66.56(13)	N(4)-C(7)-H(7A)	109.4	C(13)-C(14)-H(14A)	109.5
O(2)-Dy(1)-N(3)	130.02(14)	C(8)-C(7)-H(7A)	109.4	C(13)-C(14)-H(14B)	109.5
O(1)-Dy(1)-N(3)	142.62(14)	N(4)-C(7)-H(7B)	109.4	H(14A)-C(14)-H(14B)	109.5

C(13)-C(14)-H(14C)	109.5	C(32)-C(31)-H(31A)	109.6	C(45)-C(46)-H(46)	119.7
H(14A)-C(14)-H(14C)	109.5	N(3)-C(31)-H(31B)	109.6	C(47)-C(46)-H(46)	119.7
H(14B)-C(14)-H(14C)	109.5	C(32)-C(31)-H(31B)	109.6	C(48)-C(47)-C(46)	121.0(7)
C(16)-C(15)-C(20)	120.0(10)	H(31A)-C(31)-H(31B)	108.1	C(48)-C(47)-H(47)	119.5
C(16)-C(15)-C(13)	118.4(10)	O(3)-C(32)-N(7)	122.4(6)	C(46)-C(47)-H(47)	119.5
C(20)-C(15)-C(13)	121.6(8)	O(3)-C(32)-C(31)	119.6(5)	C(47)-C(48)-C(49)	120.0(7)
C(15)-C(16)-C(17)	117.1(14)	N(7)-C(32)-C(31)	118.0(5)	C(47)-C(48)-H(48)	120.0
C(15)-C(16)-H(16)	121.4	N(7)-C(33)-C(34)	108.9(5)	C(49)-C(48)-H(48)	120.0
C(17)-C(16)-H(16)	121.4	N(7)-C(33)-C(35)	108.8(5)	C(50)-C(49)-C(48)	118.9(7)
C(18)-C(17)-C(16)	121.0(16)	C(34)-C(33)-C(35)	114.5(5)	C(50)-C(49)-H(49)	120.6
C(18)-C(17)-H(17)	119.5	N(7)-C(33)-H(33)	108.1	C(48)-C(49)-H(49)	120.6
C(16)-C(17)-H(17)	119.5	C(34)-C(33)-H(33)	108.1	C(49)-C(50)-C(45)	121.3(7)
C(17)-C(18)-C(19)	122.0(17)	C(35)-C(33)-H(33)	108.1	C(49)-C(50)-H(50)	119.3
C(17)-C(18)-H(18)	119.0	C(33)-C(34)-H(34A)	109.5	C(45)-C(50)-H(50)	119.3
C(19)-C(18)-H(18)	119.0	C(33)-C(34)-H(34B)	109.5	F(11)-C(100)-F(12)	106.2(9)
C(18)-C(19)-C(20)	119.4(16)	H(34A)-C(34)-H(34B)	109.5	F(11)-C(100)-F(13)	107.7(8)
C(18)-C(19)-H(19)	120.3	C(33)-C(34)-H(34C)	109.5	F(12)-C(100)-F(13)	108.0(13)
C(20)-C(19)-H(19)	120.3	H(34A)-C(34)-H(34C)	109.5	F(11)-C(100)-S(1)	111.3(11)
C(15)-C(20)-C(19)	120.4(11)	H(34B)-C(34)-H(34C)	109.5	F(12)-C(100)-S(1)	111.7(7)
C(15)-C(20)-H(20)	119.8	C(40)-C(35)-C(36)	120.0(6)	F(13)-C(100)-S(1)	111.7(7)
C(19)-C(20)-H(20)	119.8	C(40)-C(35)-C(33)	119.3(6)	F(21)-C(200)-F(23)	109.9(11)
N(2)-C(21)-C(22)	112.3(5)	C(36)-C(35)-C(33)	120.6(6)	F(21)-C(200)-F(22)	104.9(9)
N(2)-C(21)-H(21A)	109.1	C(35)-C(36)-C(37)	120.7(8)	F(23)-C(200)-F(22)	107.4(8)
C(22)-C(21)-H(21A)	109.1	C(35)-C(36)-H(36)	119.6	F(21)-C(200)-S(2)	110.5(7)
N(2)-C(21)-H(21B)	109.1	C(37)-C(36)-H(36)	119.6	F(23)-C(200)-S(2)	112.8(7)
C(22)-C(21)-H(21B)	109.1	C(38)-C(37)-C(36)	118.5(9)	F(22)-C(200)-S(2)	111.0(8)
H(21A)-C(21)-H(21B)	107.9	C(38)-C(37)-H(37)	120.7	F(33)-C(300)-F(32)	108.1(9)
O(2)-C(22)-N(6)	124.0(6)	C(36)-C(37)-H(37)	120.8	F(33)-C(300)-F(31)	104.7(7)
O(2)-C(22)-C(21)	118.9(5)	C(39)-C(38)-C(37)	121.5(8)	F(32)-C(300)-F(31)	108.6(8)
N(6)-C(22)-C(21)	117.0(6)	C(39)-C(38)-H(38)	119.3	F(33)-C(300)-S(3)	115.6(6)
N(6)-C(23)-C(24)	107.5(5)	C(37)-C(38)-H(38)	119.3	F(32)-C(300)-S(3)	111.4(6)
N(6)-C(23)-C(25)	111.2(5)	C(38)-C(39)-C(40)	119.1(7)	F(31)-C(300)-S(3)	108.1(8)
C(24)-C(23)-C(25)	113.0(6)	C(38)-C(39)-H(39)	120.5	O(12)-S(1)-O(13)	114.8(3)
N(6)-C(23)-H(23)	108.3	C(40)-C(39)-H(39)	120.5	O(12)-S(1)-O(11)	116.2(4)
C(24)-C(23)-H(23)	108.3	C(35)-C(40)-C(39)	120.1(7)	O(13)-S(1)-O(11)	114.3(4)
C(25)-C(23)-H(23)	108.3	C(35)-C(40)-H(40)	120.0	O(12)-S(1)-C(100)	103.9(5)
C(23)-C(24)-H(24A)	109.5	C(39)-C(40)-H(40)	120.0	O(13)-S(1)-C(100)	101.0(5)
C(23)-C(24)-H(24B)	109.5	N(4)-C(41)-C(42)	109.5(5)	O(11)-S(1)-C(100)	103.9(5)
H(24A)-C(24)-H(24B)	109.5	N(4)-C(41)-H(41A)	109.8	O(22)-S(2)-O(23)	116.1(4)
C(23)-C(24)-H(24C)	109.5	C(42)-C(41)-H(41A)	109.8	O(22)-S(2)-O(21)	114.7(5)
H(24A)-C(24)-H(24C)	109.5	N(4)-C(41)-H(41B)	109.8	O(23)-S(2)-O(21)	111.8(4)
H(24B)-C(24)-H(24C)	109.5	C(42)-C(41)-H(41B)	109.8	O(22)-S(2)-C(200)	104.9(5)
C(30)-C(25)-C(26)	119.6(7)	H(41A)-C(41)-H(41B)	108.2	O(23)-S(2)-C(200)	103.7(4)
C(30)-C(25)-C(23)	122.3(6)	O(4)-C(42)-N(8)	123.7(6)	O(21)-S(2)-C(200)	103.9(5)
C(26)-C(25)-C(23)	118.1(7)	O(4)-C(42)-C(41)	120.6(5)	O(33)-S(3)-O(32)	116.4(3)
C(25)-C(26)-C(27)	118.3(8)	N(8)-C(42)-C(41)	115.7(5)	O(33)-S(3)-O(31)	112.4(4)
C(25)-C(26)-H(26)	120.9	N(8)-C(43)-C(45)	111.5(5)	O(32)-S(3)-O(31)	114.0(3)
C(27)-C(26)-H(26)	120.9	N(8)-C(43)-C(44)	108.4(5)	O(33)-S(3)-C(300)	106.9(4)
C(28)-C(27)-C(26)	120.9(8)	C(45)-C(43)-C(44)	111.9(5)	O(32)-S(3)-C(300)	105.0(4)
C(28)-C(27)-H(27)	119.6	N(8)-C(43)-H(43)	108.3	O(31)-S(3)-C(300)	100.3(5)
C(26)-C(27)-H(27)	119.6	C(45)-C(43)-H(43)	108.3	N(1S)-C(1S)-C(2S)	176.2(18)
C(27)-C(28)-C(29)	119.8(8)	C(44)-C(43)-H(43)	108.3	N(2S)-C(3S)-C(4S)	169(3)
C(27)-C(28)-H(28)	120.1	C(43)-C(44)-H(44A)	109.5	N(3S)-C(5S)-C(6S)	179.4(13)
C(29)-C(28)-H(28)	120.1	C(43)-C(44)-H(44B)	109.5	C(5S)-C(6S)-H(6SC)	109.5
C(30)-C(29)-C(28)	119.8(8)	H(44A)-C(44)-H(44B)	109.5	C(5S)-C(6S)-H(6SB)	109.5
C(30)-C(29)-H(29)	120.1	C(43)-C(44)-H(44C)	109.5	H(6SC)-C(6S)-H(6SB)	109.5
C(28)-C(29)-H(29)	120.1	H(44A)-C(44)-H(44C)	109.5	C(5S)-C(6S)-H(6SA)	109.5
C(25)-C(30)-C(29)	121.7(7)	H(44B)-C(44)-H(44C)	109.5	H(6SC)-C(6S)-H(6SA)	109.5
C(25)-C(30)-H(30)	119.1	C(46)-C(45)-C(50)	118.2(7)	H(6SB)-C(6S)-H(6SA)	109.5
C(29)-C(30)-H(30)	119.1	C(46)-C(45)-C(43)	121.8(6)		
N(3)-C(31)-C(32)	110.2(4)	C(50)-C(45)-C(43)	120.0(6)		
N(3)-C(31)-H(31A)	109.6	C(45)-C(46)-C(47)	120.5(7)		

***Table A.4.3.4** - Anisotropic displacement parameters ($Å^2 x\ 10^3$) for C57 H75 Dy F9 N11 O14 S3. The anisotropic displacement factor exponent takes the form: $-2\pi^2[h^2 a^{*2} U^{11} + ... + 2 h k a^* b^* U^{12}]$*

	U^{11}	U^{22}	U^{33}	U^{23}	U^{13}	U^{12}
Dy(1)	29(1)	25(1)	28(1)	0(1)	1(1)	-1(1)
O(1)	34(2)	30(2)	38(2)	7(2)	4(2)	7(2)
O(2)	33(2)	29(2)	38(2)	-3(2)	2(2)	-5(2)
O(3)	39(2)	23(2)	30(2)	1(2)	-1(2)	1(2)
O(4)	38(2)	34(2)	31(2)	-1(2)	-3(2)	-3(2)
O(5)	36(2)	37(2)	31(2)	3(2)	4(2)	-9(2)
N(1)	30(2)	25(2)	31(2)	1(2)	0(2)	2(2)
N(2)	30(2)	30(2)	32(3)	-3(2)	3(2)	2(2)
N(3)	34(3)	27(3)	27(2)	1(2)	0(2)	-2(2)
N(4)	36(2)	26(3)	32(2)	2(2)	-1(2)	-7(2)
N(5)	35(3)	34(3)	55(4)	8(3)	2(3)	5(2)
N(6)	38(3)	39(3)	36(3)	-9(2)	1(2)	-8(2)
N(7)	40(3)	29(3)	30(3)	-2(2)	-3(2)	6(2)
N(8)	43(3)	36(3)	32(3)	0(2)	-6(2)	-6(2)
C(7)	34(3)	33(3)	34(3)	3(2)	-4(2)	2(2)
C(8)	38(4)	30(3)	36(3)	4(2)	1(3)	2(3)
C(1)	35(3)	26(3)	36(3)	6(3)	-3(3)	-3(3)
C(2)	32(3)	38(4)	33(3)	5(3)	4(3)	-1(3)
C(3)	34(3)	32(3)	37(3)	-2(2)	3(2)	1(2)
C(4)	29(3)	34(3)	38(3)	3(3)	6(3)	1(3)
C(5)	44(3)	29(3)	27(3)	-3(2)	3(3)	-1(3)
C(6)	45(4)	31(3)	27(3)	-2(2)	1(3)	4(3)
C(11)	37(3)	26(3)	37(3)	3(2)	3(2)	-2(2)
C(12)	33(3)	30(3)	33(3)	1(3)	0(3)	5(3)
C(13)	33(3)	47(4)	73(5)	13(4)	9(3)	8(3)
C(14)	31(4)	61(5)	92(6)	0(4)	9(4)	14(4)
C(15)	33(4)	39(4)	131(9)	-4(5)	4(4)	1(3)
C(16)	96(8)	63(7)	184(13)	-9(8)	35(8)	-28(6)
C(17)	128(13)	110(13)	310(30)	-56(17)	93(16)	-62(11)
C(18)	96(9)	122(13)	310(30)	-80(20)	49(14)	-64(9)
C(19)	67(6)	108(9)	168(13)	-61(9)	-37(7)	17(6)
C(20)	48(5)	70(6)	103(8)	-15(5)	-23(5)	7(4)
C(21)	26(3)	29(3)	44(3)	-1(3)	-6(2)	-4(2)
C(22)	37(3)	28(3)	24(3)	-4(2)	1(2)	-3(3)
C(23)	41(3)	45(4)	38(3)	-12(3)	7(3)	-6(3)
C(24)	65(5)	50(4)	44(4)	-17(3)	3(3)	-5(4)
C(25)	43(4)	41(4)	40(3)	-13(3)	3(3)	1(3)
C(26)	41(4)	61(5)	54(4)	-15(4)	11(3)	1(4)
C(27)	47(5)	83(7)	76(6)	-26(5)	11(4)	10(4)
C(28)	66(5)	62(6)	72(5)	-6(4)	-12(4)	20(4)
C(29)	66(5)	48(4)	60(4)	-4(3)	-3(4)	4(4)
C(30)	48(4)	49(4)	56(4)	-11(3)	0(3)	-4(3)
C(31)	38(3)	22(3)	33(3)	-2(3)	-3(3)	-1(2)
C(32)	35(3)	27(3)	30(3)	3(2)	0(3)	-1(3)
C(33)	41(3)	39(4)	23(3)	-3(2)	-3(2)	6(3)
C(34)	54(4)	51(4)	33(3)	1(3)	0(3)	-12(3)
C(35)	46(3)	42(4)	26(3)	-1(3)	-3(2)	-5(3)
C(36)	44(4)	62(5)	48(4)	-9(3)	1(3)	1(4)
C(37)	44(4)	96(8)	63(5)	-24(5)	1(4)	-10(5)
C(38)	78(6)	100(8)	47(4)	-3(5)	4(4)	-47(6)
C(39)	95(6)	45(5)	43(4)	6(3)	-15(4)	-26(4)
C(40)	76(5)	45(4)	32(3)	3(3)	-8(3)	-14(4)
C(41)	40(3)	37(4)	36(3)	-3(3)	-8(3)	-1(3)
C(42)	30(3)	27(3)	34(3)	-1(2)	1(3)	0(2)
C(43)	56(4)	31(3)	32(3)	5(3)	1(3)	-14(3)
C(44)	64(5)	43(4)	59(4)	6(3)	-2(3)	-25(4)

C(45)	53(4)	28(3)	44(3)	6(3)	-7(3)	-13(3)
C(46)	63(5)	38(4)	49(4)	-4(3)	-2(3)	-6(3)
C(47)	59(4)	40(4)	70(5)	2(3)	3(4)	2(4)
C(48)	57(5)	35(4)	88(6)	14(4)	-15(4)	-4(3)
C(49)	63(5)	51(4)	67(5)	25(4)	-25(4)	-14(4)
C(50)	67(5)	47(4)	37(4)	8(3)	-3(3)	-15(4)
C(100)	52(5)	158(12)	115(9)	77(8)	-21(6)	-37(6)
C(200)	69(6)	74(6)	81(7)	14(5)	-17(5)	-18(5)
C(300)	79(6)	93(8)	68(6)	-32(5)	11(5)	-35(6)
S(1)	67(1)	88(2)	49(1)	12(1)	-6(1)	-45(1)
S(2)	85(2)	68(1)	35(1)	6(1)	-7(1)	-34(1)
S(3)	57(1)	73(1)	45(1)	-13(1)	-8(1)	-11(1)
F(11)	54(4)	361(14)	155(7)	123(8)	-35(4)	-28(6)
F(12)	55(3)	118(6)	282(11)	95(6)	26(5)	18(4)
F(13)	56(3)	174(7)	130(5)	41(5)	13(3)	-7(4)
F(21)	93(5)	138(7)	263(10)	50(7)	-13(6)	38(5)
F(22)	128(6)	205(9)	113(5)	27(5)	-32(4)	-121(6)
F(23)	63(3)	192(7)	67(3)	20(4)	3(3)	-22(4)
F(31)	188(8)	92(5)	117(5)	12(4)	46(5)	-66(5)
F(32)	57(3)	126(5)	91(4)	-45(3)	1(3)	-31(3)
F(33)	77(3)	88(4)	84(3)	-35(3)	22(3)	-23(3)
O(11)	115(6)	114(6)	72(4)	-8(4)	12(4)	-85(5)
O(12)	81(4)	142(7)	53(3)	21(4)	-3(3)	-62(4)
O(13)	70(3)	52(3)	64(3)	8(2)	-21(3)	-11(3)
O(21)	125(6)	61(4)	98(5)	8(4)	12(4)	-3(4)
O(22)	133(6)	146(6)	45(3)	30(3)	-34(4)	-83(6)
O(23)	71(3)	70(4)	52(3)	-6(3)	-15(2)	-24(3)
O(31)	72(3)	76(4)	66(4)	25(3)	-4(3)	-14(3)
O(32)	69(3)	47(3)	42(3)	-1(2)	-17(2)	-14(2)
O(33)	77(4)	96(4)	72(4)	-38(3)	-16(3)	4(4)
N(1S)	123(13)	181(17)	450(40)	-10(20)	-45(19)	-23(12)
N(2S)	420(40)	470(50)	290(30)	-30(30)	70(30)	-340(40)
N(3S)	78(6)	103(7)	92(6)	-9(5)	13(5)	10(6)
C(1S)	178(17)	70(8)	135(12)	1(8)	-27(12)	-36(10)
C(2S)	93(8)	72(7)	115(8)	10(6)	29(7)	-18(6)
C(3S)	300(30)	146(16)	104(11)	5(10)	16(16)	-44(19)
C(4S)	116(11)	202(18)	166(15)	42(13)	-42(11)	-78(12)
C(5S)	85(7)	72(6)	63(5)	-8(5)	1(5)	13(5)
C(6S)	78(7)	128(10)	97(8)	-24(7)	-9(6)	30(7)

***Table A.4.3.5** - Hydrogen coordinates (x 10^4) and isotropic displacement parameters ($Å^2$x 10^3) for $C_{57}H_{75}DyF_9N_{11}O_{14}S_3$.*

	x	y	z	U(eq)
H(5)	4387	7009	10091	49
H(6)	8111	6711	11982	45
H(7)	7747	3210	11891	39
H(8)	4127	3412	9915	44
H(7A)	5117	5624	9439	40
H(7B)	5608	5279	8899	40
H(8A)	6892	5656	9280	42
H(8B)	6288	6256	9167	42
H(1A)	7388	6627	10510	39
H(1B)	7498	6629	9792	39
H(2A)	7994	5539	9823	41
H(2B)	8575	5994	10227	41
H(3A)	8420	4556	11079	41
H(3B)	8935	4884	10543	41

H(4A)	7983	4482	9820	40
H(4B)	8334	3893	10210	40
H(5A)	6213	3534	9963	40
H(5B)	7087	3538	9618	40
H(6A)	6837	4608	9263	41
H(6B)	6089	4152	9056	41
H(11A)	5805	6895	9887	40
H(11B)	6076	6849	10581	40
H(13)	3525	6184	10851	61
H(14A)	3112	7290	10751	92
H(14B)	2340	6831	10602	92
H(14C)	2845	7167	10066	92
H(16)	2714	5255	10660	137
H(17)	2168	4469	9950	219
H(18)	2421	4566	8948	213
H(19)	3075	5461	8556	137
H(20)	3556	6281	9212	88
H(21A)	8579	5999	11214	39
H(21B)	8276	5397	11608	39
H(23)	6552	6673	12485	50
H(24A)	7700	7112	13022	79
H(24B)	6961	7628	13002	79
H(24C)	7743	7707	12563	79
H(26)	5259	7022	12127	63
H(27)	4419	7674	11473	82
H(28)	5038	8421	10814	80
H(29)	6496	8545	10805	70
H(30)	7326	7896	11427	61
H(31A)	7596	3300	10832	37
H(31B)	6603	3330	10878	37
H(33)	7155	4179	12657	41
H(34A)	6929	3100	12981	69
H(34B)	7495	3466	13465	69
H(34C)	7909	2972	12999	69
H(36)	9201	3410	12666	62
H(37)	10500	3959	12720	81
H(38)	10513	5095	12700	90
H(39)	9271	5684	12712	74
H(40)	7969	5119	12707	61
H(41A)	4787	4215	9383	45
H(41B)	4443	4801	9784	45
H(43)	4119	3255	11134	47
H(44A)	3040	2808	10521	83
H(44B)	3439	2256	10934	83
H(44C)	3683	2305	10236	83
H(46)	5300	2313	10026	60
H(47)	6560	1770	10236	67
H(48)	7050	1682	11223	72
H(49)	6355	2238	12021	72
H(50)	5112	2809	11808	60
H(6SC)	2091	6499	12414	151
H(6SB)	2263	5929	12884	151
H(6SA)	1912	5767	12227	151

***Table A.4.4.2** - Atomic coordinates (x 10^4) and equivalent isotropic displacement parameters ($Å^2$x 10^3) for C60 H73 Eu F12 N10 O13. U(eq) is defined as one third of the trace of the orthogonalized U^{ij} tensor.*

	x	y	z	U(eq)
Eu(1)	7596(1)	5598(1)	1902(1)	23(1)
O(1)	8197(2)	5302(1)	1048(1)	28(1)
O(2)	8999(2)	6152(1)	2016(1)	28(1)
O(3)	6997(2)	6491(1)	2494(1)	30(1)
O(4)	6188(2)	5699(2)	1486(1)	32(1)
O(5)	7608(2)	6716(1)	1389(1)	33(1)
N(1)	7204(2)	4247(2)	1561(1)	28(1)
N(2)	8966(2)	4650(2)	2043(1)	28(1)
N(3)	8032(2)	5410(2)	2939(1)	29(1)
N(4)	6257(2)	4979(2)	2462(1)	30(1)
N(5)	8336(2)	4632(2)	301(1)	34(1)
N(6)	10497(2)	6192(2)	2014(1)	32(1)
N(7)	6977(2)	7144(2)	3256(1)	37(1)
N(8)	4691(2)	5609(2)	1448(1)	38(1)
C(1)	7871(3)	3708(2)	1749(2)	34(1)
C(2)	8829(3)	3975(2)	1720(2)	31(1)
C(3)	9078(3)	4448(2)	2619(1)	32(1)
C(4)	8938(3)	5085(2)	3000(2)	31(1)
C(5)	7370(3)	4933(2)	3206(1)	33(1)
C(6)	6398(3)	5076(2)	3050(2)	34(1)
C(7)	6153(3)	4195(2)	2342(2)	34(1)
C(8)	6295(3)	4018(2)	1748(2)	34(1)
C(11)	7201(3)	4293(2)	966(1)	33(1)
C(12)	7964(3)	4771(2)	771(2)	28(1)
C(13)	9033(3)	5102(2)	77(2)	35(1)
C(14)	9070(4)	5011(3)	-521(2)	61(2)
C(15)	9941(3)	4962(2)	341(2)	34(1)
C(16)	10440(3)	5534(3)	533(2)	37(1)
C(17)	11263(3)	5424(3)	772(2)	50(1)
C(18)	11604(4)	4729(3)	812(2)	59(1)
C(19)	11126(4)	4146(3)	624(2)	60(2)
C(20)	10294(3)	4264(3)	382(2)	48(1)
C(21)	9776(2)	5031(2)	1846(2)	29(1)
C(22)	9743(2)	5836(2)	1971(2)	27(1)
C(23)	10487(3)	6988(2)	2104(2)	36(1)
C(24)	11406(3)	7297(2)	1953(2)	53(1)
C(25)	10216(3)	7162(2)	2675(2)	37(1)
C(26)	9504(3)	7622(2)	2781(2)	40(1)
C(27)	9248(3)	7782(3)	3304(2)	46(1)
C(28)	9706(4)	7459(3)	3726(2)	59(2)
C(29)	10407(4)	6997(3)	3634(2)	55(1)
C(30)	10665(3)	6851(3)	3100(2)	48(1)
C(31)	8025(3)	6141(2)	3186(2)	32(1)
C(32)	7278(3)	6607(2)	2955(1)	30(1)
C(33)	6279(3)	7639(2)	3061(2)	45(1)
C(34)	6257(4)	8314(3)	3417(3)	62(1)
C(35)	5378(3)	7278(3)	3040(2)	51(1)
C(36)	4851(4)	7331(4)	2578(3)	73(2)
C(37)	3995(5)	7004(5)	2570(5)	109(4)
C(38)	3672(5)	6656(5)	2993(5)	98(3)
C(39)	4184(5)	6605(4)	3451(4)	89(2)
C(40)	5048(4)	6914(3)	3481(3)	65(2)
C(41)	5435(3)	5378(2)	2304(2)	35(1)
C(42)	5455(2)	5566(2)	1711(2)	32(1)
C(43)	4661(3)	5843(3)	882(2)	43(1)
C(44)	3703(3)	6061(3)	750(2)	61(1)

C(45)	5019(3)	5270(3)	507(2)	41(1)
C(46)	5685(3)	5436(3)	136(2)	49(1)
C(47)	6015(4)	4916(4)	-217(2)	67(2)
C(48)	5685(5)	4214(4)	-202(2)	72(2)
C(49)	5026(5)	4042(4)	171(3)	73(2)
C(50)	4693(4)	4555(3)	520(2)	59(1)
F(11)	2724(3)	4587(3)	3048(2)	134(2)
F(12)	1991(4)	4038(2)	2457(2)	142(2)
F(13)	1446(2)	4953(3)	2826(2)	91(1)
F(21)	4162(5)	5998(3)	-812(2)	127(2)
F(22)	3876(4)	6705(3)	-1468(2)	107(2)
F(23)	5223(4)	6428(3)	-1271(2)	129(2)
F(31)	1943(5)	2572(3)	-405(2)	166(3)
F(32)	3262(5)	2235(3)	-503(2)	143(3)
F(33)	2963(4)	3249(2)	-102(2)	126(2)
F(41)	11464(4)	6791(3)	-1560(2)	113(2)
F(42)	10135(6)	6459(6)	-1441(3)	206(5)
F(43)	11064(6)	5942(3)	-1017(3)	178(4)
O(11)	2208(2)	5657(2)	2020(2)	59(1)
O(12)	3393(2)	4942(2)	2056(2)	65(1)
O(21)	4105(3)	7801(2)	-793(2)	62(1)
O(22)	4986(4)	7113(3)	-284(2)	86(2)
O(31)	2326(3)	2503(2)	743(1)	61(1)
O(32)	2883(3)	1519(2)	380(2)	82(1)
O(41)	10175(3)	6963(2)	-405(2)	66(1)
O(42)	11203(3)	7702(2)	-762(2)	68(1)
C(11S)	2227(3)	4683(3)	2648(2)	53(1)
C(12S)	2642(3)	5142(2)	2192(2)	39(1)
C(21S)	4417(5)	6588(3)	-1055(2)	70(2)
C(22S)	4495(4)	7241(3)	-684(2)	52(1)
C(31S)	2701(6)	2573(3)	-150(2)	85(2)
C(32S)	2649(3)	2158(2)	374(2)	44(1)
C(41S)	10897(6)	6591(4)	-1191(3)	90(3)
C(42S)	10759(4)	7144(3)	-747(2)	57(1)
N(1S)	8000(5)	6698(4)	-1316(3)	101(2)
C(1S)	7634(7)	6990(5)	-317(4)	108(2)
C(2S)	7820(5)	6810(4)	-866(3)	80(2)
C(4S)	12666(13)	4901(8)	-522(6)	192(5)
C(3S)	12350(20)	5646(11)	-527(12)	439(13)
N(2S)	12356(19)	6335(12)	-440(10)	384(11)

Table A.4.4.3 - Bond lengths [Å] and angles [°] for C60 H73 Eu F12 N10 O13.

Eu(1)-O(2)	2.352(2)	N(1)-C(1)	1.485(5)	N(8)-C(42)	1.320(5)
Eu(1)-O(4)	2.356(2)	N(1)-C(8)	1.499(5)	N(8)-C(43)	1.475(6)
Eu(1)-O(1)	2.374(3)	N(2)-C(3)	1.491(5)	C(1)-C(2)	1.518(6)
Eu(1)-O(3)	2.384(3)	N(2)-C(21)	1.484(5)	C(3)-C(4)	1.525(5)
Eu(1)-O(5)	2.426(2)	N(2)-C(2)	1.494(5)	C(5)-C(6)	1.528(6)
Eu(1)-N(3)	2.688(3)	N(3)-C(31)	1.481(5)	C(7)-C(8)	1.532(6)
Eu(1)-N(1)	2.693(3)	N(3)-C(4)	1.490(5)	C(11)-C(12)	1.523(5)
Eu(1)-N(4)	2.694(3)	N(3)-C(5)	1.482(5)	C(13)-C(14)	1.502(6)
Eu(1)-N(2)	2.716(3)	N(4)-C(7)	1.484(5)	C(13)-C(15)	1.531(6)
Eu(1)-C(42)	3.240(3)	N(4)-C(41)	1.487(5)	C(15)-C(16)	1.377(6)
Eu(1)-C(22)	3.248(3)	N(4)-C(6)	1.491(5)	C(15)-C(20)	1.395(7)
Eu(1)-C(32)	3.251(3)	N(5)-C(12)	1.323(5)	C(16)-C(17)	1.383(6)
O(1)-C(12)	1.246(5)	N(5)-C(13)	1.467(5)	C(17)-C(18)	1.382(8)
O(2)-C(22)	1.262(4)	N(6)-C(22)	1.309(5)	C(18)-C(19)	1.372(9)
O(3)-C(32)	1.244(5)	N(6)-C(23)	1.485(5)	C(19)-C(20)	1.402(8)
O(4)-C(42)	1.256(4)	N(7)-C(32)	1.320(5)	C(21)-C(22)	1.516(5)
N(1)-C(11)	1.484(5)	N(7)-C(33)	1.469(6)	C(23)-C(25)	1.513(6)

C(23)-C(24)	1.534(6)	O(1)-Eu(1)-O(5)	73.68(9)	C(11)-N(1)-C(1)	110.8(3)
C(25)-C(30)	1.380(7)	O(3)-Eu(1)-O(5)	75.05(9)	C(11)-N(1)-C(8)	108.8(3)
C(25)-C(26)	1.386(6)	O(2)-Eu(1)-N(3)	73.94(9)	C(1)-N(1)-C(8)	108.9(3)
C(26)-C(27)	1.391(7)	O(4)-Eu(1)-N(3)	130.60(9)	C(11)-N(1)-Eu(1)	105.3(2)
C(27)-C(28)	1.390(8)	O(1)-Eu(1)-N(3)	137.78(9)	C(1)-N(1)-Eu(1)	111.9(2)
C(28)-C(29)	1.370(8)	O(3)-Eu(1)-N(3)	65.55(9)	C(8)-N(1)-Eu(1)	111.1(2)
C(29)-C(30)	1.412(7)	O(5)-Eu(1)-N(3)	127.91(9)	C(3)-N(2)-C(21)	110.2(3)
C(31)-C(32)	1.522(5)	O(2)-Eu(1)-N(1)	129.31(9)	C(3)-N(2)-C(2)	109.0(3)
C(33)-C(35)	1.504(7)	O(4)-Eu(1)-N(1)	74.88(10)	C(21)-N(2)-C(2)	109.1(3)
C(33)-C(34)	1.527(7)	O(1)-Eu(1)-N(1)	65.63(9)	C(3)-N(2)-Eu(1)	111.6(2)
C(35)-C(40)	1.380(8)	O(3)-Eu(1)-N(1)	138.67(9)	C(21)-N(2)-Eu(1)	105.6(2)
C(35)-C(36)	1.398(8)	O(5)-Eu(1)-N(1)	128.26(8)	C(2)-N(2)-Eu(1)	111.2(2)
C(36)-C(37)	1.417(12)	N(3)-Eu(1)-N(1)	103.79(9)	C(31)-N(3)-C(4)	109.3(3)
C(37)-C(38)	1.325(13)	O(2)-Eu(1)-N(4)	141.75(9)	C(31)-N(3)-C(5)	110.3(3)
C(38)-C(39)	1.379(12)	O(4)-Eu(1)-N(4)	66.19(9)	C(4)-N(3)-C(5)	108.9(3)
C(39)-C(40)	1.414(9)	O(1)-Eu(1)-N(4)	130.48(9)	C(31)-N(3)-Eu(1)	106.3(2)
C(41)-C(42)	1.518(6)	O(3)-Eu(1)-N(4)	72.06(10)	C(4)-N(3)-Eu(1)	111.7(2)
C(43)-C(45)	1.509(7)	O(5)-Eu(1)-N(4)	129.62(10)	C(5)-N(3)-Eu(1)	110.2(2)
C(43)-C(44)	1.525(6)	N(3)-Eu(1)-N(4)	68.19(9)	C(7)-N(4)-C(41)	109.9(3)
C(45)-C(50)	1.405(7)	N(1)-Eu(1)-N(4)	67.14(10)	C(7)-N(4)-C(6)	109.3(3)
C(45)-C(46)	1.393(7)	O(2)-Eu(1)-N(2)	65.79(9)	C(41)-N(4)-C(6)	108.6(3)
C(46)-C(47)	1.391(8)	O(4)-Eu(1)-N(2)	141.53(10)	C(7)-N(4)-Eu(1)	112.7(2)
C(47)-C(48)	1.387(10)	O(1)-Eu(1)-N(2)	71.47(9)	C(41)-N(4)-Eu(1)	105.6(2)
C(48)-C(49)	1.391(10)	O(3)-Eu(1)-N(2)	130.42(9)	C(6)-N(4)-Eu(1)	110.7(2)
C(49)-C(50)	1.377(9)	O(5)-Eu(1)-N(2)	127.49(9)	C(12)-N(5)-C(13)	121.4(3)
F(11)-C(11S)	1.255(6)	N(3)-Eu(1)-N(2)	67.05(9)	C(12)-N(5)-H(5)	119.3
F(12)-C(11S)	1.328(7)	N(1)-Eu(1)-N(2)	67.14(9)	C(13)-N(5)-H(5)	119.3
F(13)-C(11S)	1.345(6)	N(4)-Eu(1)-N(2)	102.89(10)	C(22)-N(6)-C(23)	119.9(3)
F(21)-C(21S)	1.301(7)	O(2)-Eu(1)-C(42)	155.26(10)	C(22)-N(6)-H(6)	120.0
F(22)-C(21S)	1.327(7)	O(4)-Eu(1)-C(42)	18.56(9)	C(23)-N(6)-H(6)	120.1
F(23)-C(21S)	1.353(9)	O(1)-Eu(1)-C(42)	103.79(9)	C(32)-N(7)-C(33)	121.3(4)
F(31)-C(31S)	1.300(10)	O(3)-Eu(1)-C(42)	74.42(10)	C(32)-N(7)-H(7)	119.4
F(32)-C(31S)	1.365(9)	O(5)-Eu(1)-C(42)	86.83(10)	C(33)-N(7)-H(7)	119.3
F(33)-C(31S)	1.310(7)	N(3)-Eu(1)-C(42)	112.32(10)	C(42)-N(8)-C(43)	121.2(3)
F(41)-C(41S)	1.303(7)	N(1)-Eu(1)-C(42)	73.83(10)	C(42)-N(8)-H(8)	119.4
F(42)-C(41S)	1.323(12)	N(4)-Eu(1)-C(42)	48.19(10)	C(43)-N(8)-H(8)	119.4
F(43)-C(41S)	1.297(10)	N(2)-Eu(1)-C(42)	138.95(10)	N(1)-C(1)-C(2)	113.8(3)
O(11)-C(12S)	1.227(5)	O(2)-Eu(1)-C(22)	18.50(9)	N(1)-C(1)-H(1A)	108.8
O(12)-C(12S)	1.232(5)	O(4)-Eu(1)-C(22)	153.82(9)	C(2)-C(1)-H(1A)	108.8
O(21)-C(22S)	1.216(6)	O(1)-Eu(1)-C(22)	72.75(9)	N(1)-C(1)-H(1B)	108.8
O(22)-C(22S)	1.261(6)	O(3)-Eu(1)-C(22)	104.26(9)	C(2)-C(1)-H(1B)	108.8
O(31)-C(32S)	1.217(5)	O(5)-Eu(1)-C(22)	84.59(9)	H(1A)-C(1)-H(1B)	107.7
O(32)-C(32S)	1.228(6)	N(3)-Eu(1)-C(22)	74.11(9)	N(2)-C(2)-C(1)	112.0(3)
O(41)-C(42S)	1.264(6)	N(1)-Eu(1)-C(22)	110.92(9)	N(2)-C(2)-H(2A)	109.2
O(42)-C(42S)	1.225(7)	N(4)-Eu(1)-C(22)	139.97(9)	C(1)-C(2)-H(2A)	109.2
C(11S)-C(12S)	1.548(7)	N(2)-Eu(1)-C(22)	48.18(9)	N(2)-C(2)-H(2B)	109.2
C(21S)-C(22S)	1.522(8)	C(42)-Eu(1)-C(22)	171.35(9)	C(1)-C(2)-H(2B)	109.2
C(31S)-C(32S)	1.516(8)	O(2)-Eu(1)-C(32)	77.59(9)	H(2A)-C(2)-H(2B)	107.9
C(41S)-C(42S)	1.519(9)	O(4)-Eu(1)-C(32)	100.32(10)	N(2)-C(3)-C(4)	113.2(3)
N(1S)-C(2S)	1.172(9)	O(1)-Eu(1)-C(32)	155.52(9)	N(2)-C(3)-H(3A)	108.9
C(1S)-C(2S)	1.435(11)	O(3)-Eu(1)-C(32)	18.44(9)	C(4)-C(3)-H(3A)	108.9
C(4S)-C(3S)	1.450(17)	O(5)-Eu(1)-C(32)	86.60(9)	N(2)-C(3)-H(3B)	108.9
C(3S)-N(2S)	1.288(17)	N(3)-Eu(1)-C(32)	48.17(9)	C(4)-C(3)-H(3B)	109.0
		N(1)-Eu(1)-C(32)	138.74(9)	H(3A)-C(3)-H(3B)	107.8
O(2)-Eu(1)-O(4)	144.77(9)	N(4)-Eu(1)-C(32)	73.45(9)	N(3)-C(4)-C(3)	111.7(3)
O(2)-Eu(1)-O(1)	82.48(9)	N(2)-Eu(1)-C(32)	111.98(10)	N(3)-C(4)-H(4A)	109.2
O(4)-Eu(1)-O(1)	87.84(9)	C(42)-Eu(1)-C(32)	89.12(10)	C(3)-C(4)-H(4A)	109.2
O(2)-Eu(1)-O(3)	87.81(9)	C(22)-Eu(1)-C(32)	91.42(9)	N(3)-C(4)-H(4B)	109.3
O(4)-Eu(1)-O(3)	83.15(9)	C(12)-O(1)-Eu(1)	124.8(2)	C(3)-C(4)-H(4B)	109.3
O(1)-Eu(1)-O(3)	148.74(9)	C(22)-O(2)-Eu(1)	125.2(2)	H(4A)-C(4)-H(4B)	107.9
O(2)-Eu(1)-O(5)	71.80(9)	C(32)-O(3)-Eu(1)	124.2(2)	N(3)-C(5)-C(6)	114.8(3)
O(4)-Eu(1)-O(5)	72.97(9)	C(42)-O(4)-Eu(1)	124.8(2)	N(3)-C(5)-H(5A)	108.6

C(6)-C(5)-H(5A)	108.6	C(19)-C(20)-H(20)	119.7	C(33)-C(34)-H(34A)	109.4
N(3)-C(5)-H(5B)	108.5	C(15)-C(20)-H(20)	119.7	C(33)-C(34)-H(34B)	109.5
C(6)-C(5)-H(5B)	108.5	N(2)-C(21)-C(22)	111.6(3)	H(34A)-C(34)-H(34B)	109.5
H(5A)-C(5)-H(5B)	107.5	N(2)-C(21)-H(21A)	109.3	C(33)-C(34)-H(34C)	109.5
N(4)-C(6)-C(5)	111.4(3)	C(22)-C(21)-H(21A)	109.3	H(34A)-C(34)-H(34C)	109.5
N(4)-C(6)-H(6A)	109.4	N(2)-C(21)-H(21B)	109.3	H(34B)-C(34)-H(34C)	109.5
C(5)-C(6)-H(6A)	109.3	C(22)-C(21)-H(21B)	109.3	C(40)-C(35)-C(36)	119.2(6)
N(4)-C(6)-H(6B)	109.4	H(21A)-C(21)-H(21B)	108.0	C(40)-C(35)-C(33)	120.5(5)
C(5)-C(6)-H(6B)	109.3	O(2)-C(22)-N(6)	121.5(3)	C(36)-C(35)-C(33)	120.3(6)
H(6A)-C(6)-H(6B)	108.0	O(2)-C(22)-C(21)	119.9(3)	C(35)-C(36)-C(37)	119.5(8)
N(4)-C(7)-C(8)	112.8(3)	N(6)-C(22)-C(21)	118.6(3)	C(35)-C(36)-H(36)	120.2
N(4)-C(7)-H(7A)	109.0	O(2)-C(22)-Eu(1)	36.27(16)	C(37)-C(36)-H(36)	120.3
C(8)-C(7)-H(7A)	109.0	N(6)-C(22)-Eu(1)	157.7(3)	C(38)-C(37)-C(36)	121.7(8)
N(4)-C(7)-H(7B)	109.0	C(21)-C(22)-Eu(1)	83.61(19)	C(38)-C(37)-H(37)	119.1
C(8)-C(7)-H(7B)	109.0	N(6)-C(23)-C(25)	110.8(3)	C(36)-C(37)-H(37)	119.2
H(7A)-C(7)-H(7B)	107.8	N(6)-C(23)-C(24)	108.6(3)	C(37)-C(38)-C(39)	119.3(7)
N(1)-C(8)-C(7)	111.5(3)	C(25)-C(23)-C(24)	113.2(4)	C(37)-C(38)-H(38)	120.5
N(1)-C(8)-H(8A)	109.4	N(6)-C(23)-H(23)	108.0	C(39)-C(38)-H(38)	120.3
C(7)-C(8)-H(8A)	109.3	C(25)-C(23)-H(23)	108.1	C(38)-C(39)-C(40)	121.7(8)
N(1)-C(8)-H(8B)	109.3	C(24)-C(23)-H(23)	108.0	C(38)-C(39)-H(39)	119.2
C(7)-C(8)-H(8B)	109.3	C(23)-C(24)-H(24A)	109.4	C(40)-C(39)-H(39)	119.1
H(8A)-C(8)-H(8B)	108.0	C(23)-C(24)-H(24B)	109.5	C(35)-C(40)-C(39)	118.8(7)
N(1)-C(11)-C(12)	110.4(3)	H(24A)-C(24)-H(24B)	109.5	C(35)-C(40)-H(40)	120.6
N(1)-C(11)-H(11A)	109.5	C(23)-C(24)-H(24C)	109.5	C(39)-C(40)-H(40)	120.6
C(12)-C(11)-H(11A)	109.6	H(24A)-C(24)-H(24C)	109.5	N(4)-C(41)-C(42)	110.8(3)
N(1)-C(11)-H(11B)	109.6	H(24B)-C(24)-H(24C)	109.5	N(4)-C(41)-H(41A)	109.4
C(12)-C(11)-H(11B)	109.6	C(30)-C(25)-C(26)	118.8(4)	C(42)-C(41)-H(41A)	109.5
H(11A)-C(11)-H(11B)	108.1	C(30)-C(25)-C(23)	120.2(4)	N(4)-C(41)-H(41B)	109.5
O(1)-C(12)-N(5)	121.8(4)	C(26)-C(25)-C(23)	120.9(4)	C(42)-C(41)-H(41B)	109.5
O(1)-C(12)-C(11)	119.1(3)	C(25)-C(26)-C(27)	121.4(5)	H(41A)-C(41)-H(41B)	108.1
N(5)-C(12)-C(11)	119.0(3)	C(25)-C(26)-H(26)	119.3	O(4)-C(42)-N(8)	121.6(3)
O(1)-C(12)-Eu(1)	36.85(17)	C(27)-C(26)-H(26)	119.3	O(4)-C(42)-C(41)	119.7(3)
N(5)-C(12)-Eu(1)	158.6(3)	C(28)-C(27)-C(26)	118.8(5)	N(8)-C(42)-C(41)	118.7(3)
C(11)-C(12)-Eu(1)	82.3(2)	C(28)-C(27)-H(27)	120.6	O(4)-C(42)-Eu(1)	36.68(17)
N(5)-C(13)-C(14)	109.7(4)	C(26)-C(27)-H(27)	120.6	N(8)-C(42)-Eu(1)	158.2(3)
N(5)-C(13)-C(15)	111.7(3)	C(29)-C(28)-C(27)	121.2(5)	C(41)-C(42)-Eu(1)	83.1(2)
C(14)-C(13)-C(15)	112.0(4)	C(29)-C(28)-H(28)	119.4	N(8)-C(43)-C(45)	112.1(4)
N(5)-C(13)-H(13)	107.7	C(27)-C(28)-H(28)	119.4	N(8)-C(43)-C(44)	108.1(4)
C(14)-C(13)-H(13)	107.7	C(28)-C(29)-C(30)	119.0(5)	C(45)-C(43)-C(44)	112.6(4)
C(15)-C(13)-H(13)	107.7	C(28)-C(29)-H(29)	120.5	N(8)-C(43)-H(43)	107.9
C(13)-C(14)-H(14A)	109.5	C(30)-C(29)-H(29)	120.5	C(45)-C(43)-H(43)	107.9
C(13)-C(14)-H(14B)	109.4	C(25)-C(30)-C(29)	120.8(5)	C(44)-C(43)-H(43)	107.9
H(14A)-C(14)-H(14B)	109.5	C(25)-C(30)-H(30)	119.6	C(43)-C(44)-H(44A)	109.4
C(13)-C(14)-H(14C)	109.5	C(29)-C(30)-H(30)	119.6	C(43)-C(44)-H(44B)	109.5
H(14A)-C(14)-H(14C)	109.5	N(3)-C(31)-C(32)	111.2(3)	H(44A)-C(44)-H(44B)	109.5
H(14B)-C(14)-H(14C)	109.5	N(3)-C(31)-H(31B)	109.4	C(43)-C(44)-H(44C)	109.5
C(16)-C(15)-C(20)	118.4(4)	C(32)-C(31)-H(31B)	109.4	H(44A)-C(44)-H(44C)	109.5
C(16)-C(15)-C(13)	120.2(4)	N(3)-C(31)-H(31C)	109.4	H(44B)-C(44)-H(44C)	109.5
C(20)-C(15)-C(13)	121.4(4)	C(32)-C(31)-H(31C)	109.4	C(50)-C(45)-C(46)	118.0(5)
C(17)-C(16)-C(15)	121.4(5)	H(31B)-C(31)-H(31C)	108.0	C(50)-C(45)-C(43)	121.2(5)
C(17)-C(16)-H(16)	119.3	O(3)-C(32)-N(7)	122.6(4)	C(46)-C(45)-C(43)	120.8(4)
C(15)-C(16)-H(16)	119.3	O(3)-C(32)-C(31)	120.1(3)	C(47)-C(46)-C(45)	121.5(5)
C(16)-C(17)-C(18)	119.7(5)	N(7)-C(32)-C(31)	117.3(3)	C(47)-C(46)-H(46)	119.3
C(16)-C(17)-H(17)	120.2	O(3)-C(32)-Eu(1)	37.31(17)	C(45)-C(46)-H(46)	119.3
C(18)-C(17)-H(17)	120.1	N(7)-C(32)-Eu(1)	159.5(3)	C(46)-C(47)-C(48)	120.0(6)
C(19)-C(18)-C(17)	120.5(5)	C(31)-C(32)-Eu(1)	82.8(2)	C(46)-C(47)-H(47)	120.0
C(19)-C(18)-H(18)	119.7	N(7)-C(33)-C(35)	112.0(4)	C(48)-C(47)-H(47)	120.0
C(17)-C(18)-H(18)	119.8	N(7)-C(33)-C(34)	109.1(4)	C(49)-C(48)-C(47)	118.8(6)
C(18)-C(19)-C(20)	119.3(5)	C(35)-C(33)-C(34)	111.2(4)	C(49)-C(48)-H(48)	120.6
C(18)-C(19)-H(19)	120.3	N(7)-C(33)-H(33)	108.1	C(47)-C(48)-H(48)	120.5
C(20)-C(19)-H(19)	120.3	C(35)-C(33)-H(33)	108.1	C(48)-C(49)-C(50)	121.5(6)
C(19)-C(20)-C(15)	120.6(5)	C(34)-C(33)-H(33)	108.1	C(48)-C(49)-H(49)	119.2

C(50)-C(49)-H(49)	119.3	F(21)-C(21S)-F(23)	105.4(6)	O(31)-C(32S)-O(32)	127.1(5)
C(49)-C(50)-C(45)	120.2(6)	F(22)-C(21S)-F(23)	105.7(6)	O(31)-C(32S)-C(31S)	114.1(4)
C(49)-C(50)-H(50)	119.9	F(21)-C(21S)-C(22S)	113.6(5)	O(32)-C(32S)-C(31S)	118.7(5)
C(45)-C(50)-H(50)	119.9	F(22)-C(21S)-C(22S)	112.9(5)	F(43)-C(41S)-F(41)	111.8(7)
F(11)-C(11S)-F(12)	108.5(6)	F(23)-C(21S)-C(22S)	110.1(6)	F(43)-C(41S)-F(42)	98.9(8)
F(11)-C(11S)-F(13)	107.9(5)	O(21)-C(22S)-O(22)	127.9(5)	F(41)-C(41S)-F(42)	106.4(8)
F(12)-C(11S)-F(13)	102.6(5)	O(21)-C(22S)-C(21S)	119.9(5)	F(43)-C(41S)-C(42S)	113.6(8)
F(11)-C(11S)-C(12S)	115.0(5)	O(22)-C(22S)-C(21S)	112.2(5)	F(41)-C(41S)-C(42S)	114.4(6)
F(12)-C(11S)-C(12S)	109.3(5)	F(31)-C(31S)-F(33)	107.9(7)	F(42)-C(41S)-C(42S)	110.4(7)
F(13)-C(11S)-C(12S)	112.7(4)	F(31)-C(31S)-F(32)	102.9(6)	O(42)-C(42S)-O(41)	128.1(6)
O(11)-C(12S)-O(12)	128.2(4)	F(33)-C(31S)-F(32)	108.0(6)	O(42)-C(42S)-C(41S)	117.8(5)
O(11)-C(12S)-C(11S)	117.9(4)	F(31)-C(31S)-C(32S)	112.0(6)	O(41)-C(42S)-C(41S)	114.1(5)
O(12)-C(12S)-C(11S)	113.9(4)	F(33)-C(31S)-C(32S)	114.5(5)	N(1S)-C(2S)-C(1S)	176.3(9)
F(21)-C(21S)-F(22)	108.6(6)	F(32)-C(31S)-C(32S)	110.8(6)	N(2S)-C(3S)-C(4S)	158(3)

***Table A.4.4.4** - Anisotropic displacement parameters ($Å^2 x\ 10^3$) for C60 H73 Eu F12 N10 O13. The anisotropic displacement factor exponent takes the form: $-2\pi^2[\,h^2\,a^{*2}U^{11} + \ldots + 2\,h\,k\,a^*\,b^*\,U^{12}\,]$*

	U^{11}	U^{22}	U^{33}	U^{23}	U^{13}	U^{12}
Eu(1)	20(1)	26(1)	23(1)	1(1)	0(1)	-1(1)
O(1)	29(1)	30(1)	24(1)	-3(1)	-1(1)	-2(1)
O(2)	25(1)	30(1)	29(1)	-2(1)	1(1)	0(1)
O(3)	31(1)	31(1)	30(1)	-1(1)	3(1)	5(1)
O(4)	20(1)	41(2)	34(1)	7(1)	-2(1)	-2(1)
O(5)	28(1)	31(1)	39(1)	8(1)	2(1)	2(1)
N(1)	30(2)	30(2)	25(2)	1(1)	0(1)	-3(1)
N(2)	26(2)	27(2)	30(2)	1(1)	0(1)	3(1)
N(3)	27(2)	32(2)	27(2)	0(1)	1(1)	0(1)
N(4)	26(2)	37(2)	27(2)	4(1)	1(1)	-4(1)
N(5)	34(2)	40(2)	27(2)	-5(1)	1(1)	-7(1)
N(6)	24(2)	34(2)	39(2)	-4(1)	2(1)	0(1)
N(7)	39(2)	38(2)	33(2)	-6(1)	4(1)	4(2)
N(8)	23(2)	48(2)	45(2)	8(2)	3(1)	-7(2)
C(1)	39(2)	28(2)	34(2)	0(2)	0(2)	0(2)
C(2)	34(2)	28(2)	31(2)	1(2)	0(2)	4(2)
C(3)	35(2)	33(2)	27(2)	5(2)	-1(1)	7(2)
C(4)	32(2)	33(2)	27(2)	1(2)	-6(2)	2(2)
C(5)	37(2)	39(2)	24(2)	6(1)	1(2)	-5(2)
C(6)	32(2)	41(2)	29(2)	2(2)	9(2)	-6(2)
C(7)	34(2)	32(2)	34(2)	2(2)	6(2)	-5(2)
C(8)	32(2)	33(2)	38(2)	3(2)	0(2)	-9(2)
C(11)	36(2)	35(2)	28(2)	-2(2)	-2(2)	-6(2)
C(12)	28(2)	32(2)	25(2)	3(2)	-4(2)	-1(2)
C(13)	39(2)	41(2)	25(2)	5(2)	0(2)	-5(2)
C(14)	60(3)	98(5)	24(2)	5(2)	0(2)	-27(3)
C(15)	34(2)	40(2)	27(2)	3(2)	7(2)	-1(2)
C(16)	38(2)	40(2)	34(2)	4(2)	5(2)	-2(2)
C(17)	36(2)	66(3)	48(3)	7(2)	2(2)	-8(2)
C(18)	35(3)	76(4)	67(4)	22(3)	6(2)	1(2)
C(19)	47(3)	51(3)	82(4)	19(3)	21(3)	13(2)
C(20)	50(3)	45(3)	48(3)	4(2)	11(2)	-5(2)
C(21)	26(2)	34(2)	28(2)	-1(2)	1(2)	3(1)
C(22)	22(2)	36(2)	23(2)	1(2)	-1(1)	1(1)
C(23)	31(2)	35(2)	44(2)	-1(2)	2(2)	-4(2)
C(24)	44(2)	39(2)	74(3)	-4(2)	11(3)	-13(2)
C(25)	31(2)	37(2)	43(2)	-8(2)	-2(2)	-11(2)
C(26)	35(2)	35(2)	50(3)	-8(2)	2(2)	-7(2)
C(27)	41(2)	42(2)	55(3)	-16(2)	5(2)	-7(2)
C(28)	72(4)	57(3)	49(3)	-18(3)	16(3)	-26(3)

C(29)	63(3)	58(3)	44(3)	-5(2)	-9(2)	-12(3)
C(30)	44(2)	47(2)	52(3)	-10(2)	-9(2)	-4(2)
C(31)	32(2)	37(2)	28(2)	-8(2)	-4(2)	1(2)
C(32)	28(2)	31(2)	32(2)	-2(1)	6(2)	-2(2)
C(33)	49(2)	37(2)	49(3)	-2(2)	4(2)	11(2)
C(34)	57(3)	44(3)	83(4)	-17(3)	10(3)	8(2)
C(35)	42(2)	49(3)	64(3)	-19(3)	-1(2)	16(2)
C(36)	68(4)	73(4)	79(4)	-21(3)	-15(3)	33(3)
C(37)	60(5)	110(7)	158(9)	-77(7)	-45(5)	42(5)
C(38)	42(3)	102(6)	152(9)	-57(6)	-2(5)	2(3)
C(39)	56(4)	89(5)	122(6)	-24(5)	24(4)	-12(3)
C(40)	49(3)	75(4)	71(4)	-15(3)	10(3)	-3(3)
C(41)	22(2)	43(2)	39(2)	2(2)	3(2)	1(2)
C(42)	23(2)	31(2)	41(2)	3(2)	-1(1)	-3(2)
C(43)	26(2)	52(3)	51(3)	15(2)	-8(2)	-2(2)
C(44)	34(2)	80(4)	69(3)	22(3)	-10(2)	7(2)
C(45)	36(2)	47(2)	39(2)	8(2)	-16(2)	-2(2)
C(46)	47(3)	51(3)	49(3)	12(2)	-7(2)	-1(2)
C(47)	71(4)	94(5)	35(3)	11(3)	-3(2)	15(3)
C(48)	87(5)	80(5)	50(3)	-14(3)	-22(3)	17(4)
C(49)	84(4)	62(4)	72(4)	-14(3)	-25(4)	-7(3)
C(50)	54(3)	60(4)	64(3)	7(3)	-9(3)	-16(3)
F(11)	79(3)	219(6)	105(3)	92(4)	-19(2)	5(3)
F(12)	187(6)	68(3)	170(5)	-12(3)	98(4)	-56(3)
F(13)	60(2)	142(4)	71(2)	33(2)	28(2)	20(2)
F(21)	215(6)	82(3)	85(3)	23(2)	-32(3)	-57(4)
F(22)	164(4)	90(3)	67(2)	-2(2)	-55(3)	-11(3)
F(23)	152(5)	118(4)	117(4)	-37(3)	31(4)	30(4)
F(31)	257(8)	126(4)	114(4)	50(3)	-114(5)	-39(5)
F(32)	201(6)	143(5)	84(3)	-35(3)	82(4)	-74(4)
F(33)	229(6)	78(3)	72(2)	4(2)	33(3)	-75(3)
F(41)	140(4)	103(3)	97(3)	-27(3)	63(3)	-43(3)
F(42)	203(8)	255(10)	161(6)	-112(7)	68(6)	-143(8)
F(43)	264(9)	79(4)	192(7)	6(4)	121(7)	23(4)
O(11)	35(2)	73(2)	69(2)	16(2)	4(2)	10(2)
O(12)	33(2)	54(2)	107(3)	13(2)	19(2)	2(2)
O(21)	64(2)	57(2)	67(2)	10(2)	-27(2)	1(2)
O(22)	111(4)	74(3)	71(3)	-7(2)	-50(3)	35(3)
O(31)	87(3)	60(2)	37(2)	8(2)	9(2)	31(2)
O(32)	117(4)	69(3)	59(2)	-22(2)	-14(2)	36(2)
O(41)	67(2)	63(2)	69(3)	7(2)	28(2)	-18(2)
O(42)	71(3)	46(2)	86(3)	3(2)	36(2)	-6(2)
C(11S)	42(3)	61(3)	56(3)	11(2)	6(2)	6(2)
C(12S)	23(2)	44(2)	51(2)	-7(2)	-6(2)	2(2)
C(21S)	100(5)	57(3)	53(3)	3(3)	-12(3)	-7(3)
C(22S)	52(3)	52(3)	51(3)	6(2)	-11(2)	4(2)
C(31S)	141(7)	74(4)	41(3)	-11(3)	28(4)	-39(4)
C(32S)	44(2)	43(2)	47(2)	-15(2)	-1(2)	5(2)
C(41S)	106(6)	64(4)	98(6)	-16(4)	54(5)	-28(4)
C(42S)	56(3)	48(3)	65(3)	18(3)	16(3)	-2(2)

***Table A.4.4.5** - Hydrogen coordinates (x 10^4) and isotropic displacement parameters ($Å^2$x 10^3) for C60 H73 Eu F12 N10 O13.*

	x	y	z	U(eq)
H(5)	8160	4248	118	40
H(6)	11009	5959	1988	39
H(7)	7198	7206	3580	44

H(8)	4190	5496	1613	46
H(1A)	7816	3263	1528	40
H(1B)	7733	3575	2124	40
H(2A)	9234	3591	1855	37
H(2B)	8987	4074	1341	37
H(3A)	9686	4250	2672	38
H(3B)	8645	4060	2709	38
H(4A)	9017	4917	3374	37
H(4B)	9396	5461	2928	37
H(5A)	7430	4993	3600	40
H(5B)	7516	4422	3120	40
H(6A)	6004	4739	3249	41
H(6B)	6234	5578	3153	41
H(7A)	5545	4039	2449	40
H(7B)	6587	3916	2559	40
H(8A)	6224	3489	1691	41
H(8B)	5835	4269	1531	41
H(11A)	6624	4497	843	39
H(11B)	7264	3800	812	39
H(13)	8862	5616	154	42
H(14A)	9509	5350	-672	73
H(14B)	8480	5112	-675	73
H(14C)	9245	4512	-608	73
H(16)	10214	6014	501	45
H(17)	11592	5825	908	60
H(18)	12173	4654	971	71
H(19)	11358	3668	657	72
H(20)	9966	3863	244	57
H(21A)	9827	4963	1453	35
H(21B)	10312	4816	2015	35
H(23)	10033	7206	1858	44
H(24A)	11870	7051	2163	63
H(24B)	11420	7818	2030	63
H(24C)	11515	7217	1570	63
H(26)	9185	7832	2490	48
H(27)	8767	8107	3371	55
H(28)	9531	7562	4084	71
H(29)	10714	6777	3926	66
H(30)	11153	6534	3033	57
H(31B)	8607	6382	3122	38
H(31C)	7943	6094	3579	38
H(33)	6442	7794	2690	54
H(34A)	5829	8664	3271	74
H(34B)	6853	8534	3428	74
H(34C)	6076	8176	3781	74
H(36)	5066	7584	2272	88
H(37)	3643	7034	2254	131
H(38)	3094	6443	2981	118
H(39)	3951	6357	3755	107
H(40)	5394	6871	3799	78
H(41A)	5386	5830	2517	42
H(41B)	4904	5075	2381	42
H(43)	5046	6284	846	52
H(44A)	3677	6253	384	73
H(44B)	3503	6435	1003	73
H(44C)	3313	5636	779	73
H(46)	5920	5915	125	59
H(47)	6467	5043	-468	80
H(48)	5904	3855	-443	87
H(49)	4802	3560	186	87
H(50)	4242	4425	770	71

***Table A.4.5.2** - Atomic coordinates (x 10^4) and equivalent isotropic displacement parameters ($Å^2$x 10^3) for C64 H76 Cl N14 Na O5. U(eq) is defined as one third of the trace of the orthogonalized U^{ij} tensor.*

	x	y	z	U(eq)
Na(1)	742(2)	102(2)	8781(1)	27(1)
O(1)	1613(5)	-580(4)	9359(2)	38(1)
O(2)	1630(5)	1431(4)	9051(2)	38(1)
O(3)	1592(5)	739(4)	8205(2)	38(1)
O(4)	1619(5)	-1267(4)	8524(2)	39(1)
N(1)	-578(6)	-8(4)	9405(2)	31(2)
N(2)	-583(6)	1571(4)	8845(2)	30(2)
N(3)	-675(6)	295(4)	8169(2)	30(2)
N(4)	-662(6)	-1281(5)	8719(2)	34(2)
N(5)	1698(6)	-724(5)	10010(2)	41(2)
N(6)	1789(6)	2963(4)	9110(2)	35(2)
N(7)	1562(6)	1065(5)	7556(2)	39(2)
N(8)	1463(7)	-2744(5)	8361(2)	46(2)
N(153)	2344(9)	-3752(6)	9348(3)	66(3)
N(253)	2887(10)	1315(7)	10354(2)	64(3)
N(353)	2995(8)	3867(6)	8275(3)	55(2)
N(453)	2780(8)	-948(6)	7182(2)	57(2)
C(1)	-1429(7)	699(6)	9394(3)	38(2)
C(2)	-1025(8)	1599(6)	9248(3)	37(2)
C(3)	-1496(7)	1578(6)	8565(2)	35(2)
C(4)	-1113(7)	1225(6)	8156(2)	38(2)
C(5)	-1561(7)	-363(5)	8190(2)	35(2)
C(6)	-1161(7)	-1296(6)	8329(3)	37(2)
C(7)	-1511(7)	-1229(6)	9018(2)	33(2)
C(8)	-1066(8)	-943(6)	9413(3)	44(2)
C(11)	168(7)	117(6)	9737(3)	40(2)
C(12)	1193(7)	-418(5)	9681(2)	32(2)
C(13)	2743(7)	-1209(6)	9971(3)	38(2)
C(14)	3175(11)	-1428(8)	10396(3)	66(3)
C(15)	2625(7)	-2089(6)	9753(3)	37(2)
C(21)	155(7)	2341(6)	8776(3)	34(2)
C(22)	1244(7)	2176(5)	8999(2)	32(2)
C(23)	2883(7)	2872(6)	9278(2)	36(2)
C(24)	3344(9)	3822(7)	9357(3)	50(2)
C(25)	2859(8)	2322(6)	9641(2)	37(2)
C(31)	39(7)	168(6)	7839(2)	35(2)
C(32)	1116(7)	685(6)	7894(3)	36(2)
C(33)	2680(8)	1408(6)	7566(3)	42(2)
C(34)	3089(9)	1585(8)	7153(3)	60(3)
C(35)	2800(8)	2246(6)	7825(3)	41(2)
C(41)	73(8)	-2079(5)	8766(3)	40(2)
C(42)	1106(8)	-1981(6)	8538(3)	37(2)
C(43)	2581(8)	-2745(6)	8175(3)	44(2)
C(44)	2855(10)	-3721(7)	8041(4)	67(3)
C(45)	2632(8)	-2120(6)	7837(3)	39(2)
C(151)	1708(9)	-2623(6)	9798(3)	50(3)
C(152)	1594(10)	-3439(6)	9582(4)	63(3)
C(154)	3272(8)	-3245(7)	9291(3)	52(3)
C(155)	4089(11)	-3619(8)	9053(4)	65(3)
C(156)	5054(12)	-3128(9)	8966(4)	83(4)
C(157)	5270(10)	-2250(9)	9169(4)	69(3)

C(158)	4475(8)	-1920(7)	9417(3)	51(3)
C(159)	3475(8)	-2417(6)	9485(3)	43(2)
C(251)	1997(9)	2354(7)	9892(3)	45(2)
C(252)	2032(12)	1843(9)	10257(3)	69(4)
C(254)	3767(10)	1264(6)	10104(3)	57(3)
C(255)	4683(15)	709(9)	10208(5)	91(5)
C(256)	5519(16)	623(9)	9955(6)	103(6)
C(257)	5585(10)	1069(9)	9605(4)	73(4)
C(258)	4729(9)	1594(8)	9494(3)	58(3)
C(259)	3766(8)	1763(6)	9736(3)	41(2)
C(351)	1962(8)	2901(7)	7842(3)	46(2)
C(352)	2135(9)	3697(7)	8069(3)	52(3)
C(354)	3848(8)	3216(6)	8267(3)	41(2)
C(355)	4786(9)	3387(7)	8491(3)	52(3)
C(356)	5641(10)	2794(9)	8489(4)	65(3)
C(357)	5608(9)	2015(8)	8260(4)	61(3)
C(358)	4696(8)	1820(7)	8043(3)	50(3)
C(359)	3767(8)	2437(7)	8048(3)	49(3)
C(451)	1782(10)	-1977(7)	7577(3)	56(3)
C(452)	1869(9)	-1440(8)	7259(3)	52(3)
C(454)	3628(8)	-1038(6)	7425(3)	44(2)
C(455)	4609(9)	-509(7)	7334(3)	52(3)
C(456)	5513(9)	-565(7)	7581(3)	54(3)
C(457)	5506(9)	-1112(6)	7909(3)	49(3)
C(458)	4567(8)	-1648(7)	7990(3)	48(3)
C(459)	3609(8)	-1601(6)	7754(3)	44(2)
Cl(1)	173(2)	568(2)	6765(1)	64(1)
O(2S)	1002(7)	4807(4)	8983(2)	58(2)
C(2N)	3761(8)	35(7)	8742(3)	53(3)
N(1N)	5884(7)	-36(6)	8777(3)	61(2)
C(1N)	4915(9)	-4(6)	8759(3)	49(2)
N(2A)	3791(9)	-140(7)	5788(3)	79(2)
C(3A)	3260(20)	3(17)	6063(6)	79(2)
C(4A)	2640(19)	67(18)	6433(6)	79(2)
N(2B)	3791(9)	-140(7)	5788(3)	79(2)
C(3B)	3100(20)	-410(20)	5993(8)	79(2)
C(4B)	2200(20)	-420(20)	6278(8)	79(2)

Table A.4.5.3 - Bond lengths [Å] and angles [°] for C64 H76 Cl N14 Na O5.

Na(1)-O(3)	2.409(6)	N(1)-C(8)	1.492(11)	N(7)-C(32)	1.391(11)
Na(1)-O(2)	2.410(6)	N(2)-C(21)	1.458(11)	N(7)-C(33)	1.439(12)
Na(1)-O(4)	2.434(6)	N(2)-C(3)	1.460(11)	N(8)-C(42)	1.344(11)
Na(1)-O(1)	2.455(6)	N(2)-C(2)	1.477(11)	N(8)-C(43)	1.492(12)
Na(1)-N(4)	2.650(7)	N(3)-C(31)	1.431(10)	N(153)-C(152)	1.292(15)
Na(1)-N(1)	2.669(7)	N(3)-C(5)	1.442(10)	N(153)-C(154)	1.358(14)
Na(1)-N(2)	2.693(7)	N(3)-C(4)	1.464(11)	N(253)-C(252)	1.332(17)
Na(1)-N(3)	2.718(7)	N(4)-C(7)	1.448(10)	N(253)-C(254)	1.365(16)
O(1)-C(12)	1.234(10)	N(4)-C(6)	1.463(11)	N(353)-C(352)	1.277(14)
O(2)-C(22)	1.201(10)	N(4)-C(41)	1.478(11)	N(353)-C(354)	1.403(12)
O(3)-C(32)	1.213(10)	N(5)-C(12)	1.356(11)	N(453)-C(454)	1.323(13)
O(4)-C(42)	1.217(10)	N(5)-C(13)	1.453(12)	N(453)-C(452)	1.340(14)
N(1)-C(1)	1.459(10)	N(6)-C(22)	1.382(10)	C(1)-C(2)	1.493(13)
N(1)-C(11)	1.463(11)	N(6)-C(23)	1.445(12)	C(3)-C(4)	1.560(12)

C(5)-C(6)	1.529(12)	O(3)-Na(1)-O(2)	79.1(2)	C(12)-N(5)-C(13)	118.5(7)
C(7)-C(8)	1.517(13)	O(3)-Na(1)-O(4)	80.8(2)	C(22)-N(6)-C(23)	117.8(7)
C(11)-C(12)	1.477(12)	O(2)-Na(1)-O(4)	127.8(2)	C(32)-N(7)-C(33)	118.9(7)
C(13)-C(15)	1.499(13)	O(3)-Na(1)-O(1)	129.5(2)	C(42)-N(8)-C(43)	118.9(8)
C(13)-C(14)	1.579(13)	O(2)-Na(1)-O(1)	80.2(2)	C(152)-N(153)-C(154)	118.2(9)
C(15)-C(151)	1.364(13)	O(4)-Na(1)-O(1)	76.7(2)	C(252)-N(253)-C(254)	118.5(9)
C(15)-C(159)	1.457(13)	O(3)-Na(1)-N(4)	120.2(2)	C(352)-N(353)-C(354)	116.9(9)
C(21)-C(22)	1.540(12)	O(2)-Na(1)-N(4)	159.1(2)	C(454)-N(453)-C(452)	117.2(9)
C(23)-C(25)	1.483(12)	O(4)-Na(1)-N(4)	67.5(2)	N(1)-C(1)-C(2)	114.1(7)
C(23)-C(24)	1.525(13)	O(1)-Na(1)-N(4)	91.5(2)	N(2)-C(2)-C(1)	114.0(7)
C(25)-C(251)	1.350(13)	O(3)-Na(1)-N(1)	158.7(2)	N(2)-C(3)-C(4)	111.3(7)
C(25)-C(259)	1.404(13)	O(2)-Na(1)-N(1)	90.4(2)	N(3)-C(4)-C(3)	113.0(7)
C(31)-C(32)	1.515(11)	O(4)-Na(1)-N(1)	119.9(2)	N(3)-C(5)-C(6)	112.5(7)
C(33)-C(35)	1.523(14)	O(1)-Na(1)-N(1)	65.5(2)	N(4)-C(6)-C(5)	113.5(7)
C(33)-C(34)	1.520(14)	N(4)-Na(1)-N(1)	68.7(2)	N(4)-C(7)-C(8)	113.3(7)
C(35)-C(351)	1.395(13)	O(3)-Na(1)-N(2)	90.5(2)	N(1)-C(8)-C(7)	112.0(7)
C(35)-C(359)	1.421(14)	O(2)-Na(1)-N(2)	65.4(2)	N(1)-C(11)-C(12)	110.2(7)
C(41)-C(42)	1.476(13)	O(4)-Na(1)-N(2)	161.5(2)	O(1)-C(12)-N(5)	119.5(8)
C(43)-C(45)	1.476(13)	O(1)-Na(1)-N(2)	120.9(2)	O(1)-C(12)-C(11)	124.1(8)
C(43)-C(44)	1.539(13)	N(4)-Na(1)-N(2)	103.9(2)	N(5)-C(12)-C(11)	116.3(7)
C(45)-C(451)	1.374(14)	N(1)-Na(1)-N(2)	68.2(2)	N(5)-C(13)-C(15)	112.6(7)
C(45)-C(459)	1.432(13)	O(3)-Na(1)-N(3)	66.2(2)	N(5)-C(13)-C(14)	107.6(8)
C(151)-C(152)	1.413(15)	O(2)-Na(1)-N(3)	119.4(2)	C(15)-C(13)-C(14)	108.3(8)
C(154)-C(155)	1.391(15)	O(4)-Na(1)-N(3)	94.6(2)	C(151)-C(15)-C(159)	116.8(9)
C(154)-C(159)	1.407(14)	O(1)-Na(1)-N(3)	159.0(2)	C(151)-C(15)-C(13)	121.1(9)
C(155)-C(156)	1.401(19)	N(4)-Na(1)-N(3)	67.5(2)	C(159)-C(15)-C(13)	122.1(8)
C(156)-C(157)	1.49(2)	N(1)-Na(1)-N(3)	104.4(2)	N(2)-C(21)-C(22)	108.5(6)
C(157)-C(158)	1.367(15)	N(2)-Na(1)-N(3)	66.8(2)	O(2)-C(22)-N(6)	122.5(8)
C(158)-C(159)	1.428(13)	C(12)-O(1)-Na(1)	117.8(5)	O(2)-C(22)-C(21)	123.1(7)
C(251)-C(252)	1.456(16)	C(22)-O(2)-Na(1)	120.6(5)	N(6)-C(22)-C(21)	114.3(7)
C(254)-C(255)	1.419(19)	C(32)-O(3)-Na(1)	119.4(6)	N(6)-C(23)-C(25)	111.5(7)
C(254)-C(259)	1.457(14)	C(42)-O(4)-Na(1)	118.3(6)	N(6)-C(23)-C(24)	108.6(7)
C(255)-C(256)	1.33(2)	C(1)-N(1)-C(11)	111.2(6)	C(25)-C(23)-C(24)	110.8(7)
C(256)-C(257)	1.37(2)	C(1)-N(1)-C(8)	112.2(7)	C(251)-C(25)-C(259)	118.3(8)
C(257)-C(258)	1.342(16)	C(11)-N(1)-C(8)	110.0(7)	C(251)-C(25)-C(23)	122.0(9)
C(258)-C(259)	1.447(15)	C(1)-N(1)-Na(1)	110.9(5)	C(259)-C(25)-C(23)	119.7(9)
C(351)-C(352)	1.419(15)	C(11)-N(1)-Na(1)	104.4(5)	N(3)-C(31)-C(32)	110.6(7)
C(354)-C(359)	1.371(14)	C(8)-N(1)-Na(1)	107.9(5)	O(3)-C(32)-N(7)	121.3(8)
C(354)-C(355)	1.390(14)	C(21)-N(2)-C(3)	110.3(6)	O(3)-C(32)-C(31)	123.2(8)
C(355)-C(356)	1.349(16)	C(21)-N(2)-C(2)	110.6(7)	N(7)-C(32)-C(31)	115.4(7)
C(356)-C(357)	1.386(17)	C(3)-N(2)-C(2)	109.9(7)	N(7)-C(33)-C(35)	112.7(7)
C(357)-C(358)	1.357(16)	C(21)-N(2)-Na(1)	104.1(5)	N(7)-C(33)-C(34)	109.9(8)
C(358)-C(359)	1.440(13)	C(3)-N(2)-Na(1)	113.5(5)	C(35)-C(33)-C(34)	111.9(8)
C(451)-C(452)	1.348(15)	C(2)-N(2)-Na(1)	108.2(4)	C(351)-C(35)-C(359)	115.9(9)
C(454)-C(459)	1.398(14)	C(31)-N(3)-C(5)	113.4(6)	C(351)-C(35)-C(33)	120.7(9)
C(454)-C(455)	1.449(15)	C(31)-N(3)-C(4)	108.5(7)	C(359)-C(35)-C(33)	123.3(8)
C(455)-C(456)	1.381(15)	C(5)-N(3)-C(4)	111.0(7)	N(4)-C(41)-C(42)	111.8(7)
C(456)-C(457)	1.382(14)	C(31)-N(3)-Na(1)	102.5(5)	O(4)-C(42)-N(8)	122.4(9)
C(457)-C(458)	1.405(14)	C(5)-N(3)-Na(1)	110.9(5)	O(4)-C(42)-C(41)	122.3(8)
C(458)-C(459)	1.411(14)	C(4)-N(3)-Na(1)	110.3(4)	N(8)-C(42)-C(41)	115.3(8)
C(2N)-C(1N)	1.393(15)	C(7)-N(4)-C(6)	110.8(7)	C(45)-C(43)-N(8)	111.8(8)
N(1N)-C(1N)	1.172(13)	C(7)-N(4)-C(41)	112.9(7)	C(45)-C(43)-C(44)	109.7(9)
N(2A)-C(3A)	1.162(15)	C(6)-N(4)-C(41)	109.4(7)	N(8)-C(43)-C(44)	108.8(8)
C(3A)-C(4A)	1.471(17)	C(7)-N(4)-Na(1)	110.8(5)	C(451)-C(45)-C(459)	113.8(9)
C(3B)-C(4B)	1.457(18)	C(6)-N(4)-Na(1)	110.3(5)	C(451)-C(45)-C(43)	124.9(10)
		C(41)-N(4)-Na(1)	102.4(5)	C(459)-C(45)-C(43)	121.4(9)

C(15)-C(151)-C(152)	120.5(10)	C(256)-C(255)-C(254)	118.7(14)	C(354)-C(359)-C(358)	118.4(10)
N(153)-C(152)-C(151)	123.8(10)	C(255)-C(256)-C(257)	124.5(14)	C(35)-C(359)-C(358)	120.6(10)
N(153)-C(154)-C(155)	116.9(10)	C(258)-C(257)-C(256)	118.5(14)	C(452)-C(451)-C(45)	123.7(11)
N(153)-C(154)-C(159)	123.2(10)	C(257)-C(258)-C(259)	123.7(11)	N(453)-C(452)-C(451)	122.5(10)
C(155)-C(154)-C(159)	119.6(10)	C(25)-C(259)-C(258)	126.4(9)	N(453)-C(454)-C(459)	123.5(10)
C(154)-C(155)-C(156)	120.7(11)	C(25)-C(259)-C(254)	119.6(10)	N(453)-C(454)-C(455)	116.3(9)
C(155)-C(156)-C(157)	119.4(11)	C(258)-C(259)-C(254)	114.0(10)	C(459)-C(454)-C(455)	120.2(9)
C(158)-C(157)-C(156)	118.3(11)	C(35)-C(351)-C(352)	118.9(9)	C(456)-C(455)-C(454)	118.8(9)
C(157)-C(158)-C(159)	120.8(10)	N(353)-C(352)-C(351)	125.5(9)	C(457)-C(456)-C(455)	121.8(10)
C(154)-C(159)-C(158)	120.7(9)	C(359)-C(354)-C(355)	120.7(9)	C(456)-C(457)-C(458)	119.3(10)
C(154)-C(159)-C(15)	117.4(8)	C(359)-C(354)-N(353)	121.7(9)	C(457)-C(458)-C(459)	121.3(10)
C(158)-C(159)-C(15)	121.9(9)	C(355)-C(354)-N(353)	117.6(9)	C(454)-C(459)-C(458)	118.4(9)
C(25)-C(251)-C(252)	120.3(11)	C(356)-C(355)-C(354)	120.2(11)	C(454)-C(459)-C(45)	119.3(9)
N(253)-C(252)-C(251)	122.4(12)	C(355)-C(356)-C(357)	120.9(12)	C(458)-C(459)-C(45)	122.3(9)
N(253)-C(254)-C(255)	118.6(12)	C(358)-C(357)-C(356)	120.4(10)	N(1N)-C(1N)-C(2N)	179.6(12)
N(253)-C(254)-C(259)	120.9(10)	C(357)-C(358)-C(359)	119.4(10)	N(2A)-C(3A)-C(4A)	172(3)
C(255)-C(254)-C(259)	120.4(13)	C(354)-C(359)-C(35)	121.0(9)		

Table A.4.5.4 - Anisotropic displacement parameters ($Å^2 x\ 10^3$) for C64 H76 Cl N14 Na O5. The anisotropic displacement factor exponent takes the form: $-2p^2[\ h^2\ a^{*2}U^{11} + ... + 2\ h\ k\ a^*\ b^*\ U^{12}\ ]$

	U^{11}	U^{22}	U^{33}	U^{23}	U^{13}	U^{12}
Na(1)	34(2)	21(1)	26(2)	-4(1)	-2(1)	0(1)
O(1)	37(3)	37(3)	40(4)	8(3)	-2(3)	5(3)
O(2)	50(4)	25(3)	40(3)	-4(3)	-14(3)	5(3)
O(3)	36(3)	48(3)	29(3)	6(3)	-4(3)	-7(3)
O(4)	45(4)	24(3)	48(4)	-6(3)	5(3)	-7(3)
N(1)	42(4)	29(4)	22(3)	-1(3)	3(3)	0(3)
N(2)	35(4)	25(3)	29(4)	2(3)	-3(3)	1(3)
N(3)	39(4)	20(3)	32(4)	-12(3)	-6(3)	0(3)
N(4)	27(4)	41(4)	33(4)	-7(3)	6(3)	-5(3)
N(5)	36(4)	50(4)	35(4)	2(4)	-8(3)	6(4)
N(6)	47(4)	24(3)	35(4)	3(3)	-9(3)	-3(3)
N(7)	34(4)	51(4)	33(4)	13(3)	0(3)	0(3)
N(8)	54(5)	26(4)	58(5)	-9(4)	23(4)	1(3)
N(153)	73(7)	31(4)	94(7)	1(5)	-8(6)	7(5)
N(253)	98(8)	63(6)	32(5)	0(4)	-9(5)	-38(6)
N(353)	61(6)	46(5)	59(6)	10(4)	10(5)	9(4)
N(453)	66(6)	62(6)	43(5)	-3(4)	2(5)	17(5)
C(1)	33(5)	47(5)	35(5)	-1(4)	7(4)	12(4)
C(2)	40(5)	33(5)	38(5)	-8(4)	0(4)	14(4)
C(3)	33(5)	43(5)	29(5)	-2(4)	-2(4)	3(4)
C(4)	35(5)	53(5)	27(5)	4(4)	-14(4)	-3(4)
C(5)	34(4)	40(5)	30(4)	-7(4)	-6(4)	-6(4)
C(6)	32(5)	37(5)	42(5)	-10(4)	-9(4)	-6(4)
C(7)	29(4)	38(4)	33(5)	-2(4)	8(4)	-7(4)
C(8)	39(5)	45(5)	50(6)	9(4)	0(5)	-2(4)
C(11)	46(5)	38(5)	37(5)	-7(4)	-3(4)	8(4)
C(12)	37(5)	26(4)	32(5)	-2(4)	4(4)	0(4)
C(13)	33(5)	37(5)	45(5)	13(4)	-9(4)	-5(4)
C(14)	78(8)	75(8)	46(6)	20(6)	-35(6)	-3(6)
C(15)	40(5)	28(4)	42(5)	21(4)	0(4)	1(4)
C(21)	33(5)	36(5)	34(5)	4(4)	-6(4)	4(4)

C(22)	43(5)	17(4)	35(5)	-7(3)	-5(4)	-6(4)
C(23)	38(5)	36(5)	33(5)	-6(4)	3(4)	-7(4)
C(24)	47(6)	55(6)	46(6)	-2(5)	-1(5)	-9(5)
C(25)	48(5)	31(5)	31(5)	-2(4)	-11(4)	-3(4)
C(31)	36(5)	36(5)	31(5)	-8(4)	6(4)	-16(4)
C(32)	34(5)	33(5)	40(5)	-6(4)	-10(4)	3(4)
C(33)	40(5)	35(5)	51(6)	16(4)	9(4)	9(4)
C(34)	50(6)	63(7)	66(7)	22(6)	20(5)	4(5)
C(35)	45(5)	34(5)	43(5)	19(4)	8(5)	0(4)
C(41)	48(5)	28(4)	44(5)	-4(4)	5(5)	3(4)
C(42)	48(5)	27(5)	37(5)	1(4)	-9(4)	-1(4)
C(43)	38(5)	35(5)	57(6)	-4(5)	11(5)	3(4)
C(44)	53(6)	44(6)	102(9)	-31(6)	19(6)	7(5)
C(45)	51(6)	27(4)	40(5)	-16(4)	-2(4)	12(4)
C(151)	45(6)	40(5)	65(7)	18(5)	-2(5)	7(5)
C(152)	51(6)	27(5)	110(10)	-4(6)	-14(7)	-12(5)
C(154)	35(5)	44(6)	77(7)	8(5)	1(5)	11(5)
C(155)	77(8)	47(6)	72(8)	8(6)	7(7)	13(6)
C(156)	84(10)	79(9)	85(9)	33(8)	28(8)	39(8)
C(157)	56(7)	79(9)	71(8)	25(7)	4(6)	7(6)
C(158)	43(6)	41(5)	68(7)	13(5)	2(5)	6(4)
C(159)	43(5)	25(4)	62(6)	19(4)	-5(5)	2(4)
C(251)	52(6)	54(6)	29(5)	0(4)	-10(5)	-14(5)
C(252)	89(10)	71(8)	48(7)	-9(6)	6(7)	-39(8)
C(254)	87(8)	26(5)	56(7)	4(5)	-41(7)	-13(5)
C(255)	124(13)	47(7)	100(12)	7(7)	-86(11)	-25(9)
C(256)	106(13)	52(8)	152(17)	-8(10)	-88(13)	8(9)
C(257)	58(7)	72(8)	88(10)	-15(7)	-32(7)	14(6)
C(258)	49(6)	79(7)	45(6)	-17(5)	-12(5)	-4(6)
C(259)	61(6)	33(5)	30(5)	-6(4)	-18(5)	-20(5)
C(351)	35(5)	48(6)	55(6)	13(5)	7(5)	17(4)
C(352)	49(6)	40(6)	67(7)	23(5)	19(6)	12(5)
C(354)	48(5)	41(5)	34(5)	12(4)	7(5)	-1(4)
C(355)	52(6)	52(6)	53(6)	8(5)	3(5)	-6(5)
C(356)	50(7)	82(9)	64(7)	30(7)	6(6)	0(6)
C(357)	51(6)	52(6)	82(8)	25(6)	15(6)	15(5)
C(358)	34(5)	52(6)	63(7)	16(5)	6(5)	12(4)
C(359)	38(5)	51(6)	57(6)	26(5)	13(5)	-6(4)
C(451)	58(7)	56(6)	56(7)	-22(6)	-10(6)	15(5)
C(452)	43(6)	76(7)	36(6)	-15(5)	-5(5)	13(5)
C(454)	56(6)	49(6)	27(5)	-3(4)	0(5)	19(5)
C(455)	60(7)	44(6)	52(6)	10(5)	22(6)	16(5)
C(456)	52(6)	52(6)	57(7)	-4(5)	8(5)	4(5)
C(457)	52(6)	41(5)	55(6)	-7(5)	21(5)	-3(5)
C(458)	49(6)	55(6)	40(5)	-11(4)	0(5)	13(5)
C(459)	45(6)	37(5)	49(6)	-15(4)	12(5)	1(4)
Cl(1)	73(2)	63(2)	56(2)	-5(1)	-13(1)	12(1)
O(2S)	85(5)	37(4)	53(4)	4(3)	-3(4)	-2(4)
C(2N)	48(6)	60(6)	52(6)	-4(5)	6(5)	-2(5)
N(1N)	44(5)	74(6)	65(6)	3(5)	2(5)	7(5)
C(1N)	66(8)	41(5)	39(5)	3(5)	-8(5)	13(5)

***Table A.4.5.5** - Hydrogen coordinates (x 10^4) and isotropic displacement parameters ($Å^2$x 10^3) for C64 H76 Cl N14 Na O5.*

	x	y	z	U(eq)
H(5A)	1400	-631	10241	49
H(6A)	1481	3502	9079	42
H(7A)	1168	1095	7340	47
H(8A)	1044	-3235	8355	55
H(1A)	-1729	782	9661	46
H(1B)	-2044	491	9225	46
H(2A)	-1645	2040	9257	44
H(2B)	-436	1823	9425	44
H(3A)	-1784	2207	8538	42
H(3B)	-2105	1188	8663	42
H(4A)	-1750	1245	7974	46
H(4B)	-534	1638	8053	46
H(5B)	-1903	-427	7928	42
H(5C)	-2138	-136	8371	42
H(6B)	-1798	-1722	8331	45
H(6C)	-609	-1533	8141	45
H(7B)	-1870	-1832	9043	40
H(7C)	-2085	-787	8934	40
H(8B)	-1675	-960	9607	53
H(8C)	-491	-1382	9498	53
H(11A)	-207	-80	9980	48
H(11B)	357	771	9764	48
H(13A)	3293	-811	9834	46
H(14A)	3258	-859	10543	100
H(14B)	3894	-1737	10380	100
H(14C)	2642	-1825	10529	100
H(21A)	-197	2911	8867	41
H(21B)	308	2400	8493	41
H(23A)	3375	2561	9084	43
H(24A)	3366	4169	9113	74
H(24B)	4095	3771	9464	74
H(24C)	2866	4136	9546	74
H(31A)	-338	386	7600	41
H(31B)	199	-489	7806	41
H(33A)	3159	919	7680	51
H(34A)	3001	1031	6996	90
H(34B)	3873	1759	7161	90
H(34C)	2655	2080	7037	90
H(41A)	-324	-2634	8679	48
H(41B)	260	-2154	9045	48
H(43A)	3144	-2549	8372	52
H(44A)	3593	-3732	7921	100
H(44B)	2302	-3923	7850	100
H(44C)	2844	-4131	8267	100
H(15B)	1142	-2445	9975	75
H(15C)	927	-3777	9611	94
H(15D)	3991	-4213	8948	98
H(15E)	5566	-3354	8778	124
H(15F)	5942	-1926	9128	103
H(15G)	4590	-1354	9545	77
H(25B)	1364	2712	9831	67

H(25C)	1423	1888	10432	104
H(25D)	4701	404	10453	136
H(25E)	6109	225	10023	155
H(25F)	6222	1009	9444	109
H(25G)	4757	1869	9243	87
H(35B)	1287	2814	7704	69
H(35C)	1563	4143	8068	78
H(35D)	4826	3923	8646	79
H(35E)	6274	2912	8646	98
H(35F)	6227	1615	8255	92
H(35G)	4671	1282	7889	74
H(45B)	1094	-2274	7624	85
H(45C)	1261	-1408	7083	77
H(45D)	4631	-132	7108	78
H(45E)	6157	-217	7523	81
H(45F)	6129	-1126	8079	74
H(45G)	4578	-2049	8207	72
H(1)	3456	18	9007	95
H(2)	3482	-487	8593	95
H(3)	3534	602	8613	95

***Table A.4.6.2** - Atomic coordinates (x 10^4) and equivalent isotropic displacement parameters ($Å^2$x 10^3) for C68 H75 F3 N9 Na O6. U(eq) is defined as one third of the trace of the orthogonalized U^{ij} tensor.*

	x	y	z	U(eq)
Na	2585(1)	4916(1)	4620(1)	34(1)
O(1)	3955(3)	5436(2)	4163(2)	38(1)
O(2)	1985(3)	6096(2)	4177(2)	40(1)
O(3)	1179(3)	4463(2)	4210(2)	39(1)
O(4)	3115(3)	3692(3)	4215(2)	40(1)
N(1)	4015(3)	5037(3)	5298(2)	31(1)
N(2)	2519(3)	6197(3)	5299(2)	31(1)
N(3)	1205(3)	4863(3)	5351(2)	32(1)
N(4)	2714(3)	3706(3)	5356(2)	31(1)
N(5)	5448(3)	5627(3)	4191(2)	36(1)
N(6)	1744(3)	7393(3)	4169(2)	41(1)
N(7)	-280(3)	4153(3)	4303(2)	36(1)
N(8)	3385(3)	2390(3)	4257(2)	38(1)
C(1)	4096(4)	5833(3)	5516(3)	36(2)
C(2)	3223(4)	6170(4)	5728(3)	38(2)
C(3)	1629(4)	6238(4)	5547(3)	38(2)
C(4)	1288(4)	5473(3)	5775(3)	35(2)
C(5)	1165(4)	4085(3)	5608(3)	36(2)
C(6)	2054(4)	3774(4)	5802(2)	34(2)
C(7)	3628(4)	3683(3)	5583(2)	32(2)
C(8)	3969(4)	4479(3)	5764(3)	34(2)
C(11)	4750(4)	4865(4)	4931(3)	41(2)
C(12)	4679(4)	5338(3)	4391(3)	36(2)
C(13)	5456(4)	6008(4)	3641(3)	38(2)
C(14)	6407(4)	6208(5)	3467(3)	55(2)
C(15)	4870(4)	6736(4)	3630(2)	37(2)
C(21)	2660(4)	6851(4)	4919(2)	39(2)
C(22)	2100(4)	6742(4)	4387(2)	33(2)
C(23)	1259(4)	7359(4)	3636(3)	41(2)
C(24)	1076(4)	8185(4)	3430(3)	47(2)
C(25)	400(4)	6880(4)	3690(3)	39(2)
C(31)	413(4)	4988(4)	5004(2)	39(2)
C(32)	476(4)	4513(3)	4475(3)	34(2)
C(33)	-307(4)	3779(4)	3748(2)	33(2)
C(34)	-1271(4)	3564(4)	3620(3)	47(2)
C(35)	298(4)	3084(4)	3716(3)	37(2)
C(41)	2552(4)	3005(3)	5013(2)	34(2)
C(42)	3049(4)	3057(4)	4461(3)	35(2)
C(43)	3752(4)	2393(4)	3678(2)	38(2)
C(44)	3929(4)	1540(4)	3503(3)	46(2)
C(45)	4596(4)	2898(4)	3642(3)	37(2)
C(151)	4905(4)	7244(4)	4070(3)	42(2)
C(152)	4380(5)	7932(4)	4076(3)	50(2)
C(153)	3826(5)	8095(4)	3636(3)	48(2)
C(154)	3761(4)	7581(4)	3173(3)	43(2)
C(155)	3200(4)	7737(4)	2713(3)	42(2)
C(156)	3139(4)	7234(4)	2264(3)	48(2)
C(157)	3668(4)	6574(4)	2256(3)	43(2)
C(158)	4218(4)	6402(4)	2691(3)	48(2)
C(159)	4292(4)	6895(4)	3161(2)	34(2)
C(251)	-119(4)	6942(4)	4164(3)	45(2)
C(252)	-889(4)	6510(4)	4237(3)	51(2)
C(253)	-1164(4)	5995(4)	3837(3)	52(2)
C(254)	-691(5)	5921(4)	3334(3)	51(2)
C(255)	-969(6)	5421(4)	2889(4)	69(3)
C(256)	-509(6)	5347(5)	2404(4)	74(3)
C(257)	274(6)	5794(5)	2331(3)	65(2)

C(258)	565(4)	6294(4)	2737(3)	51(2)
C(259)	110(4)	6381(4)	3249(3)	46(2)
C(351)	396(4)	2580(4)	4167(3)	41(2)
C(352)	941(4)	1900(4)	4129(3)	53(2)
C(353)	1395(4)	1744(4)	3650(3)	45(2)
C(354)	1343(4)	2233(4)	3182(3)	43(2)
C(355)	1826(4)	2084(4)	2675(3)	47(2)
C(356)	1762(5)	2563(4)	2229(3)	52(2)
C(357)	1208(5)	3221(4)	2248(3)	50(2)
C(358)	727(4)	3391(4)	2722(3)	41(2)
C(359)	779(4)	2910(4)	3203(3)	40(2)
C(451)	5200(4)	2903(4)	4080(3)	42(2)
C(452)	5964(4)	3379(4)	4056(3)	46(2)
C(453)	6110(4)	3861(4)	3613(3)	45(2)
C(454)	5518(4)	3856(4)	3151(3)	46(2)
C(455)	5658(5)	4356(4)	2668(3)	54(2)
C(456)	5082(6)	4347(4)	2233(3)	60(2)
C(457)	4347(5)	3847(5)	2236(3)	55(2)
C(458)	4173(5)	3365(4)	2688(3)	49(2)
C(459)	4757(4)	3366(4)	3159(3)	41(2)
F(1)	6835(4)	5027(3)	5789(2)	105(2)
F(2)	8201(4)	5185(4)	5821(3)	118(2)
F(3)	7411(4)	5957(4)	5341(3)	121(2)
O(1S)	7196(3)	4882(3)	4550(2)	63(1)
O(2S)	8096(3)	4111(3)	5043(2)	50(1)
N(1S)	2644(4)	5046(3)	7034(2)	50(2)
C(1S)	7518(4)	5191(4)	5455(3)	44(2)
C(2S)	7614(4)	4693(4)	4974(3)	36(2)
C(3S)	2510(5)	5128(4)	8112(3)	52(2)
C(4S)	2578(4)	5079(4)	7509(3)	43(2)

Table A.4.6.3 -. Bond lengths [Å] and angles [°] for C68 H75 F3 N9 Na O6.

Na-O(4)	2.443(5)	N(6)-C(23)	1.469(8)	C(45)-C(451)	1.384(8)
Na-O(3)	2.453(4)	N(7)-C(32)	1.356(7)	C(45)-C(459)	1.427(9)
Na-O(2)	2.454(5)	N(7)-C(33)	1.472(7)	C(151)-C(152)	1.418(9)
Na-O(1)	2.493(4)	N(8)-C(42)	1.342(8)	C(152)-C(153)	1.370(9)
Na-N(1)	2.700(5)	N(8)-C(43)	1.489(7)	C(153)-C(154)	1.418(9)
Na-N(3)	2.712(5)	C(1)-C(2)	1.520(8)	C(154)-C(155)	1.412(9)
Na-N(4)	2.728(5)	C(3)-C(4)	1.510(8)	C(154)-C(159)	1.420(9)
Na-N(2)	2.733(5)	C(5)-C(6)	1.510(8)	C(155)-C(156)	1.379(9)
O(1)-C(12)	1.227(7)	C(7)-C(8)	1.522(8)	C(156)-C(157)	1.383(9)
O(2)-C(22)	1.228(7)	C(11)-C(12)	1.528(8)	C(157)-C(158)	1.360(9)
O(3)-C(32)	1.233(7)	C(13)-C(14)	1.527(8)	C(158)-C(159)	1.410(9)
O(4)-C(42)	1.239(7)	C(13)-C(15)	1.527(9)	C(251)-C(252)	1.383(9)
N(1)-C(11)	1.441(7)	C(15)-C(151)	1.365(8)	C(252)-C(253)	1.365(10)
N(1)-C(1)	1.465(7)	C(15)-C(159)	1.443(8)	C(253)-C(254)	1.402(10)
N(1)-C(8)	1.470(7)	C(21)-C(22)	1.536(8)	C(254)-C(255)	1.428(11)
N(2)-C(21)	1.458(7)	C(23)-C(24)	1.524(9)	C(254)-C(259)	1.453(10)
N(2)-C(3)	1.463(7)	C(23)-C(25)	1.536(9)	C(255)-C(256)	1.354(12)
N(2)-C(2)	1.473(7)	C(25)-C(251)	1.380(9)	C(256)-C(257)	1.415(12)
N(3)-C(4)	1.461(7)	C(25)-C(259)	1.425(9)	C(257)-C(258)	1.365(10)
N(3)-C(31)	1.467(7)	C(31)-C(32)	1.507(8)	C(258)-C(259)	1.410(9)
N(3)-C(5)	1.469(7)	C(33)-C(35)	1.501(8)	C(351)-C(352)	1.427(9)
N(4)-C(6)	1.459(7)	C(33)-C(34)	1.525(8)	C(352)-C(353)	1.359(9)
N(4)-C(41)	1.475(7)	C(35)-C(351)	1.388(8)	C(353)-C(354)	1.400(9)
N(4)-C(7)	1.476(7)	C(35)-C(359)	1.456(9)	C(354)-C(355)	1.436(9)
N(5)-C(12)	1.344(7)	C(41)-C(42)	1.519(8)	C(354)-C(359)	1.438(9)
N(5)-C(13)	1.468(7)	C(43)-C(45)	1.538(9)	C(355)-C(356)	1.350(10)
N(6)-C(22)	1.342(7)	C(43)-C(44)	1.544(9)	C(356)-C(357)	1.403(9)

C(357)-C(358)	1.373(9)	C(2)-N(2)-Na	111.2(3)	N(4)-C(7)-H(7B)	108.9(3)
C(358)-C(359)	1.415(9)	C(4)-N(3)-C(31)	110.9(4)	C(8)-C(7)-H(7B)	108.9(3)
C(451)-C(452)	1.409(9)	C(4)-N(3)-C(5)	111.2(5)	N(4)-C(7)-H(7A)	108.9(3)
C(452)-C(453)	1.362(9)	C(31)-N(3)-C(5)	109.6(5)	C(8)-C(7)-H(7A)	108.9(3)
C(453)-C(454)	1.418(9)	C(4)-N(3)-Na	111.0(3)	H(7B)-C(7)-H(7A)	107.8
C(454)-C(459)	1.419(9)	C(31)-N(3)-Na	104.5(3)	N(1)-C(8)-C(7)	112.6(5)
C(454)-C(455)	1.453(9)	C(5)-N(3)-Na	109.4(3)	N(1)-C(8)-H(8B)	109.1(3)
C(455)-C(456)	1.351(10)	C(6)-N(4)-C(41)	111.1(4)	C(7)-C(8)-H(8B)	109.1(3)
C(456)-C(457)	1.397(10)	C(6)-N(4)-C(7)	111.5(4)	N(1)-C(8)-H(8A)	109.1(3)
C(457)-C(458)	1.384(10)	C(41)-N(4)-C(7)	109.6(5)	C(7)-C(8)-H(8A)	109.1(3)
C(458)-C(459)	1.427(9)	C(6)-N(4)-Na	111.2(3)	H(8B)-C(8)-H(8A)	107.8
F(1)-C(1S)	1.330(8)	C(41)-N(4)-Na	104.4(3)	N(1)-C(11)-C(12)	110.6(5)
F(2)-C(1S)	1.348(8)	C(7)-N(4)-Na	108.9(3)	N(1)-C(11)-H(11B)	109.5(3)
F(3)-C(1S)	1.350(8)	C(12)-N(5)-C(13)	119.3(5)	C(12)-C(11)-H(11B)	109.5(3)
O(1S)-C(2S)	1.237(7)	C(12)-N(5)-H(5C)	120.4(3)	N(1)-C(11)-H(11A)	109.5(3)
O(2S)-C(2S)	1.243(7)	C(13)-N(5)-H(5C)	120.4(3)	C(12)-C(11)-H(11A)	109.5(3)
N(1S)-C(4S)	1.140(8)	C(22)-N(6)-C(23)	120.1(5)	H(11B)-C(11)-H(11A)	108.1
C(1S)-C(2S)	1.440(9)	C(22)-N(6)-H(6C)	119.9(3)	O(1)-C(12)-N(5)	123.6(5)
C(3S)-C(4S)	1.448(9)	C(23)-N(6)-H(6C)	119.9(3)	O(1)-C(12)-C(11)	120.6(5)
O(4)-Na-O(3)	81.45(15)	C(32)-N(7)-C(33)	119.6(5)	N(5)-C(12)-C(11)	115.8(5)
O(4)-Na-O(2)	131.0(2)	C(32)-N(7)-H(7C)	120.2(3)	N(5)-C(13)-C(14)	110.5(5)
O(3)-Na-O(2)	76.87(15)	C(33)-N(7)-H(7C)	120.2(3)	N(5)-C(13)-C(15)	111.9(5)
O(4)-Na-O(1)	82.23(15)	C(42)-N(8)-C(43)	118.2(5)	C(14)-C(13)-C(15)	110.6(5)
O(3)-Na-O(1)	130.5(2)	C(42)-N(8)-H(8C)	120.9(4)	N(5)-C(13)-H(13)	107.9(3)
O(2)-Na-O(1)	79.60(15)	C(43)-N(8)-H(8C)	120.9(3)	C(14)-C(13)-H(13)	107.9(4)
O(4)-Na-N(1)	92.5(2)	N(1)-C(1)-C(2)	113.6(5)	C(15)-C(13)-H(13)	107.9(3)
O(3)-Na-N(1)	161.6(2)	N(1)-C(1)-H(1B)	108.8(3)	C(13)-C(14)-H(14C)	109.5(4)
O(2)-Na-N(1)	119.2(2)	C(2)-C(1)-H(1B)	108.8(3)	C(13)-C(14)-H(14B)	109.5(4)
O(1)-Na-N(1)	65.06(14)	N(1)-C(1)-H(1A)	108.9(3)	H(14C)-C(14)-H(14B)	109.5
O(4)-Na-N(3)	118.4(2)	C(2)-C(1)-H(1A)	108.8(3)	C(13)-C(14)-H(14A)	109.5(3)
O(3)-Na-N(3)	65.72(15)	H(1B)-C(1)-H(1A)	107.7	H(14C)-C(14)-H(14A)	109.5
O(2)-Na-N(3)	91.5(2)	N(2)-C(2)-C(1)	113.6(5)	H(14B)-C(14)-H(14A)	109.5
O(1)-Na-N(3)	157.6(2)	N(2)-C(2)-H(2B)	108.8(3)	C(151)-C(15)-C(159)	120.0(6)
N(1)-Na-N(3)	102.9(2)	C(1)-C(2)-H(2B)	108.8(3)	C(151)-C(15)-C(13)	119.1(6)
O(4)-Na-N(4)	65.11(15)	N(2)-C(2)-H(2A)	108.8(3)	C(159)-C(15)-C(13)	120.9(6)
O(3)-Na-N(4)	94.5(2)	C(1)-C(2)-H(2A)	108.8(3)	N(2)-C(21)-C(22)	110.0(5)
O(2)-Na-N(4)	158.6(2)	H(2B)-C(2)-H(2A)	107.7	N(2)-C(21)-H(21B)	109.7(3)
O(1)-Na-N(4)	119.7(2)	N(2)-C(3)-C(4)	114.5(5)	C(22)-C(21)-H(21B)	109.7(3)
N(1)-Na-N(4)	67.32(15)	N(2)-C(3)-H(3B)	108.6(3)	N(2)-C(21)-H(21A)	109.7(3)
N(3)-Na-N(4)	67.22(15)	C(4)-C(3)-H(3B)	108.6(3)	C(22)-C(21)-H(21A)	109.7(3)
O(4)-Na-N(2)	159.5(2)	N(2)-C(3)-H(3A)	108.6(3)	H(21B)-C(21)-H(21A)	108.2
O(3)-Na-N(2)	117.4(2)	C(4)-C(3)-H(3A)	108.6(3)	O(2)-C(22)-N(6)	122.3(5)
O(2)-Na-N(2)	65.24(14)	H(3B)-C(3)-H(3A)	107.6	O(2)-C(22)-C(21)	121.7(5)
O(1)-Na-N(2)	90.2(2)	N(3)-C(4)-C(3)	113.5(5)	N(6)-C(22)-C(21)	116.0(5)
N(1)-Na-N(2)	67.04(15)	N(3)-C(4)-H(4B)	108.9(3)	N(6)-C(23)-C(24)	109.5(5)
N(3)-Na-N(2)	67.44(15)	C(3)-C(4)-H(4B)	108.9(3)	N(6)-C(23)-C(25)	111.4(5)
N(4)-Na-N(2)	103.3(2)	N(3)-C(4)-H(4A)	108.9(3)	C(24)-C(23)-C(25)	111.8(5)
C(12)-O(1)-Na	119.3(4)	C(3)-C(4)-H(4A)	108.9(3)	N(6)-C(23)-H(23)	108.0(3)
C(22)-O(2)-Na	121.0(4)	H(4B)-C(4)-H(4A)	107.7	C(24)-C(23)-H(23)	108.0(4)
C(32)-O(3)-Na	120.7(4)	N(3)-C(5)-C(6)	114.3(5)	C(25)-C(23)-H(23)	108.0(4)
C(42)-O(4)-Na	122.7(4)	N(3)-C(5)-H(5B)	108.7(3)	C(23)-C(24)-H(24C)	109.5(3)
C(11)-N(1)-C(1)	110.1(5)	C(6)-C(5)-H(5B)	108.7(3)	C(23)-C(24)-H(24B)	109.5(4)
C(11)-N(1)-C(8)	111.4(4)	N(3)-C(5)-H(5A)	108.7(3)	H(24C)-C(24)-H(24B)	109.5
C(1)-N(1)-C(8)	109.9(5)	C(6)-C(5)-H(5A)	108.7(3)	C(23)-C(24)-H(24A)	109.5(4)
C(11)-N(1)-Na	103.2(3)	H(5B)-C(5)-H(5A)	107.6	H(24C)-C(24)-H(24A)	109.5
C(1)-N(1)-Na	110.6(3)	N(4)-C(6)-C(5)	113.9(5)	H(24B)-C(24)-H(24A)	109.5
C(8)-N(1)-Na	111.5(3)	N(4)-C(6)-H(6B)	108.8(3)	C(251)-C(25)-C(259)	118.8(6)
C(21)-N(2)-C(3)	110.3(5)	C(5)-C(6)-H(6B)	108.8(3)	C(251)-C(25)-C(23)	120.2(6)
C(21)-N(2)-C(2)	110.7(5)	N(4)-C(6)-H(6A)	108.8(3)	C(259)-C(25)-C(23)	121.0(6)
C(3)-N(2)-C(2)	112.1(4)	C(5)-C(6)-H(6A)	108.8(3)	N(3)-C(31)-C(32)	110.2(5)
C(21)-N(2)-Na	104.0(3)	H(6B)-C(6)-H(6A)	107.7	N(3)-C(31)-H(31B)	109.6(3)
C(3)-N(2)-Na	108.2(3)	N(4)-C(7)-C(8)	113.2(5)	C(32)-C(31)-H(31B)	109.6(3)

N(3)-C(31)-H(31A)	109.6(3)	C(156)-C(155)-C(154)	121.8(6)	C(355)-C(356)-C(357)	120.3(7)
C(32)-C(31)-H(31A)	109.6(3)	C(156)-C(155)-H(155)	119.1(4)	C(355)-C(356)-H(356)	119.8(4)
H(31B)-C(31)-H(31A)	108.1	C(154)-C(155)-H(155)	119.1(4)	C(357)-C(356)-H(356)	119.8(4)
O(3)-C(32)-N(7)	122.0(5)	C(155)-C(156)-C(157)	118.9(6)	C(358)-C(357)-C(356)	120.6(7)
O(3)-C(32)-C(31)	121.4(5)	C(155)-C(156)-H(156)	120.6(4)	C(358)-C(357)-H(357)	119.7(4)
N(7)-C(32)-C(31)	116.5(5)	C(157)-C(156)-H(156)	120.6(4)	C(356)-C(357)-H(357)	119.7(4)
N(7)-C(33)-C(35)	112.0(5)	C(158)-C(157)-C(156)	121.1(7)	C(357)-C(358)-C(359)	121.2(6)
N(7)-C(33)-C(34)	108.2(5)	C(158)-C(157)-H(157)	119.5(4)	C(357)-C(358)-H(358)	119.4(4)
C(35)-C(33)-C(34)	111.9(5)	C(156)-C(157)-H(157)	119.5(4)	C(359)-C(358)-H(358)	119.4(4)
N(7)-C(33)-H(33)	108.2(3)	C(157)-C(158)-C(159)	121.8(6)	C(358)-C(359)-C(354)	118.3(6)
C(35)-C(33)-H(33)	108.2(3)	C(157)-C(158)-H(158)	119.1(4)	C(358)-C(359)-C(35)	122.6(6)
C(34)-C(33)-H(33)	108.2(4)	C(159)-C(158)-H(158)	119.1(4)	C(354)-C(359)-C(35)	119.1(6)
C(33)-C(34)-H(34C)	109.5(3)	C(158)-C(159)-C(154)	117.9(6)	C(45)-C(451)-C(452)	120.5(6)
C(33)-C(34)-H(34B)	109.5(4)	C(158)-C(159)-C(15)	123.6(6)	C(45)-C(451)-H(451)	119.8(4)
H(34C)-C(34)-H(34B)	109.5	C(154)-C(159)-C(15)	118.6(6)	C(452)-C(451)-H(451)	119.8(4)
C(33)-C(34)-H(34A)	109.5(3)	C(25)-C(251)-C(252)	122.2(7)	C(453)-C(452)-C(451)	120.9(6)
H(34C)-C(34)-H(34A)	109.5	C(25)-C(251)-H(251)	118.9(4)	C(453)-C(452)-H(452)	119.5(4)
H(34B)-C(34)-H(34A)	109.5	C(252)-C(251)-H(251)	118.9(4)	C(451)-C(452)-H(452)	119.5(4)
C(351)-C(35)-C(359)	118.3(6)	C(253)-C(252)-C(251)	120.8(7)	C(452)-C(453)-C(454)	120.0(6)
C(351)-C(35)-C(33)	121.3(6)	C(253)-C(252)-H(252)	119.6(4)	C(452)-C(453)-H(453)	120.0(4)
C(359)-C(35)-C(33)	120.4(6)	C(251)-C(252)-H(252)	119.6(4)	C(454)-C(453)-H(453)	120.0(4)
N(4)-C(41)-C(42)	110.8(5)	C(252)-C(253)-C(254)	120.4(7)	C(453)-C(454)-C(459)	119.9(6)
N(4)-C(41)-H(41B)	109.5(3)	C(252)-C(253)-H(253)	119.8(4)	C(453)-C(454)-C(455)	121.6(7)
C(42)-C(41)-H(41B)	109.5(3)	C(254)-C(253)-H(253)	119.8(4)	C(459)-C(454)-C(455)	118.4(6)
N(4)-C(41)-H(41A)	109.5(3)	C(253)-C(254)-C(255)	123.1(7)	C(456)-C(455)-C(454)	120.7(7)
C(42)-C(41)-H(41A)	109.5(3)	C(253)-C(254)-C(259)	119.4(7)	C(456)-C(455)-H(455)	119.6(5)
H(41B)-C(41)-H(41A)	108.1	C(255)-C(254)-C(259)	117.6(7)	C(454)-C(455)-H(455)	119.6(4)
O(4)-C(42)-N(8)	123.1(6)	C(256)-C(255)-C(254)	123.0(8)	C(455)-C(456)-C(457)	120.6(7)
O(4)-C(42)-C(41)	120.2(6)	C(256)-C(255)-H(255)	118.5(5)	C(455)-C(456)-H(456)	119.7(5)
N(8)-C(42)-C(41)	116.7(6)	C(254)-C(255)-H(255)	118.5(5)	C(457)-C(456)-H(456)	119.7(4)
N(8)-C(43)-C(45)	111.1(5)	C(255)-C(256)-C(257)	118.6(8)	C(458)-C(457)-C(456)	121.3(7)
N(8)-C(43)-C(44)	108.2(5)	C(255)-C(256)-H(256)	120.7(5)	C(458)-C(457)-H(457)	119.4(5)
C(45)-C(43)-C(44)	112.0(5)	C(257)-C(256)-H(256)	120.7(5)	C(456)-C(457)-H(457)	119.4(4)
N(8)-C(43)-H(43)	108.5(3)	C(258)-C(257)-C(256)	121.2(8)	C(457)-C(458)-C(459)	119.8(7)
C(45)-C(43)-H(43)	108.5(3)	C(258)-C(257)-H(257)	119.4(5)	C(457)-C(458)-H(458)	120.1(5)
C(44)-C(43)-H(43)	108.5(3)	C(256)-C(257)-H(257)	119.4(5)	C(459)-C(458)-H(458)	120.1(4)
C(43)-C(44)-H(44C)	109.5(3)	C(257)-C(258)-C(259)	121.9(7)	C(454)-C(459)-C(458)	119.1(6)
C(43)-C(44)-H(44B)	109.5(3)	C(257)-C(258)-H(258)	119.1(5)	C(454)-C(459)-C(45)	118.7(6)
H(44C)-C(44)-H(44B)	109.5	C(259)-C(258)-H(258)	119.1(4)	C(458)-C(459)-C(45)	122.2(6)
C(43)-C(44)-H(44A)	109.5(3)	C(258)-C(259)-C(25)	123.9(6)	F(1)-C(1S)-F(2)	101.3(6)
H(44C)-C(44)-H(44A)	109.5	C(258)-C(259)-C(254)	117.7(7)	F(1)-C(1S)-F(3)	103.6(6)
H(44B)-C(44)-H(44A)	109.5	C(25)-C(259)-C(254)	118.4(6)	F(2)-C(1S)-F(3)	103.2(6)
C(451)-C(45)-C(459)	119.8(6)	C(35)-C(351)-C(352)	121.3(6)	F(1)-C(1S)-C(2S)	115.5(6)
C(451)-C(45)-C(43)	120.1(6)	C(35)-C(351)-H(351)	119.4(4)	F(2)-C(1S)-C(2S)	115.9(6)
C(459)-C(45)-C(43)	120.1(6)	C(352)-C(351)-H(351)	119.4(4)	F(3)-C(1S)-C(2S)	115.3(6)
C(15)-C(151)-C(152)	121.1(6)	C(353)-C(352)-C(351)	120.2(7)	O(1S)-C(2S)-O(2S)	127.9(6)
C(15)-C(151)-H(151)	119.5(4)	C(353)-C(352)-H(352)	119.9(4)	O(1S)-C(2S)-C(1S)	116.6(6)
C(152)-C(151)-H(151)	119.5(4)	C(351)-C(352)-H(352)	119.9(4)	O(2S)-C(2S)-C(1S)	115.4(6)
C(153)-C(152)-C(151)	120.0(7)	C(352)-C(353)-C(354)	121.8(6)	C(4S)-C(3S)-H(3SA)	109.5(4)
C(153)-C(152)-H(152)	120.0(4)	C(352)-C(353)-H(353)	119.1(4)	C(4S)-C(3S)-H(3SB)	109.5(4)
C(151)-C(152)-H(152)	120.0(4)	C(354)-C(353)-H(353)	119.1(4)	H(3SA)-C(3S)-H(3SB)	109.5
C(152)-C(153)-C(154)	120.9(7)	C(353)-C(354)-C(355)	122.6(6)	C(4S)-C(3S)-H(3SC)	109.5(4)
C(152)-C(153)-H(153)	119.6(4)	C(353)-C(354)-C(359)	119.3(6)	H(3SA)-C(3S)-H(3SC)	109.5
C(154)-C(153)-H(153)	119.6(4)	C(355)-C(354)-C(359)	118.1(6)	H(3SB)-C(3S)-H(3SC)	109.5
C(155)-C(154)-C(153)	122.1(6)	C(356)-C(355)-C(354)	121.5(7)	N(1S)-C(4S)-C(3S)	179.0(7)
C(155)-C(154)-C(159)	118.5(6)	C(356)-C(355)-H(355)	119.2(4)		
C(153)-C(154)-C(159)	119.4(6)	C(354)-C(355)-H(355)	119.2(4)		

Table A.4.6.4 - Anisotropic displacement parameters ($Å^2 x\ 10^3$) for C68 H75 F3 N9 Na O6. The anisotropic displacement factor exponent takes the form: $-2\pi^2[\ h^2\ a^{*2}U^{11} + \ldots + 2\ h\ k\ a^*\ b^*\ U^{12}\ ]$

U^{11}	U^{22}	U^{33}	U^{23}	U^{13}	U^{12}

Na	35(1)	36(1)	30(1)	2(1)	-1(1)	-2(1)
O(1)	35(3)	42(2)	38(3)	8(2)	-3(2)	0(2)
O(2)	46(3)	37(3)	38(3)	-6(2)	-10(2)	2(2)
O(3)	33(2)	47(3)	38(3)	-8(2)	9(2)	-10(2)
O(4)	42(2)	44(3)	35(2)	6(2)	9(2)	8(2)
N(1)	31(3)	32(3)	29(3)	2(3)	2(2)	3(2)
N(2)	35(3)	30(3)	27(3)	1(2)	-2(2)	1(2)
N(3)	34(3)	30(3)	32(3)	-2(3)	1(2)	0(2)
N(4)	28(3)	40(3)	26(3)	7(2)	3(2)	-1(2)
N(5)	32(3)	49(3)	27(3)	5(3)	3(3)	-1(2)
N(6)	60(3)	25(3)	37(3)	-3(3)	-14(3)	-1(3)
N(7)	27(3)	48(3)	32(3)	-12(3)	4(3)	-8(2)
N(8)	45(3)	36(3)	33(3)	-2(3)	7(3)	4(3)
C(1)	41(4)	33(4)	33(4)	10(3)	-1(3)	-9(3)
C(2)	44(4)	40(4)	32(4)	4(3)	-7(3)	-4(3)
C(3)	34(4)	42(4)	36(4)	-2(3)	4(3)	2(3)
C(4)	36(3)	37(4)	32(4)	-7(3)	2(3)	3(3)
C(5)	38(4)	29(3)	40(4)	1(3)	5(3)	-9(3)
C(6)	38(4)	33(3)	32(4)	-1(3)	6(3)	1(3)
C(7)	43(4)	27(3)	28(3)	4(3)	0(3)	5(3)
C(8)	29(3)	40(4)	31(4)	15(3)	-6(3)	5(3)
C(11)	34(4)	49(4)	39(4)	15(3)	2(3)	2(3)
C(12)	37(4)	37(4)	32(4)	6(3)	5(3)	4(3)
C(13)	37(4)	40(4)	35(4)	9(3)	6(3)	0(3)
C(14)	38(4)	80(5)	48(4)	12(4)	6(3)	4(4)
C(15)	41(4)	44(4)	27(4)	2(3)	5(3)	-14(3)
C(21)	38(4)	41(4)	38(4)	10(3)	1(3)	-8(3)
C(22)	32(3)	39(4)	28(4)	2(3)	1(3)	1(3)
C(23)	37(4)	39(4)	45(4)	4(3)	5(3)	1(3)
C(24)	48(4)	56(5)	38(4)	6(4)	0(3)	-2(4)
C(25)	37(4)	43(4)	36(4)	11(3)	-4(3)	5(3)
C(31)	34(3)	49(4)	33(4)	-13(3)	2(3)	3(3)
C(32)	40(4)	30(3)	33(4)	2(3)	2(3)	1(3)
C(33)	31(3)	37(4)	31(4)	1(3)	2(3)	-5(3)
C(34)	37(4)	49(4)	54(4)	-2(4)	-3(3)	-6(3)
C(35)	33(4)	42(4)	37(4)	-4(3)	-6(3)	-6(3)
C(41)	45(4)	26(3)	30(3)	1(3)	1(3)	-3(3)
C(42)	33(4)	37(4)	36(4)	6(3)	-1(3)	1(3)
C(43)	38(4)	49(4)	28(4)	-9(3)	6(3)	-1(3)
C(44)	39(4)	53(4)	45(4)	-17(4)	-1(3)	4(3)
C(45)	35(4)	39(4)	36(4)	-3(3)	-7(3)	10(3)
C(151)	49(4)	41(4)	36(4)	6(4)	-7(3)	-9(3)
C(152)	65(5)	40(4)	46(5)	-3(4)	5(4)	-14(4)
C(153)	54(4)	45(4)	46(5)	14(4)	15(4)	0(4)
C(154)	49(4)	44(4)	35(4)	2(3)	2(3)	-6(4)
C(155)	43(4)	41(4)	42(4)	13(4)	6(4)	3(3)
C(156)	45(4)	66(5)	33(4)	8(4)	-7(3)	-3(4)
C(157)	51(4)	40(4)	38(4)	0(3)	-7(4)	2(3)
C(158)	43(4)	55(5)	46(4)	9(4)	10(4)	6(4)
C(159)	40(4)	32(4)	30(4)	1(3)	-4(3)	2(3)
C(251)	43(4)	51(4)	42(4)	-2(4)	2(4)	12(3)
C(252)	34(4)	70(5)	48(5)	0(4)	4(4)	12(4)
C(253)	23(4)	63(5)	70(5)	17(4)	-5(4)	0(3)
C(254)	41(4)	42(4)	69(5)	6(4)	-16(4)	3(3)
C(255)	68(6)	46(5)	94(7)	7(5)	-43(5)	-7(4)
C(256)	91(7)	66(6)	64(6)	-22(5)	-32(5)	13(5)
C(257)	79(6)	70(6)	47(5)	-12(4)	-13(5)	23(5)
C(258)	45(4)	71(5)	37(4)	-8(4)	-6(4)	15(4)
C(259)	48(4)	44(4)	47(4)	4(4)	-3(4)	14(4)
C(351)	44(4)	38(4)	41(4)	11(4)	-6(3)	-10(3)
C(352)	51(4)	42(4)	66(5)	7(4)	-6(4)	-6(4)
C(353)	44(4)	45(4)	47(4)	0(4)	-7(4)	9(3)

C(354)	39(4)	32(4)	57(5)	-3(4)	-8(4)	-1(3)
C(355)	39(4)	52(5)	51(5)	-11(4)	1(4)	-3(3)
C(356)	53(5)	53(5)	50(5)	-18(4)	5(4)	-10(4)
C(357)	59(5)	50(5)	40(4)	4(4)	5(4)	-7(4)
C(358)	46(4)	42(4)	36(4)	0(3)	4(3)	-5(3)
C(359)	33(4)	44(4)	42(4)	-2(3)	1(3)	-11(3)
C(451)	38(4)	49(4)	38(4)	10(3)	1(3)	8(3)
C(452)	46(4)	51(4)	40(4)	-2(4)	-10(3)	8(3)
C(453)	37(4)	42(4)	55(5)	-10(4)	3(4)	5(3)
C(454)	39(4)	49(4)	49(5)	-6(4)	5(4)	8(4)
C(455)	49(4)	62(5)	49(5)	9(4)	11(4)	5(4)
C(456)	72(6)	60(5)	49(5)	11(4)	12(5)	18(5)
C(457)	56(5)	78(6)	31(4)	8(4)	4(4)	21(4)
C(458)	48(4)	65(5)	34(4)	0(4)	4(4)	14(4)
C(459)	39(4)	47(4)	35(4)	3(3)	-2(3)	13(3)

***Table A.4.6.5** - Hydrogen coordinates (x 10^4) and isotropic displacement parameters ($Å^2$x 10^3) for C68H75F3N9NaO6.*

	x	y	z	U(eq)
H(5C)	5941(3)	5589(3)	4388(2)	60(23)
H(6C)	1802(3)	7841(3)	4346(2)	31(17)
H(7C)	-751(3)	4144(3)	4521(2)	40(18)
H(8C)	3388(3)	1961(3)	4460(2)	42(20)
H(1B)	4331(4)	6175(3)	5217(3)	43
H(1A)	4534(4)	5834(3)	5826(3)	43
H(2B)	3012(4)	5851(4)	6047(3)	46
H(2A)	3331(4)	6705(4)	5868(3)	46
H(3B)	1207(4)	6428(4)	5259(3)	45
H(3A)	1638(4)	6626(4)	5854(3)	45
H(4B)	1698(4)	5290(3)	6072(3)	42
H(4A)	699(4)	5560(3)	5949(3)	42
H(5B)	909(4)	3715(3)	5334(3)	43
H(5A)	757(4)	4106(3)	5933(3)	43
H(6B)	2292(4)	4124(4)	6096(2)	41
H(6A)	1964(4)	3254(4)	5972(2)	41
H(7B)	4032(4)	3468(3)	5294(2)	39
H(7A)	3642(4)	3325(3)	5908(2)	39
H(8B)	3571(4)	4691(3)	6058(3)	40
H(8A)	4569(4)	4419(3)	5930(3)	40
H(11B)	4751(4)	4301(4)	4841(3)	49
H(11A)	5317(4)	4991(4)	5122(3)	49
H(13)	5212(4)	5630(4)	3361(3)	45
H(14C)	6764(9)	5729(6)	3455(18)	83
H(14B)	6666(11)	6571(21)	3739(11)	83
H(14A)	6402(5)	6451(24)	3096(9)	83
H(21B)	3298(4)	6885(4)	4819(2)	47
H(21A)	2489(4)	7344(4)	5107(2)	47
H(23)	1650(4)	7096(4)	3355(3)	49
H(24C)	1640(5)	8465(9)	3385(16)	71
H(24B)	704(23)	8459(9)	3704(9)	71
H(24A)	765(25)	8163(4)	3070(9)	71
H(31B)	361(4)	5548(4)	4909(2)	46
H(31A)	-126(4)	4833(4)	5215(2)	46
H(33)	-106(4)	4169(4)	3464(2)	40
H(34C)	-1632(7)	4039(4)	3600(17)	70
H(34B)	-1501(9)	3225(20)	3917(9)	70
H(34A)	-1299(5)	3289(21)	3261(9)	70
H(41B)	1906(4)	2953(3)	4940(2)	41
H(41A)	2751(4)	2536(3)	5220(2)	41
H(43)	3293(4)	2618(4)	3421(2)	46

H(44C)	3367(6)	1250(7)	3498(16)	69
H(44B)	4339(21)	1297(8)	3770(10)	69
H(44A)	4195(25)	1531(4)	3128(7)	69
H(151)	5287(4)	7135(4)	4376(3)	51
H(152)	4412(5)	8279(4)	4385(3)	60
H(153)	3481(5)	8560(4)	3640(3)	58
H(155)	2854(4)	8201(4)	2712(3)	50
H(156)	2740(4)	7340(4)	1965(3)	57
H(157)	3647(4)	6234(4)	1942(3)	51
H(158)	4562(4)	5937(4)	2678(3)	57
H(251)	58(4)	7294(4)	4451(3)	54
H(252)	-1229(4)	6573(4)	4569(3)	61
H(253)	-1679(4)	5685(4)	3900(3)	62
H(255)	-1500(6)	5127(4)	2935(4)	83
H(256)	-709(6)	5002(5)	2120(4)	88
H(257)	604(6)	5746(5)	1994(3)	78
H(258)	1089(4)	6591(4)	2673(3)	61
H(351)	94(4)	2690(4)	4507(3)	49
H(352)	987(4)	1556(4)	4439(3)	64
H(353)	1756(4)	1289(4)	3632(3)	54
H(355)	2198(4)	1637(4)	2653(3)	57
H(356)	2094(5)	2454(4)	1899(3)	63
H(357)	1164(5)	3553(4)	1931(3)	60
H(358)	354(4)	3838(4)	2727(3)	49
H(451)	5098(4)	2583(4)	4398(3)	50
H(452)	6382(4)	3363(4)	4354(3)	55
H(453)	6610(4)	4202(4)	3613(3)	54
H(455)	6159(5)	4694(4)	2657(3)	64
H(456)	5178(6)	4682(4)	1923(3)	73
H(457)	3959(5)	3839(5)	1922(3)	66
H(458)	3665(5)	3034(4)	2684(3)	59
H(3SA)	2138(22)	4700(14)	8251(3)	78
H(3SB)	2241(25)	5628(11)	8216(3)	78
H(3SC)	3105(5)	5088(23)	8278(3)	78

***Table A.4.7.2** - Atomic coordinates (x 10^4) and equivalent isotropic displacement parameters ($Å^2$x 10^3) for $C_{36}H_{69}EuF_{18}N_8O_{14.5}P_3$. U(eq) is defined as one third of the trace of the orthogonalized U^{ij} tensor.*

	x	y	z	U(eq)
Eu(1)	-972(1)	22482(1)	6368(1)	20(1)
O(1)	-2132(3)	23316(3)	5865(1)	25(1)
O(2)	142(3)	23732(3)	6378(2)	29(1)
O(3)	699(3)	21747(3)	6427(1)	27(1)
O(4)	-1491(3)	21239(3)	5939(1)	26(1)
O(5)	-84(3)	22615(4)	5647(1)	27(1)
O(11)	-3999(5)	25855(3)	5421(2)	40(1)
O(12)	-4001(6)	25018(3)	6033(2)	66(2)
O(21)	3155(5)	24602(4)	6497(2)	58(2)
O(22)	1875(4)	24690(4)	7024(2)	50(1)
O(31)	2186(4)	19534(3)	6068(2)	39(1)
O(32)	1387(4)	19781(3)	6739(2)	40(1)
O(41)	-3885(5)	20223(4)	5715(2)	57(2)
O(42)	-3785(5)	20027(5)	4970(2)	72(2)
N(1)	-3011(4)	22252(3)	6515(2)	29(1)
N(2)	-1762(4)	23800(4)	6824(2)	28(1)
N(3)	-97(4)	22616(5)	7179(2)	30(1)
N(4)	-1332(4)	21085(4)	6864(2)	28(1)
N(5)	-3766(4)	23548(4)	5555(2)	28(1)
N(6)	391(4)	25180(3)	6399(2)	33(1)
N(7)	2245(4)	21422(4)	6783(2)	29(1)
N(8)	-1822(5)	19822(4)	5846(2)	34(1)
C(1)	-3409(6)	22890(5)	6855(2)	37(2)
C(2)	-2955(6)	23801(5)	6800(3)	35(2)
C(3)	-1456(6)	23759(6)	7312(2)	38(2)
C(4)	-309(7)	23487(6)	7383(3)	38(2)
C(5)	-491(6)	21925(6)	7485(2)	37(2)
C(6)	-575(6)	21043(6)	7256(2)	38(2)
C(7)	-2454(6)	21078(5)	7043(3)	35(2)
C(8)	-3251(7)	21352(6)	6685(3)	39(2)
C(11)	-3548(5)	22362(5)	6075(2)	29(2)
C(12)	-3095(5)	23124(4)	5823(2)	23(1)
C(13)	-3529(5)	24370(4)	5325(2)	27(1)
C(14)	-4090(6)	24379(5)	4864(2)	35(2)
C(15)	-3867(7)	25109(5)	5633(2)	34(2)
C(16)	-4363(7)	26589(5)	5705(3)	48(2)
C(17)	-4449(8)	27382(6)	5422(3)	68(3)
C(21)	-1351(6)	24614(5)	6615(3)	30(2)
C(22)	-212(5)	24484(4)	6458(2)	26(1)
C(23)	1497(6)	25134(5)	6255(3)	37(2)
C(24)	1905(7)	26020(5)	6100(3)	49(2)
C(25)	2177(6)	24791(5)	6639(3)	40(2)
C(26)	3865(8)	24173(12)	6867(5)	149(8)
C(27)	4411(11)	24904(11)	7047(5)	131(6)
C(31)	1075(4)	22508(6)	7116(2)	31(1)
C(32)	1318(5)	21853(4)	6751(2)	26(1)
C(33)	2616(5)	20843(4)	6431(2)	30(1)
C(34)	3811(6)	20674(5)	6495(3)	49(2)
C(35)	1982(5)	19993(5)	6439(3)	33(2)
C(36)	1659(8)	18698(6)	6031(3)	54(3)
C(37)	2123(8)	18240(5)	5630(3)	61(3)
C(41)	-1157(7)	20313(5)	6571(3)	33(2)
C(42)	-1511(5)	20490(4)	6096(2)	28(1)
C(43)	-2190(5)	19913(4)	5383(2)	35(2)
C(44)	-1838(7)	19145(5)	5097(3)	48(2)
C(45)	-3392(7)	20056(5)	5385(3)	44(2)
C(46)	-4960(8)	20276(7)	4916(4)	70(3)

C(47)	-5563(10)	19489(7)	4994(5)	113(5)
P(1)	-5805(2)	7657(3)	6858(1)	77(1)
F(1)	-5538(5)	7009(5)	7287(2)	94(2)
F(2)	-5749(8)	8448(5)	7181(2)	143(4)
F(3)	-6048(6)	8283(5)	6444(2)	110(3)
F(4)	-5891(9)	6833(6)	6538(2)	138(3)
F(5)	-7022(4)	7514(6)	6979(2)	95(2)
F(6)	-4599(4)	7656(6)	6747(2)	104(3)
P(2)	-1855(2)	22133(1)	4520(1)	32(1)
F(7)	-2912(4)	21985(5)	4261(2)	99(2)
F(8)	-2127(5)	23130(3)	4562(2)	74(2)
F(9)	-2392(7)	22003(4)	4992(2)	109(3)
F(10)	-1558(7)	21151(3)	4484(2)	108(3)
F(11)	-1273(4)	22278(4)	4055(2)	80(2)
F(12)	-750(4)	22321(6)	4768(2)	150(4)
P(3)	-1304(2)	17374(2)	6257(1)	44(1)
F(13)	-1854(7)	17130(6)	6698(2)	144(4)
F(14)	-2338(5)	17822(4)	6066(3)	105(2)
F(15)	-1608(5)	16475(3)	6042(2)	78(2)
F(16)	-947(5)	18277(3)	6470(2)	92(2)
F(17)	-663(5)	17609(6)	5815(2)	113(2)
F(18)	-216(5)	16982(3)	6451(2)	78(2)
O(1S)	-3574(11)	9327(8)	6637(4)	67(4)
O(2S)	3323(7)	21463(5)	7638(3)	79(2)

Table A.4.7.3 - Bond lengths [Å] and angles [°] for $C_{36}H_{69}EuF_{18}N_8O_{14.5}P_3$.

Eu(1)-O(2)	2.381(4)	N(4)-C(41)	1.490(10)	C(8)-H(8C)	1.02(9)
Eu(1)-O(3)	2.393(4)	N(4)-C(7)	1.507(9)	C(11)-C(12)	1.505(9)
Eu(1)-O(4)	2.394(4)	N(4)-C(6)	1.507(9)	C(13)-C(15)	1.523(10)
Eu(1)-O(5)	2.429(4)	N(5)-C(12)	1.332(8)	C(13)-C(14)	1.542(9)
Eu(1)-O(1)	2.454(4)	N(5)-C(13)	1.469(8)	C(16)-C(17)	1.488(11)
Eu(1)-N(1)	2.625(5)	N(5)-H(5)	0.81(7)	C(21)-C(22)	1.520(10)
Eu(1)-N(2)	2.635(6)	N(6)-C(22)	1.324(8)	C(23)-C(25)	1.522(11)
Eu(1)-N(4)	2.649(6)	N(6)-C(23)	1.457(9)	C(23)-C(24)	1.530(11)
Eu(1)-N(3)	2.659(5)	N(6)-H(6)	0.92(7)	C(26)-C(27)	1.423(19)
O(1)-C(12)	1.253(7)	N(7)-C(32)	1.345(8)	C(31)-C(32)	1.513(9)
O(2)-C(22)	1.265(7)	N(7)-C(33)	1.452(8)	C(33)-C(35)	1.533(9)
O(3)-C(32)	1.252(7)	N(7)-H(7)	0.92(7)	C(33)-C(34)	1.537(9)
O(4)-C(42)	1.244(7)	N(8)-C(42)	1.330(9)	C(36)-C(37)	1.505(13)
O(11)-C(15)	1.321(8)	N(8)-C(43)	1.461(9)	C(41)-C(42)	1.507(9)
O(11)-C(16)	1.486(8)	N(8)-H(8)	0.77(7)	C(43)-C(44)	1.522(10)
O(12)-C(15)	1.209(8)	C(1)-C(2)	1.524(12)	C(43)-C(45)	1.528(11)
O(21)-C(25)	1.332(9)	C(1)-H(1A)	1.00(7)	C(46)-C(47)	1.448(14)
O(21)-C(26)	1.564(15)	C(1)-H(1B)	1.02(8)	P(1)-F(2)	1.552(7)
O(22)-C(25)	1.217(9)	C(2)-H(2A)	1.08(8)	P(1)-F(6)	1.553(5)
O(31)-C(35)	1.337(9)	C(2)-H(2B)	0.71(8)	P(1)-F(5)	1.588(6)
O(31)-C(36)	1.453(9)	C(3)-C(4)	1.518(10)	P(1)-F(4)	1.592(8)
O(32)-C(35)	1.210(8)	C(3)-H(3A)	1.08(8)	P(1)-F(3)	1.594(7)
O(41)-C(45)	1.188(9)	C(3)-H(3B)	1.17(7)	P(1)-F(1)	1.657(7)
O(42)-C(45)	1.333(9)	C(4)-H(4A)	1.18(8)	P(2)-F(7)	1.554(5)
O(42)-C(46)	1.534(11)	C(4)-H(4B)	1.10(8)	P(2)-F(10)	1.563(5)
N(1)-C(11)	1.482(7)	C(5)-C(6)	1.523(12)	P(2)-F(9)	1.570(5)
N(1)-C(1)	1.497(9)	C(5)-H(5C)	0.98(8)	P(2)-F(8)	1.578(5)
N(1)-C(8)	1.506(10)	C(5)-H(5D)	1.00(8)	P(2)-F(11)	1.581(5)
N(2)-C(21)	1.492(10)	C(6)-H(6B)	0.99(8)	P(2)-F(12)	1.599(5)
N(2)-C(2)	1.501(9)	C(6)-H(6C)	0.93(8)	P(3)-F(13)	1.532(7)
N(2)-C(3)	1.503(8)	C(7)-C(8)	1.523(10)	P(3)-F(15)	1.573(6)
N(3)-C(5)	1.485(10)	C(7)-H(7B)	0.94(8)	P(3)-F(14)	1.578(6)
N(3)-C(31)	1.494(7)	C(7)-H(7C)	1.08(8)	P(3)-F(17)	1.585(5)
N(3)-C(4)	1.497(11)	C(8)-H(8B)	0.93(8)	P(3)-F(16)	1.594(5)

P(3)-F(18)	1.602(5)	O(5)-Eu(1)-C(42)	87.42(17)	C(1)-C(2)-H(2B)	107(7)
O(2S)-H(2SA)	0.91(12)	O(1)-Eu(1)-C(42)	102.61(15)	H(2A)-C(2)-H(2B)	90(7)
O(2S)-H(2SB)	0.88(13)	N(1)-Eu(1)-C(42)	73.13(16)	N(2)-C(3)-C(4)	113.0(6)
		N(2)-Eu(1)-C(42)	141.09(17)	N(2)-C(3)-H(3A)	107(4)
O(2)-Eu(1)-O(3)	82.27(15)	N(4)-Eu(1)-C(42)	48.28(18)	C(4)-C(3)-H(3A)	107(4)
O(2)-Eu(1)-O(4)	144.50(15)	N(3)-Eu(1)-C(42)	112.7(2)	N(2)-C(3)-H(3B)	101(4)
O(3)-Eu(1)-O(4)	84.21(14)	C(22)-Eu(1)-C(42)	169.18(15)	C(4)-C(3)-H(3B)	115(4)
O(2)-Eu(1)-O(5)	70.85(16)	C(32)-Eu(1)-C(42)	89.45(16)	H(3A)-C(3)-H(3B)	114(5)
O(3)-Eu(1)-O(5)	72.57(15)	C(12)-O(1)-Eu(1)	120.8(4)	N(3)-C(4)-C(3)	111.1(7)
O(4)-Eu(1)-O(5)	73.80(16)	C(22)-O(2)-Eu(1)	122.4(4)	N(3)-C(4)-H(4A)	112(4)
O(2)-Eu(1)-O(1)	86.20(15)	C(32)-O(3)-Eu(1)	122.7(4)	C(3)-C(4)-H(4A)	112(4)
O(3)-Eu(1)-O(1)	144.46(14)	C(42)-O(4)-Eu(1)	123.2(4)	N(3)-C(4)-H(4B)	108(4)
O(4)-Eu(1)-O(1)	86.04(15)	C(15)-O(11)-C(16)	115.4(6)	C(3)-C(4)-H(4B)	112(4)
O(5)-Eu(1)-O(1)	71.89(14)	C(25)-O(21)-C(26)	113.3(7)	H(4A)-C(4)-H(4B)	101(6)
O(2)-Eu(1)-N(1)	132.99(15)	C(35)-O(31)-C(36)	116.3(6)	N(3)-C(5)-C(6)	112.9(6)
O(3)-Eu(1)-N(1)	141.40(15)	C(45)-O(42)-C(46)	116.4(7)	N(3)-C(5)-H(5C)	114(4)
O(4)-Eu(1)-N(1)	73.38(15)	C(11)-N(1)-C(1)	111.7(5)	C(6)-C(5)-H(5C)	108(4)
O(5)-Eu(1)-N(1)	127.38(14)	C(11)-N(1)-C(8)	108.1(5)	N(3)-C(5)-H(5D)	116(5)
O(1)-Eu(1)-N(1)	65.89(14)	C(1)-N(1)-C(8)	108.1(6)	C(6)-C(5)-H(5D)	110(4)
O(2)-Eu(1)-N(2)	65.97(16)	C(11)-N(1)-Eu(1)	106.4(3)	H(5C)-C(5)-H(5D)	94(6)
O(3)-Eu(1)-N(2)	131.19(16)	C(1)-N(1)-Eu(1)	110.5(4)	N(4)-C(6)-C(5)	110.6(6)
O(4)-Eu(1)-N(2)	142.02(17)	C(8)-N(1)-Eu(1)	112.1(4)	N(4)-C(6)-H(6B)	102(4)
O(5)-Eu(1)-N(2)	124.24(18)	C(21)-N(2)-C(2)	109.0(6)	C(5)-C(6)-H(6B)	119(5)
O(1)-Eu(1)-N(2)	71.73(16)	C(21)-N(2)-C(3)	110.4(6)	N(4)-C(6)-H(6C)	105(5)
N(1)-Eu(1)-N(2)	69.54(17)	C(2)-N(2)-C(3)	107.4(6)	C(5)-C(6)-H(6C)	111(4)
O(2)-Eu(1)-N(4)	138.72(17)	C(21)-N(2)-Eu(1)	107.6(4)	H(6B)-C(6)-H(6C)	108(6)
O(3)-Eu(1)-N(4)	74.05(16)	C(2)-N(2)-Eu(1)	110.7(4)	N(4)-C(7)-C(8)	111.5(6)
O(4)-Eu(1)-N(4)	66.39(16)	C(3)-N(2)-Eu(1)	111.6(4)	N(4)-C(7)-H(7B)	108(5)
O(5)-Eu(1)-N(4)	129.75(18)	C(5)-N(3)-C(31)	109.0(6)	C(8)-C(7)-H(7B)	112(5)
O(1)-Eu(1)-N(4)	131.57(16)	C(5)-N(3)-C(4)	109.5(6)	N(4)-C(7)-H(7C)	119(4)
N(1)-Eu(1)-N(4)	68.31(16)	C(31)-N(3)-C(4)	109.1(6)	C(8)-C(7)-H(7C)	99(4)
N(2)-Eu(1)-N(4)	106.00(17)	C(5)-N(3)-Eu(1)	111.2(4)	H(7B)-C(7)-H(7C)	107(6)
O(2)-Eu(1)-N(3)	71.54(18)	C(31)-N(3)-Eu(1)	106.6(3)	N(1)-C(8)-C(7)	111.0(7)
O(3)-Eu(1)-N(3)	66.91(16)	C(4)-N(3)-Eu(1)	111.4(4)	N(1)-C(8)-H(8B)	107(5)
O(4)-Eu(1)-N(3)	131.21(19)	C(41)-N(4)-C(7)	109.8(6)	C(7)-C(8)-H(8B)	119(5)
O(5)-Eu(1)-N(3)	127.26(13)	C(41)-N(4)-C(6)	109.0(6)	N(1)-C(8)-H(8C)	106(4)
O(1)-Eu(1)-N(3)	139.40(18)	C(7)-N(4)-C(6)	108.5(5)	C(7)-C(8)-H(8C)	118(4)
N(1)-Eu(1)-N(3)	105.30(15)	C(41)-N(4)-Eu(1)	107.3(4)	H(8B)-C(8)-H(8C)	95(6)
N(2)-Eu(1)-N(3)	68.29(19)	C(7)-N(4)-Eu(1)	111.2(4)	N(1)-C(11)-C(12)	110.9(5)
N(4)-Eu(1)-N(3)	68.2(2)	C(6)-N(4)-Eu(1)	110.9(4)	O(1)-C(12)-N(5)	123.8(6)
O(2)-Eu(1)-C(22)	19.23(14)	C(12)-N(5)-C(13)	125.0(6)	O(1)-C(12)-C(11)	120.0(5)
O(3)-Eu(1)-C(22)	100.71(15)	C(12)-N(5)-H(5)	118(5)	N(5)-C(12)-C(11)	116.2(5)
O(4)-Eu(1)-C(22)	152.42(14)	C(13)-N(5)-H(5)	115(5)	N(5)-C(13)-C(15)	108.0(5)
O(5)-Eu(1)-C(22)	81.77(16)	C(22)-N(6)-C(23)	123.1(6)	N(5)-C(13)-C(14)	109.2(5)
O(1)-Eu(1)-C(22)	74.17(15)	C(22)-N(6)-H(6)	117(5)	C(15)-C(13)-C(14)	113.6(5)
N(1)-Eu(1)-C(22)	113.77(16)	C(23)-N(6)-H(6)	119(5)	O(12)-C(15)-O(11)	123.7(7)
N(2)-Eu(1)-C(22)	48.35(17)	C(32)-N(7)-C(33)	122.1(6)	O(12)-C(15)-C(13)	122.9(6)
N(4)-Eu(1)-C(22)	141.14(16)	C(32)-N(7)-H(7)	114(4)	O(11)-C(15)-C(13)	113.4(6)
N(3)-Eu(1)-C(22)	74.32(19)	C(33)-N(7)-H(7)	124(5)	O(11)-C(16)-C(17)	109.0(6)
O(2)-Eu(1)-C(32)	73.47(15)	C(42)-N(8)-C(43)	123.2(6)	N(2)-C(21)-C(22)	110.1(6)
O(3)-Eu(1)-C(32)	18.95(15)	C(42)-N(8)-H(8)	119(6)	O(2)-C(22)-N(6)	121.0(6)
O(4)-Eu(1)-C(32)	100.97(16)	C(43)-N(8)-H(8)	118(6)	O(2)-C(22)-C(21)	120.7(6)
O(5)-Eu(1)-C(32)	85.88(15)	N(1)-C(1)-C(2)	114.0(6)	N(6)-C(22)-C(21)	118.3(6)
O(1)-Eu(1)-C(32)	153.93(15)	N(1)-C(1)-H(1A)	102(4)	O(2)-C(22)-Eu(1)	38.3(3)
N(1)-Eu(1)-C(32)	140.18(15)	C(2)-C(1)-H(1A)	111(5)	N(6)-C(22)-Eu(1)	158.2(4)
N(2)-Eu(1)-C(32)	112.60(17)	N(1)-C(1)-H(1B)	114(4)	C(21)-C(22)-Eu(1)	82.7(4)
N(4)-Eu(1)-C(32)	73.35(16)	C(2)-C(1)-H(1B)	108(4)	N(6)-C(23)-C(25)	109.4(6)
N(3)-Eu(1)-C(32)	48.50(17)	H(1A)-C(1)-H(1B)	108(5)	N(6)-C(23)-C(24)	111.5(6)
C(22)-Eu(1)-C(32)	89.65(16)	N(2)-C(2)-C(1)	111.6(6)	C(25)-C(23)-C(24)	110.5(7)
O(2)-Eu(1)-C(42)	152.91(15)	N(2)-C(2)-H(2A)	108(4)	O(22)-C(25)-O(21)	124.0(8)
O(3)-Eu(1)-C(42)	75.74(15)	C(1)-C(2)-H(2A)	118(4)	O(22)-C(25)-C(23)	125.2(7)
O(4)-Eu(1)-C(42)	18.71(15)	N(2)-C(2)-H(2B)	122(7)	O(21)-C(25)-C(23)	110.8(7)

C(27)-C(26)-O(21)	101.9(14)	O(41)-C(45)-O(42)	125.4(8)	F(7)-P(2)-F(11)	89.0(3)
N(3)-C(31)-C(32)	111.4(5)	O(41)-C(45)-C(43)	123.5(8)	F(10)-P(2)-F(11)	88.1(3)
O(3)-C(32)-N(7)	121.9(6)	O(42)-C(45)-C(43)	110.9(7)	F(9)-P(2)-F(11)	177.8(4)
O(3)-C(32)-C(31)	121.0(5)	C(47)-C(46)-O(42)	106.2(9)	F(8)-P(2)-F(11)	91.9(3)
N(7)-C(32)-C(31)	117.1(5)	F(2)-P(1)-F(6)	95.1(5)	F(7)-P(2)-F(12)	177.1(5)
O(3)-C(32)-Eu(1)	38.4(3)	F(2)-P(1)-F(5)	90.7(5)	F(10)-P(2)-F(12)	90.0(4)
N(7)-C(32)-Eu(1)	160.2(5)	F(6)-P(1)-F(5)	171.8(6)	F(9)-P(2)-F(12)	89.2(4)
C(31)-C(32)-Eu(1)	82.7(3)	F(2)-P(1)-F(4)	178.1(5)	F(8)-P(2)-F(12)	88.6(4)
N(7)-C(33)-C(35)	110.3(5)	F(6)-P(1)-F(4)	86.4(5)	F(11)-P(2)-F(12)	88.6(4)
N(7)-C(33)-C(34)	109.2(6)	F(5)-P(1)-F(4)	87.7(5)	F(13)-P(3)-F(15)	91.3(4)
C(35)-C(33)-C(34)	111.2(6)	F(2)-P(1)-F(3)	90.7(5)	F(13)-P(3)-F(14)	92.5(5)
O(32)-C(35)-O(31)	125.8(7)	F(6)-P(1)-F(3)	91.4(4)	F(15)-P(3)-F(14)	92.2(3)
O(32)-C(35)-C(33)	124.3(7)	F(5)-P(1)-F(3)	94.3(4)	F(13)-P(3)-F(17)	176.3(5)
O(31)-C(35)-C(33)	109.8(6)	F(4)-P(1)-F(3)	90.4(4)	F(15)-P(3)-F(17)	89.3(4)
O(31)-C(36)-C(37)	107.4(8)	F(2)-P(1)-F(1)	89.2(5)	F(14)-P(3)-F(17)	91.2(4)
N(4)-C(41)-C(42)	111.1(6)	F(6)-P(1)-F(1)	88.0(4)	F(13)-P(3)-F(16)	90.0(4)
O(4)-C(42)-N(8)	120.9(6)	F(5)-P(1)-F(1)	86.3(4)	F(15)-P(3)-F(16)	177.7(4)
O(4)-C(42)-C(41)	120.9(6)	F(4)-P(1)-F(1)	89.6(5)	F(14)-P(3)-F(16)	89.6(3)
N(8)-C(42)-C(41)	118.2(6)	F(3)-P(1)-F(1)	179.3(4)	F(17)-P(3)-F(16)	89.3(4)
O(4)-C(42)-Eu(1)	38.1(3)	F(7)-P(2)-F(10)	91.6(4)	F(13)-P(3)-F(18)	89.1(4)
N(8)-C(42)-Eu(1)	159.0(5)	F(7)-P(2)-F(9)	93.2(4)	F(15)-P(3)-F(18)	91.3(3)
C(41)-C(42)-Eu(1)	82.8(4)	F(10)-P(2)-F(9)	92.3(3)	F(14)-P(3)-F(18)	176.1(3)
N(8)-C(43)-C(44)	111.1(6)	F(7)-P(2)-F(8)	89.8(4)	F(17)-P(3)-F(18)	87.2(4)
N(8)-C(43)-C(45)	108.8(6)	F(10)-P(2)-F(8)	178.6(4)	F(16)-P(3)-F(18)	86.9(3)
C(44)-C(43)-C(45)	113.8(6)	F(9)-P(2)-F(8)	87.7(3)	H2SA-O2S-H2SB	169(10)

***Table A.4.7.4** - Anisotropic displacement parameters ($Å^2 x\ 10^3$) for $C_{36}H_{69}EuF_{18}N_8O_{14.5}P_3$. The anisotropic displacement factor exponent takes the form: $-2\pi^2[\,h^2\,a^{*2}U^{11} + \ldots + 2\,h\,k\,a^*\,b^*\,U^{12}\,]$*

	U^{11}	U^{22}	U^{33}	U^{23}	U^{13}	U^{12}
Eu(1)	15(1)	27(1)	20(1)	2(1)	-1(1)	1(1)
O(1)	19(2)	31(2)	24(2)	3(2)	1(2)	2(2)
O(2)	25(2)	30(2)	32(2)	-9(2)	-2(2)	6(2)
O(3)	22(2)	31(2)	29(2)	4(2)	-4(2)	1(2)
O(4)	23(2)	26(2)	30(2)	7(2)	-2(2)	2(2)
O(5)	26(2)	30(3)	24(2)	-3(2)	-1(2)	6(2)
O(11)	52(3)	29(2)	39(3)	0(2)	-7(3)	3(3)
O(12)	116(6)	49(3)	33(3)	3(2)	4(4)	31(4)
O(21)	33(3)	91(5)	50(4)	-13(3)	0(3)	15(3)
O(22)	34(3)	75(4)	42(3)	-4(3)	-5(2)	-4(3)
O(31)	44(3)	32(3)	40(3)	5(2)	-5(2)	-3(2)
O(32)	29(3)	50(3)	43(3)	19(2)	4(2)	2(2)
O(41)	39(4)	78(4)	53(4)	-10(3)	-5(3)	-1(3)
O(42)	41(4)	114(6)	62(4)	-8(4)	-18(3)	4(4)
N(1)	28(3)	38(4)	20(2)	9(2)	-1(2)	3(2)
N(2)	15(3)	40(3)	28(3)	-5(3)	-2(2)	2(3)
N(3)	21(2)	43(4)	27(2)	4(3)	-3(2)	-6(3)
N(4)	17(3)	39(3)	29(3)	10(3)	-2(2)	4(3)
N(5)	22(3)	26(3)	36(3)	7(2)	-5(2)	-1(2)
N(6)	30(3)	22(3)	47(3)	-8(3)	-2(3)	3(2)
N(7)	21(3)	36(3)	31(3)	1(3)	-6(2)	3(2)
N(8)	35(3)	22(3)	44(4)	7(3)	-7(3)	-5(3)
C(1)	25(4)	54(5)	32(4)	5(3)	5(3)	7(3)
C(2)	24(4)	50(5)	31(4)	1(4)	6(3)	19(4)
C(3)	31(4)	60(5)	22(3)	-8(3)	-8(3)	14(4)
C(4)	41(5)	52(5)	20(4)	-7(4)	-2(3)	6(4)
C(5)	30(4)	65(6)	18(3)	7(4)	-1(3)	0(4)
C(6)	32(4)	58(5)	22(4)	13(4)	-6(3)	3(4)
C(7)	21(4)	47(5)	36(4)	12(3)	-7(3)	-2(3)
C(8)	24(4)	59(5)	35(4)	21(4)	-3(3)	-1(4)

C(11)	20(3)	34(5)	31(3)	4(3)	-6(2)	-3(3)
C(12)	21(3)	29(3)	19(3)	-3(2)	-3(2)	5(3)
C(13)	22(3)	24(3)	34(4)	12(3)	0(3)	3(3)
C(14)	31(4)	43(4)	31(3)	5(3)	3(3)	5(4)
C(15)	37(5)	35(4)	31(4)	7(3)	-10(3)	9(4)
C(16)	57(5)	44(5)	42(4)	-8(4)	-3(4)	6(4)
C(17)	84(6)	45(6)	74(5)	-7(5)	-8(5)	-2(5)
C(21)	21(4)	34(4)	34(4)	-8(3)	2(3)	6(3)
C(22)	23(3)	35(4)	20(3)	-9(3)	-5(2)	4(3)
C(23)	31(4)	36(4)	44(5)	-12(3)	6(3)	-1(3)
C(24)	47(6)	44(5)	57(5)	0(4)	7(4)	-9(4)
C(25)	26(4)	45(5)	48(5)	-15(4)	0(4)	12(3)
C(26)	27(6)	270(20)	153(13)	-139(14)	-38(7)	52(9)
C(27)	79(10)	193(17)	120(12)	55(12)	45(9)	60(11)
C(31)	23(3)	41(3)	30(2)	-2(4)	-4(2)	5(5)
C(32)	18(3)	35(4)	25(3)	6(3)	-2(2)	1(3)
C(33)	19(3)	36(4)	35(4)	3(3)	3(3)	4(3)
C(34)	20(4)	55(5)	71(6)	-8(4)	-2(4)	5(3)
C(35)	18(3)	38(4)	42(5)	13(4)	-4(3)	3(3)
C(36)	54(6)	43(5)	66(6)	5(4)	-4(5)	-15(4)
C(37)	90(7)	44(5)	48(5)	1(4)	-15(5)	-5(5)
C(41)	28(5)	33(4)	36(4)	15(3)	-3(3)	1(3)
C(42)	16(3)	26(4)	41(4)	5(3)	-1(3)	2(3)
C(43)	29(4)	32(4)	44(4)	0(3)	-7(3)	-7(3)
C(44)	55(5)	41(5)	49(5)	-6(4)	-8(4)	4(4)
C(45)	40(5)	47(5)	44(5)	-2(4)	-6(4)	-7(4)
C(46)	54(6)	81(7)	76(7)	0(6)	-12(5)	7(5)
C(47)	84(9)	73(8)	182(14)	44(9)	-43(9)	-8(7)
P(1)	50(1)	145(3)	35(1)	-7(2)	4(1)	24(2)
F(1)	84(5)	133(6)	64(4)	13(4)	30(3)	27(4)
F(2)	209(10)	137(6)	84(5)	-47(5)	53(6)	-96(7)
F(3)	89(5)	177(7)	64(4)	34(4)	18(4)	37(5)
F(4)	155(8)	176(8)	83(5)	-68(5)	48(5)	-29(7)
F(5)	73(3)	147(5)	65(3)	-26(6)	12(3)	-8(6)
F(6)	50(3)	193(8)	68(3)	23(5)	15(2)	-10(5)
P(2)	26(1)	43(1)	26(1)	2(1)	-4(1)	10(1)
F(7)	26(3)	148(6)	123(5)	-56(4)	-25(3)	13(3)
F(8)	121(5)	39(3)	62(3)	2(3)	20(4)	17(3)
F(9)	215(8)	58(4)	54(3)	5(3)	68(4)	3(4)
F(10)	218(9)	60(3)	47(3)	-4(3)	4(4)	71(4)
F(11)	88(4)	97(5)	55(3)	-25(3)	37(3)	-37(3)
F(12)	64(4)	260(10)	125(5)	-143(6)	-61(4)	93(6)
P(3)	44(1)	40(1)	49(1)	9(1)	-7(1)	8(1)
F(13)	140(7)	196(10)	95(5)	26(5)	61(5)	-38(6)
F(14)	66(4)	68(4)	181(7)	8(4)	-60(4)	8(3)
F(15)	90(4)	58(3)	86(4)	-8(3)	-27(3)	6(3)
F(16)	72(4)	51(3)	151(6)	-31(3)	-37(5)	12(3)
F(17)	111(5)	165(7)	63(3)	48(5)	3(3)	-46(6)
F(18)	77(4)	56(3)	102(4)	-6(3)	-37(4)	35(3)

***Table A.4.7.5** - Hydrogen coordinates (x 10^4) and isotropic displacement parameters ($Å^2$x 10^3) for $C_{36}H_{69}EuF_{18}N_8O_{14.5}P_3$.*

	x	y	z	U(eq)
H(5)	-4380(60)	23410(50)	5560(20)	34
H(6)	40(60)	25710(50)	6380(30)	40
H(7)	2620(60)	21540(40)	7040(20)	35
H(8)	-1800(60)	19360(50)	5950(30)	41
H(1A)	-3170(50)	22620(50)	7140(20)	45
H(1B)	-4220(60)	22940(40)	6870(20)	45

H(2A)	-3180(60)	24170(50)	6510(30)	42
H(2B)	-3270(70)	24080(50)	6940(30)	42
H(3A)	-1940(60)	23270(50)	7460(20)	46
H(3B)	-1660(60)	24470(50)	7430(20)	46
H(4A)	300(60)	24020(50)	7250(20)	45
H(4B)	-100(60)	23450(50)	7740(30)	45
H(5C)	-1170(60)	22060(50)	7630(20)	45
H(5D)	-100(70)	21860(50)	7770(30)	45
H(6B)	70(70)	20790(50)	7120(30)	45
H(6C)	-870(70)	20630(50)	7450(20)	45
H(7B)	-2480(60)	21440(50)	7300(30)	42
H(7C)	-2810(60)	20470(50)	7140(20)	42
H(8B)	-3340(60)	21000(50)	6430(30)	47
H(8C)	-4040(70)	21360(40)	6770(20)	47
H(11A)	-4319	22453	6124	34
H(11B)	-3457	21828	5894	34
H(13)	-2744	24408	5276	32
H(14A)	-3764	23944	4668	53
H(14B)	-4017	24955	4728	53
H(14C)	-4846	24244	4904	53
H(16A)	-3850	26689	5952	57
H(16B)	-5064	26452	5840	57
H(17A)	-4857	27826	5583	101
H(17B)	-4811	27238	5140	101
H(17C)	-3735	27604	5356	101
H(21A)	-1379	25092	6837	36
H(21B)	-1804	24775	6356	36
H(23)	1548	24719	5998	45
H(24A)	1444	26243	5861	74
H(24B)	2632	25960	5985	74
H(24C)	1901	26425	6354	74
H(26A)	3428	23881	7099	179
H(26B)	4367	23748	6735	179
H(27A)	4816	24726	7313	196
H(27B)	3894	25351	7132	196
H(27C)	4899	25138	6820	196
H(31A)	1398	22313	7402	38
H(31B)	1394	23074	7035	38
H(33)	2505	21131	6134	36
H(34A)	4218	21156	6365	73
H(34B)	4007	20132	6344	73
H(34C)	3971	20627	6816	73
H(36A)	884	18779	5992	65
H(36B)	1780	18351	6307	65
H(37A)	1756	17685	5585	91
H(37B)	2882	18134	5680	91
H(37C)	2032	18603	5362	91
H(41A)	-1558	19813	6692	39
H(41B)	-392	20160	6572	39
H(43)	-1853	20446	5255	42
H(44A)	-1059	19122	5088	72
H(44B)	-2114	19212	4791	72
H(44C)	-2113	18606	5228	72
H(46A)	-5159	20728	5137	84
H(46B)	-5097	20501	4610	84
H(47A)	-6162	19464	4783	170
H(47B)	-5834	19489	5303	170
H(47C)	-5103	18984	4949	170
H(2SA)	3460(100)	22020(80)	7550(40)	135
H(2SB)	3100(110)	20970(80)	7760(40)	135

***Table A.4.8.2** - Atomic coordinates (x 10^4) and equivalent isotropic displacement parameters ($Å^2$x 10^3) for C36 H68 F18 Gd N8 O14 P3. U(eq) is defined as one third of the trace of the orthogonalized U^{ij} tensor.*

	x	y	z	U(eq)
Gd(1)	-985(1)	22472(1)	6367(1)	27(1)
O(1)	-2147(4)	23313(4)	5867(2)	27(2)
O(2)	134(5)	23733(4)	6384(2)	33(2)
O(3)	694(5)	21735(4)	6430(2)	30(2)
O(4)	-1516(5)	21218(5)	5944(2)	34(2)
O(5)	-88(4)	22609(6)	5642(2)	29(2)
O(11)	-4014(7)	25857(4)	5428(3)	46(2)
O(12)	-4023(9)	25016(5)	6037(3)	72(3)
O(21)	3136(7)	24612(7)	6500(3)	70(3)
O(22)	1868(6)	24667(6)	7031(3)	57(2)
O(31)	2185(6)	19537(6)	6065(3)	49(2)
O(32)	1375(5)	19770(5)	6739(3)	47(2)
O(41)	-3887(8)	20242(7)	5721(4)	68(3)
O(42)	-3809(7)	19983(8)	4977(3)	85(3)
N(1)	-3030(6)	22230(5)	6518(3)	33(2)
N(2)	-1774(7)	23796(6)	6825(3)	31(2)
N(3)	-112(6)	22617(8)	7179(3)	35(2)
N(4)	-1349(6)	21061(6)	6863(3)	31(2)
N(5)	-3779(6)	23551(5)	5558(3)	29(2)
N(6)	382(6)	25172(6)	6404(3)	42(2)
N(7)	2232(6)	21427(6)	6777(3)	33(2)
N(8)	-1830(6)	19810(6)	5847(3)	39(2)
C(1)	-3419(8)	22873(8)	6855(4)	51(4)
C(2)	-2967(8)	23798(8)	6809(4)	40(3)
C(3)	-1475(8)	23750(9)	7307(3)	46(3)
C(4)	-323(11)	23469(10)	7395(4)	53(4)
C(5)	-510(10)	21912(10)	7475(4)	51(4)
C(6)	-619(9)	21032(9)	7256(4)	48(3)
C(7)	-2469(8)	21064(8)	7041(4)	41(3)
C(8)	-3264(9)	21331(8)	6683(4)	41(3)
C(11)	-3569(7)	22346(7)	6075(3)	30(3)
C(12)	-3132(8)	23115(6)	5819(3)	26(2)
C(13)	-3550(8)	24356(7)	5325(4)	35(3)
C(14)	-4089(10)	24379(7)	4864(4)	43(3)
C(15)	-3877(11)	25104(8)	5635(4)	40(3)
C(16)	-4361(10)	26596(8)	5708(4)	52(3)
C(17)	-4469(11)	27378(10)	5436(4)	73(4)
C(21)	-1361(9)	24616(8)	6617(4)	35(3)
C(22)	-206(8)	24486(7)	6466(3)	31(3)
C(23)	1488(9)	25146(8)	6266(5)	50(4)
C(24)	1894(11)	26020(9)	6116(5)	59(4)
C(25)	2170(10)	24777(9)	6656(5)	50(4)
C(26)	3886(10)	24257(14)	6847(6)	107(7)
C(27)	4462(13)	24985(14)	7058(6)	115(7)
C(31)	1074(6)	22488(9)	7118(3)	33(2)
C(32)	1314(7)	21854(7)	6757(3)	28(2)
C(33)	2604(7)	20844(7)	6433(4)	38(3)
C(34)	3801(8)	20663(9)	6497(5)	61(4)
C(35)	1975(8)	19992(7)	6439(4)	36(3)
C(36)	1642(12)	18694(9)	6038(6)	64(4)
C(37)	2108(13)	18241(9)	5630(5)	78(5)
C(41)	-1172(10)	20299(9)	6579(4)	40(3)
C(42)	-1538(7)	20472(7)	6098(4)	31(3)
C(43)	-2193(8)	19889(7)	5382(4)	41(3)
C(44)	-1866(11)	19138(9)	5097(4)	62(4)
C(45)	-3419(10)	20045(10)	5391(5)	53(3)
C(46)	-4987(12)	20266(13)	4922(6)	90(5)

C(47)	-5573(16)	19503(13)	5011(9)	165(11)
P(1)	-5778(3)	7734(5)	6861(1)	113(3)
F(1)	-5513(9)	7044(9)	7292(4)	133(5)
F(2)	-5786(14)	8482(10)	7178(4)	212(9)
F(3)	-6074(8)	8302(8)	6446(4)	119(4)
F(4)	-5829(17)	6859(11)	6538(5)	209(8)
F(5)	-6980(7)	7508(11)	6983(3)	124(3)
F(6)	-4617(6)	7661(13)	6740(3)	148(6)
P(2)	-1878(2)	22126(2)	4518(1)	37(1)
F(7)	-2924(5)	21987(7)	4262(3)	109(4)
F(8)	-2129(8)	23107(5)	4559(3)	82(3)
F(9)	-2426(10)	21996(6)	4989(3)	121(4)
F(10)	-1588(10)	21143(5)	4483(3)	112(4)
F(11)	-1283(6)	22270(6)	4061(2)	88(3)
F(12)	-783(6)	22312(9)	4773(3)	167(6)
P(3)	-1318(2)	17371(3)	6269(1)	53(1)
F(13)	-1849(10)	17075(10)	6698(4)	164(6)
F(14)	-2354(7)	17811(6)	6094(4)	131(5)
F(15)	-1591(7)	16481(6)	6031(3)	91(3)
F(16)	-984(8)	18257(5)	6502(4)	116(4)
F(17)	-699(8)	17664(9)	5832(3)	136(5)
F(18)	-217(7)	16984(5)	6453(4)	95(3)
O(2S)	3339(10)	21520(8)	7636(4)	88(4)

***Table A.4.8.3** - Bond lengths [Å] and angles [°] for C36 H68 F18 Gd N8 O14 P3.*

Gd(1)-O(2)	2.399(6)	N(4)-C(41)	1.464(15)	P(1)-F(5)	1.595(11)
Gd(1)-O(4)	2.400(7)	N(4)-C(6)	1.489(13)	P(1)-F(4)	1.657(15)
Gd(1)-O(3)	2.406(6)	N(4)-C(7)	1.507(13)	P(1)-F(1)	1.699(13)
Gd(1)-O(5)	2.447(6)	N(5)-C(12)	1.312(11)	P(2)-F(7)	1.537(8)
Gd(1)-O(1)	2.457(6)	N(5)-C(13)	1.449(13)	P(2)-F(8)	1.547(8)
Gd(1)-N(1)	2.641(8)	N(6)-C(22)	1.303(13)	P(2)-F(10)	1.560(8)
Gd(1)-N(2)	2.647(9)	N(6)-C(23)	1.452(13)	P(2)-F(11)	1.570(7)
Gd(1)-N(4)	2.667(9)	N(7)-C(32)	1.331(12)	P(2)-F(9)	1.578(8)
Gd(1)-N(3)	2.670(8)	N(7)-C(33)	1.440(13)	P(2)-F(12)	1.600(8)
O(1)-C(12)	1.285(11)	N(8)-C(42)	1.317(13)	P(3)-F(13)	1.514(10)
O(2)-C(22)	1.260(11)	N(8)-C(43)	1.466(14)	P(3)-F(14)	1.561(8)
O(3)-C(32)	1.263(11)	C(1)-C(2)	1.539(16)	P(3)-F(15)	1.580(10)
O(4)-C(42)	1.237(11)	C(3)-C(4)	1.537(16)	P(3)-F(17)	1.584(9)
O(11)-C(15)	1.325(13)	C(5)-C(6)	1.510(18)	P(3)-F(16)	1.587(9)
O(11)-C(16)	1.476(13)	C(7)-C(8)	1.521(14)	P(3)-F(18)	1.605(8)
O(12)-C(15)	1.218(13)	C(11)-C(12)	1.512(13)	O(2S)-H(2SA)	0.81(18)
O(21)-C(25)	1.326(14)	C(13)-C(15)	1.532(15)	O(2S)-H(2SB)	1.03(19)
O(21)-C(26)	1.504(17)	C(13)-C(14)	1.533(15)		
O(22)-C(25)	1.195(15)	C(16)-C(17)	1.456(17)	O(2)-Gd(1)-O(4)	145.6(2)
O(31)-C(35)	1.344(14)	C(21)-C(22)	1.535(15)	O(2)-Gd(1)-O(3)	82.2(2)
O(31)-C(36)	1.468(15)	C(23)-C(24)	1.507(17)	O(4)-Gd(1)-O(3)	84.6(2)
O(32)-C(35)	1.219(13)	C(23)-C(25)	1.553(18)	O(2)-Gd(1)-O(5)	71.3(3)
O(41)-C(45)	1.185(15)	C(26)-C(27)	1.48(2)	O(4)-Gd(1)-O(5)	74.5(3)
O(42)-C(45)	1.333(15)	C(31)-C(32)	1.483(14)	O(3)-Gd(1)-O(5)	72.8(2)
O(42)-C(46)	1.554(17)	C(33)-C(35)	1.533(15)	O(2)-Gd(1)-O(1)	86.4(2)
N(1)-C(1)	1.493(13)	C(33)-C(34)	1.544(13)	O(4)-Gd(1)-O(1)	86.5(2)
N(1)-C(11)	1.496(11)	C(36)-C(37)	1.52(2)	O(3)-Gd(1)-O(1)	145.0(2)
N(1)-C(8)	1.497(13)	C(41)-C(42)	1.529(15)	O(5)-Gd(1)-O(1)	72.2(2)
N(2)-C(3)	1.488(13)	C(43)-C(44)	1.491(16)	O(2)-Gd(1)-N(1)	133.1(2)
N(2)-C(21)	1.499(15)	C(43)-C(45)	1.563(16)	O(4)-Gd(1)-N(1)	72.8(2)
N(2)-C(2)	1.502(13)	C(46)-C(47)	1.41(2)	O(3)-Gd(1)-N(1)	141.0(2)
N(3)-C(4)	1.485(17)	P(1)-F(2)	1.489(13)	O(5)-Gd(1)-N(1)	127.8(2)
N(3)-C(5)	1.485(16)	P(1)-F(6)	1.510(9)	O(1)-Gd(1)-N(1)	66.3(2)
N(3)-C(31)	1.517(11)	P(1)-F(3)	1.561(11)	O(2)-Gd(1)-N(2)	65.6(2)

O(4)-Gd(1)-N(2)	141.8(3)	C(42)-N(8)-H(8)	117.9	N(5)-C(13)-H(13)	108.1
O(3)-Gd(1)-N(2)	130.7(2)	C(43)-N(8)-H(8)	117.9	C(15)-C(13)-H(13)	108.1
O(5)-Gd(1)-N(2)	124.3(3)	N(1)-C(1)-C(2)	115.6(9)	C(14)-C(13)-H(13)	108.1
O(1)-Gd(1)-N(2)	71.6(2)	N(1)-C(1)-H(1A)	108.4	C(13)-C(14)-H(14A)	109.5
N(1)-Gd(1)-N(2)	69.8(3)	C(2)-C(1)-H(1A)	108.4	C(13)-C(14)-H(14B)	109.5
O(2)-Gd(1)-N(4)	138.4(3)	N(1)-C(1)-H(1B)	108.4	H(14A)-C(14)-H(14B)	109.5
O(4)-Gd(1)-N(4)	65.7(3)	C(2)-C(1)-H(1B)	108.4	C(13)-C(14)-H(14C)	109.5
O(3)-Gd(1)-N(4)	74.0(2)	H(1A)-C(1)-H(1B)	107.4	H(14A)-C(14)-H(14C)	109.5
O(5)-Gd(1)-N(4)	129.7(3)	N(2)-C(2)-C(1)	111.4(9)	H(14B)-C(14)-H(14C)	109.5
O(1)-Gd(1)-N(4)	131.5(2)	N(2)-C(2)-H(2A)	109.4	O(12)-C(15)-O(11)	122.3(11)
N(1)-Gd(1)-N(4)	67.8(2)	C(1)-C(2)-H(2A)	109.3	O(12)-C(15)-C(13)	123.4(11)
N(2)-Gd(1)-N(4)	106.0(3)	N(2)-C(2)-H(2B)	109.3	O(11)-C(15)-C(13)	114.3(10)
O(2)-Gd(1)-N(3)	70.8(3)	C(1)-C(2)-H(2B)	109.3	C(17)-C(16)-O(11)	110.5(10)
O(4)-Gd(1)-N(3)	131.2(3)	H(2A)-C(2)-H(2B)	108.0	C(17)-C(16)-H(16A)	109.5
O(3)-Gd(1)-N(3)	66.9(3)	N(2)-C(3)-C(4)	114.6(9)	O(11)-C(16)-H(16A)	109.5
O(5)-Gd(1)-N(3)	127.2(2)	N(2)-C(3)-H(3A)	108.6	C(17)-C(16)-H(16B)	109.6
O(1)-Gd(1)-N(3)	138.7(3)	C(4)-C(3)-H(3A)	108.6	O(11)-C(16)-H(16B)	109.6
N(1)-Gd(1)-N(3)	105.0(2)	N(2)-C(3)-H(3B)	108.6	H(16A)-C(16)-H(16B)	108.1
N(2)-Gd(1)-N(3)	67.8(3)	C(4)-C(3)-H(3B)	108.6	C(16)-C(17)-H(17A)	109.5
N(4)-Gd(1)-N(3)	68.6(3)	H(3A)-C(3)-H(3B)	107.6	C(16)-C(17)-H(17B)	109.5
C(12)-O(1)-Gd(1)	121.2(6)	N(3)-C(4)-C(3)	110.2(11)	H(17A)-C(17)-H(17B)	109.5
C(22)-O(2)-Gd(1)	123.3(6)	N(3)-C(4)-H(4A)	109.6	C(16)-C(17)-H(17C)	109.5
C(32)-O(3)-Gd(1)	122.3(6)	C(3)-C(4)-H(4A)	109.6	H(17A)-C(17)-H(17C)	109.5
C(42)-O(4)-Gd(1)	123.9(7)	N(3)-C(4)-H(4B)	109.6	H(17B)-C(17)-H(17C)	109.5
C(15)-O(11)-C(16)	116.7(9)	C(3)-C(4)-H(4B)	109.6	N(2)-C(21)-C(22)	109.9(9)
C(25)-O(21)-C(26)	113.9(11)	H(4A)-C(4)-H(4B)	108.1	N(2)-C(21)-H(21A)	109.7
C(35)-O(31)-C(36)	114.5(10)	N(3)-C(5)-C(6)	115.3(11)	C(22)-C(21)-H(21A)	109.7
C(45)-O(42)-C(46)	115.4(12)	N(3)-C(5)-H(5C)	108.5	N(2)-C(21)-H(21B)	109.7
C(1)-N(1)-C(11)	111.4(8)	C(6)-C(5)-H(5C)	108.5	C(22)-C(21)-H(21B)	109.7
C(1)-N(1)-C(8)	109.1(9)	N(3)-C(5)-H(5D)	108.4	H(21A)-C(21)-H(21B)	108.2
C(11)-N(1)-C(8)	108.1(8)	C(6)-C(5)-H(5D)	108.4	O(2)-C(22)-N(6)	121.6(9)
C(1)-N(1)-Gd(1)	109.9(6)	H(5C)-C(5)-H(5D)	107.5	O(2)-C(22)-C(21)	119.9(10)
C(11)-N(1)-Gd(1)	105.9(5)	N(4)-C(6)-C(5)	111.7(10)	N(6)-C(22)-C(21)	118.4(9)
C(8)-N(1)-Gd(1)	112.2(6)	N(4)-C(6)-H(6B)	109.3	N(6)-C(23)-C(24)	112.6(10)
C(3)-N(2)-C(21)	110.6(9)	C(5)-C(6)-H(6B)	109.3	N(6)-C(23)-C(25)	109.2(12)
C(3)-N(2)-C(2)	106.5(8)	N(4)-C(6)-H(6C)	109.3	C(24)-C(23)-C(25)	111.1(11)
C(21)-N(2)-C(2)	109.4(9)	C(5)-C(6)-H(6C)	109.3	N(6)-C(23)-H(23)	107.9
C(3)-N(2)-Gd(1)	111.6(7)	H(6B)-C(6)-H(6C)	107.9	C(24)-C(23)-H(23)	107.9
C(21)-N(2)-Gd(1)	107.7(6)	N(4)-C(7)-C(8)	111.6(9)	C(25)-C(23)-H(23)	107.9
C(2)-N(2)-Gd(1)	111.1(7)	N(4)-C(7)-H(7B)	109.3	C(23)-C(24)-H(24A)	109.5
C(4)-N(3)-C(5)	109.1(10)	C(8)-C(7)-H(7B)	109.3	C(23)-C(24)-H(24B)	109.5
C(4)-N(3)-C(31)	110.1(10)	N(4)-C(7)-H(7C)	109.3	H(24A)-C(24)-H(24B)	109.5
C(5)-N(3)-C(31)	108.0(10)	C(8)-C(7)-H(7C)	109.3	C(23)-C(24)-H(24C)	109.5
C(4)-N(3)-Gd(1)	113.1(7)	H(7B)-C(7)-H(7C)	108.0	H(24A)-C(24)-H(24C)	109.5
C(5)-N(3)-Gd(1)	109.8(7)	N(1)-C(8)-C(7)	110.5(9)	H(24B)-C(24)-H(24C)	109.5
C(31)-N(3)-Gd(1)	106.5(5)	N(1)-C(8)-H(8B)	109.6	O(22)-C(25)-O(21)	126.4(14)
C(41)-N(4)-C(6)	109.7(9)	C(7)-C(8)-H(8B)	109.5	O(22)-C(25)-C(23)	125.3(11)
C(41)-N(4)-C(7)	110.4(9)	N(1)-C(8)-H(8C)	109.5	O(21)-C(25)-C(23)	108.4(12)
C(6)-N(4)-C(7)	107.4(8)	C(7)-C(8)-H(8C)	109.5	C(27)-C(26)-O(21)	109.1(16)
C(41)-N(4)-Gd(1)	107.7(7)	H(8B)-C(8)-H(8C)	108.1	C(27)-C(26)-H(26A)	109.9
C(6)-N(4)-Gd(1)	110.8(7)	N(1)-C(11)-C(12)	112.0(8)	O(21)-C(26)-H(26A)	109.9
C(7)-N(4)-Gd(1)	110.8(6)	N(1)-C(11)-H(11A)	109.2	C(27)-C(26)-H(26B)	109.8
C(12)-N(5)-C(13)	126.7(8)	C(12)-C(11)-H(11A)	109.2	O(21)-C(26)-H(26B)	109.9
C(12)-N(5)-H(5)	116.6	N(1)-C(11)-H(11B)	109.2	H(26A)-C(26)-H(26B)	108.3
C(13)-N(5)-H(5)	116.6	C(12)-C(11)-H(11B)	109.2	C(26)-C(27)-H(27A)	109.5
C(22)-N(6)-C(23)	124.3(9)	H(11A)-C(11)-H(11B)	107.9	C(26)-C(27)-H(27B)	109.5
C(22)-N(6)-H(6)	117.9	O(1)-C(12)-N(5)	123.0(9)	H(27A)-C(27)-H(27B)	109.5
C(23)-N(6)-H(6)	117.9	O(1)-C(12)-C(11)	118.7(8)	C(26)-C(27)-H(27C)	109.5
C(32)-N(7)-C(33)	124.0(9)	N(5)-C(12)-C(11)	118.3(8)	H(27A)-C(27)-H(27C)	109.5
C(32)-N(7)-H(7)	118.0	N(5)-C(13)-C(15)	107.5(9)	H(27B)-C(27)-H(27C)	109.5
C(33)-N(7)-H(7)	118.0	N(5)-C(13)-C(14)	111.2(9)	C(32)-C(31)-N(3)	112.0(8)
C(42)-N(8)-C(43)	124.2(9)	C(15)-C(13)-C(14)	113.8(9)	C(32)-C(31)-H(31A)	109.2

N(3)-C(31)-H(31A)	109.2	H(41A)-C(41)-H(41B)	108.0	F(3)-P(1)-F(4)	89.2(7)
C(32)-C(31)-H(31B)	109.2	O(4)-C(42)-N(8)	120.9(10)	F(5)-P(1)-F(4)	85.4(9)
N(3)-C(31)-H(31B)	109.2	O(4)-C(42)-C(41)	120.2(10)	F(2)-P(1)-F(1)	90.3(8)
H(31A)-C(31)-H(31B)	107.9	N(8)-C(42)-C(41)	118.9(10)	F(6)-P(1)-F(1)	86.8(6)
O(3)-C(32)-N(7)	120.0(9)	N(8)-C(43)-C(44)	112.8(10)	F(3)-P(1)-F(1)	175.1(8)
O(3)-C(32)-C(31)	121.9(8)	N(8)-C(43)-C(45)	107.7(10)	F(5)-P(1)-F(1)	83.0(7)
N(7)-C(32)-C(31)	118.0(8)	C(44)-C(43)-C(45)	113.7(10)	F(4)-P(1)-F(1)	86.5(8)
N(7)-C(33)-C(35)	110.9(9)	N(8)-C(43)-H(43)	107.4	F(7)-P(2)-F(8)	90.0(6)
N(7)-C(33)-C(34)	110.1(9)	C(44)-C(43)-H(43)	107.5	F(7)-P(2)-F(10)	91.8(6)
C(35)-C(33)-C(34)	110.4(9)	C(45)-C(43)-H(43)	107.5	F(8)-P(2)-F(10)	178.2(7)
N(7)-C(33)-H(33)	108.5	C(43)-C(44)-H(44A)	109.5	F(7)-P(2)-F(11)	89.9(5)
C(35)-C(33)-H(33)	108.4	C(43)-C(44)-H(44B)	109.5	F(8)-P(2)-F(11)	91.6(5)
C(34)-C(33)-H(33)	108.5	H(44A)-C(44)-H(44B)	109.5	F(10)-P(2)-F(11)	88.1(5)
C(33)-C(34)-H(34A)	109.4	C(43)-C(44)-H(44C)	109.5	F(7)-P(2)-F(9)	92.8(6)
C(33)-C(34)-H(34B)	109.5	H(44A)-C(44)-H(44C)	109.5	F(8)-P(2)-F(9)	88.0(5)
H(34A)-C(34)-H(34B)	109.5	H(44B)-C(44)-H(44C)	109.5	F(10)-P(2)-F(9)	92.3(5)
C(33)-C(34)-H(34C)	109.5	O(41)-C(45)-O(42)	127.1(13)	F(11)-P(2)-F(9)	177.3(6)
H(34A)-C(34)-H(34C)	109.5	O(41)-C(45)-C(43)	123.1(12)	F(7)-P(2)-F(12)	177.5(8)
H(34B)-C(34)-H(34C)	109.5	O(42)-C(45)-C(43)	109.7(12)	F(8)-P(2)-F(12)	87.9(6)
O(32)-C(35)-O(31)	125.8(11)	C(47)-C(46)-O(42)	104.2(15)	F(10)-P(2)-F(12)	90.2(7)
O(32)-C(35)-C(33)	124.6(12)	C(47)-C(46)-H(46A)	110.9	F(11)-P(2)-F(12)	88.7(5)
O(31)-C(35)-C(33)	109.6(10)	O(42)-C(46)-H(46A)	110.9	F(9)-P(2)-F(12)	88.6(6)
O(31)-C(36)-C(37)	105.7(12)	C(47)-C(46)-H(46B)	110.9	F(13)-P(3)-F(14)	92.5(8)
O(31)-C(36)-H(36A)	110.6	O(42)-C(46)-H(46B)	110.9	F(13)-P(3)-F(15)	91.3(7)
C(37)-C(36)-H(36A)	110.6	H(46A)-C(46)-H(46B)	108.9	F(14)-P(3)-F(15)	92.5(5)
O(31)-C(36)-H(36B)	110.6	C(46)-C(47)-H(47A)	109.4	F(13)-P(3)-F(17)	176.8(7)
C(37)-C(36)-H(36B)	110.6	C(46)-C(47)-H(47B)	109.5	F(14)-P(3)-F(17)	90.7(6)
H(36A)-C(36)-H(36B)	108.7	H(47A)-C(47)-H(47B)	109.5	F(15)-P(3)-F(17)	89.1(7)
C(36)-C(37)-H(37A)	109.5	C(46)-C(47)-H(47C)	109.5	F(13)-P(3)-F(16)	90.3(8)
C(36)-C(37)-H(37B)	109.5	H(47A)-C(47)-H(47C)	109.5	F(14)-P(3)-F(16)	89.7(5)
H(37A)-C(37)-H(37B)	109.5	H(47B)-C(47)-H(47C)	109.5	F(15)-P(3)-F(16)	177.2(6)
C(36)-C(37)-H(37C)	109.5	F(2)-P(1)-F(6)	102.5(10)	F(17)-P(3)-F(16)	89.2(7)
H(37A)-C(37)-H(37C)	109.5	F(2)-P(1)-F(3)	93.9(9)	F(13)-P(3)-F(18)	89.0(7)
H(37B)-C(37)-H(37C)	109.5	F(6)-P(1)-F(3)	94.7(7)	F(14)-P(3)-F(18)	176.0(6)
N(4)-C(41)-C(42)	111.0(9)	F(2)-P(1)-F(5)	91.0(8)	F(15)-P(3)-F(18)	91.1(5)
N(4)-C(41)-H(41A)	109.5	F(6)-P(1)-F(5)	163.2(11)	F(17)-P(3)-F(18)	87.8(6)
C(42)-C(41)-H(41A)	109.5	F(3)-P(1)-F(5)	94.4(6)	F(16)-P(3)-F(18)	86.6(5)
N(4)-C(41)-H(41B)	109.4	F(2)-P(1)-F(4)	175.4(8)	H(2SA)-O(2S)H(2SB)77(10)	
C(42)-C(41)-H(41B)	109.4	F(6)-P(1)-F(4)	80.7(9)		

Table A.4.8.4 - Anisotropic displacement parameters ($Å^2 x\ 10^3$) for C36 H68 F18 Gd N8 O14 P3. The anisotropic displacement factor exponent takes the form: $-2\pi^2[h^2 a^{*2} U^{11} + ... + 2 h k a^* b^* U^{12}]$

	U^{11}	U^{22}	U^{33}	U^{23}	U^{13}	U^{12}
Gd(1)	16(1)	37(1)	27(1)	2(1)	-2(1)	2(1)
O(1)	12(3)	44(4)	24(4)	4(3)	0(3)	0(3)
O(2)	23(3)	36(4)	39(4)	-5(4)	-3(4)	6(3)
O(3)	21(3)	39(4)	31(4)	5(3)	-5(3)	-2(3)
O(4)	17(3)	40(4)	45(5)	12(4)	-3(3)	-2(3)
O(5)	21(3)	32(4)	33(3)	-5(4)	-3(3)	2(4)
O(11)	50(4)	32(4)	54(5)	7(4)	-5(5)	7(4)
O(12)	120(8)	55(5)	42(5)	1(4)	1(6)	36(7)
O(21)	32(5)	118(9)	61(6)	-17(6)	-5(4)	22(5)
O(22)	32(5)	92(7)	47(5)	-19(5)	-3(4)	5(5)
O(31)	45(5)	49(5)	53(6)	4(5)	-5(4)	-6(4)
O(32)	24(4)	67(6)	49(5)	28(4)	3(4)	-4(4)
O(41)	35(5)	92(8)	76(7)	-10(6)	-5(6)	1(6)
O(42)	36(6)	136(10)	83(7)	-16(7)	-30(5)	8(6)
N(1)	17(4)	52(6)	28(4)	13(4)	-3(3)	1(4)
N(2)	23(5)	37(5)	32(5)	-12(4)	-3(4)	-4(4)
N(3)	20(3)	52(7)	33(4)	8(6)	-1(3)	1(5)

N(4)	14(4)	48(6)	30(5)	11(5)	-4(4)	9(4)
N(5)	14(4)	33(5)	39(5)	0(4)	-11(3)	1(3)
N(6)	28(5)	37(5)	61(7)	-12(6)	-1(5)	3(4)
N(7)	15(4)	49(6)	37(5)	1(5)	-6(4)	2(4)
N(8)	30(5)	35(5)	52(6)	13(5)	-13(5)	-4(4)
C(1)	25(5)	89(10)	38(7)	11(7)	12(5)	16(6)
C(2)	20(6)	69(9)	32(7)	-2(6)	4(5)	14(6)
C(3)	28(6)	82(10)	29(6)	-11(6)	-1(5)	27(6)
C(4)	47(8)	80(11)	33(8)	-19(8)	-5(6)	21(8)
C(5)	24(6)	93(11)	37(8)	10(7)	-8(5)	-4(7)
C(6)	24(6)	76(10)	45(8)	30(7)	-8(5)	9(6)
C(7)	25(6)	49(7)	49(7)	22(6)	1(6)	-6(5)
C(8)	28(6)	54(8)	41(7)	29(6)	-8(5)	-5(6)
C(11)	24(4)	34(8)	33(5)	13(5)	-11(4)	-12(5)
C(12)	29(5)	24(5)	25(5)	1(4)	1(4)	11(4)
C(13)	21(5)	36(6)	49(7)	11(6)	2(5)	5(5)
C(14)	34(6)	46(7)	48(7)	7(6)	-2(6)	7(6)
C(15)	40(8)	52(8)	29(7)	1(6)	-10(6)	9(7)
C(16)	62(8)	44(7)	49(8)	-8(6)	-4(6)	10(6)
C(17)	88(9)	56(10)	75(9)	-14(9)	-16(7)	20(10)
C(21)	22(6)	40(7)	42(8)	-13(6)	-10(5)	4(5)
C(22)	30(5)	35(6)	29(6)	-11(5)	-2(4)	5(5)
C(23)	28(6)	32(6)	90(12)	-15(7)	10(7)	-3(5)
C(24)	40(8)	74(11)	62(10)	-10(8)	3(7)	-10(8)
C(25)	33(7)	50(8)	66(10)	-25(8)	-1(7)	7(6)
C(26)	20(7)	184(19)	118(15)	-67(14)	-24(9)	42(10)
C(27)	58(11)	180(20)	107(15)	-13(15)	10(10)	50(13)
C(31)	20(4)	48(5)	30(4)	3(8)	-3(4)	3(9)
C(32)	18(5)	39(6)	25(5)	13(5)	0(4)	-1(4)
C(33)	10(4)	43(6)	60(8)	-6(6)	2(5)	2(4)
C(34)	21(6)	77(9)	87(11)	-23(8)	-9(6)	12(6)
C(35)	18(5)	38(7)	52(9)	15(6)	0(6)	7(5)
C(36)	63(9)	45(8)	84(11)	-2(8)	-19(8)	-17(7)
C(37)	110(13)	49(8)	76(10)	-10(8)	-34(10)	-21(9)
C(41)	14(6)	53(8)	53(8)	20(7)	1(5)	2(6)
C(42)	9(4)	24(6)	60(8)	8(5)	-7(5)	-4(4)
C(43)	27(6)	43(7)	52(7)	-4(6)	-8(5)	-10(5)
C(44)	63(9)	67(9)	58(9)	3(8)	-6(7)	-9(8)
C(45)	35(7)	69(10)	55(9)	1(8)	-10(7)	-9(7)
C(46)	53(10)	121(15)	97(13)	0(12)	-15(9)	8(10)
C(47)	90(15)	108(17)	300(30)	90(20)	-36(19)	-24(13)
P(1)	68(3)	233(8)	38(2)	3(4)	6(2)	74(4)
F(1)	125(9)	194(13)	81(7)	6(7)	40(6)	44(8)
F(2)	310(20)	216(14)	113(9)	-96(10)	120(12)	-183(16)
F(3)	79(6)	176(11)	101(8)	20(8)	-3(7)	44(8)
F(4)	280(20)	241(17)	105(10)	-68(11)	101(13)	-51(17)
F(5)	112(7)	183(10)	77(5)	-39(10)	17(5)	3(12)
F(6)	54(5)	310(18)	80(6)	58(11)	13(4)	8(10)
P(2)	24(1)	54(2)	32(2)	-2(1)	-5(1)	14(1)
F(7)	22(3)	167(9)	139(8)	-58(7)	-31(5)	5(5)
F(8)	122(8)	54(5)	72(6)	2(5)	26(6)	15(5)
F(9)	235(13)	71(6)	58(5)	0(5)	77(7)	5(7)
F(10)	220(12)	60(5)	57(5)	-8(4)	-9(6)	67(7)
F(11)	85(5)	114(8)	66(5)	-32(5)	36(4)	-32(5)
F(12)	58(5)	300(16)	142(8)	-160(10)	-60(5)	103(9)
P(3)	48(2)	50(2)	59(2)	15(2)	-9(1)	12(2)
F(13)	137(10)	248(18)	107(8)	44(10)	63(8)	-25(10)
F(14)	60(5)	92(8)	242(13)	3(7)	-71(7)	15(5)
F(15)	95(7)	79(6)	100(7)	-14(5)	-30(6)	17(5)
F(16)	86(6)	66(5)	195(11)	-29(6)	-71(8)	20(6)
F(17)	134(8)	194(13)	79(6)	55(8)	1(6)	-58(10)
F(18)	87(6)	59(5)	139(8)	-12(6)	-55(6)	38(5)

***Table A.4.8.5** - Hydrogen coordinates (x 10^4) and isotropic displacement parameters ($Å^2$x 10^3) for C36 H68 F18 Gd N8 O14 P3.*

	x	y	z	U(eq)
H(5)	-4418	23332	5520	34
H(6)	91	25685	6448	50
H(7)	2636	21506	7014	40
H(8)	-1807	19288	5966	47
H(1A)	-3245	22653	7158	61
H(1B)	-4202	22905	6832	61
H(2A)	-3204	24052	6521	48
H(2B)	-3246	24165	7055	48
H(3A)	-1957	23336	7460	55
H(3B)	-1588	24329	7444	55
H(4A)	170	23911	7273	64
H(4B)	-199	23424	7722	64
H(5C)	-1213	22086	7594	61
H(5D)	-22	21856	7734	61
H(6B)	89	20830	7156	58
H(6C)	-894	20610	7478	58
H(7B)	-2517	21471	7297	49
H(7C)	-2649	20475	7152	49
H(8B)	-3229	20917	6429	49
H(8C)	-3991	21311	6809	49
H(11A)	-4339	22431	6125	36
H(11B)	-3475	21813	5894	36
H(13)	-2765	24391	5278	42
H(14A)	-3842	23887	4684	64
H(14B)	-3910	24924	4712	64
H(14C)	-4861	24341	4903	64
H(16A)	-5051	26457	5850	62
H(16B)	-3835	26699	5949	62
H(17A)	-4696	27863	5627	110
H(17B)	-4999	27280	5201	110
H(17C)	-3784	27519	5298	110
H(21A)	-1399	25096	6838	42
H(21B)	-1806	24774	6356	42
H(23)	1547	24737	6006	60
H(24A)	1447	26240	5872	88
H(24B)	2627	25962	6011	88
H(24C)	1870	26427	6369	88
H(26A)	3484	23931	7077	129
H(26B)	4397	23854	6704	129
H(27A)	4955	24758	7284	173
H(27B)	3953	25377	7202	173
H(27C)	4860	25304	6829	173
H(31A)	1406	23053	7043	39
H(31B)	1386	22281	7403	39
H(33)	2500	21129	6135	45
H(34A)	4192	21213	6493	92
H(34B)	4055	20291	6252	92
H(34C)	3915	20369	6784	92
H(36A)	867	18777	6001	77
H(36B)	1772	18349	6312	77
H(37A)	1769	17672	5593	117
H(37B)	2874	18163	5672	117
H(37C)	1980	18595	5362	117
H(41A)	-1568	19798	6702	48
H(41B)	-407	20151	6578	48
H(43)	-1857	20422	5253	49

H(44A)	-1092	19077	5106	94
H(44B)	-2096	19238	4787	94
H(44C)	-2197	18606	5211	94
H(46A)	-5170	20732	5138	108
H(46B)	-5124	20478	4614	108
H(47A)	-6333	19627	4985	247
H(47B)	-5416	19302	5316	247
H(47C)	-5375	19051	4796	247
H(2SA)	3360(150)	22020(120)	7560(60)	150
H(2SB)	3270(160)	20880(130)	7730(60)	150

***Table A.4.9.2** - Atomic coordinates (x 10^4) and equivalent isotropic displacement parameters ($Å^2$x 10^3) for DTMA. U(eq) is defined as one third of the trace of the orthogonalized U^{ij} tensor.*

	x	y	z	U(eq)
O(1)	1382(1)	3830(4)	1492(2)	42(1)
O(2)	695(1)	1110(4)	-2619(2)	48(1)
O(3)	2400(1)	-4675(4)	-1117(2)	45(1)
O(4)	171(1)	-2931(4)	-596(2)	51(1)
N(1)	1259(1)	1447(4)	371(2)	32(1)
N(2)	1610(1)	880(5)	-977(2)	34(1)
N(3)	1746(1)	-2572(5)	-952(2)	31(1)
N(4)	1290(1)	-1973(5)	264(2)	30(1)
N(10)	671(2)	4154(5)	1259(2)	36(1)
N(20)	959(1)	-799(5)	-1801(2)	37(1)
N(30)	2041(2)	-5154(5)	-2312(2)	40(1)
N(40)	531(1)	-669(5)	-499(2)	34(1)
C(1)	1518(2)	2545(6)	80(3)	37(1)
C(2)	1812(2)	1852(6)	-337(3)	38(2)
C(3)	1936(2)	63(6)	-1247(3)	37(2)
C(4)	2085(2)	-1400(6)	-817(3)	34(1)
C(5)	1764(2)	-3581(6)	-317(3)	33(1)
C(6)	1694(2)	-2812(6)	366(3)	33(1)
C(7)	1295(2)	-1105(6)	944(3)	32(1)
C(8)	1505(2)	445(6)	967(3)	33(1)
C(10)	906(2)	2202(6)	559(3)	35(1)
C(11)	1011(2)	3477(6)	1155(3)	31(1)
C(12)	692(2)	5456(7)	1771(3)	46(2)
C(20)	1303(2)	1679(6)	-1577(3)	40(2)
C(21)	959(2)	638(6)	-2050(3)	37(2)
C(22)	639(2)	-1908(7)	-2174(3)	46(2)
C(30)	1711(2)	-3413(6)	-1633(3)	36(1)
C(31)	2088(2)	-4467(6)	-1653(3)	33(1)
C(32)	2366(2)	-6199(7)	-2435(3)	50(2)
C(40)	917(2)	-2964(6)	27(3)	36(1)
C(41)	512(2)	-2181(6)	-377(3)	34(1)
C(42)	166(2)	217(7)	-915(3)	43(2)
O(1W)	0	2792(6)	-2500	39(1)
O(2W)	511(1)	-5685(5)	-1200(2)	59(1)

***Table A.4.9.3** - Bond lengths [Å] and angles [°] for DTMA.*

O(1)-C(11)	1.235(6)	N(30)-C(31)	1.336(7)	C(30)-N(3)-C(4)	112.0(4)
O(2)-C(21)	1.235(6)	N(30)-C(32)	1.460(7)	C(5)-N(3)-C(4)	114.7(4)
O(3)-C(31)	1.224(6)	N(40)-C(41)	1.343(7)	C(40)-N(4)-C(6)	112.5(4)
O(4)-C(41)	1.255(6)	N(40)-C(42)	1.448(7)	C(40)-N(4)-C(7)	112.1(4)
N(1)-C(10)	1.448(7)	C(1)-C(2)	1.515(8)	C(6)-N(4)-C(7)	110.4(4)
N(1)-C(8)	1.465(7)	C(3)-C(4)	1.513(7)	C(11)-N(10)-C(12)	123.5(5)
N(1)-C(1)	1.475(7)	C(5)-C(6)	1.512(7)	C(11)-N(10)-H(10)	118.3
N(2)-C(20)	1.453(7)	C(7)-C(8)	1.510(7)	C(12)-N(10)-H(10)	118.3
N(2)-C(2)	1.462(7)	C(10)-C(11)	1.542(7)	C(21)-N(20)-C(42)	121.9(5)
N(2)-C(3)	1.477(7)	C(20)-C(21)	1.518(8)	C(21)-N(20)-H(20)	119.1
N(3)-C(30)	1.442(6)	C(30)-C(31)	1.540(8)	C(22)-N(20)-H(20)	119.1
N(3)-C(5)	1.464(6)	C(40)-C(41)	1.488(8)	C(31)-N(30)-C(32)	121.5(5)
N(3)-C(4)	1.474(7)			C(31)-N(30)-H(30)	119.2
N(4)-C(40)	1.454(7)	C(10)-N(1)-C(8)	113.0(4)	C(32)-N(30)-H(30)	119.2
N(4)-C(6)	1.468(7)	C(10)-N(1)-C(1)	111.5(4)	C(41)-N(40)-C(22)	123.0(5)
N(4)-C(7)	1.473(6)	C(8)-N(1)-C(1)	114.8(4)	C(41)-N(40)-H(40)	118.5
N(10)-C(11)	1.315(7)	C(20)-N(2)-C(2)	114.0(4)	C(42)-N(40)-H(40)	118.5
N(10)-C(12)	1.473(7)	C(20)-N(2)-C(3)	111.9(4)	N(1)-C(1)-C(2)	115.9(4)
N(20)-C(21)	1.336(7)	C(2)-N(2)-C(3)	110.7(4)	N(1)-C(1)-H(1B)	108.3
N(20)-C(22)	1.449(7)	C(30)-N(3)-C(5)	112.4(4)	C(2)-C(1)-H(1B)	108.3

N(1)-C(1)-H(1A)	108.3	N(4)-C(7)-H(7A)	109.1	N(40)-C(42)-H(42A)	109.5
C(2)-C(1)-H(1A)	108.3	C(8)-C(7)-H(7A)	109.1	H(42C)-C(42)-H(42A)	109.5
H(1B)-C(1)-H(1A)	107.4	H(7B)-C(7)-H(7A)	107.8	H(42B)-C(42)-H(42A)	109.5
N(2)-C(2)-C(1)	116.4(5)	N(1)-C(8)-C(7)	111.4(4)	N(3)-C(30)-C(31)	117.2(4)
N(2)-C(2)-H(2B)	108.2	N(1)-C(8)-H(8B)	109.4	N(3)-C(30)-H(30B)	108.0
C(1)-C(2)-H(2B)	108.2	C(7)-C(8)-H(8B)	109.4	C(31)-C(30)-H(30B)	108.0
N(2)-C(2)-H(2A)	108.2	N(1)-C(8)-H(8A)	109.3	N(3)-C(30)-H(30A)	108.0
C(1)-C(2)-H(2A)	108.2	C(7)-C(8)-H(8A)	109.3	C(31)-C(30)-H(30A)	108.0
H(2B)-C(2)-H(2A)	107.3	H(8B)-C(8)-H(8A)	108.0	H(30B)-C(30)-H(30A)	107.2
N(2)-C(3)-C(4)	112.5(4)	N(1)-C(10)-C(11)	118.1(5)	O(3)-C(31)-N(30)	122.6(5)
N(2)-C(3)-H(3B)	109.1	N(1)-C(10)-H(10B)	107.8	O(3)-C(31)-C(30)	123.6(4)
C(4)-C(3)-H(3B)	109.1	C(11)-C(10)-H(10B)	107.8	N(30)-C(31)-C(30)	113.8(5)
N(2)-C(3)-H(3A)	109.1	N(1)-C(10)-H(10A)	107.8	N(30)-C(32)-H(32C)	109.5
C(4)-C(3)-H(3A)	109.1	C(11)-C(10)-H(10A)	107.8	N(30)-C(32)-H(32B)	109.5
H(3B)-C(3)-H(3A)	107.8	H(10B)-C(10)-H(10A)	107.1	H(32C)-C(32)-H(32B)	109.5
N(3)-C(4)-C(3)	112.3(4)	O(1)-C(11)-N(10)	123.8(5)	N(30)-C(32)-H(32A)	109.5
N(3)-C(4)-H(4B)	109.2	O(1)-C(11)-C(10)	122.4(5)	H(32C)-C(32)-H(32A)	109.5
C(3)-C(4)-H(4B)	109.2	N(10)-C(11)-C(10)	113.8(5)	H(32B)-C(32)-H(32A)	109.5
N(3)-C(4)-H(4A)	109.2	N(10)-C(12)-H(12C)	109.5	N(4)-C(40)-C(41)	115.2(4)
C(3)-C(4)-H(4A)	109.2	N(10)-C(12)-H(12B)	109.5	N(4)-C(40)-H(40B)	108.5
H(4B)-C(4)-H(4A)	107.9	H(12C)-C(12)-H(12B)	109.5	C(41)-C(40)-H(40B)	108.5
N(3)-C(5)-C(6)	115.6(4)	N(10)-C(12)-H(12A)	109.5	N(4)-C(40)-H(40A)	108.5
N(3)-C(5)-H(5B)	108.4	H(12C)-C(12)-H(12A)	109.5	C(41)-C(40)-H(40A)	108.5
C(6)-C(5)-H(5B)	108.4	H(12B)-C(12)-H(12A)	109.5	H(40B)-C(40)-H(40A)	107.5
N(3)-C(5)-H(5A)	108.4	N(2)-C(20)-C(21)	113.4(4)	O(4)-C(41)-N(40)	122.3(5)
C(6)-C(5)-H(5A)	108.4	N(2)-C(20)-H(20B)	108.9	O(4)-C(41)-C(40)	120.2(5)
H(5B)-C(5)-H(5A)	107.4	C(21)-C(20)-H(20B)	108.9	N(40)-C(41)-C(40)	117.5(5)
N(4)-C(6)-C(5)	116.8(4)	N(2)-C(20)-H(20A)	108.9	N(20)-C(22)-H(22C)	109.5
N(4)-C(6)-H(6B)	108.1	C(21)-C(20)-H(20A)	108.9	N(20)-C(22)-H(22B)	109.5
C(5)-C(6)-H(6B)	108.1	H(20B)-C(20)-H(20A)	107.7	H(22C)-C(22)-H(22B)	109.5
N(4)-C(6)-H(6A)	108.1	O(2)-C(21)-N(20)	123.0(5)	N(20)-C(22)-H(22A)	109.5
C(5)-C(6)-H(6A)	108.1	O(2)-C(21)-C(20)	121.5(5)	H(22C)-C(22)-H(22A)	109.5
H(6B)-C(6)-H(6A)	107.3	N(20)-C(21)-C(20)	115.5(5)	H(22B)-C(22)-H(22A)	109.5
N(4)-C(7)-C(8)	112.5(4)	N(40)-C(42)-H(42C)	109.5	H(2WB)-O(2W)-H(2WA)	82.3
N(4)-C(7)-H(7B)	109.1	N(40)-C(42)-H(42B)	109.5		
C(8)-C(7)-H(7B)	109.1	H(42C)-C(42)-H(42B)	109.5		

***Table A.4.9.4** - Anisotropic displacement parameters ($Å^2 x\ 10^3$) for DTMA. The anisotropic displacement factor exponent takes the form: $-2\pi^2[h^2 a^{*2} U^{11} + ... + 2 h k a^* b^* U^{12}]$*

	U^{11}	U^{22}	U^{33}	U^{23}	U^{13}	U^{12}
O(1)	53(3)	38(2)	34(2)	-15(2)	13(2)	-3(2)
O(2)	73(3)	41(2)	29(2)	10(2)	10(2)	15(2)
O(3)	60(3)	42(2)	28(2)	-10(2)	3(2)	11(2)
O(4)	56(3)	32(2)	64(3)	-6(2)	15(2)	-5(2)
N(1)	52(3)	14(2)	30(3)	-1(2)	14(2)	2(2)
N(2)	55(3)	20(2)	28(3)	0(2)	15(2)	5(2)
N(3)	50(3)	21(2)	22(2)	-5(2)	9(2)	0(2)
N(4)	44(3)	21(2)	25(2)	-3(2)	10(2)	-4(2)
N(10)	51(3)	24(3)	35(3)	-8(2)	17(2)	0(2)
N(20)	54(3)	27(3)	30(3)	4(2)	10(2)	2(2)
N(30)	55(3)	38(3)	25(3)	-4(2)	9(2)	11(2)
N(40)	51(3)	25(3)	26(2)	-2(2)	9(2)	-1(2)
C(1)	63(4)	16(3)	31(3)	-4(2)	14(3)	-2(3)
C(2)	61(4)	21(3)	32(3)	0(3)	15(3)	-1(3)
C(3)	61(4)	25(3)	29(3)	2(3)	19(3)	2(3)
C(4)	53(4)	24(3)	28(3)	-3(2)	17(3)	3(3)
C(5)	48(4)	16(3)	36(3)	-1(3)	13(3)	2(3)
C(6)	55(4)	20(3)	24(3)	6(2)	10(3)	-1(3)
C(7)	52(4)	23(3)	23(3)	0(2)	13(3)	0(3)
C(8)	52(4)	26(3)	24(3)	-7(3)	15(3)	-2(3)

C(10)	53(4)	25(3)	27(3)	-3(3)	13(3)	5(3)
C(11)	51(4)	21(3)	23(3)	4(2)	15(3)	-3(3)
C(12)	69(4)	38(4)	38(3)	-14(3)	27(3)	1(3)
C(20)	65(4)	24(3)	32(3)	7(3)	17(3)	7(3)
C(21)	57(4)	32(4)	27(3)	0(3)	18(3)	7(3)
C(22)	61(4)	39(4)	36(4)	-4(3)	11(3)	2(3)
C(30)	51(4)	26(3)	29(3)	-5(3)	10(3)	6(3)
C(31)	57(4)	22(3)	19(3)	-5(3)	9(3)	-4(3)
C(32)	70(4)	50(4)	34(3)	-10(3)	20(3)	13(3)
C(40)	52(4)	20(3)	34(3)	0(3)	12(3)	0(3)
C(41)	45(4)	30(4)	29(3)	-2(3)	16(3)	-5(3)
C(42)	60(4)	36(3)	32(3)	3(3)	14(3)	3(3)
O(1W)	58(4)	25(3)	35(3)	0	12(3)	0
O(2W)	68(3)	41(3)	60(3)	-19(2)	3(2)	7(2)

Table A.4.9.5 - Hydrogen coordinates (x 10^4) and isotropic displacement parameters ($Å^2$x 10^3) for DTMA.

	x	y	z	U(eq)
H(10)	417	3810	1009	43
H(20)	1159	-1080	-1399	45
H(30)	1810	-4972	-2680	48
H(40)	777	-194	-318	41
H(1B)	1695	3149	504	24(12)
H(1A)	1322	3267	-259	41(15)
H(2B)	1962	2698	-514	42(15)
H(2A)	2032	1236	20	33(14)
H(3B)	2185	747	-1200	46(16)
H(3A)	1815	-186	-1782	34(14)
H(4B)	2333	-1815	-964	29(13)
H(4A)	2182	-1164	-276	18(12)
H(5B)	2048	-4086	-171	24(13)
H(5A)	1546	-4394	-481	45(16)
H(6B)	1710	-3606	753	15(11)
H(6A)	1932	-2086	564	10(11)
H(7B)	1450	-1705	1387	29(13)
H(7A)	997	-962	969	17(12)
H(8B)	1530	932	1457	19(12)
H(8A)	1798	311	914	20(12)
H(10B)	738	1406	729	40(15)
H(10A)	718	2648	94	30(13)
H(12C)	401	5778	1758	69
H(12B)	843	6312	1616	69
H(12A)	846	5145	2280	69
H(20B)	1458	2174	-1903	46(16)
H(20A)	1164	2498	-1359	50(16)
H(22C)	695	-2889	-1909	90(30)
H(22B)	652	-2048	-2689	55(18)
H(22A)	354	-1536	-2177	80(20)
H(30B)	1671	-2664	-2046	43
H(30A)	1449	-4047	-1737	43
H(32C)	2274	-6590	-2948	75
H(32B)	2404	-7057	-2084	75
H(32A)	2638	-5650	-2357	75
H(40B)	873	-3477	473	49(17)
H(40A)	979	-3772	-302	41(15)
H(1WA)	227	2121	-2486	80(20)
H(2WB)	237	-5841	-1587	120(30)
H(2WA)	319	-4858	-986	120(30)
H(42C)	250	1291	-936	64
H(42B)	-63	150	-668	64
H(42A)	63	-191	-1424	64

***Table A.4.10.2** - Atomic coordinates (x 10^4) and equivalent isotropic displacement parameters ($Å^2$x 10^3) for C20 H47 Dy F18 N8 O7.50 P3. U(eq) is defined as one third of the trace of the orthogonalized U^{ij} tensor.*

	x	y	z	U(eq)
Dy(1)	-8038(1)	-56(1)	-1851(1)	12(1)
O(1)	-9215(1)	1117(1)	-3087(1)	17(1)
O(2)	-9044(1)	1470(1)	-1083(1)	17(1)
O(3)	-8039(1)	-1202(1)	-126(1)	16(1)
O(4)	-8343(1)	-1533(1)	-2209(1)	18(1)
O(5)	-9995(1)	-125(1)	-1110(1)	17(1)
N(1)	-7383(2)	1703(2)	-3063(1)	16(1)
N(2)	-6657(2)	403(2)	-1094(1)	16(1)
N(3)	-6091(2)	-1829(2)	-1592(1)	16(1)
N(4)	-6795(2)	-518(2)	-3587(1)	18(1)
N(5)	-9809(2)	2715(2)	-4350(2)	23(1)
N(6)	-9232(2)	2642(2)	-146(2)	21(1)
N(7)	-7219(2)	-2828(2)	1031(1)	20(1)
N(8)	-8283(2)	-2516(2)	-3267(2)	25(1)
C(1)	-6905(2)	2179(2)	-2537(2)	18(1)
C(2)	-6077(2)	1199(2)	-1869(2)	18(1)
C(3)	-5728(2)	-694(2)	-679(2)	18(1)
C(4)	-5204(2)	-1504(2)	-1381(2)	19(1)
C(5)	-5569(2)	-2319(2)	-2497(2)	20(1)
C(6)	-5585(2)	-1355(2)	-3456(2)	21(1)
C(7)	-6716(2)	567(2)	-4361(2)	19(1)
C(8)	-6473(2)	1351(2)	-3939(2)	19(1)
C(11)	-8457(2)	2634(2)	-3419(2)	18(1)
C(12)	-9195(2)	2101(2)	-3623(2)	17(1)
C(13)	-10578(3)	2322(3)	-4615(2)	34(1)
C(21)	-7423(2)	978(2)	-278(2)	19(1)
C(22)	-8636(2)	1743(2)	-534(2)	16(1)
C(23)	-10437(2)	3377(2)	-276(2)	31(1)
C(31)	-6401(2)	-2739(2)	-731(2)	18(1)
C(32)	-7274(2)	-2204(2)	100(2)	16(1)
C(33)	-8008(2)	-2411(2)	1903(2)	27(1)
C(41)	-7407(2)	-1037(2)	-3930(2)	21(1)
C(42)	-8031(2)	-1743(2)	-3060(2)	18(1)
C(43)	-9027(3)	-3149(3)	-2552(2)	34(1)
P(1)	-7594(1)	109(1)	2963(1)	22(1)
F(1)	-8078(5)	1465(4)	2823(4)	60(1)
F(1A)	-7651(9)	1397(7)	2331(7)	62(2)
F(2)	-7116(7)	-1281(7)	3132(5)	56(2)
F(2A)	-7468(11)	-1178(10)	3520(7)	61(3)
F(3)	-6741(6)	217(6)	1923(5)	50(2)
F(3A)	-6710(9)	-303(9)	1985(8)	54(3)
F(4)	-8624(2)	238(2)	2449(1)	40(1)
F(5)	-6551(2)	-41(2)	3472(1)	40(1)
F(6)	-8450(5)	-51(5)	4036(4)	54(1)
F(6A)	-8465(6)	558(7)	3877(6)	57(2)
P(2)	-1880(1)	-4280(1)	6720(1)	23(1)
F(7)	-949(2)	-3725(2)	6648(2)	48(1)
F(8)	-2589(2)	-3921(2)	7748(1)	49(1)
F(9)	-2821(2)	-4830(2)	6775(1)	42(1)
F(10)	-1099(2)	-5514(1)	7325(1)	39(1)
F(11)	-1186(2)	-4631(2)	5674(1)	41(1)
F(12)	-2662(2)	-3056(1)	6095(1)	40(1)
P(3)	-5985(2)	4297(2)	-1494(2)	18(1)
F(13)	-5146(7)	3716(6)	-2374(5)	70(2)
F(14)	-6873(4)	4866(4)	-591(4)	48(1)
F(15)	-6468(4)	5546(4)	-2236(4)	45(1)
F(16)	-7003(4)	3931(3)	-1578(4)	35(1)

F(17)	-5521(5)	3082(4)	-740(4)	30(1)
F(18)	-4985(4)	4719(4)	-1393(5)	22(1)
P(3A)	-6165(3)	4287(3)	-1300(3)	21(1)
F(13A)	-5632(8)	4087(7)	-2485(6)	39(2)
F(14A)	-6564(6)	4479(6)	-247(5)	31(1)
F(15A)	-6852(5)	5621(5)	-1783(5)	23(1)
F(16A)	-7231(6)	3921(5)	-1220(5)	25(1)
F(17A)	-5795(10)	3213(10)	-546(9)	55(4)
F(18A)	-5103(7)	4629(7)	-1149(6)	28(2)
P(3B)	-5798(3)	4335(3)	-1726(3)	20(1)
F(13B)	-4761(9)	3629(8)	-2327(7)	43(2)
F(14B)	-6928(6)	5148(6)	-1016(6)	34(2)
F(15B)	-6062(6)	5434(5)	-2608(5)	24(1)
F(16B)	-6710(6)	3979(6)	-1975(6)	29(1)
F(17B)	-5237(7)	2967(6)	-1010(6)	30(2)
F(18B)	-4890(7)	4660(8)	-1641(6)	31(2)
O(1S)	-5766(34)	-5875(42)	-5346(22)	90(14)
O(2S)	-5912(12)	-5845(14)	-5101(11)	50(3)
O(3S)	-6832(10)	-4389(11)	-4229(8)	67(3)
O(4S)	-6539(18)	-5461(15)	-4879(10)	66(4)
O(5S)	-5536(12)	-2979(11)	-5388(9)	69(3)
O(6S)	-6481(3)	-3341(2)	-5050(2)	58(1)
O(7S)	-8058(8)	3309(14)	846(13)	55(3)
O(8S)	-8407(8)	3512(11)	852(11)	38(2)

***Table A.4.10.3** - Bond lengths [Å] and angles [°] for C20 H47 Dy F18 N8 O7.50 P3.*

Dy(1)-O(2)	2.3096(15)	N(6)-H(6)	0.80(3)	C(13)-H(13C)	0.97(4)
Dy(1)-O(4)	2.348(2)	N(7)-C(32)	1.309(3)	C(21)-C(22)	1.519(3)
Dy(1)-O(1)	2.3495(14)	N(7)-C(33)	1.461(3)	C(21)-H(21A)	1.02(3)
Dy(1)-O(3)	2.4139(14)	N(7)-H(7)	0.75(3)	C(21)-H(21B)	0.97(3)
Dy(1)-O(5)	2.427(2)	N(8)-C(42)	1.315(3)	C(23)-H(23A)	0.89(4)
Dy(1)-N(3)	2.605(2)	N(8)-C(43)	1.459(3)	C(23)-H(23B)	0.98(5)
Dy(1)-N(4)	2.640(2)	N(8)-H(8)	0.89(4)	C(23)-H(23C)	0.92(4)
Dy(1)-N(1)	2.643(2)	C(1)-C(2)	1.514(3)	C(31)-C(32)	1.510(3)
Dy(1)-N(2)	2.654(2)	C(1)-H(1A)	0.99(3)	C(31)-H(31A)	0.93(3)
O(1)-C(12)	1.257(3)	C(1)-H(1B)	0.99(3)	C(31)-H(31B)	0.93(3)
O(2)-C(22)	1.263(2)	C(2)-H(2A)	0.92(3)	C(33)-H(33A)	0.90(4)
O(3)-C(32)	1.262(2)	C(2)-H(2B)	0.95(3)	C(33)-H(33B)	1.00(3)
O(4)-C(42)	1.254(3)	C(3)-C(4)	1.520(3)	C(33)-H(33C)	0.93(3)
O(5)-H(5C)	0.78(3)	C(3)-H(3A)	0.97(3)	C(41)-C(42)	1.509(3)
O(5)-H(5D)	0.74(4)	C(3)-H(3B)	0.99(3)	C(41)-H(41A)	0.97(3)
N(1)-C(11)	1.485(3)	C(4)-H(4A)	0.97(3)	C(41)-H(41B)	0.98(3)
N(1)-C(1)	1.490(3)	C(4)-H(4B)	0.95(3)	C(43)-H(43A)	0.89(5)
N(1)-C(8)	1.491(3)	C(5)-C(6)	1.512(3)	C(43)-H(43B)	0.87(5)
N(2)-C(21)	1.482(3)	C(5)-H(5A)	0.94(3)	C(43)-H(43C)	0.92(4)
N(2)-C(3)	1.489(3)	C(5)-H(5B)	0.99(3)	P(1)-F(2A)	1.553(11)
N(2)-C(2)	1.490(3)	C(6)-H(6A)	0.93(3)	P(1)-F(6A)	1.553(7)
N(3)-C(31)	1.480(3)	C(6)-H(6B)	0.94(3)	P(1)-F(3)	1.567(6)
N(3)-C(4)	1.491(3)	C(7)-C(8)	1.514(3)	P(1)-F(1)	1.568(4)
N(3)-C(5)	1.495(3)	C(7)-H(7A)	0.96(3)	P(1)-F(1A)	1.593(8)
N(4)-C(41)	1.479(3)	C(7)-H(7B)	0.90(3)	P(1)-F(2)	1.604(8)
N(4)-C(7)	1.490(3)	C(8)-H(8A)	1.00(3)	P(1)-F(6)	1.606(5)
N(4)-C(6)	1.491(3)	C(8)-H(8B)	0.95(3)	P(1)-F(4)	1.606(2)
N(5)-C(12)	1.313(3)	C(11)-C(12)	1.510(3)	P(1)-F(5)	1.607(2)
N(5)-C(13)	1.459(3)	C(11)-H(11A)	0.95(3)	P(1)-F(3A)	1.613(10)
N(5)-H(5)	0.84(3)	C(11)-H(11B)	0.98(3)	F(1)-F(1A)	0.760(8)
N(6)-C(22)	1.307(3)	C(13)-H(13A)	0.98(4)	F(1)-F(6A)	1.659(10)
N(6)-C(23)	1.457(3)	C(13)-H(13B)	0.87(4)	F(1A)-F(3)	1.665(12)

F(2)-F(2A)	0.619(11)	N(4)-Dy(1)-N(1)	68.42(5)	C(1)-C(2)-H(2B)	108.9(17)
F(2A)-F(6)	1.710(12)	O(2)-Dy(1)-N(2)	67.11(5)	H(2A)-C(2)-H(2B)	106.2(24)
F(3)-F(3A)	0.637(10)	O(4)-Dy(1)-N(2)	144.70(5)	N(2)-C(3)-C(4)	111.3(2)
F(6)-F(6A)	0.740(8)	O(1)-Dy(1)-N(2)	130.80(5)	N(2)-C(3)-H(3A)	108.9(16)
P(2)-F(7)	1.587(2)	O(3)-Dy(1)-N(2)	72.53(5)	C(4)-C(3)-H(3A)	109.3(16)
P(2)-F(8)	1.593(2)	O(5)-Dy(1)-N(2)	128.52(6)	N(2)-C(3)-H(3B)	110.2(17)
P(2)-F(10)	1.596(2)	N(3)-Dy(1)-N(2)	68.80(5)	C(4)-C(3)-H(3B)	107.4(17)
P(2)-F(12)	1.601(2)	N(4)-Dy(1)-N(2)	105.18(6)	H(3A)-C(3)-H(3B)	109.7(23)
P(2)-F(9)	1.603(2)	N(1)-Dy(1)-N(2)	67.46(5)	N(3)-C(4)-C(3)	113.4(2)
P(2)-F(11)	1.609(2)	C(12)-O(1)-Dy(1)	123.93(14)	N(3)-C(4)-H(4A)	109.0(16)
P(3)-F(17)	1.566(5)	C(22)-O(2)-Dy(1)	125.24(13)	C(3)-C(4)-H(4A)	108.5(16)
P(3)-F(13)	1.576(7)	C(32)-O(3)-Dy(1)	121.39(13)	N(3)-C(4)-H(4B)	111.6(17)
P(3)-F(15)	1.590(5)	C(42)-O(4)-Dy(1)	124.05(14)	C(3)-C(4)-H(4B)	109.2(17)
P(3)-F(16)	1.598(5)	Dy(1)-O(5)-H(5C)	112.8(23)	H(4A)-C(4)-H(4B)	104.7(23)
P(3)-F(14)	1.611(5)	Dy(1)-O(5)-H(5D)	121.1(26)	N(3)-C(5)-C(6)	110.9(2)
P(3)-F(18)	1.638(5)	H(5C)-O(5)-H(5D)	107.5(34)	N(3)-C(5)-H(5A)	108.1(18)
P(3A)-F(17A)	1.437(12)	C(11)-N(1)-C(1)	108.4(2)	C(6)-C(5)-H(5A)	111.1(17)
P(3A)-F(14A)	1.517(7)	C(11)-N(1)-C(8)	110.0(2)	N(3)-C(5)-H(5B)	109.8(17)
P(3A)-F(16A)	1.576(7)	C(1)-N(1)-C(8)	108.2(2)	C(6)-C(5)-H(5B)	109.6(17)
P(3A)-F(15A)	1.591(7)	C(11)-N(1)-Dy(1)	106.29(12)	H(5A)-C(5)-H(5B)	107.4(25)
P(3A)-F(18A)	1.674(9)	C(1)-N(1)-Dy(1)	112.47(12)	N(4)-C(6)-C(5)	112.9(2)
P(3A)-F(13A)	1.699(8)	C(8)-N(1)-Dy(1)	111.39(12)	N(4)-C(6)-H(6A)	104.8(17)
F(14A)-F(17A)	1.658(13)	C(21)-N(2)-C(3)	110.1(2)	C(5)-C(6)-H(6A)	112.2(16)
P(3B)-F(18B)	1.431(9)	C(21)-N(2)-C(2)	109.4(2)	N(4)-C(6)-H(6B)	108.9(18)
P(3B)-F(13B)	1.479(10)	C(3)-N(2)-C(2)	108.6(2)	C(5)-C(6)-H(6B)	109.1(18)
P(3B)-F(15B)	1.541(7)	C(21)-N(2)-Dy(1)	106.48(12)	H(6A)-C(6)-H(6B)	108.8(25)
P(3B)-F(16B)	1.577(7)	C(3)-N(2)-Dy(1)	110.56(12)	N(4)-C(7)-C(8)	112.1(2)
P(3B)-F(14B)	1.681(8)	C(2)-N(2)-Dy(1)	111.74(12)	N(4)-C(7)-H(7A)	105.8(16)
P(3B)-F(17B)	1.692(8)	C(31)-N(3)-C(4)	110.4(2)	C(8)-C(7)-H(7A)	112.1(16)
O(1S)-O(4S)	1.06(5)	C(31)-N(3)-C(5)	108.0(2)	N(4)-C(7)-H(7B)	112.8(17)
O(2S)-O(4S)	0.78(2)	C(4)-N(3)-C(5)	108.8(2)	C(8)-C(7)-H(7B)	107.9(17)
O(3S)-O(6S)	1.597(13)	C(31)-N(3)-Dy(1)	106.73(12)	H(7A)-C(7)-H(7B)	106.2(23)
O(3S)-O(4S)	1.79(2)	C(4)-N(3)-Dy(1)	111.72(12)	N(1)-C(8)-C(7)	112.8(2)
O(5S)-O(6S)	1.370(13)	C(5)-N(3)-Dy(1)	111.14(12)	N(1)-C(8)-H(8A)	108.1(15)
		C(41)-N(4)-C(7)	108.9(2)	C(7)-C(8)-H(8A)	109.1(15)
O(2)-Dy(1)-O(4)	140.43(5)	C(41)-N(4)-C(6)	110.1(2)	N(1)-C(8)-H(8B)	110.4(17)
O(2)-Dy(1)-O(1)	84.68(5)	C(7)-N(4)-C(6)	109.1(2)	C(7)-C(8)-H(8B)	110.9(17)
O(4)-Dy(1)-O(1)	81.42(5)	C(41)-N(4)-Dy(1)	107.28(12)	H(8A)-C(8)-H(8B)	105.1(22)
O(2)-Dy(1)-O(3)	82.42(5)	C(7)-N(4)-Dy(1)	111.14(12)	N(1)-C(11)-C(12)	110.0(2)
O(4)-Dy(1)-O(3)	87.95(5)	C(6)-N(4)-Dy(1)	110.28(12)	N(1)-C(11)-H(11A)	112.7(17)
O(1)-Dy(1)-O(3)	144.71(5)	C(12)-N(5)-C(13)	123.4(2)	C(12)-C(11)-H(11A)	113.2(17)
O(2)-Dy(1)-O(5)	72.94(6)	C(12)-N(5)-H(5)	117.6(21)	N(1)-C(11)-H(11B)	107.0(18)
O(4)-Dy(1)-O(5)	67.63(6)	C(13)-N(5)-H(5)	119.0(21)	C(12)-C(11)-H(11B)	109.2(19)
O(1)-Dy(1)-O(5)	73.61(5)	C(22)-N(6)-C(23)	122.6(2)	H(11A)-C(11)-H(11B)	104.4(25)
O(3)-Dy(1)-O(5)	71.22(5)	C(22)-N(6)-H(6)	115.8(25)	O(1)-C(12)-N(5)	123.1(2)
O(2)-Dy(1)-N(3)	131.87(5)	C(23)-N(6)-H(6)	121.6(25)	O(1)-C(12)-C(11)	119.5(2)
O(4)-Dy(1)-N(3)	76.57(5)	C(32)-N(7)-C(33)	123.1(2)	N(5)-C(12)-C(11)	117.4(2)
O(1)-Dy(1)-N(3)	140.73(5)	C(32)-N(7)-H(7)	112.8(25)	N(5)-C(13)-H(13A)	106.8(22)
O(3)-Dy(1)-N(3)	66.70(5)	C(33)-N(7)-H(7)	123.6(25)	N(5)-C(13)-H(13B)	111.2(26)
O(5)-Dy(1)-N(3)	124.73(5)	C(42)-N(8)-C(43)	123.2(2)	H(13A)-C(13)-H(13B)	113.1(34)
O(2)-Dy(1)-N(4)	141.71(5)	C(42)-N(8)-H(8)	119.4(24)	N(5)-C(13)-H(13C)	112.2(24)
O(4)-Dy(1)-N(4)	66.95(5)	C(43)-N(8)-H(8)	117.0(24)	H(13A)-C(13)-H(13C)	105.4(31)
O(1)-Dy(1)-N(4)	72.68(5)	N(1)-C(1)-C(2)	110.6(2)	H(13B)-C(13)-H(13C)	108.0(35)
O(3)-Dy(1)-N(4)	132.85(5)	N(1)-C(1)-H(1A)	105.7(15)	N(2)-C(21)-C(22)	111.1(2)
O(5)-Dy(1)-N(4)	126.26(6)	C(2)-C(1)-H(1A)	111.3(14)	N(2)-C(21)-H(21A)	111.8(17)
N(3)-Dy(1)-N(4)	68.88(5)	N(1)-C(1)-H(1B)	109.4(16)	C(22)-C(21)-H(21A)	112.7(16)
O(2)-Dy(1)-N(1)	74.37(5)	C(2)-C(1)-H(1B)	111.2(16)	N(2)-C(21)-H(21B)	110.9(17)
O(4)-Dy(1)-N(1)	130.84(5)	H(1A)-C(1)-H(1B)	108.4(22)	C(22)-C(21)-H(21B)	104.4(17)
O(1)-Dy(1)-N(1)	66.48(5)	N(2)-C(2)-C(1)	112.5(2)	H(21A)-C(21)-H(21B)	105.6(23)
O(3)-Dy(1)-N(1)	139.02(5)	N(2)-C(2)-H(2A)	107.4(17)	O(2)-C(22)-N(6)	122.7(2)
O(5)-Dy(1)-N(1)	129.90(5)	C(1)-C(2)-H(2A)	110.1(16)	O(2)-C(22)-C(21)	119.2(2)
N(3)-Dy(1)-N(1)	105.37(5)	N(2)-C(2)-H(2B)	111.6(17)	N(6)-C(22)-C(21)	118.1(2)

N(6)-C(23)-H(23A)	109.2(26)	F(2)-P(1)-F(6)	88.0(3)	F(8)-P(2)-F(11)	178.95(10)
N(6)-C(23)-H(23B)	109.0(27)	F(2A)-P(1)-F(4)	90.7(5)	F(10)-P(2)-F(11)	89.94(9)
H(23A)-C(23)-H(23B)	111.3(36)	F(6A)-P(1)-F(4)	93.4(3)	F(12)-P(2)-F(11)	88.99(9)
N(6)-C(23)-H(23C)	112.1(26)	F(3)-P(1)-F(4)	91.8(2)	F(9)-P(2)-F(11)	89.59(10)
H(23A)-C(23)-H(23C)	109.9(35)	F(1)-P(1)-F(4)	90.0(2)	F(17)-P(3)-F(13)	87.8(4)
H(23B)-C(23)-H(23C)	105.2(36)	F(1A)-P(1)-F(4)	89.6(4)	F(17)-P(3)-F(15)	178.5(3)
N(3)-C(31)-C(32)	110.6(2)	F(2)-P(1)-F(4)	90.1(3)	F(13)-P(3)-F(15)	93.6(4)
N(3)-C(31)-H(31A)	111.0(16)	F(6)-P(1)-F(4)	88.3(2)	F(17)-P(3)-F(16)	88.9(3)
C(32)-C(31)-H(31A)	110.6(16)	F(2A)-P(1)-F(5)	88.6(5)	F(13)-P(3)-F(16)	90.0(3)
N(3)-C(31)-H(31B)	107.2(16)	F(6A)-P(1)-F(5)	87.3(3)	F(15)-P(3)-F(16)	91.7(2)
C(32)-C(31)-H(31B)	105.1(17)	F(3)-P(1)-F(5)	87.8(2)	F(17)-P(3)-F(14)	91.6(3)
H(31A)-C(31)-H(31B)	112.1(23)	F(1)-P(1)-F(5)	90.9(2)	F(13)-P(3)-F(14)	178.0(3)
O(3)-C(32)-N(7)	123.0(2)	F(1A)-P(1)-F(5)	91.0(4)	F(15)-P(3)-F(14)	87.0(3)
O(3)-C(32)-C(31)	119.3(2)	F(2)-P(1)-F(5)	89.0(3)	F(16)-P(3)-F(14)	88.1(3)
N(7)-C(32)-C(31)	117.7(2)	F(6)-P(1)-F(5)	92.1(2)	F(17)-P(3)-F(18)	92.5(3)
N(7)-C(33)-H(33A)	109.5(23)	F(4)-P(1)-F(5)	178.99(10)	F(13)-P(3)-F(18)	92.1(4)
N(7)-C(33)-H(33B)	110.7(19)	F(2A)-P(1)-F(3A)	90.2(5)	F(15)-P(3)-F(18)	86.9(3)
H(33A)-C(33)-H(33B)	107.0(29)	F(6A)-P(1)-F(3A)	177.7(5)	F(16)-P(3)-F(18)	177.6(3)
N(7)-C(33)-H(33C)	111.0(19)	F(3)-P(1)-F(3A)	23.1(4)	F(14)-P(3)-F(18)	89.8(3)
H(33A)-C(33)-H(33C)	112.2(29)	F(1)-P(1)-F(3A)	113.5(4)	F(17A)-P(3A)-F(14A)	68.2(5)
H(33B)-C(33)-H(33C)	106.3(27)	F(1A)-P(1)-F(3A)	85.8(5)	F(17A)-P(3A)-F(16A)	84.8(6)
N(4)-C(41)-C(42)	112.2(2)	F(2)-P(1)-F(3A)	67.7(4)	F(14A)-P(3A)-F(16A)	93.6(4)
N(4)-C(41)-H(41A)	111.6(18)	F(6)-P(1)-F(3A)	154.9(4)	F(17A)-P(3A)-F(15A)	159.6(6)
C(42)-C(41)-H(41A)	109.7(18)	F(4)-P(1)-F(3A)	85.8(4)	F(14A)-P(3A)-F(15A)	91.8(4)
N(4)-C(41)-H(41B)	106.1(19)	F(5)-P(1)-F(3A)	93.5(4)	F(16A)-P(3A)-F(15A)	92.3(4)
C(42)-C(41)-H(41B)	104.3(19)	F(1A)-F(1)-P(1)	78.0(8)	F(17A)-P(3A)-F(18A)	88.4(6)
H(41A)-C(41)-H(41B)	112.7(25)	F(1A)-F(1)-F(6A)	135.3(10)	F(14A)-P(3A)-F(18A)	76.1(4)
O(4)-C(42)-N(8)	123.3(2)	P(1)-F(1)-F(6A)	57.4(3)	F(16A)-P(3A)-F(18A)	169.2(5)
O(4)-C(42)-C(41)	120.1(2)	F(1)-F(1A)-P(1)	74.2(8)	F(15A)-P(3A)-F(18A)	91.0(4)
N(8)-C(42)-C(41)	116.4(2)	F(1)-F(1A)-F(3)	131.6(11)	F(17A)-P(3A)-F(13A)	111.7(6)
N(8)-C(43)-H(43A)	107.3(33)	P(1)-F(1A)-F(3)	57.4(4)	F(14A)-P(3A)-F(13A)	176.1(5)
N(8)-C(43)-H(43B)	107.7(32)	F(2A)-F(2)-P(1)	74.1(16)	F(16A)-P(3A)-F(13A)	90.3(4)
H(43A)-C(43)-H(43B)	117.1(45)	F(2)-F(2A)-P(1)	83.4(16)	F(15A)-P(3A)-F(13A)	88.4(4)
N(8)-C(43)-H(43C)	109.9(27)	F(2)-F(2A)-F(6)	142.0(20)	F(18A)-P(3A)-F(13A)	100.0(4)
H(43A)-C(43)-H(43C)	108.2(40)	P(1)-F(2A)-F(6)	58.7(4)	P(3A)-F(14A)-F(17A)	53.6(5)
H(43B)-C(43)-H(43C)	106.6(39)	F(3A)-F(3)-P(1)	82.5(14)	P(3A)-F(17A)-F(14A)	58.1(5)
F(2A)-P(1)-F(6A)	92.0(5)	F(3A)-F(3)-F(1A)	138.4(17)	F(18B)-P(3B)-F(13B)	78.8(5)
F(2A)-P(1)-F(3)	112.4(4)	P(1)-F(3)-F(1A)	59.0(4)	F(18B)-P(3B)-F(15B)	86.7(4)
F(6A)-P(1)-F(3)	155.0(4)	F(3)-F(3A)-P(1)	74.4(13)	F(13B)-P(3B)-F(15B)	94.6(5)
F(2A)-P(1)-F(1)	156.2(4)	F(6A)-F(6)-P(1)	72.5(8)	F(18B)-P(3B)-F(16B)	172.1(5)
F(6A)-P(1)-F(1)	64.2(4)	F(6A)-F(6)-F(2A)	126.8(10)	F(13B)-P(3B)-F(16B)	95.0(5)
F(3)-P(1)-F(1)	91.4(3)	P(1)-F(6)-F(2A)	55.7(4)	F(15B)-P(3B)-F(16B)	89.0(4)
F(2A)-P(1)-F(1A)	176.0(5)	F(6)-F(6A)-P(1)	80.5(9)	F(18B)-P(3B)-F(14B)	98.3(5)
F(6A)-P(1)-F(1A)	92.0(5)	F(6)-F(6A)-F(1)	137.1(11)	F(13B)-P(3B)-F(14B)	177.0(5)
F(3)-P(1)-F(1A)	63.6(4)	P(1)-F(6A)-F(1)	58.3(3)	F(15B)-P(3B)-F(14B)	86.0(4)
F(1)-P(1)-F(1A)	27.8(3)	F(7)-P(2)-F(8)	90.88(11)	F(16B)-P(3B)-F(14B)	87.9(4)
F(2A)-P(1)-F(2)	22.5(4)	F(7)-P(2)-F(10)	90.64(10)	F(18B)-P(3B)-F(17B)	92.1(5)
F(6A)-P(1)-F(2)	114.5(4)	F(8)-P(2)-F(10)	90.87(10)	F(13B)-P(3B)-F(17B)	69.9(5)
F(3)-P(1)-F(2)	89.9(3)	F(7)-P(2)-F(12)	90.09(10)	F(15B)-P(3B)-F(17B)	164.4(5)
F(1)-P(1)-F(2)	178.7(3)	F(8)-P(2)-F(12)	90.19(10)	F(16B)-P(3B)-F(17B)	90.3(4)
F(1A)-P(1)-F(2)	153.5(4)	F(10)-P(2)-F(12)	178.71(10)	F(14B)-P(3B)-F(17B)	109.5(4)
F(2A)-P(1)-F(6)	65.5(4)	F(7)-P(2)-F(9)	179.10(10)	O(6S)-O(3S)-O(4S)	106.5(7)
F(6A)-P(1)-F(6)	27.0(3)	F(8)-P(2)-F(9)	89.75(11)	O(2S)-O(4S)-O(1S)	13.8(23)
F(3)-P(1)-F(6)	177.9(3)	F(10)-P(2)-F(9)	89.99(10)	O(2S)-O(4S)-O(3S)	125.1(19)
F(1)-P(1)-F(6)	90.7(3)	F(12)-P(2)-F(9)	89.27(10)	O(1S)-O(4S)-O(3S)	130.5(29)
F(1A)-P(1)-F(6)	118.5(4)	F(7)-P(2)-F(11)	89.77(11)	O(5S)-O(6S)-O(3S)	138.1(7)

***Table A.4.10.4** - Anisotropic displacement parameters ($Å^2 x\ 10^3$) for C20 H47 Dy F18 N8 O7.50 P3. The anisotropic displacement factor exponent takes the form: $-2\pi^2[\,h^2\,a^{*2}U^{11} + \ldots + 2\,h\,k\,a^*\,b^*\,U^{12}\,]$*

	U^{11}	U^{22}	U^{33}	U^{23}	U^{13}	U^{12}
Dy(1)	11(1)	13(1)	11(1)	-3(1)	-2(1)	-4(1)
O(1)	18(1)	18(1)	15(1)	-1(1)	-4(1)	-7(1)
O(2)	16(1)	18(1)	16(1)	-6(1)	-4(1)	-5(1)
O(3)	14(1)	15(1)	15(1)	-2(1)	-3(1)	-2(1)
O(4)	19(1)	20(1)	18(1)	-6(1)	-2(1)	-8(1)
O(5)	14(1)	20(1)	17(1)	-6(1)	-1(1)	-5(1)
N(1)	15(1)	17(1)	15(1)	-2(1)	-3(1)	-7(1)
N(2)	15(1)	15(1)	17(1)	-4(1)	-4(1)	-4(1)
N(3)	14(1)	16(1)	17(1)	-4(1)	-1(1)	-4(1)
N(4)	18(1)	19(1)	15(1)	-4(1)	0(1)	-7(1)
N(5)	24(1)	25(1)	20(1)	3(1)	-10(1)	-11(1)
N(6)	21(1)	20(1)	23(1)	-11(1)	-6(1)	-4(1)
N(7)	18(1)	15(1)	18(1)	0(1)	-5(1)	-1(1)
N(8)	35(1)	24(1)	23(1)	-6(1)	-9(1)	-14(1)
C(1)	20(1)	17(1)	19(1)	-2(1)	-6(1)	-9(1)
C(2)	16(1)	21(1)	21(1)	-3(1)	-4(1)	-10(1)
C(3)	15(1)	18(1)	21(1)	-4(1)	-7(1)	-4(1)
C(4)	12(1)	19(1)	24(1)	-5(1)	-3(1)	-3(1)
C(5)	17(1)	18(1)	20(1)	-8(1)	1(1)	-2(1)
C(6)	18(1)	23(1)	18(1)	-8(1)	3(1)	-5(1)
C(7)	20(1)	22(1)	14(1)	-4(1)	2(1)	-8(1)
C(8)	18(1)	22(1)	16(1)	-3(1)	1(1)	-9(1)
C(11)	19(1)	15(1)	19(1)	0(1)	-5(1)	-6(1)
C(12)	15(1)	20(1)	15(1)	-5(1)	-2(1)	-4(1)
C(13)	35(2)	43(2)	30(1)	3(1)	-19(1)	-19(1)
C(21)	19(1)	20(1)	17(1)	-6(1)	-5(1)	-5(1)
C(22)	17(1)	16(1)	14(1)	-3(1)	-2(1)	-6(1)
C(23)	24(1)	27(1)	40(2)	-19(1)	-11(1)	4(1)
C(31)	16(1)	14(1)	19(1)	-3(1)	-3(1)	-3(1)
C(32)	15(1)	15(1)	18(1)	-4(1)	-4(1)	-5(1)
C(33)	35(1)	21(1)	16(1)	0(1)	-4(1)	-4(1)
C(41)	27(1)	25(1)	15(1)	-8(1)	-1(1)	-12(1)
C(42)	18(1)	17(1)	19(1)	-5(1)	-6(1)	-4(1)
C(43)	45(2)	32(1)	35(1)	-3(1)	-12(1)	-25(1)
P(1)	20(1)	26(1)	22(1)	-7(1)	-6(1)	-9(1)
F(1)	73(3)	30(2)	88(4)	-22(2)	-41(3)	-5(2)
F(1A)	87(7)	29(3)	70(6)	7(4)	-27(5)	-27(4)
F(2)	76(5)	27(2)	71(4)	-10(3)	-45(3)	-5(3)
F(2A)	75(7)	37(5)	78(7)	20(4)	-41(5)	-34(5)
F(3)	36(2)	100(5)	21(2)	-13(3)	-2(1)	-34(3)
F(3A)	27(3)	108(8)	42(4)	-47(5)	1(2)	-20(5)
F(4)	29(1)	53(1)	46(1)	-17(1)	-18(1)	-11(1)
F(5)	31(1)	63(1)	38(1)	-17(1)	-13(1)	-20(1)
F(6)	42(2)	106(4)	26(2)	-19(2)	5(1)	-43(3)
F(6A)	23(3)	102(6)	54(4)	-51(5)	6(2)	-13(4)
P(2)	22(1)	24(1)	21(1)	-4(1)	-6(1)	-7(1)
F(7)	44(1)	48(1)	66(1)	-8(1)	-19(1)	-26(1)
F(8)	45(1)	68(1)	29(1)	-23(1)	-4(1)	-8(1)
F(9)	43(1)	47(1)	43(1)	4(1)	-19(1)	-28(1)
F(10)	35(1)	33(1)	37(1)	6(1)	-16(1)	-6(1)
F(11)	49(1)	34(1)	27(1)	-9(1)	3(1)	-8(1)
F(12)	43(1)	26(1)	40(1)	-3(1)	-16(1)	-1(1)
O(1S)	109(24)	159(24)	28(13)	1(12)	-8(11)	-93(20)
O(2S)	38(4)	85(6)	29(7)	-3(4)	-14(4)	-29(4)
O(3S)	56(7)	70(7)	46(6)	-11(5)	-10(5)	3(6)
O(4S)	119(14)	76(10)	36(7)	9(7)	-35(9)	-71(11)
O(5S)	74(8)	70(7)	73(8)	-24(6)	-16(6)	-26(6)

O(6S)	61(2)	61(2)	53(2)	-22(1)	-16(1)	-11(1)
O(7S)	28(5)	73(7)	83(5)	-38(4)	-29(5)	-9(5)
O(8S)	27(5)	47(4)	58(3)	-22(3)	-27(4)	-10(4)

***Table A.4.10.5** - Hydrogen coordinates (x 10^4) and isotropic displacement parameters ($Å^2$x 10^3) for C20 H47 Dy F18 N8 O7.50 P3.*

	x	y	z	U(eq)
H(5C)	-10296(28)	-178(28)	-1488(24)	29(8)
H(5D)	-10438(30)	314(30)	-843(25)	30(9)
H(5)	-9741(26)	3360(27)	-4680(22)	25(7)
H(6)	-8890(30)	2775(29)	157(25)	35(9)
H(7)	-6691(30)	-3384(30)	1071(24)	34(9)
H(8)	-7925(33)	-2732(32)	-3838(28)	47(10)
H(1A)	-7600(23)	2656(22)	-2135(18)	12(6)
H(1B)	-6506(25)	2700(24)	-3043(20)	21(7)
H(2A)	-5448(25)	752(24)	-2254(20)	17(6)
H(2B)	-5757(26)	1525(25)	-1572(21)	24(7)
H(3A)	-6070(24)	-1086(23)	-32(20)	17(6)
H(3B)	-5077(27)	-516(26)	-597(22)	27(7)
H(4A)	-4822(23)	-1123(23)	-2009(20)	16(6)
H(4B)	-4584(26)	-2176(25)	-1113(21)	23(7)
H(5A)	-6000(26)	-2759(25)	-2489(21)	23(7)
H(5B)	-4751(28)	-2857(27)	-2455(22)	30(8)
H(6A)	-5177(25)	-895(24)	-3468(20)	19(6)
H(6B)	-5237(27)	-1688(27)	-4014(23)	29(8)
H(7A)	-7453(25)	942(23)	-4599(19)	17(6)
H(7B)	-6157(24)	421(23)	-4901(20)	17(6)
H(8A)	-5697(24)	931(23)	-3713(19)	14(6)
H(8B)	-6390(24)	2019(24)	-4448(20)	19(7)
H(11A)	-8287(25)	3230(25)	-3973(21)	23(7)
H(11B)	-8902(28)	3027(27)	-2878(23)	32(8)
H(13A)	-11252(35)	3017(34)	-4819(28)	51(10)
H(13B)	-10779(35)	1790(36)	-4118(30)	54(11)
H(13C)	-10212(36)	2001(35)	-5200(30)	56(11)
H(21A)	-7039(26)	1417(26)	-98(21)	25(7)
H(21B)	-7569(25)	407(25)	336(21)	22(7)
H(23A)	-10604(35)	4057(36)	-158(29)	54(11)
H(23B)	-10969(41)	2976(40)	184(34)	74(14)
H(23C)	-10560(37)	3491(36)	-909(32)	62(12)
H(31A)	-5735(24)	-3310(23)	-491(19)	16(6)
H(31B)	-6800(24)	-3043(24)	-952(20)	17(6)
H(33A)	-7839(32)	-2970(33)	2471(28)	47(10)
H(33B)	-8845(31)	-2241(29)	1877(24)	37(9)
H(33C)	-7970(28)	-1711(29)	1907(23)	30(8)
H(41A)	-6870(28)	-1517(27)	-4385(23)	31(8)
H(41B)	-8044(29)	-379(29)	-4245(23)	34(8)
H(43A)	-9221(45)	-3480(46)	-2897(38)	89(16)
H(43B)	-9602(45)	-2664(45)	-2232(36)	81(16)
H(43C)	-8611(38)	-3732(38)	-2075(32)	62(12)

***Table A.4.11.2** - Atomic coordinates (x 10^4) and equivalent isotropic displacement parameters ($Å^2$x 10^3) for C40 H74 K0.50 N4 O18.25 P4 Yb. U(eq) is defined as one third of the trace of the orthogonalized U^{ij} tensor.*

	x	y	z	U(eq)
Yb(1)	7422(1)	131(1)	4226(1)	32(1)
P(1)	8299(1)	306(1)	5131(1)	47(1)
P(2)	7963(1)	434(1)	2994(1)	38(1)
P(3)	6573(1)	484(1)	3378(1)	35(1)
P(4)	6928(1)	320(1)	5541(1)	29(1)
O(12)	8444(2)	239(3)	5793(3)	74(2)
O(11)	7827(2)	399(2)	5006(2)	34(1)
O(22)	8404(2)	398(2)	2822(3)	49(2)
O(21)	7917(2)	471(2)	3694(2)	35(1)
O(31)	7032(2)	500(2)	3514(2)	36(1)
O(32)	6425(2)	500(2)	2696(3)	48(2)
O(42)	6481(2)	307(2)	5738(2)	32(1)
O(41)	6965(2)	424(2)	4853(2)	26(1)
N(1)	8017(2)	-422(2)	4513(3)	42(2)
N(2)	7606(2)	-320(3)	3256(3)	45(2)
N(3)	6792(2)	-330(2)	3783(3)	33(2)
N(4)	7196(2)	-432(2)	5050(2)	22(1)
C(1)	8071(3)	-742(3)	4019(4)	50(2)
C(2)	8054(3)	-536(3)	3389(4)	52(3)
C(3)	7293(3)	-643(3)	3107(4)	51(2)
C(4)	6851(2)	-476(3)	3136(4)	37(2)
C(5)	6713(3)	-694(3)	4201(4)	49(2)
C(6)	6792(2)	-588(3)	4920(3)	36(2)
C(7)	7497(3)	-794(3)	5159(4)	49(2)
C(8)	7913(3)	-660(3)	5125(4)	44(2)
C(11)	8450(4)	-164(4)	4744(6)	91(4)
C(12)	8624(4)	728(4)	4807(5)	78(4)
C(13)	8436(1)	1175(1)	4963(2)	48(2)
C(14)	8281(2)	1419(2)	4458(2)	53(3)
C(15)	8151(2)	1834(2)	4551(3)	56(3)
C(16)	8173(2)	2005(2)	5149(3)	50(2)
C(17)	8327(2)	1762(2)	5655(3)	54(3)
C(18)	8458(2)	1347(2)	5562(2)	47(2)
C(21)	7619(2)	-24(2)	2722(3)	30(2)
C(22)	7714(2)	873(3)	2578(3)	32(2)
C(23)	7929(1)	1308(2)	2657(2)	36(2)
C(24)	8336(1)	1395(2)	2518(3)	52(2)
C(25)	8485(2)	1810(2)	2552(4)	63(3)
C(26)	8227(2)	2138(2)	2726(3)	68(3)
C(27)	7820(2)	2051(2)	2865(3)	79(4)
C(28)	7671(2)	1636(2)	2831(2)	47(2)
C(31)	6429(3)	-29(3)	3760(4)	39(2)
C(32)	6288(2)	891(3)	3783(4)	35(2)
C(33)	6465(1)	1344(2)	3657(2)	32(2)
C(34)	6318(2)	1553(2)	3115(2)	44(2)
C(35)	6462(2)	1959(2)	2988(3)	53(3)
C(36)	6753(2)	2155(2)	3402(4)	75(3)
C(37)	6901(2)	1945(2)	3944(3)	88(4)
C(38)	6757(2)	1539(2)	4071(2)	61(3)
C(41)	7158(3)	-216(3)	5669(3)	33(2)
C(42)	7248(3)	654(3)	6046(4)	49(2)
C(43)	7096(1)	1123(1)	6091(2)	34(2)
C(44)	6762(2)	1235(2)	6436(2)	52(3)
C(45)	6622(2)	1654(2)	6433(3)	56(3)
C(46)	6815(2)	1959(2)	6084(3)	44(2)
C(47)	7149(2)	1847(2)	5739(3)	56(3)
C(48)	7289(2)	1429(2)	5742(2)	60(3)

Yb(2)	5158(1)	2608(1)	10136(1)	35(1)
P(5)	5341(1)	2101(1)	8799(1)	43(1)
P(6)	5492(1)	3479(1)	9417(1)	47(1)
P(7)	5467(1)	3101(1)	11495(1)	31(1)
P(8)	5325(1)	1672(1)	10870(1)	34(1)
O(52)	5286(2)	1674(2)	8522(3)	53(2)
O(51)	5434(2)	2115(2)	9511(2)	34(1)
O(62)	5458(2)	3655(2)	8728(3)	59(2)
O(61)	5502(2)	3001(2)	9476(2)	27(1)
O(72)	5464(2)	3551(2)	11744(2)	35(1)
O(71)	5534(2)	3046(2)	10791(2)	33(1)
O(82)	5302(2)	1488(2)	11540(3)	46(2)
O(81)	5422(2)	2128(2)	10827(2)	28(1)
N(5)	4618(2)	2490(3)	9150(3)	47(2)
N(6)	4730(2)	3322(3)	9778(3)	46(2)
N(7)	4696(2)	2849(2)	11013(3)	26(1)
N(8)	4599(2)	2064(2)	10355(3)	40(2)
C(1A)	4354(4)	2817(4)	9053(6)	81(4)
C(2A)	4513(3)	3267(3)	9173(4)	48(2)
C(3A)	4410(3)	3402(3)	10237(4)	40(2)
C(4A)	4547(2)	3296(3)	10926(3)	31(2)
C(5A)	4341(2)	2589(3)	11101(4)	36(2)
C(6A)	4447(3)	2142(3)	10961(4)	47(2)
C(7A)	4251(3)	2017(3)	9875(4)	42(2)
C(8A)	4401(3)	2041(3)	9199(4)	42(2)
C(51)	4839(2)	2282(2)	8441(2)	0(1)
C(52)	5751(3)	2321(3)	8421(4)	49(2)
C(53)	6188(1)	2154(1)	8518(2)	54(3)
C(54)	6442(2)	2241(2)	9054(2)	45(2)
C(55)	6833(2)	2053(2)	9141(3)	82(4)
C(56)	6971(2)	1780(2)	8690(4)	49(2)
C(57)	6718(2)	1693(2)	8153(3)	53(3)
C(58)	6327(2)	1881(2)	8067(2)	52(3)
C(61)	5051(3)	3654(3)	9810(4)	51(2)
C(62)	5934(3)	3716(3)	9868(4)	39(2)
C(63)	6333(1)	3477(1)	9772(2)	38(2)
C(64)	6504(1)	3485(2)	9195(2)	42(2)
C(65)	6883(2)	3285(2)	9119(3)	41(2)
C(66)	7091(2)	3077(2)	9621(3)	45(2)
C(67)	6919(2)	3068(2)	10198(3)	59(3)
C(68)	6541(1)	3268(2)	10274(2)	37(2)
C(71)	4965(2)	2843(3)	11618(3)	31(2)
C(72)	5853(2)	2777(2)	11964(3)	26(2)
C(73)	6269(1)	2991(1)	12095(2)	41(2)
C(74)	6336(2)	3338(2)	12490(2)	51(2)
C(75)	6740(2)	3476(2)	12651(3)	88(4)
C(76)	7077(2)	3267(3)	12416(3)	68(3)
C(77)	7010(1)	2920(2)	12021(3)	64(3)
C(78)	6605(2)	2782(2)	11860(2)	37(2)
C(81)	4830(3)	1643(3)	10403(4)	44(2)
C(82)	5713(3)	1378(3)	10461(4)	43(2)
C(83)	6146(1)	1421(1)	10789(2)	32(2)
C(84)	6391(2)	1764(2)	10632(2)	48(2)
C(85)	6786(2)	1818(2)	10928(3)	63(3)
C(86)	6936(1)	1529(3)	11380(3)	52(3)
C(87)	6690(2)	1187(2)	11537(2)	53(3)
C(88)	6295(2)	1133(2)	11241(2)	45(2)
K(1)	5339(1)	73(1)	1579(1)	63(1)
O(1K)	6183(2)	-141(2)	1884(3)	48(2)
O(2K)	5664(2)	785(2)	2314(3)	56(2)
O(3K)	4808(2)	768(3)	1665(3)	66(2)
O(4K)	5789(3)	216(3)	554(4)	85(3)

O(5K)	4753(4)	-414(4)	641(6)	156(5)
O(6K)	5000	-361(7)	2500	187(8)
O(1S)	5000	1985(3)	12500	51(2)
O(2S)	5895(2)	933(2)	5411(3)	64(2)
O(3S)	5376(2)	489(3)	4553(4)	82(2)
O(4S)	9024(3)	-205(3)	2670(4)	99(3)
O(5S)	4427(2)	4447(3)	6737(3)	73(2)
O(6S)	9089(3)	-764(3)	3670(4)	95(3)
O(7S)	9545(3)	1714(4)	2427(5)	113(3)
O(8S)	9486(3)	-108(4)	4387(5)	127(4)
O(9S)	4325(3)	-918(4)	1208(4)	119(3)
O(10S)	4550(3)	1511(4)	7695(4)	117(3)
O(11S)	5000	3996(6)	12500	139(6)
O(12S)	8519(3)	-463(4)	6499(5)	122(4)
O(13S)	9768(4)	925(4)	2988(5)	143(4)
O(14S)	5780(3)	-714(4)	2564(5)	122(4)
O(15S)	9020(3)	715(3)	6534(4)	102(3)
O(16S)	9626(3)	4(3)	5635(4)	93(3)

***Table A.4.11.3** - Bond lengths [Å] and angles [°] for C40 H74 K0.50 N4 O18.25 P4 Yb.*

Yb(1)-O(11)	2.215(5)	C(1)-C(2)	1.495(13)	Yb(2)-P(6)	3.353(3)
Yb(1)-O(31)	2.231(5)	C(3)-C(4)	1.520(12)	Yb(2)-P(8)	3.365(2)
Yb(1)-O(41)	2.256(5)	C(5)-C(6)	1.581(11)	Yb(2)-P(5)	3.369(2)
Yb(1)-O(21)	2.287(5)	C(7)-C(8)	1.406(12)	Yb(2)-P(7)	3.388(2)
Yb(1)-N(2)	2.620(7)	C(12)-C(13)	1.576(13)	P(5)-O(52)	1.474(7)
Yb(1)-N(3)	2.615(7)	C(13)-C(14)	1.39	P(5)-O(51)	1.537(5)
Yb(1)-N(1)	2.626(7)	C(13)-C(18)	1.39	P(5)-C(52)	1.738(10)
Yb(1)-N(4)	2.639(6)	C(14)-C(15)	1.39	P(5)-C(51)	1.828(5)
Yb(1)-P(1)	3.355(3)	C(15)-C(16)	1.39	P(6)-O(61)	1.507(6)
Yb(1)-P(3)	3.361(2)	C(16)-C(17)	1.39	P(6)-O(62)	1.577(7)
Yb(1)-P(4)	3.383(2)	C(17)-C(18)	1.39	P(6)-C(61)	1.786(10)
Yb(1)-P(2)	3.397(2)	C(22)-C(23)	1.537(9)	P(6)-C(62)	1.822(9)
P(1)-O(12)	1.478(8)	C(23)-C(28)	1.39	P(7)-O(72)	1.514(6)
P(1)-O(11)	1.549(6)	C(23)-C(24)	1.39	P(7)-O(71)	1.549(5)
P(1)-C(11)	1.778(14)	C(24)-C(25)	1.39	P(7)-C(71)	1.841(8)
P(1)-C(12)	1.852(13)	C(25)-C(26)	1.39	P(7)-C(72)	1.847(7)
P(2)-O(22)	1.495(7)	C(26)-C(27)	1.39	P(8)-O(81)	1.475(6)
P(2)-O(21)	1.522(5)	C(27)-C(28)	1.39	P(8)-O(82)	1.555(6)
P(2)-C(22)	1.800(8)	C(32)-C(33)	1.562(9)	P(8)-C(81)	1.821(9)
P(2)-C(21)	1.883(8)	C(33)-C(34)	1.39	P(8)-C(82)	1.827(9)
P(3)-O(31)	1.486(6)	C(33)-C(38)	1.39	N(5)-C(1A)	1.339(15)
P(3)-O(32)	1.506(6)	C(34)-C(35)	1.39	N(5)-C(8A)	1.582(12)
P(3)-C(32)	1.828(8)	C(35)-C(36)	1.39	N(5)-C(51)	1.842(9)
P(3)-C(31)	1.883(9)	C(36)-C(37)	1.39	N(6)-C(2A)	1.441(11)
P(4)-O(41)	1.522(5)	C(37)-C(38)	1.39	N(6)-C(61)	1.467(12)
P(4)-O(42)	1.527(6)	C(42)-C(43)	1.557(11)	N(6)-C(3A)	1.492(11)
P(4)-C(42)	1.782(10)	C(43)-C(48)	1.39	N(7)-C(5A)	1.427(10)
P(4)-C(41)	1.855(8)	C(43)-C(44)	1.39	N(7)-C(4A)	1.491(10)
N(1)-C(1)	1.480(12)	C(44)-C(45)	1.39	N(7)-C(71)	1.510(9)
N(1)-C(8)	1.568(11)	C(45)-C(46)	1.39	N(8)-C(6A)	1.441(11)
N(1)-C(11)	1.66(2)	C(46)-C(47)	1.39	N(8)-C(7A)	1.474(10)
N(2)-C(3)	1.449(12)	C(47)-C(48)	1.39	N(8)-C(81)	1.519(12)
N(2)-C(21)	1.479(11)	Yb(2)-O(61)	2.227(5)	C(1A)-C(2A)	1.52(2)
N(2)-C(2)	1.599(12)	Yb(2)-O(81)	2.241(5)	C(3A)-C(4A)	1.550(10)
N(3)-C(5)	1.486(12)	Yb(2)-O(71)	2.256(5)	C(5A)-C(6A)	1.482(13)
N(3)-C(4)	1.487(10)	Yb(2)-O(51)	2.270(5)	C(7A)-C(8A)	1.562(11)
N(3)-C(31)	1.499(11)	Yb(2)-N(8)	2.550(7)	C(52)-C(53)	1.498(10)
N(4)-C(6)	1.400(10)	Yb(2)-N(7)	2.590(6)	C(53)-C(58)	1.39
N(4)-C(7)	1.504(11)	Yb(2)-N(5)	2.668(7)	C(53)-C(54)	1.39
N(4)-C(41)	1.503(9)	Yb(2)-N(6)	2.715(8)	C(54)-C(55)	1.39

C(55)-C(56)	1.39	O(21)-Yb(1)-P(1)	68.07(13)	O(32)-P(3)-Yb(1)	136.6(3)
C(56)-C(57)	1.39	N(2)-Yb(1)-P(1)	108.7(2)	C(32)-P(3)-Yb(1)	112.8(3)
C(57)-C(58)	1.39	N(3)-Yb(1)-P(1)	154.1(2)	C(31)-P(3)-Yb(1)	72.3(3)
C(62)-C(63)	1.513(9)	N(1)-Yb(1)-P(1)	53.4(2)	O(41)-P(4)-O(42)	114.4(3)
C(63)-C(64)	1.39	N(4)-Yb(1)-P(1)	88.92(13)	O(41)-P(4)-C(42)	112.5(4)
C(63)-C(68)	1.39	O(11)-Yb(1)-P(3)	134.12(15)	O(42)-P(4)-C(42)	111.1(4)
C(64)-C(65)	1.39	O(31)-Yb(1)-P(3)	20.31(15)	O(41)-P(4)-C(41)	106.4(3)
C(65)-C(66)	1.39	O(41)-Yb(1)-P(3)	69.58(12)	O(42)-P(4)-C(41)	107.9(3)
C(66)-C(67)	1.39	O(21)-Yb(1)-P(3)	98.16(14)	C(42)-P(4)-C(41)	103.8(4)
C(67)-C(68)	1.39	N(2)-Yb(1)-P(3)	88.2(2)	O(41)-P(4)-Yb(1)	32.6(2)
C(72)-C(73)	1.504(8)	N(3)-Yb(1)-P(3)	53.6(2)	O(42)-P(4)-Yb(1)	137.0(2)
C(73)-C(78)	1.39	N(1)-Yb(1)-P(3)	153.6(2)	C(42)-P(4)-Yb(1)	109.1(3)
C(73)-C(74)	1.39	N(4)-Yb(1)-P(3)	109.49(13)	C(41)-P(4)-Yb(1)	76.1(2)
C(74)-C(75)	1.39	P(1)-Yb(1)-P(3)	151.27(6)	P(1)-O(11)-Yb(1)	125.2(3)
C(76)-C(77)	1.39	O(11)-Yb(1)-P(4)	65.70(14)	P(2)-O(21)-Yb(1)	125.0(3)
C(77)-C(78)	1.39	O(31)-Yb(1)-P(4)	101.86(14)	P(3)-O(31)-Yb(1)	128.3(3)
C(82)-C(83)	1.519(9)	O(41)-Yb(1)-P(4)	21.34(12)	P(4)-O(41)-Yb(1)	126.0(3)
C(83)-C(84)	1.39	O(21)-Yb(1)-P(4)	135.75(14)	C(1)-N(1)-C(8)	108.5(7)
C(83)-C(88)	1.39	N(2)-Yb(1)-P(4)	154.5(2)	C(1)-N(1)-C(11)	114.1(7)
C(84)-C(85)	1.39	N(3)-Yb(1)-P(4)	90.23(14)	C(8)-N(1)-C(11)	102.0(7)
C(85)-C(86)	1.39	N(1)-Yb(1)-P(4)	107.3(2)	C(1)-N(1)-Yb(1)	113.7(5)
C(86)-C(87)	1.39	N(4)-Yb(1)-P(4)	52.60(13)	C(8)-N(1)-Yb(1)	108.6(5)
C(87)-C(88)	1.39	P(1)-Yb(1)-P(4)	84.98(6)	C(11)-N(1)-Yb(1)	109.2(6)
K(1)-O(6K)	2.694(12)	P(3)-Yb(1)-P(4)	89.04(5)	C(3)-N(2)-C(21)	109.0(6)
K(1)-O(4K)	2.750(9)	O(11)-Yb(1)-P(2)	100.09(14)	C(3)-N(2)-C(2)	110.1(7)
K(1)-O(3K)	2.788(8)	O(31)-Yb(1)-P(2)	67.37(14)	C(21)-N(2)-C(2)	109.5(6)
K(1)-O(1K)	2.824(7)	O(41)-Yb(1)-P(2)	137.62(13)	C(3)-N(2)-Yb(1)	111.2(5)
K(1)-O(2K)	2.893(7)	O(21)-Yb(1)-P(2)	21.54(13)	C(21)-N(2)-Yb(1)	107.1(5)
K(1)-O(5K)	3.067(13)	N(2)-Yb(1)-P(2)	51.5(2)	C(2)-N(2)-Yb(1)	109.8(5)
K(1)-K(1)#1	4.646(5)	N(3)-Yb(1)-P(2)	107.33(14)	C(5)-N(3)-C(4)	111.3(7)
O(6K)-K(1)#1	2.694(12)	N(1)-Yb(1)-P(2)	88.0(2)	C(5)-N(3)-C(31)	109.9(6)
O(11)-Yb(1)-O(31)	126.3(2)	N(4)-Yb(1)-P(2)	152.65(13)	C(4)-N(3)-C(31)	108.4(6)
O(11)-Yb(1)-O(41)	76.5(2)	P(1)-Yb(1)-P(2)	87.11(6)	C(5)-N(3)-Yb(1)	111.6(5)
O(31)-Yb(1)-O(41)	80.7(2)	P(3)-Yb(1)-P(2)	85.77(5)	C(4)-N(3)-Yb(1)	111.4(5)
O(11)-Yb(1)-O(21)	78.8(2)	P(4)-Yb(1)-P(2)	153.34(6)	C(31)-N(3)-Yb(1)	104.1(5)
O(31)-Yb(1)-O(21)	78.0(2)	O(12)-P(1)-O(11)	115.6(4)	C(6)-N(4)-C(7)	110.0(6)
O(41)-Yb(1)-O(21)	127.6(2)	O(12)-P(1)-C(11)	104.6(6)	C(6)-N(4)-C(41)	101.7(6)
O(11)-Yb(1)-N(2)	130.7(2)	O(11)-P(1)-C(11)	111.9(5)	C(7)-N(4)-C(41)	107.2(6)
O(31)-Yb(1)-N(2)	83.4(2)	O(12)-P(1)-C(12)	108.3(5)	C(6)-N(4)-Yb(1)	113.4(4)
O(41)-Yb(1)-N(2)	152.6(2)	O(11)-P(1)-C(12)	111.7(4)	C(7)-N(4)-Yb(1)	114.1(5)
O(21)-Yb(1)-N(2)	69.7(2)	C(11)-P(1)-C(12)	103.9(6)	C(41)-N(4)-Yb(1)	109.4(4)
O(11)-Yb(1)-N(3)	152.3(2)	O(12)-P(1)-Yb(1)	136.8(3)	N(1)-C(1)-C(2)	110.7(8)
O(31)-Yb(1)-N(3)	69.9(2)	O(11)-P(1)-Yb(1)	32.7(2)	C(1)-C(2)-N(2)	108.8(7)
O(41)-Yb(1)-N(3)	85.6(2)	C(11)-P(1)-Yb(1)	80.8(4)	N(2)-C(3)-C(4)	112.7(8)
O(21)-Yb(1)-N(3)	128.8(2)	C(12)-P(1)-Yb(1)	111.9(4)	N(3)-C(4)-C(3)	109.0(6)
N(2)-Yb(1)-N(3)	67.9(2)	O(22)-P(2)-O(21)	114.0(3)	N(3)-C(5)-C(6)	113.9(7)
O(11)-Yb(1)-N(1)	72.2(2)	O(22)-P(2)-C(22)	109.3(4)	N(4)-C(6)-C(5)	110.5(7)
O(31)-Yb(1)-N(1)	150.4(2)	O(21)-P(2)-C(22)	111.1(3)	C(8)-C(7)-N(4)	111.6(8)
O(41)-Yb(1)-N(1)	128.6(2)	O(22)-P(2)-C(21)	114.3(4)	C(7)-C(8)-N(1)	116.4(7)
O(21)-Yb(1)-N(1)	84.7(2)	O(21)-P(2)-C(21)	105.7(3)	N(1)-C(11)-P(1)	107.2(8)
N(2)-Yb(1)-N(1)	68.1(2)	C(22)-P(2)-C(21)	101.6(4)	C(13)-C(12)-P(1)	109.0(7)
N(3)-Yb(1)-N(1)	104.5(2)	O(22)-P(2)-Yb(1)	135.7(3)	C(14)-C(13)-C(12)	116.5(5)
O(11)-Yb(1)-N(4)	85.6(2)	O(21)-P(2)-Yb(1)	33.5(2)	C(18)-C(13)-C(12)	123.1(5)
O(31)-Yb(1)-N(4)	129.8(2)	C(22)-P(2)-Yb(1)	111.6(3)	N(2)-C(21)-P(2)	106.7(5)
O(41)-Yb(1)-N(4)	69.7(2)	C(21)-P(2)-Yb(1)	72.9(2)	C(23)-C(22)-P(2)	116.6(5)
O(21)-Yb(1)-N(4)	151.8(2)	O(31)-P(3)-O(32)	115.6(3)	C(28)-C(23)-C(22)	114.8(4)
N(2)-Yb(1)-N(4)	104.9(2)	O(31)-P(3)-C(32)	113.9(3)	C(24)-C(23)-C(22)	125.0(4)
N(3)-Yb(1)-N(4)	68.3(2)	O(32)-P(3)-C(32)	107.7(4)	N(3)-C(31)-P(3)	109.9(6)
N(1)-Yb(1)-N(4)	68.2(2)	O(31)-P(3)-C(31)	102.4(4)	C(33)-C(32)-P(3)	110.8(5)
O(11)-Yb(1)-P(1)	22.18(15)	O(32)-P(3)-C(31)	112.4(4)	C(34)-C(33)-C(32)	117.9(3)
O(31)-Yb(1)-P(1)	136.0(2)	C(32)-P(3)-C(31)	104.3(4)	C(38)-C(33)-C(32)	122.0(3)
O(41)-Yb(1)-P(1)	98.21(13)	O(31)-P(3)-Yb(1)	31.4(2)	N(4)-C(41)-P(4)	109.5(5)

C(43)-C(42)-P(4)	115.2(6)	O(51)-Yb(2)-P(7)	135.82(13)	C(2A)-N(6)-Yb(2)	111.1(6)
C(48)-C(43)-C(42)	117.9(4)	N(8)-Yb(2)-P(7)	108.43(15)	C(61)-N(6)-Yb(2)	103.5(5)
C(44)-C(43)-C(42)	122.0(4)	N(7)-Yb(2)-P(7)	52.41(13)	C(3A)-N(6)-Yb(2)	108.2(5)
O(61)-Yb(2)-O(81)	127.8(2)	N(5)-Yb(2)-P(7)	151.8(2)	C(5A)-N(7)-C(4A)	107.7(6)
O(61)-Yb(2)-O(71)	77.9(2)	N(6)-Yb(2)-P(7)	88.7(2)	C(5A)-N(7)-C(71)	107.0(6)
O(81)-Yb(2)-O(71)	80.6(2)	P(6)-Yb(2)-P(7)	86.48(6)	C(4A)-N(7)-C(71)	106.2(6)
O(61)-Yb(2)-O(51)	76.9(2)	P(8)-Yb(2)-P(7)	88.26(5)	C(5A)-N(7)-Yb(2)	115.7(5)
O(81)-Yb(2)-O(51)	77.6(2)	P(5)-Yb(2)-P(7)	153.01(5)	C(4A)-N(7)-Yb(2)	112.4(4)
O(71)-Yb(2)-O(51)	124.8(2)	O(52)-P(5)-O(51)	115.9(4)	C(71)-N(7)-Yb(2)	107.3(4)
O(61)-Yb(2)-N(8)	151.2(2)	O(52)-P(5)-C(52)	104.3(4)	C(6A)-N(8)-C(7A)	111.0(7)
O(81)-Yb(2)-N(8)	70.4(2)	O(51)-P(5)-C(52)	110.5(4)	C(6A)-N(8)-C(81)	106.5(7)
O(71)-Yb(2)-N(8)	130.4(2)	O(52)-P(5)-C(51)	92.2(3)	C(7A)-N(8)-C(81)	107.7(7)
O(51)-Yb(2)-N(8)	87.7(2)	O(51)-P(5)-C(51)	120.9(3)	C(6A)-N(8)-Yb(2)	109.8(5)
O(61)-Yb(2)-N(7)	129.3(2)	C(52)-P(5)-C(51)	110.9(4)	C(7A)-N(8)-Yb(2)	116.6(5)
O(81)-Yb(2)-N(7)	85.8(2)	O(52)-P(5)-Yb(2)	138.7(3)	C(81)-N(8)-Yb(2)	104.5(5)
O(71)-Yb(2)-N(7)	71.2(2)	O(51)-P(5)-Yb(2)	34.3(2)	N(5)-C(1A)-C(2A)	119.1(10)
O(51)-Yb(2)-N(7)	153.6(2)	C(52)-P(5)-Yb(2)	113.0(3)	N(6)-C(2A)-C(1A)	113.5(8)
N(8)-Yb(2)-N(7)	67.4(2)	C(51)-P(5)-Yb(2)	90.5(2)	N(6)-C(3A)-C(4A)	115.5(7)
O(61)-Yb(2)-N(5)	84.1(2)	O(61)-P(6)-O(62)	115.4(3)	N(7)-C(4A)-C(3A)	112.8(6)
O(81)-Yb(2)-N(5)	128.8(2)	O(61)-P(6)-C(61)	106.3(4)	N(7)-C(5A)-C(6A)	108.7(7)
O(71)-Yb(2)-N(5)	150.3(2)	O(62)-P(6)-C(61)	109.1(4)	N(8)-C(6A)-C(5A)	116.3(7)
O(51)-Yb(2)-N(5)	72.3(2)	O(61)-P(6)-C(62)	110.8(4)	N(8)-C(7A)-C(8A)	112.1(7)
N(8)-Yb(2)-N(5)	67.9(2)	O(62)-P(6)-C(62)	110.8(4)	C(7A)-C(8A)-N(5)	105.7(7)
N(7)-Yb(2)-N(5)	104.0(2)	C(61)-P(6)-C(62)	103.8(4)	P(5)-C(51)-N(5)	98.3(3)
O(61)-Yb(2)-N(6)	68.1(2)	O(61)-P(6)-Yb(2)	32.2(2)	C(53)-C(52)-P(5)	122.1(6)
O(81)-Yb(2)-N(6)	154.8(2)	O(62)-P(6)-Yb(2)	135.6(3)	C(58)-C(53)-C(52)	117.5(4)
O(71)-Yb(2)-N(6)	84.8(2)	C(61)-P(6)-Yb(2)	75.3(3)	C(54)-C(53)-C(52)	122.4(4)
O(51)-Yb(2)-N(6)	127.5(2)	C(62)-P(6)-Yb(2)	110.7(3)	N(6)-C(61)-P(6)	109.7(7)
N(8)-Yb(2)-N(6)	104.9(2)	O(72)-P(7)-O(71)	116.9(3)	C(63)-C(62)-P(6)	111.0(5)
N(7)-Yb(2)-N(6)	70.0(2)	O(72)-P(7)-C(71)	109.6(3)	C(64)-C(63)-C(62)	120.2(4)
N(5)-Yb(2)-N(6)	66.5(2)	O(71)-P(7)-C(71)	105.9(3)	C(68)-C(63)-C(62)	119.7(4)
O(61)-Yb(2)-P(6)	21.12(14)	O(72)-P(7)-C(72)	110.0(3)	N(7)-C(71)-P(7)	109.0(5)
O(81)-Yb(2)-P(6)	137.32(14)	O(71)-P(7)-C(72)	109.7(3)	C(73)-C(72)-P(7)	114.2(5)
O(71)-Yb(2)-P(6)	67.28(14)	C(71)-P(7)-C(72)	103.9(3)	C(78)-C(73)-C(72)	115.2(4)
O(51)-Yb(2)-P(6)	97.79(15)	O(72)-P(7)-Yb(2)	136.3(2)	C(74)-C(73)-C(72)	124.3(4)
N(8)-Yb(2)-P(6)	152.3(2)	O(71)-P(7)-Yb(2)	33.2(2)	N(8)-C(81)-P(8)	113.4(6)
N(7)-Yb(2)-P(6)	108.25(15)	C(71)-P(7)-Yb(2)	73.5(2)	C(83)-C(82)-P(8)	111.4(5)
N(5)-Yb(2)-P(6)	87.7(2)	C(72)-P(7)-Yb(2)	111.2(2)	C(84)-C(83)-C(82)	118.2(4)
N(6)-Yb(2)-P(6)	50.8(2)	O(81)-P(8)-O(82)	116.3(3)	C(88)-C(83)-C(82)	121.7(4)
O(61)-Yb(2)-P(8)	135.49(13)	O(81)-P(8)-C(81)	101.3(4)	O(6K)-K(1)-O(4K)	158.7(5)
O(81)-Yb(2)-P(8)	20.01(13)	O(82)-P(8)-C(81)	113.3(4)	O(6K)-K(1)-O(3K)	93.9(4)
O(71)-Yb(2)-P(8)	100.50(14)	O(81)-P(8)-C(82)	107.8(4)	O(4K)-K(1)-O(3K)	106.4(3)
O(51)-Yb(2)-P(8)	67.83(14)	O(82)-P(8)-C(82)	109.5(4)	O(6K)-K(1)-O(1K)	98.1(2)
N(8)-Yb(2)-P(8)	54.3(2)	C(81)-P(8)-C(82)	108.0(4)	O(4K)-K(1)-O(1K)	71.1(2)
N(7)-Yb(2)-P(8)	89.80(14)	O(81)-P(8)-Yb(2)	31.3(2)	O(3K)-K(1)-O(1K)	138.8(2)
N(5)-Yb(2)-P(8)	108.8(2)	O(82)-P(8)-Yb(2)	137.9(3)	O(6K)-K(1)-O(2K)	98.1(4)
N(6)-Yb(2)-P(8)	156.4(2)	C(81)-P(8)-Yb(2)	71.5(3)	O(4K)-K(1)-O(2K)	96.8(2)
P(6)-Yb(2)-P(8)	152.12(6)	C(82)-P(8)-Yb(2)	108.0(3)	O(3K)-K(1)-O(2K)	63.6(2)
O(61)-Yb(2)-P(5)	66.32(14)	P(5)-O(51)-Yb(2)	123.3(3)	O(1K)-K(1)-O(2K)	75.7(2)
O(81)-Yb(2)-P(5)	99.46(13)	P(6)-O(61)-Yb(2)	126.7(3)	O(6K)-K(1)-O(5K)	88.1(3)
O(71)-Yb(2)-P(5)	134.60(14)	P(7)-O(71)-Yb(2)	124.8(3)	O(4K)-K(1)-O(5K)	83.8(3)
O(51)-Yb(2)-P(5)	22.42(13)	P(8)-O(81)-Yb(2)	128.7(3)	O(3K)-K(1)-O(5K)	94.8(3)
N(8)-Yb(2)-P(5)	90.3(2)	C(1A)-N(5)-C(8A)	114.7(8)	O(1K)-K(1)-O(5K)	124.7(3)
N(7)-Yb(2)-P(5)	154.08(14)	C(1A)-N(5)-C(51)	114.9(7)	O(2K)-K(1)-O(5K)	157.8(3)
N(5)-Yb(2)-P(5)	53.2(2)	C(8A)-N(5)-C(51)	86.3(5)	O(6K)-K(1)-K(1)#1	30.4(4)
N(6)-Yb(2)-P(5)	105.4(2)	C(1A)-N(5)-Yb(2)	112.7(7)	O(4K)-K(1)-K(1)#1	169.7(2)
P(6)-Yb(2)-P(5)	85.11(6)	C(8A)-N(5)-Yb(2)	109.7(4)	O(3K)-K(1)-K(1)#1	67.5(2)
P(8)-Yb(2)-P(5)	87.30(6)	C(51)-N(5)-Yb(2)	115.9(4)	O(1K)-K(1)-K(1)#1	107.58(15)
O(61)-Yb(2)-P(7)	99.49(13)	C(2A)-N(6)-C(61)	114.8(7)	O(2K)-K(1)-K(1)#1	73.08(14)
O(81)-Yb(2)-P(7)	70.34(13)	C(2A)-N(6)-C(3A)	107.6(7)	O(5K)-K(1)-K(1)#1	104.7(2)
O(71)-Yb(2)-P(7)	22.06(13)	C(61)-N(6)-C(3A)	111.4(7)	K(1)#1-O(6K)-K(1)	119.2(8)

***Table A.4.11.4** - Anisotropic displacement parameters ($Å^2 x\ 10^3$) for C40 H74 K0.50 N4 O18.25 P4 Yb. The anisotropic displacement factor exponent takes the form: $-2\pi^2[h^2 a^{*2} U^{11} + ... + 2 h k a^* b^* U^{12}]$*

	U^{11}	U^{22}	U^{33}	U^{23}	U^{13}	U^{12}
Yb(1)	47(1)	16(1)	33(1)	3(1)	11(1)	2(1)
P(1)	39(1)	30(1)	72(2)	-5(1)	-2(1)	0(1)
P(2)	57(1)	29(1)	30(1)	2(1)	13(1)	-2(1)
P(3)	56(1)	21(1)	27(1)	1(1)	1(1)	12(1)
P(4)	37(1)	26(1)	25(1)	2(1)	6(1)	3(1)
Yb(2)	35(1)	48(1)	22(1)	-1(1)	-3(1)	7(1)
P(5)	33(1)	73(2)	21(1)	-8(1)	-11(1)	-6(1)
P(6)	47(1)	59(2)	34(1)	-1(1)	-4(1)	3(1)
P(7)	37(1)	36(1)	21(1)	-3(1)	3(1)	-4(1)
P(8)	39(1)	35(1)	28(1)	-4(1)	2(1)	-3(1)

***Table A.4.11.5** - Hydrogen coordinates ($x\ 10^4$) and isotropic displacement parameters ($Å^2 x\ 10^3$) for C40 H74 K0.50 N4 O18.25 P4 Yb.*

	x	y	z	U(eq)
H(1A)	7848(3)	-959(3)	4027(4)	60
H(1B)	8343(3)	-887(3)	4100(4)	60
H(2A)	8100(3)	-752(3)	3065(4)	63
H(2B)	8276(3)	-318(3)	3378(4)	63
H(3A)	7337(3)	-882(3)	3404(4)	62
H(3B)	7329(3)	-753(3)	2682(4)	62
H(4A)	6803(2)	-237(3)	2839(4)	45
H(4B)	6648(2)	-704(3)	3017(4)	45
H(5A)	6896(3)	-933(3)	4097(4)	59
H(5B)	6421(3)	-788(3)	4119(4)	59
H(6A)	6586(2)	-374(3)	5042(3)	44
H(6B)	6753(2)	-849(3)	5169(3)	44
H(7A)	7463(3)	-919(3)	5576(4)	58
H(7B)	7433(3)	-1018(3)	4842(4)	58
H(8A)	8095(3)	-913(3)	5173(4)	52
H(8B)	7985(3)	-471(3)	5485(4)	52
H(11B)	8609(4)	-90(4)	4379(6)	110
H(11C)	8629(4)	-343(4)	5032(6)	110
H(12A)	8914(4)	706(4)	4992(5)	94
H(12B)	8627(4)	693(4)	4349(5)	94
H(14A)	8266(2)	1301(2)	4049(2)	64
H(15A)	8046(3)	2000(2)	4205(3)	67
H(16A)	8083(3)	2289(2)	5213(4)	60
H(17A)	8343(3)	1879(2)	6064(3)	65
H(18A)	8564(2)	1181(2)	5908(2)	57
H(21B)	7335(2)	78(2)	2592(3)	36
H(21C)	7734(2)	-168(2)	2361(3)	36
H(22A)	7692(2)	801(3)	2127(3)	38
H(22B)	7427(2)	900(3)	2712(3)	38
H(24A)	8513(2)	1171(2)	2399(3)	62
H(25A)	8764(2)	1869(3)	2457(5)	76
H(26A)	8329(3)	2421(2)	2749(4)	81
H(27A)	7644(3)	2275(2)	2984(4)	94
H(28A)	7393(2)	1576(2)	2926(3)	57
H(31B)	6349(3)	28(3)	4190(4)	46
H(31C)	6187(3)	-159(3)	3521(4)	46
H(32A)	5989(2)	881(3)	3637(4)	42
H(32B)	6312(2)	833(3)	4237(4)	42
H(34A)	6119(2)	1419(2)	2832(2)	53

H(35A)	6361(3)	2102(2)	2618(3)	64
H(36A)	6852(3)	2432(2)	3315(5)	90
H(37A)	7100(2)	2079(2)	4227(4)	106
H(38A)	6858(2)	1396(2)	4441(3)	73
H(41B)	7437(3)	-191(3)	5893(3)	40
H(41C)	6979(3)	-388(3)	5929(3)	40
H(42A)	7264(3)	529(3)	6470(4)	59
H(42B)	7533(3)	656(3)	5900(4)	59
H(44A)	6630(2)	1026(2)	6674(3)	62
H(45A)	6394(2)	1730(2)	6669(4)	67
H(46A)	6719(3)	2245(2)	6082(4)	53
H(47A)	7281(3)	2056(2)	5501(3)	67
H(48A)	7517(2)	1352(2)	5506(3)	72
H(1AA)	4118(4)	2771(4)	9317(6)	97
H(1AB)	4240(4)	2803(4)	8613(6)	97
H(2AA)	4704(3)	3344(3)	8847(4)	57
H(2AB)	4274(3)	3466(3)	9134(4)	57
H(3AA)	4159(3)	3231(3)	10111(4)	49
H(3AB)	4329(3)	3705(3)	10211(4)	49
H(4AA)	4773(2)	3492(3)	11075(3)	37
H(4AB)	4308(2)	3343(3)	11186(3)	37
H(5AA)	4102(2)	2684(3)	10820(4)	43
H(5AB)	4263(2)	2613(3)	11538(4)	43
H(6AA)	4661(3)	2044(3)	11283(4)	56
H(6AB)	4195(3)	1966(3)	11001(4)	56
H(7AA)	4044(3)	2245(3)	9930(4)	50
H(7AB)	4112(3)	1740(3)	9933(4)	50
H(8AA)	4161(3)	2016(3)	8885(4)	50
H(8AB)	4601(3)	1810(3)	9128(4)	50
H(51B)	4671(2)	2045(2)	8252(2)	0
H(51C)	4872(2)	2507(2)	8125(2)	0
H(52A)	5673(3)	2305(3)	7967(4)	59
H(52B)	5762(3)	2626(3)	8531(4)	59
H(54A)	6347(2)	2428(2)	9362(2)	54
H(55A)	7006(2)	2113(3)	9508(3)	99
H(56A)	7239(2)	1652(3)	8749(5)	58
H(57A)	6813(2)	1506(3)	7845(4)	64
H(58A)	6154(2)	1822(2)	7700(2)	62
H(61B)	5137(3)	3719(3)	10252(4)	61
H(61C)	4937(3)	3917(3)	9610(4)	61
H(62A)	5966(3)	4016(3)	9738(4)	46
H(62B)	5881(3)	3714(3)	10317(4)	46
H(64A)	6362(2)	3627(2)	8852(2)	50
H(65A)	7000(2)	3291(3)	8725(3)	49
H(66A)	7350(2)	2940(3)	9569(4)	54
H(67A)	7061(2)	2926(3)	10541(4)	71
H(68A)	6423(2)	3262(2)	10668(2)	44
H(71B)	5013(2)	2546(3)	11758(3)	37
H(71C)	4823(2)	2996(3)	11946(3)	37
H(72A)	5737(2)	2706(2)	12367(3)	31
H(72B)	5896(2)	2507(2)	11741(3)	31
H(74A)	6105(2)	3481(2)	12650(3)	61
H(75A)	6786(3)	3713(3)	12921(4)	106
H(76A)	7353(2)	3362(3)	12525(4)	81
H(77A)	7240(2)	2777(3)	11861(4)	77
H(78A)	6559(2)	2544(2)	11590(3)	45
H(81B)	4883(3)	1545(3)	9977(4)	53
H(81C)	4650(3)	1428(3)	10589(4)	53
H(82A)	5634(3)	1074(3)	10438(4)	52
H(82B)	5717(3)	1487(3)	10028(4)	52
H(84A)	6288(2)	1961(2)	10323(3)	58
H(85A)	6954(2)	2052(2)	10821(4)	76

H(86A)	7206(2)	1566(3)	11583(3)	63
H(87A)	6793(2)	989(3)	11846(3)	64
H(88A)	6127(2)	899(2)	11348(3)	54

***Table A.4.12.2** - Atomic coordinates (x 10^4) and equivalent isotropic displacement parameters ($Å^2$x 10^3) for C40 H66 La N4 O17 P4. U(eq) is defined as one third of the trace of the orthogonalized U^{ij} tensor.*

	x	y	z	U(eq)
La(1)	2849(1)	2193(1)	348(1)	65(1)
P(1)	2346(4)	1588(4)	1792(5)	57(3)
P(2)	4007(5)	2872(5)	1189(6)	84(4)
P(3)	3614(5)	2470(5)	-1085(5)	72(3)
P(4)	1959(4)	1199(6)	-459(6)	87(4)
O(5)	3565(9)	1287(9)	450(11)	68(7)
O(12)	1844(11)	1242(9)	2061(11)	76(7)
O(11)	2458(8)	1481(8)	1111(8)	42(6)
O(22)	4124(10)	3099(9)	1852(13)	80(8)
O(21)	3587(10)	2356(9)	1153(10)	65(7)
O(32)	4037(12)	2870(11)	-1354(11)	89(8)
O(31)	3677(10)	2360(9)	-404(10)	65(7)
O(42)	1722(14)	1043(16)	-1096(14)	148(14)
O(41)	2568(9)	1484(9)	-428(11)	70(7)
N(1)	2078(13)	2663(12)	1266(13)	70(9)
N(2)	3031(12)	3307(11)	659(13)	59(8)
N(3)	2528(16)	2978(15)	-618(15)	93(10)
N(4)	1646(13)	2259(12)	0(14)	67(8)
C(1)	2049(14)	3265(14)	1323(16)	61(10)
C(2)	2748(17)	3425(17)	1252(18)	86(13)
C(3)	2794(18)	3747(17)	143(18)	92(14)
C(4)	2887(20)	3491(20)	-516(21)	112(16)
C(5)	1895(23)	3056(23)	-748(25)	138(18)
C(6)	1613(19)	2529(17)	-658(18)	88(13)
C(7)	1325(15)	2597(14)	470(15)	62(10)
C(8)	1476(14)	2481(15)	1121(15)	60(10)
C(11)	2222(16)	2336(14)	1885(16)	73(11)
C(12)	2991(15)	1470(14)	2252(17)	71(11)
C(13)	3250(11)	891(9)	2272(11)	67(11)
C(14)	2957(9)	450(12)	2587(12)	97(14)
C(15)	3214(13)	-93(10)	2639(12)	138(19)
C(16)	3765(13)	-195(9)	2377(13)	94(13)
C(17)	4058(9)	246(11)	2062(11)	105(14)
C(18)	3800(10)	789(10)	2009(10)	63(10)
C(21)	3694(17)	3442(16)	690(19)	90(13)
C(22)	4663(16)	2663(15)	802(17)	77(12)
C(23)	4946(10)	2142(8)	1005(12)	74(11)
C(24)	5228(11)	2148(9)	1587(11)	84(12)
C(25)	5488(11)	1647(11)	1818(9)	100(14)
C(26)	5466(10)	1140(9)	1467(12)	79(12)
C(27)	5184(11)	1133(8)	885(11)	75(12)
C(28)	4924(10)	1634(11)	654(9)	85(12)
C(31)	2864(14)	2672(14)	-1193(16)	63(10)
C(32)	3629(17)	1812(15)	-1524(18)	81(12)
C(33)	4171(12)	1454(11)	-1417(12)	63(10)
C(34)	4090(12)	1018(12)	-975(13)	99(14)
C(35)	4568(16)	695(11)	-768(12)	158(21)
C(36)	5126(13)	808(14)	-1002(16)	132(18)
C(37)	5208(11)	1245(15)	-1444(16)	166(23)
C(38)	4730(15)	1568(11)	-1652(12)	156(21)
C(41)	1449(16)	1684(15)	-19(17)	70(11)
C(42)	1961(17)	548(16)	44(19)	85(12)
C(43)	2533(10)	212(10)	6(14)	76(11)
C(44)	2820(13)	80(12)	567(10)	114(16)
C(45)	3335(13)	-244(13)	557(12)	115(16)
C(46)	3562(10)	-437(12)	-14(15)	141(19)
C(47)	3275(12)	-306(11)	-575(12)	88(13)

C(48)	2761(12)	19(11)	-565(11)	91(13)
O(1AS)	3349(16)	2927(15)	2831(17)	45(11)
O(1BS)	2837(30)	3867(28)	2851(31)	138(24)
O(2S)	4994(19)	3330(17)	-750(19)	177(15)
O(3AS)	3730(21)	4031(19)	-1813(21)	73(14)
O(3BS)	5101(33)	4115(31)	182(32)	149(26)
O(4S)	4445(23)	2904(19)	-2504(25)	235(21)
O(5AS)	6100(22)	4293(20)	2822(22)	82(15)
O(5BS)	6625(36)	5065(33)	3303(37)	181(30)
O(6S)	4269(22)	3835(19)	-3303(22)	216(19)
O(7AS)	5170(32)	4646(31)	2030(32)	157(26)
O(7BS)	5098(27)	3579(16)	2366(27)	83(17)
O(8S)	3951(30)	5015(27)	-1504(31)	139(24)
O(9S)	5588(24)	3909(22)	1401(25)	99(18)

Table A.4.12.3 - Bond lengths [Å] and angles [°] for C40 H66 La N4 O17 P4.

La(1)-O(41)	2.41(2)	C(14)-C(15)	1.39	O(31)-La(1)-N(3)	68.5(8)
La(1)-O(21)	2.42(2)	C(15)-C(16)	1.39	O(5)-La(1)-N(3)	136.1(8)
La(1)-O(11)	2.47(2)	C(16)-C(17)	1.39	N(2)-La(1)-N(3)	66.7(9)
La(1)-O(31)	2.50(2)	C(17)-C(18)	1.39	O(41)-La(1)-N(1)	124.4(8)
La(1)-O(5)	2.66(2)	C(22)-C(23)	1.43(4)	O(21)-La(1)-N(1)	83.4(8)
La(1)-N(2)	2.69(3)	C(23)-C(24)	1.39	O(11)-La(1)-N(1)	65.4(7)
La(1)-N(3)	2.83(3)	C(23)-C(28)	1.39	O(31)-La(1)-N(1)	147.7(8)
La(1)-N(1)	2.84(3)	C(24)-C(25)	1.39	O(5)-La(1)-N(1)	128.6(8)
La(1)-N(4)	2.84(3)	C(25)-C(26)	1.39	N(2)-La(1)-N(1)	63.9(8)
P(1)-O(11)	1.49(2)	C(26)-C(27)	1.39	N(3)-La(1)-N(1)	95.2(9)
P(1)-O(12)	1.51(2)	C(27)-C(28)	1.39	O(41)-La(1)-N(4)	66.6(7)
P(1)-C(11)	1.76(3)	C(32)-C(33)	1.50(4)	O(21)-La(1)-N(4)	147.5(8)
P(1)-C(12)	1.78(3)	C(33)-C(38)	1.39	O(11)-La(1)-N(4)	81.9(7)
P(2)-O(22)	1.52(3)	C(33)-C(34)	1.39	O(31)-La(1)-N(4)	123.5(7)
P(2)-O(21)	1.53(2)	C(34)-C(35)	1.39	O(5)-La(1)-N(4)	130.7(7)
P(2)-C(22)	1.77(4)	C(35)-C(36)	1.39	N(2)-La(1)-N(4)	99.3(8)
P(2)-C(21)	1.83(4)	C(36)-C(37)	1.39	N(3)-La(1)-N(4)	61.9(9)
P(3)-O(32)	1.45(3)	C(37)-C(38)	1.39	N(1)-La(1)-N(4)	64.0(8)
P(3)-O(31)	1.47(2)	C(42)-C(43)	1.52(4)	O(11)-P(1)-O(12)	114.1(13)
P(3)-C(32)	1.78(4)	C(43)-C(44)	1.39	O(11)-P(1)-C(11)	107.5(15)
P(3)-C(31)	1.78(3)	C(43)-C(48)	1.39	O(12)-P(1)-C(11)	110.9(15)
P(4)-O(42)	1.50(3)	C(44)-C(45)	1.39	O(11)-P(1)-C(12)	111.4(14)
P(4)-O(41)	1.53(2)	C(45)-C(46)	1.39	O(12)-P(1)-C(12)	109.5(16)
P(4)-C(42)	1.85(4)	C(46)-C(47)	1.39	C(11)-P(1)-C(12)	102.8(17)
P(4)-C(41)	1.87(4)	C(47)-C(48)	1.39	O(22)-P(2)-O(21)	115.1(14)
N(1)-C(1)	1.40(4)			O(22)-P(2)-C(22)	112.0(16)
N(1)-C(8)	1.47(4)	O(41)-La(1)-O(21)	140.4(7)	O(21)-P(2)-C(22)	107.0(16)
N(1)-C(11)	1.55(4)	O(41)-La(1)-O(11)	84.1(7)	O(22)-P(2)-C(21)	110.6(16)
N(2)-C(2)	1.44(4)	O(21)-La(1)-O(11)	83.8(6)	O(21)-P(2)-C(21)	106.7(16)
N(2)-C(21)	1.54(4)	O(41)-La(1)-O(31)	82.5(7)	C(22)-P(2)-C(21)	104.9(18)
N(2)-C(3)	1.59(4)	O(21)-La(1)-O(31)	84.4(7)	O(32)-P(3)-O(31)	115.5(16)
N(3)-C(4)	1.46(5)	O(11)-La(1)-O(31)	142.3(6)	O(32)-P(3)-C(32)	109.1(17)
N(3)-C(5)	1.48(6)	O(41)-La(1)-O(5)	71.4(7)	O(31)-P(3)-C(32)	111.2(16)
N(3)-C(31)	1.60(4)	O(21)-La(1)-O(5)	69.0(7)	O(32)-P(3)-C(31)	114.7(16)
N(4)-C(41)	1.40(4)	O(11)-La(1)-O(5)	69.1(6)	O(31)-P(3)-C(31)	105.3(15)
N(4)-C(7)	1.46(4)	O(31)-La(1)-O(5)	73.2(6)	C(32)-P(3)-C(31)	100.0(17)
N(4)-C(6)	1.53(4)	O(41)-La(1)-N(2)	149.3(8)	O(42)-P(4)-O(41)	117.9(18)
C(1)-C(2)	1.64(5)	O(21)-La(1)-N(2)	64.6(8)	O(42)-P(4)-C(42)	109.0(21)
C(3)-C(4)	1.53(5)	O(11)-La(1)-N(2)	122.2(7)	O(41)-P(4)-C(42)	108.9(16)
C(5)-C(6)	1.39(5)	O(31)-La(1)-N(2)	83.9(8)	O(42)-P(4)-C(41)	111.8(17)
C(7)-C(8)	1.45(4)	O(5)-La(1)-N(2)	129.7(7)	O(41)-P(4)-C(41)	106.4(15)
C(12)-C(13)	1.46(4)	O(41)-La(1)-N(3)	82.8(9)	C(42)-P(4)-C(41)	101.7(17)
C(13)-C(14)	1.39	O(21)-La(1)-N(3)	126.0(9)	P(1)-O(11)-La(1)	125.8(11)
C(13)-C(18)	1.39	O(11)-La(1)-N(3)	143.8(8)	P(2)-O(21)-La(1)	126.1(12)

P(3)-O(31)-La(1)	125.4(13)	C(4)-N(3)-La(1)	105.7(25)	N(1)-C(11)-P(1)	114.7(23)
P(4)-O(41)-La(1)	124.2(14)	C(5)-N(3)-La(1)	117.7(27)	C(13)-C(12)-P(1)	119.2(23)
C(1)-N(1)-C(8)	105.1(27)	C(31)-N(3)-La(1)	98.2(19)	C(14)-C(13)-C(12)	119.5(22)
C(1)-N(1)-C(11)	115.1(27)	C(41)-N(4)-C(7)	111.5(28)	C(18)-C(13)-C(12)	120.4(22)
C(8)-N(1)-C(11)	103.6(25)	C(41)-N(4)-C(6)	110.2(29)	N(2)-C(21)-P(2)	105.0(24)
C(1)-N(1)-La(1)	118.0(21)	C(7)-N(4)-C(6)	112.3(27)	C(23)-C(22)-P(2)	118.0(24)
C(8)-N(1)-La(1)	108.8(20)	C(41)-N(4)-La(1)	105.4(20)	C(24)-C(23)-C(22)	117.7(23)
C(11)-N(1)-La(1)	105.3(18)	C(7)-N(4)-La(1)	109.4(20)	C(28)-C(23)-C(22)	122.3(23)
C(2)-N(2)-C(21)	111.3(28)	C(6)-N(4)-La(1)	107.8(21)	N(3)-C(31)-P(3)	118.4(24)
C(2)-N(2)-C(3)	109.2(27)	N(1)-C(1)-C(2)	99.9(27)	C(33)-C(32)-P(3)	114.0(25)
C(21)-N(2)-C(3)	103.4(26)	N(2)-C(2)-C(1)	118.1(30)	C(38)-C(33)-C(32)	126.4(26)
C(2)-N(2)-La(1)	109.1(21)	C(4)-C(3)-N(2)	109.5(32)	C(34)-C(33)-C(32)	113.1(26)
C(21)-N(2)-La(1)	110.8(20)	N(3)-C(4)-C(3)	111.8(37)	N(4)-C(41)-P(4)	112.6(25)
C(3)-N(2)-La(1)	113.0(20)	C(6)-C(5)-N(3)	108.5(41)	C(43)-C(42)-P(4)	112.8(25)
C(4)-N(3)-C(5)	118.4(37)	C(5)-C(6)-N(4)	117.4(38)	C(44)-C(43)-C(42)	117.9(24)
C(4)-N(3)-C(31)	101.8(31)	C(8)-C(7)-N(4)	115.6(29)	C(48)-C(43)-C(42)	122.0(24)
C(5)-N(3)-C(31)	112.2(33)	C(7)-C(8)-N(1)	111.7(28)		

***Table A.4.12.4** - Anisotropic displacement parameters ($Å^2 x\ 10^3$) for C40 H66 La N4 O17 P4. The anisotropic displacement factor exponent takes the form: $-2\pi^2[h^2 a^{*2} U^{11} + ... + 2 h k a^* b^* U^{12}]$*

	U^{11}	U^{22}	U^{33}	U^{23}	U^{13}	U^{12}
La(1)	71(2)	61(2)	63(2)	-3(1)	-13(1)	17(1)
P(1)	26(6)	71(7)	74(8)	11(6)	0(5)	22(5)
P(2)	97(9)	70(8)	85(9)	4(7)	-34(7)	7(7)
P(3)	63(8)	86(8)	66(8)	20(6)	1(6)	30(7)
P(4)	41(7)	141(11)	77(9)	-38(8)	-6(6)	15(7)
O(5)	46(14)	61(15)	98(19)	2(13)	19(14)	1(12)
O(12)	89(20)	63(16)	76(18)	-6(14)	21(15)	-2(15)
O(11)	27(12)	69(15)	30(13)	-17(11)	-12(10)	34(11)
O(22)	58(17)	58(15)	124(24)	7(15)	-47(15)	-5(13)
O(21)	65(16)	55(15)	75(17)	12(12)	-27(13)	-20(13)
O(32)	89(21)	97(20)	80(19)	33(16)	13(16)	35(18)
O(31)	68(16)	75(16)	51(16)	24(13)	-16(12)	39(13)
O(42)	105(25)	230(38)	109(26)	-109(26)	10(20)	18(24)
O(41)	28(13)	66(16)	116(20)	-15(14)	-40(14)	-7(12)

***Table A.4.12.5** - Hydrogen coordinates ($x\ 10^4$) for C40 H66 La N4 O17 P4.*

	x	y	z	U(eq)
H(1A)	1891(14)	3385(14)	1738(16)	73
H(1B)	1811(14)	3440(14)	982(16)	73
H(2A)	2793(17)	3843(17)	1341(18)	103
H(2B)	2964(17)	3214(17)	1585(18)	103
H(3A)	2370(18)	3821(17)	212(18)	110
H(3B)	3006(18)	4119(17)	179(18)	110
H(4A)	2786(20)	3786(20)	-837(21)	134
H(4B)	3307(20)	3389(20)	-569(21)	134
H(5C)	1728(23)	3350(23)	-460(25)	165
H(5D)	1838(23)	3189(23)	-1187(25)	165
H(6A)	1780(19)	2249(17)	-963(18)	106
H(6B)	1193(19)	2580(17)	-767(18)	106
H(7A)	1396(15)	3013(14)	386(15)	74
H(7B)	900(15)	2525(14)	414(15)	74
H(8A)	1436(14)	2062(15)	1204(15)	72
H(8B)	1198(14)	2688(15)	1400(15)	72
H(11B)	1892(16)	2390(14)	2184(16)	87

H(11C)	2576(16)	2512(14)	2077(16)	87
H(12A)	3298(15)	1739(14)	2097(17)	85
H(12B)	2900(15)	1584(14)	2692(17)	85
H(14)	2581(11)	519(17)	2767(17)	117
H(15)	3014(17)	-395(13)	2855(17)	166
H(16)	3940(17)	-567(10)	2412(18)	113
H(17)	4434(11)	177(16)	1882(16)	126
H(18)	4001(14)	1091(12)	1794(15)	76
H(21B)	3763(17)	3828(16)	878(19)	107
H(21C)	3871(17)	3433(16)	263(19)	107
H(22A)	4575(16)	2624(15)	347(17)	93
H(22B)	4949(16)	2983(15)	847(17)	93
H(24)	5243(16)	2495(11)	1827(15)	101
H(25)	5681(15)	1651(16)	2215(11)	120
H(26)	5644(15)	797(11)	1625(16)	95
H(27)	5168(16)	787(10)	646(15)	90
H(28)	4731(14)	1630(15)	257(11)	101
H(31B)	2845(14)	2935(14)	-1560(16)	76
H(31C)	2642(14)	2319(14)	-1306(16)	76
H(32A)	3280(17)	1579(15)	-1409(18)	97
H(32B)	3599(17)	1905(15)	-1979(18)	97
H(34)	3708(14)	940(19)	-815(19)	118
H(35)	4512(23)	396(14)	-466(16)	190
H(36)	5453(17)	588(19)	-861(23)	158
H(37)	5590(13)	1323(22)	-1604(23)	199
H(38)	4785(22)	1867(15)	-1953(17)	187
H(41B)	1057(16)	1673(15)	-222(17)	85
H(41C)	1405(16)	1539(15)	418(17)	85
H(42A)	1892(17)	665(16)	488(19)	102
H(42B)	1633(17)	292(16)	-85(19)	102
H(44)	2665(19)	212(18)	957(12)	137
H(45)	3531(18)	-334(19)	940(14)	138
H(46)	3914(13)	-659(16)	-21(22)	169
H(47)	3431(17)	-438(17)	-965(14)	106
H(48)	2565(16)	108(16)	-949(13)	109

***Table A.4.13.2** - Atomic coordinates (x 10^4) and equivalent isotropic displacement parameters ($Å^2$x 10^3) for C28 H49 Eu N4 O20.25. U(eq) is defined as one third of the trace of the orthogonalized U^{ij} tensor.*

	x	y	z	U(eq)
Eu(1)	4179(1)	2765(1)	2664(1)	12(1)
O(5)	1958(4)	3118(3)	2960(3)	29(1)
O(12A)	6645(7)	6099(5)	4956(3)	18(1)
O(12B)	7164(10)	5885(7)	5062(5)	16(2)
O(12C)	6325(16)	6337(12)	4732(9)	24(3)
O(122)	5037(3)	4390(2)	3985(2)	22(1)
O(151)	10854(3)	9080(2)	3929(2)	25(1)
O(152)	10813(3)	9216(2)	5316(2)	28(1)
O(221)	3539(3)	795(2)	4634(2)	25(1)
O(222)	3240(3)	1607(2)	3553(2)	17(1)
O(251)	7682(3)	4467(2)	6461(2)	32(1)
O(252)	6139(3)	3806(2)	7275(2)	28(1)
O(321)	719(4)	-461(2)	445(2)	28(1)
O(322)	1951(3)	1311(2)	1470(2)	17(1)
O(351)	386(4)	-4377(3)	1393(3)	55(1)
O(352)	2209(4)	-3773(3)	745(2)	36(1)
O(421)	2991(3)	4414(2)	616(2)	29(1)
O(422)	3780(3)	4092(2)	1892(2)	18(1)
O(451)	2692(4)	813(3)	-1269(2)	41(1)
O(452)	1180(4)	1294(3)	-2199(2)	51(1)
O(1SA)	10045(5)	9130(4)	6817(3)	52(1)
O(1SB)	10457(19)	8960(14)	7000(11)	46(4)
O(2SA)	139(12)	3580(9)	1920(7)	37(2)
O(2SB)	-215(13)	3199(10)	802(7)	71(3)
O(3SB)	-1001(10)	1666(8)	1452(6)	72(2)
O(3SA)	-968(11)	1872(8)	1881(7)	48(2)
O(3SC)	-1631(15)	1284(11)	882(9)	50(3)
N(1)	7001(3)	4447(2)	2955(2)	18(1)
N(2)	6387(3)	2543(2)	3835(2)	17(1)
N(3)	4369(3)	705(2)	2075(2)	14(1)
N(4)	4998(3)	2594(2)	1175(2)	14(1)
C(1)	8215(4)	4111(3)	3397(2)	23(1)
C(2)	7875(4)	3626(3)	4149(2)	24(1)
C(3)	6682(4)	1505(3)	3422(2)	21(1)
C(4)	5236(4)	438(3)	2822(2)	17(1)
C(5)	5229(4)	766(3)	1408(2)	16(1)
C(6)	4770(4)	1350(3)	741(2)	16(1)
C(7)	6678(4)	3375(3)	1388(2)	17(1)
C(8)	7214(4)	4566(3)	2080(2)	19(1)
C(11)	7053(4)	5576(3)	3507(2)	21(1)
C(12)	6233(5)	5322(3)	4207(2)	31(1)
C(13)	8661(4)	6616(3)	3895(3)	25(1)
C(14)	8555(4)	7816(3)	4111(3)	30(1)
C(15)	10178(4)	8782(3)	4515(2)	23(1)
C(21)	5756(4)	2391(3)	4603(2)	16(1)
C(22)	4043(4)	1516(3)	4240(2)	17(1)
C(23)	6724(4)	2094(3)	5314(2)	19(1)
C(24)	6399(4)	2362(3)	6205(2)	20(1)
C(25)	6825(4)	3656(3)	6647(2)	22(1)
C(31)	2735(4)	-226(3)	1705(2)	16(1)
C(32)	1735(4)	256(3)	1168(2)	16(1)
C(33)	2577(4)	-1466(3)	1237(2)	20(1)
C(34)	1092(4)	-2449(3)	1241(3)	28(1)
C(35)	1173(4)	-3640(3)	1134(2)	24(1)
C(41)	3967(4)	2927(3)	558(2)	16(1)
C(42)	3562(4)	3906(3)	1054(2)	18(1)
C(43)	4537(4)	3190(3)	-231(2)	19(1)

C(44)	3243(5)	2868(3)	-1074(2)	25(1)
C(45)	2349(5)	1553(3)	-1514(2)	26(1)

Table A.4.13.3 - Bond lengths [Å] and angles [°] for C28 H49 Eu N4 O20.25.

Eu(1)-O(222)	2.354(2)	N(4)-C(6)	1.501(4)	C(43)-H(43A)	0.95(4)
Eu(1)-O(422)	2.391(2)	C(1)-C(2)	1.520(5)	C(44)-C(45)	1.510(5)
Eu(1)-O(122)	2.393(2)	C(1)-H(1A)	0.99	C(44)-H(44A)	0.98(5)
Eu(1)-O(322)	2.412(2)	C(1)-H(1B)	0.99	C(44)-H(44B)	0.98(4)
Eu(1)-O(5)	2.447(3)	C(2)-H(2A)	0.96(4)		
Eu(1)-N(3)	2.664(3)	C(2)-H(2B)	1.01(5)	O(222)-Eu(1)-O(422)	145.19(8)
Eu(1)-N(4)	2.667(3)	C(3)-C(4)	1.518(5)	O(222)-Eu(1)-O(122)	84.31(8)
Eu(1)-N(1)	2.681(3)	C(3)-H(3B)	0.99	O(422)-Eu(1)-O(122)	85.84(8)
Eu(1)-N(2)	2.696(3)	C(3)-H(3A)	0.99	O(222)-Eu(1)-O(322)	85.83(8)
Eu(1)-H(5D)	2.81(6)	C(4)-H(4B)	1.00(4)	O(422)-Eu(1)-O(322)	83.23(8)
O(5)-H(5D)	0.64(6)	C(4)-H(4A)	0.99(4)	O(122)-Eu(1)-O(322)	144.73(8)
O(5)-H(5C)	0.76(9)	C(5)-C(6)	1.516(4)	O(222)-Eu(1)-O(5)	72.73(9)
O(12A)-O(12B)	0.660(8)	C(5)-H(5B)	0.97(4)	O(422)-Eu(1)-O(5)	72.52(9)
O(12A)-O(12C)	0.622(13)	C(5)-H(5A)	0.93(4)	O(122)-Eu(1)-O(5)	70.15(11)
O(12A)-C(12)	1.274(6)	C(6)-H(6A)	1.03(4)	O(322)-Eu(1)-O(5)	74.58(10)
O(12B)-O(12C)	1.25(2)	C(6)-H(6B)	0.93(3)	O(222)-Eu(1)-N(3)	72.75(8)
O(12B)-C(12)	1.367(9)	C(7)-C(8)	1.518(5)	O(422)-Eu(1)-N(3)	130.35(8)
O(12C)-C(12)	1.343(14)	C(7)-H(7B)	0.99(4)	O(122)-Eu(1)-N(3)	140.88(9)
O(122)-C(12)	1.249(4)	C(7)-H(7A)	1.00(4)	O(322)-Eu(1)-N(3)	65.85(8)
O(151)-C(15)	1.300(4)	C(8)-H(8B)	0.96(4)	O(5)-Eu(1)-N(3)	128.46(9)
O(151)-H(151)	0.91(6)	C(8)-H(8A)	1.00(4)	O(222)-Eu(1)-N(4)	140.90(8)
O(152)-C(15)	1.227(4)	C(11)-C(12)	1.530(5)	O(422)-Eu(1)-N(4)	65.16(8)
O(221)-C(22)	1.242(4)	C(11)-C(13)	1.540(5)	O(122)-Eu(1)-N(4)	131.41(8)
O(222)-C(22)	1.277(4)	C(11)-H(11)	1.00	O(322)-Eu(1)-N(4)	72.43(8)
O(251)-C(25)	1.213(4)	C(13)-C(14)	1.531(5)	O(5)-Eu(1)-N(4)	128.38(11)
O(252)-C(25)	1.331(4)	C(13)-H(13B)	1.00(4)	N(3)-Eu(1)-N(4)	68.80(8)
O(252)-H(252)	0.85(6)	C(13)-H(13A)	0.98(4)	O(222)-Eu(1)-N(1)	129.88(8)
O(321)-C(32)	1.275(4)	C(14)-C(15)	1.514(5)	O(422)-Eu(1)-N(1)	74.11(8)
O(322)-C(32)	1.248(4)	C(14)-H(14B)	0.99	O(122)-Eu(1)-N(1)	65.34(8)
O(351)-C(35)	1.193(5)	C(14)-H(14A)	0.99	O(322)-Eu(1)-N(1)	141.10(8)
O(352)-C(35)	1.319(4)	C(21)-C(23)	1.532(5)	O(5)-Eu(1)-N(1)	125.29(10)
O(352)-H(352)	0.91(6)	C(21)-C(22)	1.537(4)	N(3)-Eu(1)-N(1)	106.20(8)
O(421)-C(42)	1.230(4)	C(21)-H(21)	0.98(4)	N(4)-Eu(1)-N(1)	69.47(8)
O(422)-C(42)	1.287(4)	C(23)-C(24)	1.527(5)	O(222)-Eu(1)-N(2)	65.39(8)
O(451)-C(45)	1.214(5)	C(23)-H(23B)	0.98(4)	O(422)-Eu(1)-N(2)	141.58(8)
O(452)-C(45)	1.304(5)	C(23)-H(23A)	0.94(4)	O(122)-Eu(1)-N(2)	73.13(9)
O(452)-H(452)	0.77(9)	C(24)-C(25)	1.511(5)	O(322)-Eu(1)-N(2)	131.54(8)
O(1SA)-O(1SB)	0.58(2)	C(24)-H(24B)	0.93(4)	O(5)-Eu(1)-N(2)	125.97(11)
O(2SA)-O(2SB)	1.701(15)	C(24)-H(24A)	0.93(4)	N(3)-Eu(1)-N(2)	68.63(8)
O(3SB)-O(3SA)	0.677(11)	C(31)-C(33)	1.532(4)	N(4)-Eu(1)-N(2)	105.62(8)
O(3SB)-O(3SC)	0.915(12)	C(31)-C(32)	1.539(4)	N(1)-Eu(1)-N(2)	67.98(9)
O(3SA)-O(3SC)	1.52(2)	C(31)-H(31A)	0.93(4)	O(222)-Eu(1)-H(5D)	75.7(12)
N(1)-C(1)	1.488(5)	C(33)-C(34)	1.539(5)	O(422)-Eu(1)-H(5D)	69.9(12)
N(1)-C(11)	1.494(4)	C(33)-H(33B)	0.99(4)	O(122)-Eu(1)-H(5D)	81.2(12)
N(1)-C(8)	1.501(4)	C(33)-H(33A)	1.02(4)	O(322)-Eu(1)-H(5D)	63.5(12)
N(2)-C(3)	1.489(4)	C(34)-C(35)	1.515(5)	O(5)-Eu(1)-H(5D)	11.4(11)
N(2)-C(2)	1.497(4)	C(34)-H(34A)	0.95(5)	N(3)-Eu(1)-H(5D)	121.2(12)
N(2)-C(21)	1.507(4)	C(34)-H(34B)	0.96(6)	N(4)-Eu(1)-H(5D)	119.2(11)
N(3)-C(5)	1.483(4)	C(41)-C(42)	1.540(4)	N(1)-Eu(1)-H(5D)	132.0(12)
N(3)-C(4)	1.501(4)	C(41)-C(43)	1.542(4)	N(2)-Eu(1)-H(5D)	134.8(11)
N(3)-C(31)	1.503(4)	C(41)-H(41)	0.98(4)	Eu(1)-O(5)-H(5D)	119.0(53)
N(4)-C(7)	1.496(4)	C(43)-C(44)	1.523(5)	Eu(1)-O(5)-H(5C)	118.7(66)
N(4)-C(41)	1.500(4)	C(43)-H(43B)	0.96(4)	H(5D)-O(5)-H(5C)	98.3(76)

O(12B)-O(12A)-O(12C)	153.5(19)	N(3)-C(4)-C(3)	112.7(3)	N(2)-C(21)-C(22)	108.7(2)
O(12B)-O(12A)-C(12)	83.6(9)	N(3)-C(4)-H(4B)	111.5(21)	C(23)-C(21)-C(22)	113.7(3)
O(12C)-O(12A)-C(12)	82.5(14)	C(3)-C(4)-H(4B)	105.0(21)	N(2)-C(21)-H(21)	103.5(23)
O(12A)-O(12B)-O(12C)	12.9(9)	N(3)-C(4)-H(4A)	110.5(22)	C(23)-C(21)-H(21)	107.8(23)
O(12A)-O(12B)-C(12)	67.8(8)	C(3)-C(4)-H(4A)	111.6(22)	C(22)-C(21)-H(21)	107.3(23)
O(12C)-O(12B)-C(12)	61.6(7)	H(4B)-C(4)-H(4A)	105.1(30)	O(221)-C(22)-O(222)	125.1(3)
O(12A)-O(12C)-O(12B)	13.7(10)	N(3)-C(5)-C(6)	114.3(3)	O(221)-C(22)-C(21)	118.6(3)
O(12A)-O(12C)-C(12)	70.1(14)	N(3)-C(5)-H(5B)	112.0(21)	O(222)-C(22)-C(21)	116.3(3)
O(12B)-O(12C)-C(12)	63.6(8)	C(6)-C(5)-H(5B)	106.8(21)	C(24)-C(23)-C(21)	113.3(3)
C(12)-O(122)-Eu(1)	125.7(2)	N(3)-C(5)-H(5A)	111.3(21)	C(24)-C(23)-H(23B)	108.3(22)
C(15)-O(151)-H(151)	110.9(34)	C(6)-C(5)-H(5A)	107.4(21)	C(21)-C(23)-H(23B)	110.3(22)
C(22)-O(222)-Eu(1)	126.7(2)	H(5B)-C(5)-H(5A)	104.5(29)	C(24)-C(23)-H(23A)	106.6(23)
C(25)-O(252)-H(252)	112.5(38)	N(4)-C(6)-C(5)	112.3(3)	C(21)-C(23)-H(23A)	111.5(24)
C(32)-O(322)-Eu(1)	124.1(2)	N(4)-C(6)-H(6A)	110.5(21)	H(23B)-C(23)-H(23A)	106.6(32)
C(35)-O(352)-H(352)	113.1(38)	C(5)-C(6)-H(6A)	107.6(21)	C(25)-C(24)-C(23)	114.5(3)
C(42)-O(422)-Eu(1)	124.6(2)	N(4)-C(6)-H(6B)	110.8(21)	C(25)-C(24)-H(24B)	106.0(25)
C(45)-O(452)-H(452)	107.8(68)	C(5)-C(6)-H(6B)	111.2(21)	C(23)-C(24)-H(24B)	109.6(25)
O(3SA)-O(3SB)-O(3SC)	146.0(19)	H(6A)-C(6)-H(6B)	104.1(29)	C(25)-C(24)-H(24A)	109.0(25)
O(3SB)-O(3SA)-O(3SC)	19.6(11)	N(4)-C(7)-C(8)	114.6(3)	C(23)-C(24)-H(24A)	111.2(25)
O(3SB)-O(3SC)-O(3SA)	14.4(8)	N(4)-C(7)-H(7B)	104.7(21)	H(24B)-C(24)-H(24A)	106.0(35)
C(1)-N(1)-C(11)	112.3(3)	C(8)-C(7)-H(7B)	110.0(21)	O(251)-C(25)-O(252)	123.5(3)
C(1)-N(1)-C(8)	109.0(3)	N(4)-C(7)-H(7A)	112.1(21)	O(251)-C(25)-C(24)	124.9(3)
C(11)-N(1)-C(8)	109.8(3)	C(8)-C(7)-H(7A)	108.5(21)	O(252)-C(25)-C(24)	111.7(3)
C(1)-N(1)-Eu(1)	110.0(2)	H(7B)-C(7)-H(7A)	106.6(29)	N(3)-C(31)-C(33)	115.1(3)
C(11)-N(1)-Eu(1)	107.1(2)	N(1)-C(8)-C(7)	112.3(3)	N(3)-C(31)-C(32)	108.4(2)
C(8)-N(1)-Eu(1)	108.7(2)	N(1)-C(8)-H(8B)	110.1(23)	C(33)-C(31)-C(32)	115.6(3)
C(3)-N(2)-C(2)	108.8(3)	C(7)-C(8)-H(8B)	107.3(23)	N(3)-C(31)-H(31A)	108.0(23)
C(3)-N(2)-C(21)	111.8(3)	N(1)-C(8)-H(8A)	107.8(24)	C(33)-C(31)-H(31A)	103.8(23)
C(2)-N(2)-C(21)	109.4(2)	C(7)-C(8)-H(8A)	107.2(24)	C(32)-C(31)-H(31A)	105.1(23)
C(3)-N(2)-Eu(1)	110.2(2)	H(8B)-C(8)-H(8A)	112.1(33)	O(322)-C(32)-O(321)	124.2(3)
C(2)-N(2)-Eu(1)	111.4(2)	N(1)-C(11)-C(12)	109.2(3)	O(322)-C(32)-C(31)	118.3(3)
C(21)-N(2)-Eu(1)	105.2(2)	N(1)-C(11)-C(13)	115.9(3)	O(321)-C(32)-C(31)	117.4(3)
C(5)-N(3)-C(4)	107.8(2)	C(12)-C(11)-C(13)	113.1(3)	C(31)-C(33)-C(34)	112.7(3)
C(5)-N(3)-C(31)	112.9(2)	N(1)-C(11)-H(11)	105.9(2)	C(31)-C(33)-H(33B)	108.8(23)
C(4)-N(3)-C(31)	109.3(2)	C(12)-C(11)-H(11)	105.9(2)	C(34)-C(33)-H(33B)	113.7(23)
C(5)-N(3)-Eu(1)	109.7(2)	C(13)-C(11)-H(11)	105.9(2)	C(31)-C(33)-H(33A)	108.4(24)
C(4)-N(3)-Eu(1)	110.4(2)	O(122)-C(12)-O(12A)	120.7(4)	C(34)-C(33)-H(33A)	107.3(24)
C(31)-N(3)-Eu(1)	106.8(2)	O(122)-C(12)-O(12B)	123.2(4)	H(33B)-C(33)-H(33A)	105.6(33)
C(7)-N(4)-C(41)	112.6(2)	O(12A)-C(12)-O(12B)	28.6(3)	C(35)-C(34)-C(33)	114.3(3)
C(7)-N(4)-C(6)	107.9(2)	O(122)-C(12)-O(12C)	120.9(6)	C(35)-C(34)-H(34A)	107.1(31)
C(41)-N(4)-C(6)	108.6(2)	O(12A)-C(12)-O(12C)	27.3(6)	C(33)-C(34)-H(34A)	112.4(30)
C(7)-N(4)-Eu(1)	109.4(2)	O(12B)-C(12)-O(12C)	54.8(7)	C(35)-C(34)-H(34B)	106.9(33)
C(41)-N(4)-Eu(1)	107.4(2)	O(122)-C(12)-C(11)	117.9(3)	C(33)-C(34)-H(34B)	111.4(34)
C(6)-N(4)-Eu(1)	110.9(2)	O(12A)-C(12)-C(11)	120.9(4)	H(34A)-C(34)-H(34B)	104.0(44)
N(1)-C(1)-C(2)	114.2(3)	O(12B)-C(12)-C(11)	114.3(4)	O(351)-C(35)-O(352)	123.5(4)
N(1)-C(1)-H(1A)	108.7(2)	O(12C)-C(12)-C(11)	109.9(7)	O(351)-C(35)-C(34)	122.7(3)
C(2)-C(1)-H(1A)	108.7(2)	C(14)-C(13)-C(11)	112.3(3)	O(352)-C(35)-C(34)	113.8(3)
N(1)-C(1)-H(1B)	108.7(2)	C(14)-C(13)-H(13B)	112.3(25)	N(4)-C(41)-C(42)	112.2(3)
C(2)-C(1)-H(1B)	108.7(2)	C(11)-C(13)-H(13B)	108.9(25)	N(4)-C(41)-C(43)	114.3(3)
H(1A)-C(1)-H(1B)	107.6	C(14)-C(13)-H(13A)	109.2(24)	C(42)-C(41)-C(43)	112.7(3)
N(2)-C(2)-C(1)	111.5(3)	C(11)-C(13)-H(13A)	107.9(24)	N(4)-C(41)-H(41)	106.5(23)
N(2)-C(2)-H(2A)	109.8(26)	H(13B)-C(13)-H(13A)	106.0(34)	C(42)-C(41)-H(41)	103.9(22)
C(1)-C(2)-H(2A)	111.2(26)	C(15)-C(14)-C(13)	108.8(3)	C(43)-C(41)-H(41)	106.2(22)
N(2)-C(2)-H(2B)	109.3(26)	C(15)-C(14)-H(14B)	109.9(2)	O(421)-C(42)-O(422)	124.9(3)
C(1)-C(2)-H(2B)	107.2(26)	C(13)-C(14)-H(14B)	109.9(2)	O(421)-C(42)-C(41)	117.8(3)
H(2A)-C(2)-H(2B)	107.8(35)	C(15)-C(14)-H(14A)	109.9(2)	O(422)-C(42)-C(41)	117.2(3)
N(2)-C(3)-C(4)	114.3(3)	C(13)-C(14)-H(14A)	109.9(2)	C(44)-C(43)-C(41)	114.3(3)
N(2)-C(3)-H(3B)	108.7(2)	H(14B)-C(14)-H(14A)	108.3	C(44)-C(43)-H(43B)	106.1(24)
C(4)-C(3)-H(3B)	108.7(2)	O(152)-C(15)-O(151)	123.2(3)	C(41)-C(43)-H(43B)	109.7(24)
N(2)-C(3)-H(3A)	108.7(2)	O(152)-C(15)-C(14)	123.3(3)	C(44)-C(43)-H(43A)	111.9(26)
C(4)-C(3)-H(3A)	108.7(2)	O(151)-C(15)-C(14)	113.4(3)	C(41)-C(43)-H(43A)	107.2(26)
H(3B)-C(3)-H(3A)	107.6	N(2)-C(21)-C(23)	115.0(3)	H(43B)-C(43)-H(43A)	107.6(35)

C(45)-C(44)-C(43)	113.6(3)	C(45)-C(44)-H(44B)	107.6(25)	O(451)-C(45)-O(452)	123.4(4)
C(45)-C(44)-H(44A)	109.9(27)	C(43)-C(44)-H(44B)	107.6(25)	O(451)-C(45)-C(44)	123.9(3)
C(43)-C(44)-H(44A)	110.0(26)	H(44A)-C(44)-H(44B)	107.8(36)	O(452)-C(45)-C(44)	112.8(3)

***Table A.4.13.4** - Anisotropic displacement parameters ($Å^2 x\ 10^3$) for C28 H49 Eu N4 O20.25. The anisotropic displacement factor exponent takes the form: $-2\pi^2[\ h^2\ a^{*2}U^{11} + ...\ + 2\ h\ k\ a^*\ b^*\ U^{12}\ ]$*

	U^{11}	U^{22}	U^{33}	U^{23}	U^{13}	U^{12}
Eu(1)	12(1)	11(1)	13(1)	2(1)	5(1)	3(1)
O(5)	24(2)	17(1)	48(2)	6(1)	18(2)	9(1)
O(122)	22(1)	16(1)	21(1)	-1(1)	13(1)	0(1)
O(151)	20(1)	24(1)	20(1)	2(1)	3(1)	1(1)
O(152)	27(1)	27(1)	27(1)	8(1)	7(1)	9(1)
O(221)	19(1)	25(1)	26(1)	14(1)	4(1)	0(1)
O(222)	16(1)	20(1)	15(1)	6(1)	5(1)	5(1)
O(251)	40(2)	22(1)	30(1)	8(1)	12(1)	7(1)
O(252)	34(2)	21(1)	29(1)	2(1)	13(1)	12(1)
O(321)	29(2)	17(1)	25(1)	1(1)	-10(1)	6(1)
O(322)	15(1)	14(1)	19(1)	3(1)	3(1)	7(1)
O(351)	58(2)	31(2)	106(3)	38(2)	59(2)	24(2)
O(352)	47(2)	23(1)	58(2)	20(1)	34(2)	23(1)
O(421)	45(2)	29(1)	28(1)	14(1)	15(1)	28(1)
O(422)	24(1)	14(1)	18(1)	4(1)	9(1)	10(1)
O(451)	55(2)	26(2)	35(2)	4(1)	-3(1)	19(1)
O(452)	53(2)	48(2)	36(2)	-8(2)	-16(2)	31(2)
N(1)	16(1)	14(1)	17(1)	1(1)	7(1)	1(1)
N(2)	14(1)	20(1)	15(1)	5(1)	5(1)	4(1)
N(3)	14(1)	12(1)	15(1)	4(1)	3(1)	6(1)
N(4)	15(1)	13(1)	15(1)	5(1)	6(1)	5(1)
C(1)	17(2)	22(2)	23(2)	4(1)	7(1)	2(1)
C(2)	17(2)	28(2)	19(2)	5(1)	4(1)	2(1)
C(3)	18(2)	27(2)	16(2)	6(1)	4(1)	9(1)
C(4)	19(2)	19(2)	18(2)	7(1)	6(1)	12(1)
C(5)	17(2)	16(2)	18(2)	4(1)	8(1)	8(1)
C(6)	21(2)	15(2)	15(2)	3(1)	7(1)	10(1)
C(7)	17(2)	20(2)	17(2)	6(1)	8(1)	8(1)
C(8)	17(2)	17(2)	21(2)	7(1)	10(1)	2(1)
C(11)	19(2)	16(2)	20(2)	1(1)	8(1)	1(1)
C(12)	34(2)	22(2)	24(2)	-3(2)	20(2)	-2(2)
C(13)	19(2)	18(2)	31(2)	4(2)	7(2)	2(1)
C(14)	23(2)	20(2)	38(2)	2(2)	8(2)	5(2)
C(15)	21(2)	16(2)	28(2)	2(1)	5(1)	7(1)
C(21)	14(1)	17(2)	15(2)	4(1)	5(1)	4(1)
C(22)	16(2)	17(2)	15(2)	2(1)	5(1)	4(1)
C(23)	19(2)	22(2)	18(2)	6(1)	5(1)	11(1)
C(24)	24(2)	20(2)	18(2)	7(1)	6(1)	10(1)
C(25)	24(2)	21(2)	16(2)	4(1)	1(1)	8(1)
C(31)	16(2)	13(1)	18(2)	4(1)	4(1)	6(1)
C(32)	13(1)	16(2)	18(2)	5(1)	4(1)	6(1)
C(33)	21(2)	12(2)	28(2)	5(1)	10(1)	8(1)
C(34)	23(2)	13(2)	49(2)	8(2)	17(2)	5(1)
C(35)	22(2)	19(2)	28(2)	5(1)	9(1)	6(1)
C(41)	19(2)	13(1)	15(2)	3(1)	6(1)	8(1)
C(42)	18(2)	13(1)	21(2)	5(1)	7(1)	6(1)
C(43)	22(2)	19(2)	19(2)	8(1)	10(1)	9(1)
C(44)	37(2)	27(2)	19(2)	11(2)	12(2)	19(2)
C(45)	35(2)	30(2)	17(2)	7(1)	8(2)	19(2)

***Table A.4.13.5** - Hydrogen coordinates (x 10^4) and isotropic displacement parameters ($Å^2$x 10^3) for C28 H49 Eu N4 O20.25.*

	x	y	z	U(eq)
H(5D)	1313(67)	2873(52)	2657(37)	39(19)
H(5C)	2015(100)	3752(80)	3077(56)	117(33)
H(151)	11783(67)	9708(50)	4193(36)	56(16)
H(252)	6316(65)	4528(51)	7502(36)	55(16)
H(352)	2288(70)	-4471(55)	711(39)	68(18)
H(452)	753(106)	614(79)	-2382(60)	125(36)
H(1A)	9215(4)	4814(3)	3632(2)	28
H(1B)	8333(4)	3507(3)	2948(2)	28
H(2A)	7840(49)	4209(38)	4620(29)	28(11)
H(2B)	8762(54)	3416(39)	4390(29)	34(12)
H(3B)	7197(4)	1272(3)	3898(2)	25
H(3A)	7406(4)	1745(3)	3072(2)	25
H(4B)	5614(42)	-172(32)	2599(23)	12(9)
H(4A)	4540(45)	94(34)	3161(25)	18(9)
H(5B)	5100(41)	-15(33)	1070(24)	12(9)
H(5A)	6288(42)	1172(30)	1677(22)	7(8)
H(6A)	5428(43)	1337(32)	312(24)	16(9)
H(6B)	3760(41)	904(30)	383(22)	5(8)
H(7B)	7231(42)	2919(32)	1603(23)	12(9)
H(7A)	6970(42)	3512(32)	849(24)	14(9)
H(8B)	8286(47)	4996(34)	2147(25)	19(10)
H(8A)	6561(48)	4964(36)	1859(27)	24(10)
H(11)	6402(4)	5831(3)	3102(2)	25
H(13B)	9255(50)	6504(37)	4422(29)	28(11)
H(13A)	9227(47)	6572(35)	3457(27)	22(10)
H(14B)	8031(4)	7922(3)	3564(3)	36
H(14A)	7943(4)	7857(3)	4532(3)	36
H(21)	5786(45)	3171(36)	4873(26)	20(10)
H(23B)	7830(46)	2536(33)	5407(24)	16(9)
H(23A)	6534(44)	1284(36)	5141(25)	18(10)
H(24B)	6976(47)	2127(35)	6601(26)	21(10)
H(24A)	5363(51)	1931(37)	6152(27)	24(10)
H(31A)	2338(43)	-321(32)	2177(25)	14(9)
H(33B)	2684(46)	-1498(35)	636(27)	22(10)
H(33A)	3498(50)	-1593(37)	1565(28)	28(11)
H(34A)	813(59)	-2255(44)	1767(34)	45(14)
H(34B)	214(67)	-2566(49)	779(37)	57(16)
H(41)	2972(45)	2241(34)	304(25)	17(9)
H(43B)	5123(47)	2738(36)	-382(26)	22(10)
H(43A)	5219(50)	4000(39)	-41(28)	28(11)
H(44A)	2533(53)	3233(40)	-947(29)	34(12)
H(44B)	3719(50)	3198(38)	-1494(29)	30(11)

***Table A.4.14.2** - Atomic coordinates (x 10^4) and equivalent isotropic displacement parameters ($Å^2$x 10^3) for (C28 H42 N4 O20 Tb)$^-$.(H30)$^+$.2(H20). U(eq) is defined as one third of the trace of the orthogonalized U^{ij} tensor.*

	x	y	z	U(eq)
Tb(1)	795(1)	-7763(1)	2339(1)	16(1)
O(5)	3017(5)	-8097(4)	2060(3)	32(1)
O(121)	1981(5)	-9419(4)	4361(3)	31(1)
O(122)	1200(4)	-9082(3)	3090(2)	22(1)
O(151)	2335(6)	-5805(4)	6262(3)	43(1)
O(152)	3797(7)	-6313(5)	7196(3)	56(2)
O(22A)	-1634(11)	-11104(7)	37(5)	21(2)
O(22B)	-2130(16)	-10915(11)	-49(8)	20(3)
O(22C)	-1310(20)	-11349(16)	269(12)	19(4)
O(222)	-36(4)	-9377(3)	1027(2)	25(1)
O(251)	-5832(5)	-14229(4)	-315(3)	31(1)
O(252)	-5846(5)	-14073(4)	1073(2)	28(1)
O(321)	1463(4)	-5803(3)	382(2)	27(1)
O(322)	1746(4)	-6615(3)	1465(2)	20(1)
O(352)	-1141(5)	-8818(4)	-2266(3)	32(1)
O(351)	-2684(5)	-9483(4)	-1460(3)	36(1)
O(421)	4283(5)	-4547(3)	4560(3)	31(1)
O(422)	3010(4)	-6323(3)	3524(2)	19(1)
O(451)	4625(7)	-607(4)	3621(5)	63(2)
O(452)	2777(6)	-1231(4)	4249(4)	44(1)
N(1)	-17(5)	-7595(3)	3820(3)	17(1)
N(2)	-2013(5)	-9452(4)	2044(3)	21(1)
N(3)	-1403(5)	-7554(4)	1166(3)	19(1)
N(4)	609(5)	-5714(3)	2922(3)	15(1)
C(1)	-1700(6)	-8374(4)	3604(3)	20(1)
C(2)	-2239(6)	-9573(4)	2918(3)	21(1)
C(3)	-3233(6)	-9127(5)	1600(4)	24(1)
C(4)	-2904(6)	-8642(5)	852(4)	25(1)
C(5)	-1710(6)	-6522(5)	1582(3)	24(1)
C(6)	-255(6)	-5446(4)	2178(3)	19(1)
C(7)	-247(6)	-5768(4)	3590(3)	19(1)
C(8)	206(6)	-6345(4)	4252(3)	21(1)
C(11)	1026(6)	-7922(4)	4438(3)	18(1)
C(12)	1413(6)	-8896(4)	3932(3)	20(1)
C(13)	447(6)	-8186(5)	5226(3)	22(1)
C(14)	1748(7)	-7873(5)	6062(4)	26(1)
C(15)	2653(7)	-6556(5)	6508(4)	30(1)
C(21)	-2067(7)	-10584(4)	1487(4)	26(1)
C(22)	-1232(7)	-10316(5)	799(4)	34(1)
C(23)	-3652(7)	-11620(5)	1098(4)	29(1)
C(24)	-3555(7)	-12824(5)	887(5)	34(1)
C(25)	-5179(7)	-13794(5)	488(4)	28(1)
C(31)	-762(6)	-7399(4)	411(3)	20(1)
C(32)	956(6)	-6523(4)	775(3)	20(1)
C(33)	-1724(7)	-7099(5)	-308(3)	22(1)
C(34)	-1399(7)	-7370(5)	-1199(3)	23(1)
C(35)	-1834(6)	-8670(5)	-1641(3)	23(1)
C(41)	2251(6)	-4775(4)	3300(3)	20(1)
C(42)	3238(6)	-5266(4)	3835(3)	20(1)
C(43)	2408(6)	-3537(4)	3764(4)	24(1)
C(44)	3904(7)	-2550(5)	3760(5)	34(1)
C(45)	3823(7)	-1346(5)	3870(4)	30(1)
O(1WA)	5015(10)	-4154(7)	8200(5)	33(2)
O(1WB)	4690(17)	-4024(12)	8075(9)	28(3)
O(2WA)	-4004(14)	-6656(11)	3559(10)	39(3)
O(2WB)	-3420(30)	-6280(20)	4075(16)	46(5)
O(2WC)	-4072(16)	-6864(12)	3173(10)	32(3)

O(3WA)	5130(20)	-1426(18)	6927(13)	120(6)
O(3WB)	4800(20)	-1782(16)	5790(12)	108(5)

***Table A.4.14.3** - Bond lengths [Å] and angles [°] for (C28 H42 N4 O20 Tb)$^-$.(H30)$^+$.2(H20).*

Tb(1)-O(322)	2.335(3)	C(4)-H(4A)	0.75(7)	O(122)-Tb(1)-O(222)	85.38(13)
Tb(1)-O(122)	2.368(4)	C(4)-H(4B)	0.98(7)	O(322)-Tb(1)-O(422)	85.78(12)
Tb(1)-O(222)	2.371(3)	C(5)-C(6)	1.518(7)	O(122)-Tb(1)-O(422)	83.04(12)
Tb(1)-O(422)	2.386(3)	C(5)-H(5A)	0.85(7)	O(222)-Tb(1)-O(422)	144.00(12)
Tb(1)-O(5)	2.427(4)	C(5)-H(5B)	1.08(6)	O(322)-Tb(1)-O(5)	72.46(14)
Tb(1)-N(4)	2.644(4)	C(6)-H(6A)	0.91(6)	O(122)-Tb(1)-O(5)	71.91(14)
Tb(1)-N(1)	2.654(4)	C(6)-H(6B)	0.98(6)	O(222)-Tb(1)-O(5)	70.16(14)
Tb(1)-N(2)	2.665(4)	C(7)-C(8)	1.506(7)	O(422)-Tb(1)-O(5)	73.84(14)
Tb(1)-N(3)	2.686(4)	C(7)-H(7A)	0.98(6)	O(322)-Tb(1)-N(4)	72.76(12)
O(5)-H(5D)	0.64(9)	C(7)-H(7B)	0.97(6)	O(122)-Tb(1)-N(4)	131.03(12)
O(5)-H(5C)	0.61(8)	C(8)-H(8A)	1.07(6)	O(222)-Tb(1)-N(4)	140.94(13)
O(121)-C(12)	1.238(6)	C(8)-H(8B)	0.98(6)	O(422)-Tb(1)-N(4)	66.25(12)
O(122)-C(12)	1.296(6)	C(11)-C(12)	1.529(6)	O(5)-Tb(1)-N(4)	128.06(13)
O(151)-C(15)	1.218(7)	C(11)-C(13)	1.546(7)	O(322)-Tb(1)-N(1)	141.17(12)
O(152)-C(15)	1.298(7)	C(11)-H(11)	1.04(6)	O(122)-Tb(1)-N(1)	65.54(12)
O(152)-H(152)	0.94(10)	C(13)-C(14)	1.522(7)	O(222)-Tb(1)-N(1)	131.71(12)
O(22A)-O(22B)	0.611(12)	C(13)-H(13A)	0.98(6)	O(422)-Tb(1)-N(1)	72.40(12)
O(22A)-O(22C)	0.638(18)	C(13)-H(13B)	1.09(6)	O(5)-Tb(1)-N(1)	127.81(15)
O(22A)-C(22)	1.292(9)	C(14)-C(15)	1.507(8)	N(4)-Tb(1)-N(1)	69.15(12)
O(22B)-O(22C)	1.21(2)	C(14)-H(14A)	1.09(7)	O(322)-Tb(1)-N(2)	130.28(12)
O(22B)-C(22)	1.353(14)	C(14)-H(14B)	1.00(7)	O(122)-Tb(1)-N(2)	74.10(13)
O(22C)-C(22)	1.366(18)	C(21)-C(23)	1.518(7)	O(222)-Tb(1)-N(2)	65.65(12)
O(222)-C(22)	1.249(7)	C(21)-C(22)	1.527(7)	O(422)-Tb(1)-N(2)	141.07(12)
O(251)-C(25)	1.231(7)	C(21)-H(21)	1.01(7)	O(5)-Tb(1)-N(2)	125.39(14)
O(252)-C(25)	1.289(7)	C(23)-C(24)	1.531(8)	N(4)-Tb(1)-N(2)	106.51(13)
O(252)-H(252)	0.92(8)	C(23)-H(23A)	1.14(7)	N(1)-Tb(1)-N(2)	69.57(12)
O(321)-C(32)	1.242(6)	C(23)-H(23B)	1.02(7)	O(322)-Tb(1)-N(3)	65.60(12)
O(322)-C(32)	1.276(6)	C(24)-C(25)	1.510(8)	O(122)-Tb(1)-N(3)	141.70(13)
O(352)-C(35)	1.331(7)	C(24)-H(24A)	0.97(8)	O(222)-Tb(1)-N(3)	73.21(13)
O(352)-H(352)	0.71(8)	C(24)-H(24B)	1.02(8)	O(422)-Tb(1)-N(3)	131.99(12)
O(351)-C(35)	1.207(7)	C(31)-C(32)	1.536(7)	O(5)-Tb(1)-N(3)	126.09(15)
O(421)-C(42)	1.284(6)	C(31)-C(33)	1.545(7)	N(4)-Tb(1)-N(3)	68.71(12)
O(422)-C(42)	1.247(6)	C(31)-H(31)	0.77(6)	N(1)-Tb(1)-N(3)	106.07(13)
O(451)-C(45)	1.191(7)	C(33)-C(34)	1.528(7)	N(2)-Tb(1)-N(3)	68.24(13)
O(452)-C(45)	1.312(7)	C(33)-H(33A)	0.93(7)	Tb(1)-O(5)-H(5D)	117(8)
O(452)-H(452)	0.68(9)	C(33)-H(33B)	0.95(7)	Tb(1)-O(5)-H(5C)	129(8)
N(1)-C(1)	1.492(6)	C(34)-C(35)	1.511(7)	H(5D)-O(5)-H(5C)	103(10)
N(1)-C(8)	1.505(6)	C(34)-H(34A)	0.91(7)	C(12)-O(122)-Tb(1)	124.2(3)
N(1)-C(11)	1.507(6)	C(34)-H(34B)	0.90(7)	C(15)-O(152)-H(152)	111(6)
N(2)-C(3)	1.487(7)	C(41)-C(43)	1.524(7)	O(22B)-O(22A)-O(22C)	150(3)
N(2)-C(21)	1.495(6)	C(41)-C(42)	1.542(7)	O(22B)-O(22A)-C(22)	82.2(15)
N(2)-C(2)	1.508(6)	C(41)-H(41)	0.99(6)	O(22C)-O(22A)-C(22)	82.7(19)
N(3)-C(5)	1.490(7)	C(43)-C(44)	1.543(8)	O(22A)-O(22B)-O(22C)	15.2(14)
N(3)-C(31)	1.496(6)	C(43)-H(43A)	1.06(6)	O(22A)-O(22B)-C(22)	71.2(15)
N(3)-C(4)	1.501(6)	C(43)-H(43B)	1.05(6)	O(22C)-O(22B)-C(22)	64.2(10)
N(4)-C(7)	1.483(6)	C(44)-C(45)	1.530(8)	O(22A)-O(22C)-O(22B)	14.5(14)
N(4)-C(6)	1.500(6)	C(44)-H(44A)	0.98(8)	O(22A)-O(22C)-C(22)	69.7(18)
N(4)-C(41)	1.507(6)	C(44)-H(44B)	0.92(8)	O(22B)-O(22C)-C(22)	63.0(10)
C(1)-C(2)	1.516(7)	C(45)-H(452)	1.50(10)	C(22)-O(222)-Tb(1)	125.6(3)
C(1)-H(1A)	1.03(6)	O(2WA)-O(2WC)	0.604(15)	C(25)-O(252)-H(252)	106(4)
C(1)-H(1B)	0.90(6)	O(2WA)-O(2WB)	0.83(2)	C(32)-O(322)-Tb(1)	127.0(3)
C(2)-H(2A)	1.05(6)	O(2WB)-O(2WC)	1.39(3)	C(35)-O(352)-H(352)	116(7)
C(2)-H(2B)	1.05(6)	O(3WA)-O(3WB)	1.73(3)	C(42)-O(422)-Tb(1)	124.3(3)
C(3)-C(4)	1.515(8)			C(45)-O(452)-H(452)	92(8)
C(3)-H(3A)	0.99(7)	O(322)-Tb(1)-O(122)	144.33(12)	C(1)-N(1)-C(8)	107.4(4)
C(3)-H(3B)	0.84(7)	O(322)-Tb(1)-O(222)	84.08(12)	C(1)-N(1)-C(11)	113.2(4)

C(8)-N(1)-C(11)	108.9(4)	C(8)-C(7)-H(7A)	114(4)	C(23)-C(24)-H(24B)	114(4)
C(1)-N(1)-Tb(1)	109.4(3)	N(4)-C(7)-H(7B)	109(3)	H(24A)-C(24)-H(24B)	96(6)
C(8)-N(1)-Tb(1)	110.7(3)	C(8)-C(7)-H(7B)	110(3)	O(251)-C(25)-O(252)	123.3(5)
C(11)-N(1)-Tb(1)	107.5(3)	H(7A)-C(7)-H(7B)	96(5)	O(251)-C(25)-C(24)	123.3(6)
C(3)-N(2)-C(21)	111.8(4)	N(1)-C(8)-C(7)	112.5(4)	O(252)-C(25)-C(24)	113.3(5)
C(3)-N(2)-C(2)	108.7(4)	N(1)-C(8)-H(8A)	116(3)	N(3)-C(31)-C(32)	109.3(4)
C(21)-N(2)-C(2)	109.9(4)	C(7)-C(8)-H(8A)	105(3)	N(3)-C(31)-C(33)	115.3(4)
C(3)-N(2)-Tb(1)	110.0(3)	N(1)-C(8)-H(8B)	110(4)	C(32)-C(31)-C(33)	113.3(4)
C(21)-N(2)-Tb(1)	107.4(3)	C(7)-C(8)-H(8B)	111(4)	N(3)-C(31)-H(31)	108(5)
C(2)-N(2)-Tb(1)	109.0(3)	H(8A)-C(8)-H(8B)	102(5)	C(32)-C(31)-H(31)	105(5)
C(5)-N(3)-C(31)	112.2(4)	N(1)-C(11)-C(12)	111.4(4)	C(33)-C(31)-H(31)	106(5)
C(5)-N(3)-C(4)	108.0(4)	N(1)-C(11)-C(13)	114.0(4)	O(321)-C(32)-O(322)	125.7(5)
C(31)-N(3)-C(4)	110.1(4)	C(12)-C(11)-C(13)	113.3(4)	O(321)-C(32)-C(31)	118.5(4)
C(5)-N(3)-Tb(1)	110.0(3)	N(1)-C(11)-H(11)	106(3)	O(322)-C(32)-C(31)	115.8(4)
C(31)-N(3)-Tb(1)	105.0(3)	C(12)-C(11)-H(11)	103(3)	C(34)-C(33)-C(31)	113.8(4)
C(4)-N(3)-Tb(1)	111.5(3)	C(13)-C(11)-H(11)	108(3)	C(34)-C(33)-H(33A)	107(4)
C(7)-N(4)-C(6)	107.8(4)	O(121)-C(12)-O(122)	124.0(4)	C(31)-C(33)-H(33A)	113(4)
C(7)-N(4)-C(41)	112.3(4)	O(121)-C(12)-C(11)	117.9(4)	C(34)-C(33)-H(33B)	107(4)
C(6)-N(4)-C(41)	109.3(4)	O(122)-C(12)-C(11)	118.0(4)	C(31)-C(33)-H(33B)	106(4)
C(7)-N(4)-Tb(1)	109.7(3)	C(14)-C(13)-C(11)	113.8(4)	H(33A)-C(33)-H(33B)	111(5)
C(6)-N(4)-Tb(1)	110.8(3)	C(14)-C(13)-H(13A)	106(4)	C(35)-C(34)-C(33)	114.3(4)
C(41)-N(4)-Tb(1)	106.9(3)	C(11)-C(13)-H(13A)	112(4)	C(35)-C(34)-H(34A)	108(4)
N(1)-C(1)-C(2)	114.5(4)	C(14)-C(13)-H(13B)	108(3)	C(33)-C(34)-H(34A)	106(4)
N(1)-C(1)-H(1A)	107(3)	C(11)-C(13)-H(13B)	109(3)	C(35)-C(34)-H(34B)	109(4)
C(2)-C(1)-H(1A)	107(3)	H(13A)-C(13)-H(13B)	108(5)	C(33)-C(34)-H(34B)	112(4)
N(1)-C(1)-H(1B)	110(4)	C(15)-C(14)-C(13)	113.3(4)	H(34A)-C(34)-H(34B)	109(6)
C(2)-C(1)-H(1B)	108(4)	C(15)-C(14)-H(14A)	107(4)	O(351)-C(35)-O(352)	123.3(5)
H(1A)-C(1)-H(1B)	111(5)	C(13)-C(14)-H(14A)	110(3)	O(351)-C(35)-C(34)	125.5(5)
N(2)-C(2)-C(1)	111.6(4)	C(15)-C(14)-H(14B)	106(4)	O(352)-C(35)-C(34)	111.2(5)
N(2)-C(2)-H(2A)	106(3)	C(13)-C(14)-H(14B)	102(4)	N(4)-C(41)-C(43)	115.2(4)
C(1)-C(2)-H(2A)	111(3)	H(14A)-C(14)-H(14B)	118(5)	N(4)-C(41)-C(42)	107.9(4)
N(2)-C(2)-H(2B)	106(3)	O(151)-C(15)-O(152)	123.8(6)	C(43)-C(41)-C(42)	116.1(4)
C(1)-C(2)-H(2B)	107(3)	O(151)-C(15)-C(14)	124.1(5)	N(4)-C(41)-H(41)	113(4)
H(2A)-C(2)-H(2B)	115(5)	O(152)-C(15)-C(14)	112.0(5)	C(43)-C(41)-H(41)	101(3)
N(2)-C(3)-C(4)	114.6(4)	N(2)-C(21)-C(23)	116.3(4)	C(42)-C(41)-H(41)	103(3)
N(2)-C(3)-H(3A)	111(4)	N(2)-C(21)-C(22)	108.8(4)	O(422)-C(42)-O(421)	123.9(5)
C(4)-C(3)-H(3A)	112(4)	C(23)-C(21)-C(22)	113.5(5)	O(422)-C(42)-C(41)	118.2(4)
N(2)-C(3)-H(3B)	107(4)	N(2)-C(21)-H(21)	104(4)	O(421)-C(42)-C(41)	117.8(4)
C(4)-C(3)-H(3B)	109(4)	C(23)-C(21)-H(21)	111(4)	C(41)-C(43)-C(44)	112.5(4)
H(3A)-C(3)-H(3B)	102(6)	C(22)-C(21)-H(21)	102(4)	C(41)-C(43)-H(43A)	114(3)
N(3)-C(4)-C(3)	111.5(4)	O(222)-C(22)-O(22A)	120.4(6)	C(44)-C(43)-H(43A)	107(4)
N(3)-C(4)-H(4A)	105(5)	O(222)-C(22)-O(22B)	124.1(7)	C(41)-C(43)-H(43B)	110(3)
C(3)-C(4)-H(4A)	111(5)	O(22A)-C(22)-O(22B)	26.6(5)	C(44)-C(43)-H(43B)	111(4)
N(3)-C(4)-H(4B)	111(4)	O(222)-C(22)-O(22C)	120.9(9)	H(43A)-C(43)-H(43B)	102(5)
C(3)-C(4)-H(4B)	114(4)	O(22A)-C(22)-O(22C)	27.6(7)	C(45)-C(44)-C(43)	114.1(5)
H(4A)-C(4)-H(4B)	104(6)	O(22B)-C(22)-O(22C)	52.7(10)	C(45)-C(44)-H(44A)	106(4)
N(3)-C(5)-C(6)	113.8(4)	O(222)-C(22)-C(21)	118.2(5)	C(43)-C(44)-H(44A)	113(4)
N(3)-C(5)-H(5A)	105(4)	O(22A)-C(22)-C(21)	120.9(6)	C(45)-C(44)-H(44B)	99(5)
C(6)-C(5)-H(5A)	117(4)	O(22B)-C(22)-C(21)	114.1(7)	C(43)-C(44)-H(44B)	115(5)
N(3)-C(5)-H(5B)	113(3)	O(22C)-C(22)-C(21)	109.3(9)	H(44A)-C(44)-H(44B)	109(6)
C(6)-C(5)-H(5B)	109(3)	C(21)-C(23)-C(24)	112.9(5)	O(451)-C(45)-O(452)	124.4(5)
H(5A)-C(5)-H(5B)	98(5)	C(21)-C(23)-H(23A)	116(3)	O(451)-C(45)-C(44)	122.4(6)
N(4)-C(6)-C(5)	112.2(4)	C(24)-C(23)-H(23A)	110(3)	O(452)-C(45)-C(44)	113.1(5)
N(4)-C(6)-H(6A)	110(4)	C(21)-C(23)-H(23B)	108(4)	O(451)-C(45)-H(452)	98(4)
C(5)-C(6)-H(6A)	103(4)	C(24)-C(23)-H(23B)	110(4)	O(452)-C(45)-H(452)	27(4)
N(4)-C(6)-H(6B)	111(3)	H(23A)-C(23)-H(23B)	100(5)	C(44)-C(45)-H(452)	138(4)
C(5)-C(6)-H(6B)	108(3)	C(25)-C(24)-C(23)	109.0(5)	O(2WC)-O(2WA)-O(2WB)	148(3)
H(6A)-C(6)-H(6B)	112(5)	C(25)-C(24)-H(24A)	113(4)	O(2WA)-O(2WB)-O(2WC)	13.2(13)
N(4)-C(7)-C(8)	114.5(4)	C(23)-C(24)-H(24A)	111(4)	O(2WA)-O(2WC)-O(2WB)	18.4(18)
N(4)-C(7)-H(7A)	112(3)	C(25)-C(24)-H(24B)	113(4)		

***Table A.4.14.4** - Anisotropic displacement parameters ($Å^2 x\ 10^3$) for (C28 H42 N4 O20 Tb)$^-$.(H30)$^+$.2(H20). The anisotropic displacement factor exponent takes the form: $-2\pi^2[h^2 a^{*2} U^{11} + ... + 2 h k a^* b^* U^{12}]$*

	U^{11}	U^{22}	U^{33}	U^{23}	U^{13}	U^{12}
Tb(1)	18(1)	11(1)	14(1)	1(1)	5(1)	3(1)
O(5)	32(2)	18(2)	48(3)	6(2)	18(2)	11(2)
O(121)	46(3)	30(2)	32(2)	15(2)	15(2)	26(2)
O(122)	31(2)	15(2)	22(2)	3(1)	13(2)	11(2)
O(151)	55(3)	25(2)	36(2)	2(2)	-7(2)	16(2)
O(152)	70(4)	43(3)	38(3)	-8(2)	-18(3)	33(3)
O(222)	27(2)	15(2)	25(2)	-2(1)	14(2)	0(2)
O(251)	34(2)	30(2)	27(2)	8(2)	8(2)	14(2)
O(252)	28(2)	27(2)	18(2)	2(2)	0(2)	5(2)
O(321)	24(2)	25(2)	24(2)	12(2)	3(2)	0(2)
O(322)	17(2)	21(2)	18(2)	6(1)	4(1)	5(1)
O(352)	39(2)	22(2)	31(2)	-3(2)	14(2)	12(2)
O(351)	45(3)	23(2)	31(2)	6(2)	11(2)	6(2)
O(421)	31(2)	16(2)	28(2)	-2(2)	-9(2)	3(2)
O(422)	19(2)	15(2)	22(2)	5(1)	2(1)	7(1)
O(451)	63(4)	33(3)	119(5)	39(3)	60(4)	25(3)
O(452)	60(3)	25(2)	69(3)	23(2)	40(3)	25(2)
N(1)	23(2)	12(2)	14(2)	3(2)	7(2)	6(2)
N(2)	26(2)	18(2)	16(2)	2(2)	9(2)	5(2)
N(3)	16(2)	21(2)	14(2)	2(2)	3(2)	3(2)
N(4)	16(2)	12(2)	15(2)	3(2)	2(2)	4(2)
C(1)	22(3)	20(2)	20(2)	4(2)	10(2)	9(2)
C(2)	25(3)	16(2)	17(2)	2(2)	7(2)	3(2)
C(3)	18(3)	24(3)	22(3)	4(2)	5(2)	2(2)
C(4)	20(3)	25(3)	17(2)	0(2)	1(2)	-1(2)
C(5)	20(3)	33(3)	16(2)	4(2)	1(2)	13(2)
C(6)	25(3)	19(2)	16(2)	6(2)	4(2)	14(2)
C(7)	23(3)	16(2)	19(2)	5(2)	6(2)	9(2)
C(8)	28(3)	19(2)	16(2)	5(2)	8(2)	10(2)
C(11)	24(3)	13(2)	16(2)	4(2)	9(2)	8(2)
C(12)	22(3)	14(2)	25(3)	7(2)	7(2)	7(2)
C(13)	27(3)	22(2)	19(2)	8(2)	8(2)	10(2)
C(14)	36(3)	23(3)	21(3)	8(2)	5(2)	17(2)
C(15)	43(3)	32(3)	20(3)	7(2)	8(2)	21(3)
C(21)	27(3)	16(2)	26(3)	-2(2)	13(2)	2(2)
C(22)	41(3)	20(3)	26(3)	-4(2)	19(3)	-1(2)
C(23)	24(3)	22(3)	33(3)	3(2)	10(2)	5(2)
C(24)	30(3)	22(3)	43(4)	2(2)	12(3)	5(2)
C(25)	33(3)	17(2)	29(3)	4(2)	6(2)	9(2)
C(31)	23(3)	16(2)	17(2)	3(2)	5(2)	6(2)
C(32)	21(2)	17(2)	18(2)	3(2)	5(2)	5(2)
C(33)	27(3)	21(2)	17(2)	7(2)	6(2)	8(2)
C(34)	26(3)	22(2)	18(2)	5(2)	5(2)	8(2)
C(35)	24(3)	22(2)	17(2)	3(2)	-2(2)	7(2)
C(41)	21(2)	13(2)	23(2)	7(2)	5(2)	5(2)
C(42)	18(2)	14(2)	23(2)	7(2)	4(2)	4(2)
C(43)	25(3)	13(2)	31(3)	4(2)	8(2)	7(2)
C(44)	28(3)	19(3)	54(4)	6(3)	17(3)	10(2)
C(45)	29(3)	19(2)	35(3)	5(2)	9(2)	6(2)

***Table A.4.14.5** - Hydrogen coordinates (x 10^4) and isotropic displacement parameters ($Å^2$x 10^3) for (C28 H42 N4 O20 Tb)$^-$.(H30)$^+$.2(H20).*

	x	y	z	U(eq)
H(5D)	3670(100)	-7820(80)	2370(60)	48
H(5C)	3050(100)	-8560(80)	1880(60)	48
H(152)	4160(110)	-5530(90)	7570(60)	84
H(252)	-6850(90)	-14610(70)	760(50)	42
H(352)	-1360(100)	-9410(70)	-2520(50)	48
H(452)	2780(110)	-770(80)	4100(60)	67
H(1A)	-2320(70)	-7940(50)	3350(40)	24
H(1B)	-1920(70)	-8500(50)	4100(40)	24
H(2A)	-1600(70)	-10040(50)	3110(40)	25
H(2B)	-3440(70)	-10010(50)	2800(40)	25
H(3A)	-4280(80)	-9790(60)	1410(40)	29
H(3B)	-3320(70)	-8610(60)	1990(40)	29
H(4A)	-2800(80)	-9080(60)	510(40)	30
H(4B)	-3760(80)	-8500(60)	530(40)	30
H(5A)	-2270(80)	-6430(60)	1150(40)	29
H(5B)	-2550(70)	-6740(50)	1940(40)	29
H(6A)	-630(70)	-4920(50)	2400(40)	23
H(6B)	400(70)	-5160(50)	1810(40)	23
H(7A)	-1370(70)	-6070(50)	3310(40)	23
H(7B)	-110(70)	-4970(50)	3890(40)	23
H(8A)	1360(70)	-5740(50)	4650(40)	25
H(8B)	-370(70)	-6330(50)	4690(40)	25
H(11)	2100(70)	-7190(50)	4690(40)	21
H(13A)	-160(70)	-7740(60)	5390(40)	29
H(13B)	-300(70)	-9130(60)	5040(40)	29
H(14A)	2580(80)	-8230(60)	5900(40)	33
H(14B)	1160(80)	-8170(60)	6470(40)	33
H(21)	-1330(80)	-10770(60)	1900(40)	31
H(23A)	-4470(80)	-11590(60)	500(40)	37
H(23B)	-4260(80)	-11570(60)	1540(40)	37
H(24A)	-2890(90)	-12860(70)	510(50)	44
H(24B)	-2900(90)	-12940(70)	1410(50)	44
H(31)	-750(70)	-8000(60)	170(40)	23
H(33A)	-1560(70)	-6310(60)	-140(40)	29
H(33B)	-2780(80)	-7600(60)	-410(40)	29
H(34A)	-2000(80)	-7140(60)	-1560(40)	29
H(34B)	-390(80)	-6960(60)	-1150(40)	29
H(41)	2770(70)	-4610(50)	2840(40)	23
H(43A)	1460(70)	-3350(60)	3490(40)	31
H(43B)	2350(70)	-3470(60)	4410(40)	31
H(44A)	4820(90)	-2400(60)	4230(50)	44
H(44B)	4130(90)	-2660(70)	3230(50)	44

***Table A.4.15.2** - Atomic coordinates (x 10^4) and equivalent isotropic displacement parameters ($Å^2$x 10^3) for C28 H49 Gd N4 O20. U(eq) is defined as one third of the trace of the orthogonalized U^{ij} tensor.*

	x	y	z	U(eq)
Gd(1)	806(1)	-7765(1)	2335(1)	11(1)
O(5)	3017(2)	-8109(2)	2045(2)	28(1)
O(121)	1991(2)	-9421(2)	4368(1)	28(1)
O(122)	1205(2)	-9092(1)	3097(1)	18(1)
O(151)	2317(3)	-5815(2)	6268(1)	40(1)
O(152)	3802(3)	-6310(2)	7201(1)	48(1)
O(22A)	-1636(5)	-11099(3)	40(2)	19(1)
O(22B)	-2157(6)	-10901(4)	-60(3)	14(1)
O(22C)	-1326(11)	-11326(8)	243(6)	24(2)
O(222)	-45(2)	-9382(1)	1015(1)	22(1)
O(251)	-5817(2)	-14221(2)	-315(1)	25(1)
O(252)	-5855(2)	-14076(2)	1073(1)	25(1)
O(321)	1460(2)	-5793(2)	375(1)	25(1)
O(322)	1753(2)	-6607(1)	1454(1)	16(1)
O(352)	-1132(2)	-8810(2)	-2265(1)	29(1)
O(351)	-2678(2)	-9471(2)	-1454(1)	33(1)
O(421)	4284(2)	-4548(2)	4555(1)	27(1)
O(422)	3028(2)	-6319(1)	3524(1)	16(1)
O(452)	2765(2)	-1238(2)	4237(2)	37(1)
O(451)	4633(3)	-612(2)	3626(2)	58(1)
N(1)	-5(2)	-7593(2)	3822(1)	14(1)
N(2)	-2007(2)	-9445(2)	2043(1)	17(1)
N(3)	-1390(2)	-7547(2)	1167(1)	16(1)
N(4)	625(2)	-5708(2)	2923(1)	13(1)
C(1)	-1688(2)	-8373(2)	3607(1)	16(1)
C(2)	-2221(3)	-9571(2)	2914(2)	18(1)
C(3)	-3228(2)	-9112(2)	1605(2)	20(1)
C(4)	-2878(3)	-8631(2)	854(2)	22(1)
C(5)	-1693(3)	-6507(2)	1583(2)	19(1)
C(6)	-244(3)	-5438(2)	2185(1)	17(1)
C(7)	-238(2)	-5769(2)	3594(1)	16(1)
C(8)	227(3)	-6352(2)	4258(1)	16(1)
C(11)	1024(2)	-7930(2)	4435(1)	15(1)
C(12)	1421(2)	-8908(2)	3932(1)	17(1)
C(13)	456(3)	-8195(2)	5222(2)	19(1)
C(14)	1751(3)	-7875(2)	6065(2)	25(1)
C(15)	2644(3)	-6559(2)	6512(2)	25(1)
C(21)	-2060(3)	-10578(2)	1487(2)	20(1)
C(22)	-1232(3)	-10322(2)	791(2)	31(1)
C(23)	-3662(3)	-11614(2)	1101(2)	23(1)
C(24)	-3558(3)	-12818(2)	882(2)	28(1)
C(25)	-5175(3)	-13786(2)	484(2)	21(1)
C(31)	-760(2)	-7391(2)	404(1)	15(1)
C(32)	954(2)	-6515(2)	769(1)	16(1)
C(33)	-1719(3)	-7091(2)	-306(2)	19(1)
C(34)	-1394(3)	-7361(2)	-1197(2)	20(1)
C(35)	-1826(3)	-8657(2)	-1642(2)	21(1)
C(41)	2264(2)	-4778(2)	3297(1)	16(1)
C(42)	3254(2)	-5263(2)	3832(1)	16(1)
C(43)	2426(3)	-3536(2)	3767(2)	21(1)
C(44)	3905(3)	-2552(2)	3755(2)	31(1)
C(45)	3817(3)	-1363(2)	3866(2)	25(1)
O(1WA)	5010(4)	-4153(3)	8197(2)	30(1)
O(1WB)	4657(7)	-4022(6)	8058(4)	20(1)
O(2WA)	-4005(7)	-6685(5)	3517(5)	30(1)
O(2WB)	-3421(9)	-6303(7)	4071(5)	42(2)
O(2WC)	-4051(6)	-6877(5)	3133(4)	27(1)

O(3WA)	5147(9)	-1421(7)	6922(5)	90(2)
O(3WB)	4797(8)	-1784(6)	5791(4)	76(2)

***Table A.4.15.3** - Bond lengths [Å] and angles [°] for C28 H49 Gd N4 O20.*

Gd(1)-O(322)	2.3492(15)	C(3)-H(3B)	0.95(3)	O(322)-Gd(1)-O(122)	144.86(5)
Gd(1)-O(222)	2.383(2)	C(4)-H(4B)	0.93(3)	O(222)-Gd(1)-O(122)	85.82(6)
Gd(1)-O(122)	2.385(2)	C(4)-H(4A)	1.00(3)	O(322)-Gd(1)-O(422)	85.68(5)
Gd(1)-O(422)	2.4028(15)	C(5)-C(6)	1.520(3)	O(222)-Gd(1)-O(422)	144.47(5)
Gd(1)-O(5)	2.432(2)	C(5)-H(5B)	0.95(3)	O(122)-Gd(1)-O(422)	83.14(5)
Gd(1)-N(4)	2.655(2)	C(5)-H(5A)	1.05(3)	O(322)-Gd(1)-O(5)	72.57(6)
Gd(1)-N(1)	2.662(2)	C(6)-H(6B)	0.98(3)	O(222)-Gd(1)-O(5)	70.33(7)
Gd(1)-N(2)	2.674(2)	C(6)-H(6A)	0.99(3)	O(122)-Gd(1)-O(5)	72.34(6)
Gd(1)-N(3)	2.689(2)	C(7)-C(8)	1.516(3)	O(422)-Gd(1)-O(5)	74.14(6)
O(5)-H(5D)	0.75(6)	C(7)-H(7A)	0.98(2)	O(322)-Gd(1)-N(4)	72.59(5)
O(5)-H(5C)	0.68(5)	C(7)-H(7B)	0.99(3)	O(222)-Gd(1)-N(4)	140.73(6)
O(121)-C(12)	1.235(3)	C(8)-H(8A)	1.01(3)	O(122)-Gd(1)-N(4)	130.66(5)
O(122)-C(12)	1.282(3)	C(8)-H(8B)	1.02(3)	O(422)-Gd(1)-N(4)	66.02(5)
O(151)-C(15)	1.213(3)	C(11)-C(12)	1.538(3)	O(5)-Gd(1)-N(4)	128.11(6)
O(152)-C(15)	1.307(3)	C(11)-C(13)	1.538(3)	O(322)-Gd(1)-N(1)	140.92(5)
O(152)-H(152)	1.03(7)	C(11)-H(11)	0.98(3)	O(222)-Gd(1)-N(1)	131.61(5)
O(22A)-O(22C)	0.587(9)	C(13)-C(14)	1.527(3)	O(122)-Gd(1)-N(1)	65.28(5)
O(22A)-O(22B)	0.645(5)	C(13)-H(13A)	0.99(3)	O(422)-Gd(1)-N(1)	72.43(5)
O(22A)-C(22)	1.275(4)	C(13)-H(13B)	1.02(3)	O(5)-Gd(1)-N(1)	128.11(6)
O(22B)-O(22C)	1.199(11)	C(14)-C(15)	1.510(4)	N(4)-Gd(1)-N(1)	69.03(5)
O(22B)-C(22)	1.363(6)	C(14)-H(14A)	1.04(3)	O(322)-Gd(1)-N(2)	130.09(5)
O(22C)-C(22)	1.346(9)	C(14)-H(14B)	0.97(3)	O(222)-Gd(1)-N(2)	65.47(5)
O(222)-C(22)	1.250(3)	C(21)-C(22)	1.529(3)	O(122)-Gd(1)-N(2)	74.17(6)
O(251)-C(25)	1.225(3)	C(21)-C(23)	1.534(3)	O(422)-Gd(1)-N(2)	141.16(5)
O(252)-C(25)	1.305(3)	C(21)-H(21)	0.95(2)	O(5)-Gd(1)-N(2)	125.48(6)
O(252)-H(252)	0.86(4)	C(23)-C(24)	1.535(3)	N(4)-Gd(1)-N(2)	106.36(5)
O(321)-C(32)	1.244(3)	C(23)-H(23A)	0.99(3)	N(1)-Gd(1)-N(2)	69.56(5)
O(322)-C(32)	1.275(3)	C(23)-H(23B)	0.98(3)	O(322)-Gd(1)-N(3)	65.51(5)
O(352)-C(35)	1.330(3)	C(24)-C(25)	1.511(3)	O(222)-Gd(1)-N(3)	72.95(6)
O(352)-H(352)	0.83(5)	C(24)-H(24A)	0.97(2)	O(122)-Gd(1)-N(3)	141.63(5)
O(351)-C(35)	1.216(3)	C(24)-H(24B)	0.98(3)	O(422)-Gd(1)-N(3)	131.78(5)
O(421)-C(42)	1.280(3)	C(31)-C(33)	1.532(3)	O(5)-Gd(1)-N(3)	125.97(6)
O(422)-C(42)	1.246(3)	C(31)-C(32)	1.539(3)	N(4)-Gd(1)-N(3)	68.72(5)
O(452)-C(45)	1.313(3)	C(31)-H(31)	0.97(3)	N(1)-Gd(1)-N(3)	105.89(5)
O(452)-H(452)	0.98(5)	C(33)-C(34)	1.528(3)	N(2)-Gd(1)-N(3)	68.03(5)
O(451)-C(45)	1.198(3)	C(33)-H(33B)	0.95(3)	Gd(1)-O(5)-H(5D)	122.4(39)
N(1)-C(8)	1.495(3)	C(33)-H(33A)	0.94(3)	Gd(1)-O(5)-H(5C)	118.4(42)
N(1)-C(1)	1.497(3)	C(34)-C(35)	1.512(3)	H(5D)-O(5)-H(5C)	102.2(52)
N(1)-C(11)	1.501(3)	C(34)-H(34A)	0.95(3)	C(12)-O(122)-Gd(1)	124.52(13)
N(2)-C(3)	1.492(3)	C(34)-H(34B)	0.93(3)	C(15)-O(152)-H(152)	106.8(36)
N(2)-C(21)	1.498(3)	C(41)-C(43)	1.531(3)	O(22C)-O(22A)-O(22B)	153.7(13)
N(2)-C(2)	1.500(3)	C(41)-C(42)	1.538(3)	O(22C)-O(22A)-C(22)	83.9(10)
N(3)-C(5)	1.496(3)	C(41)-H(41)	0.99(3)	O(22B)-O(22A)-C(22)	83.6(6)
N(3)-C(4)	1.498(3)	C(43)-C(44)	1.540(3)	O(22A)-O(22B)-O(22C)	12.5(6)
N(3)-C(31)	1.500(3)	C(43)-H(43B)	1.02(3)	O(22A)-O(22B)-C(22)	68.4(6)
N(4)-C(7)	1.491(3)	C(43)-H(43A)	0.99(3)	O(22C)-O(22B)-C(22)	63.0(5)
N(4)-C(6)	1.497(3)	C(44)-C(45)	1.515(3)	O(22A)-O(22C)-O(22B)	13.8(7)
N(4)-C(41)	1.507(3)	C(44)-H(42B)	1.01(4)	O(22A)-O(22C)-C(22)	70.4(10)
C(1)-C(2)	1.522(3)	C(44)-H(42A)	0.92(4)	O(22B)-O(22C)-C(22)	64.5(5)
C(1)-H(1B)	0.95(3)	O(2WA)-O(2WC)	0.604(6)	C(22)-O(222)-Gd(1)	125.88(14)
C(1)-H(1A)	0.95(2)	O(2WA)-O(2WB)	0.883(8)	C(25)-O(252)-H(252)	114.6(24)
C(2)-H(2B)	1.00(3)	O(2WB)-O(2WC)	1.434(9)	C(32)-O(322)-Gd(1)	126.64(13)
C(2)-H(2A)	1.00(3)	O(3WA)-O(3WB)	1.722(9)	C(35)-O(352)-H(352)	109.8(31)
C(3)-C(4)	1.520(3)			C(42)-O(422)-Gd(1)	124.31(13)
C(3)-H(3A)	0.94(3)	O(322)-Gd(1)-O(222)	84.22(5)	C(45)-O(452)-H(452)	113.2(30)

C(8)-N(1)-C(1)	107.9(2)	N(4)-C(7)-C(8)	114.1(2)	C(23)-C(24)-H(24A)	113.4(14)
C(8)-N(1)-C(11)	108.7(2)	N(4)-C(7)-H(7A)	107.7(14)	C(25)-C(24)-H(24B)	108.3(20)
C(1)-N(1)-C(11)	112.8(2)	C(8)-C(7)-H(7A)	108.3(14)	C(23)-C(24)-H(24B)	113.3(20)
C(8)-N(1)-Gd(1)	110.87(12)	N(4)-C(7)-H(7B)	113.0(15)	H(24A)-C(24)-H(24B)	103.5(23)
C(1)-N(1)-Gd(1)	109.20(12)	C(8)-C(7)-H(7B)	109.7(15)	O(251)-C(25)-O(252)	123.0(2)
C(11)-N(1)-Gd(1)	107.41(11)	H(7A)-C(7)-H(7B)	103.4(20)	O(251)-C(25)-C(24)	123.3(2)
C(3)-N(2)-C(21)	112.2(2)	N(1)-C(8)-C(7)	112.3(2)	O(252)-C(25)-C(24)	113.6(2)
C(3)-N(2)-C(2)	108.8(2)	N(1)-C(8)-H(8A)	110.4(16)	N(3)-C(31)-C(33)	115.4(2)
C(21)-N(2)-C(2)	109.5(2)	C(7)-C(8)-H(8A)	109.6(16)	N(3)-C(31)-C(32)	108.8(2)
C(3)-N(2)-Gd(1)	110.29(12)	N(1)-C(8)-H(8B)	109.7(16)	C(33)-C(31)-C(32)	113.5(2)
C(21)-N(2)-Gd(1)	107.13(12)	C(7)-C(8)-H(8B)	106.8(15)	N(3)-C(31)-H(31)	105.1(16)
C(2)-N(2)-Gd(1)	108.81(12)	H(8A)-C(8)-H(8B)	107.9(21)	C(33)-C(31)-H(31)	107.3(16)
C(5)-N(3)-C(4)	108.4(2)	N(1)-C(11)-C(12)	112.0(2)	C(32)-C(31)-H(31)	106.0(16)
C(5)-N(3)-C(31)	111.8(2)	N(1)-C(11)-C(13)	114.4(2)	O(321)-C(32)-O(322)	125.2(2)
C(4)-N(3)-C(31)	109.8(2)	C(12)-C(11)-C(13)	112.9(2)	O(321)-C(32)-C(31)	118.5(2)
C(5)-N(3)-Gd(1)	110.20(12)	N(1)-C(11)-H(11)	104.8(15)	O(322)-C(32)-C(31)	116.3(2)
C(4)-N(3)-Gd(1)	111.33(13)	C(12)-C(11)-H(11)	104.0(14)	C(34)-C(33)-C(31)	113.4(2)
C(31)-N(3)-Gd(1)	105.36(12)	C(13)-C(11)-H(11)	107.8(14)	C(34)-C(33)-H(33B)	107.8(15)
C(7)-N(4)-C(6)	107.5(2)	O(121)-C(12)-O(122)	124.8(2)	C(31)-C(33)-H(33B)	110.3(16)
C(7)-N(4)-C(41)	112.7(2)	O(121)-C(12)-C(11)	117.5(2)	C(34)-C(33)-H(33A)	108.1(18)
C(6)-N(4)-C(41)	109.7(2)	O(122)-C(12)-C(11)	117.5(2)	C(31)-C(33)-H(33A)	106.4(18)
C(7)-N(4)-Gd(1)	109.45(12)	C(14)-C(13)-C(11)	114.3(2)	H(33B)-C(33)-H(33A)	110.8(24)
C(6)-N(4)-Gd(1)	110.83(12)	C(14)-C(13)-H(13A)	107.2(17)	C(35)-C(34)-C(33)	114.5(2)
C(41)-N(4)-Gd(1)	106.69(11)	C(11)-C(13)-H(13A)	109.0(17)	C(35)-C(34)-H(34A)	105.4(18)
N(1)-C(1)-C(2)	114.5(2)	C(14)-C(13)-H(13B)	109.0(16)	C(33)-C(34)-H(34A)	111.1(17)
N(1)-C(1)-H(1B)	105.9(16)	C(11)-C(13)-H(13B)	109.7(15)	C(35)-C(34)-H(34B)	106.7(18)
C(2)-C(1)-H(1B)	110.2(16)	H(13A)-C(13)-H(13B)	107.3(23)	C(33)-C(34)-H(34B)	111.9(17)
N(1)-C(1)-H(1A)	111.3(15)	C(15)-C(14)-C(13)	113.7(2)	H(34A)-C(34)-H(34B)	106.8(25)
C(2)-C(1)-H(1A)	108.5(16)	C(15)-C(14)-H(14A)	110.0(18)	O(351)-C(35)-O(352)	123.3(2)
H(1B)-C(1)-H(1A)	106.2(21)	C(13)-C(14)-H(14A)	110.2(18)	O(351)-C(35)-C(34)	125.0(2)
N(2)-C(2)-C(1)	111.8(2)	C(15)-C(14)-H(14B)	108.3(19)	O(352)-C(35)-C(34)	111.7(2)
N(2)-C(2)-H(2B)	108.8(15)	C(13)-C(14)-H(14B)	109.0(19)	N(4)-C(41)-C(43)	115.0(2)
C(1)-C(2)-H(2B)	108.4(16)	H(14A)-C(14)-H(14B)	105.2(25)	N(4)-C(41)-C(42)	108.5(2)
N(2)-C(2)-H(2A)	110.9(14)	O(151)-C(15)-O(152)	123.6(3)	C(43)-C(41)-C(42)	115.6(2)
C(1)-C(2)-H(2A)	106.7(15)	O(151)-C(15)-C(14)	124.0(2)	N(4)-C(41)-H(41)	109.2(16)
H(2B)-C(2)-H(2A)	110.2(22)	O(152)-C(15)-C(14)	112.4(2)	C(43)-C(41)-H(41)	103.0(17)
N(2)-C(3)-C(4)	113.4(2)	N(2)-C(21)-C(22)	109.2(2)	C(42)-C(41)-H(41)	104.7(16)
N(2)-C(3)-H(3A)	110.2(17)	N(2)-C(21)-C(23)	115.8(2)	O(422)-C(42)-O(421)	124.1(2)
C(4)-C(3)-H(3A)	110.3(16)	C(22)-C(21)-C(23)	113.5(2)	O(422)-C(42)-C(41)	118.1(2)
N(2)-C(3)-H(3B)	107.8(15)	N(2)-C(21)-H(21)	105.3(14)	O(421)-C(42)-C(41)	117.8(2)
C(4)-C(3)-H(3B)	108.8(16)	C(22)-C(21)-H(21)	105.5(13)	C(41)-C(43)-C(44)	112.8(2)
H(3A)-C(3)-H(3B)	106.0(22)	C(23)-C(21)-H(21)	106.6(14)	C(41)-C(43)-H(43B)	108.2(16)
N(3)-C(4)-C(3)	111.8(2)	O(222)-C(22)-O(22A)	120.6(2)	C(44)-C(43)-H(43B)	107.4(15)
N(3)-C(4)-H(4B)	108.8(19)	O(222)-C(22)-O(22C)	120.8(4)	C(41)-C(43)-H(43A)	108.5(18)
C(3)-C(4)-H(4B)	112.0(19)	O(22A)-C(22)-O(22C)	25.7(4)	C(44)-C(43)-H(43A)	112.4(18)
N(3)-C(4)-H(4A)	110.0(15)	O(222)-C(22)-O(22B)	123.6(3)	H(43B)-C(43)-H(43A)	107.3(23)
C(3)-C(4)-H(4A)	109.3(14)	O(22A)-C(22)-O(22B)	28.0(2)	C(45)-C(44)-C(43)	114.1(2)
H(4B)-C(4)-H(4A)	104.8(23)	O(22C)-C(22)-O(22B)	52.6(5)	C(45)-C(44)-H(42B)	107.3(23)
N(3)-C(5)-C(6)	114.0(2)	O(222)-C(22)-C(21)	117.9(2)	C(43)-C(44)-H(42B)	111.3(23)
N(3)-C(5)-H(5B)	112.3(17)	O(22A)-C(22)-C(21)	121.1(2)	C(45)-C(44)-H(42A)	108.9(24)
C(6)-C(5)-H(5B)	107.1(18)	O(22C)-C(22)-C(21)	111.3(4)	C(43)-C(44)-H(42A)	112.2(25)
N(3)-C(5)-H(5A)	109.4(15)	O(22B)-C(22)-C(21)	113.9(3)	H(42B)-C(44)-H(42A)	102.4(30)
C(6)-C(5)-H(5A)	111.0(15)	C(21)-C(23)-C(24)	112.2(2)	O(451)-C(45)-O(452)	123.5(2)
H(5B)-C(5)-H(5A)	102.6(22)	C(21)-C(23)-H(23A)	111.2(18)	O(451)-C(45)-C(44)	122.4(2)
N(4)-C(6)-C(5)	112.7(2)	C(24)-C(23)-H(23A)	109.7(18)	O(452)-C(45)-C(44)	114.2(2)
N(4)-C(6)-H(6B)	111.6(15)	C(21)-C(23)-H(23B)	107.3(19)	O(2WC)-O(2WA)-O(2WB)	148.9(12)
C(5)-C(6)-H(6B)	106.9(15)	C(24)-C(23)-H(23B)	107.9(20)	O(2WA)-O(2WB)-O(2WC)	12.6(5)
N(4)-C(6)-H(6A)	107.2(15)	H(23A)-C(23)-H(23B)	108.3(25)	O(2WA)-O(2WC)-O(2WB)	18.6(8)
C(5)-C(6)-H(6A)	112.3(15)	C(25)-C(24)-C(23)	108.9(2)		
H(6B)-C(6)-H(6A)	106.1(22)	C(25)-C(24)-H(24A)	109.0(14)		

***Table A.4.15.4** - Anisotropic displacement parameters ($Å^2 x\ 10^3$) for C28 H49 Gd N4 O20. The anisotropic displacement factor exponent takes the form: $-2\pi^2[h^2 a^{*2} U^{11} + ... + 2 h k a^* b^* U^{12}]$*

	U^{11}	U^{22}	U^{33}	U^{23}	U^{13}	U^{12}
Gd(1)	11(1)	10(1)	12(1)	2(1)	5(1)	4(1)
O(5)	24(1)	18(1)	45(1)	7(1)	19(1)	10(1)
O(121)	44(1)	28(1)	27(1)	13(1)	14(1)	27(1)
O(122)	25(1)	15(1)	18(1)	5(1)	9(1)	10(1)
O(151)	52(1)	25(1)	33(1)	5(1)	-5(1)	19(1)
O(152)	52(1)	44(1)	35(1)	-6(1)	-15(1)	29(1)
O(222)	21(1)	16(1)	21(1)	0(1)	12(1)	1(1)
O(251)	24(1)	25(1)	24(1)	7(1)	6(1)	10(1)
O(252)	20(1)	25(1)	21(1)	3(1)	4(1)	3(1)
O(321)	21(1)	25(1)	24(1)	13(1)	4(1)	1(1)
O(322)	13(1)	18(1)	17(1)	6(1)	5(1)	5(1)
O(352)	34(1)	23(1)	31(1)	2(1)	14(1)	12(1)
O(351)	39(1)	23(1)	31(1)	8(1)	13(1)	6(1)
O(421)	27(1)	16(1)	25(1)	-1(1)	-9(1)	6(1)
O(422)	14(1)	13(1)	21(1)	4(1)	3(1)	6(1)
O(452)	48(1)	24(1)	58(1)	19(1)	34(1)	23(1)
O(451)	58(2)	31(1)	114(2)	39(1)	60(2)	24(1)
N(1)	17(1)	12(1)	14(1)	3(1)	5(1)	7(1)
N(2)	17(1)	15(1)	15(1)	2(1)	7(1)	3(1)
N(3)	12(1)	18(1)	15(1)	4(1)	5(1)	3(1)
N(4)	12(1)	13(1)	15(1)	4(1)	3(1)	6(1)
C(1)	15(1)	18(1)	17(1)	4(1)	7(1)	6(1)
C(2)	18(1)	16(1)	19(1)	5(1)	9(1)	3(1)
C(3)	13(1)	22(1)	20(1)	5(1)	5(1)	2(1)
C(4)	14(1)	25(1)	17(1)	5(1)	3(1)	0(1)
C(5)	16(1)	25(1)	17(1)	6(1)	4(1)	11(1)
C(6)	20(1)	18(1)	16(1)	7(1)	7(1)	11(1)
C(7)	18(1)	14(1)	16(1)	3(1)	6(1)	9(1)
C(8)	20(1)	13(1)	14(1)	2(1)	5(1)	8(1)
C(11)	18(1)	14(1)	15(1)	5(1)	6(1)	8(1)
C(12)	17(1)	11(1)	22(1)	5(1)	8(1)	5(1)
C(13)	24(1)	19(1)	19(1)	8(1)	10(1)	10(1)
C(14)	36(1)	27(1)	19(1)	11(1)	9(1)	18(1)
C(15)	33(1)	30(1)	18(1)	6(1)	8(1)	19(1)
C(21)	19(1)	15(1)	21(1)	1(1)	10(1)	2(1)
C(22)	37(1)	19(1)	26(1)	-2(1)	21(1)	0(1)
C(23)	17(1)	17(1)	28(1)	4(1)	7(1)	0(1)
C(24)	20(1)	20(1)	37(1)	2(1)	7(1)	3(1)
C(25)	20(1)	17(1)	27(1)	4(1)	6(1)	9(1)
C(31)	14(1)	17(1)	14(1)	4(1)	4(1)	5(1)
C(32)	15(1)	15(1)	16(1)	4(1)	6(1)	5(1)
C(33)	19(1)	20(1)	17(1)	5(1)	4(1)	8(1)
C(34)	24(1)	20(1)	16(1)	7(1)	5(1)	8(1)
C(35)	23(1)	22(1)	17(1)	6(1)	1(1)	8(1)
C(41)	14(1)	13(1)	20(1)	4(1)	3(1)	5(1)
C(42)	13(1)	15(1)	19(1)	5(1)	3(1)	5(1)
C(43)	21(1)	12(1)	28(1)	3(1)	8(1)	7(1)
C(44)	24(1)	15(1)	55(2)	8(1)	19(1)	7(1)
C(45)	23(1)	19(1)	30(1)	5(1)	10(1)	6(1)

***Table A.4.15.5** - Hydrogen coordinates (x 10^4) and isotropic displacement parameters ($Å^2$x 10^3) for C28 H49 Gd N4 O20.*

	x	y	z	U(eq)
H(5D)	3814(64)	-7793(50)	2369(34)	85(18)
H(5C)	2949(58)	-8675(48)	1916(32)	78(17)
H(152)	4264(77)	-5406(62)	7500(43)	144(24)
H(252)	-6763(46)	-14650(36)	855(24)	54(11)
H(352)	-1341(53)	-9522(43)	-2475(29)	76(14)
H(452)	2529(61)	-563(49)	4166(33)	101(17)
H(1B)	-2235(31)	-7942(24)	3405(17)	18(6)
H(1A)	-1952(29)	-8501(23)	4122(17)	14(6)
H(2B)	-1593(32)	-9992(26)	3134(18)	23(7)
H(2A)	-3337(30)	-10018(23)	2854(16)	14(6)
H(3A)	-4192(32)	-9757(25)	1402(17)	20(7)
H(3B)	-3314(29)	-8525(24)	2040(17)	14(6)
H(4B)	-2829(34)	-9192(28)	395(20)	30(8)
H(4A)	-3754(30)	-8448(23)	579(17)	17(6)
H(5B)	-2193(33)	-6250(26)	1156(18)	24(7)
H(5A)	-2509(32)	-6766(25)	1922(18)	22(7)
H(6B)	-577(30)	-4810(24)	2411(17)	17(6)
H(6A)	485(30)	-5119(24)	1860(17)	18(6)
H(7A)	-1338(28)	-6225(22)	3276(15)	9(5)
H(7B)	-188(30)	-4992(25)	3910(17)	20(7)
H(8A)	1346(33)	-5860(26)	4625(18)	22(7)
H(8B)	-444(32)	-6352(25)	4671(18)	22(7)
H(11)	2014(29)	-7234(23)	4673(16)	14(6)
H(13A)	-158(34)	-7737(27)	5366(19)	29(7)
H(13B)	-256(33)	-9066(27)	5049(18)	25(7)
H(14A)	2506(37)	-8264(29)	5930(20)	37(8)
H(14B)	1307(36)	-8223(29)	6483(21)	35(8)
H(21)	-1435(26)	-10809(21)	1873(15)	4(5)
H(23A)	-4277(36)	-11545(28)	569(20)	33(8)
H(23B)	-4199(38)	-11579(30)	1552(21)	38(8)
H(24A)	-3028(26)	-12959(20)	1390(15)	3(5)
H(24B)	-2963(40)	-12907(31)	461(22)	43(9)
H(31)	-767(31)	-8152(26)	125(18)	21(7)
H(33B)	-1519(30)	-6271(25)	-116(17)	17(6)
H(33A)	-2767(36)	-7566(28)	-389(19)	29(7)
H(34A)	-1966(35)	-7122(27)	-1611(20)	30(8)
H(34B)	-357(34)	-6963(26)	-1146(18)	22(7)
H(41)	2710(32)	-4662(26)	2805(18)	24(7)
H(43B)	1504(31)	-3416(24)	3442(17)	20(7)
H(43A)	2363(35)	-3495(28)	4377(21)	34(8)
H(42B)	4838(47)	-2431(36)	4239(26)	59(11)
H(42A)	4182(44)	-2757(35)	3248(26)	56(11)

***Table A.4.16.2** - Atomic coordinates (x 10^4) and equivalent isotropic displacement parameters ($Å^2$x 10^3) for C28 H67 N4 O23.50. U(eq) is defined as one third of the trace of the orthogonalized U^{ij} tensor.*

	x	y	z	U(eq)
O(121)	2965(2)	-5334(3)	2381(2)	28(1)
O(122)	2908(2)	-3874(3)	3258(2)	25(1)
O(151)	771(2)	-5916(3)	326(2)	38(1)
O(152)	496(1)	-3863(3)	537(2)	31(1)
O(221)	276(2)	216(4)	690(2)	43(1)
O(222)	1217(1)	-306(3)	468(2)	24(1)
O(251)	1414(2)	-380(4)	3451(2)	42(1)
O(252)	390(2)	-930(4)	3400(2)	41(1)
O(321)	2569(2)	3036(3)	-947(2)	33(1)
O(322)	2507(2)	4088(3)	74(2)	33(1)
O(351)	1367(2)	621(3)	-2528(2)	39(1)
O(352)	1211(2)	-1159(3)	-1932(2)	28(1)
O(421)	2499(1)	-2614(3)	180(2)	24(1)
O(422)	3189(2)	-3916(3)	-194(2)	26(1)
O(451)	4510(2)	-910(4)	-1416(2)	37(1)
O(452)	4265(1)	217(3)	-495(2)	26(1)
N(1)	2805(2)	-1846(3)	2113(2)	16(1)
N(2)	1991(2)	562(3)	1810(2)	17(1)
N(3)	2682(2)	1363(3)	693(2)	18(1)
N(4)	3499(2)	-1124(3)	1011(2)	16(1)
C(1)	2565(2)	-1253(4)	2704(2)	18(1)
C(2)	2477(2)	226(4)	2589(2)	19(1)
C(3)	2072(2)	1966(4)	1592(2)	20(1)
C(4)	2690(2)	2151(4)	1363(2)	20(1)
C(5)	3351(2)	1276(4)	629(2)	20(1)
C(6)	3782(2)	254(4)	1170(2)	19(1)
C(7)	3802(2)	-2009(4)	1689(2)	20(1)
C(8)	3534(2)	-1742(4)	2343(2)	18(1)
C(11)	2578(2)	-3213(4)	1916(2)	16(1)
C(12)	2825(2)	-4155(4)	2603(2)	19(1)
C(13)	1822(2)	-3298(4)	1521(2)	19(1)
C(14)	1635(2)	-4554(4)	1048(2)	21(1)
C(15)	911(2)	-4726(4)	626(2)	24(1)
C(21)	1279(2)	250(4)	1744(2)	19(1)
C(22)	895(2)	44(4)	882(2)	21(1)
C(23)	978(2)	1256(4)	2151(2)	24(1)
C(24)	486(2)	608(5)	2482(2)	27(1)
C(25)	823(2)	-267(4)	3160(2)	25(1)
C(31)	2188(2)	1815(4)	-41(2)	18(1)
C(32)	2434(2)	3048(4)	-359(2)	20(1)
C(33)	2021(2)	707(4)	-632(2)	20(1)
C(34)	1347(2)	930(4)	-1258(2)	24(1)
C(35)	1302(2)	145(4)	-1966(2)	26(1)
C(41)	3548(2)	-1728(4)	275(2)	18(1)
C(42)	3034(2)	-2864(4)	61(2)	20(1)
C(43)	4266(2)	-2101(4)	365(2)	21(1)
C(44)	4389(2)	-2141(4)	-401(2)	25(1)
C(45)	4379(2)	-825(5)	-768(2)	25(1)
O(1S)	396(4)	-2224(9)	1758(5)	61(2)
O(2S)	1167(1)	-2232(3)	-622(2)	25(1)
O(3S)	3483(2)	-7027(3)	3506(2)	31(1)
O(4S)	4331(2)	1148(4)	3095(2)	48(1)
O(5A)	4417(5)	-5552(9)	206(6)	39(2)
O(5B)	4292(7)	-5472(14)	-362(8)	40(4)
O(5C)	4262(10)	-5540(20)	-150(14)	41(5)
O(6S)	4551(2)	1221(4)	-2185(2)	39(1)
O(7A)	4507(4)	931(8)	-2851(4)	47(2)
O(7B)	4545(4)	1863(8)	-3281(5)	54(2)
O(8A)	4518(5)	403(10)	-3600(6)	73(3)
O(8B)	4448(4)	-240(8)	-3095(5)	50(2)

***Table A.4.16.3** - Bond lengths [Å] and angles [°] for C28 H67 N4 O23.50.*

O(121)-C(12)	1.336(5)	C(41)-C(42)	1.555(5)	C(23)-C(21)-C(22)	115.6(3)
O(122)-C(12)	1.201(5)	C(43)-C(44)	1.527(6)	O(222)-C(22)-O(221)	127.7(4)
O(151)-C(15)	1.327(5)	C(44)-C(45)	1.502(6)	O(222)-C(22)-C(21)	117.6(3)
O(152)-C(15)	1.221(5)	O(5A)-O(5C)	0.63(2)	O(221)-C(22)-C(21)	114.7(3)
O(221)-C(22)	1.266(5)	O(5A)-O(5B)	0.999(18)	C(24)-C(23)-C(21)	111.4(3)
O(222)-C(22)	1.241(5)	O(6S)-O(7A)	1.243(8)	C(25)-C(24)-C(23)	112.7(3)
O(251)-C(25)	1.205(5)	O(7A)-O(7B)	1.261(11)	O(251)-C(25)-O(252)	122.9(4)
O(252)-C(25)	1.337(5)	O(7A)-O(8B)	1.268(11)	O(251)-C(25)-C(24)	124.6(4)
O(321)-C(32)	1.216(5)	O(7A)-O(8A)	1.496(13)	O(252)-C(25)-C(24)	112.5(4)
O(322)-C(32)	1.307(5)	O(7B)-O(8A)	1.595(13)	N(3)-C(31)-C(33)	110.5(3)
O(351)-C(35)	1.198(5)	O(8A)-O(8B)	1.193(12)	N(3)-C(31)-C(32)	111.7(3)
O(352)-C(35)	1.348(5)			C(33)-C(31)-C(32)	110.7(3)
O(421)-C(42)	1.262(5)	C(8)-N(1)-C(11)	111.6(3)	O(321)-C(32)-O(322)	122.9(4)
O(422)-C(42)	1.258(5)	C(8)-N(1)-C(1)	110.4(3)	O(321)-C(32)-C(31)	122.9(4)
O(451)-C(45)	1.324(5)	C(11)-N(1)-C(1)	113.4(3)	O(322)-C(32)-C(31)	114.2(3)
O(452)-C(45)	1.236(5)	C(2)-N(2)-C(3)	111.5(3)	C(31)-C(33)-C(34)	111.6(3)
N(1)-C(8)	1.479(4)	C(2)-N(2)-C(21)	112.5(3)	C(35)-C(34)-C(33)	110.5(3)
N(1)-C(11)	1.480(5)	C(3)-N(2)-C(21)	112.1(3)	O(351)-C(35)-O(352)	120.0(4)
N(1)-C(1)	1.486(5)	C(4)-N(3)-C(5)	111.1(3)	O(351)-C(35)-C(34)	123.2(4)
N(2)-C(2)	1.511(5)	C(4)-N(3)-C(31)	114.0(3)	O(352)-C(35)-C(34)	116.7(4)
N(2)-C(3)	1.514(5)	C(5)-N(3)-C(31)	110.9(3)	N(4)-C(41)-C(43)	111.5(3)
N(2)-C(21)	1.521(5)	C(7)-N(4)-C(6)	110.9(3)	N(4)-C(41)-C(42)	105.9(3)
N(3)-C(4)	1.476(5)	C(7)-N(4)-C(41)	111.3(3)	C(43)-C(41)-C(42)	116.1(3)
N(3)-C(5)	1.478(5)	C(6)-N(4)-C(41)	113.8(3)	O(422)-C(42)-O(421)	127.2(4)
N(3)-C(31)	1.492(5)	N(1)-C(1)-C(2)	110.8(3)	O(422)-C(42)-C(41)	118.5(3)
N(4)-C(7)	1.508(5)	N(2)-C(2)-C(1)	111.8(3)	O(421)-C(42)-C(41)	114.2(3)
N(4)-C(6)	1.520(5)	N(2)-C(3)-C(4)	112.2(3)	C(44)-C(43)-C(41)	112.4(3)
N(4)-C(41)	1.531(5)	N(3)-C(4)-C(3)	113.4(3)	C(45)-C(44)-C(43)	114.6(3)
C(1)-C(2)	1.526(5)	N(3)-C(5)-C(6)	112.2(3)	O(452)-C(45)-O(451)	124.0(4)
C(3)-C(4)	1.527(5)	N(4)-C(6)-C(5)	112.9(3)	O(452)-C(45)-C(44)	123.8(4)
C(5)-C(6)	1.525(5)	N(4)-C(7)-C(8)	112.6(3)	O(451)-C(45)-C(44)	112.2(4)
C(7)-C(8)	1.528(5)	N(1)-C(8)-C(7)	113.3(3)	O(5C)-O(5A)-O(5B)	15(2)
C(11)-C(13)	1.541(5)	N(1)-C(11)-C(13)	112.2(3)	O(6S)-O(7A)-O(7B)	116.7(8)
C(11)-C(12)	1.541(5)	N(1)-C(11)-C(12)	112.9(3)	O(6S)-O(7A)-O(8B)	123.0(8)
C(13)-C(14)	1.528(5)	C(13)-C(11)-C(12)	112.1(3)	O(7B)-O(7A)-O(8B)	120.2(8)
C(14)-C(15)	1.496(5)	O(122)-C(12)-O(121)	123.5(4)	O(6S)-O(7A)-O(8A)	171.3(8)
C(21)-C(23)	1.537(5)	O(122)-C(12)-C(11)	125.5(4)	O(7B)-O(7A)-O(8A)	70.1(7)
C(21)-C(22)	1.549(5)	O(121)-C(12)-C(11)	110.9(3)	O(8B)-O(7A)-O(8A)	50.3(6)
C(23)-C(24)	1.533(6)	C(14)-C(13)-C(11)	110.7(3)	O(7A)-O(7B)-O(8A)	61.9(6)
C(24)-C(25)	1.513(6)	C(15)-C(14)-C(13)	115.2(3)	O(8B)-O(8A)-O(7A)	54.9(7)
C(31)-C(33)	1.530(5)	O(152)-C(15)-O(151)	123.3(4)	O(8B)-O(8A)-O(7B)	102.8(9)
C(31)-C(32)	1.553(5)	O(152)-C(15)-C(14)	124.5(4)	O(7A)-O(8A)-O(7B)	48.0(5)
C(33)-C(34)	1.539(5)	O(151)-C(15)-C(14)	112.1(3)	O(8A)-O(8B)-O(7A)	74.8(8)
C(34)-C(35)	1.512(6)	N(2)-C(21)-C(23)	113.2(3)		
C(41)-C(43)	1.537(5)	N(2)-C(21)-C(22)	106.6(3)		

***Table A.4.16.4** - Anisotropic displacement parameters ($Å^2 x\ 10^3$) for C28 H67 N4 O23.50. The anisotropic displacement factor exponent takes the form: $-2\pi^2[h^2 a^{*2} U^{11} + ... + 2 h k a^* b^* U^{12}]$*

	U^{11}	U^{22}	U^{33}	U^{23}	U^{13}	U^{12}
O(121)	38(2)	15(1)	26(2)	-1(1)	5(1)	6(1)
O(122)	34(2)	20(2)	22(1)	3(1)	9(1)	5(1)
O(151)	21(2)	22(2)	56(2)	-16(2)	-5(1)	-2(1)
O(152)	21(1)	21(2)	43(2)	-6(1)	-1(1)	0(1)
O(221)	20(2)	82(3)	21(2)	-11(2)	0(1)	13(2)
O(222)	25(1)	25(2)	22(1)	-6(1)	8(1)	-1(1)
O(251)	28(2)	58(2)	37(2)	17(2)	4(1)	-6(2)
O(252)	27(2)	53(2)	44(2)	19(2)	15(2)	3(2)
O(321)	56(2)	20(2)	31(2)	5(1)	25(2)	2(1)
O(322)	57(2)	14(1)	37(2)	-3(1)	29(2)	-8(1)
O(351)	66(2)	32(2)	25(2)	5(1)	23(2)	7(2)
O(352)	34(2)	23(2)	27(2)	-3(1)	9(1)	-1(1)
O(421)	23(1)	21(2)	27(2)	-1(1)	7(1)	-3(1)
O(422)	31(2)	17(1)	32(2)	-3(1)	13(1)	-3(1)
O(451)	36(2)	51(2)	28(2)	-2(2)	17(1)	-11(2)
O(452)	25(2)	25(2)	27(2)	1(1)	6(1)	-3(1)
N(1)	15(1)	14(2)	18(2)	-2(1)	3(1)	-3(1)
N(2)	21(2)	13(2)	18(2)	0(1)	5(1)	0(1)
N(3)	24(2)	13(2)	19(2)	2(1)	9(1)	1(1)
N(4)	17(2)	12(2)	19(2)	-1(1)	5(1)	-1(1)
C(1)	21(2)	15(2)	17(2)	2(2)	5(1)	2(2)
C(2)	20(2)	17(2)	16(2)	-1(2)	1(1)	-3(2)
C(3)	30(2)	11(2)	21(2)	-1(2)	11(2)	1(2)
C(4)	28(2)	10(2)	22(2)	-1(2)	9(2)	-3(2)
C(5)	24(2)	13(2)	27(2)	3(2)	11(2)	2(2)
C(6)	19(2)	12(2)	24(2)	0(2)	5(2)	-2(1)
C(7)	17(2)	17(2)	21(2)	3(2)	2(1)	0(2)
C(8)	16(2)	16(2)	19(2)	3(2)	1(1)	-4(1)
C(11)	19(2)	13(2)	17(2)	-2(1)	7(1)	-2(1)
C(12)	14(2)	18(2)	24(2)	1(2)	6(1)	-1(1)
C(13)	17(2)	17(2)	21(2)	0(2)	4(1)	-1(1)
C(14)	17(2)	19(2)	23(2)	-4(2)	3(2)	0(2)
C(15)	21(2)	23(2)	25(2)	-2(2)	4(2)	-4(2)
C(21)	21(2)	18(2)	18(2)	-1(2)	9(1)	1(2)
C(22)	23(2)	20(2)	19(2)	-3(2)	5(2)	0(2)
C(23)	30(2)	22(2)	22(2)	-3(2)	11(2)	5(2)
C(24)	25(2)	34(2)	23(2)	-3(2)	9(2)	5(2)
C(25)	26(2)	30(2)	22(2)	-3(2)	12(2)	-2(2)
C(31)	24(2)	14(2)	18(2)	2(2)	8(2)	2(2)
C(32)	24(2)	14(2)	23(2)	3(2)	11(2)	1(2)
C(33)	30(2)	13(2)	16(2)	1(2)	7(2)	1(2)
C(34)	28(2)	21(2)	23(2)	-4(2)	9(2)	3(2)
C(35)	25(2)	29(2)	23(2)	-1(2)	7(2)	5(2)
C(41)	19(2)	16(2)	18(2)	0(2)	6(1)	-1(2)
C(42)	20(2)	18(2)	18(2)	2(2)	3(1)	-1(2)
C(43)	20(2)	18(2)	25(2)	2(2)	7(2)	1(2)
C(44)	22(2)	25(2)	30(2)	-7(2)	11(2)	-1(2)
C(45)	15(2)	38(3)	23(2)	-3(2)	6(2)	-6(2)

***Table A.4.16.5** - Hydrogen coordinates (x 10^4) and isotropic displacement parameters ($Å^2$x 10^3) for C28 H67 N4 O23.50.*

	x	y	z	U(eq)
H(121)	3066	-5851	2756	50
H(151)	359	-5997	124	50
H(221)	105	145	213	50
H(252)	596	-1465	3742	50
H(322)	2657	4708	-119	50
H(451)	4493	-160	-1609	50
H(2)	2095	30	1459	27(12)
H(4)	3050	-1061	946	18(11)
H(1A)	2887	-1434	3218	4(9)
H(1B)	2136	-1656	2676	22(11)
H(2A)	2317	597	2989	14(10)
H(2B)	2911	631	2645	4(9)
H(3A)	2102	2548	2029	16(10)
H(3B)	1677	2228	1159	21(11)
H(4A)	2730	3090	1249	17(11)
H(4B)	3085	1910	1802	22(11)
H(5A)	3569	2144	746	16(10)
H(5B)	3311	1047	97	12(10)
H(6A)	4229	263	1123	14(10)
H(6B)	3829	495	1703	11(10)
H(7A)	4288	-1885	1876	17(11)
H(7B)	3711	-2934	1524	18(11)
H(8A)	3737	-2374	2762	6(9)
H(8B)	3670	-849	2545	16(10)
H(11)	2782	-3518	1533	17(10)
H(13A)	1600	-3285	1912	18(11)
H(13B)	1667	-2527	1183	31(13)
H(14A)	1873	-4567	672	21(11)
H(14B)	1793	-5314	1393	12(10)
H(21)	1285	-613	2003	27(12)
H(23A)	1337	1679	2569	32(13)
H(23B)	747	1947	1783	12(10)
H(24A)	235	1300	2643	49(16)
H(24B)	165	80	2078	27(12)
H(31)	1773	2057	62	19(11)
H(33A)	2012	-137	-371	19(11)
H(33B)	2371	652	-870	13(10)
H(34A)	987	662	-1065	25(12)
H(34B)	1291	1874	-1389	28(12)
H(41)	3401	-1050	-136	11(10)
H(43A)	4570	-1456	704	15(10)
H(43B)	4366	-2973	612	14(10)
H(44A)	4825	-2556	-322	50(16)
H(44B)	4047	-2705	-757	32(13)

***Table A.4.17.2** - Atomic coordinates (x 10^4) and equivalent isotropic displacement parameters ($Å^2$x 10^3) for (C29 H54.50 N4 O20.25), the RRRS-isomer. U(eq) is defined as one third of the trace of the orthogonalized U^{ij} tensor.*

	x	y	z	U(eq)
O(12B)	-6375(2)	6280(4)	-167(2)	61(1)
O(12A)	-5094(3)	6667(5)	-274(2)	89(2)
O(22B)	-8082(2)	8106(3)	-343(2)	42(1)
O(22A)	-8049(2)	7189(3)	621(1)	51(1)
O(25A)	-7186(6)	3367(10)	1070(4)	46(2)
O(251)	-7026(8)	3896(13)	950(6)	51(3)
O(252)	-7376(10)	2862(16)	1081(7)	54(4)
O(25B)	-7731(2)	3070(3)	19(2)	60(1)
O(32B)	-10776(2)	9386(3)	-2082(1)	40(1)
O(32A)	-10789(2)	9234(3)	-1026(1)	44(1)
O(35B)	-9912(2)	12080(3)	-9(1)	42(1)
O(35A)	-10046(2)	12352(3)	-1072(2)	51(1)
O(42B)	-6475(2)	8579(4)	-1067(2)	56(1)
O(42A)	-6961(8)	10577(8)	-1045(4)	82(4)
O(421)	-6395(7)	10521(10)	-1181(5)	72(3)
O(45B)	-7729(2)	13333(3)	-2679(1)	46(1)
O(45A)	-8401(2)	11501(3)	-2849(1)	41(1)
N(1)	-6963(2)	5844(3)	-1445(2)	35(1)
N(2)	-8541(2)	5938(3)	-1015(1)	28(1)
N(3)	-9193(2)	8177(3)	-1783(1)	28(1)
N(4)	-7678(2)	8200(3)	-2186(1)	29(1)
C(1)	-7367(3)	4694(4)	-1245(2)	35(1)
C(2)	-8294(3)	4820(4)	-1324(2)	32(1)
C(3)	-9428(2)	6164(4)	-1249(2)	31(1)
C(4)	-9609(2)	6922(4)	-1870(2)	29(1)
C(5)	-9166(3)	8747(4)	-2435(2)	29(1)
C(6)	-8453(2)	8216(4)	-2688(2)	30(1)
C(7)	-7074(2)	7359(4)	-2380(2)	33(1)
C(8)	-7194(3)	6017(4)	-2177(2)	35(1)
C(11)	-6035(3)	5842(5)	-1188(2)	49(1)
C(12)	-5813(4)	6312(6)	-483(3)	64(2)
C(13)	-5665(3)	4557(6)	-1268(2)	57(2)
C(14A)	-4702(9)	5023(15)	-1266(7)	46(2)
C(15A)	-4346(8)	3838(13)	-1469(6)	41(2)
O(15A)	-4580(6)	3454(10)	-2050(4)	48(3)
O(15B)	-3810(6)	3175(9)	-1061(4)	42(2)
C(14B)	-4758(5)	4413(8)	-1234(4)	46(2)
C(15B)	-4490(5)	3131(8)	-1342(3)	41(2)
O(151)	-4711(4)	2582(7)	-1874(3)	74(2)
O(152)	-4035(4)	2535(6)	-857(3)	55(2)
C(21)	-8295(3)	5872(4)	-300(2)	36(1)
C(22)	-8141(3)	7186(4)	-19(2)	36(1)
C(23)	-8862(3)	5074(4)	24(2)	40(1)
C(24)	-8415(3)	4432(5)	643(2)	47(1)
C(25)	-7771(3)	3574(5)	525(2)	48(1)
C(31)	-9507(3)	9016(4)	-1309(2)	30(1)
C(32)	-10428(3)	9227(4)	-1495(2)	34(1)
C(33)	-9009(3)	10218(4)	-1178(2)	41(1)
C(34)	-9066(3)	10827(4)	-539(2)	34(1)
C(35)	-9725(3)	11796(4)	-582(2)	35(1)
C(41)	-7354(3)	9475(4)	-2022(2)	36(1)
C(42)	-6779(4)	9451(5)	-1354(2)	55(2)
C(43)	-6920(3)	10092(4)	-2518(2)	40(1)
C(44)	-6919(3)	11526(5)	-2488(2)	50(1)
C(45)	-7759(3)	12086(4)	-2690(2)	39(1)
O(1SA)	-2171(4)	697(6)	-1205(3)	60
O(1SB)	-2411(11)	389(17)	-1043(8)	60

O(2S)	-4106(5)	-2256(7)	-832(4)	62(2)
C(1S)	-4388(9)	-619(15)	-2104(7)	85(4)
O(3S)	-4198(5)	272(7)	-1991(3)	57(2)
C(2S)	-4986(6)	-1615(9)	-1961(5)	47(2)
O(4SA)	-4994(7)	-637(11)	249(5)	52(3)
O(4SB)	-4411(5)	-921(8)	17(4)	48(2)
O(4SC)	-5112(8)	-1260(13)	577(6)	57(3)
O(5SA)	-3429(7)	-349(11)	-258(5)	52(3)
O(5SB)	-3266(6)	326(10)	-409(4)	59(2)
O(5SC)	-3450(8)	-810(13)	-957(6)	58(3)
O(6S)	-5073(9)	1182(14)	-1873(7)	59(4)

***Table A.4.17.3** - Bond lengths [Å] and angles [°] for (C29 H54.50 N4 O20.25), the RRRS-isomer.*

O(12B)-C(12)	1.267(7)	C(15B)-O(152)	1.302(9)	C(4)-N(3)-C(31)	113.0(3)
O(12A)-C(12)	1.245(7)	C(21)-C(22)	1.529(6)	C(5)-N(3)-C(31)	116.3(3)
O(22B)-C(22)	1.218(5)	C(21)-C(23)	1.544(6)	C(4)-N(3)-H(3)	105.2
O(22A)-C(22)	1.327(5)	C(23)-C(24)	1.523(6)	C(5)-N(3)-H(3)	105.2
O(25A)-O(252)	0.632(16)	C(24)-C(25)	1.478(7)	C(31)-N(3)-H(3)	105.2
O(25A)-O(251)	0.698(13)	C(31)-C(32)	1.518(6)	C(7)-N(4)-C(6)	110.5(3)
O(25A)-C(25)	1.355(9)	C(31)-C(33)	1.526(6)	C(7)-N(4)-C(41)	113.0(3)
O(251)-O(252)	1.31(2)	C(33)-C(34)	1.524(5)	C(6)-N(4)-C(41)	111.9(3)
O(251)-C(25)	1.409(13)	C(34)-C(35)	1.501(6)	N(1)-C(1)-C(2)	113.7(3)
O(252)-C(25)	1.435(16)	C(41)-C(42)	1.523(6)	N(1)-C(1)-H(1A)	108.8
O(25B)-C(25)	1.213(5)	C(41)-C(43)	1.548(6)	C(2)-C(1)-H(1A)	108.8
O(32B)-C(32)	1.261(4)	C(43)-C(44)	1.539(6)	N(1)-C(1)-H(1B)	108.8
O(32A)-C(32)	1.270(5)	C(44)-C(45)	1.499(7)	C(2)-C(1)-H(1B)	108.8
O(35B)-C(35)	1.353(5)	O(1SA)-O(1SB)	0.669(18)	H(1A)-C(1)-H(1B)	107.7
O(35A)-C(35)	1.213(5)	C(1S)-O(3S)	1.019(15)	N(2)-C(2)-C(1)	113.7(3)
O(42B)-C(42)	1.168(6)	C(1S)-C(2S)	1.537(18)	N(2)-C(2)-H(2A)	108.8
O(42A)-O(421)	1.049(13)	O(4SA)-O(4SC)	1.012(14)	C(1)-C(2)-H(2A)	108.8
O(42A)-C(42)	1.437(11)	O(4SA)-O(4SB)	1.222(12)	N(2)-C(2)-H(2B)	108.8
O(421)-C(42)	1.326(10)	O(4SA)-O(4SA)#1	1.72(2)	C(1)-C(2)-H(2B)	108.8
O(45B)-C(45)	1.338(5)	O(5SA)-O(5SB)	0.859(12)	H(2A)-C(2)-H(2B)	107.7
O(45A)-C(45)	1.224(5)	O(5SA)-O(5SC)	1.552(16)	N(2)-C(3)-C(4)	111.9(3)
N(1)-C(1)	1.510(5)	O(5SB)-O(5SC)	1.662(16)	N(2)-C(3)-H(3A)	109.2
N(1)-C(8)	1.522(5)			C(4)-C(3)-H(3A)	109.2
N(1)-C(11)	1.525(5)	C(22)-O(22A)-H(22A)	109.5	N(2)-C(3)-H(3B)	109.2
N(2)-C(2)	1.467(5)	O(252)-O(25A)-O(251)	161(3)	C(4)-C(3)-H(3B)	109.2
N(2)-C(3)	1.475(5)	O(252)-O(25A)-C(25)	84.1(19)	H(3A)-C(3)-H(3B)	107.9
N(2)-C(21)	1.479(5)	O(251)-O(25A)-C(25)	79.7(15)	N(3)-C(4)-C(3)	112.0(3)
N(3)-C(4)	1.507(5)	O(25A)-O(251)-O(252)	8.8(14)	N(3)-C(4)-H(4A)	109.2
N(3)-C(5)	1.519(4)	O(25A)-O(251)-C(25)	71.1(14)	C(3)-C(4)-H(4A)	109.2
N(3)-C(31)	1.524(5)	O(252)-O(251)-C(25)	63.6(9)	N(3)-C(4)-H(4B)	109.2
N(4)-C(7)	1.477(5)	O(25A)-O(252)-O(251)	9.8(15)	C(3)-C(4)-H(4B)	109.2
N(4)-C(6)	1.482(5)	O(25A)-O(252)-C(25)	69.9(18)	H(4A)-C(4)-H(4B)	107.9
N(4)-C(41)	1.483(5)	O(251)-O(252)-C(25)	61.5(9)	N(3)-C(5)-C(6)	110.6(3)
C(1)-C(2)	1.526(6)	O(421)-O(42A)-C(42)	62.2(9)	N(3)-C(5)-H(5A)	109.5
C(3)-C(4)	1.517(5)	O(42A)-O(421)-C(42)	73.4(8)	C(6)-C(5)-H(5A)	109.5
C(5)-C(6)	1.520(5)	C(45)-O(45B)-H(45A)	109.5	N(3)-C(5)-H(5B)	109.5
C(7)-C(8)	1.527(6)	C(1)-N(1)-C(8)	110.9(3)	C(6)-C(5)-H(5B)	109.5
C(11)-C(13)	1.535(7)	C(1)-N(1)-C(11)	112.4(3)	H(5A)-C(5)-H(5B)	108.1
C(11)-C(12)	1.539(7)	C(8)-N(1)-C(11)	111.9(3)	N(4)-C(6)-C(5)	112.4(3)
C(13)-C(14B)	1.509(9)	C(1)-N(1)-H(1)	107.1	N(4)-C(6)-H(6A)	109.1
C(13)-C(14A)	1.683(15)	C(8)-N(1)-H(1)	107.1	C(5)-C(6)-H(6A)	109.1
C(14A)-C(15A)	1.51(2)	C(11)-N(1)-H(1)	107.1	N(4)-C(6)-H(6B)	109.1
C(15A)-O(15A)	1.273(15)	C(2)-N(2)-C(3)	110.2(3)	C(5)-C(6)-H(6B)	109.1
C(15A)-O(15B)	1.307(16)	C(2)-N(2)-C(21)	112.0(3)	H(6A)-C(6)-H(6B)	107.9
C(14B)-C(15B)	1.479(11)	C(3)-N(2)-C(21)	112.5(3)	N(4)-C(7)-C(8)	110.9(3)
C(15B)-O(151)	1.251(9)	C(4)-N(3)-C(5)	110.7(3)	N(4)-C(7)-H(7A)	109.5

C(8)-C(7)-H(7A)	109.5	O(152)-C(15B)-C(14B)	118.6(7)	H(33A)-C(33)-H(33B)	107.8
N(4)-C(7)-H(7B)	109.5	N(2)-C(21)-C(22)	109.8(3)	C(35)-C(34)-C(33)	115.6(4)
C(8)-C(7)-H(7B)	109.5	N(2)-C(21)-C(23)	114.9(3)	C(35)-C(34)-H(34A)	108.4
H(7A)-C(7)-H(7B)	108.0	C(22)-C(21)-C(23)	114.0(4)	C(33)-C(34)-H(34A)	108.4
N(1)-C(8)-C(7)	112.4(3)	N(2)-C(21)-H(21A)	105.8	C(35)-C(34)-H(34B)	108.4
N(1)-C(8)-H(8A)	109.1	C(22)-C(21)-H(21A)	105.8	C(33)-C(34)-H(34B)	108.4
C(7)-C(8)-H(8A)	109.1	C(23)-C(21)-H(21A)	105.8	H(34A)-C(34)-H(34B)	107.5
N(1)-C(8)-H(8B)	109.1	O(22B)-C(22)-O(22A)	124.5(4)	O(35A)-C(35)-O(35B)	120.6(4)
C(7)-C(8)-H(8B)	109.1	O(22B)-C(22)-C(21)	123.7(4)	O(35A)-C(35)-C(34)	124.9(4)
H(8A)-C(8)-H(8B)	107.8	O(22A)-C(22)-C(21)	111.7(4)	O(35B)-C(35)-C(34)	114.3(3)
N(1)-C(11)-C(13)	111.3(4)	C(24)-C(23)-C(21)	113.5(4)	N(4)-C(41)-C(42)	109.0(3)
N(1)-C(11)-C(12)	110.7(4)	C(24)-C(23)-H(23A)	108.9	N(4)-C(41)-C(43)	115.9(3)
C(13)-C(11)-C(12)	112.6(4)	C(21)-C(23)-H(23A)	108.9	C(42)-C(41)-C(43)	110.0(4)
N(1)-C(11)-H(11A)	107.3	C(24)-C(23)-H(23B)	108.9	N(4)-C(41)-H(41A)	107.2
C(13)-C(11)-H(11A)	107.3	C(21)-C(23)-H(23B)	108.9	C(42)-C(41)-H(41A)	107.2
C(12)-C(11)-H(11A)	107.3	H(23A)-C(23)-H(23B)	107.7	C(43)-C(41)-H(41A)	107.2
O(12A)-C(12)-O(12B)	126.1(5)	C(25)-C(24)-C(23)	111.9(4)	O(42B)-C(42)-O(421)	114.9(6)
O(12A)-C(12)-C(11)	116.8(6)	C(25)-C(24)-H(24A)	109.2	O(42B)-C(42)-O(42A)	123.2(5)
O(12B)-C(12)-C(11)	117.0(4)	C(23)-C(24)-H(24A)	109.2	O(421)-C(42)-O(42A)	44.4(5)
C(14B)-C(13)-C(11)	120.7(5)	C(25)-C(24)-H(24B)	109.2	O(42B)-C(42)-C(41)	127.4(4)
C(14B)-C(13)-C(14A)	23.3(5)	C(23)-C(24)-H(24B)	109.2	O(421)-C(42)-C(41)	114.2(6)
C(11)-C(13)-C(14A)	98.1(6)	H(24A)-C(24)-H(24B)	107.9	O(42A)-C(42)-C(41)	104.7(5)
C(14B)-C(13)-H(13A)	104.4	O(25B)-C(25)-O(25A)	120.5(6)	C(44)-C(43)-C(41)	113.4(4)
C(11)-C(13)-H(13A)	112.1	O(25B)-C(25)-O(251)	117.3(7)	C(44)-C(43)-H(43A)	108.9
C(14A)-C(13)-H(13A)	112.1	O(25A)-C(25)-O(251)	29.2(5)	C(41)-C(43)-H(43A)	108.9
C(14B)-C(13)-H(13B)	96.2	O(25B)-C(25)-O(252)	112.4(8)	C(44)-C(43)-H(43B)	108.9
C(11)-C(13)-H(13B)	112.1	O(25A)-C(25)-O(252)	26.0(7)	C(41)-C(43)-H(43B)	108.9
C(14A)-C(13)-H(13B)	112.2	O(251)-C(25)-O(252)	54.9(8)	H(43A)-C(43)-H(43B)	107.7
H(13A)-C(13)-H(13B)	109.8	O(25B)-C(25)-C(24)	127.6(4)	C(45)-C(44)-C(43)	113.3(4)
C(15A)-C(14A)-C(13)	100.7(10)	O(25A)-C(25)-C(24)	111.9(5)	C(45)-C(44)-H(44A)	108.9
C(15A)-C(14A)-H(14A)	111.6	O(251)-C(25)-C(24)	108.2(6)	C(43)-C(44)-H(44A)	108.9
C(13)-C(14A)-H(14A)	111.6	O(252)-C(25)-C(24)	114.3(7)	C(45)-C(44)-H(44B)	108.9
C(15A)-C(14A)-H(14B)	111.6	C(32)-C(31)-C(33)	113.7(4)	C(43)-C(44)-H(44B)	108.9
C(13)-C(14A)-H(14B)	111.6	C(32)-C(31)-N(3)	113.2(3)	H(44A)-C(44)-H(44B)	107.7
H(14A)-C(14A)-H(14B)	109.4	C(33)-C(31)-N(3)	111.4(3)	O(45A)-C(45)-O(45B)	122.9(5)
O(15A)-C(15A)-O(15B)	118.7(12)	C(32)-C(31)-H(31A)	105.9	O(45A)-C(45)-C(44)	125.6(4)
O(15A)-C(15A)-C(14A)	119.4(12)	C(33)-C(31)-H(31A)	105.9	O(45B)-C(45)-C(44)	111.5(4)
O(15B)-C(15A)-C(14A)	121.9(12)	N(3)-C(31)-H(31A)	105.9	O(3S)-C(1S)-C(2S)	142.1(15)
C(15B)-C(14B)-C(13)	115.0(7)	O(32B)-C(32)-O(32A)	125.0(4)	O4SC-O4SA-O4SB	113.8(13)
C(15B)-C(14B)-H(14C)	108.5	O(32B)-C(32)-C(31)	119.7(4)	O4SC-O4SA-O4SA#1	164.6(16)
C(13)-C(14B)-H(14C)	108.5	O(32A)-C(32)-C(31)	115.3(3)	O(4SB)-O(4SA)-O4SA#1	81.6(9)
C(15B)-C(14B)-H(14D)	108.5	C(31)-C(33)-C(34)	112.6(3)	O(5SB)-O(5SA)-O(5SC)	81.7(12)
C(13)-C(14B)-H(14D)	108.5	C(31)-C(33)-H(33A)	109.1	O(5SA)-O(5SB)-O(5SC)	67.5(11)
H(14C)-C(14B)-H(14D)	107.5	C(34)-C(33)-H(33A)	109.1	O(5SA)-O(5SC)-O(5SB)	30.8(5)
O(151)-C(15B)-O(152)	118.9(7)	C(31)-C(33)-H(33B)	109.1		
O(151)-C(15B)-C(14B)	122.5(7)	C(34)-C(33)-H(33B)	109.1		

***Table A.4.17.4** - Anisotropic displacement parameters ($Å^2 x\ 10^3$) for (C29 H54.50 N4 O20.25), the RRRS-isomer. The anisotropic displacement factor exponent takes the form: $-2\pi^2[h^2 a^{*2} U^{11} + ... + 2 h k a^* b^* U^{12}]$*

	U^{11}	U^{22}	U^{33}	U^{23}	U^{13}	U^{12}
O(12B)	56(2)	79(3)	40(2)	-23(2)	-12(2)	17(2)
O(12A)	59(3)	106(4)	79(3)	-37(3)	-35(2)	3(2)
O(22B)	45(2)	35(2)	45(2)	-6(1)	8(1)	-5(2)
O(22A)	70(2)	48(2)	30(2)	-12(1)	1(2)	3(2)
O(25B)	88(3)	38(2)	48(2)	-7(2)	3(2)	9(2)
O(32B)	55(2)	37(2)	27(1)	4(1)	8(1)	15(2)
O(32A)	54(2)	51(2)	30(2)	3(1)	16(1)	20(2)
O(35B)	50(2)	46(2)	35(2)	3(1)	18(1)	16(2)
O(35A)	67(2)	48(2)	37(2)	13(2)	7(2)	13(2)
O(42B)	68(2)	52(2)	40(2)	-8(2)	-7(2)	2(2)
O(42A)	156(11)	28(4)	36(4)	-8(3)	-35(6)	-7(6)
O(421)	100(8)	50(5)	50(5)	2(4)	-19(5)	-38(6)
O(45B)	54(2)	32(2)	44(2)	1(1)	-3(2)	-17(2)
O(45A)	42(2)	38(2)	41(2)	-1(1)	2(1)	-14(2)
N(1)	32(2)	40(2)	27(2)	-9(2)	-2(1)	2(2)
N(2)	33(2)	29(2)	23(2)	-5(1)	5(1)	2(2)
N(3)	35(2)	25(2)	26(2)	-1(1)	9(1)	-1(1)
N(4)	34(2)	30(2)	23(2)	-7(1)	4(1)	-5(2)
C(1)	40(2)	31(2)	29(2)	-5(2)	0(2)	8(2)
C(2)	37(2)	27(2)	29(2)	-3(2)	2(2)	1(2)
C(3)	34(2)	25(2)	33(2)	1(2)	11(2)	2(2)
C(4)	32(2)	25(2)	29(2)	0(2)	6(2)	1(2)
C(5)	43(2)	24(2)	21(2)	-1(2)	8(2)	2(2)
C(6)	35(2)	33(2)	23(2)	-5(2)	10(2)	-6(2)
C(7)	28(2)	40(2)	30(2)	-8(2)	5(2)	-6(2)
C(8)	36(2)	40(2)	24(2)	-8(2)	0(2)	0(2)
C(11)	33(3)	64(3)	42(2)	-13(2)	-8(2)	0(2)
C(12)	51(3)	69(4)	54(3)	-23(3)	-24(3)	8(3)
C(13)	32(3)	93(4)	40(3)	-10(3)	-4(2)	17(3)
C(21)	50(3)	30(2)	27(2)	-4(2)	9(2)	-1(2)
C(22)	34(2)	39(3)	30(2)	-9(2)	1(2)	1(2)
C(23)	54(3)	39(3)	27(2)	3(2)	9(2)	-5(2)
C(24)	62(3)	44(3)	35(2)	-1(2)	7(2)	-1(3)
C(25)	52(3)	57(3)	32(2)	5(2)	2(2)	1(3)
C(31)	45(2)	25(2)	23(2)	-2(2)	11(2)	0(2)
C(32)	51(3)	25(2)	24(2)	-2(2)	5(2)	11(2)
C(33)	67(3)	30(2)	29(2)	-6(2)	19(2)	-5(2)
C(34)	47(3)	26(2)	31(2)	-3(2)	12(2)	5(2)
C(35)	42(2)	34(2)	28(2)	-2(2)	8(2)	-2(2)
C(41)	53(3)	30(2)	24(2)	-5(2)	7(2)	-12(2)
C(42)	95(4)	31(3)	31(2)	-2(2)	-2(2)	-21(3)
C(43)	38(2)	40(3)	35(2)	5(2)	-2(2)	-13(2)
C(44)	50(3)	47(3)	46(3)	14(2)	-6(2)	-22(2)
C(45)	48(3)	38(3)	27(2)	-1(2)	-1(2)	-16(2)

***Table A.4.17.5** - Hydrogen coordinates (x 10^4) and isotropic displacement parameters ($Å^2$x 10^3) for (C29 H54.50 N4 O20.25), the RRRS-isomer.*

	x	y	z	U(eq)
H(22A)	-7971	7923	760	76
H(45A)	-8209	13620	-2755	69
H(1)	-7170	6526	-1262	39(12)
H(3)	-8649	8011	-1586	36(12)
H(1A)	-7117	4508	-785	42
H(1B)	-7254	3978	-1508	42
H(2A)	-8554	4841	-1792	38
H(2B)	-8502	4074	-1136	38
H(3A)	-9639	6613	-911	37
H(3B)	-9717	5354	-1326	37
H(4A)	-9421	6454	-2213	34
H(4B)	-10209	7043	-2012	34
H(5A)	-9106	9663	-2390	35
H(5B)	-9688	8570	-2749	35
H(6A)	-8589	7355	-2845	36
H(6B)	-8374	8723	-3061	36
H(7A)	-6512	7639	-2176	39
H(7B)	-7137	7396	-2856	39
H(8A)	-7776	5777	-2338	41
H(8B)	-6854	5455	-2381	41
H(11A)	-5796	6446	-1456	59
H(13A)	-5932	4153	-1682	68
H(13B)	-5686	3993	-902	68
H(14A)	-4696	5705	-1580	55
H(14B)	-4408	5296	-829	55
H(14C)	-4605	4969	-1562	55
H(14D)	-4454	4697	-803	55
H(21A)	-7750	5445	-200	43
H(23A)	-9298	5615	125	48
H(23B)	-9131	4432	-288	48
H(24A)	-8161	5072	963	57
H(24B)	-8815	3958	831	57
H(31A)	-9401	8555	-888	36
H(33A)	-9208	10812	-1537	49
H(33B)	-8426	10031	-1171	49
H(34A)	-9161	10166	-237	41
H(34B)	-8531	11219	-348	41
H(41A)	-7831	10016	-1990	43
H(43A)	-6346	9793	-2436	47
H(43B)	-7198	9824	-2959	47
H(44A)	-6672	11793	-2040	60
H(44B)	-6571	11852	-2774	60

***Table A.4.18.2** - Atomic coordinates (x 10^5) and equivalent isotropic displacement parameters ($Å^2$ x 10^4) for C28 H60 N4 O22. U_{eq} is defined as one third of the trace of the orthogonalized U_{ij} tensor.*

	x	y	z	U_{eq}
O(121)	45340(4)	-5320(5)	32760(4)	289(11)
O(122)	69660(5)	-890(5)	30500(4)	274(10)
O(151)	16270(5)	-34160(5)	51150(4)	335(11)
O(152)	39260(5)	-37990(5)	57270(3)	280(10)
O(221)	63900(5)	-17070(5)	700(3)	306(10)
O(222)	83790(5)	6640(5)	11740(4)	269(10)
O(251)	86620(6)	-47660(5)	12460(4)	436(12)
O(252)	77600(7)	-57990(6)	-6920(5)	432(14)
N(1)	77320(5)	-17320(5)	46000(4)	200(11)
N(2)	96210(5)	-6420(5)	29090(4)	181(11)
C(1)	80000(7)	-26690(6)	37140(5)	200(13)
C(2)	97240(6)	-17550(7)	36430(5)	193(13)
C(3)	113030(6)	7330(6)	31880(5)	197(13)
C(4)	82440(7)	-20140(6)	57610(5)	202(13)
C(11)	60050(6)	-18330(7)	42200(5)	199(13)
C(12)	59030(7)	-7410(7)	34530(5)	209(13)
C(13)	45390(6)	-34940(6)	36120(5)	211(13)
C(14)	28560(7)	-37180(7)	37250(5)	227(14)
C(15)	28850(7)	-36440(6)	49520(5)	215(13)
C(21)	87500(6)	-15250(6)	16010(5)	180(13)
C(22)	77570(7)	-7760(7)	9070(5)	193(13)
C(23)	99780(7)	-17330(7)	10600(5)	224(13)
C(24)	90620(7)	-30980(6)	-360(5)	222(13)
C(25)	84750(7)	-46420(7)	2530(6)	239(14)
O(1S)	63880(6)	15290(5)	-4090(4)	315(11)
O(2S)	57740(5)	-14500(5)	-21820(4)	286(11)
O(3S)	14580(7)	-32560(7)	72320(5)	395(14)
O(4S)	52090(19)	-47900(17)	7400(13)	250(4)

***Table A.4.18.3** - Bond lengths [Å] and angles [°] for C28 H60 N4 O22.*

O(121)-C(12)	1.321(6)	C(2)-H(2A)	0.99	C(23)-H(23A)	0.99
O(121)-H(121)	0.84	C(2)-H(2B)	0.99	C(23)-H(23B)	0.99
O(122)-C(12)	1.221(6)	C(3)-C(4)#1	1.511(8)	C(24)-C(25)	1.520(8)
O(151)-C(15)	1.331(6)	C(3)-H(3A)	0.99	C(24)-H(24A)	0.99
O(151)-H(151)	0.97(7)	C(3)-H(3B)	0.99	C(24)-H(24B)	0.99
O(152)-C(15)	1.214(6)	C(4)-C(3)#1	1.511(8)	O(1S)-H(1SA)	0.76(5)
O(221)-C(22)	1.262(7)	C(4)-H(4A)	0.99	O(1S)-H(1SB)	0.92(7)
O(222)-C(22)	1.251(7)	C(4)-H(4B)	0.99	O(2S)-H(2SA)	0.82(8)
O(251)-C(25)	1.211(7)	C(11)-C(12)	1.523(7)	O(2S)-H(2SB)	0.96(7)
O(252)-C(25)	1.306(7)	C(11)-C(13)	1.555(8)	O(3S)-H(3SA)	0.61(8)
O(252)-H(252)	0.72(8)	C(11)-H(11A)	1.00	O(3S)-H(3SB)	0.98(13)
N(1)-C(4)	1.465(7)	C(13)-C(14)	1.535(7)	O(4S)-O(4S)#2	1.71(3)
N(1)-C(1)	1.474(7)	C(13)-H(13A)	0.99	C(12)-O(121)-H(121)	109.5(3)
N(1)-C(11)	1.486(6)	C(13)-H(13B)	0.99	C(15)-O(151)-H(151)	106(4)
N(2)-C(3)	1.511(6)	C(14)-C(15)	1.494(8)	C(25)-O(252)-H(252)	104(7)
N(2)-C(2)	1.512(6)	C(14)-H(14A)	0.99	C(4)-N(1)-C(1)	112.1(4)
N(2)-C(21)	1.529(7)	C(14)-H(14B)	0.99	C(4)-N(1)-C(11)	112.1(4)
N(2)-H(2)	0.93	C(21)-C(22)	1.529(7)	C(1)-N(1)-C(11)	114.3(4)
C(1)-C(2)	1.528(7)	C(21)-C(23)	1.538(7)	C(3)-N(2)-C(2)	113.7(4)
C(1)-H(1A)	0.99	C(21)-H(21A)	1.00	C(3)-N(2)-C(21)	112.9(4)
C(1)-H(1B)	0.99	C(23)-C(24)	1.521(8)	C(2)-N(2)-C(21)	109.3(4)

C(3)-N(2)-H(2)	106.8(3)	H(4A)-C(4)-H(4B)	107.4	N(2)-C(21)-C(23)	112.9(4)
C(2)-N(2)-H(2)	106.8(3)	N(1)-C(11)-C(12)	109.4(4)	C(22)-C(21)-C(23)	112.1(4)
C(21)-N(2)-H(2)	106.8(2)	N(1)-C(11)-C(13)	114.8(4)	N(2)-C(21)-H(21A)	106.9(2)
N(1)-C(1)-C(2)	110.3(5)	C(12)-C(11)-C(13)	111.9(5)	C(22)-C(21)-H(21A)	106.9(3)
N(1)-C(1)-H(1A)	109.6(3)	N(1)-C(11)-H(11A)	106.8(3)	C(23)-C(21)-H(21A)	106.9(3)
C(2)-C(1)-H(1A)	109.6(3)	C(12)-C(11)-H(11A)	106.8(3)	O(222)-C(22)-O(221)	126.3(5)
N(1)-C(1)-H(1B)	109.6(3)	C(13)-C(11)-H(11A)	106.8(3)	O(222)-C(22)-C(21)	118.7(5)
C(2)-C(1)-H(1B)	109.6(3)	O(122)-C(12)-O(121)	122.2(5)	O(221)-C(22)-C(21)	114.9(5)
H(1A)-C(1)-H(1B)	108.1	O(122)-C(12)-C(11)	124.9(5)	C(24)-C(23)-C(21)	111.8(4)
N(2)-C(2)-C(1)	109.8(4)	O(121)-C(12)-C(11)	112.9(4)	C(24)-C(23)-H(23A)	109.3(3)
N(2)-C(2)-H(2A)	109.7(3)	C(14)-C(13)-C(11)	114.2(4)	C(21)-C(23)-H(23A)	109.3(3)
C(1)-C(2)-H(2A)	109.7(3)	C(14)-C(13)-H(13A)	108.7(3)	C(24)-C(23)-H(23B)	109.3(3)
N(2)-C(2)-H(2B)	109.7(3)	C(11)-C(13)-H(13A)	108.7(3)	C(21)-C(23)-H(23B)	109.3(3)
C(1)-C(2)-H(2B)	109.7(3)	C(14)-C(13)-H(13B)	108.7(3)	H(23A)-C(23)-H(23B)	107.9
H(2A)-C(2)-H(2B)	108.2	C(11)-C(13)-H(13B)	108.7(3)	C(25)-C(24)-C(23)	112.7(5)
N(2)-C(3)-C(4)#1	113.1(4)	H(13A)-C(13)-H(13B)	107.6	C(25)-C(24)-H(24A)	109.1(3)
N(2)-C(3)-H(3A)	109.0(3)	C(15)-C(14)-C(13)	113.7(5)	C(23)-C(24)-H(24A)	109.1(3)
C(4)#1-C(3)-H(3A)	109.0(3)	C(15)-C(14)-H(14A)	108.8(3)	C(25)-C(24)-H(24B)	109.1(3)
N(2)-C(3)-H(3B)	109.0(3)	C(13)-C(14)-H(14A)	108.8(3)	C(23)-C(24)-H(24B)	109.1(3)
C(4)#1-C(3)-H(3B)	109.0(3)	C(15)-C(14)-H(14B)	108.8(3)	H(24A)-C(24)-H(24B)	107.8
H(3A)-C(3)-H(3B)	107.8	C(13)-C(14)-H(14B)	108.8(3)	O(251)-C(25)-O(252)	124.7(6)
N(1)-C(4)-C(3)#1	116.3(4)	H(14A)-C(14)-H(14B)	107.7	O(251)-C(25)-C(24)	123.4(5)
N(1)-C(4)-H(4A)	108.2(2)	O(152)-C(15)-O(151)	122.8(5)	O(252)-C(25)-C(24)	111.9(5)
C(3)#1-C(4)-H(4A)	108.2(3)	O(152)-C(15)-C(14)	124.0(5)	H(1SA)-O(1S)-H(1SB)	79(5)
N(1)-C(4)-H(4B)	108.2(3)	O(151)-C(15)-C(14)	113.2(5)	H(2SA)-O(2S)-H(2SB)	124(6)
C(3)#1-C(4)-H(4B)	108.2(3)	N(2)-C(21)-C(22)	110.7(4)	H(3SA)-O(3S)-H(3SB)	80(9)

***Table A.4.18.4** - Anisotropic displacement parameters ($Å^2 \times 10^4$) for C28 H60 N4 O22. The anisotropic displacement factor exponent takes the form: $-2\pi^2 [h^2 a^{*2} U_{11} + ... + 2 h k a^* b^* U_{12}]$*

	U_{11}	U_{22}	U_{33}	U_{23}	U_{13}	U_{12}
O(121)	170(2)	360(3)	480(3)	270(2)	190(2)	170(2)
O(122)	210(2)	310(3)	460(3)	260(2)	240(2)	140(2)
O(151)	250(2)	430(3)	470(3)	230(2)	230(2)	200(2)
O(152)	240(2)	280(3)	350(3)	140(2)	120(2)	120(2)
O(221)	170(2)	320(3)	310(2)	10(2)	-20(2)	100(2)
O(222)	190(2)	250(3)	380(3)	160(2)	120(2)	80(2)
O(251)	670(3)	250(3)	370(3)	140(2)	220(3)	140(3)
O(252)	550(3)	240(3)	410(3)	120(3)	160(3)	90(3)
N(1)	130(2)	190(3)	330(3)	120(2)	120(2)	90(2)
N(2)	110(2)	180(3)	270(3)	110(2)	110(2)	50(2)
C(1)	170(3)	180(3)	280(3)	120(3)	120(3)	70(3)
C(2)	130(3)	250(4)	250(3)	160(3)	100(3)	90(3)
C(3)	140(3)	180(3)	240(3)	80(3)	100(3)	20(3)
C(4)	130(3)	180(3)	330(4)	150(3)	110(3)	60(3)
C(11)	120(3)	250(3)	270(3)	110(3)	110(3)	90(3)
C(12)	150(3)	210(3)	240(3)	50(3)	50(3)	80(3)
C(13)	70(3)	180(3)	290(3)	50(3)	60(2)	-20(3)
C(14)	120(3)	200(3)	340(4)	120(3)	90(3)	40(3)
C(15)	140(3)	70(3)	330(4)	30(3)	70(3)	-20(3)
C(21)	110(3)	150(3)	270(3)	100(3)	80(3)	30(3)
C(22)	120(3)	260(4)	220(3)	70(3)	120(3)	60(3)
C(23)	170(3)	200(3)	290(3)	70(3)	100(3)	60(3)
C(24)	230(3)	170(3)	300(3)	90(3)	160(3)	80(3)
C(25)	220(3)	160(4)	310(4)	50(3)	90(3)	60(3)

***Table A.4.18.5** - Hydrogen coordinates (x 10^3) and isotropic displacement parameters (Å ^{2} x 10^3) for C28 H60 N4 O22.*

	x	y	z	U_{eq}
H(121)	453(1)	8(1)	285(1)	95(34)
H(151)	179(9)	-335(8)	594(7)	63(24)
H(252)	745(10)	-647(10)	-48(7)	60(31)
H(2)	892(1)	-26(1)	309(1)	57(22)
H(1A)	710(1)	-297(1)	293(1)	24
H(1B)	794(1)	-362(1)	393(1)	24
H(2A)	1058(1)	-118(1)	445(1)	23
H(2B)	1007(1)	-247(1)	328(1)	23
H(3A)	1127(1)	114(1)	249(1)	24
H(3B)	1220(1)	39(1)	335(1)	24
H(4A)	923(1)	-222(1)	587(1)	24
H(4B)	731(1)	-296(1)	576(1)	24
H(11A)	586(1)	-144(1)	495(1)	24
H(13A)	436(1)	-375(1)	276(1)	25
H(13B)	489(1)	-423(1)	396(1)	25
H(14A)	257(1)	-291(1)	346(1)	27
H(14B)	195(1)	-473(1)	320(1)	27
H(21A)	791(1)	-258(1)	154(1)	22
H(23A)	1057(1)	-78(1)	85(1)	27
H(23B)	1084(1)	-189(1)	165(1)	27
H(24A)	807(1)	-303(1)	-57(1)	27
H(24B)	983(1)	-304(1)	-47(1)	27
H(1SA)	594(6)	163(5)	0(4)	6(13)
H(1SB)	692(9)	128(8)	24(6)	56(21)
H(2SA)	525(9)	-225(9)	-273(7)	53(22)
H(2SB)	602(8)	-142(7)	-137(6)	48(19)
H(3SA)	199(10)	-331(10)	763(7)	57(27)
H(3SB)	191(15)	-226(15)	780(11)	149(45)

***Table A.5.1.2** - Atomic coordinates (x 10^4) and equivalent isotropic displacement parameters ($Å^2$x 10^3) for C2 H10 B12 O2 at 150 K. U(eq) is defined as one third of the trace of the orthogonalized U^{ij} tensor.*

	x	y	z	U(eq)
O(1)	1100(2)	4195(1)	3896(2)	40(1)
C(1)	2126(3)	4422(2)	2877(3)	29(1)
B(1)	4588(3)	3475(2)	413(3)	31(1)
B(2)	6892(4)	4002(2)	64(3)	32(1)
B(3)	7185(4)	5563(2)	987(3)	32(1)
B(4)	5064(3)	5996(2)	1893(4)	32(1)
B(5)	3530(3)	4720(2)	1467(3)	30(1)
B(6)	5987(3)	4437(2)	2188(4)	31(1)

***Table A.5.1.3** - Anisotropic displacement parameters ($Å^2$x 10^3) for C2 H10 B12 O2 at 150 K. The anisotropic displacement factor exponent takes the form: $-2\pi^2[h^2 a^{*2}U^{11} + ... + 2 h k a^* b^* U^{12}]$*

	U^{11}	U^{22}	U^{33}	U^{23}	U^{13}	U^{12}
O(1)	40(1)	44(1)	37(1)	2(1)	13(1)	-4(1)
C(1)	31(1)	25(1)	29(1)	-1(1)	0(1)	1(1)

***Table A.5.1.4** - Hydrogen coordinates (x 10^4) and isotropic displacement parameters ($Å^2$x 10^3) for C2 H10 B12 O2 at 150 K.*

	x	y	z	U(eq)
H(1)	4202(27)	2492(18)	759(28)	33(5)
H(2)	8172(28)	3395(20)	31(29)	40(6)
H(3)	8636(29)	5932(19)	1520(30)	35(5)
H(4)	5018(31)	6617(22)	3174(31)	49(6)
H(6)	6521(28)	4066(18)	3652(28)	31(5)

***Table A.5.2.2** - Atomic coordinates (x 10^4) and equivalent isotropic displacement parameters ($Å^2$x 10^3) for C2 H10 B12 O2 at 100 K. U(eq) is defined as one third of the trace of the orthogonalized U^{ij} tensor.*

	x	y	z	U(eq)
O(1)	0	1091(1)	5817(1)	24(1)
C(1)	0	2114(1)	5583(1)	18(1)
B(1)	0	3529(1)	5281(1)	17(1)
B(2)	0	4586(1)	6522(1)	18(1)
B(3)	1594(1)	4397(1)	5563(1)	18(1)
B(4)	986(1)	4083(1)	4004(1)	18(1)

***Table A.5.2.3** - Anisotropic displacement parameters ($Å^2$x 10^3) for C2 H10 B12 O2 at 100 K. The anisotropic displacement factor exponent takes the form: $-2\pi^2[h^2 a^{*2}U^{11} + ... + 2 h k a^* b^* U^{12}]$*

	U^{11}	U^{22}	U^{33}	U^{23}	U^{13}	U^{12}
O(1)	28(1)	17(1)	27(1)	4(1)	0	0
C(1)	17(1)	21(1)	15(1)	-1(1)	0	0
B(1)	19(1)	14(1)	17(1)	1(1)	0	0
B(2)	21(1)	16(1)	16(1)	1(1)	0	0
B(3)	16(1)	18(1)	21(1)	2(1)	-1(1)	0(1)
B(4)	21(1)	16(1)	18(1)	1(1)	3(1)	1(1)

***Table A.5.2.4** - Hydrogen coordinates (x 10^4) and isotropic displacement parameters ($Å^2$x 10^3) for C2 H10 B12 O2 at 100 K.*

	x	y	z	U(eq)
H(2)	0	4219(15)	7456(15)	26(4)
H(3)	2542(16)	3964(10)	5907(10)	24(3)
H(4)	1605(13)	3439(11)	3409(12)	30(3)

***Table A.5.3.2** - Atomic coordinates (x 10^4) and equivalent isotropic displacement parameters ($Å^2$x 10^3) for C2 H22 B12 O8 at 90 K. U(eq) is defined as one third of the trace of the orthogonalized U^{ij} tensor.*

	x	y	z	U(eq)
O(1)	8448(1)	2832(1)	6663(1)	13(1)
O(2)	9452(1)	713(1)	6422(1)	14(1)
C(1)	9127(1)	2370(1)	6277(1)	10(1)
B(1)	9563(1)	3662(2)	5660(1)	9(1)
B(2)	8737(1)	5252(2)	4958(1)	10(1)
B(3)	9732(1)	6045(2)	5871(1)	9(1)
B(4)	10822(1)	4558(2)	5997(1)	10(1)
B(5)	10497(1)	2839(2)	5158(1)	10(1)
B(6)	9214(1)	3260(2)	4519(1)	10(1)
O(1S)	8623(1)	-1150(1)	7470(1)	13(1)
O(2S)	7500(1)	5866(1)	6640(1)	13(1)

***Table A.5.3.3** - Anisotropic displacement parameters ($Å^2$x 10^3) for C2 H22 B12 O8 at 90 K. The anisotropic displacement factor exponent takes the form: $-2\pi^2[h^2 a^{*2}U^{11} + ... + 2 h k a^* b^* U^{12}]$*

	U^{11}	U^{22}	U^{33}	U^{23}	U^{13}	U^{12}
O(1)	16(1)	10(1)	17(1)	2(1)	10(1)	3(1)
O(2)	17(1)	10(1)	18(1)	4(1)	10(1)	3(1)
C(1)	10(1)	10(1)	8(1)	-1(1)	2(1)	-1(1)
B(1)	11(1)	8(1)	10(1)	1(1)	4(1)	0(1)
B(2)	10(1)	9(1)	10(1)	0(1)	3(1)	1(1)
B(3)	11(1)	9(1)	9(1)	0(1)	4(1)	0(1)
B(4)	11(1)	9(1)	10(1)	0(1)	3(1)	1(1)
B(5)	11(1)	9(1)	10(1)	1(1)	4(1)	1(1)
B(6)	11(1)	9(1)	10(1)	-1(1)	4(1)	-1(1)
O(1S)	14(1)	12(1)	13(1)	2(1)	6(1)	2(1)
O(2S)	14(1)	11(1)	13(1)	1(1)	3(1)	1(1)

***Table A.5.3.4** - Hydrogen coordinates (x 10^4) and isotropic displacement parameters ($Å^2$x 10^3) for $C_2H_{22}B_{12}O_8$ at 90 K*

	x	y	z	U(eq)
H(10)	8214(14)	3936(26)	6571(12)	40(5)
H(20)	9138(14)	168(25)	6736(13)	41(5)
H(2)	7932(11)	5378(20)	4930(9)	20(3)
H(3)	9561(11)	6696(19)	6432(9)	19(3)
H(4)	11324(10)	4288(19)	6634(9)	18(3)
H(5)	10791(10)	1425(18)	5254(9)	15(3)
H(6)	8707(11)	2126(20)	4234(9)	21(3)
H(1SB)	9038(14)	-1627(23)	7897(12)	35(4)
H(1SA)	8261(14)	-461(24)	7705(12)	37(4)
H(2SB)	7091(13)	6194(22)	6170(12)	31(4)
H(2SA)	7811(14)	6769(27)	6876(13)	42(5)

***Table A.6.1.2** - Atomic coordinates (x 10^4) and equivalent isotropic displacement parameters ($Å^2$x 10^3) for C57 H75 Dy F9 N11 O14 S3. U(eq) is defined as one third of the trace of the orthogonalized U^{ij} tensor.*

	x	y	z	U(eq)
Dy(1)	3802(1)	5091(1)	9171(1)	18(1)
O(1)	3102(2)	4498(1)	8418(1)	23(1)
O(2)	4734(2)	4175(1)	9224(1)	25(1)
O(3)	5003(2)	5728(1)	9366(1)	27(1)
O(4)	3386(2)	5983(1)	8566(1)	25(1)
O(5)	4650(2)	5118(1)	8250(1)	29(1)
O(11)	6741(4)	1002(2)	8641(2)	83(2)
O(12)	6767(2)	-148(2)	8792(2)	55(1)
O(13)	6256(3)	285(3)	7829(2)	98(2)
O(21)	-898(3)	7898(2)	5943(2)	59(1)
O(22)	-1497(2)	7404(2)	6869(2)	45(1)
O(23)	-1139(3)	6722(2)	5999(2)	65(1)
O(31)	10807(3)	7180(3)	8284(2)	86(2)
O(32)	9945(3)	7954(3)	8855(2)	93(2)
O(33)	10898(3)	7227(2)	9388(2)	54(1)
N(1)	2894(2)	4103(2)	9614(1)	22(1)
N(2)	4262(2)	4803(2)	10298(1)	23(1)
N(3)	3518(2)	6085(2)	9936(1)	21(1)
N(4)	2154(2)	5384(2)	9272(1)	22(1)
N(5)	2452(2)	3602(2)	8044(1)	25(1)
N(6)	5607(2)	3487(2)	9746(2)	29(1)
N(7)	5676(2)	6617(2)	9737(2)	33(1)
N(8)	2435(2)	6615(2)	8069(2)	30(1)
C(1)	3317(3)	3817(2)	10171(2)	25(1)
C(2)	3639(3)	4356(2)	10593(2)	27(1)
C(3)	4357(2)	5404(2)	10684(2)	25(1)
C(4)	3631(2)	5876(2)	10591(2)	24(1)
C(5)	2650(2)	6364(2)	9862(2)	26(1)
C(6)	1995(3)	5814(2)	9815(2)	27(1)
C(7)	1635(2)	4776(2)	9332(2)	25(1)
C(8)	2030(3)	4295(2)	9782(2)	27(1)
C(11)	2873(2)	3600(2)	9119(2)	24(1)
C(12)	2803(2)	3933(2)	8492(2)	22(1)
C(13)	2385(3)	3866(2)	7406(2)	25(1)
C(14)	2516(3)	3310(2)	6962(2)	38(1)
C(15)	1537(3)	4218(2)	7340(2)	29(1)
C(16)	1517(3)	4897(2)	7311(2)	42(1)
C(17)	751(5)	5224(3)	7302(2)	66(2)
C(18)	7(4)	4888(4)	7305(2)	68(2)
C(19)	27(4)	4198(3)	7307(3)	55(2)
C(20)	795(3)	3876(3)	7327(2)	46(1)
C(21)	5102(3)	4468(2)	10254(2)	27(1)
C(22)	5128(3)	4019(2)	9697(2)	25(1)
C(23)	5714(3)	3017(2)	9239(2)	32(1)
C(24)	6453(3)	2557(3)	9413(2)	46(1)
C(25)	4911(3)	2640(2)	9114(2)	34(1)
C(26)	4592(4)	2609(2)	8516(2)	43(1)
C(27)	3846(4)	2260(3)	8392(3)	58(2)
C(28)	3429(4)	1939(3)	8876(3)	56(2)
C(29)	3742(4)	1979(2)	9452(3)	51(1)
C(30)	4485(3)	2317(2)	9583(2)	42(1)
C(31)	4142(2)	6597(2)	9775(2)	25(1)
C(32)	4982(3)	6289(2)	9620(2)	25(1)
C(33)	6514(3)	6370(2)	9565(3)	43(1)

C(34)	7116(3)	6950(3)	9537(3)	58(2)
C(35)	6817(3)	5837(3)	10016(4)	62(2)
C(36)	7190(5)	5271(4)	9786(5)	105(3)
C(37)	7474(8)	4785(7)	10179(9)	163(7)
C(38)	7366(7)	4865(6)	10783(9)	156(6)
C(39)	6992(5)	5417(4)	11045(5)	92(3)
C(40)	6706(4)	5899(3)	10647(4)	66(2)
C(41)	1907(2)	5730(2)	8702(2)	26(1)
C(42)	2632(3)	6137(2)	8443(2)	24(1)
C(43)	3091(3)	6992(2)	7727(2)	34(1)
C(44)	2624(4)	7401(3)	7238(2)	48(1)
C(45)	3621(3)	7404(2)	8157(2)	36(1)
C(46)	4492(3)	7343(3)	8145(3)	50(1)
C(47)	5009(4)	7726(4)	8538(3)	71(2)
C(48)	4628(4)	8181(3)	8929(3)	67(2)
C(49)	3760(4)	8237(3)	8940(3)	56(1)
C(50)	3265(3)	7857(2)	8568(2)	44(1)
C(100)	5311(4)	416(4)	8801(3)	70(2)
C(200)	71(5)	7217(4)	6629(3)	72(2)
C(300)	9584(5)	6731(5)	8938(4)	111(4)
S(1)	6378(1)	377(1)	8472(1)	53(1)
S(2)	-982(1)	7315(1)	6335(1)	46(1)
S(3)	10401(1)	7344(1)	8851(1)	58(1)
F(11)	4918(4)	-123(4)	8695(4)	158(3)
F(12)	4853(4)	860(4)	8525(2)	148(3)
F(13)	5315(3)	541(3)	9383(2)	107(2)
F(21)	116(4)	6703(2)	7005(2)	115(2)
F(22)	632(2)	7129(2)	6167(2)	85(1)
F(23)	338(3)	7729(2)	6949(2)	78(1)
F(31)	9199(3)	6764(3)	9475(3)	125(2)
F(32)	9879(3)	6116(3)	8884(4)	152(3)
F(33)	8990(3)	6774(5)	8510(3)	199(4)
N(9)	7943(11)	3697(9)	8937(9)	243(7)
C(401)	8647(10)	3865(8)	8958(8)	175(6)
C(402)	9475(8)	4162(6)	8964(5)	119(3)
N(10)	7701(10)	4452(10)	7646(9)	252(8)
C(403)	6945(10)	4317(9)	7637(9)	187(7)
C(404)	6086(6)	4119(4)	7601(4)	93(2)
N(11)	6218(5)	5946(4)	7957(3)	100(2)
C(405)	6879(6)	5996(4)	7778(3)	80(2)
C(406)	7725(5)	6057(5)	7559(5)	105(3)

Table A.6.1.3 - Bond lengths [Å] and angles [°] for C57 H75 Dy F9 N11 O14 S3.

Dy(1)-O(1)	2.312(3)	O(13)-S(1)	1.422(4)	N(3)-C(4)	1.495(5)
Dy(1)-O(4)	2.330(3)	O(21)-S(2)	1.463(4)	N(4)-C(41)	1.475(5)
Dy(1)-O(3)	2.332(3)	O(22)-S(2)	1.427(3)	N(4)-C(7)	1.486(5)
Dy(1)-O(2)	2.372(3)	O(23)-S(2)	1.428(4)	N(4)-C(6)	1.487(5)
Dy(1)-O(5)	2.406(3)	O(31)-S(3)	1.425(4)	N(5)-C(12)	1.306(5)
Dy(1)-N(2)	2.617(3)	O(32)-S(3)	1.432(5)	N(5)-C(13)	1.489(5)
Dy(1)-N(1)	2.645(3)	O(33)-S(3)	1.423(4)	N(6)-C(22)	1.320(5)
Dy(1)-N(3)	2.649(3)	N(1)-C(8)	1.462(5)	N(6)-C(23)	1.466(5)
Dy(1)-N(4)	2.676(3)	N(1)-C(11)	1.482(5)	N(7)-C(32)	1.306(5)
O(1)-C(12)	1.248(5)	N(1)-C(1)	1.497(5)	N(7)-C(33)	1.463(6)
O(2)-C(22)	1.242(5)	N(2)-C(2)	1.483(5)	N(8)-C(42)	1.303(5)
O(3)-C(32)	1.264(5)	N(2)-C(3)	1.486(5)	N(8)-C(43)	1.486(5)
O(4)-C(42)	1.259(5)	N(2)-C(21)	1.493(5)	C(1)-C(2)	1.515(5)
O(11)-S(1)	1.438(5)	N(3)-C(31)	1.472(5)	C(3)-C(4)	1.505(5)
O(12)-S(1)	1.411(4)	N(3)-C(5)	1.490(5)	C(5)-C(6)	1.525(6)

C(7)-C(8)	1.516(5)	O(1)-Dy(1)-O(5)	71.93(9)	C(22)-N(6)-H(6C)	118.7
C(11)-C(12)	1.523(5)	O(4)-Dy(1)-O(5)	70.78(9)	C(23)-N(6)-H(6C)	118.7
C(13)-C(14)	1.497(6)	O(3)-Dy(1)-O(5)	71.71(9)	C(32)-N(7)-C(33)	122.2(4)
C(13)-C(15)	1.523(6)	O(2)-Dy(1)-O(5)	73.33(10)	C(32)-N(7)-H(7C)	118.9
C(15)-C(20)	1.361(7)	O(1)-Dy(1)-N(2)	132.65(9)	C(33)-N(7)-H(7C)	118.9
C(15)-C(16)	1.379(6)	O(4)-Dy(1)-N(2)	141.10(10)	C(42)-N(8)-C(43)	121.9(4)
C(16)-C(17)	1.379(8)	O(3)-Dy(1)-N(2)	74.26(10)	C(42)-N(8)-H(8C)	119.0
C(17)-C(18)	1.357(10)	O(2)-Dy(1)-N(2)	66.94(9)	C(43)-N(8)-H(8C)	119.0
C(18)-C(19)	1.398(10)	O(5)-Dy(1)-N(2)	128.85(9)	N(1)-C(1)-C(2)	111.0(3)
C(19)-C(20)	1.377(8)	O(1)-Dy(1)-N(1)	66.65(9)	N(1)-C(1)-H(1B)	109.4
C(21)-C(22)	1.513(5)	O(4)-Dy(1)-N(1)	129.83(10)	C(2)-C(1)-H(1B)	109.4
C(23)-C(25)	1.505(6)	O(3)-Dy(1)-N(1)	142.58(10)	N(1)-C(1)-H(1A)	109.4
C(23)-C(24)	1.540(6)	O(2)-Dy(1)-N(1)	74.01(10)	C(2)-C(1)-H(1A)	109.4
C(25)-C(30)	1.384(7)	O(5)-Dy(1)-N(1)	128.35(10)	H(1B)-C(1)-H(1A)	108.0
C(25)-C(26)	1.393(7)	N(2)-Dy(1)-N(1)	68.99(10)	N(2)-C(2)-C(1)	113.7(3)
C(26)-C(27)	1.400(8)	O(1)-Dy(1)-N(3)	139.33(9)	N(2)-C(2)-H(2B)	108.8
C(27)-C(28)	1.401(9)	O(4)-Dy(1)-N(3)	73.44(9)	C(1)-C(2)-H(2B)	108.8
C(28)-C(29)	1.347(8)	O(3)-Dy(1)-N(3)	66.59(10)	N(2)-C(2)-H(2A)	108.8
C(29)-C(30)	1.388(8)	O(2)-Dy(1)-N(3)	132.11(10)	C(1)-C(2)-H(2A)	108.8
C(31)-C(32)	1.505(6)	O(5)-Dy(1)-N(3)	126.69(10)	H(2B)-C(2)-H(2A)	107.7
C(33)-C(35)	1.534(8)	N(2)-Dy(1)-N(3)	68.35(9)	N(2)-C(3)-C(4)	111.6(3)
C(33)-C(34)	1.513(7)	N(1)-Dy(1)-N(3)	104.89(10)	N(2)-C(3)-H(3B)	109.3
C(35)-C(40)	1.386(10)	O(1)-Dy(1)-N(4)	73.11(9)	C(4)-C(3)-H(3B)	109.3
C(35)-C(36)	1.383(10)	O(4)-Dy(1)-N(4)	66.42(9)	N(2)-C(3)-H(3A)	109.3
C(36)-C(37)	1.379(17)	O(3)-Dy(1)-N(4)	130.67(9)	C(4)-C(3)-H(3A)	109.3
C(37)-C(38)	1.33(2)	O(2)-Dy(1)-N(4)	140.54(9)	H(3B)-C(3)-H(3A)	108.0
C(38)-C(39)	1.386(16)	O(5)-Dy(1)-N(4)	127.12(9)	N(3)-C(4)-C(3)	113.5(3)
C(39)-C(40)	1.381(10)	N(2)-Dy(1)-N(4)	104.02(9)	N(3)-C(4)-H(4B)	108.9
C(41)-C(42)	1.517(6)	N(1)-Dy(1)-N(4)	67.17(10)	C(3)-C(4)-H(4B)	108.9
C(43)-C(45)	1.505(7)	N(3)-Dy(1)-N(4)	67.37(9)	N(3)-C(4)-H(4A)	108.9
C(43)-C(44)	1.535(6)	C(12)-O(1)-Dy(1)	124.5(2)	C(3)-C(4)-H(4A)	108.9
C(45)-C(46)	1.381(7)	C(22)-O(2)-Dy(1)	123.4(2)	H(4B)-C(4)-H(4A)	107.7
C(45)-C(50)	1.397(7)	C(32)-O(3)-Dy(1)	123.8(3)	N(3)-C(5)-C(6)	110.6(3)
C(46)-C(47)	1.412(9)	C(42)-O(4)-Dy(1)	125.3(3)	N(3)-C(5)-H(5B)	109.5
C(47)-C(48)	1.391(10)	C(8)-N(1)-C(11)	110.1(3)	C(6)-C(5)-H(5B)	109.5
C(48)-C(49)	1.375(9)	C(8)-N(1)-C(1)	108.5(3)	N(3)-C(5)-H(5A)	109.5
C(49)-C(50)	1.362(8)	C(11)-N(1)-C(1)	109.2(3)	C(6)-C(5)-H(5A)	109.5
C(100)-F(11)	1.279(10)	C(8)-N(1)-Dy(1)	113.2(2)	H(5B)-C(5)-H(5A)	108.1
C(100)-F(13)	1.286(8)	C(11)-N(1)-Dy(1)	105.6(2)	N(4)-C(6)-C(5)	111.5(3)
C(100)-F(12)	1.300(8)	C(1)-N(1)-Dy(1)	110.2(2)	N(4)-C(6)-H(6B)	109.3
C(100)-S(1)	1.830(8)	C(2)-N(2)-C(3)	108.9(3)	C(5)-C(6)-H(6B)	109.3
C(200)-F(23)	1.319(8)	C(2)-N(2)-C(21)	109.7(3)	N(4)-C(6)-H(6A)	109.3
C(200)-F(21)	1.324(9)	C(3)-N(2)-C(21)	108.7(3)	C(5)-C(6)-H(6A)	109.3
C(200)-F(22)	1.350(8)	C(2)-N(2)-Dy(1)	110.9(2)	H(6B)-C(6)-H(6A)	108.0
C(200)-S(2)	1.791(7)	C(3)-N(2)-Dy(1)	111.8(2)	N(4)-C(7)-C(8)	111.4(3)
C(300)-F(33)	1.322(10)	C(21)-N(2)-Dy(1)	106.7(2)	N(4)-C(7)-H(7B)	109.4
C(300)-F(31)	1.316(10)	C(31)-N(3)-C(5)	108.7(3)	C(8)-C(7)-H(7B)	109.4
C(300)-F(32)	1.337(10)	C(31)-N(3)-C(4)	110.2(3)	N(4)-C(7)-H(7A)	109.4
C(300)-S(3)	1.800(11)	C(5)-N(3)-C(4)	108.7(3)	C(8)-C(7)-H(7A)	109.4
N(9)-C(401)	1.162(15)	C(31)-N(3)-Dy(1)	106.0(2)	H(7B)-C(7)-H(7A)	108.0
C(401)-C(402)	1.438(14)	C(5)-N(3)-Dy(1)	112.1(2)	N(1)-C(8)-C(7)	113.2(3)
N(10)-C(403)	1.223(15)	C(4)-N(3)-Dy(1)	111.1(2)	N(1)-C(8)-H(8B)	108.9
C(403)-C(404)	1.416(14)	C(41)-N(4)-C(7)	108.8(3)	C(7)-C(8)-H(8B)	108.9
N(11)-C(405)	1.119(10)	C(41)-N(4)-C(6)	109.9(3)	N(1)-C(8)-H(8A)	108.9
C(405)-C(406)	1.422(12)	C(7)-N(4)-C(6)	108.9(3)	C(7)-C(8)-H(8A)	108.9
		C(41)-N(4)-Dy(1)	107.1(2)	H(8B)-C(8)-H(8A)	107.8
O(1)-Dy(1)-O(4)	82.57(10)	C(7)-N(4)-Dy(1)	111.0(2)	N(1)-C(11)-C(12)	110.1(3)
O(1)-Dy(1)-O(3)	143.61(9)	C(6)-N(4)-Dy(1)	111.1(2)	N(1)-C(11)-H(11B)	109.6
O(4)-Dy(1)-O(3)	84.33(10)	C(12)-N(5)-C(13)	122.6(3)	C(12)-C(11)-H(11B)	109.6
O(1)-Dy(1)-O(2)	85.55(9)	C(12)-N(5)-H(5D)	118.7	N(1)-C(11)-H(11A)	109.6
O(4)-Dy(1)-O(2)	144.10(9)	C(13)-N(5)-H(5D)	118.7	C(12)-C(11)-H(11A)	109.6
O(3)-Dy(1)-O(2)	85.50(10)	C(22)-N(6)-C(23)	122.5(3)	H(11B)-C(11)-H(11A)	108.2

O(1)-C(12)-N(5)	122.4(3)	C(26)-C(27)-H(27)	120.5	C(45)-C(43)-H(43)	108.5
O(1)-C(12)-C(11)	119.7(3)	C(29)-C(28)-C(27)	119.7(5)	C(44)-C(43)-H(43)	108.5
N(5)-C(12)-C(11)	117.9(3)	C(29)-C(28)-H(28)	120.1	C(43)-C(44)-H(44C)	109.5
N(5)-C(13)-C(14)	108.5(3)	C(27)-C(28)-H(28)	120.1	C(43)-C(44)-H(44B)	109.5
N(5)-C(13)-C(15)	108.5(3)	C(28)-C(29)-C(30)	122.0(5)	H(44C)-C(44)-H(44B)	109.5
C(14)-C(13)-C(15)	114.5(3)	C(28)-C(29)-H(29)	119.0	C(43)-C(44)-H(44A)	109.5
N(5)-C(13)-H(13)	108.4	C(30)-C(29)-H(29)	119.0	H(44C)-C(44)-H(44A)	109.5
C(14)-C(13)-H(13)	108.4	C(29)-C(30)-C(25)	119.5(5)	H(44B)-C(44)-H(44A)	109.5
C(15)-C(13)-H(13)	108.4	C(29)-C(30)-H(30)	120.2	C(46)-C(45)-C(50)	118.1(5)
C(13)-C(14)-H(14C)	109.5	C(25)-C(30)-H(30)	120.2	C(46)-C(45)-C(43)	119.4(5)
C(13)-C(14)-H(14B)	109.5	N(3)-C(31)-C(32)	110.5(3)	C(50)-C(45)-C(43)	122.5(4)
H(14C)-C(14)-H(14B)	109.5	N(3)-C(31)-H(31B)	109.6	C(45)-C(46)-C(47)	121.0(6)
C(13)-C(14)-H(14A)	109.5	C(32)-C(31)-H(31B)	109.6	C(45)-C(46)-H(46)	119.5
H(14C)-C(14)-H(14A)	109.5	N(3)-C(31)-H(31A)	109.6	C(47)-C(46)-H(46)	119.5
H(14B)-C(14)-H(14A)	109.5	C(32)-C(31)-H(31A)	109.6	C(48)-C(47)-C(46)	119.0(6)
C(20)-C(15)-C(16)	119.2(4)	H(31B)-C(31)-H(31A)	108.1	C(48)-C(47)-H(47)	120.5
C(20)-C(15)-C(13)	121.3(4)	O(3)-C(32)-N(7)	121.5(4)	C(46)-C(47)-H(47)	120.5
C(16)-C(15)-C(13)	119.5(4)	O(3)-C(32)-C(31)	119.6(4)	C(49)-C(48)-C(47)	119.7(6)
C(15)-C(16)-C(17)	120.1(6)	N(7)-C(32)-C(31)	118.8(4)	C(49)-C(48)-H(48)	120.1
C(15)-C(16)-H(16)	119.9	N(7)-C(33)-C(35)	111.1(4)	C(47)-C(48)-H(48)	120.2
C(17)-C(16)-H(16)	119.9	N(7)-C(33)-C(34)	108.1(4)	C(50)-C(49)-C(48)	120.9(6)
C(16)-C(17)-C(18)	121.0(6)	C(35)-C(33)-C(34)	112.2(5)	C(50)-C(49)-H(49)	119.5
C(16)-C(17)-H(17)	119.5	N(7)-C(33)-H(33)	108.4	C(48)-C(49)-H(49)	119.5
C(18)-C(17)-H(17)	119.5	C(35)-C(33)-H(33)	108.4	C(49)-C(50)-C(45)	121.3(5)
C(17)-C(18)-C(19)	118.9(6)	C(34)-C(33)-H(33)	108.4	C(49)-C(50)-H(50)	119.3
C(17)-C(18)-H(18)	120.5	C(33)-C(34)-H(34C)	109.5	C(45)-C(50)-H(50)	119.3
C(19)-C(18)-H(18)	120.5	C(33)-C(34)-H(34B)	109.4	F(11)-C(100)-F(13)	110.3(9)
C(20)-C(19)-C(18)	119.6(6)	H(34C)-C(34)-H(34B)	109.5	F(11)-C(100)-F(12)	103.8(7)
C(20)-C(19)-H(19)	120.2	C(33)-C(34)-H(34A)	109.5	F(13)-C(100)-F(12)	108.6(6)
C(18)-C(19)-H(19)	120.2	H(34C)-C(34)-H(34A)	109.5	F(11)-C(100)-S(1)	109.8(5)
C(15)-C(20)-C(19)	121.1(5)	H(34B)-C(34)-H(34A)	109.5	F(13)-C(100)-S(1)	112.8(5)
C(15)-C(20)-H(20)	119.4	C(40)-C(35)-C(36)	119.1(7)	F(12)-C(100)-S(1)	111.2(6)
C(19)-C(20)-H(20)	119.4	C(40)-C(35)-C(33)	121.8(5)	F(23)-C(200)-F(21)	106.2(5)
N(2)-C(21)-C(22)	110.5(3)	C(36)-C(35)-C(33)	119.1(8)	F(23)-C(200)-F(22)	106.6(7)
N(2)-C(21)-H(21B)	109.6	C(37)-C(36)-C(35)	120.6(11)	F(21)-C(200)-F(22)	108.6(5)
C(22)-C(21)-H(21B)	109.6	C(37)-C(36)-H(36)	119.7	F(23)-C(200)-S(2)	113.3(4)
N(2)-C(21)-H(21A)	109.5	C(35)-C(36)-H(36)	119.7	F(21)-C(200)-S(2)	110.9(6)
C(22)-C(21)-H(21A)	109.6	C(38)-C(37)-C(36)	118.7(12)	F(22)-C(200)-S(2)	111.0(4)
H(21B)-C(21)-H(21A)	108.1	C(38)-C(37)-H(37)	120.7	F(33)-C(300)-F(31)	107.0(6)
O(2)-C(22)-N(6)	124.1(4)	C(36)-C(37)-H(37)	120.6	F(33)-C(300)-F(32)	104.2(8)
O(2)-C(22)-C(21)	119.6(3)	C(37)-C(38)-C(39)	123.8(12)	F(31)-C(300)-F(32)	106.5(10)
N(6)-C(22)-C(21)	116.3(4)	C(37)-C(38)-H(38)	118.1	F(33)-C(300)-S(3)	112.9(9)
N(6)-C(23)-C(25)	111.7(3)	C(39)-C(38)-H(38)	118.1	F(31)-C(300)-S(3)	112.9(6)
N(6)-C(23)-C(24)	107.4(4)	C(40)-C(39)-C(38)	117.0(11)	F(32)-C(300)-S(3)	112.7(5)
C(25)-C(23)-C(24)	112.0(4)	C(40)-C(39)-H(39)	121.5	O(12)-S(1)-O(13)	116.3(3)
N(6)-C(23)-H(23)	108.6	C(38)-C(39)-H(39)	121.5	O(12)-S(1)-O(11)	111.5(3)
C(25)-C(23)-H(23)	108.6	C(35)-C(40)-C(39)	120.8(8)	O(13)-S(1)-O(11)	114.8(4)
C(24)-C(23)-H(23)	108.6	C(35)-C(40)-H(40)	119.6	O(12)-S(1)-C(100)	103.9(3)
C(23)-C(24)-H(24C)	109.5	C(39)-C(40)-H(40)	119.6	O(13)-S(1)-C(100)	105.3(3)
C(23)-C(24)-H(24B)	109.5	N(4)-C(41)-C(42)	111.7(3)	O(11)-S(1)-C(100)	103.2(3)
H(24C)-C(24)-H(24B)	109.5	N(4)-C(41)-H(41B)	109.3	O(22)-S(2)-O(23)	115.0(2)
C(23)-C(24)-H(24A)	109.5	C(42)-C(41)-H(41B)	109.3	O(22)-S(2)-O(21)	114.9(2)
H(24C)-C(24)-H(24A)	109.5	N(4)-C(41)-H(41A)	109.3	O(23)-S(2)-O(21)	113.6(3)
H(24B)-C(24)-H(24A)	109.5	C(42)-C(41)-H(41A)	109.3	O(22)-S(2)-C(200)	104.6(3)
C(30)-C(25)-C(26)	119.2(5)	H(41B)-C(41)-H(41A)	107.9	O(23)-S(2)-C(200)	104.5(3)
C(30)-C(25)-C(23)	121.0(4)	O(4)-C(42)-N(8)	122.7(4)	O(21)-S(2)-C(200)	102.4(3)
C(26)-C(25)-C(23)	119.7(4)	O(4)-C(42)-C(41)	120.0(3)	O(33)-S(3)-O(31)	114.8(2)
C(25)-C(26)-C(27)	120.4(5)	N(8)-C(42)-C(41)	117.1(4)	O(33)-S(3)-O(32)	114.5(3)
C(25)-C(26)-H(26)	119.8	N(8)-C(43)-C(45)	111.3(3)	O(31)-S(3)-O(32)	115.6(3)
C(27)-C(26)-H(26)	119.8	N(8)-C(43)-C(44)	106.8(4)	O(33)-S(3)-C(300)	101.2(4)
C(28)-C(27)-C(26)	119.0(5)	C(45)-C(43)-C(44)	113.3(4)	O(31)-S(3)-C(300)	104.6(4)
C(28)-C(27)-H(27)	120.5	N(8)-C(43)-H(43)	108.4	O(32)-S(3)-C(300)	103.6(4)

N(9)-C(401)-C(402) 172(2) N(10)-C(403)-C(404) 176(2) N(11)-C(405)-C(406) 179.1(10)

***Table A.6.1.4** - Anisotropic displacement parameters ($Å^2 x\ 10^3$) for C57 H75 Dy F9 N11 O14 S3. The anisotropic displacement factor exponent takes the form: $-2\pi^2[h^2 a^{*2} U^{11} + ... + 2 h k a^* b^* U^{12}]$*

	U^{11}	U^{22}	U^{33}	U^{23}	U^{13}	U^{12}
Dy(1)	22(1)	15(1)	17(1)	0(1)	1(1)	1(1)
O(1)	30(1)	21(1)	19(1)	3(1)	0(1)	-2(1)
O(2)	32(1)	25(1)	19(1)	0(1)	-2(1)	5(1)
O(3)	29(1)	26(1)	25(1)	-3(1)	2(1)	1(1)
O(4)	27(1)	22(1)	25(1)	5(1)	3(1)	3(1)
O(5)	33(1)	31(2)	23(1)	1(1)	3(1)	6(1)
O(11)	120(4)	52(3)	77(3)	-3(2)	2(3)	-7(3)
O(12)	62(2)	59(2)	43(2)	-3(2)	-17(2)	24(2)
O(13)	126(4)	134(4)	32(2)	-27(2)	-30(2)	82(4)
O(21)	64(2)	58(2)	54(2)	15(2)	5(2)	13(2)
O(22)	62(2)	37(2)	35(2)	-2(1)	13(2)	11(2)
O(23)	67(2)	66(2)	61(2)	-30(2)	14(2)	3(2)
O(31)	76(3)	137(5)	44(2)	-13(3)	3(2)	63(3)
O(32)	109(4)	113(4)	57(3)	5(3)	9(3)	81(4)
O(33)	67(2)	44(2)	50(2)	-7(2)	-18(2)	11(2)
N(1)	29(2)	22(2)	17(2)	1(1)	1(1)	-2(1)
N(2)	31(2)	19(2)	19(1)	-1(1)	-1(1)	4(1)
N(3)	26(2)	19(1)	20(2)	-2(1)	2(1)	0(1)
N(4)	26(1)	18(1)	22(2)	1(1)	2(1)	-2(1)
N(5)	35(2)	21(2)	18(2)	1(1)	-3(1)	-4(1)
N(6)	35(2)	25(2)	26(2)	-1(1)	-3(1)	8(1)
N(7)	30(2)	23(2)	46(2)	-8(2)	1(2)	-6(1)
N(8)	32(2)	28(2)	30(2)	9(2)	1(1)	8(2)
C(1)	35(2)	20(2)	18(2)	4(1)	-1(2)	-3(2)
C(2)	39(2)	23(2)	19(2)	0(1)	-1(2)	-2(2)
C(3)	34(2)	23(2)	18(2)	-2(1)	-3(1)	-2(2)
C(4)	31(2)	21(2)	20(2)	-4(1)	4(2)	-1(2)
C(5)	27(2)	23(2)	26(2)	-3(2)	4(2)	4(2)
C(6)	24(2)	29(2)	29(2)	-2(2)	5(2)	4(2)
C(7)	25(2)	25(2)	26(2)	-1(1)	3(1)	-5(2)
C(8)	30(2)	24(2)	26(2)	1(2)	6(2)	-7(2)
C(11)	36(2)	19(2)	18(2)	1(2)	-3(2)	-1(1)
C(12)	25(2)	23(2)	18(2)	0(2)	0(2)	4(2)
C(13)	34(2)	26(2)	16(2)	5(2)	-1(2)	-2(2)
C(14)	46(3)	44(3)	23(2)	-4(2)	-5(2)	11(2)
C(15)	43(2)	29(2)	17(2)	1(2)	0(2)	8(2)
C(16)	64(3)	39(2)	23(2)	-5(2)	-6(2)	11(2)
C(17)	112(6)	54(4)	33(3)	-12(2)	-13(3)	38(4)
C(18)	64(4)	100(6)	41(3)	4(3)	1(2)	38(4)
C(19)	41(3)	72(4)	52(3)	22(3)	1(2)	1(3)
C(20)	49(3)	54(3)	34(2)	11(2)	3(2)	1(2)
C(21)	31(2)	25(2)	24(2)	-1(2)	-6(2)	5(2)
C(22)	27(2)	22(2)	26(2)	3(2)	1(2)	3(2)
C(23)	43(2)	26(2)	27(2)	0(2)	1(2)	12(2)
C(24)	50(3)	39(3)	48(3)	-3(2)	0(2)	23(2)
C(25)	45(2)	23(2)	35(2)	-5(2)	-4(2)	14(2)
C(26)	61(3)	32(2)	37(2)	-5(2)	-1(2)	11(2)
C(27)	68(4)	44(3)	63(3)	-27(3)	-31(3)	19(3)
C(28)	56(3)	25(2)	85(4)	-5(3)	-12(3)	1(2)
C(29)	57(3)	30(2)	67(3)	1(2)	-2(3)	-1(3)

C(30)	59(3)	25(2)	40(3)	3(2)	-1(2)	5(2)
C(31)	31(2)	19(2)	26(2)	-1(2)	3(2)	-2(2)
C(32)	31(2)	23(2)	22(2)	0(2)	2(2)	-5(2)
C(33)	29(2)	40(3)	60(3)	-13(2)	8(2)	-8(2)
C(34)	35(3)	56(3)	85(4)	2(3)	11(3)	-13(2)
C(35)	31(2)	37(3)	119(6)	11(3)	10(3)	0(2)
C(36)	82(5)	74(5)	159(9)	11(6)	39(6)	30(4)
C(37)	121(9)	99(8)	268(19)	34(11)	65(12)	67(7)
C(38)	95(7)	107(9)	270(20)	53(14)	4(10)	49(6)
C(39)	68(4)	87(6)	121(7)	37(5)	-30(4)	-1(4)
C(40)	41(3)	62(4)	93(5)	11(3)	-26(3)	-8(3)
C(41)	26(2)	25(2)	27(2)	2(2)	-4(2)	1(2)
C(42)	30(2)	20(2)	22(2)	-2(2)	3(2)	6(2)
C(43)	41(2)	35(2)	28(2)	13(2)	7(2)	4(2)
C(44)	65(3)	45(3)	32(2)	18(2)	-3(2)	3(2)
C(45)	36(2)	33(2)	38(2)	18(2)	5(2)	-1(2)
C(46)	43(3)	55(3)	54(3)	17(3)	18(2)	1(2)
C(47)	42(3)	92(5)	79(5)	36(4)	-3(3)	-23(3)
C(48)	72(4)	59(4)	70(4)	8(3)	-8(3)	-28(3)
C(49)	72(4)	38(3)	58(3)	0(2)	-1(3)	-6(3)
C(50)	43(3)	38(3)	49(3)	4(2)	6(2)	2(2)
C(100)	58(4)	81(5)	70(4)	-17(4)	-18(3)	20(4)
C(200)	78(4)	82(5)	57(4)	-23(4)	-16(3)	41(4)
C(300)	53(4)	163(9)	119(7)	-91(7)	-13(4)	45(5)
S(1)	77(1)	57(1)	26(1)	-6(1)	-9(1)	32(1)
S(2)	52(1)	52(1)	34(1)	-9(1)	7(1)	12(1)
S(3)	55(1)	78(1)	42(1)	-14(1)	-7(1)	41(1)
F(11)	92(4)	157(6)	225(8)	-48(6)	-29(4)	-32(4)
F(12)	136(5)	207(7)	100(4)	-32(4)	-40(3)	132(5)
F(13)	68(3)	199(6)	53(2)	-19(3)	7(2)	23(3)
F(21)	164(5)	76(3)	104(4)	7(3)	-47(3)	61(3)
F(22)	59(2)	119(4)	77(3)	-38(2)	0(2)	37(2)
F(23)	72(2)	90(3)	72(2)	-36(2)	-24(2)	26(2)
F(31)	60(3)	154(5)	160(5)	-49(4)	24(3)	4(3)
F(32)	53(2)	110(4)	294(9)	-99(5)	25(4)	-25(3)
F(33)	53(3)	372(12)	173(6)	-149(7)	-50(3)	42(5)
N(11)	93(5)	124(6)	83(5)	17(4)	-12(4)	-21(5)
C(405)	112(7)	71(5)	57(4)	18(4)	13(4)	-4(5)
C(406)	71(5)	119(7)	123(7)	29(6)	-4(5)	-25(5)

***Table A.6.1.5** - Hydrogen coordinates (x 10^4) and isotropic displacement parameters ($Å^2$x 10^3) for C57 H75 Dy F9 N11 O14 S3.*

	x	y	z	U(eq)
H(5D)	2247	3207	8122	30
H(6C)	5872	3413	10096	34
H(7C)	5637	7000	9926	39
H(8C)	1898	6718	8017	36
H(1B)	3797	3536	10039	29
H(1A)	2909	3536	10397	29
H(2B)	3151	4620	10739	32
H(2A)	3906	4149	10958	32
H(3B)	4895	5628	10578	30
H(3A)	4385	5275	11124	30

H(4B)	3102	5663	10736	29
H(4A)	3728	6272	10848	29
H(5B)	2630	6639	9485	31
H(5A)	2516	6650	10219	31
H(6B)	2012	5545	10195	33
H(6A)	1422	6010	9781	33
H(7B)	1581	4563	8923	30
H(7A)	1059	4895	9476	30
H(8B)	2039	4497	10197	32
H(8A)	1673	3894	9804	32
H(11B)	2382	3303	9181	29
H(11A)	3396	3331	9134	29
H(13)	2848	4196	7343	30
H(14C)	2520	3482	6540	56
H(14B)	2055	2989	7007	56
H(14A)	3059	3094	7049	56
H(16)	2032	5139	7298	51
H(17)	744	5692	7293	79
H(18)	-518	5117	7306	82
H(19)	-486	3954	7295	66
H(20)	807	3408	7331	55
H(21B)	5204	4206	10632	32
H(21A)	5557	4803	10220	32
H(23)	5873	3266	8859	39
H(24C)	6986	2806	9407	68
H(24B)	6486	2194	9116	68
H(24A)	6359	2378	9827	68
H(26)	4884	2825	8190	52
H(27)	3625	2241	7984	70
H(28)	2927	1694	8798	67
H(29)	3445	1769	9779	61
H(30)	4700	2327	9992	50
H(31B)	4212	6903	10127	30
H(31A)	3934	6853	9418	30
H(33)	6475	6171	9145	51
H(34C)	7169	7147	9948	87
H(34B)	6895	7280	9249	87
H(34A)	7673	6799	9397	87
H(36)	7251	5217	9353	126
H(37)	7741	4400	10022	195
H(38)	7556	4525	11050	187
H(39)	6936	5461	11479	111
H(40)	6430	6278	10808	79
H(41B)	1420	6023	8789	31
H(41A)	1725	5403	8390	31
H(43)	3471	6672	7512	41
H(44C)	2225	7701	7441	72
H(44B)	2314	7106	6962	72
H(44A)	3036	7658	7000	72
H(46)	4748	7040	7867	60
H(47)	5607	7673	8535	85
H(48)	4967	8452	9188	80
H(49)	3501	8545	9211	67
H(50)	2666	7901	8588	52

***Table A.6.2.1** - Atomic coordinates (x 10^4) and equivalent isotropic displacement parameters ($Å^2$x 10^3) for C60 H73 Eu F12 N10 O13. U(eq) is defined as one third of the trace of the orthogonalized U^{ij} tensor.*

	x	y	z	U(eq)
Eu(1)	2599(1)	-599(1)	-1903(1)	16(1)
O(1)	3197(2)	-305(2)	-1049(1)	22(1)
O(2)	1192(2)	-702(2)	-1488(1)	26(1)
O(3)	2002(2)	-1491(2)	-2496(1)	25(1)
O(4)	4004(2)	-1151(1)	-2016(1)	21(1)
O(5)	2609(2)	-1717(1)	-1388(1)	26(1)
O(11)	2212(2)	5649(2)	2022(2)	53(1)
O(12)	3397(2)	4937(2)	2057(2)	60(1)
O(21)	9106(3)	7203(2)	795(2)	57(1)
O(22)	9993(4)	7883(3)	284(2)	81(2)
O(31)	-2670(3)	2504(2)	-741(1)	57(1)
O(32)	-2126(4)	3485(2)	-376(2)	74(2)
O(41)	10174(3)	6965(2)	-407(2)	60(1)
O(42)	11195(3)	7704(2)	-762(2)	62(1)
N(1)	2201(2)	750(2)	-1562(1)	23(1)
N(2)	1259(2)	17(2)	-2464(1)	24(1)
N(3)	3034(2)	-413(2)	-2941(1)	22(1)
N(4)	3970(2)	347(2)	-2043(1)	21(1)
N(5)	3335(2)	367(2)	-303(1)	27(1)
N(6)	-309(2)	-617(2)	-1453(2)	33(1)
N(7)	1978(3)	-2140(2)	-3258(1)	31(1)
N(8)	5499(2)	-1193(2)	-2013(1)	27(1)
C(1)	1296(3)	980(2)	-1750(2)	27(1)
C(2)	1157(3)	803(2)	-2344(2)	27(1)
C(3)	1399(3)	-76(2)	-3053(2)	28(1)
C(4)	2374(3)	68(2)	-3208(2)	27(1)
C(5)	3940(3)	-90(2)	-3001(2)	26(1)
C(6)	4081(3)	548(2)	-2622(2)	25(1)
C(7)	3830(3)	1021(2)	-1721(2)	25(1)
C(8)	2869(3)	1289(2)	-1752(2)	27(1)
C(11)	2200(3)	702(2)	-967(2)	27(1)
C(12)	2964(3)	227(2)	-771(2)	22(1)
C(13)	4031(3)	-99(3)	-78(2)	30(1)
C(14)	4070(4)	-3(4)	521(2)	54(2)
C(15)	4939(3)	38(2)	-341(2)	28(1)
C(16)	5441(3)	-528(3)	-532(2)	32(1)
C(17)	6265(3)	-421(3)	-771(2)	45(1)
C(18)	6607(4)	272(3)	-811(2)	52(2)
C(19)	6128(4)	848(3)	-625(3)	54(2)
C(20)	5292(4)	737(3)	-383(2)	43(1)
C(21)	457(2)	-569(3)	-1714(2)	27(1)
C(22)	438(3)	-380(3)	-2305(2)	30(1)
C(23)	-337(3)	-844(3)	-887(2)	37(1)
C(24)	-1297(3)	-1069(4)	-753(3)	56(2)
C(25)	10(3)	-266(3)	-512(2)	37(1)
C(26)	-310(4)	448(3)	-529(3)	53(2)
C(27)	17(5)	953(4)	-186(3)	68(2)
C(28)	664(5)	791(4)	190(3)	70(2)
C(29)	1004(5)	82(4)	216(2)	61(2)
C(30)	676(4)	-436(3)	-140(2)	44(1)
C(31)	3026(3)	-1140(2)	-3189(2)	26(1)
C(32)	2283(3)	-1606(2)	-2957(2)	24(1)
C(33)	1284(3)	-2640(3)	-3062(2)	40(1)
C(34)	1263(4)	-3316(3)	-3414(3)	58(2)

C(35)	379(3)	-2278(3)	-3047(2)	47(1)
C(36)	-140(5)	-2335(4)	-2581(3)	67(2)
C(37)	-990(6)	-2015(6)	-2572(5)	106(4)
C(38)	-1319(5)	-1666(5)	-2995(5)	103(4)
C(39)	-809(5)	-1612(5)	-3456(4)	88(3)
C(40)	49(4)	-1920(4)	-3481(3)	59(2)
C(41)	4778(2)	-32(2)	-1849(2)	23(1)
C(42)	4745(2)	-836(2)	-1973(2)	19(1)
C(43)	5492(3)	-1984(2)	-2107(2)	30(1)
C(44)	6413(3)	-2293(3)	-1957(3)	45(1)
C(45)	5218(3)	-2164(3)	-2672(2)	30(1)
C(46)	5671(3)	-1852(3)	-3101(2)	43(1)
C(47)	5406(4)	-2001(3)	-3635(2)	52(2)
C(48)	4716(5)	-2455(3)	-3730(2)	53(2)
C(49)	4252(4)	-2780(3)	-3304(2)	42(1)
C(50)	4510(3)	-2619(3)	-2779(2)	34(1)
C(101)	2641(3)	5138(2)	2193(2)	32(1)
C(102)	2231(4)	4682(3)	2643(2)	50(1)
C(201)	9500(4)	7757(3)	685(2)	46(1)
C(202)	9431(5)	8412(4)	1056(3)	67(2)
C(301)	-2360(4)	2849(3)	-373(2)	40(1)
C(302)	-2306(7)	2427(4)	153(2)	82(3)
C(401)	10752(4)	7149(3)	-751(3)	51(1)
C(402)	10876(7)	6594(4)	-1193(4)	87(3)
F(11)	2730(3)	4592(4)	3049(2)	129(2)
F(12)	1991(5)	4040(3)	2454(3)	142(3)
F(13)	1454(3)	4947(3)	2828(2)	86(1)
F(21)	9190(5)	9012(3)	816(2)	123(2)
F(22)	8881(4)	8298(3)	1467(2)	104(2)
F(23)	10238(5)	8561(3)	1280(2)	129(2)
F(31)	-3063(6)	2434(4)	403(3)	170(4)
F(33)	-2035(4)	1757(2)	98(2)	122(2)
F(32)	-1744(5)	2768(4)	503(2)	147(3)
F(41)	11449(4)	6796(3)	-1563(2)	112(2)
F(42)	10102(7)	6486(6)	-1444(3)	213(5)
F(43)	11035(7)	5952(3)	-1022(3)	171(4)
N(9)	-2638(20)	-1165(11)	427(10)	354(8)
C(501)	-2582(23)	-414(13)	497(14)	354(8)
C(502)	-2317(19)	324(12)	615(11)	354(8)
N(10)	7979(6)	6674(4)	-1310(4)	115(3)
C(601)	7821(5)	6803(4)	-852(4)	75(2)
C(602)	7638(7)	6975(5)	-330(4)	107(3)

***Table A.6.2.3** - Bond lengths [Å] and angles [°] for C60 H73 Eu F12 N10 O13.*

Eu(1)-O(4)	2.346(3)	O(3)-C(32)	1.240(5)	N(2)-C(3)	1.487(6)
Eu(1)-O(2)	2.348(3)	O(4)-C(42)	1.253(5)	N(2)-C(2)	1.483(6)
Eu(1)-O(1)	2.365(3)	O(11)-C(101)	1.214(5)	N(3)-C(31)	1.471(5)
Eu(1)-O(3)	2.376(3)	O(12)-C(101)	1.233(6)	N(3)-C(4)	1.479(5)
Eu(1)-O(5)	2.420(2)	O(21)-C(201)	1.208(7)	N(3)-C(5)	1.484(5)
Eu(1)-N(3)	2.682(3)	O(22)-C(201)	1.260(7)	N(4)-C(41)	1.473(5)
Eu(1)-N(1)	2.687(3)	O(31)-C(301)	1.206(6)	N(4)-C(7)	1.490(5)
Eu(1)-N(2)	2.687(3)	O(32)-C(301)	1.219(6)	N(4)-C(6)	1.494(5)
Eu(1)-N(4)	2.707(3)	O(41)-C(401)	1.261(6)	N(5)-C(12)	1.315(5)
Eu(1)-C(21)	3.231(4)	O(42)-C(401)	1.216(7)	N(5)-C(13)	1.459(5)
Eu(1)-C(42)	3.235(4)	N(1)-C(11)	1.480(5)	N(6)-C(21)	1.317(5)
Eu(1)-C(12)	3.242(4)	N(1)-C(8)	1.482(5)	N(6)-C(23)	1.468(6)
O(1)-C(12)	1.246(5)	N(1)-C(1)	1.490(5)	N(7)-C(32)	1.315(5)
O(2)-C(21)	1.255(5)	N(2)-C(22)	1.480(5)	N(7)-C(33)	1.468(6)

N(8)-C(42)	1.306(5)			N(1)-Eu(1)-C(12)	48.03(10)
N(8)-C(43)	1.473(6)	O(4)-Eu(1)-O(2)	144.80(9)	N(2)-Eu(1)-C(12)	112.17(10)
C(1)-C(2)	1.527(6)	O(4)-Eu(1)-O(1)	82.50(9)	N(4)-Eu(1)-C(12)	71.57(10)
C(3)-C(4)	1.527(6)	O(2)-Eu(1)-O(1)	87.79(10)	C(21)-Eu(1)-C(12)	91.83(10)
C(5)-C(6)	1.519(6)	O(4)-Eu(1)-O(3)	87.83(9)	C(42)-Eu(1)-C(12)	86.76(10)
C(7)-C(8)	1.519(6)	O(2)-Eu(1)-O(3)	83.18(10)	C(12)-O(1)-Eu(1)	124.8(3)
C(11)-C(12)	1.516(5)	O(1)-Eu(1)-O(3)	148.76(9)	C(21)-O(2)-Eu(1)	124.6(3)
C(13)-C(14)	1.499(6)	O(4)-Eu(1)-O(5)	71.98(9)	C(32)-O(3)-Eu(1)	124.4(3)
C(13)-C(15)	1.526(6)	O(2)-Eu(1)-O(5)	72.81(10)	C(42)-O(4)-Eu(1)	125.3(2)
C(15)-C(16)	1.366(7)	O(1)-Eu(1)-O(5)	73.59(9)	C(11)-N(1)-C(8)	111.1(3)
C(15)-C(20)	1.393(7)	O(3)-Eu(1)-O(5)	75.17(9)	C(11)-N(1)-C(1)	109.2(3)
C(16)-C(17)	1.380(7)	O(4)-Eu(1)-N(3)	73.97(9)	C(8)-N(1)-C(1)	108.6(3)
C(17)-C(18)	1.375(8)	O(2)-Eu(1)-N(3)	130.49(10)	C(11)-N(1)-Eu(1)	105.1(2)
C(18)-C(19)	1.359(9)	O(1)-Eu(1)-N(3)	137.99(10)	C(8)-N(1)-Eu(1)	111.6(2)
C(19)-C(20)	1.399(8)	O(3)-Eu(1)-N(3)	65.33(10)	C(1)-N(1)-Eu(1)	111.3(2)
C(21)-C(22)	1.509(6)	O(5)-Eu(1)-N(3)	127.97(10)	C(22)-N(2)-C(3)	108.8(3)
C(23)-C(25)	1.505(8)	O(4)-Eu(1)-N(1)	129.39(10)	C(22)-N(2)-C(2)	110.0(3)
C(23)-C(24)	1.528(7)	O(2)-Eu(1)-N(1)	74.81(10)	C(3)-N(2)-C(2)	108.9(3)
C(25)-C(30)	1.391(7)	O(1)-Eu(1)-N(1)	65.75(9)	C(22)-N(2)-Eu(1)	105.6(2)
C(25)-C(26)	1.398(8)	O(3)-Eu(1)-N(1)	138.51(10)	C(3)-N(2)-Eu(1)	110.9(2)
C(26)-C(27)	1.352(10)	O(5)-Eu(1)-N(1)	128.17(9)	C(2)-N(2)-Eu(1)	112.5(2)
C(27)-C(28)	1.377(10)	N(3)-Eu(1)-N(1)	103.84(10)	C(31)-N(3)-C(4)	110.6(3)
C(28)-C(29)	1.399(10)	O(4)-Eu(1)-N(2)	141.71(10)	C(31)-N(3)-C(5)	109.2(3)
C(29)-C(30)	1.390(8)	O(2)-Eu(1)-N(2)	66.20(10)	C(4)-N(3)-C(5)	108.8(3)
C(31)-C(32)	1.515(6)	O(1)-Eu(1)-N(2)	130.52(10)	C(31)-N(3)-Eu(1)	106.5(2)
C(33)-C(35)	1.505(7)	O(3)-Eu(1)-N(2)	71.97(10)	C(4)-N(3)-Eu(1)	110.2(2)
C(33)-C(34)	1.519(7)	O(5)-Eu(1)-N(2)	129.51(10)	C(5)-N(3)-Eu(1)	111.6(2)
C(35)-C(40)	1.355(9)	N(3)-Eu(1)-N(2)	68.11(10)	C(41)-N(4)-C(7)	109.4(3)
C(35)-C(36)	1.397(9)	N(1)-Eu(1)-N(2)	67.07(10)	C(41)-N(4)-C(6)	110.0(3)
C(36)-C(37)	1.397(12)	O(4)-Eu(1)-N(4)	65.63(10)	C(7)-N(4)-C(6)	109.0(3)
C(37)-C(38)	1.326(14)	O(2)-Eu(1)-N(4)	141.66(10)	C(41)-N(4)-Eu(1)	105.8(2)
C(38)-C(39)	1.377(14)	O(1)-Eu(1)-N(4)	71.55(9)	C(7)-N(4)-Eu(1)	111.1(2)
C(39)-C(40)	1.401(9)	O(3)-Eu(1)-N(4)	130.29(9)	C(6)-N(4)-Eu(1)	111.5(2)
C(41)-C(42)	1.511(5)	O(5)-Eu(1)-N(4)	127.49(10)	C(12)-N(5)-C(13)	121.6(4)
C(43)-C(45)	1.499(6)	N(3)-Eu(1)-N(4)	67.16(10)	C(21)-N(6)-C(23)	121.1(4)
C(43)-C(44)	1.533(6)	N(1)-Eu(1)-N(4)	67.35(10)	C(32)-N(7)-C(33)	121.5(4)
C(45)-C(50)	1.372(7)	N(2)-Eu(1)-N(4)	102.99(10)	C(42)-N(8)-C(43)	120.1(3)
C(45)-C(46)	1.386(7)	O(4)-Eu(1)-C(21)	155.32(10)	N(1)-C(1)-C(2)	111.5(3)
C(46)-C(47)	1.412(8)	O(2)-Eu(1)-C(21)	18.64(10)	N(2)-C(2)-C(1)	112.8(3)
C(47)-C(48)	1.346(9)	O(1)-Eu(1)-C(21)	103.81(10)	N(2)-C(3)-C(4)	111.2(3)
C(48)-C(49)	1.397(9)	O(3)-Eu(1)-C(21)	74.40(11)	N(3)-C(4)-C(3)	114.7(3)
C(49)-C(50)	1.393(7)	O(5)-Eu(1)-C(21)	86.75(10)	N(3)-C(5)-C(6)	111.9(3)
C(101)-C(102)	1.526(7)	N(3)-Eu(1)-C(21)	112.14(10)	N(4)-C(6)-C(5)	113.0(3)
C(102)-F(11)	1.264(7)	N(1)-Eu(1)-C(21)	73.73(11)	N(4)-C(7)-C(8)	112.0(3)
C(102)-F(12)	1.320(8)	N(2)-Eu(1)-C(21)	48.12(10)	N(1)-C(8)-C(7)	113.7(3)
C(102)-F(13)	1.339(7)	N(4)-Eu(1)-C(21)	139.05(11)	N(1)-C(11)-C(12)	110.7(3)
C(201)-C(202)	1.520(9)	O(4)-Eu(1)-C(42)	18.42(9)	O(1)-C(12)-N(5)	121.7(4)
C(202)-F(21)	1.304(8)	O(2)-Eu(1)-C(42)	153.88(9)	O(1)-C(12)-C(11)	119.0(4)
C(202)-F(22)	1.327(8)	O(1)-Eu(1)-C(42)	72.88(9)	N(5)-C(12)-C(11)	119.2(3)
C(202)-F(23)	1.355(10)	O(3)-Eu(1)-C(42)	104.17(10)	O(1)-C(12)-Eu(1)	36.8(2)
C(301)-C(302)	1.521(8)	O(5)-Eu(1)-C(42)	84.73(9)	N(5)-C(12)-Eu(1)	158.6(3)
C(302)-F(31)	1.289(11)	N(3)-Eu(1)-C(42)	74.13(9)	C(11)-C(12)-Eu(1)	82.2(2)
C(302)-F(33)	1.303(8)	N(1)-Eu(1)-C(42)	111.09(10)	N(5)-C(13)-C(14)	109.7(4)
C(302)-F(32)	1.362(10)	N(2)-Eu(1)-C(42)	139.91(10)	N(5)-C(13)-C(15)	111.8(3)
C(401)-C(402)	1.509(10)	N(4)-Eu(1)-C(42)	48.08(10)	C(14)-C(13)-C(15)	111.9(4)
C(402)-F(43)	1.278(11)	C(21)-Eu(1)-C(42)	171.44(10)	C(16)-C(15)-C(20)	118.0(5)
C(402)-F(41)	1.309(8)	O(4)-Eu(1)-C(12)	99.02(10)	C(16)-C(15)-C(13)	120.6(4)
C(402)-F(42)	1.327(13)	O(2)-Eu(1)-C(12)	78.85(10)	C(20)-C(15)-C(13)	121.3(4)
N(9)-C(501)	1.39(2)	O(1)-Eu(1)-C(12)	18.40(10)	C(15)-C(16)-C(17)	121.9(5)
C(501)-C(502)	1.44(2)	O(3)-Eu(1)-C(12)	157.41(9)	C(16)-C(17)-C(18)	119.6(5)
N(10)-C(601)	1.185(11)	O(5)-Eu(1)-C(12)	86.45(9)	C(19)-C(18)-C(17)	120.2(5)
C(601)-C(602)	1.364(12)	N(3)-Eu(1)-C(12)	137.24(10)	C(18)-C(19)-C(20)	120.1(5)

C(15)-C(20)-C(19)	120.2(5)	C(36)-C(35)-C(33)	119.0(6)	F(12)-C(102)-C(101)	109.8(5)
O(2)-C(21)-N(6)	121.6(4)	C(35)-C(36)-C(37)	119.0(9)	F(13)-C(102)-C(101)	113.5(4)
O(2)-C(21)-C(22)	119.7(3)	C(38)-C(37)-C(36)	121.8(9)	O(21)-C(201)-O(22)	128.1(6)
N(6)-C(21)-C(22)	118.6(4)	C(37)-C(38)-C(39)	119.3(8)	O(21)-C(201)-C(202)	119.9(5)
O(2)-C(21)-Eu(1)	36.7(2)	C(38)-C(39)-C(40)	120.9(9)	O(22)-C(201)-C(202)	112.0(5)
N(6)-C(21)-Eu(1)	158.2(3)	C(35)-C(40)-C(39)	119.5(7)	F(21)-C(202)-F(22)	108.4(6)
C(22)-C(21)-Eu(1)	83.1(2)	N(4)-C(41)-C(42)	111.6(3)	F(21)-C(202)-F(23)	105.1(7)
N(2)-C(22)-C(21)	111.0(3)	O(4)-C(42)-N(8)	121.4(3)	F(22)-C(202)-F(23)	105.4(6)
N(6)-C(23)-C(25)	112.5(4)	O(4)-C(42)-C(41)	120.0(3)	F(21)-C(202)-C(201)	114.3(6)
N(6)-C(23)-C(24)	108.2(4)	N(8)-C(42)-C(41)	118.6(3)	F(22)-C(202)-C(201)	112.6(6)
C(25)-C(23)-C(24)	112.3(4)	O(4)-C(42)-Eu(1)	36.3(2)	F(23)-C(202)-C(201)	110.4(6)
C(30)-C(25)-C(26)	118.4(6)	N(8)-C(42)-Eu(1)	157.5(3)	O(31)-C(301)-O(32)	127.5(5)
C(30)-C(25)-C(23)	119.9(5)	C(41)-C(42)-Eu(1)	83.7(2)	O(31)-C(301)-C(302)	113.7(5)
C(26)-C(25)-C(23)	121.8(5)	N(8)-C(43)-C(45)	111.6(4)	O(32)-C(301)-C(302)	118.8(5)
C(27)-C(26)-C(25)	120.1(6)	N(8)-C(43)-C(44)	108.7(4)	F(31)-C(302)-F(33)	109.4(8)
C(26)-C(27)-C(28)	122.2(7)	C(45)-C(43)-C(44)	113.0(4)	F(31)-C(302)-F(32)	103.1(7)
C(27)-C(28)-C(29)	119.2(6)	C(50)-C(45)-C(46)	118.6(5)	F(33)-C(302)-F(32)	108.1(7)
C(30)-C(29)-C(28)	118.7(6)	C(50)-C(45)-C(43)	121.7(4)	F(31)-C(302)-C(301)	111.2(7)
C(29)-C(30)-C(25)	121.4(6)	C(46)-C(45)-C(43)	119.7(4)	F(33)-C(302)-C(301)	114.2(5)
N(3)-C(31)-C(32)	111.2(3)	C(45)-C(46)-C(47)	120.4(5)	F(32)-C(302)-C(301)	110.2(7)
O(3)-C(32)-N(7)	122.5(4)	C(48)-C(47)-C(46)	120.0(6)	O(42)-C(401)-O(41)	127.7(6)
O(3)-C(32)-C(31)	120.1(3)	C(47)-C(48)-C(49)	120.7(5)	O(42)-C(401)-C(402)	118.9(5)
N(7)-C(32)-C(31)	117.4(4)	C(50)-C(49)-C(48)	118.8(5)	O(41)-C(401)-C(402)	113.4(5)
O(3)-C(32)-Eu(1)	37.2(2)	C(45)-C(50)-C(49)	121.6(5)	F(43)-C(402)-F(41)	111.9(8)
N(7)-C(32)-Eu(1)	159.4(3)	O(11)-C(101)-O(12)	128.2(5)	F(43)-C(402)-F(42)	100.4(8)
C(31)-C(32)-Eu(1)	82.9(2)	O(11)-C(101)-C(102)	118.1(4)	F(41)-C(402)-F(42)	106.3(9)
N(7)-C(33)-C(35)	111.4(4)	O(12)-C(101)-C(102)	113.7(4)	F(43)-C(402)-C(401)	113.9(8)
N(7)-C(33)-C(34)	109.7(5)	F(11)-C(102)-F(12)	109.1(6)	F(41)-C(402)-C(401)	113.6(6)
C(35)-C(33)-C(34)	111.0(4)	F(11)-C(102)-F(13)	106.5(5)	F(42)-C(402)-C(401)	109.7(8)
C(40)-C(35)-C(36)	119.6(6)	F(12)-C(102)-F(13)	102.2(5)	N(9)-C(501)-C(502)	166.6(39)
C(40)-C(35)-C(33)	121.4(5)	F(11)-C(102)-C(101)	114.9(5)	N(10)-C(601)-C(602)	178.0(9)

***Table A.6.2.4** - Anisotropic displacement parameters ($Å^2 x\ 10^3$) for C60 H73 Eu F12 N10 O13. The anisotropic displacement factor exponent takes the form: $-2\pi^2[h^2 a^{*2} U^{11} + ... + 2 h k a^* b^* U^{12}]$*

	U^{11}	U^{22}	U^{33}	U^{23}	U^{13}	U^{12}
Eu(1)	10(1)	19(1)	19(1)	1(1)	0(1)	1(1)
O(1)	20(1)	25(1)	21(1)	1(1)	2(1)	3(1)
O(2)	11(1)	35(2)	31(1)	7(1)	1(1)	3(1)
O(3)	23(2)	26(2)	26(2)	-1(1)	-2(1)	-4(1)
O(4)	12(1)	24(1)	26(2)	-1(1)	1(1)	0(1)
O(5)	19(1)	25(1)	35(1)	8(1)	-1(1)	-2(1)
O(11)	24(2)	71(3)	65(2)	18(2)	3(2)	10(2)
O(12)	24(2)	48(2)	109(4)	13(2)	18(2)	3(2)
O(21)	52(2)	53(2)	67(3)	12(2)	27(2)	-1(2)
O(22)	107(4)	68(3)	67(3)	-6(2)	50(3)	-39(3)
O(31)	82(3)	58(2)	30(2)	8(2)	-10(2)	-34(2)
O(32)	105(4)	60(3)	58(3)	-22(2)	14(3)	-33(3)
O(41)	61(3)	59(3)	61(3)	5(2)	29(2)	-19(2)
O(42)	61(3)	40(2)	84(3)	5(2)	40(2)	-6(2)
N(1)	22(2)	24(2)	23(2)	2(1)	1(1)	4(1)
N(2)	16(2)	30(2)	25(2)	2(2)	-2(1)	4(1)
N(3)	17(2)	26(2)	21(2)	-1(1)	-1(1)	0(1)
N(4)	18(2)	23(2)	22(2)	1(1)	1(1)	-2(1)

N(5)	28(2)	34(2)	20(2)	-3(1)	0(1)	10(2)
N(6)	13(2)	41(2)	44(2)	10(2)	0(1)	6(2)
N(7)	30(2)	34(2)	30(2)	-6(2)	-3(1)	-4(2)
N(8)	14(2)	29(2)	38(2)	-5(2)	-1(1)	-2(1)
C(1)	24(2)	27(2)	29(2)	2(2)	0(2)	11(2)
C(2)	25(2)	28(2)	28(2)	3(2)	-6(2)	7(2)
C(3)	23(2)	36(2)	26(2)	1(2)	-11(2)	5(2)
C(4)	29(2)	32(2)	21(2)	7(2)	0(2)	6(2)
C(5)	22(2)	32(2)	22(2)	4(2)	5(2)	-4(2)
C(6)	26(2)	25(2)	24(2)	7(2)	4(2)	-7(2)
C(7)	25(2)	20(2)	30(2)	-1(2)	0(2)	-3(2)
C(8)	31(2)	19(2)	32(2)	-1(2)	2(2)	1(2)
C(11)	28(2)	33(2)	20(2)	-3(2)	2(2)	8(2)
C(12)	20(2)	24(2)	22(2)	2(2)	5(2)	1(2)
C(13)	32(2)	35(2)	22(2)	6(2)	0(2)	7(2)
C(14)	49(4)	89(5)	23(2)	5(3)	1(2)	25(3)
C(15)	27(2)	35(2)	22(2)	4(2)	-6(2)	2(2)
C(16)	30(2)	33(2)	33(2)	5(2)	-5(2)	4(2)
C(17)	26(2)	63(4)	45(3)	10(3)	-2(2)	8(2)
C(18)	26(3)	69(4)	62(4)	23(3)	-6(2)	-2(3)
C(19)	42(3)	49(3)	73(4)	23(3)	-24(3)	-16(3)
C(20)	41(3)	37(3)	50(3)	5(2)	-11(2)	3(2)
C(21)	15(2)	29(2)	36(2)	2(2)	2(2)	3(2)
C(22)	13(2)	39(3)	36(2)	3(2)	-5(2)	0(2)
C(23)	18(2)	48(3)	46(3)	15(2)	8(2)	3(2)
C(24)	25(3)	73(4)	69(4)	21(3)	11(3)	-8(3)
C(25)	28(2)	44(3)	40(3)	11(2)	18(2)	2(2)
C(26)	43(3)	51(4)	64(4)	6(3)	13(3)	16(3)
C(27)	75(5)	57(4)	73(5)	-10(3)	28(4)	12(4)
C(28)	81(5)	80(5)	49(4)	-14(3)	25(4)	-17(4)
C(29)	63(4)	88(5)	33(3)	10(3)	4(3)	-15(4)
C(30)	40(3)	49(3)	42(3)	13(2)	6(2)	0(2)
C(31)	23(2)	30(2)	26(2)	-4(2)	3(2)	1(2)
C(32)	20(2)	24(2)	27(2)	-1(1)	-7(2)	3(2)
C(33)	42(3)	32(2)	46(3)	-2(2)	-4(3)	-12(2)
C(34)	52(4)	38(3)	83(4)	-20(3)	-12(3)	-7(3)
C(35)	36(3)	44(3)	59(3)	-19(3)	-2(3)	-18(2)
C(36)	58(4)	67(4)	76(4)	-24(4)	16(3)	-34(3)
C(37)	49(5)	104(7)	164(10)	-77(7)	43(6)	-42(5)
C(38)	29(4)	101(7)	179(11)	-66(7)	5(5)	-2(4)
C(39)	44(4)	94(6)	126(7)	-27(5)	-19(5)	14(4)
C(40)	43(3)	66(4)	67(4)	-15(3)	-10(3)	3(3)
C(41)	15(2)	29(2)	26(2)	-1(2)	1(2)	-4(2)
C(42)	15(2)	25(2)	16(2)	1(2)	2(2)	0(1)
C(43)	22(2)	27(2)	40(2)	0(2)	-1(2)	6(2)
C(44)	30(2)	38(3)	68(4)	-5(3)	-12(3)	15(2)
C(45)	21(2)	28(2)	42(3)	-7(2)	2(2)	12(2)
C(46)	38(3)	45(3)	45(3)	-7(3)	10(3)	3(2)
C(47)	58(4)	54(4)	43(3)	-9(3)	11(3)	11(3)
C(48)	64(4)	49(3)	48(3)	-17(3)	-10(3)	21(3)
C(49)	36(3)	36(3)	55(3)	-19(2)	-11(2)	10(2)
C(50)	26(3)	29(2)	48(3)	-8(2)	-2(2)	9(2)
C(101)	12(2)	36(2)	48(2)	-7(2)	-4(2)	1(2)
C(102)	37(3)	59(3)	55(3)	15(3)	7(2)	9(3)
C(201)	46(3)	49(3)	42(3)	7(3)	11(2)	-2(3)
C(202)	90(5)	60(4)	50(3)	3(3)	13(4)	7(4)
C(301)	37(3)	41(2)	43(2)	-13(2)	1(2)	-2(2)
C(302)	135(8)	74(4)	38(3)	-13(3)	-25(4)	37(5)
C(401)	45(3)	47(3)	60(3)	16(3)	17(3)	-2(3)
C(402)	109(7)	60(5)	92(6)	-15(4)	58(5)	-25(4)
F(11)	74(3)	214(6)	99(3)	87(4)	-21(3)	6(4)
F(12)	181(6)	67(3)	178(6)	-5(3)	96(5)	-56(3)

F(13)	53(2)	136(4)	70(2)	34(2)	30(2)	20(2)
F(21)	212(7)	77(3)	80(3)	26(3)	36(4)	60(4)
F(22)	165(5)	82(3)	64(2)	-2(2)	61(3)	10(3)
F(23)	150(6)	114(4)	123(5)	-43(4)	-36(4)	-26(4)
F(31)	263(10)	130(5)	117(5)	54(4)	122(6)	46(5)
F(33)	222(7)	73(3)	70(3)	3(2)	-36(3)	76(4)
F(32)	215(7)	145(5)	81(3)	-38(3)	-92(4)	84(5)
F(41)	137(5)	101(4)	97(3)	-24(3)	65(3)	-47(3)
F(42)	194(8)	294(13)	150(6)	-106(7)	49(6)	-157(9)
F(43)	255(10)	72(4)	185(7)	8(4)	127(7)	18(5)
N(10)	123(7)	73(5)	150(7)	-46(5)	-58(6)	37(4)
C(601)	65(5)	54(4)	105(6)	-29(4)	-22(4)	10(3)
C(602)	116(8)	86(6)	119(7)	-1(5)	7(7)	-18(6)

***Table A.6.2.5** - Hydrogen coordinates (x 10^4) and isotropic displacement parameters ($Å^2$x 10^3) for C60 H73 Eu F12 N10 O13.*

	x	y	z	U(eq)
H(5)	3158(2)	751(2)	-120(1)	33
H(6)	-812(2)	-512(2)	-1620(2)	39
H(7)	2196(3)	-2199(2)	-3585(1)	37
H(8)	6012(2)	-960(2)	-1984(1)	33
H(1A)	1226(3)	1510(2)	-1694(2)	32
H(1B)	833(3)	729(2)	-1533(2)	32
H(2A)	549(3)	961(2)	-2453(2)	33
H(2B)	1595(3)	1082(2)	-2561(2)	33
H(3A)	1004(3)	264(2)	-3251(2)	34
H(3B)	1234(3)	-578(2)	-3158(2)	34
H(4A)	2435(3)	11(2)	-3602(2)	33
H(4B)	2521(3)	579(2)	-3118(2)	33
H(5A)	4021(3)	77(2)	-3377(2)	31
H(5B)	4397(3)	-467(2)	-2927(2)	31
H(6A)	4692(3)	746(2)	-2677(2)	30
H(6B)	3648(3)	937(2)	-2712(2)	30
H(7A)	4237(3)	1406(2)	-1855(2)	30
H(7B)	3986(3)	923(2)	-1341(2)	30
H(8A)	2812(3)	1737(2)	-1534(2)	33
H(8B)	2731(3)	1418(2)	-2130(2)	33
H(11A)	1623(3)	496(2)	-844(2)	33
H(11B)	2261(3)	1196(2)	-812(2)	33
H(13)	3860(3)	-616(3)	-152(2)	35
H(14A)	4486(20)	-359(14)	675(2)	65
H(14B)	3471(7)	-76(20)	674(3)	65
H(14C)	4278(24)	490(8)	605(2)	65
H(16)	5215(3)	-1009(3)	-500(2)	39
H(17)	6595(3)	-823(3)	-907(2)	54
H(18)	7179(4)	348(3)	-969(2)	63
H(19)	6361(4)	1327(3)	-659(3)	65
H(20)	4964(4)	1140(3)	-247(2)	51
H(22A)	388(3)	-832(3)	-2520(2)	36
H(22B)	-93(3)	-75(3)	-2382(2)	36
H(23)	54(3)	-1283(3)	-847(2)	45
H(24A)	-1317(6)	-1274(20)	-389(7)	67

H(24B)	-1501(10)	-1435(16)	-1012(10)	67
H(24C)	-1690(6)	-642(5)	-771(15)	67
H(26)	-760(4)	579(3)	-782(3)	63
H(27)	-206(5)	1437(4)	-206(3)	82
H(28)	878(5)	1155(4)	429(3)	84
H(29)	1450(5)	-43(4)	473(2)	73
H(30)	910(4)	-916(3)	-130(2)	52
H(31A)	3611(3)	-1380(2)	-3125(2)	31
H(31B)	2942(3)	-1091(2)	-3582(2)	31
H(33)	1444(3)	-2791(3)	-2688(2)	48
H(34A)	833(20)	-3666(9)	-3265(9)	69
H(34B)	1860(7)	-3537(12)	-3423(13)	69
H(34C)	1080(26)	-3182(4)	-3779(5)	69
H(36)	81(5)	-2588(4)	-2275(3)	80
H(37)	-1340(6)	-2048(6)	-2254(5)	127
H(38)	-1900(5)	-1456(5)	-2981(5)	124
H(39)	-1043(5)	-1364(5)	-3760(4)	106
H(40)	397(4)	-1877(4)	-3799(3)	70
H(41A)	4833(2)	38(2)	-1455(2)	28
H(41B)	5314(2)	184(2)	-2021(2)	28
H(43)	5040(3)	-2204(2)	-1858(2)	35
H(44A)	6877(4)	-2052(13)	-2171(10)	54
H(44B)	6423(8)	-2817(4)	-2030(13)	54
H(44C)	6527(10)	-2208(17)	-1574(4)	54
H(46)	6164(3)	-1537(3)	-3035(2)	51
H(47)	5714(4)	-1781(3)	-3927(2)	62
H(48)	4543(5)	-2557(3)	-4090(2)	64
H(49)	3769(4)	-3104(3)	-3372(2)	51
H(50)	4189(3)	-2829(3)	-2488(2)	41
H(50A)	-2793(81)	658(16)	502(106)	531
H(50B)	-1764(111)	440(54)	420(89)	531
H(50C)	-2214(192)	375(41)	1002(20)	531
H(60A)	8183(15)	6921(41)	-113(7)	161
H(60B)	7172(39)	6649(29)	-192(11)	161
H(60C)	7427(50)	7479(15)	-309(5)	161

***Table A.6.3.2** - Atomic coordinates (x 10^4) and equivalent isotropic displacement parameters ($Å^2$x 10^3) for $C_{16}H_{21}NO_8$. U(eq) is defined as one third of the trace of the orthogonalized U^{ij} tensor.*

	x	y	z	U(eq)
C(1)	3897(1)	6698(3)	-737(1)	21(1)
C(2)	4275(1)	6566(3)	233(1)	21(1)
C(3)	3941(1)	5773(3)	1482(1)	26(1)
C(4)	3174(1)	4779(3)	1603(2)	27(1)
C(5)	1492(1)	4751(3)	1084(2)	33(1)
C(6)	1148(2)	3487(3)	277(2)	35(1)
C(7)	647(2)	3491(3)	-1327(1)	32(1)
C(8)	303(1)	4752(3)	-2137(2)	31(1)
C(9)	1611(1)	5159(3)	-2484(2)	29(1)
C(10)	2524(1)	6198(3)	-2170(1)	28(1)
C(11)	4415(1)	7489(3)	-1139(1)	23(1)
C(12)	5321(1)	8126(3)	-558(1)	22(1)
C(13)	5700(1)	7971(3)	382(1)	22(1)
C(14)	5184(1)	7205(3)	802(1)	22(1)
C(15)	6672(1)	8776(3)	787(1)	24(1)
C(17)	6034(1)	9059(3)	-780(1)	24(1)
O(1)	3016(1)	5954(2)	-1196(1)	26(1)
O(2)	3679(1)	5768(2)	521(1)	25(1)
O(3)	2306(1)	5786(2)	1188(1)	27(1)
O(4)	848(1)	4544(2)	-532(1)	30(1)
O(5)	1039(1)	5948(2)	-2103(1)	28(1)
O(6)	5966(1)	9482(2)	-1527(1)	32(1)
O(7)	7241(1)	8918(2)	1589(1)	30(1)
N(1)	6820(1)	9362(2)	54(1)	25(1)
O(1S)	8309(1)	11737(2)	379(1)	39(1)

***Table A.6.3.3** - Bond lengths [Å] and angles [°] for $C_{16}H_{21}NO_8$.*

C(1)-O(1)	1.357(2)	N(1)-H(1)	0.87(3)	C(7)-C(8)-H(8A)	106.8(12)
C(1)-C(11)	1.378(3)	O(1S)-H(1SB)	0.95(4)	H(8B)-C(8)-H(8A)	108.4(17)
C(1)-C(2)	1.423(3)	O(1S)-H(1SA)	0.88(4)	O(5)-C(9)-C(10)	109.14(18)
C(2)-O(2)	1.352(2)			O(5)-C(9)-H(9B)	111.2(12)
C(2)-C(14)	1.389(3)	O(1)-C(1)-C(11)	125.23(17)	C(10)-C(9)-H(9B)	107.4(12)
C(3)-O(2)	1.432(2)	O(1)-C(1)-C(2)	113.65(16)	O(5)-C(9)-H(9A)	110.6(12)
C(3)-C(4)	1.494(3)	C(11)-C(1)-C(2)	121.11(16)	C(10)-C(9)-H(9A)	109.7(11)
C(3)-H(3B)	1.00(2)	O(2)-C(2)-C(14)	125.10(17)	H(9B)-C(9)-H(9A)	108.7(17)
C(3)-H(3A)	0.98(2)	O(2)-C(2)-C(1)	114.00(15)	O(1)-C(10)-C(9)	105.80(17)
C(4)-O(3)	1.427(2)	C(14)-C(2)-C(1)	120.90(17)	O(1)-C(10)-H(10B)	108.5(12)
C(4)-H(4B)	0.98(2)	O(2)-C(3)-C(4)	106.71(16)	C(9)-C(10)-H(10B)	111.5(11)
C(4)-H(4A)	1.01(2)	O(2)-C(3)-H(3B)	109.7(12)	O(1)-C(10)-H(10A)	110.9(12)
C(5)-O(3)	1.429(2)	C(4)-C(3)-H(3B)	108.6(12)	C(9)-C(10)-H(10A)	108.5(12)
C(5)-C(6)	1.506(3)	O(2)-C(3)-H(3A)	111.0(12)	H(10B)-C(10)-H(10A)	111.5(17)
C(5)-H(5B)	1.01(2)	C(4)-C(3)-H(3A)	111.9(12)	C(1)-C(11)-C(12)	117.17(17)
C(5)-H(5A)	0.96(2)	H(3B)-C(3)-H(3A)	109.0(17)	C(1)-C(11)-H(11)	121.3(11)
C(6)-O(4)	1.421(3)	O(3)-C(4)-C(3)	109.19(18)	C(12)-C(11)-H(11)	121.5(11)
C(6)-H(6B)	1.01(2)	O(3)-C(4)-H(4B)	109.3(12)	C(13)-C(12)-C(11)	122.07(17)
C(6)-H(6A)	0.98(2)	C(3)-C(4)-H(4B)	107.5(12)	C(13)-C(12)-C(17)	108.14(16)
C(7)-O(4)	1.422(3)	O(3)-C(4)-H(4A)	109.4(12)	C(11)-C(12)-C(17)	129.78(17)
C(7)-C(8)	1.508(3)	C(3)-C(4)-H(4A)	111.5(12)	C(12)-C(13)-C(14)	121.68(17)
C(7)-H(7B)	1.01(2)	H(4B)-C(4)-H(4A)	109.9(17)	C(12)-C(13)-C(15)	107.95(16)
C(7)-H(7A)	1.00(2)	O(3)-C(5)-C(6)	113.03(18)	C(14)-C(13)-C(15)	130.35(17)
C(8)-O(5)	1.434(2)	O(3)-C(5)-H(5B)	106.1(13)	C(2)-C(14)-C(13)	117.04(17)
C(8)-H(8B)	1.02(2)	C(6)-C(5)-H(5B)	109.1(13)	C(2)-C(14)-H(14)	122.1(11)
C(8)-H(8A)	1.01(2)	O(3)-C(5)-H(5A)	110.7(13)	C(13)-C(14)-H(14)	120.9(11)
C(9)-O(5)	1.420(2)	C(6)-C(5)-H(5A)	109.7(14)	O(7)-C(15)-N(1)	125.36(18)
C(9)-C(10)	1.497(3)	H(5B)-C(5)-H(5A)	108.1(18)	O(7)-C(15)-C(13)	128.79(19)
C(9)-H(9B)	0.97(2)	O(4)-C(6)-C(5)	107.95(19)	N(1)-C(15)-C(13)	105.85(16)
C(9)-H(9A)	1.02(2)	O(4)-C(6)-H(6B)	109.2(13)	O(6)-C(17)-N(1)	125.75(18)
C(10)-O(1)	1.434(2)	C(5)-C(6)-H(6B)	107.2(13)	O(6)-C(17)-C(12)	128.54(18)
C(10)-H(10B)	0.98(2)	O(4)-C(6)-H(6A)	108.5(13)	N(1)-C(17)-C(12)	105.71(17)
C(10)-H(10A)	0.97(2)	C(5)-C(6)-H(6A)	111.6(13)	C(1)-O(1)-C(10)	118.07(15)
C(11)-C(12)	1.390(3)	H(6B)-C(6)-H(6A)	112(2)	C(2)-O(2)-C(3)	118.22(14)
C(11)-H(11)	0.988(19)	O(4)-C(7)-C(8)	107.74(19)	C(4)-O(3)-C(5)	112.51(16)
C(12)-C(13)	1.380(3)	O(4)-C(7)-H(7B)	108.9(12)	C(6)-O(4)-C(7)	112.90(17)
C(12)-C(17)	1.486(3)	C(8)-C(7)-H(7B)	107.8(12)	C(9)-O(5)-C(8)	112.23(16)
C(13)-C(14)	1.391(3)	O(4)-C(7)-H(7A)	109.3(12)	C(17)-N(1)-C(15)	112.31(17)
C(13)-C(15)	1.486(3)	C(8)-C(7)-H(7A)	111.9(12)	C(17)-N(1)-H(1)	122.6(16)
C(14)-H(14)	0.949(19)	H(7B)-C(7)-H(7A)	111.0(19)	C(15)-N(1)-H(1)	124.0(16)
C(15)-O(7)	1.214(2)	O(5)-C(8)-C(7)	112.56(16)	H(1SB)-O(1S)-H(1SA)	110(3)
C(15)-N(1)	1.385(3)	O(5)-C(8)-H(8B)	109.0(12)		
C(17)-O(6)	1.216(2)	C(7)-C(8)-H(8B)	112.0(13)		
C(17)-N(1)	1.385(3)	O(5)-C(8)-H(8A)	107.8(12)		

***Table A.6.3.4** - Anisotropic displacement parameters ($Å^2 x\ 10^3$) for $C_{16}H_{21}NO_8$. The anisotropic displacement factor exponent takes the form: $-2\pi^2[h^2 a^{*2}U^{11} + ... + 2\,h\,k\,a^*\,b^*\,U^{12}]$*

	U^{11}	U^{22}	U^{33}	U^{23}	U^{13}	U^{12}
C(1)	18(1)	18(1)	23(1)	-1(1)	6(1)	5(1)
C(2)	22(1)	18(1)	23(1)	1(1)	10(1)	6(1)
C(3)	28(1)	28(1)	19(1)	0(1)	9(1)	1(1)
C(4)	28(1)	28(1)	26(1)	2(1)	12(1)	4(1)
C(5)	28(1)	44(2)	29(1)	3(1)	14(1)	-3(1)
C(6)	33(1)	34(1)	32(1)	5(1)	10(1)	-7(1)
C(7)	34(1)	29(1)	30(1)	-4(1)	10(1)	-7(1)
C(8)	23(1)	34(1)	28(1)	-1(1)	6(1)	-6(1)

C(9)	27(1)	31(1)	22(1)	-2(1)	5(1)	0(1)
C(10)	26(1)	34(1)	19(1)	2(1)	6(1)	0(1)
C(11)	25(1)	21(1)	21(1)	1(1)	9(1)	5(1)
C(12)	25(1)	16(1)	25(1)	0(1)	12(1)	5(1)
C(13)	21(1)	16(1)	24(1)	-2(1)	7(1)	5(1)
C(14)	24(1)	21(1)	19(1)	-1(1)	8(1)	6(1)
C(15)	25(1)	18(1)	28(1)	-3(1)	11(1)	5(1)
C(17)	26(1)	18(1)	28(1)	-1(1)	11(1)	4(1)
O(1)	22(1)	32(1)	19(1)	2(1)	5(1)	-2(1)
O(2)	24(1)	32(1)	19(1)	0(1)	9(1)	-1(1)
O(3)	24(1)	26(1)	29(1)	-1(1)	11(1)	1(1)
O(4)	35(1)	27(1)	25(1)	0(1)	10(1)	-4(1)
O(5)	24(1)	25(1)	30(1)	0(1)	9(1)	0(1)
O(6)	35(1)	32(1)	29(1)	2(1)	16(1)	-1(1)
O(7)	27(1)	32(1)	26(1)	-4(1)	6(1)	0(1)
N(1)	23(1)	24(1)	28(1)	-1(1)	12(1)	-1(1)
O(1S)	37(1)	29(1)	47(1)	2(1)	14(1)	-4(1)

***Table A.6.3.5** - Hydrogen coordinates (x 10^4) and isotropic displacement parameters ($Å^2$x 10^3) for $C_{16}H_{21}NO_8$*

	x	y	z	U(eq)
H(3B)	4557(15)	5110(30)	1820(14)	32(6)
H(3A)	4017(14)	7010(30)	1719(14)	26(5)
H(4B)	3085(14)	3610(30)	1289(15)	33(6)
H(4A)	3350(15)	4580(30)	2274(16)	35(6)
H(5B)	970(16)	5650(30)	988(15)	36(6)
H(5A)	1625(15)	4080(30)	1634(16)	34(6)
H(6B)	582(17)	2820(30)	263(15)	46(7)
H(6A)	1658(16)	2670(30)	312(14)	35(6)
H(7B)	108(16)	2630(30)	-1426(15)	38(6)
H(7A)	1235(15)	2830(30)	-1243(14)	33(6)
H(8B)	28(15)	4070(30)	-2746(16)	35(6)
H(8A)	-220(15)	5510(30)	-2112(14)	30(6)
H(9B)	1293(14)	5210(30)	-3146(15)	31(6)
H(9A)	1758(14)	3850(30)	-2285(14)	30(6)
H(10B)	2403(13)	7490(30)	-2299(13)	28(6)
H(10A)	2890(14)	5700(30)	-2465(14)	25(5)
H(11)	4164(13)	7540(30)	-1812(13)	17(5)
H(14)	5450(13)	7120(30)	1450(13)	20(5)
H(1)	7301(17)	10030(40)	107(16)	46(7)
H(1SB)	8480(20)	12360(50)	940(30)	99(12)
H(1SA)	8130(20)	12510(50)	-80(20)	88(12)

Appendix B

Conferences, Courses, Seminars attended and Other Periods spent Working away from Host Institution and List of Publications arising from this Thesis.

B.1 Conferences Attended

1995 - 1996

17/11/95	BCA CCG group Autumn meeting: Structural Refinement (Siemens House, Manchester.)
15/12/95–16/12/95	Fourth UK Charge Density meeting, (Trevelyan College, University of Durham.)
1/4/96–4/4/96	BCA Annual Spring meeting (University of Cambridge, U.K.) Poster presented entitled "Structural Studies of Small Ring Containing Compounds."
9/5/96–19/5/96	International School of Crystallography 24th Course; Experimental and Computational Approaches to Structure-Based Drug Design; (EMCSC, Erice, Sicily), Poster presented entitled "Solid-State Characterisation of Lanthanide Complexes based on N-Substituted Cyclododecanes."
8/8/96–18/8/96	International Union of Crystallography XVII International World Congress, (Seattle, USA), Poster presented entitled "Crystal Growth and X-ray Structure Determination of a Series of Biologically Interesting Compounds."

1996 - 1997

14/11/96	BCA CCG group Autumn meeting: Dynamic Crystallography (Daresbury Laboratory, Cheshire, U.K.)
17/3/97-18/3/97	SMART User Meeting (University of Warwick, U.K.)
14/4/97-17/4/97	BCA Annual Spring meeting (University of Leeds, U.K.), Poster presented in the CCG session entitled "Solid-State Characterisation of Lanthanide Macrocycles, with Luminescent Properties."

1997 - 1998

9/9/97-10/9/97	Synchrotron Radiation Users Meeting (Daresbury Laboratory, Cheshire, U.K.) Poster presented entitled "X-ray Structure

	Determination of Small Molecular Crystals using Station 9.8 at Daresbury SRS."
22/9/97-23/9/97	RSC Structural Fluids Conference, (Grey College, University of Durham, U.K.), Lecture: Dr. Daan Frenkel, What Van der Waals could have told us about Protein Crystallisation.
12/11/97	BCA CCG Autumn meeting: Disorder, Twinning and Incommensurate Structures (University of Bristol, U.K.)
15/11/97	84th Meeting of the Scottish Protein Structure Group (University of Edinburgh, U.K.)
1/12/97-2/12/97	British Assoc. for Crystal Growth (BACG), Polymorphism in Molecular Crystals: 100 years of Ostwald's Rule, (UMIST, Manchester, U.K.)
9/1/98-10/1/98	CCP4 organised meeting, Databases for Macromolecular Crystallographers (University of Reading, U.K.)
5/4/98-8/4/98	BCA Annual Spring meeting (University of St. Andrews, U.K.), Posters presented in the BSG poster session entitled "Ultra Low-Temperature Crystallographic Studies on CEW-Lysozyme, using the *Fddd* Cryo-Diffractometer at Durham" and the CCG poster session entitled "The Effect of Boranes on the Carbonyl Group and Hydrogen-Bonding in Carborane Derivatives."
9/4/98	RSC National Congress, (University of Durham, U.K.), Lecture: Prof. Sir Jack Baldwin,

B.2 First year induction courses (October 1995)

The course consisted of one hour lectures on the services available in the department

1. Departmental Safety
2. Safety Matters
3. Library Facilities
4. Nuclear Magnetic Resonance Spectroscopy
5. Glass Blowing Techniques

B.3 Courses completed

27/11/95 - 01/12/95 Practical nuclear-magnetic resonance; Six lecture course given by Dr. A.M. Kenwright, Examination date 14/12/95.

08/01/96 - 12/02/96 Diffraction and scattering methods; Six lecture course given by Prof. J.A.K. Howard.

12/01/96 - 16/02/96 Synthetic methodology in organometallic and coordination chemistry; Six lecture course given by Prof. D. Parker, Examination date 12/03/96.

09/01/96 - 13/02/96 Advanced mass spectrometry; Six lecture course given by Dr. M. Jones and Dr. C.A. Woodward, Examination date 19/02/96.

6/2/96: Trip to the University of York, Protein Crystallisation Group: Dr. R.C.B. Copley and I went to York Chemistry department to speak with Dr. Marek Bryzozolski about the different crystallisation techniques that had been used with success in York. I saw their experimental setup and spoke with him about the main variables in crystallisation, and cocrystallisation techniques.

B.4 Seminars attended

1995 - 1996

09/11/95	Prof. R. J. P. Williams, (Oxford U.K.), Metals in Health and Disease.
11/10/95	Prof. P. Lugar, (Frei. Univ. Berlin, F.R.G.), Low Temperature Crystallography.
18/10/95	Prof. A. Alexakis, (Univ. Pierre et Madame Curie, Paris, France) Synthetic and Analytical Uses of Chiral Diamines.
15/11/95	Dr. Andrea Sella (UCL, London), Chemistry of Lanthanides with Polypyrazoylborate Ligands.
10/01/96	Dr. Bill Henderson, (Waikato University, New Zealand), Electrospray Mass Spectrometry - a new sporting technique.
11/01/96	Dr. J. K. M. Sanders, (Oxford U.K.), Enzyme Mimics.
17/01/96	Prof. J. W. Emsley, (Southampton U.K.), Liquid Crystals: More than Meets the Eye.

14/02/96 Prof. Roeland J. M. Nolte, (University of Nijmegen), Helical Poly(isocyanides.)

21/02/96 Dr. Colin Pulham, (Edinburgh, U.K.) Heavy Metal Hydrides – an exploration of the chemistry of stannanes and plumbanes

28/02/96 Prof. E. W. Randall, (Queen Mary and Westfield College, U.K.), New Perpectives in NMR Imaging.

6/3/96 Dr. Richard Whitby, (University of Southampton), New Approaches to Chiral Catalysts. Induction of Planar and Metal Centred Asymmetry.

12/03/96 RSC Endowed Lecture - Prof. V. Balzani, (University of Bologna, Italy), Supramolecular Photochemistry.

13/03/96 Prof. Dave Garner, (Manchester University), Mushrooming in Chemistry.

30/4/96 Dr. L.D. Pettit, Chairman, IUPAC Commission of Equilibrium Data; pH-metric studies using very small quantities of uncertain purity.

1996 - 1997

1/10/96 Prof. L.K. Thompson, (Memorial University, Canada), Unusual Magnetic Behavior of Open Chain and Macrocyclic Dinuclear Cu(II) Complexes.

4/10/96 Prof. Terry Sabine, (ANSTO, Australia), Small-angle Neutron Scattering Studies of Hydrating Cement Paste.

9/10/96 Prof. G. Bowmaker, Visiting Professor (University of Auckland, New Zealand), Coordination and Materials Chemistry of the Group 11 and Group 12 Metals: Some recent Vibrational and Solid-State NMR studies.

22/10/96 Prof. B.J. Tighe, (Department of Molecular Sciences and Chemistry, University of Aston), Durham University Chemical Society (DUCS) Lecture; Making Polymers for Biomedical Application: Can we meet Nature's Challenge?

23/10/96 Prof. H. Ringsdorf, (Johannes Gutenburg Universitat, Mainz, Germany), Function based on Self-Organisation and Molecular Recognition.

29/10/96 Prof. D.M. Knight, (University of Durham, Dept. of Physics), Durham University Chemical Society (DUCS) Lecture; The Purpose of Experiment: a look at Davy and Faraday.

18/11/96 Prof. G.A. Olah, (Loker Hydrocarbon Research Inst., USA) Crossing Conventional Lines in my Chemistry of the Elements.

4/12/96 Prof. Klaus Muller-Dethlefs, (York University), Chemical Applications of Very High Resolution ZEKE Photoelectron Spectroscopy.

4/2/97 Dr. A.J. Bannister, (University of Durham), Durham University Chemical Society (DUCS) Lecture; From Runways to Non-Metallic Metals – A new Chemistry based on Sulphur.

18/2/97 Prof. Sir James Black, (James Black Foundation/KCL, U.K.), Lecture sponsored by Durham University Chemical Society (DUCS) and Lancaster Synthesis; My Dialogues with Medicinal Chemists.

25/2/97 Prof. Sykes, (University of Newcastle, U.K.),), Durham University Chemical Society (DUCS) Lecture; The Synthesis and Structure of Copper Blue Protein.

26/2/96 Dr. Tony Ryan, (UMIST), Making Hairpins from Rings and Chains.

11/3/97 Dr. A.D. Taylor, (ISIS Facility, Rutherton Appleton Laboratory), Durham University Chemical Society (DUCS) Lecture; Expanding the Frontiers of Neutron Scattering.

23/6/97 Prof. Sasha Bagaturyants, (Inst. Of Organometallic Research, Moscow), *Ab-inito* Calculations on some small Semi-conductor Clusters.

1997 - 1998

8/10/97 Prof. E. Atkins, (Department of Physics, University of Bristol), Advances in the Control of Architecture of Polyamides: From Nylons to Genetically Engineered Silks to Monodisperse Oligoamides.

23/10/97 Prof. M.R. Bryce, (University of Durham, Inaugural lecture), New Tetrathiafulvalene Derivatives in Molecular, Supramolecular and Macromolecular Chemistry; Controlling the Electronic Properties of Electronic Solids.

27/10/97 Prof. Warren Roper FRS, (University of Auckland, New Zealand), Silyl Complexes of Rutheium and Osmium.

29/10/97 Prof. Bob Peacock, (University of Glasgow), Probing Chirality with Circular Dichroism.

26/11/97 Prof. R.W. Richards, (University of Durham, Inaugural Lecture), A Random Walk in Polymer Science.

3/12/97 Prof. A.P. Davis, (Trinity College Dublin, Ireland), Steroid-based Frameworks for Supramolecular Chemistry.

21/1/98 Prof. D. Cardin, (University of Reading), Aspects of Metal and Carbon Cluster Chemistry.

17/2/98 Dr. S. Topham, (ICI Chemicals), Durham University Chemical Society (DUCS) Lecture; Perseption of Environmental Risk; The River Tees, Two different rivers.

24/2/98 Prof. R. Ramage, (University of Edinburgh) Durham University Chemical Society (DUCS) Lecture; Synthesis and Folding of Proteins.

11/3/98 Prof. M.J. Cook, (Department of Chemistry, UEA), How to make Phthalocyanine Films and what to do with them.

17/3/98 Prof. V. Rotello, (University of Massachusetts, Amherst, USA), The Interplay of Recognition and Redox Processes: From Flavoenzymes to Devices.

2/4/98 Visiting Professor L.K. Thompson (Memorial University, Canada); Crossing the Border Between Ferromagnetism and Antiferromagnetism.

29/6/98 Main Group Symposium in honour of Dr. Arthur Banister and Profs. Evelyn Ebsworth and Ken Wade. *Lectures:* Dr. R. Snaith

(Cambridge, UK) "Still Wading into Lithium Aluminates, Thirty Years On". Prof. G. M. Sheldrick (Göttingen, Germany) "Is the Crystallographic Phase Problem Solved?"

12/8/98 Dr. Mark Johnson, (Institut Laue Langevin, France); Neutrons and numerical methods: from crystal structures and atom-atom potentials to vibrational and tunnelling dynamics in molecular crystals.

B.5 Publication list

1. *Structural rigidity and luminescence of chiral lanthanide tetraamide complexes based on 1,4,7,10-tetraazacyclododecane*
   R.S. Dickins, J.A.K. Howard, C.W. Lehmann, J. Moloney, D. Parker, and R.D. Peacock; *Angew. Chem., Int. Ed. Engl.*, 1997, **36**, 521.

2. *Strong exciton coupling and circularly polarised luminescence in rigid complexes of chiral macrocyclic tetranaphthlamides*
   R.S. Dickins, J.A.K. Howard, J.M. Moloney, D. Parker, R.D. Peacock and G. Siligardi; *J. Chem. Soc. Chem. Commun.*, 1997, 1747.

3. *Nuclear magnetic resonance, luminescence and structural studies of lanthanide complexes with octadentate macrocyclic ligands bearing benzylphosphinate groups*
   S. Aime, A.S. Batsanov, M. Botta, R.S. Dickins, S. Faulkner, C.E. Foster, A. Harrison, J.A.K. Howard, J.M. Moloney, T.J. Norman, D. Parker, L. Royle and J.A.G. Williams; *J. Chem. Soc. Dalton Trans.*, 1997, 3623 - 3636.

4. *Structure and dynamics of all the stereoisomers of europium complexes of tetra(carboxyethyl) derivatives of dota: ring inversion is decoupled from cooperative arm rotation in the RRRR and RRRS isomers*
   J.A.K. Howard, A.M. Kenwright, J.M. Moloney, D. Parker, M. Port, M. Navet, O. Rosseau and M. Woods. *J. Chem. Soc. Chem. Commun.*, 1998, 1381.

5. *Ground and excited state chiroptical of enantiopure macrocyclic tetranaphthyl lanthanide complexes: controlled modulation of the frequency and polarisation of emitted light*
   R.S. Dickins, J.A.K. Howard, C.L. Maupin, J.M. Moloney, D. Parker, R.D. Peacock, J.P. Riehl and G. Siligardi, *New Journal of Chemistry*, 1998, 891 - 900.

6. *Synthesis, time-resolved luminescence, NMR, circular dichroism and circularly polarised luminescence studies of enantiopure macrocyclic lanthanide tetraamide complexes.*

R.S. Dickins, J.A.K. Howard, C.L. Maupin, J.M. Moloney, D. Parker, J.P. Riehl and G. Siligardi and J.A.G. Williams, *Chem. Eur. J.*, 1998, **5**, 1095 - 1105.

7. *Dimethyl thiophosphoryl hydrazide ligands: ligand and complex structural studies and an investigation of their solution behaviour by electrospray mass spectrometry.*

   A.S. Batsanov, M.A.M. Easson, L.J. Govenlock, J.A.K. Howard, J.M. Moloney and D. Parker. *J. Chem. Soc. Dalton Trans.*, 1999, 323 - 329.

8. *Correlation of Water Exchange Rate with Isomeric Composition in Diastereomeric Gadolinium Complexes of Tetra(carboxyethyl) dota and Related Macrocyclic Ligands.*

   M. Woods, S. Aime, M. Botta, J.A.K. Howard, J.M. Moloney, M. Navet, D. Parker, M. Port and O. Rosseau, J. Amer. Chem. Soc., 2000, Submitted.

9. *Dependence of the relaxivity and luminescence of gadolinium and europium amino-acid complexes on hydrogencarbonate and pH.*

   S. Aime, A. Barge, M. Botta, J.A.K. Howard, R. Kataky, M.P. Lowe, J.M. Moloney, D. Parker and A.S. de Sousa, (1999), *J. Chem. Soc., Chem. Commun.*, 1047 – 1048.

10. *NMR, Relaxometric and Structural Studies of the Hydration and Exchange of Cationic Lanthanide Complexes of Macrocyclic Tetraamide Ligands.*

    M. Woods, S. Aime, A. Barge, M. Botta, J.A.K. Howard, J.M. Moloney, D. Parker and A.S. de Sousa, *J. Amer. Chem. Soc.*, 1999, **121**, 5762 - 5772.

11. *Chiroptical Features and Luminescence Behaviour of Macrocyclic Tetra-(-4-quinolyl)- Complexes: surprising absence of exciton compling.*

    Linda J. Govenlock, J.A.K. Howard, J.M. Moloney, D. Parker, R.D. Peacock and G. Siligardi, *J. Chem. Soc., Perkin Trans. 2*, 1999, 2415 – 2419.

12. *Molecular Structures of 1,12-$B_{12}H_{10}CO_2$ and its dihydrate 1,12-$B_{12}H_{10}[C(OH)_2]_2$ – a novel bis-carbene complex.*

    M.A. Fox, J.A.K. Howard, J.M. Moloney and K. Wade. *J. Chem. Soc., Chem. Commun.*, 1998, 2487 – 2488.